PhytoKeys 237: 1–22 (2024)
DOI: 10.3897/phytokeys.237.113773

Research Article

Description of five new *Luticola* D.G.Mann (Bacillariophyta, Diadesmidaceae) species from Indonesia with comments on the morphological boundaries of the genus

Mateusz Rybak[1], Łukasz Peszek[1], Oktiyas Muzaky Luthfi[2,4], Sulastri Arsad[2,4], John Patrick Kociolek[3], Andrzej Witkowski[4†]

1 Department of Agroecology and Forest Utilization, University of Rzeszów, ul. Ćwiklinskiej 1A, 35-601 Rzeszów, Poland
2 University of Brawijaya, Department of Marine Science, Malang, East Java, Indonesia
3 Museum of Natural History and Department of Ecology and Evolutionary Biology, University of Colorado, Boulder, CO, USA
4 University of Szczecin, Institute of Marine and Environmental Sciences, Mickiewicza 16A, 70-383 Szczecin, Poland
Corresponding author: Mateusz Rybak (matrybak91@gmail.com; mrybak@ur.edu.pl)

Abstract

During a survey of the Indonesian diatoms, five *Luticola* D.G.Mann taxa that could not be identified, based on the available literature were discovered. Based on light microscopy, scanning electron microscope observations and comparisons with similar taxa, all of them are described as new species. All taxa were found on mosses growing on tree trunks and concrete on the islands of Banda Besar and Seram and from spring on Java Island. *Luticola insularis* **sp. nov.** is most similar to *L. aequatorialis* and *L. simplex*, but it can easily be distinguished from both taxa, based on the lower striae density, the narrower valves and the well-developed silica ridges on the valve face/mantle junction. *Luticola bandanensis* **sp. nov.** resembles *L. frequentissima*, but they can be easily distinguished, based on their valve widths and the direction of the grooves located on the distal and proximal raphe endings. *Luticola elliptica* **sp. nov.** is most similar to *L. sparsipunctata*, *L. tenuis* and *L. bryophila*. Amongst all the species compared, *L. elliptica* **sp. nov.** is the only one with a highly asymmetrical central area, with the isolated pore located on the wider side. *Luticola malukuana* **sp. nov.** shares similarities with *L. dismutica* and *L. areolata*, but it has a notably higher stria density. From *L. areolata*, it can also be separated by the morphology of striae and the lack of ghost areolae in the central area. *Luticola poliporea* **sp. nov.** is unique in the whole genus due to the presence of multiple isolated pores.

Key words: Diatoms, morphology, Southeast Asia, taxonomy

Academic editor: Kalina Manoylov
Received: 6 October 2023
Accepted: 4 December 2023
Published: 5 January 2024

Citation: Rybak M, Peszek Ł, Luthfi OM, Arsad S, Kociolek JP, Witkowski A (2024) Description of five new *Luticola* D.G.Mann (Bacillariophyta, Diadesmidaceae) species from Indonesia with comments on the morphological boundaries of the genus. PhytoKeys 237: 1–22. https://doi.org/10.3897/phytokeys.237.113773

Introduction

The study of terrestrial diatoms in Southeast Asia began at the end of the 19th century (Grunow 1865) and continues to this day. The result of this work is over 100 scientific publications focusing on diatoms in this area (Glushchenko et al. 2021). Despite a relatively long history of diatom research, terrestrial and aerophytic diatoms have received much less attention. The first and, for a long time, the only mention of this ecological group in Southeast Asia was the work of Kolkwitz and Krieger (1936), in which they mention the results from a single soil sample collected under trees, in which they found just a few diatom species. However, the situation has been changing in recent years, reflected in the descriptions of many new species from terrestrial environments of this region like soils or tufts of mosses (Kezlya et al. 2020a, b, 2022a, b; Rybak et al. 2020, 2022a, b, c; Glushchenko et al. 2022).

Many genera of diatoms are recorded in terrestrial and aerophytic environments and *Luticola* D.G. Mann (in Round et al. (1990: 148)) seems to be one of the most diverse (Chattová 2018; Bishop et al. 2021; Rybak et al. 2021a, 2023; Radhakrishnan et al. 2022; Chattová et al. 2022). However, representatives of this genus can also be found in other environments such as fresh-, brackish and marine water and even as epizoic on turtles (Wetzel et al. 2010; Levkov et al. 2013; Wu and Bergey 2017; Rybak et al. 2021b). The genus *Luticola* was distinguished from *Navicula* to accommodate species included in the *Naviculae* sect. Punctatae with *Luticola mutica* (Kützing) D.G.Mann (in Round et al. (1990: 532)) selected as the generitype. Features common to all species are the distinctly punctate, uniseriate striae composed of rounded to elongated areolae covered internally by perforated hymenes, an evident and morphologically unique isolated pore in the central area and a marginal longitudinal channel positioned internally between the valve face and the valve mantle (Round et al. 1990; Levkov et al. 2013). Since the publication of the Levkov’s et al. (2013) monograph on the genus, in which almost 200 species are treated, the genus has attracted the attention of many taxonomists from around the world. As a result of their work, the number of currently-known taxa has increased to 262 (Guiry and Guiry 2023), amongst which 23 species have been described from tropical Asia (Glushchenko et al. 2017; Liu et al. 2017; Lokhande et al. 2020; Rybak et al. 2021b; Yang et al. 2022) or transferred to the genus (Glushchenko and Kulikovskiy 2015; Kale et al. 2017).

In this paper, five new *Luticola* taxa are described from terrestrial and water mosses in Indonesia and separated from other similar taxa, based on their combinations of morphological features as documented with light and scanning electron microscopy.

Material and methods

The Maluku Islands (Spice Islands or Moluccas) are an archipelago in the northeast of Indonesia. The climate of the study area is almost entirely tropical and is dominated by a tropical rainforest climate with wet and dry seasons. Samples of terrestrial mosses from concrete and tree trunks were collected, placed in paper envelopes and left to dry. Moss samples from springs were collected with a spoon and placed in a plastic container. Three samples, in which unidentified *Luticola* taxa were observed, were selected for this study:

- 2018/440 – 4°31'29.93"S, 129°56'51.69"E, terrestrial orthotropic mosses collected from the base of a tree trunk on Banda Besar, Indonesia, in a forest near the shore at an elevation of 19 m a.s.l. The pH measured was 5.8 and conductivity was 1250 µS/l/cm.
- 2018/447 – 3°19'12.2"S, 128°56'6.94"E, terrestrial plagiotropic mosses collected from concrete in Amahai, Seram, Indonesia, at an elevation of 14 m a.s.l. The pH measured was 6.7 and conductivity was 680 µS/l/cm.

- 2023/81 – 7°50'26.2"S, 112°31'43.0"E, plagiotropic mosses from an unnamed spring collected in Malang, East Java, Indonesia.

The samples were used for preparation of diatom slides and filtrates for pH and conductivity measurements. The filtrates were obtained by soaking pieces of moss in deionised water (at a 1:10 weight ratio) for 24 h. pH and electrical conductivity were measured with a MARTINI pH56 pH meter and a MARTINI EC59 conductivity meter (Szeged, Hungary).

For diatom slides preparation, a small part of each moss sample was digested with a mixture of sulphuric acid and potassium dichromate. After dissolving all organic matter, the suspension was centrifuged at 2500 rpm to remove the dissolving mixture and subsequently washed 3–5 times with centrifugation in distilled water. The cleaned diatom suspension was pipetted on to coverslips, left to dry overnight at room temperature and then mounted with Naphrax (Brunel Microscopes Ltd, Wiltshire, U.K.). Identification, counting and the measurements of the diatoms' basic morphological features were performed under a Carl Zeiss Axio Imager A2 light microscope (LM), equipped with a 100× Plan Apochromatic objective with differential interference contrast (DIC) for oil immersion (NA 1.4) and captured with a Zeiss AxioCam ICc5 camera. For scanning electron microscope (SEM) observations, several drops of the samples were placed on a polycarbonate membrane filter with a 3 μm mesh, attached to aluminium stubs and sputtered with 20 nm of gold using a Turbo-Pumped Sputter Coater Quorum Q 150OT ES. The diatoms were observed using a Hitachi SU 8010 SEM. Diatom terminology follows Barber and Haworth (1981), Round et al. (1990) and Levkov et al. (2013).

Results

Luticola insularis **M.Rybak & Peszek, sp. nov.**
Figs 1A–S, 4A–H

Description. LM observations (Fig. 1A–S). Valves elliptic-lanceolate to lanceolate with narrowly rounded apices. Range of valve dimensions (n = 35): 8.5–24.0 μm long, 4.5–7.0 μm wide and 16–20 striae in 10 μm. Striae clearly punctate, composed of 3–4 areolae. Central area rectangular to slightly bow-tie shaped axial area linear and narrow Isolated pore clearly visible in central area located halfway between the margin and the centre. Raphe filiform with proximal endings slightly bent away from isolated pore, distal raphe endings barely visible.

SEM observations (Fig. 4A–H). ***External view***: Striae composed of 3–4 areolae round, becoming larger and more elongated near the margins (Fig. 4A–E). Single row of elongated areolae, interrupted at valve apices, present on valve mantle (Fig. 4D, F). Central area bordered by 2–3 areolae (Fig. 4A–D). Raphe filiform with weakly hooked distal ends continuing on to valve mantle (Fig. 4A, C–E). Proximal raphe ends slightly bent opposite to the isolate pore bearing side, then shortly hooked to the pore and finishing with a small, elongated shallow depressions (Fig. 4B, D, E). Opening of isolated pore small and slightly elongated (Fig. 4A–D). Girdle bands open with two rows of poroids (Fig. 4D, F). Distinct silica ridge visible along valve face/mantle junction (Fig. 1D, F).

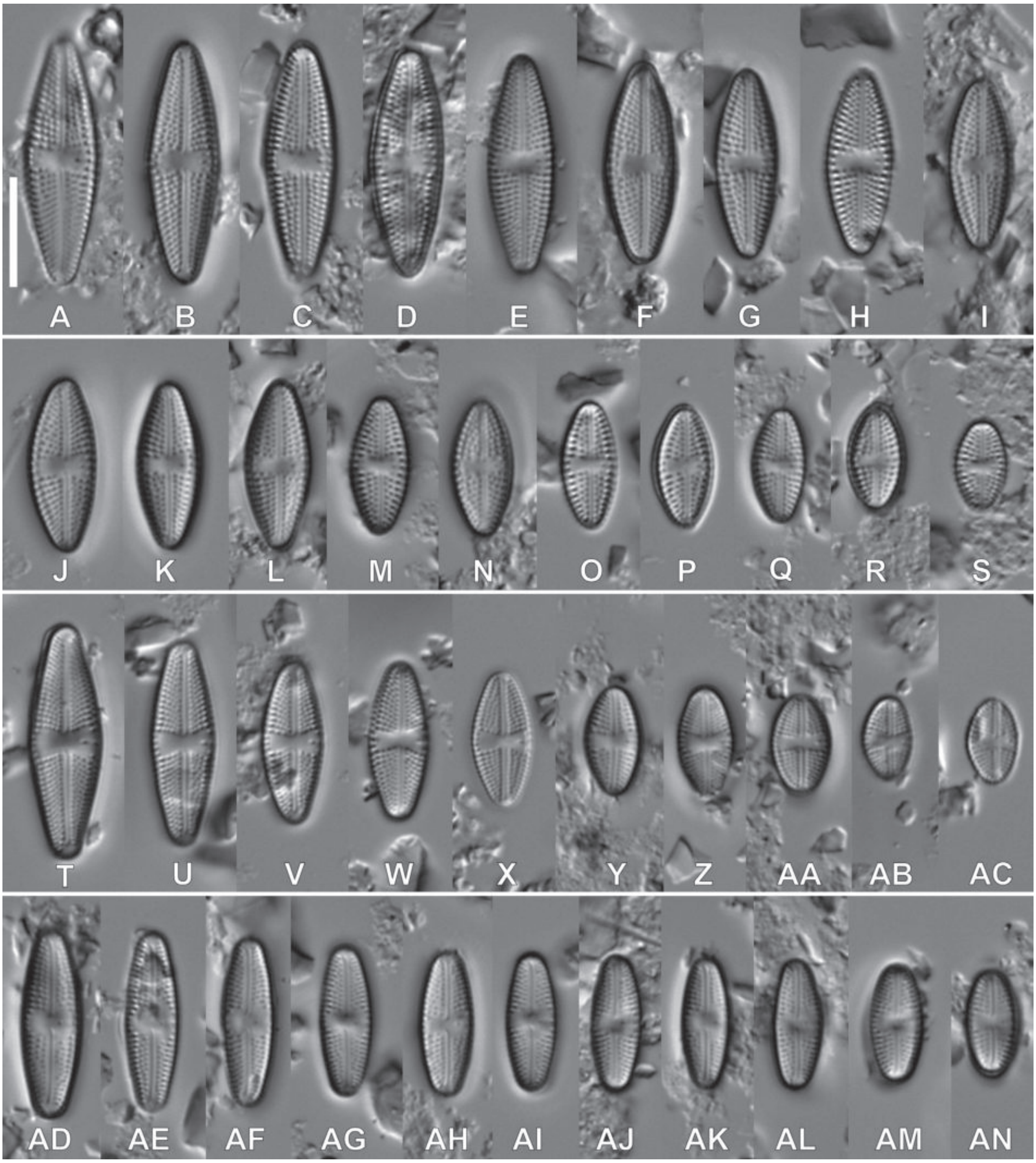

Figure 1. LM microphotographs of three new *Luticola* taxa in size diminution series. *Luticola insularis* sp. nov. (**A–S**), *Luticola bandanensis* sp. nov. (**T–AC**), *Luticola eliptica* sp. nov. (**AD–AN**). Scale bar: 10 µm.

***Internal view*:** Areolae occluded by hymenes forming a continuous strip (Fig. 4G, H). Raphe slits straight (Fig. 4G, H). Proximal raphe endings simple and straight (Fig. 4G, H), distal raphe endings finishing on to weakly developed helictoglossae (Fig. 4G, H). Isolated pore opening with small lipped structure (Fig. 4G, H). Longitudinal channels visible along valve (Fig. 4G, H).

Table 1. Comparison of valve features between *Luticola insularis* sp. nov. and similar species. *- indicates data obtained from photography in original description.

	***L. insularis* sp. nov.**	***L. aequatorialis***	***L. pseudoimbricata***	***L. simplex***
length [µm]	8.5–24.0	15.5–32.5	9.0–22.0	9.5–26.0
width [µm]	4.6–6.7	5.2–8.6	5.0–7.0	5.0–8.0
striae [in 10 µm]	16–20	20–22	20–24	19–21
areolae [per stria]	3–4	3–4	2–4*	3–5
proximal raphe endings	deflected with small, shallow grooves	clearly deflected	short, curved and slightly expanded	doubly curved
distal raphe endings	weakly hooked	strongly hooked	short, bent	hooked
source	this study	Levkov et al. (2013)	Levkov et al. (2013)	Metzeltin et al. (2005); Levkov et al. (2013)

Type. Indonesia, Banda Besar, 4°31'29.93"S, 129°56'51.69"E, 19 m a.s.l., coll. 23 June 2018, holotype slide no. SZCZ29103! and the unmounted material with the same number in the Szczecin Diatom Collection (University of Szczecin, Poland), isotype slide no. 2018/440 and the unmounted material with the same number at the University of Rzeszów, Poland. The type population is illustrated in Figs 1A–S, 4A–H.

Etymology. The name refers to the fact that the species was found on one of many Asian islands (lat. *insula* – island).

Distribution. So far, this species has been observed only in the type locality.

Ecology and associated diatom flora. The species was observed in a sample characterised by a slightly acidic pH (5.8) and conductivity was 1250 µS/cm. The species described herein co-occurred with: *Luticola bandanensis* sp. nov., *L. elliptica* sp. nov., *L. minima* Levkov, Metzeltin & Pavlov, two unidentified small-celled *Nitzschia* sp., *Nitzschia vitrea* G.Norman and *Tryblionella debilis* Arnott ex O'Meara.

Luticola bandanensis M.Rybak & Peszek, sp. nov.

Figs 1T–AC, 5A–H

Description. LM observations (Fig. 1T–AC). Valves elliptic-lanceolate to rhombic-lanceolate with narrowly rounded apices in larger specimens becoming elliptic with broadly rounded apices in smaller specimens. Range of valve dimensions (n = 25): 6.8–21.5 µm long, 4.5–6.5 µm wide and 21–23 striae in 10 µm. Striae clearly punctate composed of 3–5 areolae. Central area bow-tie shaped, axial area linear and narrow. Isolated pore clearly visible in central area, shifted slightly to valve margin. Raphe filiform with proximal endings slightly bent away from isolated pore, distal raphe endings barely visible.

SEM observations (Fig. 5A–H). ***External view*:** Striae composed of 3–5 round to slightly elongated areolae (Fig. 5A–F). Single row of round areolae present on valve mantle uninterrupted at the apices (Fig. 5D, E). Central area bordered by 2–4 areolae (Fig. 5A–F). raphe straight and filiform with distal raphe endings hooked with irregular shallow grooves on valve face on isolated pore side

Table 2. Comparison of valve features between *Luticola bandanensis* sp. nov. and similar species. *- indicates data obtained from photography in original description.

	***L. bandanensis* sp. nov.**	***L. frequentissima***	***L. pitranensis***	***L. rapanuiensis***
length [μm]	6.8–21.5	12.0–27.0	13.5–27.0	5.2–15.9
width [μm]	4.5–6.5	6.5–9.0	5.0–7.0	4.3–7.6
striae [in 10 μm]	21–23	20–24	18–21	16–19
areolae [per stria]	3–5	4–6	4–5	2–3(4)
proximal raphe endings	deflected with irregular shallow grooves on side opposite to isolated pore	short with irregular shallow grooves on isolated pore side	hooked with irregular shallow grooves* on isolated pore side	curved towards stigma with irregular shallow grooves
distal raphe endings	hooked with irregular shallow grooves on isolated pore side	curved with irregular shallow grooves on isolated pore side	hooked	curved to tightly hooked to isolated pore side
source	this study	Levkov et al. (2013); Noga et al. (2017)	Levkov et al. (2013)	Peszek et al. (2021)

(Fig. 5A–F). Proximal raphe endings deflected finishing with varying in length shallow grooves extending to the first or second row of areolae on the opposite side of the isolated pore (Fig. 5A–F). Distal raphe endings hooked with irregular shallow grooves on isolated pore side (Fig. 5A–F). Small, transacially elongated opening of isolated pore shifted slightly to valve margin (Fig. 5A–F). Girdle bands open with two rows of poroids (Fig. 5D).

***Internal view*:** Areolae occluded by hymenes forming a continuous strip (Fig. 5H). Raphe slits straight (Fig. 5G, H). Proximal raphe endings simple and straight (Fig. 5G, H), distal raphe endings finishing on to weakly developed helictoglossae (Fig. 5G, H). Isolated pore opening with small lipped structure (Fig. 5G, H). Narrow longitudinal channels visible around valve (Fig. 5G, H).

Type. Indonesia, Banda Besar, 4°31'29.93"S, 129°56'51.69"E, 19 m a.s.l., coll. 23 June 2018, holotype slide no. SZCZ29103! and the unmounted material with the same number in the Szczecin Diatom Collection (University of Szczecin, Poland), isotype slide no. 2018/440 and the unmounted material with the same number at the University of Rzeszów, Poland. The type population is illustrated in Figs 1T–AC, 5A–H.

Etymology. Name refers to type locality, the island of Banda Besar in the Banda Island archipelago in the Banda Sea.

Distribution. So far, species observed only in the type locality.

Ecology and associated diatom flora. The species was observed in a sample characterised by a slightly acidic pH (5.8) and conductivity was 1250 μS/cm. The species co-occurred with: *Luticola insularis* sp. nov., *L. elliptica* sp. nov., *L. minima* Levkov, Metzeltin & Pavlov, two unidentified small-celled *Nitzschia* sp., *Nitzschia vitrea* G.Norman and *Tryblionella debilis* Arnott ex O'Meara.

Luticola elliptica **M.Rybak & Peszek, sp. nov.**

Figs 1AD–AN, 6A–H

Description. LM observations (Fig. 1AD–AN). Valves elliptic with broadly rounded apices. Range of valve dimensions (n = 20): 9.0–20.0 μm long, 4.3–

5.5 µm wide and 20–24 striae in 10 µm. Striae clearly punctate. Central area asymmetrical, side with isolated pore wider than the opposite site, axial area linear and narrow becoming slightly wider near to central area. Isolated pore clearly visible in central area located halfway between the margin and the centre. Raphe filiform with proximal endings slightly bent away from isolated pore, hooked distal raphe endings visible.

SEM observations (Fig. 6A–H). ***External view*:** striae composed of 2–3 round to slightly elongated areolae (Fig. 6A–G). Single row of round areolae, interrupted at valve apices, present on valve mantle (Fig. 6A–D, F). Central area bordered by 4–7 areolae on side with isolated pore and 2–4 on opposite side (Fig. 6A–G). Raphe filiform with weakly-hooked distal endings continuing on to valve mantle (Fig. 6A–G). Proximal raphe endings deflected away from isolated pore and slightly enlarged (Fig. 6A–G). Opening of isolated pore round and not connected by areolae with striae (Fig. 6A–G). Girdle bands open with two rows of poroids.

***Internal view*:** Areolae occluded by hymenes forming a continuous strip (Fig. 6H). Raphe slits straight (Fig. 6H). Proximal raphe endings simple and straight (Fig. 6H), distal raphe endings forming finishing on to weakly-developed helictoglossae (Fig. 6H). Isolated pore opening with small lipped structure (Fig. 6H). Longitudinal channels visible along valve (Fig. 6H).

Type. INDONESIA, Banda Besar, 4°31'29.93"S, 129°56'51.69"E, 19 m a.s.l., coll. 23 June 2018, holotype slide no. SZCZ29103! and the unmounted material with the same number in the Szczecin Diatom Collection (University of Szczecin, Poland), isotype slide no. 2018/440 and the unmounted material with the same number at the University of Rzeszów, Poland. The type population is illustrated in Figs 1AD–AN, 6A–H.

Etymology. Name refers to the valve shape of the species.

Distribution. Species has been observed in various locations in Southeast Asia. It was also observed on Borneo Island, Palambak Island, Sulawesi Island and Banda Besar (Rybak – unpublished data).

Ecology and associated diatom flora. The species was observed in a sample characterised by a slightly acidic pH (5.8) and conductivity was 1250 µS/cm.

Table 3. Comparison of valve features between *Luticola eliptica* sp. nov. and similar species. *- indicates data obtained from photography in original description.

	***L. eliptica* sp. nov.**	***L. sparsipunctata***	***L. tenuis***	***L. bryophila***	***Luticola* sp.**
length [µm]	9.0–20.0	11.0–28.0	11.0–30.0	10.0–25.0	10.7–20.5
width [µm]	4.3–5.5	5.0–7.0	4.0–6.0	4–6	4.5–6.5
striae [in 10 µm]	20–24	17–20	18–20	18–20	20–24
areolae [per stria]	2–3	1–2	2–4	2–3	3–4*
proximal raphe endings	deflected away from the isolated pore	deflected away from the isolated pore	distinctly deflected away from the isolated pore	deflected away from the isolated pore	deflected away from the isolated pore
distal raphe endings	weakly hooked	short and weakly deflected or hooked	weakly hooked	deflected	deflected
source	this study	Levkov et al. (2013)	Levkov et al. (2013)	Rybak et al. (2023)	Chattová et al. (2017)

The species co-occurred with: *Luticola insularis* sp. nov., *L. bandanensis* sp. nov., *L. minima* Levkov, Metzeltin & Pavlov, two unidentified small-celled *Nitzschia* sp., *Nitzschia vitrea* G.Norman and *Tryblionella debilis* Arnott ex O'Meara.

Luticola malukuana **M.Rybak & J.P. Kociolek, sp. nov.**

Figs 2A–S, 7A–H

Description. LM observations (Fig. 2A–S). Frustules rectangular in girdle view, larger valves linear-lanceolate with weakly-protracted apices and slightly undulating margin, smaller valves elliptic-lanceolate. Range of valve dimensions (n = 35): 12.0–28.0 µm long, 5.5–7.0 µm wide and 18–21 striae in 10 µm. Striae clearly punctate. Central area rectangular to slightly bow-tie-shaped, axial area linear and narrow. Isolated pore clearly visible in central area. Raphe filiform with proximal endings slightly bent away from isolated pore, distal raphe endings barely visible.

SEM observations (Fig. 7A–H). ***External view*****:** Striae composed of 3–4 round to slightly elongated areolae (Fig. 7A–D). Single row of elongated areolae, interrupted at valve apices, present on valve mantle (Fig. 7B, D). Central area bordered by 3–4 areolae (Fig. 7A–D). Raphe filiform with weakly-hooked distal endings continuing on to valve mantle (Fig. 7A–D). Proximal raphe endings deflected away from isolated pore (Fig. 7A–D). External opening of isolated pore round and not associated with striae (Fig. 7A–D). Girdle bands numerous and open with two rows of poroids (Fig. 7E, F).

Internal view**:** Areolae occluded by hymenes forming continuous strips (Fig. 7G, H). Raphe slits straight (Fig. 7G, H). Proximal raphe endings simple and straight (Fig. 7G, H). Isolated pore opening with small circular structure (Fig. 7G, H). Longitudinal channels visible along valve (Fig. 7G).

Type. INDONESIA, Seram, Amahai City, 3°19'12.2"S, 128°56'6.94"E, 14 m a.s.l., coll. 29 June 2018, holotype slide no. SZCZ29104! Additionally, the unmounted material with the same number in the Szczecin Diatom Collection (University of Szczecin, Poland), isotype slide no. 2018/447 and the unmounted material with the same number at the University of Rzeszów, Poland. The type population is illustrated on Figs 2A–S, 7A–H.

Table 4. Comparison of valve features between *Luticola malukuana* sp. nov. and similar species. *- indicates data obtained from photography in original description.

	L. malukuana **sp. nov.**	***L. dismutica***	***L. areolata***
length [µm]	12.0–28.0	18.0–40.0	23.0–37.0
width [µm]	5.5–7.0	6.0–9.5	5.5–8.5
striae [in 10 µm]	18–21	16–18	13–16
areolae [per stria]	3–4	3–4	2–3*
proximal raphe endings	deflected away from the isolated pore	weakly curved	deflected away from the isolated pore
distal raphe endings	hooked	hooked	deflected
source	this study	Levkov et al. (2013)	Lokhande et al. (2020)

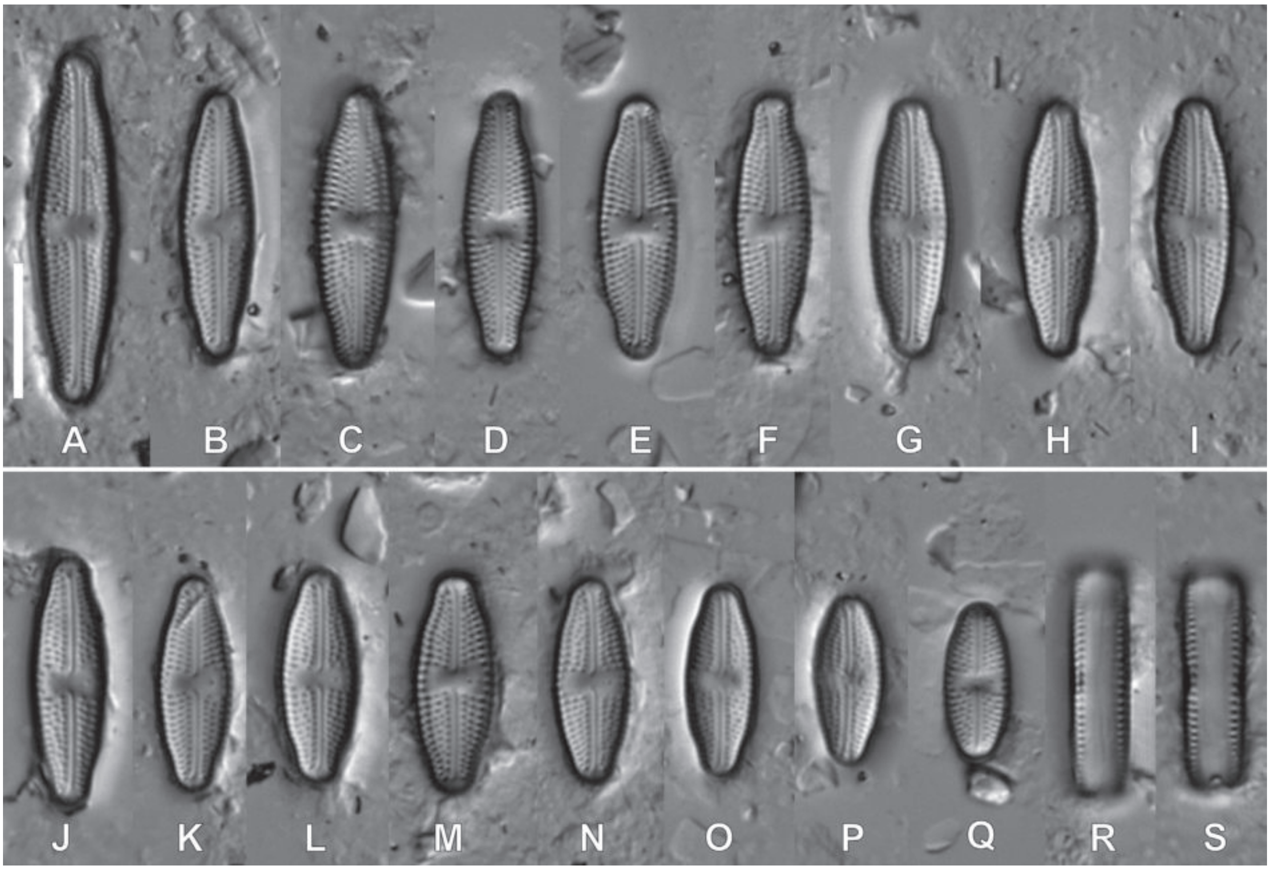

Figure 2. LM microphotographs of *Luticola malukuana* sp. nov. in size diminution series. W, S – frustule in girdle view. Scale bar: 10 µm.

Etymology. Name refers to Maluku Islands where the species was found.

Distribution. So far, this species has been observed only in the type locality.

Ecology and associated diatom flora. The species was observed in a sample characteried by a circum-neutral pH (6.7) and conductivity of 680 µS/cm. The species was the most abundant taxon in an assemblage including: *Humidophila lacunosa* (Moser, Lange-Bertalot & Metzeltin) Lowe, Kociolek, Johansen, Van de Vijver, Lange-Bertalot and Kopalová, *Luticola hustedtii* Levkov, Metzeltin & Pavlov, *Luticola intermedia* Levkov, Metzeltin & Pavlov and *Luticola sublagerheimii* Levkov, Metzeltin & Pavlov.

Luticola poliporea **M.Rybak, Peszek, Luthfi, Arsad & A.Witkowski sp. nov.**
Figs 3A–W, 8A–G, 9A–G

Description. LM observations (Fig. 3A–W). Frustules rectangular in girdle view, lanceolate or linear-lanceolate with rostrate apices. Range of valve dimensions (n = 100): 12.5–39.0 µm long, 5.3–9.0 µm wide and 20–24 striae in 10 µm. Striae clearly punctate. Central area slightly bow-tie-shaped, axial area linear and narrow. Isolated pores clearly visible in central area. Usually two isolated pores are present, in about 2% of the type population, a third isolated pore occurs (Fig. 3C, J, K, T, A, C).

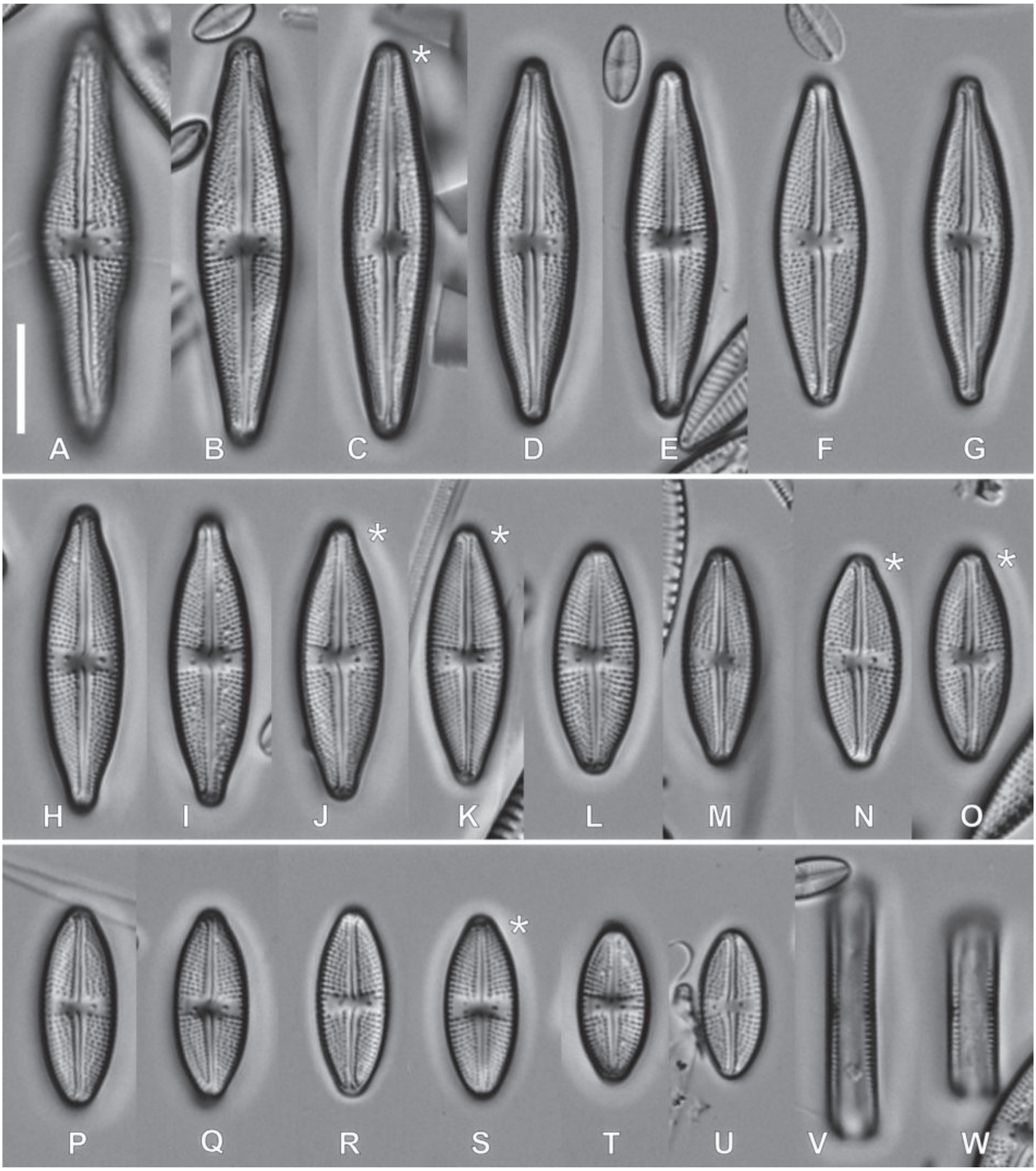

Figure 3. LM microphotographs of *Luticola poliporea* sp. nov. in size diminution series. * – indicates valves with triple isolated pores. **A** initial valve, **V, W** frustule in girdle view. Scale bar: 10 µm.

SEM observations (Figs 8A–G, 9A–G). ***External view*:** Striae composed of 4–5 slightly elongated areolae, almost equal in size (Fig. 8A–G). Single row of elongated areolae, interrupted at valve apices, present on the valve mantle (Fig. 8G, 9G). Central area bordered by three areolae (Fig. 8A–F), ghost areolae commonly present in central area (Fig. 8A–F). Raphe filiform located on distinct raphe sternum (Fig. 8A–G). Distal raphe endings hooked and continued on

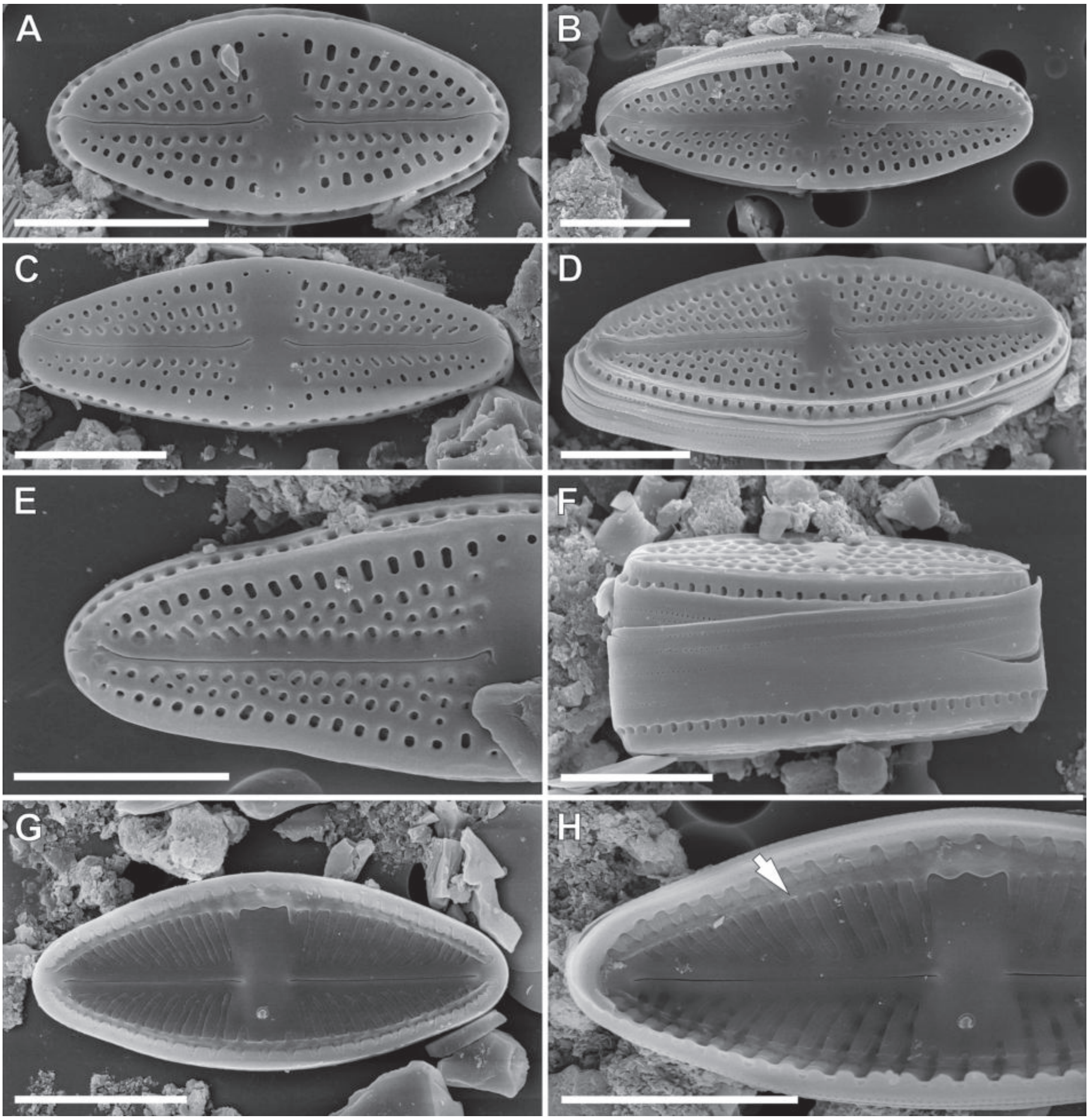

Figure 4. SEM microphotographs of *Luticola insularis* sp. nov. external (**A–F**) and internal (**G, H**) views. Arrow indicate a longitudinal channel. Scale bars: 5 μm.

to valve mantle (Fig. 8G), proximal raphe endings weakly deflected and finishing slightly pore-like enlarged (Fig. 8A–E). External openings of isolated pores elongated located in mid-way between valve margin and valve centre. Isolated pore opening on side where raphe endings are deflected commonly are smaller and shifted from centre part into striae (Fig. 8A–E). Edge of the valve mantle notched approximately half-way between centre and pole in each quadrant of the valve (Fig. 9C).

***Internal view*:** Areolae occluded by hymenes forming continuous strip (Fig. 9A–D). Raphe slits straight (Fig. 9A–E). Proximal raphe endings simple

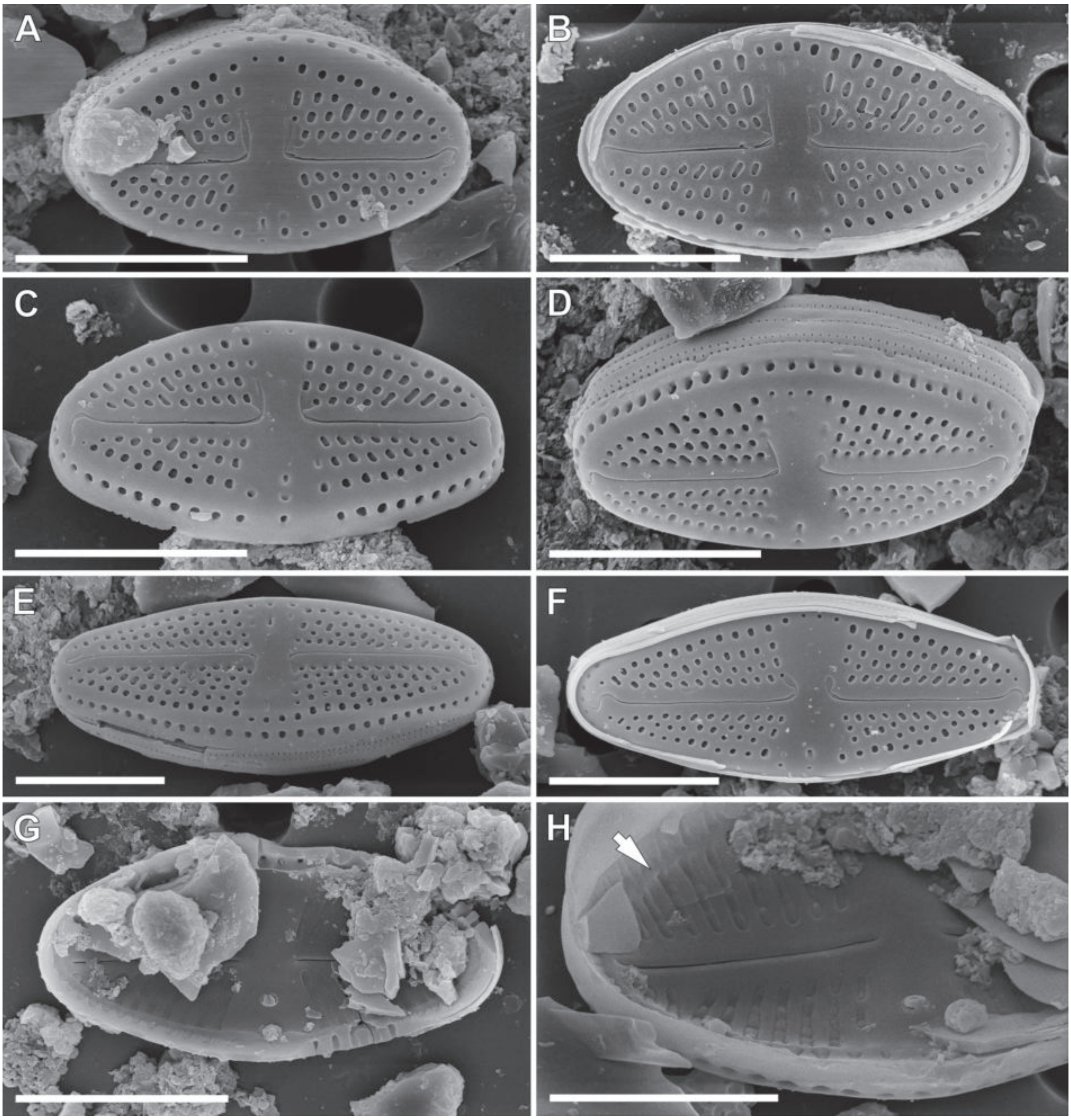

Figure 5. SEM microphotographs of *Luticola bandanensis* sp. nov. external (**A–F**) and internal (**G, H**) views. Arrow indicate a longitudinal channel. Scale bars: 5 µm (**A–G**); 3 µm (**H**).

and straight (Fig. 9A–C, E, F), distal raphe endings forming small helictoglossa (Fig. 9C, D). Isolated pore openings with large circular structure (Fig. 9A–C, E, F), openings of additional pores commonly reduced (Fig. 9B, C, F). Longitudinal channels visible along valve (Fig. 9A–F).

Type. Indonesia, Malang, East Java, unnamed spring, 7°50'26.2"S, 112°31'43.0"E, coll. 2 July 2023. Holotype slide no. SZCZ28794! and unmounted material with the same number in the Szczecin Diatom Collection (University of Szczecin, Poland), isotype slide no. 2023/81 and the unmounted material with the same number at the University of Rzeszów, Poland. The type population is illustrated in Figs 3A–W, 8A–G, 9A–G.

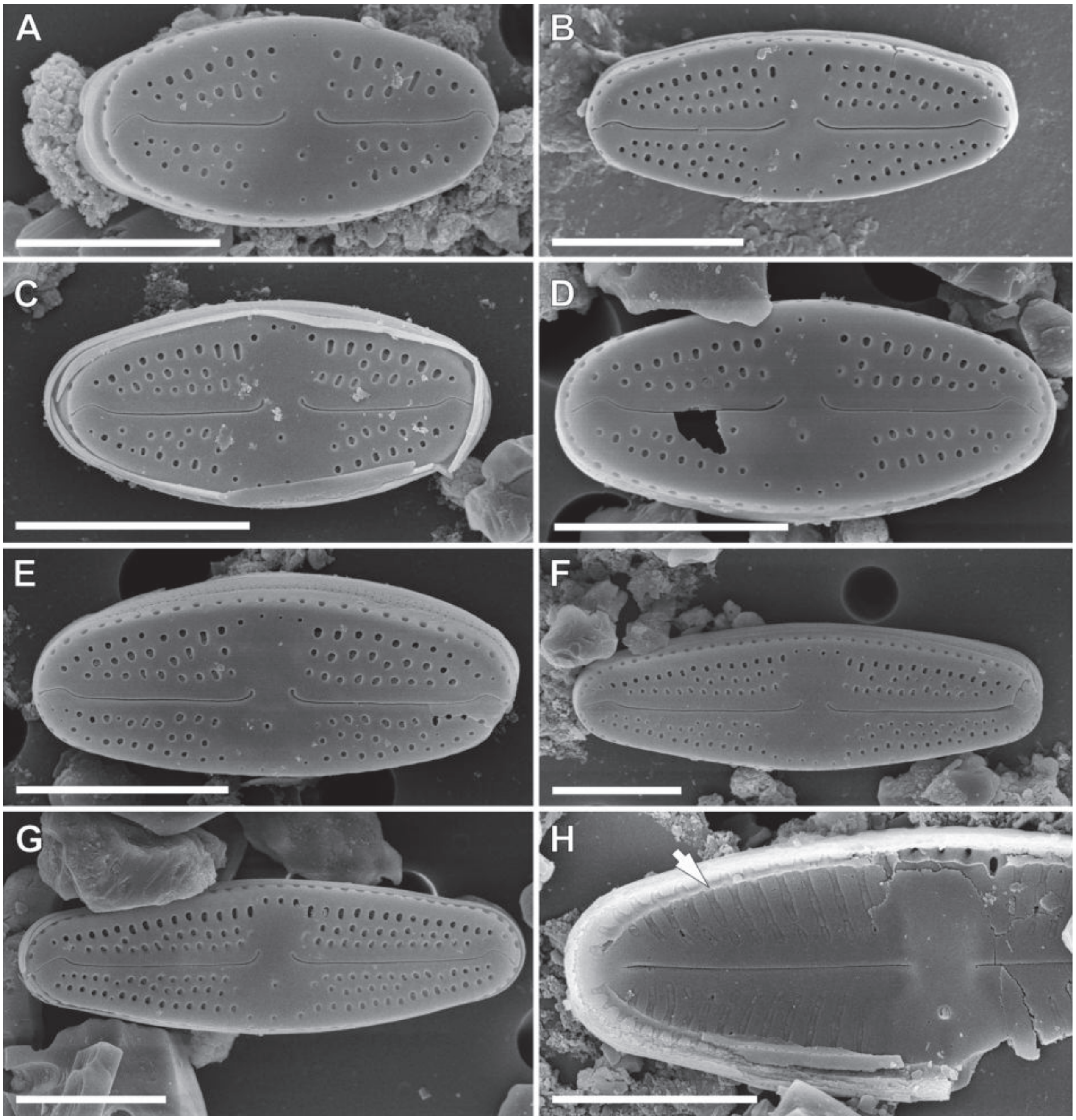

Figure 6. SEM microphotographs of *Luticola eliptica* sp. nov. external (**A–G**) and internal (**H**) views. Arrow indicate a longitudinal channel. Scale bars: 4 µm (**A, C–G**); 5 µm (**B, H**).

Etymology. Name refers to the unusual feature of bearing multiple isolated pores.

Distribution. So far, species observed only in the type locality.

Ecology and associated diatom flora. The species was most abundant in a sample of moss from collected from spring – where it reached 30% of the total share in diatom assemblage; together with the described species, also occurred: *Diadesmis confervacea* Kützing, *Mayamaea* sp., various *Nitzschia* spp., *Navicula* cf. *germainii* Wallace and *Sellaphora nigrii* (De Notaris) Wetzel & Ector. The species was also observed in samples of other habitats from the same spring (sediments, epilithon), but in lower numbers.

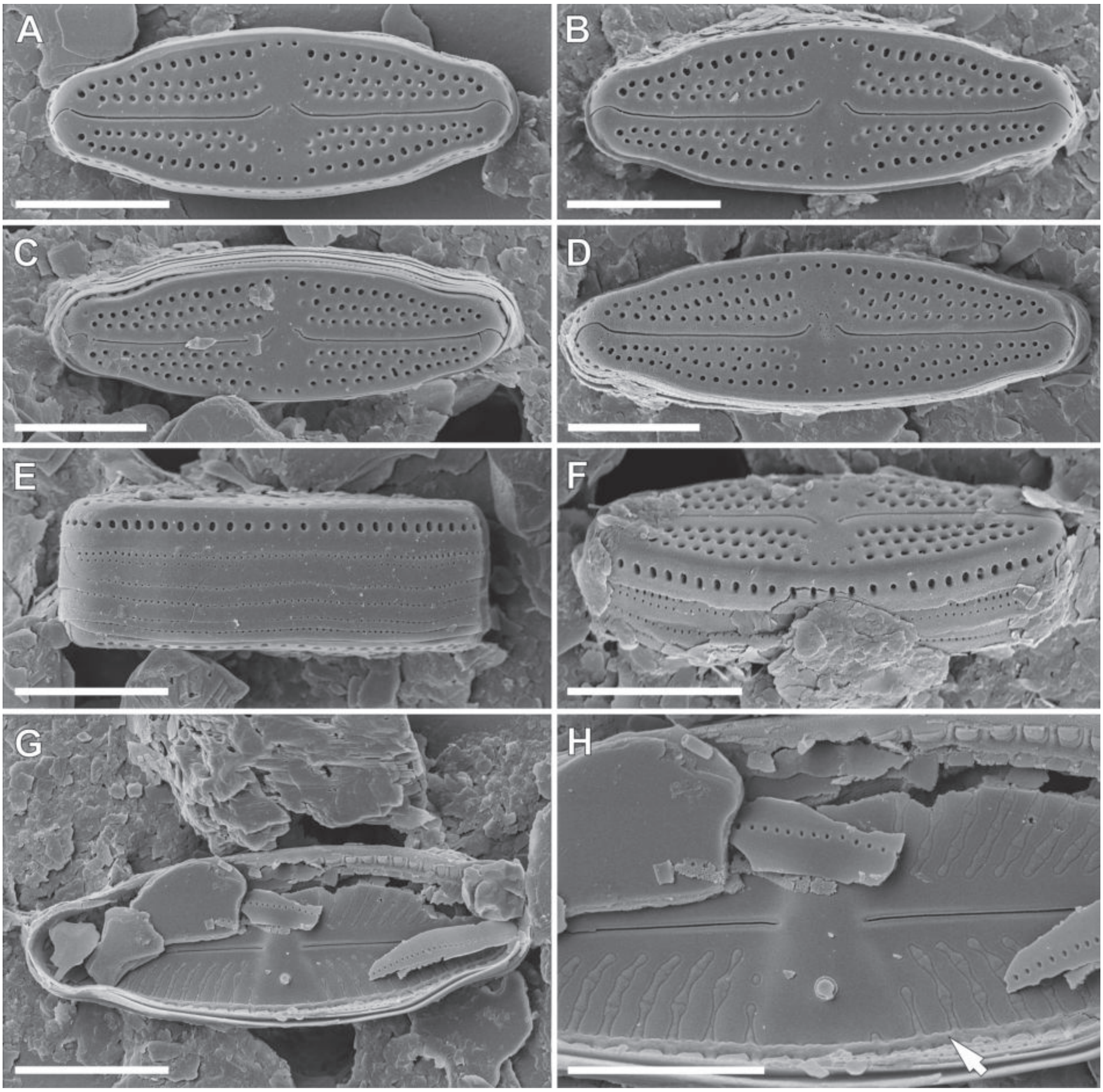

Figure 7. SEM microphotographs of *Luticola malukuana* sp. nov. external (**A–F**) and internal (**G, H**) views. Arrow indicate a longitudinal channel. Scale bars: 5 µm (**A–G**); 3 µm (**H**).

Table 5. Comparison of valve features between *Luticola poliporea* sp. nov. and similar species.

	***L. poliporea* sp. nov**	***L. tuji***	***L. burmensis***
length [µm]	12.5–39.0	14.0–23.0	20.0–36.0
width [µm]	5.3–9.0	5.0–6.5	7.0–10.5
striae [in 10 µm]	20–24	22–28	19–22
areolae [per stria]	4–5	3–5	4–5
proximal raphe endings	deflected to the side opposite to isolated pore	deflected to the side opposite to isolated pore	deflected to the side opposite to isolated pore
distal raphe endings	hooked	hooked	hooked
source	this study	Levkov et al. (2013)	Levkov et al. (2013)

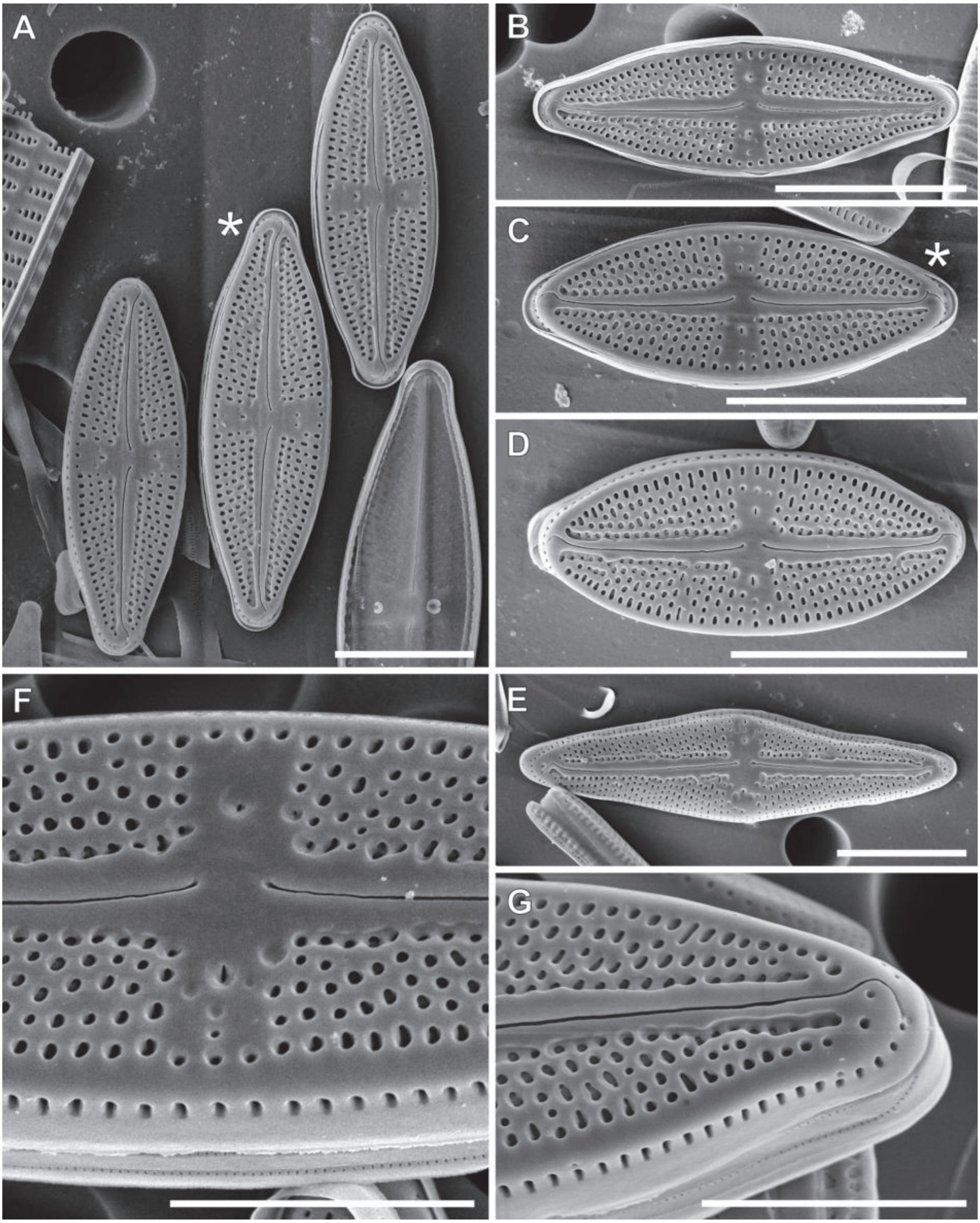

Figure 8. SEM microphotographs of *Luticola poliporea* sp. nov. in external views. * – indicates valves with triple isolated pores. Scale bars: 10 µm (**A–E**); 5 µm (**F, G**).

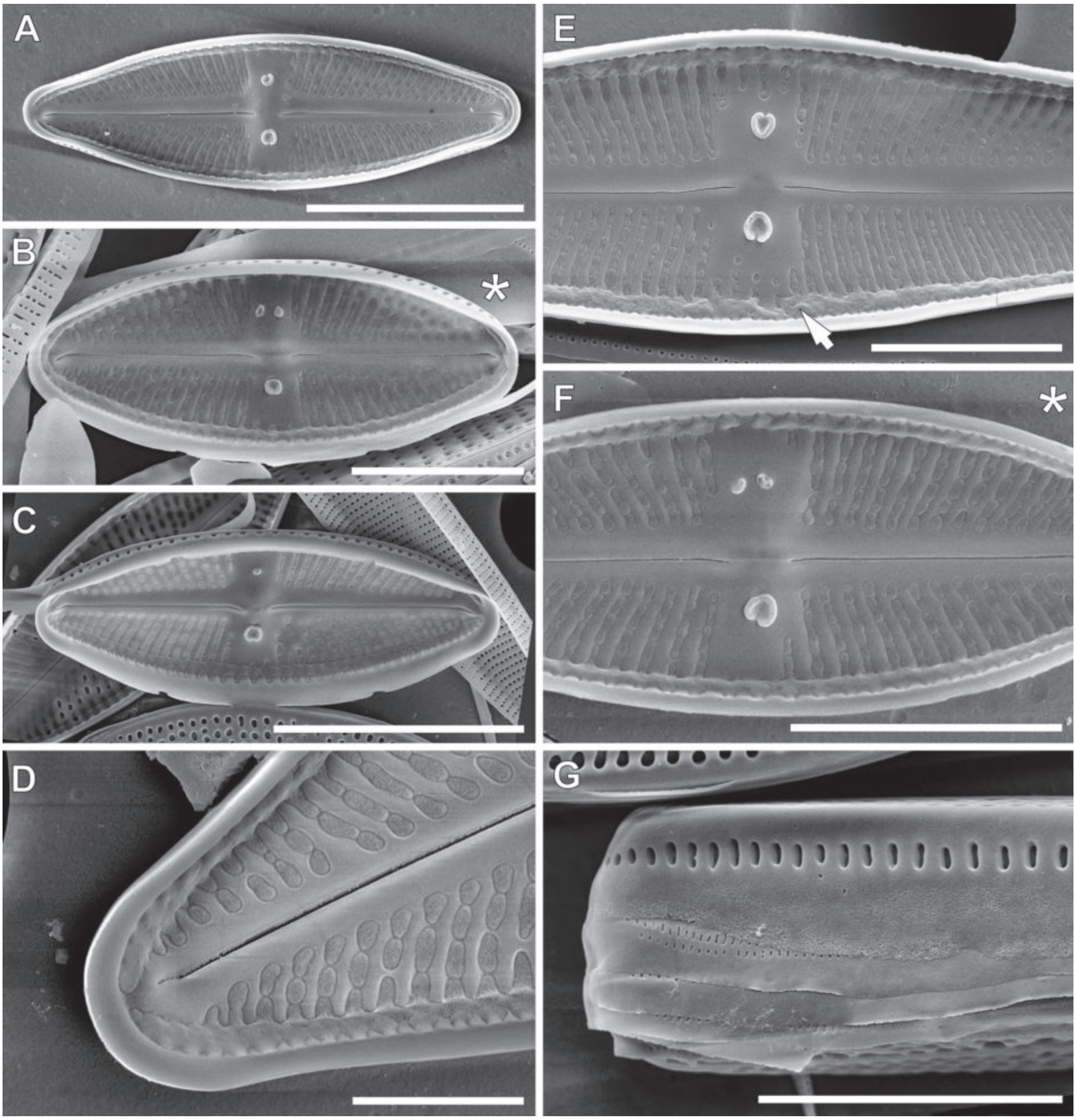

Figure 9. SEM microphotographs of *Luticola poliporea* sp. nov. in internal views (**A–F**) and external details of valve mantle and girdle band (**G**). * – indicates valves with triple isolated pores, arrow indicates a longitudinal channel. Scale bars: 10 µm (**A, C**); 5 µm (**B, E–G**); 2 µm (**D**).

Discussion

Five *Luticola* observed and described in the study show specific features that separate them from all other described *Luticola* species so far. Tables 1–5 present morphological comparisons amongst all of the new species and the most similar taxa worldwide.

Luticola insularis sp. nov. is morphologically most similar to *L. aequatorialis* (Heiden) Lange-Bertalot & T.Ohtsuka and *L. simplex* Metzeltin, Lange-Bertalot & García-Rodríguez, since they share similar valve outlines, areolae densities and distal raphe ending morphologies (Metzeltin et al. 2005; Levkov et al. 2013).

However, *L. insularis* sp. nov. can be easily distinguished from the other two taxa by a lower striae density and narrower valves (Table 1). Moreover, *L. insularis* sp. nov. shows well-developed silica ridges along the valve face/mantle junction (Fig. 4D–F), which are absent in both *L. aequatorialis* and *L. simplex* (Metzeltin et al. 2005; Levkov et al. 2013). Additionally, the European *L. pseudoimbricata* Levkov, Metzeltin & Pavlov shows some degree of similarity and the dimensions of the two taxa overlap. However, *L. insularis* has different proximal and distal raphe endings. In *L. insularis*, the external proximal raphe endings are deflected with small, shallow grooves (Fig. 4A–E), while in *L. pseudoimbricata*, proximal raphe endings are short, curved and slightly expanded (Levkov et al. 2013; pl 16, figs 1–3, 5). Additionally, *L. insularis* has a lower striae density (16–20/10 µm vs. 20–24/10 µm) (see Table 1).

Luticola bandanensis sp. nov. resembles two European species: *L. frequentissima* Levkov, Metzeltin & Pavlov, *L. pitranensis* Levkov, Metzeltin & Pavlov and also with *L. rapanuiensis* M.Rybak, Peszek, A.Witkowski & Lange-Bertalot, which was recently described from Easter Island (Table 2). *Luticola frequentissima* seems the most morphologically similar to *L. bandanensis* sp. nov. The two taxa can be separated, based on the valve width (4.5–6.5 µm in *L. bandanensis* sp. nov. vs. 6.5–9.0 µm in *L. frequentissima*; Levkov et al. (2013)). Additionally, *L. bandanensis* sp. nov. has symmetrical valves, while the valves of *L. frequentissima* are commonly more bulged on the side opposite the isolated pore (Levkov et al. 2013; Noga et al. 2017). Both species show irregular grooves on both distal and proximal raphe endings. In *L. bandanensis* sp. nov., these grooves are present on the side opposite to the isolated pore, while in *L. frequentissima*, the grooves extend to the isolated pore side (Levkov et al. 2013: pl. 9, figs 1–4, Noga et al. 2017: fig. 3). *Luticola pitranensis* can be distinguished from *L. bandanensis* sp. nov., based on its lower striae density (18–21/10 µm vs. 21–23/10 µm), more cuneate valve apices and, as in *L. frequentissima*, the grooves on the proximal raphe endings that extend to the isolate pore side (Levkov et al. 2013: pl. 9, figs 1–5). *Luticola rapanuiensis* can be separated from *L. bandanensis* sp. nov. by its lower striae density (16–19/10 µm vs. 21–23/10 µm), central area that is more rectangular in shape (Peszek et al. 2021: fig. 3A–P) and the presence of irregular silica ridges on the valve face/mantle junction (Peszek et al. 2021: fig. 3U, X–Z) (absent in *L. bandanensis* sp. nov.).

Luticola elliptica sp. nov. shows some degree of similarity to *L. bryophila* M.Rybak, Czarnota & Noga, *Luticola sparsipunctata* Levkov, Metzeltin & Pavlov, *L. tenuis* Levkov, Metzeltin & Pavlov and an unidentified species from the Île Saint-Paul (Chattová et al. 2017: p. 10, figs 72–82). The European *L. sparsipunctata* can be distinguished from *L. elliptica* sp. nov., based on its wider valves with lower striae and areolae density (see Table 3) and a more lanceolate valve shape, especially in larger specimens (Levkov et al. 2013: pl. 32). Both *L. tenuis* and *L. bryophila* have a lower striae density than *L. elliptica* sp. nov. The distal endings in *L. bryophila* are short and deflected to the side opposite the isolated pore (Rybak et al. 2023: fig. 2Y–AA), while the raphe endings in *L. elliptica* sp. nov. are weakly hooked and continue on to the valve mantle (Fig. 5A–G). Finally, *Luticola elliptica* sp. nov. is the only species with a strongly asymmetrical central area. The side bearing the isolated pore is almost two times wider than the other side. This very rare feature was only observed in a single unnamed species from Île Saint-Paul Island in the south Indian Ocean

(Chattová et al. 2017). Both taxa overlap in valve shape, basic dimensions and raphe ending morphology (Table 3). However, because of the lack of SEM documentation for *Luticola* sp., it is impossible to determine definitively whether it is an isolated population of the same taxon or a similar, but different species.

Luticola malukuana sp. nov. most closely resembles *L. dismutica* (Hustedt) D.G.Mann and *L. areolata* V.Lokhande, Lowe, Kociolek & B.Karthick. The basic feature separating it from both species is the notably higher density of striae (Table 4). *L. malukuana* sp. nov. can also be distinguished from *L. dismutica* based on valve outline, which is more undulate in the latter species (see Levkov et al. 2013, pl. 151, figs 15–33, pl. 155, figs 26–35). *Luticola malukuana* sp. nov. and *L. areolata* share a similar, slightly undulating valve outline; however, *L. areolata* has more elongated, narrower valve apices (Lokhande et al. 2020: figs 52–61). Additionally, these taxa differ in striae morphology. Striae of *L. areolata* are composed of fewer areolae (2–3 vs. 3–4) with a clearly reduced external opening (Lokhande et al. 2020: fig. 76). *Luticola areolata* also commonly has ghost areolae in the central area (Lokhande et al. 2020: 52–61) and these are absent or rare in *L. malukuana* sp. nov. (Fig. 7A–D).

Luticola poliporea sp. nov. most closely resembles taxa from the group of *Luticola goeppertiana* (Bleisch) D.G.Mann ex Rarick, S.Wu, S.S.Lee & Edlund. Amongst them, *Luticola tujii* Levkov, Metzeltin & Pavlov and *Luticola burmensis* Metzeltin & Levkov (Levkov et al. 2013) are most similar to the new taxon (Table 5). *Luticola poliporea* sp. nov., together with the taxa it most closely resembles, are characterised by having the raphe located on a clearly visible raphe sternum (Levkov et al. 2013: pl. 63, figs 1–7, Pl. 69, figs 1–5). However, due to the presence of multiple isolated pores in the central area, *Luticola poliporea* sp. nov. is distinguished from both mentioned taxa. Additionally, *Luticola tuji* in contrast to newly-described species, has narrower and usually shorter valves with denser striae (Levkov et al. 2013). *Luticola burmensis* can be distinguished from *L. poliporea* sp. nov. by less rostrate apices and mostly wider valves (Levkov et al. 2013). Moreover, multiple isolated pores make this species unique amongst the entire genus. So far, all taxa described in the genus *Luticola* have a single isolated pore on each valve (Round et al 1990).

Species of the genus *Luticola* described in recent years, especially those representing the *L. goeppertiana* group (Simonato et al. 2020; Yang et al. 2022) clearly show that the morphological boundaries of the genus are much wider than previously documented (Round et al. 1990; Levkov et al. 2013). The original description of the genus by Round et al. (1990) indicated several distinguishing features of the genus *Luticola*, such as: mainly solitary life habit, single plastid with two lobes, single central pyrenoid, mantle margin notched halfway between the apices and valve middle, uniseriate striae, single row of areolae on valve mantle, poroids on valve face and mantle covered by hymenes, presence of a longitudinal canal, narrow raphe-sternum and short stauros, presence of single isolated pore (called stigma) with lipped external opening, deflected raphe endings and open girdle bands with 1 or 2 row of poroids. Since the genus was described, several species with multiple rows of areolae on the mantle have been described or transferred to the genus (Mayama and Kawashima 1998; Pavlov et al. 2009; Wetzel et al. 2010; Da Silva Lehmkuhl et al. 2019; Simonato et al. 2020).

Levkov et al. (2013), in their monograph of the genus, draw attention to the great heterogeneity of the genus in terms of the shape of frustules, areolae and raphe ends. They also draw attention to individual taxa that deviate from the general pattern of frustule structure due to the presence of distinct ridges or spines on the edge. Additionally, Levkov et al. (2013) noted that *L. mutica* (which is the type species of the genus), unlike the other species known at that time, does not have simple areoles, but has a recessed cribrum (Levkov et al. 2013). However, since the publication of the monograph of the genus, several additional species possessing a cribrum have been described, i.e. *Luticola ivetana* Chattova & B.Van de Vijver, *L. cribriareolata* M.Rybak, Witkowski, Risjani & Yunianta and *L. jinshaensis* L.Yang & Q.X.Wang (Chattová et al. 2017; Rybak et al. 2021b; Yang et al. 2022). Additionally, Simonato et al. (2020) shed some light on the morphological variability of the genus, pointing out the occurrence of pseudosepta in some species group, as well as the absence of longitudinal/marginal channels in others. Observations of various species show that the range of morphological variability of the genus is much broader than originally assumed by Round et al. (1990), within which taxa demonstrating certain differences from many characteristic valve features are found (i.e. taxa without longitudinal/marginal canals, having additional rows of areolae on the mantle, additional isolated pores, cribra-bearing). Despite the significant expansion of knowledge about the diversity of morphological features found within *Luticola*, observations of living cells so far show that features, such as the shape of the plastid, the number of its lobes and the presence of a single pyrenoid, seem to be constant (Denys and De Smet 1996; Poulíčková 2008; Bagmet et al. 2023).

A significant number of new diatom taxa have been described in the last few years from both terrestrial and freshwater environments in Southeast Asia. The discovery of five new species of *Luticola* in just three samples presented herein, shows that the poorly-explored terrestrial environments hide interesting and yet undescribed species.

Additional information

Conflict of interest

The authors have declared that no competing interests exist.

Ethical statement

No ethical statement was reported.

Funding

The work was supported by the programme of the Ministry of Science and Higher Education named “Regional Initiative of Excellence” in the years 2019–2023, project number 026/RID/2018/19.

Author contributions

Conceptualization: MR, AW, ŁP. Data curation: SA, MR. Formal analysis: MR. Investigation: MR. Methodology: ŁP. Validation: OL, SA. Visualization: ŁP. Writing – original draft: MR, ŁP, AW. Writing – review and editing: AW, JPK.

Author ORCIDs

Mateusz Rybak https://orcid.org/0000-0001-8998-9537
Łukasz Peszek https://orcid.org/0000-0002-9132-2210
Oktiyas Muzaky Luthfi https://orcid.org/0000-0002-9550-9381

Sulastri Arsad https://orcid.org/0000-0002-7322-7834
John Patrick Kociolek https://orcid.org/0000-0001-9824-7164
Andrzej Witkowski http://orcid.org/0000-0003-1714-218X

Data availability

All of the data that support the findings of this study are available in the main text.

References

Bagmet VB, Abdullin SR, Nikulin AY, Nikulin VY, Gontcharov AA (2023) *Luticola tenera* sp. nov. (Diadesmidaceae, Naviculales) – A new diatom from the soil of the State Nature Reserve "Bastak" (Jewish Autonomous Region, Russia). Life 13(1937): 1–13. https://doi.org/10.3390/life13091937

Barber HG, Haworth EY (1981) A guide to the morphology of the diatom frustule with a key to the British freshwater genera. Scientific Publication – Freshwater Biological Association 44: 1–112.

Bishop J, Wasley J, Waterman M, Kohler T, Van de Vijver B, Robinson S, Kopalová K (2021) Diatom communities differ among Antarctic moss and lichen vegetation types. Antarctic Science 33(2): 118–132. https://doi.org/10.1017/S0954102020000620

Chattová B (2018) Diatoms (Bacillariophyta) associated with lichens from Ulu Peninsula (James Ross Island, NE Antarctic Peninsula). Czech Polar Reports 8(2): 151–161. https://doi.org/10.5817/CPR2018-2-12

Chattová B, Lebouvier M, De Haan M, Van de Vijver B (2017) The genus *Luticola* (Bacillariophyta) on Ile Amsterdam and Ile Saint-Paul (Southern Indian Ocean) with the description of two new species. European Journal of Taxonomy 387(387): 1–17. https://doi.org/10.5852/ejt.2017.387

Chattová B, Cahová T, Pinseel E, Kopalová K, Kohler TJ, Hrbacek F, Van de Vijver B, Nývlt D (2022) Diversity, ecology, and community structure of the terrestrial diatom flora from Ulu Peninsula (James Ross Island, NE Antarctic Peninsula). Polar Biology 45(1): 873–894. https://doi.org/10.1007/s00300-022-03038-z

Da Silva Lehmkuhl AM, Ludwig TAV, Tremarin PI, Bicudo D (2019) On *Luticola* Mann (Bacillariophyceae) in southeastern Brazil: Taxonomy, ecology and description of two new species. Phytotaxa 402(4): 165–186. https://doi.org/10.11646/phytotaxa.402.4.1

Denys L, De Smet WH (1996) Observations on the subaerial diatom *Navicula spinifera* Bock, and its transfer to *Luticola* Mann. Cryptogamie. Algologie 17: 77–93.

Glushchenko AM, Kulikovskiy MS (2015) Species of the genus *Luticola* in waterbodies of Laos and Vietnam. Botanicheskii Zhurnal 100(8): 799–804.

Glushchenko AM, Kulikovskiy MS, Kociolek JP (2017) New and interesting species from the genus *Luticola* (Bacillariophyceae) in waterbodies of Southeastern Asia. Nova Hedwigia. Beiheft 146: 157–173. https://doi.org/10.1127/1438-9134/2017/157

Glushchenko AM, Kuznetsova IV, Kulikovskiy MS (2021) The Diatoms of Southeast Asia. Yaroslavl, Filigran, 320 pp.

Glushchenko A, Kezlya E, Maltsev Y, Genkal S, Kociolek JP, Kulikovskyi M (2022) Description of the Soil Diatom *Sellaphora terrestris* sp. nov. (Bacillariophyceae, Sellaphoraceae) from Vietnam, with Remarks on the Phylogeny and Taxonomy of *Sellaphora* and Systematic Position of *Microcostatus*. Plants 11(16): e2148. https://doi.org/10.3390/plants11162148

Grunow A (1865) Über die von Herrn Gerstenberger in Rabenhorst›s Decaden ausgegeben Süsswasser Diatomaceen und Desmidiaceen von der Insel Banka, nebst Untersuchungen über die Gattungen *Ceratoneis* und *Frustulia*. In: Rabenhorst L (Ed.)

Beiträge zur Näheren Kenntniss und Verbreitung der Algen. Verlag von Eduard Kummer, Leipzig, Heft II, 16 pp.

Guiry MD, Guiry GM (2023) AlgaeBase. World-wide electronic publication, National University of Ireland, Galway. https://www.algaebase.org [Accessed 6 February 2023]

Kale A, Levkov Z, Karthick B (2017) Typification of two species of *Luticola* (Bacillariophyta) from aerophilic habitats of the Western Ghats, India. Phytotaxa 298(1): 29–42. https://doi.org/10.11646/phytotaxa.298.1.3

Kezlya E, Glushchenko A, Maltsev Y, Gusev E, Genkal S, Kuznetsov A, Kociolek JP, Kulikovskyi M (2020a) *Placoneis cattiensis* sp. nov.—a new, diatom (Bacillariophyceae: Cymbellales) soil species from Cát Tiên National Park (Vietnam). Phytotaxa 460(4): 237–248. https://doi.org/10.11646/phytotaxa.460.4.1

Kezlya E, Glushchenko A, Kociolek JP, Maltsev Y, Martynenko N, Genkal S, Kulikovskyi M (2020b) *Mayamaea vietnamica* sp. nov.: A new, terrestrial diatom (Bacillariophyceae) species from Vietnam. Algae – Korean Phycological Society 35(4): 325–335. https://doi.org/10.4490/algae.2020.35.11.23

Kezlya E, Glushchenko A, Kociolek JP, Maltsev Y, Genkal S, Kulikovskyi M (2022a) A new species of *Placoneis* Mereschkowsky (Bacillariophyceae: Cymbellales) from wet soils in southern Vietnam. Cryptogamie. Algologie 43(11): 177–188. https://doi.org/10.5252/cryptogamie-algologie2022v43a11

Kezlya E, Maltsev Y, Genkal S, Krivova Z, Kulikovskyi M (2022b) Phylogeny and fatty acid profiles of new *Pinnularia* (Bacillariophyta) species from Soils of Vietnam. Cells 11(15): e2446. https://doi.org/10.3390/cells11152446

Kolkwitz R, Krieger W (1936) Zur Ökologie der Pflanzenwelt, insbesondere der Algen, des Vulkans Pangerango in West-Java. Berichte der Deutschen Botanischen Gesellschaft 54(2): 65–91. https://doi.org/10.1111/j.1438-8677.1936.tb01946.x

Levkov Z, Metzeltin D, Pavlov A (2013) *Luticola* and *Luticolopsis*. Diatoms of the European inland waters and comparable habitats. Diatoms of Europe 7: 1–698.

Liu B, Williams DM, Blanco S, Jiang X (2017) Two new species of *Luticola* (Bacillariophyta) from the Wuling Mountains Area, China. Nova Hedwigia. Beiheft 146: 197–208. https://doi.org/10.1127/1438-9134/2017/197

Lokhande V, Radhakrishnan C, Kociolek JP, Lowe R, Karthic B (2020) The diatom genus *Luticola* D.G.Mann (Bacillariophyceae) in the Western Ghats of India and its biogeography. European Journal of Phycology 56(2): 142–158. https://doi.org/10.1080/09670262.2020.1783460

Mayama S, Kawashima A (1998) New combinations for some taxa of *Navicula* and *Stauroneis*, and an avowed substitute for a taxon of *Eunotia*. Diatom. The Japanese Journal of Diatomology 14: 69–71. https://doi.org/10.11464/diatom1985.14.0_69

Metzeltin D, Lange-Bertalot H, García-Rodriguez F (2005) Diatoms of Uruguay. Compared with other taxa from South America and elsewhere. Iconographia Diatomologica 15: 1–736.

Noga T, Stanek-Tarkowska J, Kochman-Kędziora N, Rybak M, Peszek Ł, Poradowska A (2017) *Luticola frequentissima* Levkov, Metzeltin & Pavlov – morphological and ecological characteristics of a population from Southern Poland. Oceanological and Hydrobiological Studies 46(2): 237–243. https://doi.org/10.1515/ohs-2017-0024

Pavlov A, Nakov T, Levkov Z, Furey P, Lowe R, Ector L (2009) *Luticola grupcei* (Bacillariophyceae) – a new freshwater diatom from Mountain Baba (Macedonia) and Great Smoky Mountains National Park (U.S.A.): Comparison with the type material of *L. goeppertiana* (Bleisch) D.G.Mann. Nova Hedwigia 89(1/2): 147–164. https://doi.org/10.1127/0029-5035/2009/0089-0147

Peszek Ł, Rybak M, Lange-Bertalot H, Kociolek JP, Witkowski A (2021) Three new *Luticola* D.G.Mann (Bacillariophyta) species from Rapa Nui (Easter Island) found in terrestrial diatom assemblages dominated by widely distributed taxa. PeerJ 9: e11142. https://doi.org/10.7717/peerj.11142

Poulíčková A (2008) Morphology, cytology and sexual reproduction in the aerophytic cave diatom *Luticola dismutica* (Bacillariophyceae). Preslia 80(1): 87–99.

Radhakrishnan C, Yogeshwaran M, Karthick B (2022) Hanging in the air: Tree moss diatoms from Indo-Burma biodiversity hot spot of India. Aerobiologia 38(1): 557–566. https://doi.org/10.1007/s10453-022-09766-3

Round FE, Crawford RM, Mann DG (1990) The Diatoms. Biology & Morphology of the Genera. Cambridge University Press, Cambridge, 747 pp.

Rybak M, Solak CN, Noga T, Glushchenko A, Williams DM, Kulikovskyi M (2020) *Nupela brevistriata* sp. nov. – a new, terrestrial diatom species from Southeast Asia. Diatom Research 34(4): 1–8. https://doi.org/10.1080/0269249X.2019.1698467

Rybak M, Kochman-Kędziora N, Peszek Ł (2021a) Description of four new terrestrial diatom species from *Luticola* and *Microcostatus* genera from South Africa. PhytoKeys 182: 1–26. https://doi.org/10.3897/phytokeys.181.65326

Rybak M, Witkowski A, Peszek Ł, Kociolek JP, Risjani T, Nguyen HD, Zhang J, Yunianta, Nguyen VD, Gastineau R, Duong TT, Rosa P, Meleder V (2021b) Marine and brackish *Luticola* D.G.Mann (Bacillariophyta) species from the Java Sea and South China Sea coasts with the description of three new species. PhytoKeys 183: 115–142. https://doi.org/10.3897/phytokeys.183.71049

Rybak M, Glushchenko A, Witkowski A, Lange-Bertalot H, Kulikovskyi M (2022a) Diversity of the genus *Orthoseira* Thwaites (Bacillariophyceae) from Southeast Asia and Rapa Nui Island with descriptions of four new taxa. Diatom Research 37(1): 1–16. https://doi.org/10.1080/0269249X.2022.2043448

Rybak M, Kochman-Kędziora N, Luthfi OM (2022b) Four novel species from the genus *Hantzschia* Grunow (Bacillariophyta: Bacillariaceae) from rural areas of Southeast Asia. Phytotaxa 567(3): 207–221. https://doi.org/10.11646/phytotaxa.567.3.1

Rybak M, Kochman-Kędziora N, Luthfi OM (2022c) A new diatom (Bacillariophyta) species from Indonesian urban areas, description of *Microcostatus labrisicus* sp. nov. Phytotaxa 555(1): 87–94. https://doi.org/10.11646/phytotaxa.555.1.6

Rybak M, Czarnota P, Noga T (2023) Study of terrestrial diatoms in corticolous assemblages from deciduous trees in Central Europe with descriptions of two new *Luticola* D.G.Mann taxa. PhytoKeys 7(221): 1–40. https://doi.org/10.3897/phytokeys.221.95248

Simonato J, Kociolek JP, Sala SE, Díaz YP, Núñez-Avellaneda M (2020) Three new *Luticola* species from the Andean-Amazonian transition in Colombia: Taxonomy, morphology and preliminary considerations of biogeography of the genus. Diatom Research 35(4): 377–393. https://doi.org/10.1080/0269249X.2020.1813205

Wetzel CE, Van de Vijver B, Ector L (2010) *Luticola denisae* sp. nov. A new epizoic diatom from the Rio Negro (Amazon hydrographic basin). Vie et Milieu 60(3): 177–184.

Wu SC, Bergey EA (2017) Diatoms on the carapace of common snapping turtles: *Luticola* spp. dominate despite spatial variation in assemblages. PLoS ONE 12(2): e0171910. https://doi.org/10.1371/journal.pone.0171910

Yang L, Yu P, Wang Q, Kociolek JP, You Q (2022) *Luticola jinshaensis* sp. nov. (Bacillariophyta), a new freshwater species from Jinsha River, China. Fottea 22(1): 152–161. https://doi.org/10.5507/fot.2021.021

PhytoKeys 237: 23–35 (2024)
DOI: 10.3897/phytokeys.237.112939

Research Article

A new species of genus *Crenotia* (Bacillariophyta) from Tibet, China

Xinyuan Na[1], Jiaming Liu[1], Ying Zhang[1], John Patrick Kociolek[2], Maxim Kulikovskiy[3], Xinxin Lu[1], Fengyang Sui[1], Huan Zhu[4], Guoxiang Liu[4], Yawen Fan[1], Yan Liu[1]

1 *College of Life Science and Technology, Harbin Normal University, Harbin, 150025, China*
2 *Museum of Natural History and Department of Ecology and Evolutionary Biology, University of Colorado, Boulder, CO 80309, USA*
3 *K. A. Timiryazev Institute of Plant Physiology RAS, IPP RAS, Moscow 127276, Russia*
4 *Key Laboratory of Algal Biology, Institute of Hydrobiology, Chinese Academy of Sciences, Wuhan 430072, China*
Corresponding authors: Yawen Fan (fanyaw@163.com); Yan Liu (yanliuhrb@hotmail.com)

Abstract

During the investigation of the freshwater diatoms from Tibet, a monoraphid species was observed from a hot spring near Anduo County, located on a plateau in the central portion of Tibet. This species shares the diagnostic features of *Crenotia*, such as the valve bent along the transapical axis, striae uniseriate to biseriate from centre to the apices and areolae with special structures located at the end of each stria. We compared the morphological characters of this new species with the others in this genus and show it to be new; it is named *Crenotia tibetia* **sp. nov.** This species has small valves with slightly protracted ends with nearly capitate apices, lanceolate axial area, central area unilaterally expanded to the margin, striae uniseriate to biseriate, but, in some valves, the striae are only uniseriate. Areolae are round small to irregular in shape and, at the end of each stria, there is a horseshoe-shaped areola present. Observations of developing valves show all the striae begin biseriate, then they become covered by silica to form uniseriate striae. Comparisons are made amongst the species in this genus and with genera assigned to the Achnanthidiaceae.

Key words: Freshwater diatoms, hot spring, monoraphid, taxonomy

OPEN ACCESS

Academic editor: Bing Liu
Received: 19 September 2023
Accepted: 8 December 2023
Published: 11 January 2024

Citation: Na X, Liu J, Zhang Y, Kociolek JP, Kulikovskiy M, Lu X, Sui F, Zhu H, Liu G, Fan Y, Liu Y (2024) A new species of genus *Crenotia* (Bacillariophyta) from Tibet, China. PhytoKeys 237: 23–35. https://doi.org/10.3897/phytokeys.237.112939

Introduction

Raphid diatoms that possess a raphe on only one of the valves are very diverse and recent systematic revisions of this group have led to a marked increase in the number of genera, from two (e.g. Hustedt (1930); Patrick and Reimer (1966)) to 27 genera (De Stefano and Marino 2003; Wojtal 2013; Kulikovskiy et al. 2020a; Al-Handal et al. 2021; Ge et al. 2022). Traditionally, these genera have been assigned to one of three families, Achnanthaceae Kützing (1844), Cocconeidaceae Kützing (1844) or Achnanthidiaceae Mann in Round et al. (1990). Recent phylogenetic studies have shown these groups to be unrelated, widely dispersed across the raphid diatom tree of life (Thomas et al. 2016; Kulikovskiy et al. 2019). Even genera within the Achnanthidiaceae have been shown to be non-monophyletic (Kociolek et al. 2019; Kulikovskiy et al. 2019).

Crenotia was established in 2013 by Wojtal, when species assigned to it were split from the genus *Achnanthidium*. The type species of *Crenotia*, *C. thermalis* (Rabenhorst) Wojtal, was originally described as a species of *Achnanthidium* (as *A. thermalis* Rabenhorst) and then assigned to the genus *Achnanthes* (as *Achnanthes thermalis* (Rabenhorst) Schoenfeld). Eight species have been suggested to belong to *Crenotia* so far. Like other monoraphid diatoms, *Crenotia* has heterovalvar frustules; however, it is distinguished from other monoraphid genera by lacking a cavum on both valves, having biseriate or uniseriate striae, presence of specialised structures at the end of each stria and no ornamentation on the girdle bands. This genus has been reported to have a worldwide distribution (Rioual et al. 2019), usually being found from benthic or periphytic habitats in lakes, springs and swamps and preferring neutral to alkaline waters (Stockner 1968; Hindáková 2009; Wojtal 2013; Kulikovskiy et al. 2016; Coste et al. 2019; Rioual et al. 2019; Wetzel et al. 2019; Liu et al. 2020).

Tibet is one of the biodiversity hotspots of the world and, in this region, the biodiversity of *Crenotia* is also relatively high, with five of the eight species of the genus being reported from Tibet. These species include *C. gibberula* (Grunow) Wojtal, *C. grimmei* (Krasske) Wojtal, *C. hedinii* (Hustedt) Rioual, Ector & Wetzel, as well as three species that are endemic to Tibet, namely, *C. hedinii* (Hustedt) Rioual, *C. distincta* Liu, Kociolek & Xie and *C. oblonga* Liu, Kociolek & Xie (Rioual et al. 2019; Liu et al. 2020). During the investigation of freshwater biodiversity of the Tibetan Plateau, samples were collected from a hot spring in Anduo County, specifically, Nagqu City. One species was observed with light microscopy (LM) and scanning electron microscopy (SEM), based on its morphological features, demonstrated to be a new species belonging to the genus *Crenotia*. Herein we describe this Tibetan diatom as new to science.

Materials and methods

Samples were collected from Tibet, during a biodiversity investigation initiated in 2021. Benthic diatoms were collected from Anduo County, Nagqu City, which is located in about the middle of Tibet. Samples were taken from a hot spring located at 31°40'51.24"N, 91°51'20.52"E and 31°40'52.32"N, 91°51'20.52"E, at an elevation of 4570 m above sea level. At the time of collection, the water temperature was around 20 °C, pH ranged from 6.55 to 7.77, conductivity ranged from 2790 to 3200 $\mu S \cdot cm^{-1}$(determined by YSI 6920 multiparameter probe). This locality has a cold climate, with dry, windy and cold weather and an annual precipitation of only ca. 100–200 mm.

Samples were fixed with 4% formaldehyde in the field. The samples were cleaned with nitric acid (HNO_3), then washed and settled using distilled water until the pH was neutral. For LM observations, cleaned diatoms were mounted to make permanent slides with Naphrax. These permanent slides were examined with a Zeiss Imager A2 microscope, equipped with a digital camera (AxioCam MRc 5) and observed with DIC (differential interference contrast) optics (Zeiss, Jena, Germany at Harbin Normal University).

For SEM observations, cleaned material was air-dried and coated with gold-palladium and observations made with a Hitachi S-4800 field emission SEM (Hitachi, Tokyo, Japan at Harbin Normal University) at an operating voltage of 15 kv. Diatom images were compiled with Photoshop 7.0. The holotype slides are deposited in the Key Laboratory of Algal Biology, Institute of Hydrobiology, Chinese Academy of Sciences, Wuhan, China and isotype slides are kept in the College of Life Science and Technology, Harbin Normal University, Harbin, China. Terminology used in the description were referenced by Round et al. (1990), Kingston (2003) and Kulikovskiy et al. (2022).

Results

***Crenotia tibetia* Liu & Kociolek, sp. nov.**
Figs 1–5

Holotype. Slide THXZ2021BYQX1–4#, the holotype specimen circled on the slide, illustrated here as Fig. 1A and 1A'; isotype, slide QX1–4#, illustrated here as Fig. 1C and 1C'.

Type locality. CHINA. Tibet, Anduo County, Nagqu City, hot spring, periphyton, 31°41'51.24"N, 91°51'20.52"E, 4570 m a.s.l., collected by Huan Zhu, 31 January 2021.

Description. LM (Fig. 1). Frustule slightly bent along the transapical axis ("V" shaped), monoraphid, with raphe valve concave, rapheless valve convex. Valve lanceolate with slightly protracted ends, slightly asymmetrical to the apical axis, apices nearly capitate. Length 11.8–19.7 μm, breadth 4.1–5.3 μm (n = 30). Raphe valve: straight raphe positioned in the middle of the valve, axial area lanceolate, with asymmetrical, rectangular to rhombic central area. Striae slightly radiating in the centre, becoming parallel towards the apices. Rapheless valve: Axial area lanceolate, central area expanded unilaterally to the margin. Striae 19–21 per 10 μm on both valves.

SEM (Figs 2–5). Raphe valve: Externally, raphe straight, proximal raphe ends slightly deflected to the same side, with distal raphe ends curved to the other side. Axial area lanceolate, nearly 1/3 of the valve width, formed by short striae along the margin. The 3 – 4 striae near the apices are biseriate and become uniseriate towards the valve centre. Areolae openings round to elongate, to irregularly-shaped externally. Internally, proximal raphe ends slightly bent to opposite side, helictoglossae slightly elongated. Areolae covered by hymens, forming two rows of "C"-shaped openings for each stria. Along the axial area, at the end of each stria, there is one horseshoe-shaped structure, open with fine radiating slit-like openings. One developing valve was observed; all the striae were biseriate.

Rapheless valve: Internally, axial area lanceolate, narrow at the apices and becoming wider towards the centre, centre area enlarged unilaterally and reaching the margin. Striae uniseriate to biseriate, mostly biseriate at the apices and becoming uniseriate at the centre. Areolae openings round to irregular in shape. Mantle and girdle bands without ornamentation.

Internally, the axial area is lanceolate, wide in the centre and enlarged at one side extending to the margin. Areolae were occluded by hymens with double rows of "C"-shaped openings; at the end of each stria, there is horseshoe-shaped structure, with fine slit-like openings. A developing valve was observed, all the striae were biseriate, with a "C- shaped structure at the end of each stria.

Etymology. Named after the type locality from which it was found.

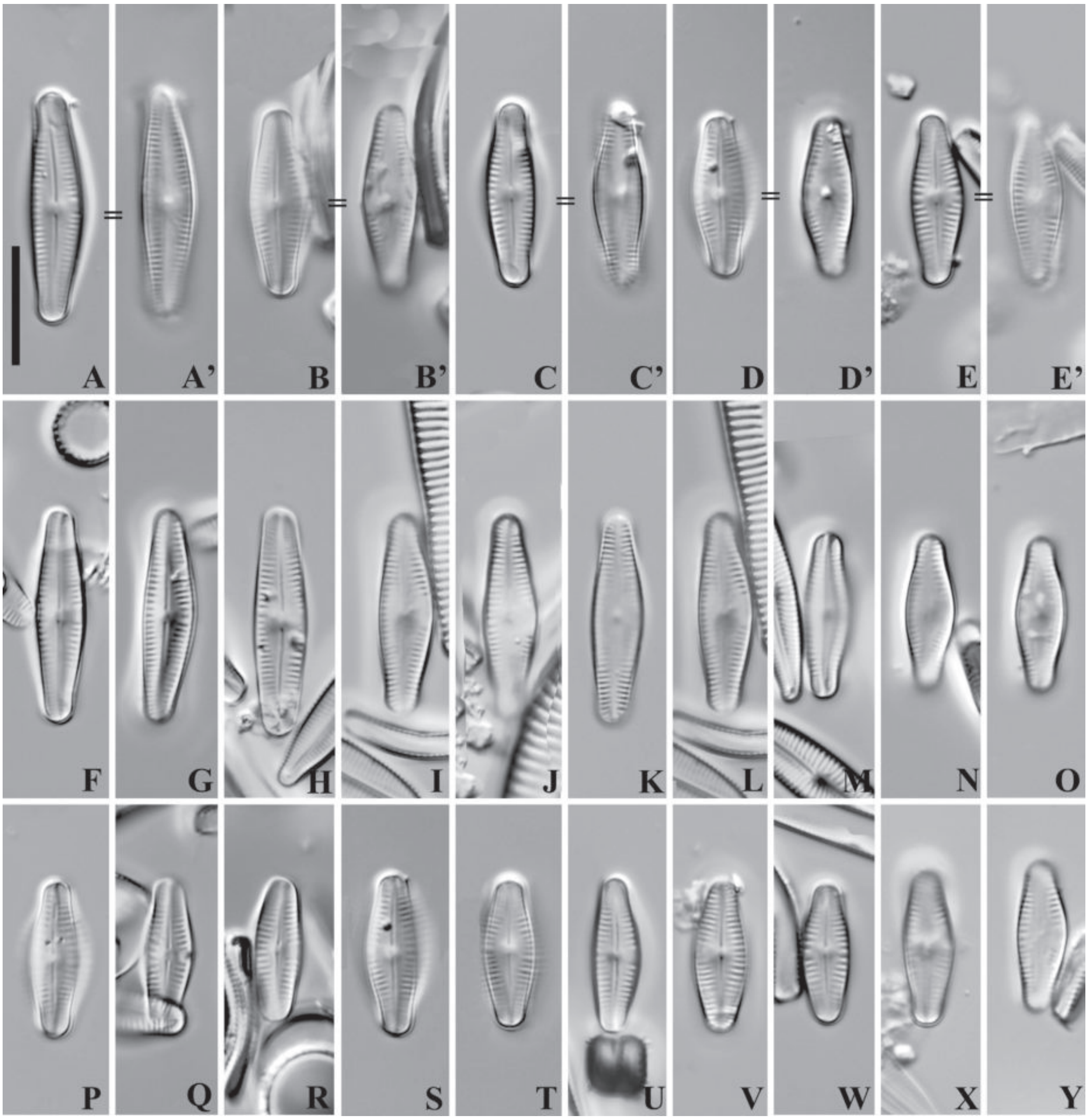

Figure 1. *Crenotia tibetia* sp. nov., LM. Raphe and rapheless valves from the type population. A, A' illustrations of the holotype. "=" means the raphe valve and rapheless valve are from the same frustule. Scale bar: 10 μm.

Discussion

Based on the morphological features of the valve and striae structure, this new species appears to be best placed in the genus *Crenotia*. This small genus currently is known to have nine species, including eight previously-described taxa. The previously-described taxa are: *C. angustior* (Grunow) Wojtal, *C. distincta*, *C. hedinii*, *C. oblonga*, *C. rumrichorum* (Lange-Bertalot) Wojtal, *C. thermalis*, *C. gibberula* and *C. grimmei*.

In comparing this new species with other known taxa (Table 1), *C. angustior* differs by its small frustule and capitate ends. *Crenotia hedinii* was formally transferred to *Crenotia* by Rioual et al. (2019); it has more slender valves and more acutely-rounded ends than our new species.

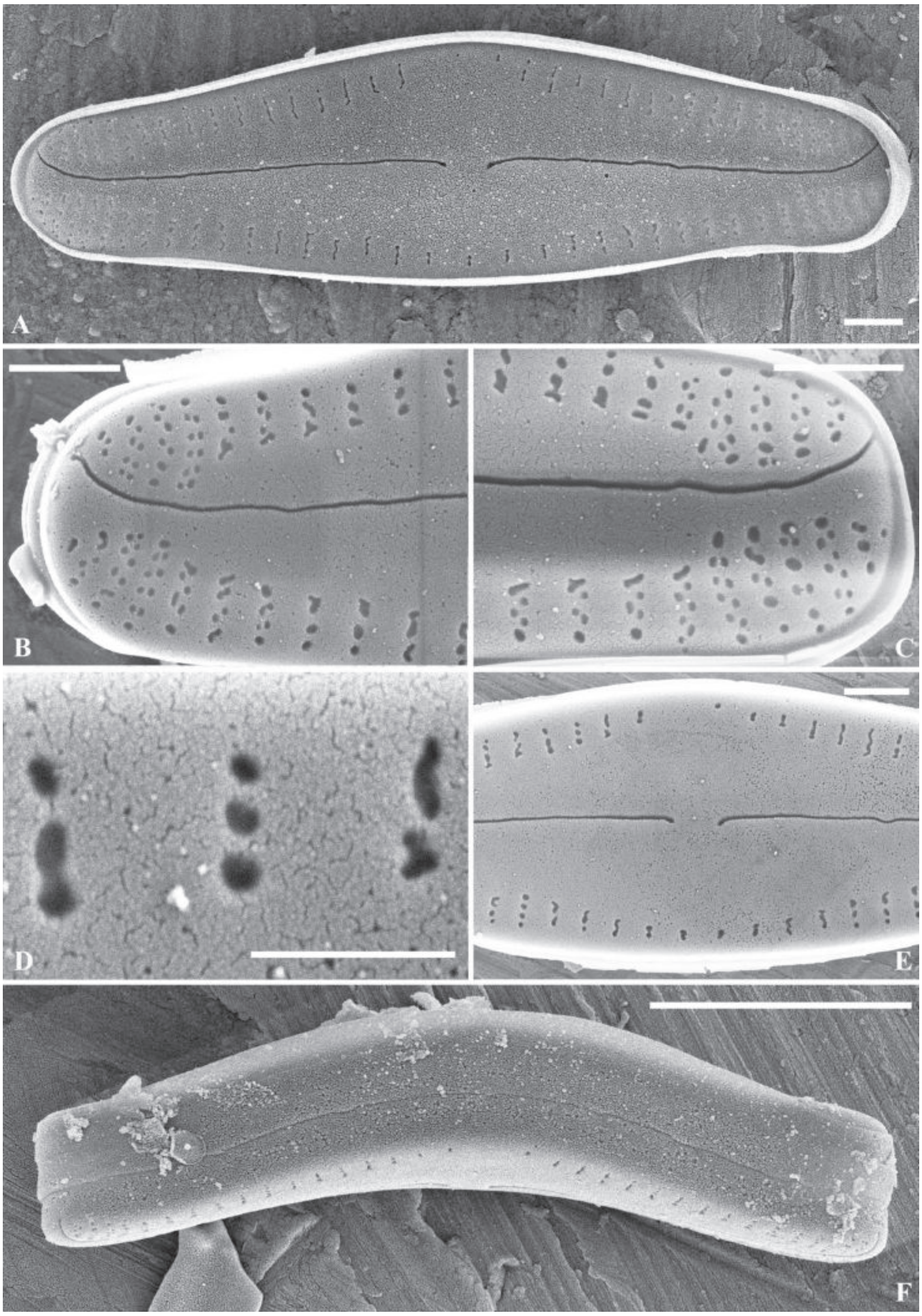

Figure 2. *Crenotia tibetia* sp. nov. SEM, external view of the raphe valve **A** external view of the whole valve **B, C** apices of the valve **D** magnification of areolae **E** central area of the valve **F** girdle view of the valve. Scale bar: 1 μm (**A, B, C, E, F**); 500 nm (**D**).

Crenotia grimmei, *C. gibberula* and *C. rumrichorum*, the former two species being designated as synonyms of *Achnanthes thermalis* (Rabenhorst) Schoenfeld (Krammer and Lange-Bertalot 2004), are the type species of *Crenotia*. All these three species were transferred to *Crenotia* by Wojtal (2013) when the genus was established.

Crenotia grimmei, first reported by Krasske (1925), was originally named *Achnanthes grimmei* Krasske; however, Lange-Bertalot and his colleagues rechecked the type and lectotype (Lange-Bertalot and Ruppel (1980), tafel 2, figs

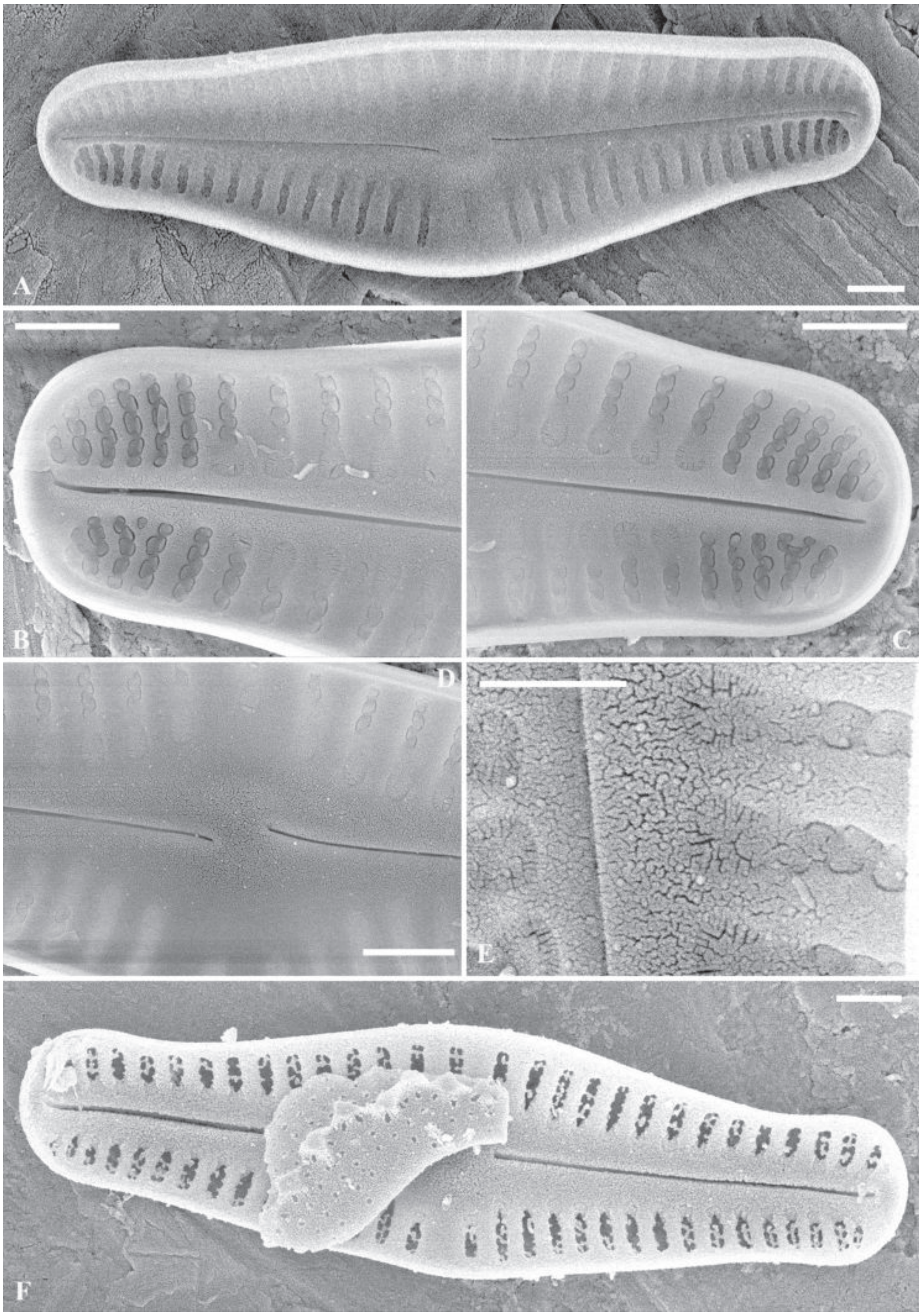

Figure 3. *Crenotia tibetia* sp. nov. SEM internal view of the raphe valve **A** internal view of the whole view **B, C** apices of the valve **D** central area of the valve internally **E** magnification of the areolae, showing the horseshoes areola at the end of striae **F** internal view of a developing valve. Scale bar: 1 μm (**A, B, C, D, F**); 500 nm (**E**).

46–50; Lange-Bertalot et al. (1996), tafel 4, figs 8–13) and suggested it is synonymous with *A. thermalis*. *Crenotia. gibberula* was described originally as *Achnanthes gibberula* Grunow in Cleve & Grunow. Lange-Bertalot and Ruppel (1980) suggested that *A. grimmei* and its varieties should be considered synonymous with *A. gibberula* and illustrated *A. gibberula* as a morphologically variable taxon (Håkansson 1982). Although Lange-Bertalot and Ruppel (1980) presented the type material of *Crenotia grimmei* and *C. gibberula*, it is hard to suggest that they belong to the

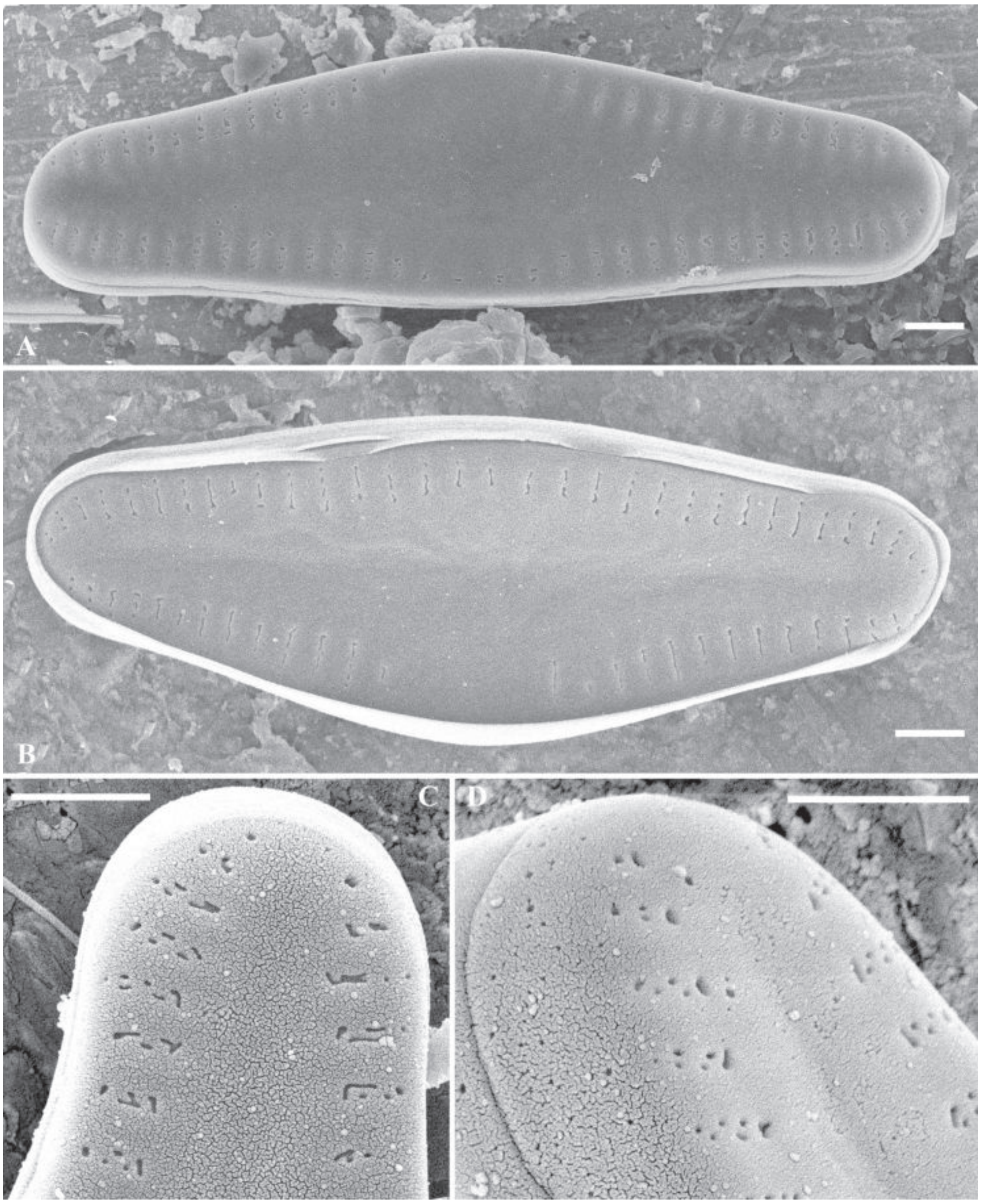

Figure 4. *Crenotia tibetia* sp. nov. SEM external view of the rapheless valve **A, B** external view of whole valve **C, D** apices of the valve, showing the areolae. Scale bar: 1 µm.

same species, at least based on LM morphology. Based on the illustrations of Lange-Bertalot and Ruppel (1980), Lange-Bertalot et al. (1996) and Wojtal (2013), we can separate *C. thermalis*, *C. grimmei* and *C. gibberula*, based on the morphology of the valves. *Crenotia thermalis* has elliptical-lanceolate or linear valves and the raphe valve face is flat, slightly convex in the central area and the rapheless valves are concave along the apical axis; *C. grimmei* has linear valves with protracted ends that form capitate apices; *C. gibberula* has more rhombic-shaped valves and they have capitate apices and the centre of the valves is obviously enlarged.

LM and SEM images were also presented by Håkansson (1982, plate I: 3–6) for *A. gibberula*, but the striae showed a “macroareolae”-like structure on both valves, similar to those shown in the genus *Madinithidium* Witkowski, Desrosiers & Riaux-Gobin (Desrosiers et al. 2014) or, probably, similar to developing valves of *Achnanthidium* species. Okuno (1974, pl. 855–856), also showed

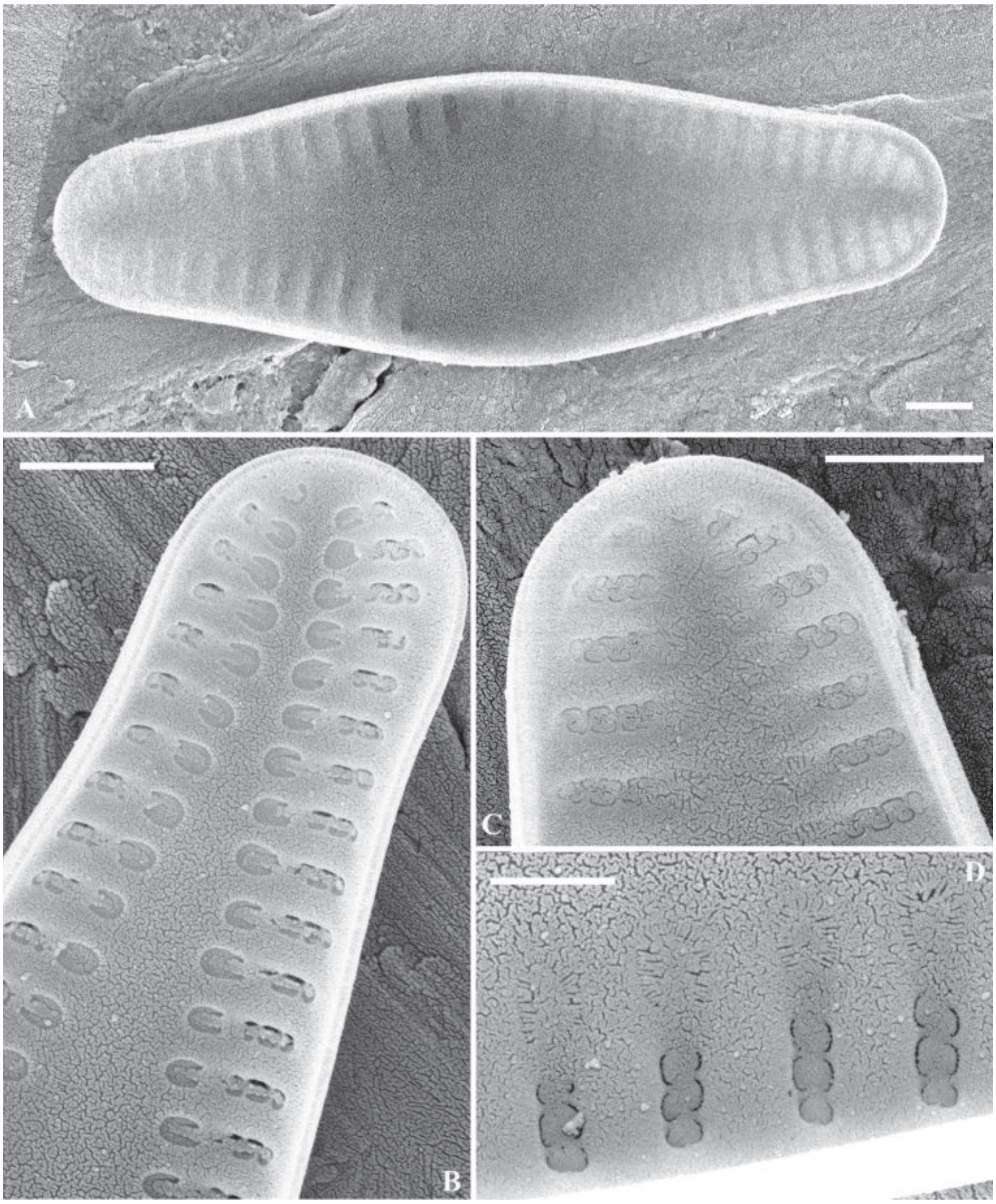

Figure 5. *Crenotia tibetia* sp. nov. SEM internal view of the rapheless valve **A** internal view of the whole valve **B** apex of the developing valve **C** apex of the valve **D** magnification of the areolae, showing the horseshoe-shaped structure at the end of the areolae. Scale bar: 1 μm.

a SEM of *A. grimmei*, but, based on the stria pattern and areola structure, the specimen presented was more similar to *Achnanthidium* rather than *Crenotia*.

Compared with the former three species, *C. tibetia* is morphologically most similar to *C. grimmei*, but *C. tibetia* has a more highly deflected frustule about the transapical axis, the raphe valve is more concave and is larger than *C. grimmei* (Lange-Bertlaot et al. (1996) report length 13.0–16.7 μm, breadth 3.6–4.7 μm, striae 16–19/10 μm, for this taxon), striae are denser on both valves, with shorter capitate ends and axial area are wider on the rapheless valves.

Crenotia grimmei and *C. gibberula* were also recorded in Tibet by Zhu and Chen (2000), as *Achnanthes grimmei* and *A. gibberula*, respectively, plate 46: 11–14), but, based on the published line drawings, their specimens do not match well either of these species.

Table 1. Comparison of morphological characteristics of *Crenotia tibetia* sp. nov. and closely related taxa.

	***C. tibetia* sp. nov.**	***C. angustior***	***C. distincta***	***C. gibberula***	***C. grimmei***	***C. hedinii***	***C. oblonga***	***C. rumrichorum***	***C. thermalis***
Length (µm)	11.8–19.7	10–19.5	14.0–31.5	13.5–39.5	16–24	7–30	8.0–21.0	12–13.4	7–34
Breadth (µm)	4.1–5.3	4.1–5.2	5.0–8.0	3.6–8	3.6–5	3.2–4.6	4.0–6.0	3.4–4	3.3–5.5
Valve shape	lanceolate	linear to lanceolate	lanceolate	rhombic-shaped	linear	lanceolate	elliptical-lanceolate	narrow lanceolate	elliptical-lanceolate or linear
Valve apices	capitate	small capitate	rounded	capitate	capitate	acutely rounded	rounded	acutely rounded	rounded
Striae	Slightly radiate to parallel / uni to biseriate	Slightly radiate / biseriate	Radiate / multiseriate	slightly radiate	slightly radiate	Slightly radiate / uni to biseriate	Parallel / bi to triseriate	Radiate / uni to biseriate	almost parallel / uni to biseriate
Raphe valve									
Axial area	lanceolate	narrow lanceolate	very narrow at the apices, broadly lanceolate in shape	lanceolate	narrow lanceolate	narrow lanceolate	very narrow at the apices, broadly lanceolate in shape	lanceolate, both ends are slightly curved ipsilaterally	linear
Central area	asymmetrical, rectangular to rhombic	small rectangle	absent	obviously enlarged	rectangular	small	absent	small rectangle	rectangular
Raphe	straight	filiform, straight	filiform, straight	filiform, straight	filiform, straight	filiform, straight	filiform, straight	filiform, slightly curved	straight, slightly curved at the end
Striae / 10 µm	19–21	12–16	17–18	14–32	20–22	17–25	22–26	25–27	20–26
Rapheless valve									
Axial area	lanceolate	narrow lanceolate	broadly lanceolate	narrow lanceolate	narrow lanceolate	broadly lanceolate	broadly lanceolate	broadly lanceolate	needle lanceolate
Central area	expanded unilaterally to the margin	absent	absent	absent	absent	asymmetry	absent	absent	absent
Striae / 10 µm	19–21	14–18	17–19	12–30	18–22	17–25	22–26	25–27	18–20

The morphology of *C. rumrichorum* was observed in detail by Hindáková (2009) as *Achnanthes thermalis* var. *rumrichorum*. Based on the structure, this species was found to belong to the genus *Crenotia*. *Crenotia rumrichorum* has more acute apices, distinguishing it from *C. tibetia*.

Within the genus, *C. distincta* and *C. oblonga* are endemic to Tibet so far and these two species have chambered and multiseriate striae on both valves, which easily distinguish them from our new species. However, these two species do not share the typical features of *Crenotia* and the valve structure resembles the genus *Haloroundia* Diaz & Maidana (2006), a monotypic genus described from Chile. The differences between *Crenotia* and *Haloroundia* can be seen in terms of striae structure, raphe system and degree of flexure of the frustules, but further investigations on the relationships between these two genera are warranted.

The work from Lake Baikal (Kulikovskiy et al. 2013, 2020a, b) established many new genera within Achnanthidiaceae. In research on monoraphid diatoms, curvature of the valve, valve shape and raphe system have been considered as critical features used to separate genera within this family (e.g. Yu et al. (2019); You et al. (2021)). However, molecular data showed the raphe number of frustules does not play such an important role in diatom taxonomy and its reduction or loss occurred many times during the evolution of raphid diatoms (Kulikovskiy et al. 2016). Features such as the “cavum” seem to have played important roles in the evolution of this group. Both morphological features and molecular data were used to identify this group and recognise: 1) species with a sinus; 2) species with a cavum; 3) species without these features (Kulikovskiy et al. 2022). Since more and more "intermediate species" between genera have been observed (You et al. 2021), the relationships between some uniseriate genera, such as *Achnanthidium*, *Gomphothidium* and *Psammothidium* (Round et al. 1990; Bukhtiyarova and Round 1996; Kociolek et al. 2021); and multiseriate genera such as *Platebaikalia*, *Lemnicola* and *Haloroundia* (Diaz and Maidana 2006; Kulikovskiy et al. 2020b) and those with macroareolae, such as *Scalariella*, *Madinithidium*, *Karayevia* and *Kolbesia* (Riaux-Gobin et al. 2012; Desrosiers et al. 2014; Kulikovskiy et al. 2022), appear to be in need of revision. Investigations with formal analyses of both morphological and molecular data may clarify the systematic position and diagnostic features amongst these genera.

Additional information

Conflict of interest

The authors have declared that no competing interests exist.

Ethical statement

No ethical statement was reported.

Funding

This research was supported by National Science Foundation of China (Grant no. 31970213, 32370215); Natural Science Foundation of Heilongjiang Province for Excellent Young Scholars (Grant no. YQ2020C032) and The Second Tibetan Plateau Scientific Expedition and Research Program (Grant no. 2019QZKK0304).

Author contributions

Validation: John Patrick Kociolek, Maxim Kulikovskiy. Resources: Huan Zhu, Guoxiang Liu. Data Curation: Jiaming Liu, Ying Zhang. Investigation: Xinyuan Na. Writing - Original draft: Xinyuan Na. Writing - Review and Editing: Yawen Fan, Yan Liu. Supervision: Yawen Fan, Yan Liu, Xinxin Lu, Fengyang Sui

Author ORCIDs

Xinyuan Na https://orcid.org/0009-0005-1425-7610
John Patrick Kociolek https://orcid.org/0000-0001-9824-7164
Maxim Kulikovskiy https://orcid.org/0000-0003-0999-9669
Fengyang Sui https://orcid.org/0000-0002-6734-6570
Guoxiang Liu https://orcid.org/0000-0001-8565-2363

Data availability

All of the data that support the findings of this study are available in the main text.

References

Al-Handal AY, Romero OE, Eggers SL, Wulff A (2021) *Navithidium* gen. nov., a new monoraphid diatom (Bacillariophyceae) genus based on *Achnanthes delicatissima* Simonsen. Diatom Research 36(2): 133–141. https://doi.org/10.1080/0269249X.2021.1921039

Bukhtiyarova L, Round FE (1996) Revision of the genus *Achnanthes* sensu lato. *Psammothidium*, a new genus based on *A. marginulatum.* Diatom Research 11(1): 1–30. https://doi.org/10.1080/0269249X.1996.9705361

Coste M, Riaux-Gobin C, Riaux J, Saenz-Agudelo P, Massuel S, Ector L, Calvez R, Ben AÏssa N (2019) AÏn Bou Rkhiss and AÏn Kibrit, two springs from the Merguellil Basin (Kairouan, Central Tunisia): diatom assemblages, biological pollusensitivity indices, hydrogeology and societal aspects. Vie et Milieu – life and Environment 69(1): 1–17.

De Stefano M, Marino D (2003) Morphology and taxonomy of *Amphicocconeis* gen. nov. (Achnanthales, Bacillariophyceae, Bacillariophyta) with considerations on its relationship to other monoraphid diatom genera. European Journal of Phycology 38(4): 361–370. https://doi.org/10.1080/09670260310001612646

Desrosiers C, Witkowski A, Riaux-Gobin C, Zglobicka I, Kurzydlowski KJ, Eulin A, Leflaive J, Ten-Hage L (2014) *Madinithidium gen. nov.* (Bacillariophyceae), a new monoraphid diatom genus from the tropical marine coastal zone. Phycologia 53(6): 583–592. https://doi.org/10.2216/14-21R2

Diaz CA, Maidana NI (2006) A new monoraphid diatom genus: *Haloroundia* Diaz & Maidana. Nova Hedwigia. Beiheft 130: 177–184.

Ge DY, Zhang SM, Liu HY, Liu Y, Kociolek JP, Zhu H, Liu GX, Fan YW (2022) One new species of *Achnanthidium* Kützing (Bacillariophyta, Achnanthidiaceae) from Tibet, China. Phytotaxa 538(4): 268–280. https://doi.org/10.11646/phytotaxa.538.4.1

Håkansson H (1982) Taxonomical discussion on four diatom taxa from an ancient lagoon in Spjälkö, South Sweden. In: Håkansson H (Ed.) Rapport från diatomésymposium i Lund, Maj 1981, University of Lund, Department of Quarternary Geology 22: 65–81.

Hindáková A (2009) On the occurrence of *Achnanthes thermalis* var. *rumrichorum* (Bacillariophyceae) in Slovakia. Fottea 9(2): 193–198. https://doi.org/10.5507/fot.2009.020

Hustedt F (1930) Die susswasser-Flora Mitteleuropas Heft. Bacillariophyta (diatomeae), Fischer, Jena, Germany, 466 pp.

Kingston JC (2003) Araphid and Monoraphid Diatoms. Freshwater Algae of North America. Ecology and Classification. Elsevier Science, 595–636 https://doi.org/10.1016/B978-012741550-5/50017-9

Kociolek JP, Williams DM, Stepanek J, Liu Q, Liu Y, You QM, Karthick B, Kulikovskiy M (2019) Rampant homoplasy and adaptive radiation in pennate diatoms. Plant Ecology and Evolution 152(2): 131–141. https://doi.org/10.5091/plecevo.2019.1612

Kociolek JP, You QM, Li YL, Wang YL, Lowe R, Wang QX (2021) Description of *Gomphothidium* gen. nov., with light and scanning electron microscopy: A new freshwater monoraphid diatom genus from Asia. Fottea 21(1): 1–7. https://doi.org/10.5507/fot.2020.011

Krammer K, Lange-Bertalot H (1991b) Suesswasserflora von Mitteleuropa. Bacillariophyceae. 4. Teil: Achnanthaceae, vol. 2/4, Gustav Fischer, Stuttgart, Germany, 437 pp.

Krammer K, Lange-Bertalot H (2004) Bacillariophyceae 4. Teil: Achnanthaceae, Kritische Erganzungen zu *Navicula* (Lineolatae), *Gomphonema* Gesamtliteraturverzeichnis [second revised edition] In: Ettl et al. Suesswasserflora von Mitteleuropa. Spektrum Akademischer Verlad Heidelberg, 2, 4, 468 pp.

Krasske G (1925) Die Bacillariaceen-Vegetation Niederhessens. Abhandlungen und Bericht LVI des Vereins für Naturkunde zu Cassel, 84–89 Vereinsjahr 1919–1925, 56: 1–119.

Kulikovskiy M, Andreeva S, Gusev E, Kuznetsova I, Annenkova N (2016) Molecular phylogeny of monoraphid diatoms and raphe significance in Evolution and taxonomy. Botany 43(5): 398–407. https://doi.org/10.1134/S1062359016050046

Kulikovskiy M, Lange-Bertalot H, Witkowski A (2013) *Gliwiczia* gen. nov. a new monoraphid diatom genus from Lake Baikal with a description of four species new for science. Phytotaxa 109(1): 1–16. https://doi.org/10.11646/phytotaxa.109.1.1

Kulikovskiy M , Glushchenko A , Genkal S, Kuznetsova I (2016) Identification book of diatoms from Russia. Filigran, Yaroslavl, Russia, 804 pp.

Kulikovskiy M, Maltsev Y, Andreeva S, Glushchenko A, Pudonay Y, Ludwig T, Tusset E, Kociolek JP (2019) Splitting of the diatom genus *Navicula sensu lato*: Description of *Dorofeyukae* gen. nov., remarks on the phylogeny of stauroneioid diatoms, and implications for the higher classification of raphid diatoms. Journal of Phycology 55: 173–185. https://doi.org/10.1111/jpy.12810

Kulikovskiy M, Glushchenko A, Kuznetsova I, Genkal S, Kociolek JP (2020a) *Gololobovia* gen. nov. a new genus from Lake Baikal with comments on pore occlusion in monoraphid diatoms. Phycologia 59(6): 1–18. https://doi.org/10.1080/00318884.2020.1830596

Kulikovskiy M, Glushchenko A, Genkal S, Kuznetsova I, Kociolek J (2020b) *Platebaikalia*–A new monoraphid diatom genus from ancient Lake Baikal with comments on the genus *Platessa*. Fottea 2020(20): 58–67. https://doi.org/10.5507/fot.2019.014

Kulikovskiy M, Glushchenko A, Kuznetsova I, Kociolek J (2022) *Planoplatessa* gen. nov. – A new, neglected monoraphid diatom genus with a cavum. Plants 11(17): 2314. https://doi.org/10.3390/plants11172314

Kützing FT (1844) Die Kieselschaligen. Bacillarien oder Diatomeen. Nordhausen, 152 pp. https://doi.org/10.5962/bhl.title.64360

Lange-Bertalot H, Ruppel M (1980) A revision of some taxonomically most problematic groups in *Achnanthes* Bory, important from the ecological point of view. Algological Studies 26: 1–31.

Lange-Bertalot H, Külbs K, Lauser T, Nörpel-Schempp M, Willmann M (1996) Iconographia Diatomologica, Volume 3: Dokumentation und Revision der von Georg Krasske beschriebenen Diatomeen-Taxa. Koeltz Botanical Books, Kapellenbergstr, Germany, 358 pp.

Liu Q, Xiang YD, Yu P, Xie SL, Kociolek JP (2020) New and interesting diatoms from Tibet. II. Description of two new species of monoraphid diatoms. Diatom Research 35(4): 353–361. https://doi.org/10.1080/0269249X.2020.1810781

Okuno H (1974) Freshwater diatoms. In: Helmcke J-G, Krieger W, Gerloff J (Eds) Diatomeenschalen im elektronenmikroskopischen Bild. Vol. IX: 825–923. [J. Cramer, Vaduz]

Patrick R, Reimer CW (1966) The diatoms of the United States, exclusive of Alaska and Hawaii. Volume 1. Fragilariaceae, Eunotiaceae, Achnanthaceae, Naviculaceae. The Academy of Natural Sciences of Philadelphia, America, 688 pp.

Riaux-Gobin C, Witkowski A, Ruppel M (2012) *Scalariella* a new genus of monoraphid diatom (Bacillariophyta) with a bipolar distribution. Fottea 12(1): 13–25. https://doi.org/10.5507/fot.2012.002

Rioual P, Ector L, Wetzel CE (2019) Transfer of *Achnanthes hedinii* Hustedt to the genus *Crenotia* Wojtal (Achnanthidiaceae, Bacillariophyceae). Notulae Algarum 106: 1–6. https://doi.org/10.5507/fot.2012.002

Round FE, Crawford RM, Mann DG (1990) The Diatoms. Biology and Morphology of the Genera. Cambridge University Press, 747 pp.

Stockner JG (1968) The ecology of a diatom community in a thermal stream. British Phycological Bulletin 3(3): 501–514. https://doi.org/10.1080/00071616800650101

Thomas E, Stepanek J, Kociolek JP (2016) Historical and current perspectives on the systematics of the 'Enigmatic' diatom genus *Rhoicosphenia* (Bacillariophyta), with single and multi-molecular marker and morphological analyses and discussion on the monophyly of 'Monoraphid' Diatoms. PLOS ONE 11(4): e0152797. https://doi.org/10.1371/journal.pone.0152797

Wetzel CE, Beauger A, Ector L (2019) *Cocconeis rouxii* Héribaud & Brun a forgotten, but common benthic diatom species from the Massif Central, France. Botany Letters 166(2): 221–233. https://doi.org/10.1080/23818107.2019.1584865

Wojtal AZ (2013) Bibliotheca Diatomologica, Volume 59: Species composition and distribution of diatom assemblages in spring waters from various geological formation in southern Poland. J. Cramer in Borntraeger Science, Johannesstr, Germany, 436 pp.

You QM, Zhao K,Wang YL,Yu P, Kociolek JP, Pang WT, Wang QX (2021) Four new species of monoraphid diatoms from western sichuan plateau in China. Phytotaxa 479(3): 257–274. https://doi.org/10.11646/phytotaxa.479.3.3

Yu P, You QM, Pang WT, Cao Y, Wang QX (2019) Five new Achnanthidiaceae species (Bacillariophyta) from Jiuzhai Valley, Sichuan Province, Southwestern China. Phytotaxa 405(3):147–170. https://doi.org/10.11646/phytotaxa.405.3.5

Zhu HZ, Chen JY (2000) Bacillariophyta of the Xizang Plateau. Science Press, Beijing, China, 353 pp.

PhytoKeys 237: 37–49 (2024)
DOI: 10.3897/phytokeys.237.110482

Research Article

Hypericum liboense (Hypericaceae), a new species from Guizhou, China

Tian-Rou Wu[1*], Jian Xu[2*], Ming-Tai An[1], Jiang-Hong Yu[1], Feng Liu[3], Zheng-Ren Chen[4]

1 *College of Forestry, Guizhou University, Guiyang 550025, Guizhou, China*
2 *Guizhou Botanical Garden, Guiyang, 550000, Guizhou, China*
3 *College of Life Sciences, Guizhou University, Guiyang 550025, Guizhou, China*
4 *Guizhou Maolan National Nature Reserve Administration, Libo 558400, Guizhou, China*
Corresponding author: Ming-Tai An (gdanmingtai@126.com)

Abstract

Hypericum liboense M.T.An & T.R.Wu, **sp. nov.** (Hypericaceae) is a newly described species found in the Maolan National Nature Reserve of Guizhou Province, where it grows in rocky habitats without soil on karst mountain tops. In this study, key morphological characters were compared between the new species and the other known *Hypericum* species of Hypericaceae. DNA sequences were extracted from the leaves of the new species, with nuclear gene sequences (ITS) generated to reconstruct phylogenetic trees and describe its phylogenetic position in relation to other species of *Hypericum*. Our results show that the proposed new species has the typical characteristics of the genus *Hypericum* in morphology being similar to *Hypericum monogynum*, but differing in its sessile and semi-clasped leaves, long elliptical to long circular leaf blades, thickly papery to thinly leathery, with entire and wavy leaf margins. The abaxial side of the leaves is covered with white powder, giving them a grey-white appearance. The main lateral veins of the leaves are 8–15-paired, and the midvein on both sides is convex. The main lateral veins and midvein branch are conspicuous, with tertiary venation forming a network on the leaf surface and appearing prominently sunken. The inflorescences are 1–3-flowered, with a large calyx and conspicuous veins. The molecular phylogenetic analysis (PP = 1.00) provided substantial evidence for the proposition of *H. liboense* as a new species within *Hypericum*. Morphological and molecular evidence is presented, corroborating the proposition of the new species, including a comprehensive account of the distinctive morphological attributes of *H. liboense*, along with its key distinguishing features from similar species.

Key words: Molecular evidence, morphology, phylogeny, taxonomy

Academic editor: Rafael F. Almeida
Received: 3 August 2023
Accepted: 15 December 2023
Published: 12 January 2024

Citation: Wu T-R, Xu J, An M-T, Yu J-H, Liu F, Chen Z-R (2024) *Hypericum liboense* (Hypericaceae), a new species from Guizhou, China. PhytoKeys 237: 37–49. https://doi.org/10.3897/phytokeys.237.110482

Introduction

Hypericum L. is the largest genus of the family Hypericaceae, with approximately 470 species worldwide (Dauncey et al. 2019), especially in temperate regions of the Northern Hemisphere and on tropical high-altitude mountains (Crockett and Robson 2011). In China, the genus is known to include a total

---

[*] These authors contributed equally to this work.

of 68 species and nine subspecies, of which 33 species are endemic to the country. About 46 species and four subspecies are abundant in the western and southern regions of China, with few distributed in Xinjiang (Robson 2012). *Hypericum* plants are mostly herbs or shrubs, less often trees, and the flowers are often yellow or golden and occasionally white. Some species of this genus are cultivated around the world due to ornamental value, while some species have high medicinal value (Galeotti 2017; Bertoli et al. 2018; Marrelli et al. 2020; Revuru et al. 2020; Caldeira et al. 2022; Fang et al. 2023; Luo et al. 2023; Zheng et al. 2023).

The genus *Hypericum* was originally classified under the family Guttiferae based on morphological studies (Bessey 1915). However, the morphological characteristics of plants grown in different regions vary widely, leading to controversy among scholars regarding the main morphological basis for species identification. The rapid development of molecular technology (ITS), particularly the emergence of molecular marker technology, has provided compelling evidence for the study of classification, genetic relationship and developmental position of many plants (Yu et al. 2022; Deng et al. 2023; Ya et al. 2023), and the construction of phylogenetic trees is widely employed to demonstrate genetic relationships among species in the classification of *Hypericum*.

The APG IV system (The Angiosperm Phylogeny Group 2016) split the broad Guttiferae family into three families, namely Guttiferae, Hypericaceae, and Calophyllaceae, based on molecular evidence. Furthermore, the family Hypericaceae was divided into three tribes and ten genera (including the genus *Hypericum*). Robson (1972, 1977, 1985, 1990, 2001, 2006, 2010a, 2010b, 2012, 2016) has provided detailed monographic and molecular phylogenetic assessments of *Hypericum* and has classified the genus into 36 sections and 469 species. Nürk et al. (2015) utilized ITS sequence to establish the phylogenetic relationships within *Hypericum*; their findings demonstrated that sect. *Ascyreia* was non-monophyletic. It was exhibited as a division into two sects: eastern *Ascyreia* and western *Ascyreia* (Meseguer et al. 2013). The completion of the taxonomic part of the *Hypericum* provides not only a taxonomic baseline and valuable tool for the identification of taxa, but also a rich resource for research into many other aspects of the biology and evolution of the genus. However, relationships between the more complete branches in *Hypericum* remained unresolved, and the classification problem of *Hypericum* still needs further in-depth research.

In 2022, we participated in a plant survey in a karst area of the Maolan National Nature Reserve in Guizhou, China, and discovered an unusual specimen of Hypericaceae. After field investigation and collection of specimens, we conducted detailed morphological analyses and realised that the morphological characteristics of this species were similar to those of *Hypericum*, but there were obvious differences in the leaf and calyx from the species occurring in China. To effectively differentiate species *H. liboense* from others within the genus *Hypericum*, this study utilized phylogenetic analysis based on morphological identification and description, combined with ITS sequences. As a result, a conclusion was reached, designating it as a novel species within the realm of scientific understanding.

Material and methods

Phylogenetic analysis

The ITS sequence, a highly reiterated tandem sequence in the nuclear genome, exhibits rapid changes, providing abundant variation and informative sites (Meseguer et al. 2013; Nürk et al. 2015). This sequence also demonstrates the highest level of species resolution accuracy (Chinese Plant Bol Group et al. 2011). In this study, we extracted DNA sequences from fresh leaves of *H. liboense*, followed by PCR amplification and instrument detection to obtain ITS sequences. A total of 55 *Hypericum* species were included in the analysis dataset, with ITS sequences obtained from NCBI (https://www.ncbi.nlm.nih.gov/). These 55 species represented 34 taxa of the genus *Hypericum* (Table 1), with 1–10 species selected as representatives for each taxon (Nürk et al. 2013). However, species of sect. *Umbraculoides* and sect. *Thasia* were not included in the analysis due to lack of ITS sequence data. *Thornea calcicole* Standl. & Steyerm was used as the outgroup (Park and Kim 2004).

The sequences were imported into BioEdit 7.0 for manual alignment and sorting, resulting in a refined sequence matrix, which was then exported (Hall 1999). The ITS matrix (Miller et al. 2010) was imported into the CIPRES supercomputer, and the optimal tree model was constructed using the appropriate Bayesian method (Ronquist and Huelsenbeck 2003; Ruchisansakun et al. 2016). The most suitable alternative model for base evolution was chosen based on the Bayesian Information Criterion (BIC). For the ITS sequence of nuclear genes, the GTR+I+G model was identified as the best model. The successful construction of the phylogenetic tree was achieved by analysing the ITS dataset using Bayesian inference (BI).

Table 1. Information of samples used for phylogenetic inference in this study.

Section number	Specie number	Species	GenBank No.	Section
1	1	*Hypericum quartinianum* A.Rich.	HE653603.1	*Campylosporus*
2	2	*Hypericum balearicum* L.	AY555862.1	*Psorophytum*
3	3	*Hypericum bellum* subsp. *latisepalum* N.Robson	HE653426.1	*Ascyreia*
	4	*Hypericum calycinum* L.	HE653431.1	
	5	*Hypericum forrestii* (Chittenden) N. Robson	HE653476.1	
	6	*Hypericum hookerianum* Wight et Arn.	KC709450.1	
	7	*Hypericum kouytchense* Lévl.	FJ694210.1	
	8	*Hypericum lagarocladum* N. Robson	HE662703.1	
	9	*Hypericum patulum* Thunb. ex Murray	FJ694214.1	
	10	*Hypericum pseudohenryi* N. Robson	KC709447.1	
	11	*Hypericum wilsonii* N. Robson	HE653658.1	
	12	*Hypericum monogynum* L.	HE653544.1	
4	13	*Hypericum geminiflorum* Hemsl.	HM162838.1	*Takasagoya*
5	14	*Hypericum androsaemum* L.	KC709337.1	*Androsaemum*
	15	*Hypericum grandifolium* Choisy	KC709385.1	
	16	*Hypericum* × *inodorum* Mill.	HE653565.1	
6	17	*Hypericum xylosteifolium* N. Robson	HE653659.1	*Lnodora*
7	18	*Hypericum przewalskii* Maxim.	JF976672.1	*Roscyna*
8	19	*Hypericum bupleuroides* Griseb.	HE653429.1	*Bupleuroides*

Section number	Specie number	Species	GenBank No.	Section
9	20	*Hypericum attenuatum* Choisy	HE662752.1	*Hypericum*
	21	*Hypericum kamtschaticum* Ledeb.	HE653516.1	
	22	*Hypericum perforatum* L.	JN811136.1	
	23	*Hypericum perforatum* subsp. *veronense* (Schrank) H. Lindb.	MN036448.1	
	24	*Hypericum pseudopetiolatum* R. Keller	AY573002.1	
	25	*Hypericum yezoense* Maxim.	AY573004.1	
10	26	*Hypericum concinnum* Benth.	HE653442.1	*Concinna*
11	27	*Hypericum pseudomaculatum* Bush	HE653595.1	*Graveolentia*
12	28	*Hypericum sampsonii* Hance	HE653620.1	*Sampsonia*
13	29	*Hypericum elodeoides* Choisy	HE653457.1	*Elodeoida*
14	30	*Hypericum monanthemum* Hook. f. et Thoms. ex Dyer	HE653542.1	*Monanthema*
15	31	*Hypericum polyphyllum* Boiss. & Balansa	HE662730.1	*Olympia*
16	32	*Hypericum cerastoides* (Spach) N.Robson	AY555884.1	*Campylopus*
17	33	*Hypericum papillare* Boiss. & Heldr.	HE653570.1	*Origanifolia*
18	34	*Hypericum barbatum* Jacq.	FJ694192.1	*Drosocarpium*
	35	*Hypericum richeri* subsp. *grisebachii* (Boiss.) Nyman	FJ694222.1	
	36	*Hypericum rumeliacum* Boiss.	HE653616.1	
19	37	*Hypericum humifusum* L.	HE653507.1	*Oligostema*
20	38	*Hypericum orientale* L.	HE653565.1	*Crossophyllum*
21	39	*Hypericum pseudolaeve* N.Robson	HE653594.1	*Hirtella*
22	40	*Hypericum hirsutum* L.	HE653500.1	*Taeniocarpium*
	41	*Hypericum pulchrum* L.	FJ694219.1	
23	42	*Hypericum empetrifolium* Willd.	HE653464.1	*Coridium*
24	43	*Hypericum hypericoides* (L.) Crantz	KC709376.1	*Myriandra*
	44	*Hypericum kalmianum* L.	FJ694209.1	
	45	*Hypericum prolificum* L.	MT551029.1	
25	46	*Hypericum canariense* L.	KC709387.1	*Webbia*
26	47	*Hypericum vacciniifolium* Hayek & Siehe	HE653656.1	*Arthrophyllum*
27	48	*Hypericum pallens* Banks & Sol.	AY555848.1	*Triadenioides*
28	49	*Hypericum heterophyllum* Vent.	HE653492.1	*Heterophylla*
29	50	*Hypericum aegypticum* subsp. *webbii* L.	KC709380.1	*Adenotrias*
30	51	*Hypericum papuanum* Ridl.	HE653571.1	*Humifusoideum*
31	52	*Hypericum reflexum* L.f.	HE662747.1	*Adenosepalum*
32	53	*Hypericum elodes* L.	FJ694200.1	*Elodes*
33	54	*Hypericum mexicanum* L.	LT904662.1	*Brathys*
34	55	*Hypericum japonicum* Thunb. ex Murray	HE653513.1	*Trigynobrathys*
Outgroup		*Thornea calcicole* Standl. & Steyerm	AY573028.1	–

Morphology

During the period of 2022–2023, we conducted a field investigation on *H. liboense* in Maolan National Nature Reserve, Guizhou Province, including photographing its characteristics and collecting seven live specimens. The type specimen is deposited in the Tree Herbaria, College of Forestry, Guizhou University, Huaxi District, Guiyang City, Guizhou Province, China (GZAC, GZAC–LB–0001). The morphological comparison of *H. liboense* specimens with similar species, such as *H. monogynum*, was conducted by studying various materials including leaves, flowers, fructus, and branches. This comparison was primarily based on authoritative plant literature, specifically descriptions found in Flora of China (Li et al. 1990) and Flora of Guizhou (Li 1986). Additionally, the identification process involved referencing sample images from the website (http://plants.jstor.org/) and detailed plant morphological descriptions available at Plant Information System (http://www.iplant.cn/). After measuring the traits with Vernier callipers, the data were analysed and compared with those from specimens of similar species. We directly collected fresh leaf materials in the field, placing them into FAA fixation solution.

Results

Phylogenetic analyses indicated that the 34 included taxa of *Hypericum* formed a well-supported monophyletic group (Fig. 1). Two individuals of the inferred new species from the sites in Libo County were resolved as a strongly-supported monophyletic lineage (PP = 1.00), which further clustered with *H. monogynum*, *H. patulum* and *H. geminiflorum* into a subclade (PP = 0.99). The tree shows that *H. liboense* is the sister species of *H. monogynum*, with relatively strong support (PP = 1.00). These two species also showed certain morphological similarities, especially those of the petals, stamens and pistils (Fig. 2; Table 2). *H. patulum* has the closest relationship to *H. liboense* and *H. monogynum*, although with relatively poor support (PP = 0.62), followed by *H. geminiflorum* (PP = 0.99).

Discussion

The results of our phylogenetic tree showed that all species of sect. *Asian* (including *H. patulum*, *H. kouytchense* and *H. monogynum*, etc) clustered together into a single clade with strong support (PP = 1.00), and the results were consistent with previous studies (Nürk et al.2013; Meseguer et al. 2014). In the phylogenetic tree the new species and *H. monogynum* were placed along with the species of sect. *Asian*. The phylogenetic trees (ITS; Fig. 2) indicate that *H. liboense* is a distinct member of *Hypericum*, and furthermore, support its sister taxon relationship with *H. monogynum*, thus corroborating the evidence provided by the morphological observations. There are two populations of *H. liboense* that have been recorded and observed, and we find that the morphological characters of the species present consistency between the two populations, especially with respect to the morphology of leaves, inflorescence, and calyx. *H. liboense* is similar to *H. monogynum* in having whole leaf margins, glandular, yellow petals, whole and flat calyx margins, stamen fascicles each with 25–35 stamens, styles united nearly to apices, then out curved free. but differs from *H. monogynum* in that the leaf edges are wavy (vs. flat), the midvein are raised on both sides (vs. raised on lower epidermis of leaves), the tertiary venation is sunken on both surfaces (vs. surface not sunken), and the abaxial leaf surface are greyish-white (vs. without grey), inflorescences with 1–3 flowers (vs. 1–15(–30) flowers), calyx are elliptic or broad-ovate (vs. broad or narrowly elliptic or oblong to lanceolate or oblanceolate), and veins obvious (vs. obscure), wholly punctiform glands (vs. laminar glands basally lines to streaks). This feature of wavy leaf edges, obvious veins of leaves and calyx, inflorescence 1–3-flowered is crucial for distinguishing *H. liboense* from *H. monogynum* and other related species (Table 2), and supports its standing as a separate, and new species. Furthermore, to our knowledge, most calyx of *Hypericum* species have obscure thin veins; there is also no report of variation in the leaf edges of *H. liboense*. Therefore, we believe that the wavy leaf

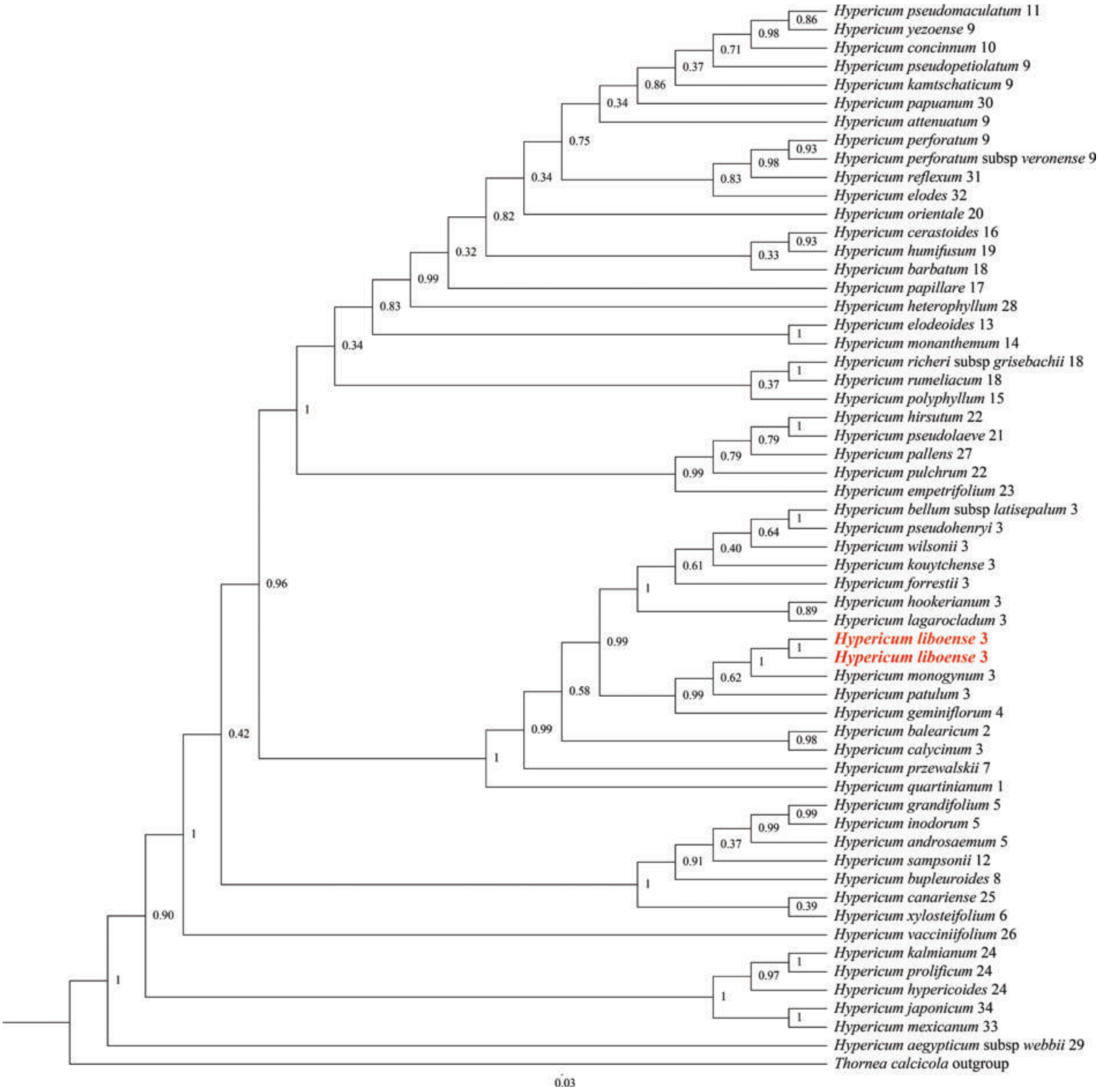

Figure 1. Partial Bayesian consensus phylogram based on ITS sequences. Numbers above branches are Bayesian posterior probabilities (The number after the species name represents the section of *Hypericum*; Table 1).

edges and distinctly thin veined of calyx are reliable trait for this purpose and that the recognition of *H. liboense* as a new species is strongly supported (PP = 1.00) by ITS phylogenetic tree.

In recent years, new species of the genus Hypericaceae have been gradually discovered and reported (Ocak et al. 2009; Bacchetta et al. 2010; Tan et al. 2010; Ely and Boldrini 2015; Ely et al. 2015; Marinho et al. 2016; Trigas 2018; Galindon et al. 2021), indicating the important potential role of discovering and documenting new species in enriching regional species diversity and prioritizing conservation efforts in biodiversity hotspots. As time progresses, the discovery of new species is increasingly receiving attention. The discovery location of *H. liboense* is in the karst landscape-rich area of Guizhou Province, China. The discovery and description of this species further highlight the ability

Table 2. Morphological comparison of *Hypericum liboense* and similar species.

	H. liboense	***H. monogynum***	***H. kouytchense***	***H. patulum***
Petiole	Leaves sessile, semi-amplexicaul	Leaves sessile or brachy petiolate	Leaves petiolate, 0.5–1.5 mm long	Leaves petiolate, 0.5–2 mm long
Leaf texture	Thickly papery to thinly leathery	Thickly papery	Thickly papery	Thickly papery
Leaf morphology	Long elliptical to long circular	Oblanceolate or elliptic to long circular	Elliptic, lanceolate to ovate or triangular ovate	Blade lanceolate or oblong-lanceolate to ovate or oblong-ovate
Leaf margin	Slight undulation	Flat	Flat	Flat
Leaf lower epidermis character	Greyish white with white powder	Light green, not grey	Light green, not grey	Abaxially rather glaucous
Midvein	Midvein raised on both sides of the leaf surface	Midvein flat on the leaf surface	Midvein flat on the leaf surface	Midvein flat on the leaf surface
Main lateral veins	8–15-paired	4–6-paired	3–4-paired	3-paired
Tertiary reticulation	Conspicuous, sunken on the leaf surface	Not very conspicuous	Obscure or invisible	Scarcely visible
Inflorescence	1–3-flowered	1–15(–30)-flowered	1–7(–11)-flowered	1–15-flowered
Anther	Yellow, glandular	Yellow to dark orange, glandular	Yellow, glandular	Yellow, glandless
Calyx size	Elliptic or broad ovate, larger, 10–14×4–6 mm	Broad or narrowly elliptic or oblong to lanceolate or oblanceolate, smaller, 4.5–13×1.2–2 mm	Oblong-ovate to lanceolate, larger, 7–15×2.5–7 mm	Broadly ovate or broadly elliptic or subcircular to oblong-elliptic or obovate-spatulate, 5–10×3.5–7 mm
Calyx margin	Margin entire	Margin entire	Margin entire	Margin eroded-denticulate to ciliolate with markedly hyaline margin
Thin veins of calyx	Obvious	Obscure	Obscure	Obscure

of the karst limestone region to support rich species diversity and endemism, while also providing favourable conditions for the survival of *H. liboense*. Therefore, conducting a comprehensive investigation and study of the phylogeny and morphology of *H. liboense* in the karst limestone region of southern China will provide important scientific insights into the plant diversity and the implementation of conservation strategies in this region.

Taxonomy

Hypericum liboense **M.T.An & T.R.Wu, sp. nov.**
urn:lsid:ipni.org:names:77334341-1
Fig. 2

Type. China, Guizhou Province, Libo County, Maolan National Nature Reserve, elev. 947, 25°16'N, 107°57'E, 21 April 2022, Jian Xu, Mingtai An and Tianrou Wu 220421(Holotype: GZAC–LB–0001, Isotype: GZAC–LB–0002).

Diagnosis. This species is similar to *H. monogynum* in terms of morphology. The main difference between the two species is that the leaves of *H. liboense* are sessile and semi-clasped (vs. leaves sessile or brachypetiolate). The leaves of *H. liboense* are long elliptical to long circular, and the edges are whole and wavy (vs. oblanceolate or elliptic to long circular, flat). *H. liboense* leaves are thickly papery to thinly leathery (vs. thickly papery), with a white powder on the abaxial side leading to a grey-white appearance (vs. abaxially without grey).

Main lateral veins of leaves 8–15 pairs (vs. 4–6 pairs), with the midvein on both sides convex, the main lateral veins obvious branches from the midvein, the main lateral veins and tertiary vein forming an obvious network and obviously sagging (vs. tertiary vein obscure and not sunken). Inflorescences with 1–3 flowers (vs. 1–15(–30) flowers), calyx are elliptic or broad-ovate (vs. broad or narrowly elliptic or oblong to lanceolate or oblanceolate), 10–14 mm long, 4–6 mm wide (vs. 4.5–13 mm long and 1.2–2 mm wide), and veins obvious (vs. obscure) (Table 2).

Description. ***Plants*** Erect shrub, 0.5–1.3 m tall. Young branches reddish brown with a light white powder. Old branches dark reddish-brown or grey, cylindrical, with a lumpy rind after cracking off, and the cortex light red. ***Leaves*** opposite, sessile, with semi-clasping branchlets. The leaves are long elliptical to long circular, 4–8 cm long and 2–4 cm wide, with the middle entire part of the leaf usually the widest, the apex blunt round, with a fine cusp; leaf blade base cuneate to rounded, margin entire and slightly ruffled; thickly papery to thinly leathery, glabrous, the surface of the leaves green or dark green, the back of the leaves white and greyish-white; the main lateral veins of the leaves in 8–15 pairs, the midvein raised on both sides, and the base reddish; main lateral veins and midvein branching obviously, main lateral veins and tertiary vein forming an obvious network and concave on the leaf surface; wholly punctiform glands. ***Inflorescence*** with 1–3 flowers, emanating from the first segment of the stem; ***peduncle*** yellow-green, 1.3–3 cm long. ***Flowers*** 4–7 cm in diameter; bud ovular, apex subacute. ***Calyx*** 5, free, ovate to broadly ovate, 1–1.4 cm long, 0.4–0.6 cm wide, wholly punctiform glands, apex acute to rounded, entire margin, base light green, margin purplish red, midvein and veining obvious, and calyx enlarged in the fruit stage. ***Petals*** 5, yellow, without flush, open, triangular obovate, slightly curved, 2.8–3.5 cm long, 1.6–2.2 cm wide, approximately, margin entire, glandular. ***Stamens*** in 5 fascicles, each with 23–40 stamens, 1.3–3.4 cm long, several times the length of the petal, anthers yellow to dark orange, with glands. ***Ovary*** ovulate or sub-globular, 3–5 mm long, 2.5–5 mm wide. ***Style*** 1.3–2.2 cm long, styles partly united (style confluent almost to apex and then curved outwards into 5 splits), stigma small, lavender. ***Capsule*** broadly oval-shaped or oval-shaped and conical, 10–14 mm long and 6–10 mm wide, light green, dark brown when ripe.

Phenology. Flowering from April to June; fruiting from June to September.

Distribution and ecology. This species is known to be found only in Libo County, Guizhou Province, China, on the top of a mountain in a karst landscape, alt. 947 m.

Etymology. The species name “liboense” refers to the origin of the type specimen, Libo County, Guizhou Province.

Conservation status. In the 2022–2023 period, we sampled the *H. liboense* population and found two more sites around the location where the species was first discovered, each with a population of approximately 20 plants. The habitat of *H. liboense* is mainly from the exposed rock gully area above the middle of the mountain to the top of the mountain. The soil in the plant habitat is poor, the soil layer is weak in its ability to retain water, and drought is common. At present, *H. liboense* is not known to be distributed in the low-altitude areas below the foot of the mountain and the middle of the mountain, so we hypothesize that the current availability of habitat for *H. liboense* is relatively poor and the

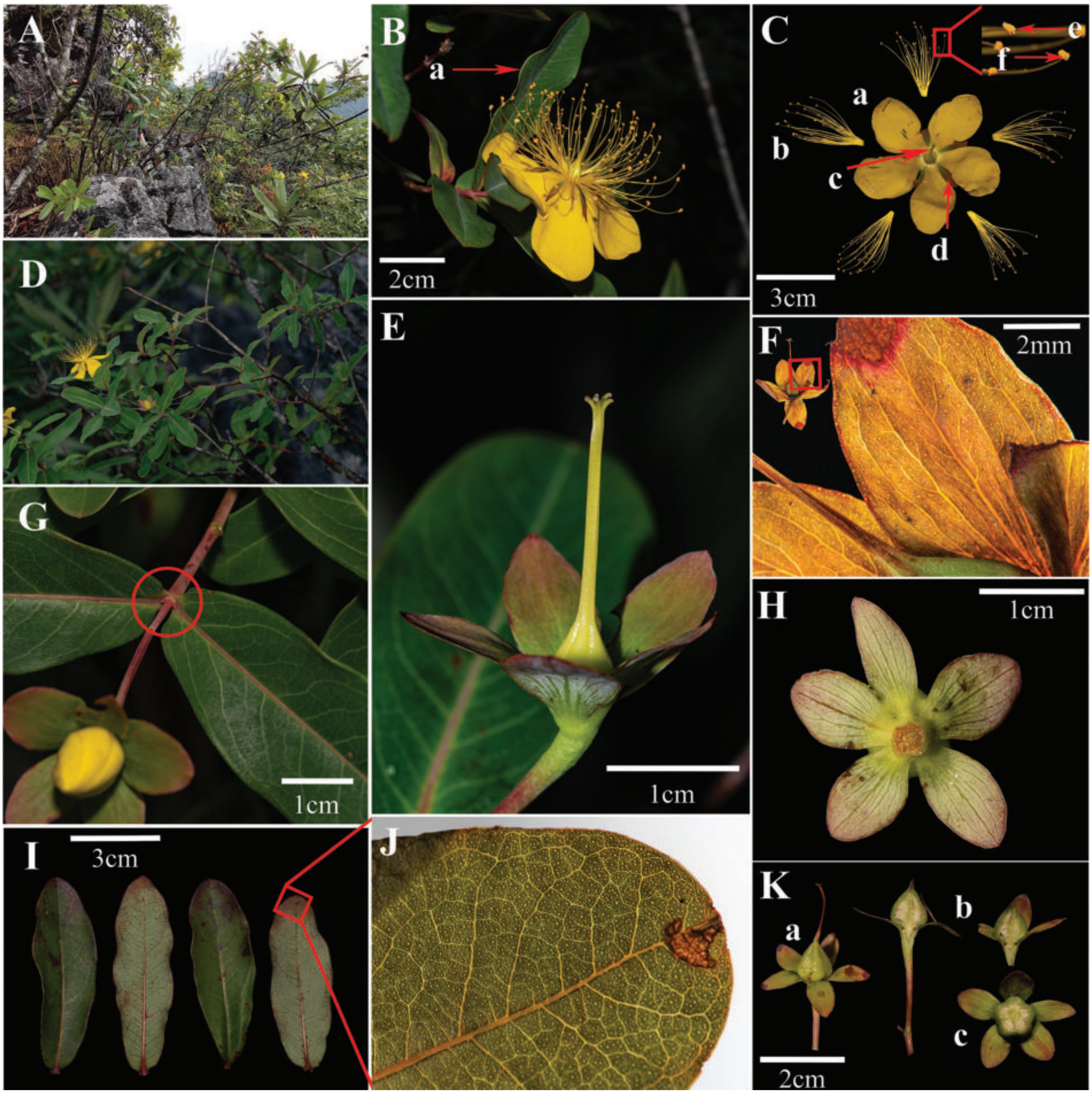

Figure 2. *Hypericum liboense* **A** habitat **B** flower (a) undulating leaf margins **C** flower anatomy (a) petal (b) stamens (c) pistil (d) calyx (e) anther (f) gland **D** *H. liboense* branch with flowers **E** stylus **F** veins and glandular points of calyx **G** leaf blade half-clasping twig **H** abaxial side of calyx **I** blade **J** veins and glands **K** anatomy of fructus (a) whole fructus (b) longitudinal section of fructus (c) cross-section of fructus

population is relatively endangered. However, because our current investigation of the survival status and threat factors of *H. liboense* is not sufficiently comprehensive to provide information on the specific distribution of this population, we recommend that *H. liboense* be classified as “data missing” (IUCN 2017).

Conclusions

According to the morphological characteristics and molecular evidence of *Hypericum*, the findings indicate that *H. liboense* should be categorized within sect. *Ascyreia*. It is evident that *H. liboense* is a distinct member of

Hypericum and forms a strongly supported clade (PP = 1.00) within the *Hypericum* phylogenetic tree. Moreover, *H. liboense* exhibits distinct morphological features that differentiate it from all currently accepted species in *Hypericum*. Therefore, it is deemed necessary to classify *H. liboense* as a new species.

Acknowledgements

The authors would like to thank Kun Wang, Xing-Yong Cui, Xi-Hong Yang and Hong-Fen Hu for their help with species investigation and specimen collection. Thanks to Ling-Bin Yan for his help with photographing the species.

Additional information

Conflict of interest

The authors have declared that no competing interests exist.

Ethical statement

No ethical statement was reported.

Funding

This work was supported by the "Survey and Assessment of Newly Added National Key Protected Wild Plant Resources in Guizhou Province (Second stage) (MCHC–ZD20232020)", "Research on the diversity of Corybas fanjingshanensis mycorrhizal fungi of rare and endangered orchids endemic in Guizhou (QKHJC [2023]1Y235)" and "Investigation and Monitoring Project of Maolan Large-scale Dynamic Plot of Karst Forest Eco-system in South China (2023–23)".

Author contributions

Tian-Rou Wu and Jian Xu completed all the work of this paper together, they contributed equally to this work and are the co-first authors of this paper. Ming-Tai An planned and guided the writing of the whole paper, participated in the field investigation and identification work, acted as the corresponding author of the paper. Jiang-Hong Yu participated in the field investigation and completed part of the data processing and content writing. Feng Liu Collect plant specimens in the field and take photographs for identification. Zheng-Ren Chen participated in field investigation and compared plant specimens to identify species and guide the writing of the paper.

Author ORCIDs

Tian-Rou Wu https://orcid.org/0009-0001-5223-0567
Jian Xu https://orcid.org/0000-0002-0714-0917
Ming-Tai An https://orcid.org/0000-0003-3886-0287
Jiang-Hong Yu https://orcid.org/0000-0003-1765-8557
Feng Liu https://orcid.org/0009-0003-7031-4494

Data availability

All of the data that support the findings of this study are available in the main text.

References

Bacchetta G, Brullo S, Salmeri C (2010) *Hypericum scruglii* sp. nov. (Guttiferae) from Sardinia. Nordic Journal of Botany 28(4): 469–474. https://doi.org/10.1111/j.1756-1051.2009.00736.x

Bertoli A, Cirak C, Seyis F (2018) *Hypericum* spp. volatile profiling and the potential significance in the quality control of new valuable raw material. Microchemical Journal 136: 94–100. https://doi.org/10.1016/j.microc.2017.01.006

Bessey CE (1915) The phylogenetic taxonomy of flowering plants. Annals of the Missouri Botanical Garden 2(1/2): 109–164. https://doi.org/10.2307/2990030

Caldeira GI, Gouveia LP, Serrano R, Silva OD (2022) *Hypericum* genus as a natural source for biologically active compounds. Plants 11(19): 2509. https://doi.org/10.3390/plants11192509

Chinese Plant Bol Group, Li DZ, Gao LM, Li HT, Wang H, Ge XJ, Liu JQ, Chen ZD, Zhou SL, Chen SL, Yang JB, Fu CX, Zeng CX, Yan HF, Zhu YJ, Sun YS, Chen SY, Zhao L, Wang K, Yang T, Duan GW (2011) Comparative analysis of a large dataset indicates that internal transcribed spacer (ITS) should be incorporated into the core barcode for seed plants. Proceedings of the National Academy of Sciences of the United States of America 108(49): 19641–19646 https://doi.org/10.1073/pnas.1104551108

Crockett SL, Robson NKB (2011) Taxonomy and chemotaxonomy of the genus *Hypericum*. Medicinal and Aromatic Plant Science and Biotechnology 5(1): 1–13.

Dauncey EA, Irving JTW, Allkin R (2019) A review of issues of nomenclature and taxonomy of *Hypericum perforatum* L. and Kew's Medicinal Plant Names Services. The Journal of Pharmacy and Pharmacology 71(1): 4–14. https://doi.org/10.1111/jphp.12831

Deng T, Wen F, Xie DJ, Wei RX, He L, Dou QL, Qian ZM, Zhang RB (2023) *Paraboea zunyiensis* (Gesneriaceae), a new species from north Guizhou, China. PhytoKeys 235: 21–29. https://doi.org/10.3897/phytokeys.235.111412

Ely CV, Boldrini II (2015) A new threatened species of *Hypericum* from the south Brazilian Pampa Biome. Systematic Botany 40(4): 989–994. http://www.bioone.org/doi/full/10.1600/036364415X690021

Ely CV, Boldrini II, Bordignon SADL (2015) A new species of *Hypericum* (Hypericaceae) from southern Brazil. Phytotaxa 192(4): 290–295. https://doi.org/10.11646/phytotaxa.192.4.6

Fang SL, Xu B, Zhang L, He ZR, Zhou XM (2023) *Selaginella densiciliata* (subg. *Heterostachys*, Selaginellaceae), a new spikemoss species from China based on morphological and molecular data. PhytoKeys 227: 135–149. https://doi.org/10.3897/phytokeys.227.101222

Galeotti N (2017) *Hypericum perforatum* (St John's wort) beyond depression: A therapeutic perspective for pain conditions. Journal of Ethnopharmacology 200: 136–147. https://doi.org/10.1016/j.jep.2017.02.016

Galindon JMM, Penneys DS, Lagunday NE, Tandang DN, Coritico FP, Amoroso VB, Fritsch PW (2021) *Hypericum perryongii* (Hypericaceae), a new species from Philippines. Phytotaxa 478(1): 61–66. https://doi.org/10.11646/phytotaxa.478.1.4

Hall FR (1999) Precision farming: Technologies and information as risk-reduction tools. Nucleic Acids Symposium Series 41: 96–116. https://doi.org/10.1021/bk-1999-0734.ch008

IUCN (2017) Guidelines for Using the IUCN Red List Categories and Criteria. Version 13. http://cmsdocs.s3.amazonaws.com/RedListGuidelines.pdf

Li YK (1986) Flora of Guizhou (vol. 2), Guizhou People Press, 151–171.

Li XW, Li YH, Tong SQ, Tao GD, Zhang PY, Zhang YJ (1990) Flora of China (vol. 50). Science Press, 8–71.

Luo JJ, Zhang MK, Liu XF, Chen H, Li TY, Ma XD, Huang K, Fu ZX (2023) *Primula xilingensis* (Primulaceae), a new species from Sichuan, China. PhytoKeys 234: 135–143. https://doi.org/10.3897/phytokeys.234.108411

Marinho LC, Martins MV, Amorim AMA, Bittrich V (2016) *Vismia atlantica* (Hypericaceae), a new species previously thought to be well-known from the Brazilian Atlantic forest. The Journal of the Torrey Botanical Society 143(3): 330–337. https://doi.org/10.3159/TORREY-D-15-00041

Marrelli M, Statti G, Conforti F (2020) *Hypericum* spp.: An update on the biological activities and metabolic profiles. Mini-Reviews in Medicinal Chemistry 20(1): 66–87. https://doi.org/10.2174/1389557519666190926120211

Meseguer AS, Aldasoro JJ, Sanmartín I (2013) Bayesian inference of phylogeny, morphology and range evolution reveals a complex evolutionary history in St. John's Wort (*Hypericum*). Molecular Phylogenetics and Evolution 67(2): 379–403. https://doi.org/10.1016/j.ympev.2013.02.007

Meseguer AS, Sanmartín I, Marcussen T, Pfeil BE (2014) Utility of low-copy nuclear markers in phylogenetic reconstruction of *Hypericum* L. (Hypericaceae). Plant Systematics and Evolution 300(6): 1503–1514. https://doi.org/10.1007/s00606-013-0977-5

Miller MA, Pfeiffer W, Schwartz T (2010) Creating the CIPRES science gateway for inference of large phylogenetic trees. Gateway Computing Environments Workshop 14: 1–8. https://doi.org/10.1109/GCE.2010.5676129

Nürk NM, Madriñán S, Carine MA, Chase MW, Blattner FR (2013) Molecular phylogenetics and morphological evolution of St. John's Wort (*Hypericum*; Hypericaceae). Molecular Phylogenetics and Evolution 66(1): 1–16. https://doi.org/10.1016/j.ympev.2012.08.022

Nürk NM, Uribe-Convers S, Gehrke B, Tank DC, Blattner FR (2015) Oligocene niche shift, miocene diversification-cold tolerance and accelerated speciation rates in the St. John's Worts (*Hypericum*, Hypericaceae). BMC Evolutionary Biology 15(1): 80. https://doi.org/10.1186/s12862-015-0359-4

Ocak A, Savaroglu F, Erkara İP, Koyuncu O (2009) *Hypericum sechmenii* (Hypericaceae), a new species from central Anatolia, Turkey. Annales Botanici Fennici 46(6): 591–594. https://doi.org/10.5735/085.046.0616

Park SJ, Kim KJ (2004) Molecular phylogeny of the genus *Hypericum* (Hypericaceae) from Korea and Japan: Evidence from nuclear rDNA ITS sequence data. Journal of Plant Biology 47(4): 366–374. https://doi.org/10.1007/BF03030553

Revuru B, Bálintová M, Henzelyová J, Eva Č, Kusari S (2020) MALDI–HRMS imaging maps the localization of skyrin, the precursor of Hypericin, and pathway intermediates in leaves of *Hypericum* species. Molecules (Basel, Switzerland) 25(17): 3964. https://doi.org/10.3390/molecules25173964

Robson NKB (1972) Evolutionary recall in *Hypericum* (Guttiferae). Transactions of the Botanical Society of Edinburgh 41(3): 365–383. https://doi.org/10.1080/03746607208685239

Robson NKB (1977) Studies in the genus *Hypericum* L. (Guttiferae): 1. Infrageneric classification. Bulletin of the British Museum (Natural History). Botany 5: 293–355.

Robson NKB (1985) Studies in the genus *Hypericum* L. (Guttiferae): 3. Sections: 1. *Campylosporus* to: 6a. *Umbraculoides*. Bulletin of the British Museum (Natural History). Botany 12: 163–325.

Robson NKB (1990) Studies in the genus *Hypericum* L. (Guttiferae): 8. Sections 29. *Brathys* (part 2) and 30. *Trigynobrathys*. Bulletin of the British Museum (Natural History). Botany 20: 1–150.

Robson NKB (2001) Studies in the genus *Hypericum* L. (Guttiferae) 4(1). section 7. *Roscyna* to 9. *Hypericum sensu lato* (part 1). Bulletin of the Natural History Museum Botany Series 31: 37–88. https://doi.org/10.1017/S096804460200004X

Robson NKB (2006) Studies in the genus *Hypericum* L. (Clusiaceae). section 9. *Hypericum sensu lato* (part 3): Subsection 1. *Hypericum* series 2. *Senanensia*, subsection 2. *Erecta* and section 9b. *Graveolentia*. Systematics and Biodiversity 4(1): 19–98. https://doi.org/10.1017/S1477200005001842

Robson NKB (2010a) Studies in the genus *Hypericum* L. (Hypericaceae) 5(1). sections 10. *Olympia* to 15/16. *Crossophyllum*. Phytotaxa 4(1): 5–126. https://doi.org/10.11646/phytotaxa.4.1.2

Robson NKB (2010b) Studies in the genus *Hypericum* L (Hypericaceae) 5(2). sections 17. *Hirtella* to 19. *Coridium*. Phytotaxa 4(1): 127–258. https://doi.org/10.11646/phytotaxa.4.1.3

Robson NKB (2012) Studies in the genus *Hypericum* L. (Hypericaceae) 9. addenda, corrigenda, keys, lists and general discussion. Phytotaxa 72(1): 1–111. https://doi.org/10.11646/phytotaxa.72.1.1

Robson NKB (2016) And then came molecular phylogenetics–reactions to a monographic study of *Hypericum* (Hypericaceae). Phytotaxa 255(3): 181–198. https://doi.org/10.11646/phytotaxa.255.3.1

Ronquist F, Huelsenbeck JP (2003) MrBayes 3: Bayesian phylogenetic inference under mixed models. Bioinformatics 19(12): 1572–1574. https://doi.org/10.1093/bioinformatics/btg180

Ruchisansakun S, van der Niet T, Janssens SB, Triboun P, Techaprasan J, Jenjittikul T, Suksathan P (2016) Phylogenetic analyses of molecular data and reconstruction of morphological character evolution in Asian *Impatiens* section *Semeiocardium* (Balsaminaceae). Systematic Botany 40(4): 1063–1074. https://doi.org/10.1600/036364415X690102

Tan K, Iatrou G, Vold G, Strid A (2010) *Hypericum boehlingraabei* (Hypericaceae), a new species from the northern Peloponnese (Greece). Phytologia Balcanica 16(2): 227–331. http://www.bio.bas.bg/~phytolbalcan/PDF/16_2/16_2_06_Kit_Tan_&_al.pdf

The Angiosperm Phylogeny Group (2016) An update of the angiosperm phylogeny group classification for the orders and families of flowering plants: APG IV. Botanical Journal of the Linnean Society 181(1): 1–20. https://doi.org/10.1111/boj.12385

Trigas P (2018) A new *Hypericum* (sect. *Drosocarpium*, *Hypericaceae*) from the Cyclades Islands (Greece). Nordic Journal of Botany 36(11): e2205. https://doi.org/10.1111/njb.02205

Ya JD, Wang WT, Liu YL, Jiang H, Han ZD, Zhang T, Huang H, Cai J, Li DZ (2023) Five new and noteworthy species of Epidendroideae (Orchidaceae) from southwestern China based on morphological and phylogenetic evidence. PhytoKeys 235: 211–236. https://doi.org/10.3897/phytokeys.235.111230

Yu JH, Zhang WD, Qin F, Xia CY, Qin Y, An MT, Gadagkar SR, Yu SX (2022) *Impatiens yunlingensis* (Balsaminaceae), a new species from Yunnan, China. PhytoKeys 212: 13–27. https://doi.org/10.3897/phytokeys.212.89347

Zheng LN, Luo L, Tang YW, Yu C, Lyu PF, Liu XS, Zhang QX, Yang YY (2023) *Rosa funingensis* (Rosaceae), a new species from Yunnan, China. PhytoKeys 229: 61–70. https://doi.org/10.3897/phytokeys.229.101052

PhytoKeys 237: 51–77 (2024)
DOI: 10.3897/phytokeys.237.112860

Research Article

From morphology to molecules: A comprehensive study of a novel *Derris* species (Fabaceae) with a rare flowering habit and reddish leaflet midribs, discovered in Peninsular Thailand

Punvarit Boonprajan[1], Charan Leeratiwong[2], Yotsawate Sirichamorn[1]

1 *Department of Biology, Faculty of Science, Silpakorn University, Sanam Chandra Palace Campus, Nakhon Pathom 73000, Thailand*
2 *Division of Biological Science, Faculty of Science, Prince of Songkla University, Songkhla 90112, Thailand*
Corresponding author: Yotsawate Sirichamorn (sirichamorn_y@su.ac.th)

Abstract

Derris rubricosta Boonprajan & Sirich., **sp. nov.**, a new species of the genus *Derris* Lour. (Fabaceae) was discovered in Peninsular Thailand. The overall morphology demonstrates that the species most resembles *D. pubipetala*. Nevertheless, the species has several autapomorphies differentiating it from other *Derris* species, e.g., the presence of reddish midribs of the mature leaflets, sparsely hairy stamen filaments, prominent hairs at the base of the anthers, and presence of glandular trichomes along the leaflet midrib. Additionally, HPLC fingerprints of this species showed a distinction from *D. pubipetala* by the absence of phytochemical compound peaks after 13 min. Retention Time (RT). Results from molecular phylogenetic analyses also strongly supported the taxonomic status as a new species.

Key words: Anatomy, *Derris*, HPLC fingerprint, molecular phylogeny, morphology, phytochemical

Academic editor: Patrick Herendeen
Received: 21 September 2023
Accepted: 13 December 2023
Published: 15 January 2024

Citation: Boonprajan P, Leeratiwong C, Sirichamorn Y (2024) From morphology to molecules: A comprehensive study of a novel *Derris* species (Fabaceae) with a rare flowering habit and reddish leaflet midribs, discovered in Peninsular Thailand. PhytoKeys 237: 51–77. https://doi.org/10.3897/phytokeys.237.112860

Introduction

The genus *Derris* Lour. is a papilionoid legume, comprising approximately 50 species (Adema 2000, 2003; Sirichamorn 2020; POWO 2023). It is a taxonomically complex genus in the tribe Millettieae of Fabaceae. Species of *Derris* are important sources of a toxic substance, Rotenone, which is traditionally used as a fish poison and commercially used as an insecticide. In addition, many species of *Derris* are used as local medicines for a variety of ailments in many South-East Asian countries (Hamid 1999).

Derris was first described by Loureiro (1790), based on the type species *D. trifoliata* Lour. Bentham (1860) recognised the genus in a taxonomically broad sense and his concept has been widely followed since then. After revisions of the genus based mainly on morphological and molecular phylogenetic analyses, the circumscription of *Derris* became taxonomically narrower (Geesink 1985; Adema 2000, 2003; Sirichamorn et al. 2012a; Sirichamorn et al. 2012b; Sirichamorn et al. 2014b).

All *Derris* species are lianas, with imparipinnate leaves and opposite leaflets, its inflorescences are pseudoracemes/pseudopanicles, or rarely panicles, the androecium is monadelphous and the stamens generally glabrous, the fruits are indehiscent, laterally compressed, leathery pods, usually with marginal wings. However, tardily dehiscent, wingless, and inflated pods were also reported in *D. montana* Benth. (Sirichamorn et al. 2012a) and recently in *D. taiwaniana* (Hayata) Z.Q.Song and *D. entadoides* (Z.Wei) Z.Q.Song (Song and Pan 2022). Some genera in the tribe Millettieae such as the Asiatic *Aganope* Miq. and *Brachypterum* (Wight & Arn.) Benth. or the American *Deguelia* Aubl. are, however, morphologically very similar to *Derris* and are sometimes referred to as *Derris*-like plants (Sirichamorn et al. 2012a). Species of *Derris* are found mainly in South-East Asia. Seventeen species were reported in the Flora of Thailand (Sirichamorn 2020). In addition, previously unknown Thai taxa have been discovered in different parts of the country.

Thailand is a part of the ancestral center of *Derris* (Sirichamorn et al. 2014a, sits at the nexus of three key floristic regions: Indo-Chinese, Indo-Burmese and Malesian elements. Southern Thailand, positioned on the Malay Peninsula and bordered northward by the Kra Isthmus, predominantly lies within the Tenasserim-South Thailand semi-evergreen rainforest ecoregion. This stretch spans the western Andaman Sea coast and the eastern Gulf of Thailand coast. Conversely, the southernmost border with Malaysia falls under the Peninsular Malaysian rainforest and montane rainforest ecoregions (Wikramanayake et al. 2002). Areas such as the Hala-Bala Wildlife Sanctuary, straddling the Thai-Malaysian border, house an array of rare and indigenous flora and fauna (ICEM 2003). A variety of new plant taxa have been discovered and reported from the area in the past two decades including the legume species such as *Derris glabra* Sirich. (Sirichamorn et al. 2012a) and *Millettia calcicola* Mattapha, G.P. Lewis & Hawkins (Mattapha et al. 2023).

During a field expedition in 2019, the authors of this article discovered and collected an unrecognised “*Derris*-like” species along the stream at Pha Dam Forest Ranger Unit (Ton Nga Chang Wildlife Sanctuary), Songkhla province. However, the plant showed some unusual morphological characteristics compared with other known species of *Derris* and *Derris*-like taxa. During comprehensive field surveys in the following years, two more populations were found by the stream at the entrance of Tone Prew waterfall (Ton Nga Chang Wildlife Sanctuary, also in Songkhla province) and Krung Ching waterfall (in Khao Luang National Park in Nakhon Si Thammarat province). The latter two populations had very similar vegetative characters, but unfortunately were never observed producing flowers. The flowering specimen from Pha Dam Forest Ranger Unit only once produced inflorescences in 2019, but no seed pod was produced. The specimens were compared with the type specimens of all *Derris*-like taxa, including the descriptions in several taxonomic publications, including the Flora of Thailand (Sirichamorn 2020), the Flora of the Malay Peninsula (Ridley 1922), the Flora of China (Chen and Pedley 2010), the Flora of India (Thothathri 1982), the Flora of British India (Baker 1878) and a taxonomic revision of the genus in India (Thothathri 1961). Preliminary morphological studies pointed to the plant being an undescribed species of *Derris*.

The main objectives of this work were to investigate and verify the exact taxonomic status of this unknown *Derris*-like species using more critical macro- and micro-morphological studies, molecular phylogenetic analyses, and phytochemical evidence from high-performance liquid chromatography (HPLC) fingerprinting. A full species description and revised key to the species of *Derris* in Thailand are provided, together with photographs and a line drawing of the new taxon.

Materials and methods

Taxon collection, preparation, and taxonomic study

Samples from three localities of the putative new taxon, and three samples of *D. pubipetala* from three different localities (represented by accessions nos. 1 to 6 in Table 1), were collected for morphological, anatomical, phytochemical, and molecular investigation. Voucher specimens were deposited in the BKF herbarium and duplicates were distributed to other herbaria. Three mature leaflets per accession were fixed in 70% ethyl alcohol for anatomical study. Young leaves of the three putative new taxon samples were collected and stored in silica gel for later DNA extraction. Stems and roots were also collected, cleaned, cut into smaller pieces and then dried at 50–60 °C in a hot air oven, and then stored at room temperature for phytochemical study.

Voucher specimens were examined using a stereomicroscope. The species description was prepared following the format of the Flora of Thailand (Sirichamorn 2020). Morphological measurements and comparison of specimens with (type) specimens of *Derris*-like plants housed in Thai herbaria (BK, BKF, and PSU) or available as online digital images (K, L, and P) were carried out.

Scanning electron microscopy (SEM)

Three lateral leaflets of mature leaves for each accession were used. Samples of 5 × 5 mm were taken from the center of the leaflets (from midrib to margin, including the midrib). Sections were cleaned, dehydrated in a series of ethyl alcohol, dried by critical point drying (CPD) in liquid CO_2, and preserved in a desiccator for subsequent observation by SEM. Samples were mounted directly on aluminum stubs using double-sided carbon tape, then sputter-coated with gold using an SPI module sputter coater. The samples were photographed using a Tescan Mira3 scanning electron microscope (SEM) at the Scientific and Technological Equipment Center, Faculty of Science, Silpakorn University.

Anatomical study of leaves

Leaf epidermis was studied using the leaf scraping technique (modified from Johansen 1940). Mesophyll was scraped from the upper and lower surfaces with a razor blade, followed by epidermal bleaching using 10% sodium hypochlorite. Samples were cleaned three times in distilled water, then stained with 1% Safranin-O before washing again and dehydrating in a graded series of ethyl alcohol and a series of xylene. Samples were mounted on slides using DePeX mounting media (VWR international Ltd., England).

Table 1. Species, localities, and vouchers of the material in Thailand used for morphological and phytochemical analysis.

Accession No.	Species	Locality	Voucher specimen	Herbarium
1	*Derris* sp.	Pha Dam Forest Ranger Unit, Ton Nga Chang Wildlife Sanctuary, Padang Besar sub-district, Sadao district, Songkhla Province (Locality code; SS)	C. Leeratiwong 19-1666	BKF
2	*Derris* sp.	Tone Prew waterfall, Ton Nga Chang Wildlife Sanctuary, Kamphaeng Phet sub-district, Rattaphum district, Songkhla Province (Locality code; RS)	YSM2021-15	BKF
3	*Derris* sp.	Krung Ching waterfall, Nopphitam sub-district, Nopphitam district, Nakhon Si Thammarat Province (Locality code; NN)	YSM2021-16	BKF
4	*D. pubipetala*	Surat Thani, Ko Samui district, Ang Thong sub-district (Hin Lad Waterfall)*	Leeratiwong et al. 18-1192	PSU
5	*D. pubipetala*	Nakhon Si Thammarat, Khanom district, Khanom sub-district (Samedchun Waterfall)	YSM2022-5	BKF
6	*D. pubipetala*	Nakhon Si Thammarat, Khanom district, Khanom sub-district (Hin Lad Waterfall)*	YSM2022-6	BKF

Note: *The name of both waterfalls is the same, but they are different locations.

Three leaflets from 3 mature leaves for each accession were sectioned by hand to produce transverse sections, then stained with 1% Safranin-O, dehydrated in a graded series of ethyl alcohol and series of xylene. Finally, the sections were mounted on slides using DePeX. All leaf epidermal surfaces and sectioned parts were digitally photographed with an Olympus BX53 microscope with a DP27 camera attachment. Each leaf anatomical character was measured using ImageJ (Rueden et al. 2017).

Phytochemical analyses

Dried stems and roots of each accession were ground separately into a powder using a high-speed blender. The maceration process (modified from da Costa et al. 2016) involved soaking 5 grams of each plant sample in 250 mL of Dichloromethane in the dark at room temperature for 72 hrs. After maceration, the solvent extract of each accession was then filtered and subsequently evaporated in a dark fume hood at room temperature for 24 hrs. The crude extract was transferred into a sealed plastic tube, protected from light and stored in a refrigerator at 0–5 °C for further analysis.

The qualitative phytochemical analysis of rotenone and deguelin was analyzed using high-performance liquid chromatography (Agilent Technologies, Germany) consisting of a 1260 Infinity II LC system controller fitted with 1260 Infinity II Quaternary, 1260 Infinity Binary pump, 1260 Infinity II degasser, and 1260 Infinity II Diode Array UV-Visible detector. An Agilent 5 TC-C18 (4.6 × 150 mm, particle size 5 μm) reversed-phase analytical column was used. The isocratic method was performed for separating chemical substances using a mobile phase of acetonitrile/water (60:40; v/v) for 35 min. The injection volume was 10 μL, and the flow rate was 1.0 mL/min. The liquid chromatography system had to be stabilised for 15 min with the mobile phase before injecting the analyte. The analysis was performed at a wavelength of 294 nm. The control and data elaboration used Agilent OpenLAB ChemStation Edition.

Approximately 0.01 g of crude extract was dissolved and diluted with 1 mL of acetonitrile in a 2 mL microcentrifuge tube. The extracted solution was filtered using a syringe filter nylon membrane of 0.22 µm pore size. The chemical patterns of the two mains chemical markers were carried out using the HPLC system.

Molecular analyses

Taxon sampling for this study were selected based on the phylogeny reconstructed by Sirichamorn et al. (2012a) (Suppl. material 1). Additional DNA samples were extracted from dried young leaves of the three populations of the putative new species using the DNeasy Plant mini kit and modified protocol (Qiagen, Hilden, Germany). Two chloroplast regions [*trnL-F* intergenic spacer (IGS) and *trnK-matK*] and one nuclear region [the ribosomal internal transcribed spacer (ITS/5.8S)] were amplified using universal primers (Table 2). PCR reagents were carried out in a 25 µL reaction mixture which contained 1 µL (10 µM) of each forward and reverse primer, 12.5 µL GoTag Green Master Mix (Promega), 2 µL (< 250 ng) of total DNA and Nuclease-free water to 25 µL. PCR conditions for *trnL-F* IGS and *trnK-matK* followed a modified protocol of Hu et al. (2000). The ITS/5.8S region was amplified following Wojciechowski et al. (1993, 1999). Quality, quantity, and size of PCR products were tested by gel electrophoresis and genomic absorption. Samples were sent to Celemics, Inc. (http://www.celemics.com) for purifying and sequencing. Each purified fragment was treated using a Barcode-Tagged Sequencing (BTSeq) technique of Next-Generation Sequencing (NGS) (CELEMICS, Seoul, Republic of Korea) technology for automated dsDNA sequencing. All newly generated sequences in this study have been deposited in GenBank (Suppl. material 1).

Sequence alignments were performed using the program Bioedit v. 7.0.9 (Hall 1999) with the CLUSTAL W multiple alignment (default settings; Thompson et al. 1994) together with subsequent manual adjustment. Sequences of each marker were firstly aligned separately. Then, the combined data matrix was made by concatenating those already aligned datasets. Phylogenetic relationship was reconstructed using Maximum Parsimony (MP), Maximum Likelihood (ML), and Bayesian Inference (BI). For MP analyses, phylogenetic trees were constructed with the program PAUP* v. 4.0a169 (Swofford 2002) under heuristic search with 10,000 replicates of random taxon additions. The process employed Tree Bisection-Reconnection (TBR) branch swapping and Multrees activated, with all parsimonious trees saved. Bootstrap percentage

Table 2. Sequences of the primers used for PCR amplification and sequencing.

Primers	Amplified region	Direction	Sequence (5 ' to 3 ')	References
trnKIL	*trnK-matK* (Ch)	forward	CTC AAT GGT AGA GTA CTC G	Hu et al. 2000
trnK2R	*trnK-matK* (Ch)	reverse	AAC TAG TCG GAT GGA GTA G	Hu et al. 2000
e	*trnL-F* IGS (Ch)	forward	GGT TCA AGT CCC TCT ATC CC	Taberlet et al. 1991
f	*trnL-F* IGS (Ch)	reverse	ATT TGA ACT GGT GAC ACG AG	Taberlet et al. 1991
ITS1	ITS/5.8S (Nr)	forward	TCC GTA GGT GAA CCT GCG G	White et al. 1990
ITS4	ITS/5.8S (Nr)	reverse	TCC TCC GCT TAT TGA TAT GC	Wojciechowski et al. 1993

Ch = chloroplast marker; Nr = nuclear marker.

analysis was used for the evaluation of MP clade support and calculated using the same settings (Felsenstein 1985). Maximum Parsimony Bootstrap Support (MPBS) is described as high (85–100%), moderate (75–84%), low (50–74%), or none (< 50%). The jModelTest v. 2 (Darriba et al. 2012) on the CIPRES web portal was used to find the best-fit substitution model chosen by the Akaike Information Criterion (AIC) scores (Akaike 1974). The General Time Reversible (GTR) (Tavaré 1985) nucleotide substitution model with a gamma distribution for among-site rate variation was selected for all DNA regions. ML analyses were performed for the combined data sets using the program IQ-TREE v. 2.2.0 (Nguyen et al. 2015) under GTR+G partition models implemented with the "-p" command. Bootstrap (Felsenstein 1985) clade support was calculated using a non-parametric bootstrap resampling with 2,000 replicates. Maximum Likelihood Bootstrap Support (MLBS) values are described as high (85–100%), moderate (75–84%), low (50–74%), or none (< 50%). Bayesian Markov Chain Monte Carlo (MCMC) (Yang and Rannala 1997) phylogenetic analyses were reconstructed using the program MrBayes v. 3.2.7a (Ronquist et al. 2012) via the CIPRES Science Gateway v.3.3 (Miller et al. 2010). The majority-rule consensus tree was started from random trees and run for 10,000,000 generations until stationarity, with MCMC sampled every 1,000 generations. The first 25% of all trees were discarded as burn-in and each BI clade was supported by posterior probabilities (PP) estimation from the remaining sampled trees. PPs are described as high (0.95–1), moderate (0.9–0.94), low (0.5–0.89), or none (< 0.5) support.

Morphological study

Three putative new *Derris* samples were morphologically studied and photographed as shown in Figs 1–3. They were collected from three localities in Songkhla and Nakhon Si Thammarat provinces (Fig. 4, a yellow square and 2 light-blue triangles). Their overall vegetative morphology is the same and they presumably represent a single species. The most remarkable characteristic found in all three samples is the reddish midribs of the mature leaflets. Only the sample collected from Pha Dam Forest Ranger Unit in Songkhla province had flowers. Morphologically, the most similar species in Peninsular Thailand is *D. pubipetala*, although this differs by several morphological characters. In general, the putative new *Derris* samples have paler bark and more leaflets per leaf, and the inflorescence is longer than that of *D. pubipetala*. Shape, curvature, and the lower auricle of the wing petals are also different. Stamens of the new *Derris* are hairy on the free part of their filaments and, more importantly, hairs at the base of the anthers are not present in *D. pubipetala* or any other species of *Derris*. Comparisons between the morphological characters of the new *Derris* and *D. pubipetala* are summarised in Table 3.

Anatomical study of leaves/leaflets

As seen in *D. pubipetala*, all samples of the putative new *Derris* (Table 1) showed no significant differences in their leaf anatomy. Micro-morphological and anatomical characteristics are summarised in Table 4 and presented in Figs 5–7.

Table 3. Comparative morphological characters of the new *Derris* and *D. pubipetala*.

Morphological characters	Species	
	***Derris* sp. nov.**	***D. pubipetala***
Vegetative parts		
Colour of roots	brownish to black-gray	slightly pinkish or reddish
Colour of bark	pale brownish-gray to gray	dark reddish-brown
Colour of leaves when young	reddish	light green to brownish
Number of leaflets per leaf	9–11	5–9
Colour of midrib of leaves when mature	reddish	green
Adaxial leaf surface	glabrous except for slightly strigose along midrib and lateral veins	glabrous to slightly strigose
Reproductive parts		
Length of inflorescence (cm)	40–50	5–28
Position of bracteoles	at the base of calyx tube	on pedicel
Colour of corolla	pale pink to pink	white
Shape of wing petals	elliptic to narrowly ovate	elliptic to semi-hastate
Apex of wing petals	obtuse	rounded
Upper auricle of wing petals	indistinct, 0.5–0.9 mm long	evident, 1–2.5 mm long
Lower auricle of wing petals	absent	present
Curvature of wing petals	straight	curved backward
Apex of keel petals	retuse	rounded
Anthers with some basal hairs	present	absent
Free part of filaments with hairs	present	absent
Shape of floral disc	indistinct or more or less 10-lobed	annular
Indumentum on style	sericeous at the base and gradually becoming glabrous apically	glabrous

Leaf epidermis (Fig. 6A–L); Leaf epidermal cells of the three new *Derris* samples and those of *D. pubipetala* were quite similar on both leaflet surfaces, i.e., lobed or jigsaw-like in shape because of their undulate anticlinal cell walls (slightly more deeply undulate in the new *Derris* samples). The width and length of the epidermal cells on both surfaces ranged between 21.91–41.53 μm and 31.15–56.60 μm, respectively. Ratios of epidermal cell size (width: length) of the new *Derris* species were 0.77 (±0.20) for the adaxial and 0.66 (±0.12) for the abaxial surface, whereas the ratios of *D. pubipetala* were 0.83 (±0.09) for adaxial and 0.78 (±0.36) for abaxial surfaces, respectively. Leaflets of all taxa were hypostomatic with commonly paracytic and rarely anomocytic stomata. The width and length of stomata in the new species of *Derris* (w = 17.47±1.01 μm; l = 22.95±1.03 μm) was greater than in *D. pubipetala* (w = 12.43±0.73 μm; l = 15.04±0.52 μm), whereas the stomatal density of *D. pubipetala* (230±15.62 per mm^2) was higher than for the new *Derris* (104.66±3.05 per mm^2). The stomatal index of the new species was also higher (17.02±0.75) than that of *D. pubipetala* (16.52±1.04). Guard cell size of the new *Derris* was c. 22.65 μm long and c. 8.24 μm wide (ratio = 0.36±0.01). For *D. pubipetala*, guard cells were clearly smaller, c. 15.41 μm long and c. 5.17 μm wide (ratio = 0.33±00). Only unicellular non-glandular trichomes occurred on both leaflet

Figure 1. *Derris rubricosta*, sp. nov. **A** habit and habitat **B** leaves **C** stem **D** young reddish leaflets **E** reddish midribs of mature leaflets **F**, **G** close-up of midrib on adaxial and abaxial surface respectively **H** inflorescences and foliage **I**, **J** close-up of inflorescence, showing flower buds and brachyblasts **K** close-up of flower and buds. All photos were taken at Pha Dam Forest Ranger Unit in Songkhla province. Photos by Punvarit Boonprajan (**A**, **B**, **D**–**G**) and Charan Leeratiwong (**C**, **H**–**K**).

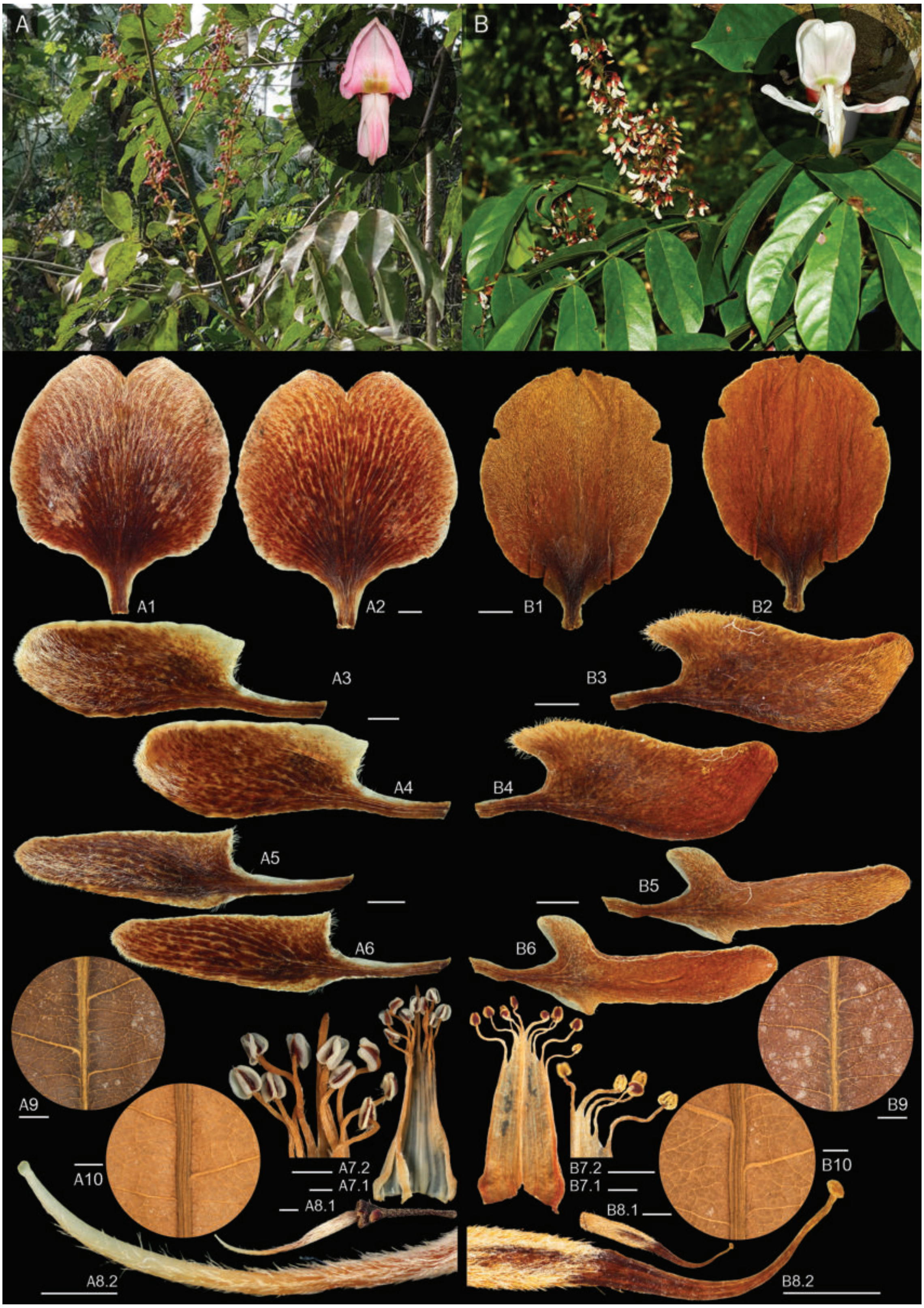

Figure 2. Comparative macro- and micro-morphological characters of leaflets and flowers of *Derris rubricosta* (**A, A1–A10**) and *D. pubipetala* (**B**, **B1–B10**) **A, B** a branch with leaves and inflorescences **A1, B1** outer surface and **A2, B2** inner surface of standard petal **A3, B3** outer surface and **A4, B4** inner surface of keel petals **A5, B5** outer surface and **A6, B6** inner surface of wing petals **A7.1, B7.1** stamens and **A7.2, B7.2** close-up stamens **A8.1, B8.1** pistil and **A8.2, B8.2** close-up pistil apex **A9, B9** adaxial and **A10, B10** abaxial leaflet surfaces. Photos by Charan Leeratiwong (**A, B**) and Punvarit Boonprajan (**A1–A10, B1–B10**). Scale bars: 1 mm.

surfaces in the new *Derris*. In *D. pubipetala*, unicellular non-glandular trichomes occurred only on the adaxial side and three different lengths (large: more than 400 μm; medium: > 100–400 μm, and small: less than 100 μm) of bicellular non-glandular trichomes were found only on the abaxial surface. No significant differences in leaflet epidermis were found among the three accessions of the new *Derris* or among populations of *D. pubipetala*.

Transverse sections (Fig. 7A–P); the adaxial leaflet surface midrib of the new *Derris* samples is convex, while it is flat or slightly concave in *D. pubipetala*. The midrib transverse section of the new *Derris* species is larger (w = 1200.15±234.88 μm; h = 1241.50±244.61 μm) than in *D. pubipetala* (w = 616.44±85.36 μm; h = 593.48±80.23 μm). The height of the epidermal cells on the adaxial and abaxial surface of the midrib ranged from 8.41–13.9 μm. in both species. The midrib of both taxa shows an elliptic or semi-circular shaped vascular bundle, surrounded by perivascular fibers. Inside the vascular bundle, vascular tissue is presented in two groups; smaller and fan-shaped on the adaxial surface and larger and horseshoe-shaped on the abaxial surface. The vascular bundle of all samples of the new *Derris* was larger (w = 1067.22±240.35 μm; h = 923.20±240.47 μm) than was found in *D. pubipetala* (w = 481.48±64.20 μm; h = 406.98±52.31 μm). Bicellular non-glandular and glandular trichomes were restricted to the midrib of the new *Derris* (Fig. 5E, F, M, N). In *D. pubipetala*, on the other hand, only bicellular non-glandular trichomes were found (Fig. 5O, P, 7C, D).

All taxa had dorsiventral leaves (Fig. 7M, O), with palisade mesophyll adaxially and spongy mesophyll abaxially. The new *Derris* samples have a greater leaflet thickness (204.27±37.90 μm) than in *D. pubipetala* (150.35±8.43 μm). The epidermal cell heights on the adaxial and abaxial surfaces of leaflet blades in all studied samples were between 9.22–23.49 μm. Furthermore, the mesophyll of the new *Derris* has a thicker 2–3-layered palisade parenchyma (105.14±19.70 μm) than in *D. pubipetala* (59.62±7.51 μm). However, spongy parenchyma in *D. pubipetala* was thicker (69.85±5.19 μm) than in samples of the new *Derris* (64.48±20.24 μm). Spongy mesophyll of *D. pubipetala* consists of variously-shaped, loosely arranged cells with larger intercellular air spaces than in the new *Derris*, which possessed fewer and smaller intercellular air spaces.

Transverse sections of the leaflet margin in all samples revealed them as being slightly revolute (Fig. 7N, P). The leaflet margin of the new *Derris* was thicker (143.98±5.86 μm) than in *D. pubipetala* (138.04±4.19 μm). Height of the epidermal layer on the adaxial and abaxial surfaces ranged from 7.73–14.10 μm. Thickness of palisade and spongy parenchyma at the leaflet margin of the new *Derris* samples and *D. pubipetala* were (74.57±6.01 vs. 31.88±2.27 μm) and (49.54±7.35 vs. 54.42±11.82 μm), respectively.

Leaflet transverse sections of all samples demonstrated the accumulation of prismatic crystals, generally associated with vascular bundles, and particularly in the leaflet midribs. Rhomboidal prisms and styroid prisms were two types of crystal observed in the leaflets of the new *Derris* species, whereas only rhomboidal di-pyramid prisms were seen in *D. pubipetala*. The reddish substance present in cortical parenchyma cells of the leaflet midrib on the abaxial leaflet surface is a unique characteristic observed only in the new *Derris*.

Figure 3. *D. rubricosta* **A** inflorescence with leaf **B** close-up of inflorescence **C** flowers (top and side view) **D** outer surface and **E** inner surface of standard petal **F** outer surface and **G** inner surface of keel petals **H** outer surface and **I** inner surface of wing petals **J** staminal sheath **K** anthers **L** pistil **M** adaxial and **N** abaxial leaflet surfaces. Drawn by Punvarit Boonprajan from C. Leeratiwong 19-1666 (BKF). Scale bars: 5 mm (**A, B**); 1 mm (**C–N**).

Table 4. Comparison of selected anatomical characters of the new *Derris* species and *D. pubipetala*. [Quantitative data; Mean value ± standard deviation (SD)].

Anatomical characters	Species	
	***Derris* sp. nov.**	***D. pubipetala***
Leaflet epidermis		
Adaxial leaflet surface		
Pattern of epidermal cell walls	undulate	undulate
Width of epidermal cell walls (µm)	41.53±5.52	35.73±3.94
Length of epidermal cell walls (µm)	55.05±6.50	43.22±4.71
Indumentum	glabrous, slightly strigose along midrib and lateral veins	thinly strigose
Ratio of epidermal cell walls (width: length)	0.77±0.20	0.83±0.09
Abaxial leaflet surface		
Pattern of epidermal cell walls	undulate	undulate
Width of epidermal cell walls (µm)	37.28±2.71	21.91±2.42
Length of epidermal cell walls (µm)	56.60±6.81	31.15±10.43
Ratio of epidermal cell walls (width: length)	0.66±0.12	0.78±0.36
Types of stomata	Ps, rarely As	Ps, rarely As
Width of stomata (µm)	17.47±1.01	12.43±0.73
Length of stomata (µm)	22.95±1.03	15.04±0.52
Ratio of stomatal (width: length)	0.76±0.04	0.82±0.07
Stomatal density (per mm^2)	104.66±3.05	230±15.62
Number of epidermal cells per unit area (mm^2)	511.33±38.27	1161.33±20.42
Stomatal Index (SI)	17.02±0.75	16.52±1.04
Width of guard cell (µm)	8.24±0.76	5.17±0.08
Length of guard cell (µm)	22.65±1.46	15.41±0.34
Ratio of guard cell (width: length)	0.36±0.01	0.33±0.00
Indumentum	glabrous to thinly strigose	strigose
Types of indumentum	Ut	Bt
Length of indumentum hairs (µm)	204.70±80.00	ST = 60.10±16.26 MT = 265.02±39.15 LT = 457.25±30.70
Ratio of epidermal cell width on adaxial leaflet surface to epidermal cell width on abaxial leaflet surface (width: width)	1.11±0.07	1.64±0.25
Ratio of epidermal cell length on adaxial leaflet surface to epidermal cell length on abaxial leaflet surface (length: length)	0.97±0.07	1.54±0.72
Leaflet transverse sections		
Transverse section of Midribs		
Outline of midribs	convex on the abaxial surface with an adaxial ridge	convex on the abaxial surface, either flat or slightly concave on the adaxial surface
Width of midrib (µm)	1200.15±234.88	616.44±85.36
Height of midrib (µm)	1241.50±244.61	593.48±80.23
Ratio of midrib (width: height)	0.96±0.00	1.04±0.10
Height of epidermal cells on adaxial leaflet surface (µm)	9.96±3.59	13.9±0.92
Height of epidermal cells on abaxial leaflet surface (µm)	8.55±0.38	8.41±0.72
Width of vascular bundle (µm)	1067.22±240.35	481.48±64.20
Height of vascular bundle (µm)	923.20±240.47	406.98±52.31
Ratio of vascular bundle (width: height)	1.16±0.05	1.18±0.08
Types of indumentum	UT, BT, GT	BT

Anatomical characters	Species	
	***Derris* sp. nov.**	***D. pubipetala***
Transverse section of Leaflet Blades		
Thickness of leaflet blade (µm)	204.27±37.90	150.35±8.43
Height of epidermal cells on adaxial leaflet surface (µm)	23.49±5.80	11.59±1.03
Height of epidermal cells on abaxial leaflet surface (µm)	13.06±0.99	9.22±1.49
Thickness of palisade mesophyll (µm)	105.14±19.70	59.62±7.51
Thickness of spongy mesophyll (µm)	64.48±20.24	69.85±5.19
Thickness ratio of palisade mesophyll to spongy mesophyll	1.68±0.31	0.85±0.13
Number of palisade mesophyll layers	2 or rarely 3	2
Transverse section of Leaflet Margin		
Outline of leaflet margin	downward	downward
Thickness of leaflet margin (µm)	143.98±5.86	138.04±4.19
Height of epidermal cells on adaxial leaflet margin (µm)	10.84±1.33	14.10±2.61
Height of epidermal cells on abaxial leaflet margin (µm)	7.73±1.19	10.34±0.21
Thickness of palisade mesophyll (µm)	74.57±6.01	49.54±7.35
Thickness of spongy mesophyll (µm)	31.88±2.27	54.42±11.82
Thickness ratio of palisade mesophyll to spongy mesophyll	2.35±0.34	0.95±0.31
Number of palisade mesophyll layers	2	2
Angle of leaflet margin curvation	9.16±1.68	16.01±3.04

Note: As = anomocytic stomata; BT = bicellular non-glandular trichome; GT = glandular trichome; LT = long trichome; MT = medium trichome; Ps = paracytic stomata; ST = short trichome; UT = unicellular non-glandular trichome.

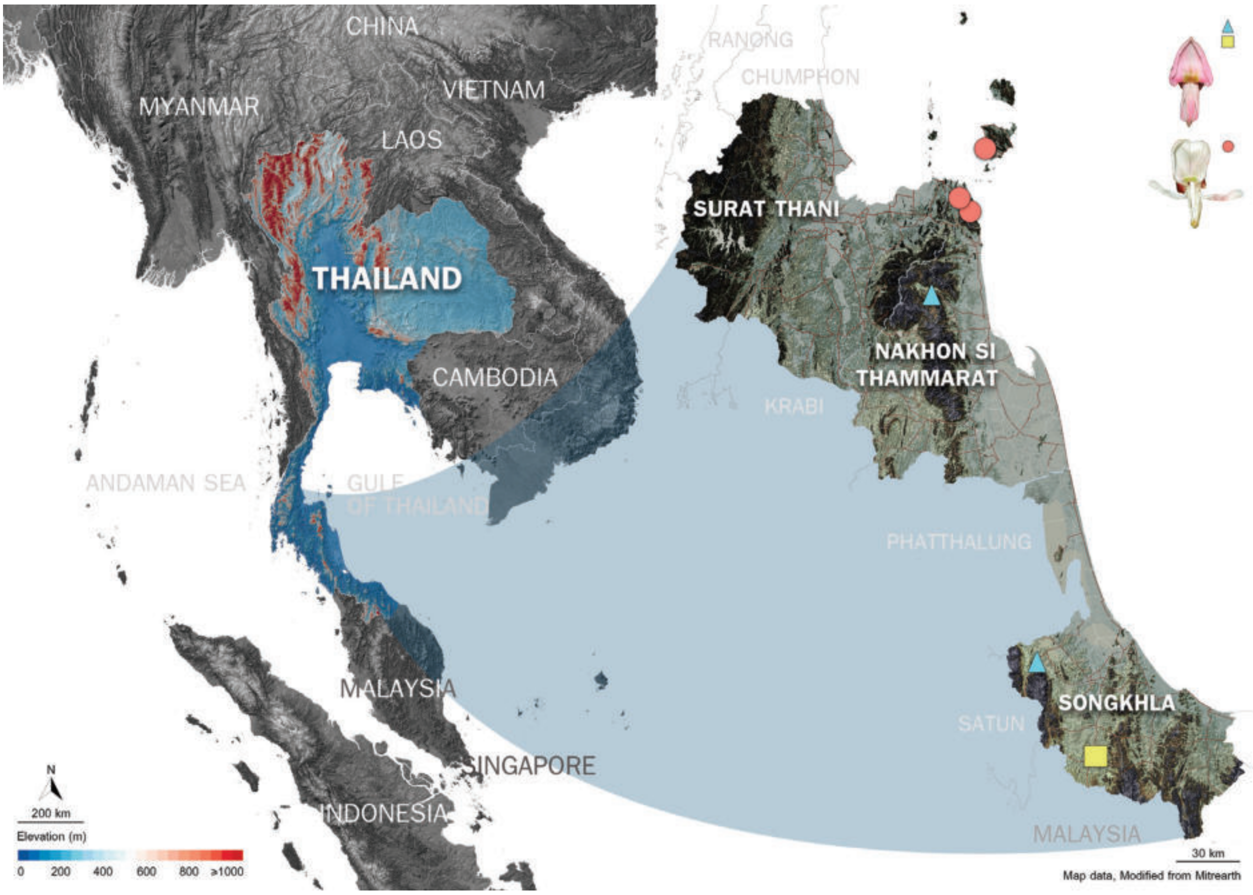

Figure 4. Collection sites of the new *Derris* samples, represented by a yellow square (flowering specimen) and light-blue triangle (specimen without flowers) and *D. pubipetala* (orange circles) in Peninsular Thailand.

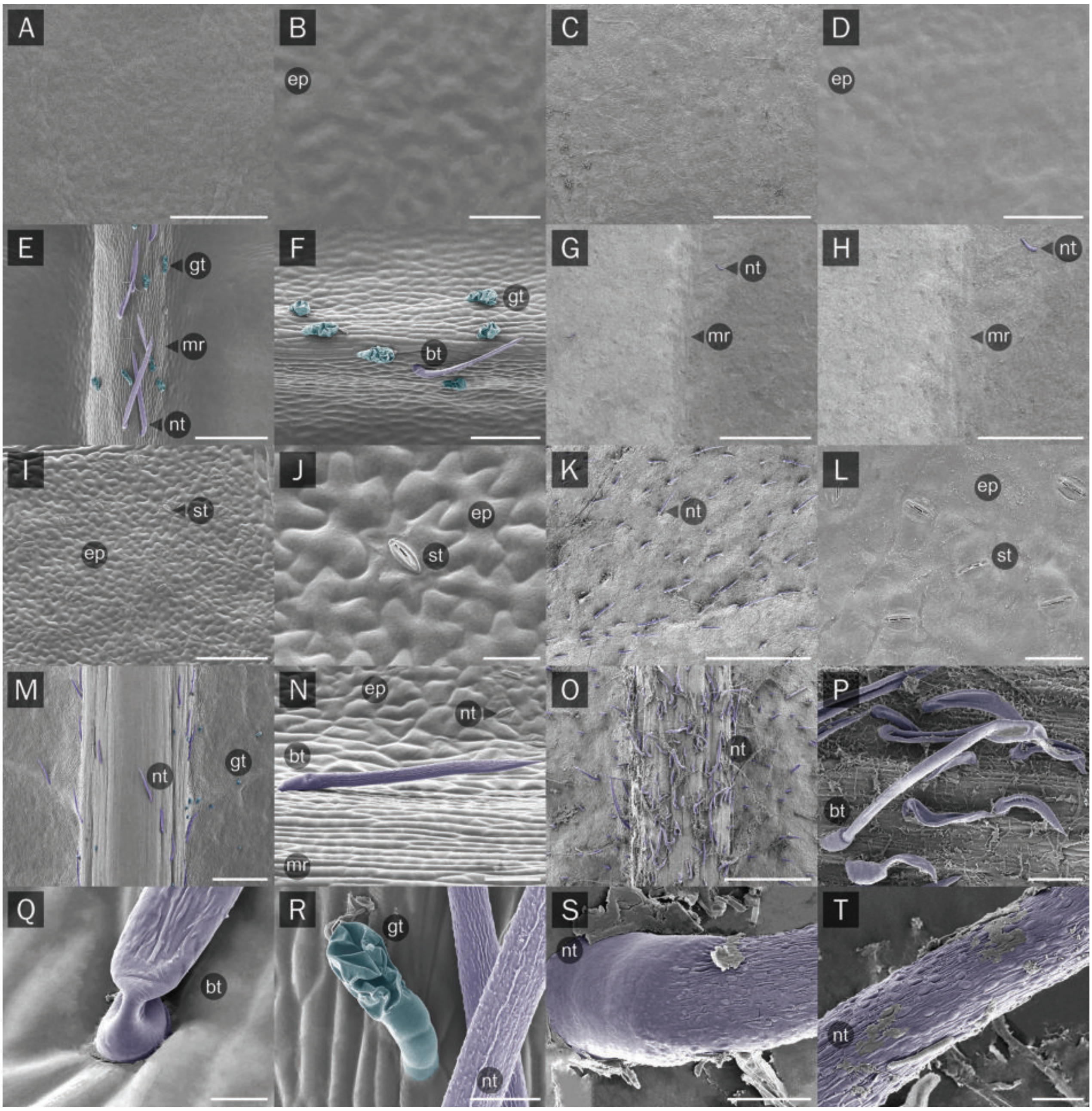

Figure 5. Scanning electron microscope (SEM) photographs showing leaflet micromorphology **A–D**) adaxial and **I–L** abaxial surfaces of leaflet lamina **E–H** adaxial and (**M–P**) abaxial surfaces of midrib **Q–T** non-glandular and glandular trichomes **A, B, E, F, I, J, M, N, Q, R** the new *Derris* samples and **C, D, G, H, K, L, O, P, S, T** *D. pubipetala*; bt = bicellular non-glandular trichome; ep = epidermal cell; gt = glandular trichome; mr = midrib; nt = non-glandular trichome; st = stoma. Scale bars: 5 µm (**T**); 10 µm (**Q, S**); 20 µm (**J, L, R**); 50 µm (**B, D, N, P**); 100 µm (**F, I**); 200 µm (**E**); 500 µm (**A, C, H, K, M, O**); 1000 µm (**G**).

Chemical fingerprinting

HPLC chromatograms (Fig. 8) revealed intra- and inter-specific differences in chemical compounds of the root and stem crude extracts. Under optimal HPLC conditions, the peaks of two chemical markers showed acceptable resolution (Fig. 8A). The standard peaks of rotenone and deguelin were detected at 6.1 (peak **I**) and 6.7 (peak **II**) min, respectively. Most of the HPLC chromatograms (8 of the 12) of the new *Derris* (Fig. 8B) and *D. pubipetala* (Fig. 8C) displayed two common chemical markers, i.e., Rotenone (**I**) and Deguelin (**II**). Exceptions were noted in

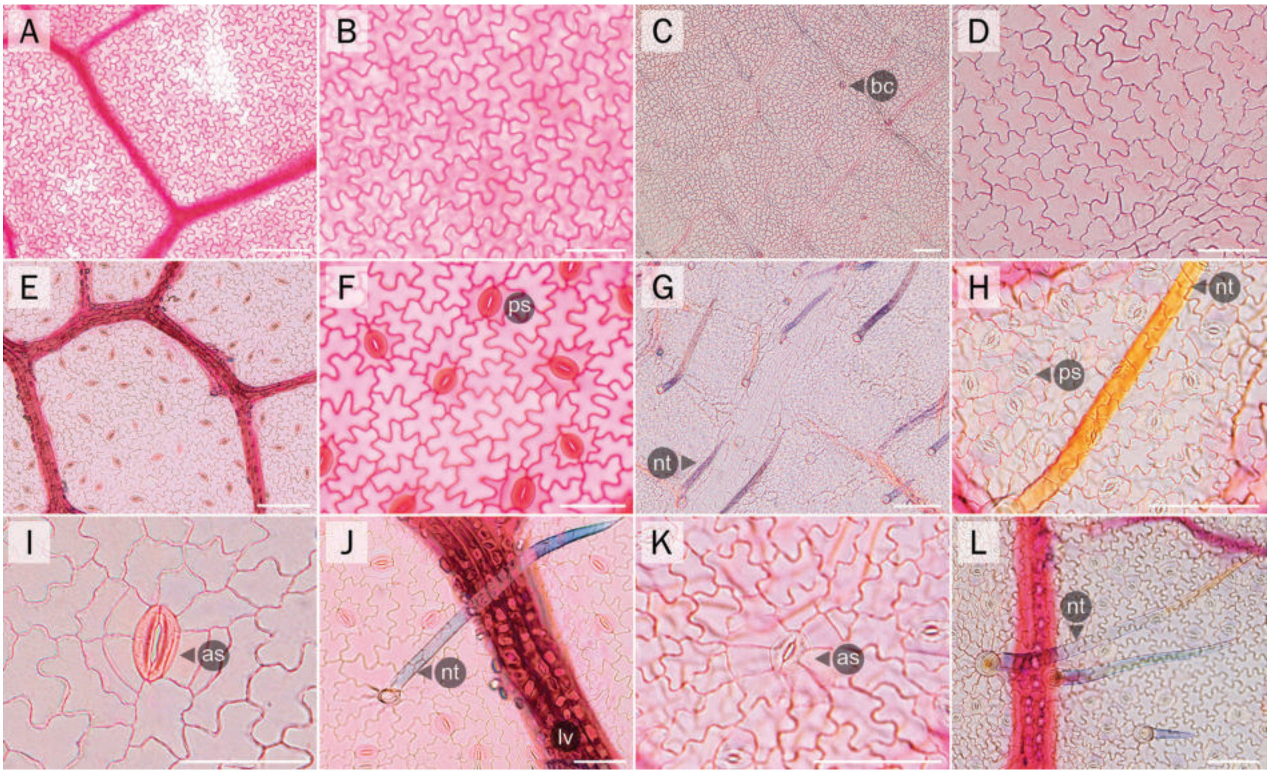

Figure 6. Comparative anatomical characters of the leaflet epidermis **A–D** adaxial leaflet epidermis **E–H** abaxial leaflet epidermis **A, B, E, F, I, J** the new *Derris* samples and **C, D, G, H, K, L** *D. pubipetala*. as = anomocytic stomata; bc = basal cell of trichome; nt = non-glandular trichome; ps = paracytic stomata. Scale bars: 50 µm (**B, D, F, H–L**); 100 µm (**A, C, E, G**).

the *Derris* new species' accession no. 2 (both root and stem extract), in the stem extract of the new *Derris* accession no. 1, and in the stem extract of *D. pubipetala* accession no. 5. Peaks of unknown chemical compounds (III–XI) were detected only in *D. pubipetala*, and were absent in all samples of the new *Derris*.

Molecular phylogeny

A phylogeny based on combined nuclear and chloroplast sequences using three analyses (MP, ML, and BI) demonstrated different degrees of resolution and support, but with compatible tree topologies. According to the cladogram of the Bayesian analysis (Fig. 9), the clade of the genus *Derris* has very high support (PP 1.00, MLBS 99%, MPBS 98%) and is sister to the clade consisting of members of the genus *Brachypterum* including *Millettia pinnata* (L.) Panigrahi and *Fordia splendidissima* (Blume ex Miq.) Buijsen. The *Derris* clade is divided into several subclades with varying clade support.

Samples of the putative new *Derris* species from three separate populations, however, did not form a clade in the Maximum Likelihood and Bayesian analyses because the sample from Nakhon Si Thammarat province (NN in Fig. 9) was separate from the other two samples from Songkhla province (SS and RS). Those two samples formed a strongly supported clade in all three analyses (PP 1.00, MLBS 100%, MPBS 100%). The clade emerged as sister to the clade consisting of *D. elegans* Benth., *D. ferruginea* Benth., *D. glabra* Sirich., *D. laxiflora* Benth., *D. laotica* Gagnep., *D. laxiflora* Benth., *D. longiracemosa* (sp. nov., in press), *D. reticulata* Craib, *D. rubrocalyx* Verdc., *D. trifoliata* and the new taxon

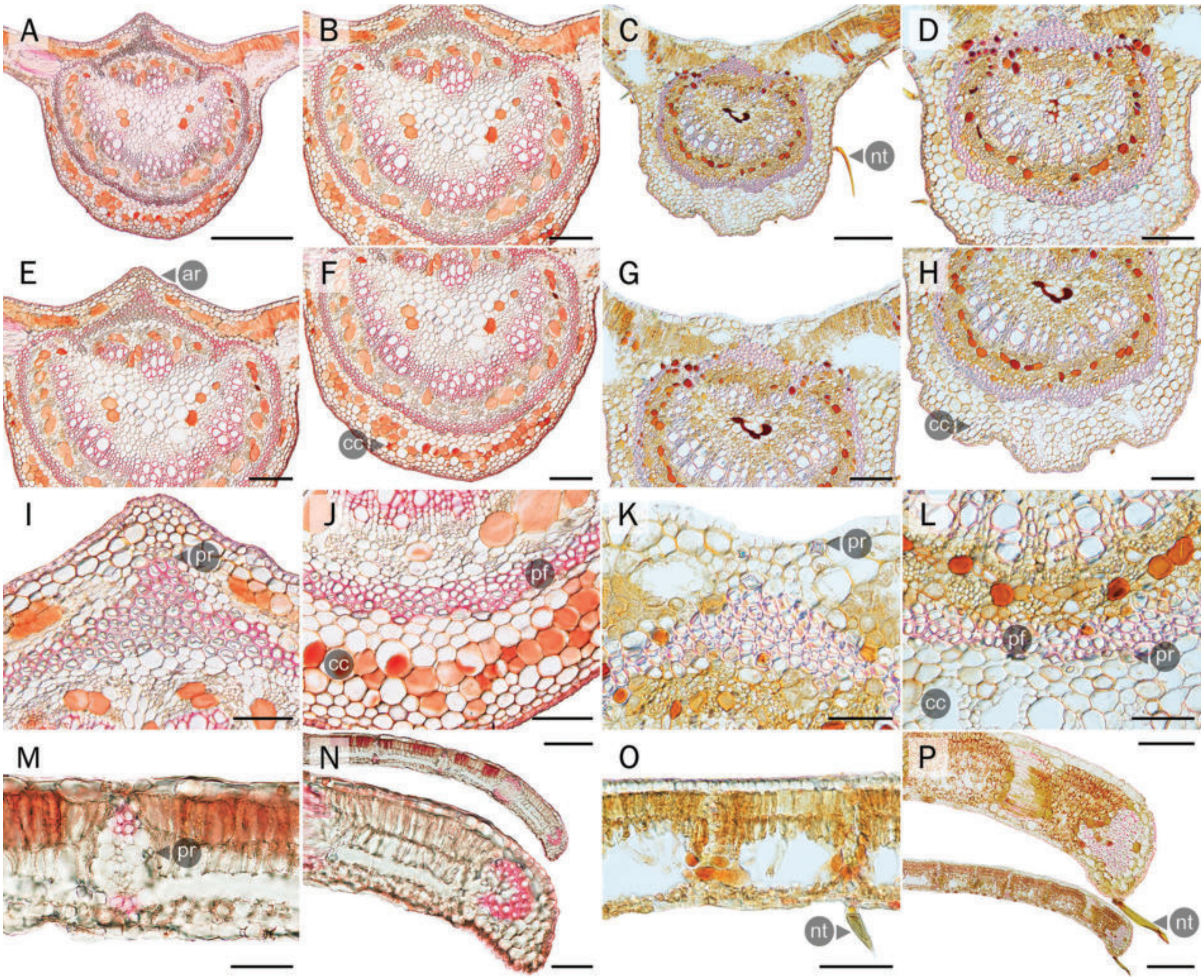

Figure 7. Comparative anatomical characters of leaflet transverse sections **A–L** midrib **M, O** leaflet blade and **N, P** leaflet margin **A, B, E, F, I, J, M, N** the new *Derris* and **C, D, G, H, K, L, O, P** *D. pubipetala*. ar = adaxial ridge; cc = cortical cells; nt = non-glandular trichome; pf = perivascular fibers; pr = prism. Scale bars: 50 μm (**M, N** (below), **O, P** (above)); 100 μm (**I–L**); 200 μm (**B, D, E–H, N** (above), **P** (below)); 500 μm (**A, C**).

sample from Nakhon Si Thammarat province, with high PP (0.97) but low MLBS (51%) and MPBS (< 50%) clade support. A slightly different topology emerged in the Maximum Parsimony (MP) analysis, where the three new species samples formed a moderately supported clade (MPBS 72%, see Suppl. material 2).

Discussion

Based on morphological, anatomical, phytochemical, and phylogenetic investigations of the new *Derris* samples, it is evident that they represent a novel and distinct species.

Macro- and micro-morphologically, the new *Derris* is similar to *D. pubipetala*. The two species also share the same distribution area and thrive in very similar habitats. (Fig. 4; Southern Thailand) (Sirichamorn et al. 2014a; Sirichamorn 2020). The reddish colour of the leaflet midrib is the most distinctive vegetative character of the new species.

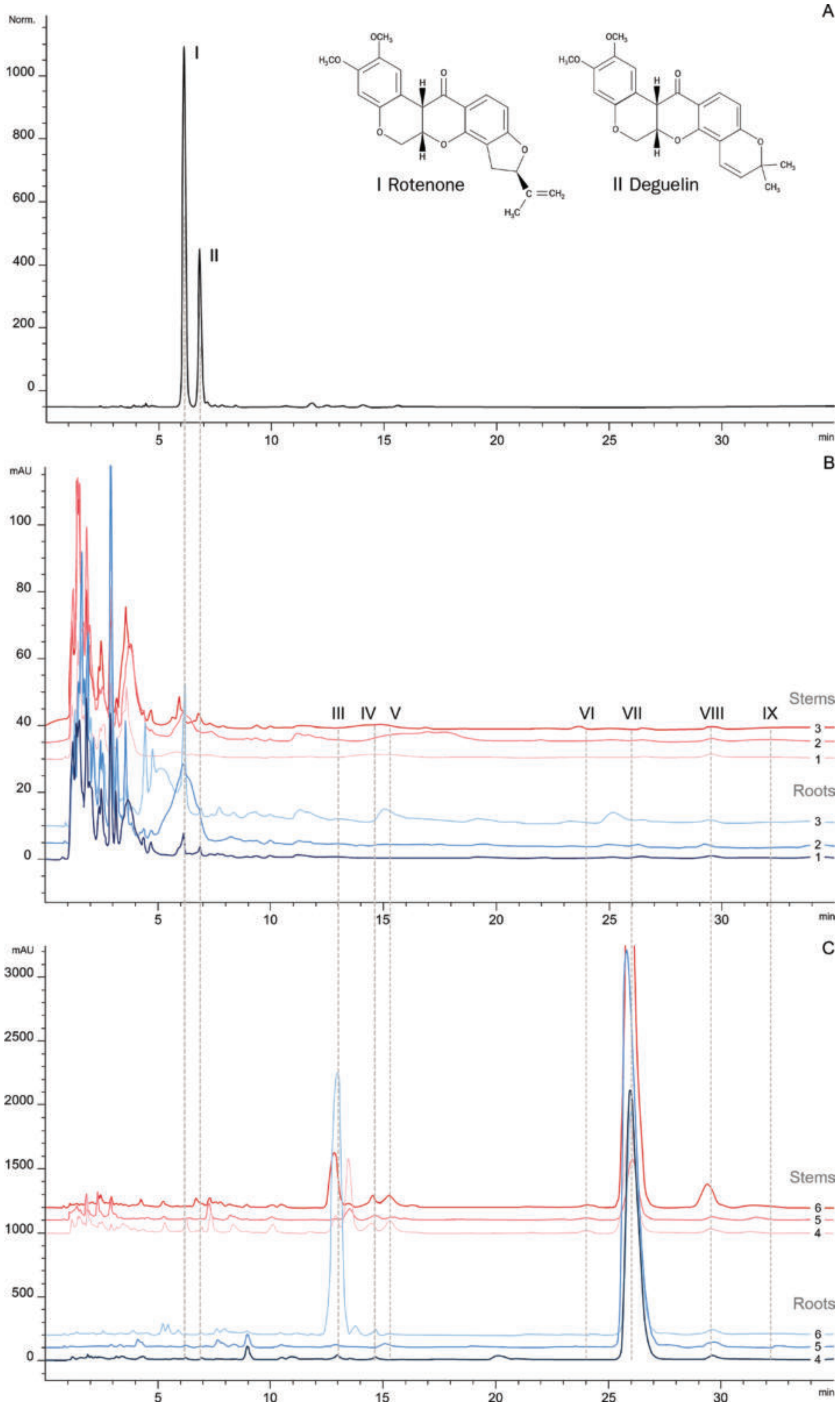

Figure 8. High-performance liquid chromatography (HPLC) chromatograms of the new *Derris* samples and *D. pubipetala* roots (the lower, blueish lines) and stems (the upper, reddish lines) extracts **A** two standard compounds **B** The new *Derris* species samples **C** *D. pubipetala*; Each Arabic numeral represents the accession number of each sample presented in Table 1. Each Roman numeral represents each peak of HPLC chromatograms (chemical compound) with its retention time, i.e., (**I**) RT, 6.1 min; (**II**) DG, 6.7 min; (**III**) UK1, 13.3 min; (**IV**) UK2, 14.4 min; (**V**) UK3, 15.3 min; (**VI**) UK4, 24.0 min; (**VII**) UK5, 26.1 min; (**VIII**) UK6, 29.5 min; (**IX**) UK7, 32.2 min; RT = rotenone; DG = deguelin; UK = unknown.

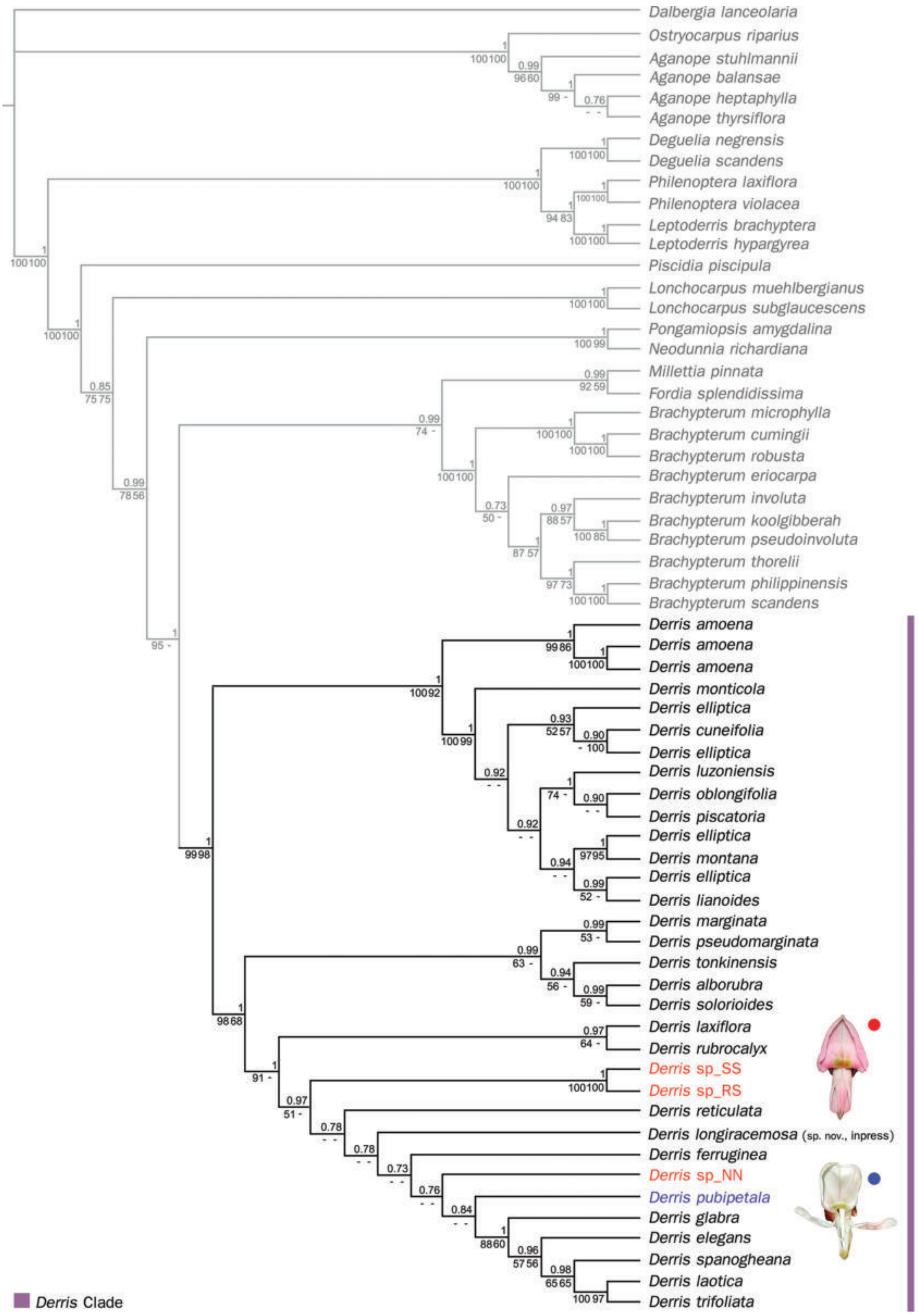

Figure 9. Consensus tree from Bayesian Inference analysis (BI) of concatenated two plastid and one nuclear dataset. The posterior probabilities (PP) are shown above the branches. Bootstrap percentage support values of Maximum likelihood (MLBS) and Maximum parsimony (MPBS) are shown below the branches, respectively (- = MPBS and/or MLBS < 50%). Abbreviations and numbers after the scientific names indicate locality codes following Table 1: NN = Nopphitam district, Nakhon Si Thammarat province; RS = Rattaphum district, Songkhla province; SS = Sadao district, Songkhla province, Thailand. Red and blue lettering highlight the position of the three samples of the new *Derris* and *D. pubipetala*, respectively.

Microscopic studies of leaflets revealed additional unique characters of the new species. Small glandular trichomes are distributed mainly on the midrib on both surfaces of the leaflets; together with uni- and bicellular non-glandular hairs (Fig. 5E, F, M, N, Q, R). Glandular trichomes usually function as herbivore deterrents and protect against oxidative stress due to their ability to produce, store, or secrete chemical substances, as reported for many plants (Peiffer et al. 2009; LoPresti 2016; Murungi et al. 2016; Stojičić et al. 2016; Zhao and Chen 2016; Tozin and Rodrigues 2017; Jachuła et al. 2018; Li et al. 2018), but their presence in species of *Derris* is quite rare. A few species, e.g., *D. elegans*, *D. elliptica* (Wall.) Benth., *D. ferruginea*, and *D. pubipetala*, have been reported as having hairy leaves, but only non-glandular trichomes.

Several characteristics of the reproductive parts of the new species differ from *D. pubipetala*. For example, prominent hairs on stamen filaments, below the anthers, have never been reported for any other *Derris* species, including *D. pubipetala*. Hairs at the base of the anthers do occur, however, in some members of the genus *Millettia* Wight & Arn., e.g., *M. extensa* (Benth.) Benth. ex Baker and *M. pinnata* (Mattapha 2020; Sirichamorn 2020). The function of these stamen hairs needs further investigation.

Pod traits, such as the number of wings on the margin of the pods or the density of the hairs covering the pod surface, are among the most important characters for identifying members of *Derris*. Most species of *Derris* have two-winged pods. For example, pods of *D. pubipetala* are two-winged and densely covered with golden-brown hairs (Sirichamorn 2020). Based on the phylogenetic position of the new species, we may assume that its pods are also two-winged, although the collection of mature fruits is needed to confirm this.

Epidermal cell size of the new *Derris* is larger than in *D. pubipetala*, notably on the lower leaflet surface. Additionally, larger stomata were also observed. The Stomatal Index (SI) of *D. pubipetala* is lower because the size of epidermal cells and stomata are both smaller than in the new *Derris*.

Leaflet thickness of the new *Derris* samples is positively correlated with the height of the epidermal cells and palisade mesophyll, which were generally greater than in *D. pubipetala*. In contrast, the height of the spongy mesophyll in *D. pubipetala* is greater. Palisade mesophyll on the adaxial surface of the leaflets is the primary site of photosynthesis and cells of this layer are directly exposed to light. The plants growing in more sunlight may develop a thicker palisade layer, not only to increase photosynthesis but also to prevent the deeper leaflet tissue from sunlight damage (Terashima et al. 2011; Gotoh et al. 2018).

Our study presents the first report of HPLC fingerprinting of the new *Derris* species and *D. pubipetala*. Results showed peaks of unique chemical markers that can be used for the rapid identification of *Derris rubricosta* and *D. pubipetala*. Intra-specific variation of chemical constituents was noted among populations, a phenomenon commonly found in other plant studies (Chen et al. 2015; Saraf and Shinede 2016, 2018). Production and accumulation of phytochemicals are not only dependent on plant species, but also on environmental factors (Qaderi et al. 2023).

Cladograms from all phylogenetic analyses, based on 62 accessions, exhibit similar topologies to the previous study by Sirichamorm et al. (2012a) (Fig. 9). *Derris* is strongly supported as monophyletic. The phylogenetic positions of three newly collected accessions demonstrated that they are members of the genus

Derris. However (and surprisingly), the samples apparently are not representative of a single taxon, at least based on molecular analysis. The three accessions, of what we are recognizing as *D. rubricosta*, from three localities separated into two groups, i.e., one from Songkhla province (consisting of *Derris* sp_SS and *Derris* sp_RS) and the other from Nakhon Si Thammarat province (*Derris* sp_NN). Nevertheless, vegetative morphology (and leaflet anatomy) of these three accessions was almost identical. It is possible that two taxa should be recognized but this will only be resolved when more reproductive parts are collected.

Here we preliminarily accept the two accessions from Songkhla province (one with flowers, *Derris* sp_SS, and the other without reproductive parts, *Derris* sp_RS) as a species new to science. The accession from Nakhon Si Thammarat province (*Derris* sp_NN) is considered as a taxon of unknown status to be further reviewed pending development of flowers.

Taxonomic treatment

Derris rubricosta **Boonprajan & Sirich., sp. nov.**
urn:lsid:ipni.org:names:77334641-1
Figs 1–3

Type. Thailand. Songkhla, Sadao district, Padang Besar sub-district, Pha Dam Forest Ranger Unit, Ton Nga Chang Wildlife Sanctuary, c. 150 m elevation, GPS coordinate 6°47'16.7"N, 100°13'51.8"E, 22 January 2019, *C. Leeratiwong 19-1666* (holotype BKF!; isotypes K!).

Diagnosis. The species has several autapomorphies distinguishing it from other *Derris* species. It is the only species that has reddish midribs on the lower surface of mature leaflets. Its style is sericeous at the base and gradually becomes glabrous apically (vs. thinly hairy at the base and mostly glabrous throughout in other *Derris* species). *Derris rubricosta* has prominent hairs below the anthers (vs. glabrous anthers in all other *Derris* species). It is morphologically similar to *D. pubipetala* Miq., but differs by its leaflet midrib colour (reddish vs. green), number of leaflets er leaf (9–11 vs. 5–9), colour of its corolla (pale pink to pink vs. white), wing petal margin (straight vs. revolute), stamen filament indumentum (sparsely hairy vs. glabrous), indumentum presence below the anthers (present vs. absent), floral disc shape (indistinct to more-or-less 10-lobed vs. annular).

Description. Woody climber. ***Bark*** pale brownish-gray to gray, lenticellate. ***Leaves*** with 9–11 leaflets, reddish when young, chartaceous to sub-coriaceous. ***Stipules*** caducous (not present on herbarium specimens); petiole 6–10.8 cm long, grooved above, thinly strigose to almost glabrous; rachis 10–18 cm long, grooved above, thinly strigose to glabrous; pulvinus 9–15 mm long, thinly strigose; stipellae absent; terminal leaflet elliptic to obovate or narrowly oblong, 10–18.3 × 3.0–4.3 cm, length/width ratio 3.2–4.3, base cuneate, apex acuminate, acumen 7.2–18 mm long, emarginate, upper surface glabrous but slightly strigose along midrib and lateral veins, lower surface glabrous to sparsely strigose along midrib, lateral veins and lamina, sometimes slightly strigose to glabrous at the margin, midrib (reddish on fresh mature leaflets) and secondary veins slightly raised or flat above, raised below, 7–9 each side of the midvein, 0.7–2.7 cm a part, curving towards the apex and almost reaching the margins, sometimes anastomosing near the margins, tertiary venation reticulate, pulvinus 5.0–6.5 mm long, sparsely strigose; lateral leaflets mostly like the terminal one, narrowly elliptic to obovate, rarely ovate, 10–18.8 × 3–4.4 cm, length/width ratio 3–4.3; pulvinus of petiolules 4.5–6.5 mm long, sparsely strigose to sericeous. ***Inflorescence*** a pseudoracemes or pseudopanicle, axillary or terminal, 40–50 cm long; peduncle 2–7 cm long, lenticellate, strigose; bracts subtending inflorescence triangular, 2–2.6 × 1.8–2.5 mm, outside with some hairs at base and along margin apically, inside glabrous; bracts subtending lateral branches triangular, ovate, 2–2.5 × 1.8–2.4 mm, outside with some hairs at base and along margin apically, inside glabrous; lateral branches 3.4.–15 cm long, sparsely strigose at base, lenticellate; bracts subtending brachyblasts ovate-triangular, 1–2.5 × 0.8–1.4 mm, outside with some hairs at base and along margin apically, inside glabrous. ***Brachyblasts*** knob-like to elongate-cylindrical, 1–12 mm long, 2-flowered, strigose; bracts subtending flowers ovate-triangular, 0.7–0.9 × 0.7–1 mm, outside sparsely hairy at base and along margin, inside glabrous; pedicels 3.5–5.2 mm long, strigose; bracteoles 2, at base of calyx, ovate, semi-circular, orbicular to narrowly triangular, 0.6–0.9 × 0.5–0.7 mm, outside sparsely strigose, with some hairs along the margin, inside glabrous. ***Calyx*** red- to maroonish, cup-shaped 3.4–4.2 mm long, outside sparsely strigose, with some hairs along the margin, inside glabrous; tube 3–3.2 mm long; upper lip with 2 short lobes, 0.2–0.4 × 1.5–2 mm; lateral lobes short-triangular, 0.2–0.6 × 0.7–1 mm; lower lobes triangular 0.3–1.3 × 0.8–1.2 mm. ***Corolla*** pale pink to pink; standard orbicular or broadly ovate, with a greenish-yellow spot at the base on the inner surface, 8.5–10 × 8.6–9.3 mm, apex emarginate, basal callosities absent, outside hairy from the middle part to apex, inside with some hairs near apex, claw 1.5–2.8 mm long; wings elliptic to narrowly ovate, 7.3–8.2 × 3.1–4 mm, apex obtuse, upper auricle indistinct, pubescent, 0.5–0.9 mm long, lower auricle absent, lateral pocket 1.4–2.2 mm long, outside hairy in the middle part of the petal to the apex, inside hairy near the apex, claw 1.8–3.5 mm long; keels boat-shaped 7–7.8 × 2.3–3 mm, apex retuse, upper auricle pubescent, 0.5–1 mm long, lower auricle absent, lateral pocket 1–2.1 mm long, outside and inside hairy near the apex, sometimes also with sparse hairs along the veins ventrally, claw 1–2.9 mm long. ***Stamens*** 10, monadelphous, 2.8–4.6 mm long, free part 1.5–3.1 mm long, sparsely hairy, anthers 0.5–0.6 × 0.2–0.3 mm, with some basal hairs. ***Disc*** indistinct, or more or less 10-lobed, glabrous. ***Ovary*** 3.5–5 mm long, sericeous; stipe usually indistinct, sericeous; style 5.6–7.4 mm long, sericeous at the base and gradually become glabrous apically. ***Pod*** and seeds unknown.

Phenology. Flowering from November-February and fruiting possibly from March-April.

Vernacular names. “Khruea lai leeratiwong” (เครือไหลลีรติวงศ์) means “Leeratiwong’s *Derris*”, in Thai, in honor of Associate Professor Dr. Charan Leeratiwong, who discovered and collected the type specimens.

Etymology. The specific epithet refers to the striking reddish colour of the midrib of the mature leaflets which has never been found in other species of *Derris*.

Distribution. Peninsular Thailand: Songkhla (Rattaphum district, Sadao district) (Fig. 4). Estimated population of more than 2,500 mature individuals were found during field survey between 2019 and 2022 in its type locality and nearby areas.

Habitat and ecology. Usually near streams, in semi-shaded to fully exposed areas of tropical evergreen rainforest. The species, especially in the type locality, thrives on sandy or sandy-loam soils.

Proposed IUCN conservation assessment. This new species is only known from two locations in Songkhla province. The estimated number of mature individuals might be more than 2,500 but less than 10,000. The Area of Occupancy (AOO) is about 2,000 km^2. Although its type locality and overall distribution are located within conservation areas, the species is still threatened by human disturbance. Therefore, we provisionally assess its conservation status to be "Vulnerable (VU), B2 b(ii) c(ii)", following the criteria of the IUCN Standards and Petitions Committee (2022, v. 15.1)

Representative specimens examined (paratypes). THAILAND. Songkhla: Rattaphum district, Kamphaeng Phet sub-district, 27 October 2021, *Sirichamorn Y. and Boonprajan P. YSM2021-15* (BKF!); Sadao district, Padang Besar sub-district, Pha Dam Forest Ranger Unit, 27 October 2021, *Sirichamorn Y. and Boonprajan P. YSM2021-14* (BKF!).

Addition of *Derris rubricosta* to the key to Thai species of *Derris*

The new taxon is inserted as couplet 7 in a modified key to species of *Derris* in the Flora of Thailand (Sirichamorn 2020; 391–392).

6 Brachyblasts variable in shape and length, usually with more than 3 flowers. Standard less than 10 mm long, rarely with basal callosities
  7 Mature leaflets with reddish midribs. Stamen filament sparsely hairy. Anther base with a tuft of hairs .... **18. *D. rubricosta***
  7' Mature leaflets without reddish midribs. Stamen filament glabrous. Anther base glabrous
    8 Pods single winged or wingless
      9 Leaflets hirsute to velvety underneath; stipels present .... **4. *D. elegans***
      9' Leaflets glabrous underneath; stipels usually absent
        10 Leaflets 3.3–7.5 × 0.9–3.5 cm; petiolules 3–5 mm long ...... **8. *D. laotica***
        10' Leaflets 3.5–16 × 1.5–8.5 cm; petiolules 5–10 mm long.. **17. *D. trifoliata***
    8' Pods two-winged
      11 Pods velvety or sericeous
        12 Leaflets slightly strigose to velvety below, apex rounded, obtuse, or cuspidate to short-acuminate. Pods with upper wing 4–10 mm wide, lower wing 4–7 mm wide. North-eastern Thailand .... **6. *D. ferruginea***
        12' Leaflets usually strigose to almost glabrous below, apex distinctly acuminate. Pods with upper wing 5–9 mm wide, lower wing 2–4 mm wide. Southern Thailand... **13. *D. pubipetala***
      11' Pods mostly glabrous
        13 Leaflets 9–11 per leaf, narrowly obovate, base narrowly cuneate to attenuate .... **11. *D. monticola***
        13' Leaflets 3–7(–9) per leaf, elliptic, ovate, or obovate, base cuneate to obtuse
          14 Leaflets sometimes glaucous below. Lateral veins reaching leaflet margin .... **2. *D. amoena***
          14' Leaflets never glaucous below. Lateral veins not reaching leaflet margin but curving toward leaf apex, sometimes forming an intramarginal vein

15 Leaflets 3–5 per leaf. Terminal leaflet distinctly longer and wider than lateral ones. Calyx glabrous outside .... **7. *D. glabra***

15’ Leaflets 5–7 per leaf. Terminal leaflet slightly longer but not wider than lateral the others. Calyx thinly sericeous outside .... **12. *D. pseudomarginata***

6’ Brachyblasts slender with 2 or 3 flowers at apex. Standard usually more than 10 mm long, usually with basal callosities

Acknowledgments

We would like to thank all staff of the Khao Luang National Park and Ton Nga Chang Wildlife Sanctuary, Department of National Parks, Wildlife and Plant Conservation, for their help during fieldwork. The authors wish to express gratitude to Dr. Tanawat Chaowasku for his advice on the phylogenetic analysis. All staff at BK, BKF, and PSU herbaria and Scientific and Technological Equipment Center, Faculty of Science, Silpakorn University are thanked for their invaluable assistance and support. We also thank the anonymous reviewer for their helpful comments which greatly improved our article.

Additional information

Conflict of interest

The authors have declared that no competing interests exist.

Ethical statement

No ethical statement was reported.

Funding

This research was financially supported by the Faculty of Science, Silpakorn University, grant number SCSU-STA-2564-02 and SRIF-JRG-2564-06.

Author contributions

Conceptualization: Punvarit Boonprajan and Yotsawate Sirichamorn. Fieldwork and specimen collection: Punvarit Boonprajan, Charan Leeratiwong, and Yotsawate Sirichamorn. Methodology and Experimental Work: Punvarit Boonprajan. Original Draft Preparation: Punvarit Boonprajan and Yotsawate Sirichamorn. Response to Reviewers and Manuscript Revision: Punvarit Boonprajan and Yotsawate Sirichamorn. Funding Acquisition: Punvarit Boonprajan and Yotsawate Sirichamorn

Author ORCIDs

Punvarit Boonprajan https://orcid.org/0009-0006-7251-1928
Charan Leeratiwong https://orcid.org/0000-0002-0752-4275
Yotsawate Sirichamorn https://orcid.org/0000-0002-3026-3894

Data availability

All of the data that support the findings of this study are available in the main text or Supplementary Information.

References

Adema F (2000) Notes on Malesian Fabaceae XX. *Derris* in Thailand and Malesia. Thai Forest Bulletin (Botany) 28: 2–16.

Adema F (2003) Notes on Malesian Fabaceae (Leguminosae-Papilionoideae). 11. The genus *Derris.* Blumea 48(2): 393–419. https://doi.org/10.3767/000651903X675035

Akaike H (1974) A new look at the statistical model identification. IEEE Transactions on Automatic Control 19(6): 716–723. https://doi.org/10.1109/TAC.1974.1100705

Baker JG (1878) L. Leguminosae, 89. *Derris*. In: Hooker JD (Ed.) Flora of British India. Reeve and Co., Ltd., London, 2: 240–246.

Bentham G (1860) Synopsis of Dalbergieae, a tribe of Leguminosae. In: Proceedings of the Linnean Society, Botany, London, UK, 1–134. https://doi.org/10.1111/j.1095-8339.1860.tb02464.x

Chen D, Pedley L (2010). *Derris* Lour. In: Wu ZY, Raven PH, Hong DY (Eds) Flora of China: Beijing, Science Press, China, 10: 166–170.

Chen XJ, Meng ZY, Wang P, Chen S, Ren L (2015) Chemical chromatography fingerprints of insecticidal plant *Derris* root. Journal of Yangzhou University. Agricultural and Life Sciences 36(2): 79–82.

da Costa D, Silva CE, Pinheiro A, Frommenwiler D, Arruda M, Guilhon G, Alves C, Arruda A, Da Silva M (2016) Using LC and Hierarchical Cluster Analysis as Tools to Distinguish Timbó Collections into two *Deguelia* Species: A Contribution to Chemotaxonomy. Molecules (Basel, Switzerland) 21(5): 569. https://doi.org/10.3390/molecules21050569

Darriba D, Taboada GL, Doallo R, Posada D (2012) jModelTest 2: More models, new heuristics and parallel computing. Nature Methods 9(8): 772. https://doi.org/10.1038/nmeth.2109

Felsenstein J (1985) Confidence Limits on Phylogenies: An Approach Using the Bootstrap. Evolution; International Journal of Organic Evolution 39(4): 783–791. https://doi.org/10.2307/2408678

Geesink R (1985) Scala Millettiearum: A survey of the genera of the Tribe Millettieae (Legum.–Pap.), with Methodological Considerations. Brittonia 37(2): 178. https://doi.org/10.2307/2806098

Gotoh E, Suetsugu N, Higa T, Matsushita T, Tsukaya H, Wada M (2018) Palisade cell shape affects the light-induced chloroplast movements and leaf photosynthesis. Scientific Reports 8(1): 1472. https://doi.org/10.1038/s41598-018-19896-9

Hall TA (1999) Bioedit: A user-friendly biological sequence alignment editor and analysis program for Windows 9.5/98/NT. Nucleic Acids Symposium Series 41: 95–98.

Hamid A (1999) *Derris* Lour. In: de Padua LS, Bunyapraphatsara N, Lemmens RHMJ (Eds) PROSEA: Plant Resources of South–East Asia 12, Medical and Poisonous Plants. Backhuys. Leiden, Netherlands 1: 234–242.

Hu J-M, Lavin M, Wojciechowski MF, Sanderson MJ (2000) Phylogenetic systematics of the tribe Millettieae (Leguminosae) based on chloroplast *trnK/matK* sequences and its implications for evolutionary patterns in Papilionoideae. American Journal of Botany 87(3): 418–430. https://doi.org/10.2307/2656638

ICEM (2003) Thailand National Report on Protected Areas and Development. Review of Protected Areas and Development in the Lower Mekong River Region, Indooroopilly, Queensland, Australia, 131 pp.

IUCN Standards and Petitions Committee (2022) Guidelines for Using the IUCN Red List Categories and Criteria, Version 15.1. Prepared by the Standards and Petitions Committee.

Jachuła J, Konarska A, Denisow B (2018) Micromorphological and histochemical attributes of flowers and floral reward in *Linaria vulgaris* (Plantaginaceae). Protoplasma 255(6): 1763–1776. https://doi.org/10.1007/s00709-018-1269-2

Johansen DA (1940) Plant Microtechnique. McGraw-Hill, New York.

Li S, Tosens T, Harley PC, Jiang Y, Kanagendran A, Grosberg M, Jaamets K, Niinemets Ü (2018) Glandular trichomes as a barrier against atmospheric oxidative stress: Relationships with ozone uptake, leaf damage, and emission of LOX products across a diverse set of species. Plant, Cell & Environment 41(6): 1263–1277. https://doi.org/10.1111/pce.13128

LoPresti EF (2016) Chemicals on plant surfaces as a heretofore unrecognized, but ecologically informative, class for investigations into plant defence. Biological Reviews of the Cambridge Philosophical Society 91(4): 1102–1117. https://doi.org/10.1111/brv.12212

Loureiro J de (1790) Flora Cochinchinensis. 432. Lissabon, J. de Loureiro.

Mattapha S (2020) *Millettia* Wight & Arn. In: Chayamarit K, Balslev H (Eds) Flora of Thailand: Bangkok, Thailand 4(3.2): 421–450.

Mattapha S, Forest F, Schrire BD, Lewis GP, Hawkins J, Suddee S (2023) Three new species of *Millettia* (Leguminosae-Papilionoideae: Millettieae) from the Indo-Chinese region. Kew Bulletin 78(2): 175–187. https://doi.org/10.1007/s12225-023-10084-1

Miller MA, Pfeiffer W, Schwartz T (2010) Creating the CIPRES Science Gateway for inference of large phylogenetic trees. In: 2010 Gateway Computing Environments Workshop (GCE). New Orleans, LA, USA, 1–8. https://doi.org/10.1109/GCE.2010.5676129

Murungi LK, Kirwa H, Salifu D, Torto B (2016) Opposing Roles of Foliar and Glandular Trichome Volatile Components in Cultivated Nightshade Interaction with a Specialist Herbivore. PLOS ONE 11(8): e0160383. https://doi.org/10.1371/journal.pone.0160383

Nguyen LT, Schmidt HA, von Haeseler A, Minh BQ (2015) IQ-TREE: A Fast and Effective Stochastic Algorithm for Estimating Maximum-Likelihood Phylogenies. Molecular Biology and Evolution 32(1): 268–274. https://doi.org/10.1093/molbev/msu300

Peiffer M, Tooker JF, Luthe DS, Felton GW (2009) Plants on early alert: Glandular trichomes as sensors for insect herbivores. The New Phytologist 184(3): 644–656. https://doi.org/10.1111/j.1469-8137.2009.03002.x

POWO (2023) Plants of the World Online. Facilitated by the Royal Botanic Gardens, Kew. http://www.plantsoftheworldonline.org/

Qaderi MM, Martel AB, Strugnell CA (2023) Environmental Factors Regulate Plant Secondary Metabolites. Plants 12(3): 447. https://doi.org/10.3390/plants12030447

Ridley HN (1922) Flora of the Malay Peninsula 1. London, L. Reeve and Co., Ltd., 964 pp. https://doi.org/10.5962/bhl.title.10921

Ronquist F, Teslenko M, van der Mark P, Ayres DL, Darling A, Höhna S, Larget B, Liu L, Suchard MA, Huelsenbeck JP (2012) MrBayes 3.2: Efficient Bayesian Phylogenetic Inference and Model Choice Across a Large Model Space. Systematic Biology 61(3): 539–542. https://doi.org/10.1093/sysbio/sys029

Rueden CT, Schindelin J, Hiner MC, DeZonia BE, Walter AE, Arena ET, Eliceiri KW (2017) ImageJ2: ImageJ for the next generation of scientific image data. BMC Bioinformatics 18(1): 529. https://doi.org/10.1186/s12859-017-1934-z

Saraf A, Shinede P (2016) HPTLC fingerprint profile, isolation and validation of marker compound lupeol in *Derris heyneana* (Wight and Arn.) Benth. International Journal of Pharma and Bio Sciences 7(7): 14–21. https://doi.org/10.22376/ijpbs.2016.7.4.b714-721

Saraf A, Shinede P (2018) Phytochemical analysis and chemical fingerprinting of *Derris heyneana* (Wight and Arn.) Benth. Journal of Pharmacognosy and Phytochemistry 7(3): 740–747.

Sirichamorn Y (2020) *Derris* Lour. In: Chayamarit K, Balslev H (Eds) Flora of Thailand: Bangkok, Thailand 4(3.2): 390–417.

Sirichamorn Y, Adema F, Welzen PC (2012a) The Genera *Aganope*, *Derris*, and *Paraderris* (Fabaceae, Millettieae) in Thailand. Systematic Botany 37(2): 404–436. https://doi.org/10.1600/036364412X635467

Sirichamorn Y, Adema FA, Gravendeel B, van Welzen PC (2012b) Phylogeny of palaeotropic *Derris*-like taxa (Fabaceae) based on chloroplast and nuclear DNA sequences shows reorganization of (infra) generic classifications is needed. American Journal of Botany 99(11): 1793–1808. https://doi.org/10.3732/ajb.1200390

Sirichamorn Y, Adema F, Roos M, Welzen PC (2014a) Molecular and morphological phylogenetic reconstruction reveals a new generic delimitation of Asian *Derris* (Fabaceae): Reinstatement of *Solori* and synonymisation of *Paraderris* with *Derris*. Taxon 63(3): 522–538. https://doi.org/10.12705/633.13

Sirichamorn Y, Thomas D, Adema F, Welzen PC (2014b) Historical biogeography of *Aganope*, *Brachypterum* and *Derris* (Fabaceae, tribe Millettieae): Insights into the origins of Palaeotropical intercontinental disjunctions and general biogeographical patterns in Southeast Asia. Journal of Biogeography 41(5): 882–893. https://doi.org/10.1111/jbi.12262

Song S, Pan B (2022) Transfer of *Millettia pachycarpa* and *M. entadoides* to *Derris* (Fabaceae), supported by morphological and molecular data. Phytotaxa 531(3): 230–248. https://doi.org/10.11646/phytotaxa.531.3.4

Stojičić D, Tošić S, Slavkovska V, Zlatković B, Budimir S, Janošević D, Uzelac B (2016) Glandular trichomes and essential oil characteristics of in vitro propagated *Micromeria pulegium* (Rochel) Benth. (Lamiaceae). Planta 244(2): 393–404. https://doi.org/10.1007/s00425-016-2513-7

Swofford D (2002) PAUP*. Phylogenetic Analysis Using Parsimony (*and Other Methods). Version 4.0b10. Sinauer, Sunderland, Massachusetts, USA, 2003.

Taberlet P, Gielly L, Pautou G, Bouvet J (1991) Universal primers for amplification of three non-coding regions of chloroplast DNA. Plant Molecular Biology 17(5): 1105–1109. https://doi.org/10.1007/BF00037152

Tavaré S (1985) Some Probabilistic and Statistical Problems in the Analysis of DNA Sequences. Lectures on Mathematics in the Life Sciences 17: 57–86.

Terashima I, Hanba YT, Tholen D, Niinemets Ü (2011) Leaf Functional Anatomy in Relation to Photosynthesis. Plant Physiology 155(1): 108–116. https://doi.org/10.1104/pp.110.165472

Thompson JD, Higgins DG, Gibson TJ (1994) CLUSTAL W: Improving the sensitivity of progressive multiple sequence alignment through sequence weighting, position-specific gap penalties and weight matrix choice. Nucleic Acids Research 22(22): 4673–4680. https://doi.org/10.1093/nar/22.22.4673

Thothathri K (1961) Studies in Leguminosae 1. A taxonomic revision of the genus *Derris* Lour. in India. Bulletin of the Botanical Survey of India 3: 175–200.

Thothathri K (1982) Leguminosae: Genus *Derris*. Fascicles of Flora of India. 8: 1–33.

Tozin LR, Rodrigues T (2017) Morphology and histochemistry of glandular trichomes in *Hyptis villosa* Pohl ex Benth. (Lamiaceae) and differential labeling of cytoskeletal elements. Acta Botanica Brasílica 31(3): 330–343. https://doi.org/10.1590/0102-33062016abb0292

White TJ, Bruns T, Lee S, Taylor J (1990) 38-Amplification and direct sequencing of fungal ribosomal RNA genes for phylogenetics. In: Innis MA, Gelfand DH, Sninsky JJ, White TJ (Eds) PCR Protocols. Academic Press, San Diego, 315–322. https://doi.org/10.1016/B978-0-12-372180-8.50042-1

Wikramanayake E, Dinerstein E, Loucks CJ, Olson MD, Morrison J, Lamoreaux J, Hamilton-Smith E (2002) Terrestrial Ecoregions of the Indo-Pacific: A Conservation Assessment. Electronic Green Journal 1(17): 1–643. https://doi.org/10.5070/G311710489

Wojciechowski MF, Sanderson MJ, Baldwin BG, Donoghue MJ (1993) Monophyly of aneuploid *Astragalus* (Fabaceae): Evidence from nuclear ribosomal DNA internal transcribed spacer sequences. American Journal of Botany 80(6): 711–722. https://doi.org/10.1002/j.1537-2197.1993.tb15241.x

Wojciechowski MF, Sanderson MJ, Hu JM (1999) Evidence on the monophyly of *Astragalus* (Fabaceae) and its major subgroups based on nuclear ribosomal DNA ITS and chloroplast DNA *trnL* intron data. Systematic Botany 24(3): 409–437. https://doi.org/10.2307/2419698

Yang Z, Rannala B (1997) Bayesian phylogenetic inference using DNA sequences: A Markov Chain Monte Carlo Method. Molecular Biology and Evolution 14(7): 717–724. https://doi.org/10.1093/oxfordjournals.molbev.a025811

Zhao Q, Chen XY (2016) Development: A new function of plant trichomes. Nature Plants 2(7): 16096. https://doi.org/10.1038/nplants.2016.96

Supplementary material 1

Species, voucher specimen, and GenBank accession for sequence data reported in the study

Authors: Punvarit Boonprajan, Charan Leeratiwong, Yotsawate Sirichamorn

Data type: pdf

Link: https://doi.org/10.3897/phytokeys.237.112860.suppl1

Supplementary material 2

Maximum Parsimony (MP) analysis

Authors: Punvarit Boonprajan, Charan Leeratiwong, Yotsawate Sirichamorn

Data type: jpg

Link: https://doi.org/10.3897/phytokeys.237.112860.suppl2

PhytoKeys 237: 79–89 (2024)
DOI: 10.3897/phytokeys.237.115037

Research Article

Aletris guangxiensis (Nartheciaceae), a new species from Guangxi, China

You Nong[1], Ke-Dao Lai[1], Yun-Rui Qin[2], Gui-Yuan Wei[1], Ke-Jian Yan[1], Chuan-Gui Xu[1], Zi-Yi Zhao[1], Ren-Chuan Hu[1], Yun-Feng Huang[1]

1 *Guangxi Key Laboratory of Traditional Chinese Medicine Quality Standards, Guangxi Institute of Chinese Medicine & Pharmaceutical Science, No. 20–1 Dongge Road, Nanning, Guangxi, China*
2 *Xishuangbanna Tropical Botanical Garden, Chinese Academy of Sciences, Menglun Town, Mengla County, Yunnan, China*
Corresponding author: Yun-Feng Huang (huangyunfeng2000@126.com)

Abstract

Aletris guangxiensis Y. Nong & Y. F. Huang (Nartheciaceae), a new species from Guangxi, China, is described and illustrated. This new species is most similar to *A. scopulorum*, but it can be easily distinguished by its sparsely glandular, 5–18 cm long scape, glandular inflorescence axis, distinctly pedicellate flowers, sparsely glandular, 5–10 mm long pedicel, bract borne at base of pedicel, glabrous perianth divided to the base, strongly recurved or revolute perianth lobes and turbinate, obovoid to oblong-obovoid capsule. An identification key for 24 species and 1 hybrid of *Aletris* is also provided.

Key words: Conservation, flora of China, limestone, Nartheciaceae, taxonomy

Academic editor: Michal Hroneš
Received: 1 November 2023
Accepted: 21 December 2023
Published: 19 January 2024

Citation: Nong Y, Lai K-D, Qin Y-R, Wei G-Y, Yan K-J, Xu C-G, Zhao Z-Y, Hu R-C, Huang Y-F (2024) *Aletris guangxiensis* (Nartheciaceae), a new species from Guangxi, China. PhytoKeys 237: 79–89. https://doi.org/10.3897/phytokeys.237.115037

Introduction

The family Nartheciaceae Fr. ex Bjurzon comprises five genera (Caddick et al. 2002). All species in this family are perennial herbs with short tuberculate or creeping rhizomes, erect stems and terminal spikes or racemes. Various researchers have continuously enhanced its classification (Li and Zhang 2011, Fuse et al. 2012; Tobe et al. 2018). In this family, *Aletris* L. is the largest genus, which contains approximately 21 species distributed in East Asia and North America (Zhao et al. 2012). However, a total of 23 species and 1 hybrid have been accepted according to the Plants of the World Online (POWO 2023).

The genus *Aletris* is characterised by perennial herbs with leaves in basal rosettes, lanceolate to linear blades, racemose to spicate inflorescences, scape simple, erect, usually with a few small, bractlike leaves, flowers bisexual, perianth white, yellow, or golden orange, cylindrical, campanulate or obovoid, with rough abaxial surfaces, six basally connate tepals, six stamens with basifixed anthers, obscurely 3-lobed stigma and fruits capsular, 3-locular, beaked.

During our field surveys in Guangxi in 2020, we found an unusual *Aletris* population that was morphologically similar to the species *A. scopulorum* Dunn. However, this special population is distinctly different from *A. scopulorum*, based on sparsely glandular, 5–18 cm long scape, glandular inflorescence axis, distinctly pedicellate flowers with sparsely glandular, 5–10 mm long pedicel, glabrous perianth divided to the base, strongly recurved or revolute perianth lobes and turbinate, obovoid to oblong-obovoid capsule (Table 1). Therefore, we proposed that this special population may represent a new species. In order to test this hypothesis, we conducted a literature search (Noltie 1994; Yang 1997; Liang and Turland 2000) and examined many specimens of *Aletris* from the Herbaria PE, IBK, GXMI and KUN. Finally, we continued to carry out multiple rounds of field surveys to confirm that this special population represents a new species.

Materials and methods

The new species were described based on field observations that were conducted in March to May and examination of herbarium specimens at GXMI. Other related *Aletris* species were examined based on online images from Kew Herbarium Catalogue (http://apps.kew.org/herbcat/gotoHomePage.do) and JSTOR Global Plants (http://plants.jstor.org/) and Chinese Virtual Herbarium (https://www.cvh.ac.cn/). Morphological characters that distinguish it from all other species in the genus of *Aletris* are used. We also observed living plants of the new species at flowering and fruiting time (March to May). We observed characters of stems, leaves, pedicels, flowers, receptacles, petals, stamens, gynoecium, carpels, size of flowers, size and shape of petals, number of stamens and the shape of gynoecium and fruit.

Descriptions were written from herbarium specimens. Measurements were made with a tape measure and calipers. The structure of the indumentum and its distribution were observed and described under a dissecting microscope at magnifications of more than 20×. Additional information on locality, habitat, ecology, plant form and fruits were collected in the field and taken from herbarium labels. Conservation threat assessment followed IUCN Categories and Criteria (IUCN 2022).

Results and discussion

Taxonomy

***Aletris guangxiensis* Y.Nong & Y.F.Huang, sp. nov.**
urn:lsid:ipni.org:names:77334668-1
Figs 1–4
Chinese name: guǎng xī fèi jīn cǎo (广西肺筋草)

Diagnosis. *Aletris guangxiensis* is most similar to *A. scopulorum*, but it differs by inflorescence axis sparsely glandular (vs. pubescent), pedicel 5–8 mm (vs. 0.5–3.5 mm), bract borne at base of pedicel (vs. bract borne on the proximal 1/2 of the pedicel), lobes strongly recurved or revolute, linear, 4–7 × 0.2–0.5 mm (vs. erect

Table 1. Main morphological differences amongst *Aletris guangxiensis*, *A. scopulorum*, *A. gracilis* and *A. cinerascens*.

Morphological traits	*A. guangxiensis*	*A. scopulorum*	*A. gracilis*	*A. cinerascens*
Plant	sparsely glandular	inflorescence axis pubescent	glabrous throughout	glabrous throughout
Leaves	in lax basal rosette, narrowly linear to lanceolate, 4–9 cm × 2–5 mm	in lax basal rosette, linear, 3–15 cm × 2–4.5 mm.	in lax basal rosette, linear, 2–20 cm × 2–7(–9) mm	densely tufted, linear–lanceolate, 4–13 cm × 3–12.5 mm
Scape	5–18 cm	10–35 cm	7–40 cm	8–30 cm
Pedicel	5–8 mm	0.5–3.5 mm	1–10 mm	1–10 mm
Bract and bracteole	bract borne at base of pedicel, bracteole borne on proximal 1/3 of pedicel	bract and bracteole borne on proximal 1/2 of pedicel	bract borne at or near base of pedicel, bracteole borne on proximal 1/2 of pedicel	bract borne at or near base of pedicel, bracteole borne on proximal 1/2 of pedicel
Perianth	White	White	yellowish, whitish or pinkish	yellowish
Perianth lobes	strongly recurved or revolute, linear, 4–7 × 0.2–0.5 mm	erect or slightly recurved, narrowly oblong–lanceolate to linear, 1.5–2.5 × 0.3–0.7 mm	strongly recurved or revolute, narrowly oblong or oblong, 2–3 × 1 mm	strongly recurved or revolute, narrowly lanceolate, 3–4.5 × 1–1.5 mm
Capsule	turbinate, obovoid or oblong–obovoid, distinctly angular, 2–4 × 2–3 mm	subglobose, 3–3.5 × 2.5–3 mm	narrowly ovoid, 4.5–7 × 2.5–3.5 mm	oblong–ovoid or ± ellipsoid, 5–7 × 3–3.5 mm

or slightly recurved, narrowly oblong–lanceolate to linear, 1.5–2.5 × 0.3–0.7 mm). At first glance, it also looks similar to *A. gracilis* Rendle and *A. cinerascens* Wang & Tang, but differs by its inflorescence axis sparsely glandular (vs. glabrous), pedicel 5–8 mm (vs. 1–10 mm), perianth white (vs. yellowish, whitish or pinkish/yellowish). More detailed morphological differences amongst the four species are provided in Table 1.

Holotype. China. Guangxi: Cenxi, 22°44'5"N, 110°51'59"E, alt. 320 m, on the cliff next to the stream, 23 April 2020 *Y Nong NY2020042301* (holotype GXMI! isotypes IBK!).

Description. Herbs. Roots usually fibrous. Leaves in basal rosette, narrowly linear to lanceolate, 4–9 cm × 2–5 mm. Scape 5–18 cm, sparsely glandular, bract–like leaves 3–10 mm long in the middle and lower part. Raceme 2.5–9 cm, laxly 2–10(or more)–flowered; axis glandular. Flowers distinctly pedicellate; pedicel 5–8 mm, sparsely glandular, subtended by a bract borne at base of pedicel and bracteole borne on proximal 1/3 of pedicel above bract; bract and bracteole lanceolate, 2–4 mm, shorter than flower, apex subacute. Perianth white, glabrous, divided to the base; lobes strongly recurved or revolute, linear, 4–7 × 0.2–0.5 mm, apex obtuse. Filaments of stamens adnate to perianth, 3–4 mm. Style 0.2–0.5 mm; stigma conspicuously thickened, capitate. Fruits capsular, 3–locular; capsule turbinate, obovoid or oblong–obovoid, distinctly angular, 2–4 × 2–3 mm.

Phenology. Flowering and fruiting in March to April.

Etymology. Guangxi is located in the southwest of China and is a biodiversity hotspot where many new species or new species records have been found (Hu et al. 2019; Luo et al. 2020; Feng et al. 2021; Xin et al. 2021; Huang et al. 2022; Nong et al. 2023). The new species, *A. guangxiensis*, is found in this region and is named after the geographic location.

Figure 1. Habitat of *Aletris guangxiensis* on the moist cliffs next to streams. [Photographed by You Nong and Ke–Jian Yan].

Distribution and habit. Known only from the southeast of Guangxi, China (Fig. 5). The new species mainly occurs at elevations of 320 m. It has been mainly found on moist cliffs next to streams.

IUCN Red List Category. Data available for the new species are still insufficient to assess its conservation status. According to the IUCN Criteria (IUCN 2022), it is considered Data Deficient (DD) until more information becomes available. Although the population of *A. guangxiensis* is currently in relatively good conditions, further collection and monitoring are necessary to allow more conclusive estimations about the rarity and vulnerability of the species. Therefore, special attention should be given to the conservation of the new species of *Aletris*.

Additional specimen. Cenxi. Southeast Guangxi: limestone hills, fl. 30 March 2023, *G.Y. Wei WGY2023033001* (GXMI!).

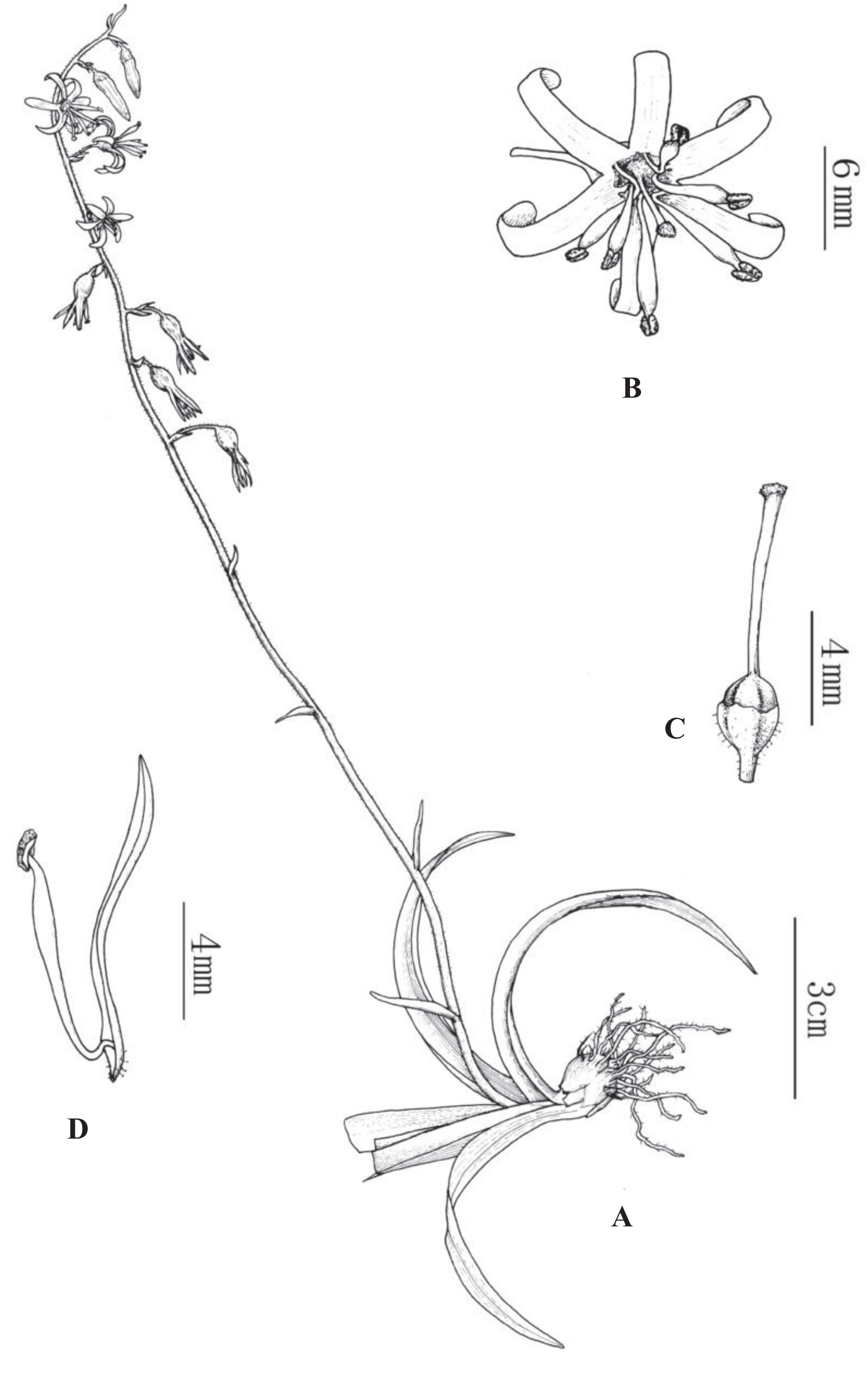

Figure 2. Line drawing of *Aletris guangxiensis* **A** flowering branch **B** flowers **C** Ovary and stigma **D** Filaments of stamens and perianth [Drawn by Xin–cheng Qu from *Y Nong NY2020042301* (GXMI)].

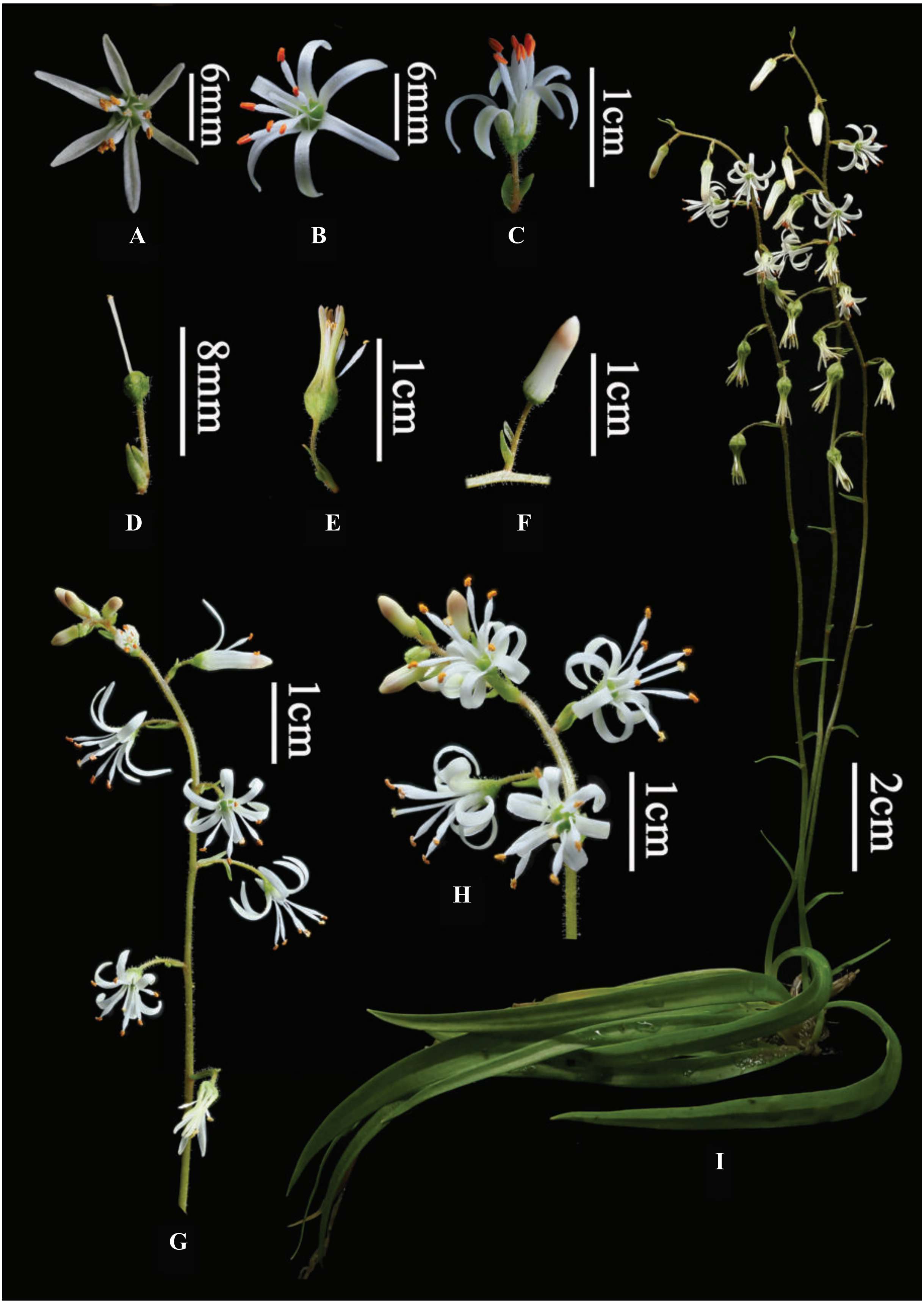

Figure 3. *Aletris guangxiensis* **A** flower (front view) **B, C** flower (lateral view) **D** ovary and stigma **E** young fruit **F** inflorescence node with flower-subtending bract and flower bud, pedicel with bracteole in its proximal part **G** inflorescence **H** flowers **I** plant [Photographed by Ke–Jian Yan from *G.Y. Wei WGY2023033001* (GXMI), edited by Yuan Fang].

Figure 4. Digital images of type specimens **A** *Aletris guangxiensis* [*Y Nong NY2020042301* (GXMI!)] **B** *A. scopulorum* [*Dunn 3556* (K!)] **C** *A. gracilis* [*Younghusband s.n.* (K!)] **D** *A. cinerascens* [*Guangxi Investigation Team 4248* (PE!)].

Figure 5. The distribution of *Aletris guangxiensis* (red circle) in Guangxi, China.

Key to species of *Aletris*

1 Flowers usually solitary, rarely densely 2–or 3–flowered forming a raceme.. **1. *A. simpliciflora***
– Flowers usually densely 4–14–flowered forming a raceme **2**
2 Perianth abaxial surfaces rough...**3**
– Perianth glabrous or pubescent **8**
3 Perianth usually wholly yellow to golden yellow, rarely white.....................**4**
– Perianth white to creamy–white, lobes sometimes tipped with orange or pinkish–orange...**6**
4 Perianth campanulate, 6–7 mm, 2 times or less as long as broad............. ....**2. *A. aurea***
– Perianth cylindrical, 9–12 mm, more than 2.5 times as long as broad **5**
5 Lobes spreading ....**3. *A. lutea***
– Lobes erect ....**4. *A. × tottenii* (*A. lutea ×A. obovata*)**
6 Perianth campanulate or obovoid, lobes turned slightly inwards ....**5. *A. obovata***
– Perianth cylindrical, lobes spreading **7**
7 Leaves dull greyish–green, 0.6–1 cm wide; beaks of fruits gradually tapering from body to tip .... **6. *A. bracteata***
– Leaves bright yellowish–green, 0.5–2.6 cm wide; beaks of fruits abruptly narrowed distally .... **7. *A. farinosa***
8 Perianth pubescent, sometimes sparsely or minutely so...........................**9**
– Perianth glabrous, rarely papillose **15**
9 Leaves 1–1.5 cm wide; perianth 7–10 mm .... **8. *A. megalantha***
– Leaves less than 1 cm wide; perianth less than 7 mm **10**
10 Bracts 2–5 × flower length.. **9. *A. glandulifera***
– Bracts shorter than or subequalling flower length, sometimes a few bracts near base of raceme to 2 × flower length **11**

11 Flowers usually subsessile, pedicels absent to 1(–2) mm, bract and bracteole borne on distal 1/2 of pedicel (often near apex); perianth lobes linear–lanceolate or narrowly oblong–lanceolate to linear; capsule turbinate, oblong–obovoid, obovoid or ovoid **12**

– Flowers distinctly pedicellate, pedicels 0.5–3.5 mm, bract and bracteole borne on proximal 1/2 of pedicel (often near base); perianth lobes ovate to lanceolate; capsule subglobose **13**

12 Capsule turbinate, oblong–obovoid or obovoid, distinctly angular, 3–5 × 2–3 mm, abruptly contracted distally when dehisced; leaves 2–4(–5) mm wide .... **10. *A. spicata***

– Capsule ovoid, not angular, 4–6 × 3–4.5 mm, not or only slightly contracted distally when dehisced; leaves (2–)3–5(–8) mm wide...... **11. *A. stenoloba***

13 Leaves 1–5, laxly tufted; rhizome cormlike, 3–7 mm in diam .... **12. *A. scopulorum***

– Leaves numerous, densely tufted; rhizome not corm–like **14**

14 Perianth lobes oblong–lanceolate, 2–3 mm .... **13. *A. pedicellata***

– Perianth lobes ovate, ca. 1 mm .... **14. *A. yaanica***

15 Raceme axis and pedicels glabrous **16**

– Raceme axis and pedicels pubescent or puberulent **20**

16 Raceme covered with viscid secretion;perianth tube urceolate, strongly constricted at apex, lobes erect **17**

– Raceme not covered with viscid secretion; perianth tube broadly funnelform, lobes strongly recurved or revolute **18**

17 Pedicel 0.5–3(–4.5) mm; bract 2–16 mm, perianth yellowish–green or cream 3–6 mm .... **15. *A. glabra***

– Pedicels 1 mm; bracts 5–15 mm long, yellow green corollas 6–7 mm long.......... **16. *A. foliata***

18 Rhizome surrounded by mass of fibres from disintegrated leaf bases; capsule with persistent stigma conspicuously thickened and capitate .... **17. *A. gracilis***

– Rhizome not surrounded by mass of fibres, but sometimes by persistent, dead leaves; capsule with persistent stigma not or only slightly thickened **19**

19 Capsule oblong–ovoid or ± ellipsoid, 5–7 × 3–3.5 mm .... **18. *A. cinerascens***

– Capsule ellipsoid or ovoid, to 7 mm long .... **19. *A. foliolosa***

20 Bracteole borne on proximal 1/2 of pedicel (often near base) .... **20. *A. guangxiensis***

– Bracteole usually borne on distal 1/2 of pedicel (often near apex) **21**

21 Rhizome often surrounded by mass of fibres from disintegrated leaf bases; roots thickened, fleshy; leaves usually rather few (5–10) and laxly tufted; capsule ovoid ellipsoid or ovoid–conical .... **21. *A. pauciflora***

– Rhizome not surrounded by mass of fibres; roots fibrous; leaves numerous and densely tufted; capsule narrowly ovoid to subglobose **22**

22 Raceme densely capitate or oblong–capitate; bract and bracteole borne on proximal 1/2 of pedicel (often near base) .... **22. *A. capitata***

– Raceme elongate and lax to short and dense, but not capitate; bract and bracteole usually borne at or near apex of pedicel **23**

23 Perianth 4–7.5 mm, lobes 2–5.5 mm, erect, spreading, recurved or revolute, 1–5× tube length .... **23. *A. laxiflora***

– Perianth 3–4.5 mm, lobes 1–2 mm, erect or recurved, 0.3–1× tube length **24**

24 Scape very slender, wiry, often somewhat flexuous, 7–20 cm; bract shorter than perianth; perianth often densely papillose, lobes recurved .... **24. *A. alpestris***

– Scape relatively stout, not wiry, straight and erect, 1.5–10 cm; bract equalling or longer than perianth; perianth not or scarcely papillose, lobes erect or slightly recurved .... **25. *A. nana***

Acknowledgements

We are grateful to Lan Xiangchun for fieldwork assistance and Qu Xincheng for the line drawing (Guangxi Institute of Traditional Medical and Pharmaceutical Sciences, Nanning).

Additional information

Conflict of interest

The authors have declared that no competing interests exist.

Ethical statement

No ethical statement was reported.

Funding

This work was supported by the National Natural Science Foundation of China (32000264), the Survey and Collection of Germplasm Resources of Woody & Herbaceous Plants in Guangxi, China (GXFS–2021–34).

Author contributions

Data curation: YN, RCH. Funding acquisition: YN, RCH, and YRQ. Investigation: YN, GYW, CGX, KJY. Methodology: YN, KJY, ZYZ. Project administration: YN, KDL. Supervision: KDL, KJY. Visualization: YN, YF, YFH. Writing – original draft: YN. Writing – review and editing: YN.

Author ORCIDs

You Nong https://orcid.org/0000-0001-7004-0946
Yun-Rui Qin https://orcid.org/0000-0003-2692-9048
Gui-Yuan Wei https://orcid.org/0000-0003-0652-1213
Ke-Jian Yan https://orcid.org/0000-0002-4927-4665
Chuan-Gui Xu https://orcid.org/0009-0000-6263-3821
Zi-Yi Zhao https://orcid.org/0000-0003-2513-0728
Ren-Chuan Hu https://orcid.org/0000-0002-0941-7203

Data availability

All of the data that support the findings of this study are available in the main text.

References

Caddick LR, Rudall PJ, Wilkin P, Hedderson TAJ, Chase MW(2002)Phylogenetics of Dioscoreales based on combined analyses of morphological and molecular data. Botanical Journal of the Linnean Society 138: 123–144. https://doi.org/10.1046/j.1095-8339.2002.138002123.x

Feng XX, Xiao Y, Liu ZX, Li RK, Wei D, Tian DK (2021) *Begonia pseudoedulis*, a new species in *Begonia* sect. Platycentrum (Begoniaceae) from southern Guangxi of China. PhytoKeys 182: 113–124. https://doi.org/10.3897/phytokeys.182.69074

Fuse S, Lee NS, Tamura MN (2012) Biosystematic studies on the family Nartheciaceae (Dioscoreales) I. Phylogenetic relationships, character evolution and taxonomic re-examination 298(8): 1575–1584. https://doi.org/10.1007/s00606-012-0660-2

Hu R, Wei S, Liufu Y, Nong Y, Fang W (2019) *Camellia debaoensis* (Theaceae), a new species of yellow camellia from limestone karsts in southwestern China. PhytoKeys 135: 49–58. https://doi.org/10.3897/phytokeys.135.38756

Huang YS, Nong SY, Li XK, Xie G, Tong YH (2022) *Vaccinium bangliangense*, a new species of Ericaceae from limestone areas in Guangxi, China. PhytoKeys 194: 23–31. https://doi.org/10.3897/phytokeys.194.81018

IUCN (2022) Guidelines for using the IUCN Red List categories and criteria, version 14. Prepared by the Standards and Petitions Committee. https://www.iucnredlist.org/resources/redlistguidelines [Accessed 28 October 2023]

Li R, Zhang SD (2011) *Aletris simpliciflora* sp. nov. (Nartheciaceae) from southwest Xizang, China. Nordic Journal of Botany 29(4): 440–442. https://doi.org/10.1111/j.1756-1051.2011.01222.x

Liang S, Turland NJ (2000) *Aletris* Linnaeus. In: Wu ZY, Raven PH (Eds) Flora of China. Science Press, Beijing & Missouri Botanical Garden Press, St Louis, 77–82.

Luo YJ, Ni SD, Jiang Q, Huang BG, Liu Y, Huang YS (2020) *Aristolochia yachangensis*, a new species of Aristolochiaceae from limestone areas in Guangxi, China. PhytoKeys 153: 49–61. https://doi.org/10.3897/phytokeys.153.52796

Noltie HJ (1994) *Aletris* Linnaeus. In: Noltie HJ (Ed.) Flora of Bhutan. Royal Botanic Garden, Edinburgh, 87–89.

Nong Y, Xu CG, Wei GY, Yan KJ, Qu XC, Zhang ZJ, Hu RC, Huang YF (2023) *Walsura guangxiensis* (Meliaceae), a new species from Guangxi, China. PhytoKeys 234: 219–227. https://doi.org/10.3897/phytokeys.234.106205

POWO (2023) Plants of the World Online. Facilitated by the Royal Botanic Gardens, Kew. http://www.plantsoftheworldonline.org/

Tobe H, Huang YL, Kadokawa T, Tamura MN (2018) Floral structure and development in Nartheciaceae (Dioscoreales), with special reference to ovary position and septal nectaries. Journal of Plant Research 131(3): 411–428. https://doi.org/10.1007/s10265-018-1026-9

Xin ZB, Chou WC, Maciejewski S, Fu LF, Wen F (2021) *Primulina papillosa* (Gesneriaceae), a new species from limestone areas of Guangxi, China. PhytoKeys 177: 55–61. https://doi.org/10.3897/phytokeys.177.63878

Yang YP (1997) *Aletris* Linnaeus. In: Wu ZY (Ed.) Flora Yunnanica. Science Press, Beijing, 649–655.

Zhao YM, Wang W, Zhang SR (2012) Delimitation and phylogeny of *Aletris* (Nartheciaceae) with implications for perianth evolution. Journal of Systematics and Evolution 50(2): 135–145. https://doi.org/10.1111/j.1759-6831.2011.00172.x

PhytoKeys 237: 91–102 (2024)
DOI: 10.3897/phytokeys.237.114105

Research Article

Re-evaluating monotypic *Eleutherostylis* from New Guinea and the Moluccas and its inclusion in *Grewia* (Malvaceae, Grewioideae)

Laurence J. Dorr[1], Kenneth J. Wurdack[1]

1 *National Museum of Natural History, Department of Botany, MRC-166, Smithsonian Institution, P.O. Box 37012, Washington, D.C. 20013-7012, USA*
Corresponding author: Laurence J. Dorr (dorrl@si.edu)

Abstract

Morphological and molecular phylogenetic evidence indicate that *Eleutherostylis* Burret (Malvaceae, Grewioideae), a monotypic genus described from New Guinea, is best considered a synonym of *Grewia* L., a species-rich genus widespread across the Paleotropics and found in Africa, Arabia, Asia, Australia and the western Pacific. A new combination, based on *E. renistipulata* Burret, *G. renistipulata* (Burret) Dorr, **comb. nov.**, is proposed. Original material of the basionym could not be located and a neotype is designated. A lectotype is designated for *G. morotaiensis* Kosterm., a synonym of *G. renistipulata*.

Key words: *Eleutherostylis*, *Grewia*, lectotype, Malvaceae, neotype, phylogeny

Academic editor: S. K. Ganesan
Received: 12 October 2023
Accepted: 18 December 2023
Published: 19 January 2024

Citation: Dorr LJ, Wurdack KJ (2024) Re-evaluating monotypic *Eleutherostylis* from New Guinea and the Moluccas and its inclusion in *Grewia* (Malvaceae, Grewioideae). PhytoKeys 237: 91–102. https://doi.org/10.3897/phytokeys.237.114105

Introduction

Generic circumscriptions in Malvaceae s.l. remain surprisingly unsettled and many genera of clearly uncertain circumscription have not had their monophyly tested in well-sampled phylogenies. Sufficient taxon sampling in such phylogenies, even with limited genetic loci, can often identify problems and suggest alternative taxonomies (e.g. *Eriolaena* DC., see Dorr and Wurdack (2021)). *Grewia* L. (Malvaceae, Grewioideae), one of the largest genera in the family, with 280–300 species distributed across Africa, Arabia, Asia, Australia and the western Pacific has a history of generic circumscription problems with multiple segregates. One of those segregates, the monotypic genus *Eleutherostylis* Burret, endemic to New Guinea and the Moluccas, is the focus of this study. When Burret (1926) created *Eleutherostylis*, he stated how it differed from *Grewia* while tacitly admitting the two genera were closely allied. He observed that his new genus differed by having several styles that are free to the base and a gynoecium with more locules. *Eleutherostylis* has 4(5) locules while *Grewia* sensu Burret has 1–2(3) locules. These two genera along with *Vincentia* Bojer (non Gaud.) and *Microcos* L. were the only genera Burret (1926) included in his circumscription of Grewieae Endl. (Grewioideae).

Hutchinson (1967) retained *Eleutherostylis* in an expanded circumscription of Grewieae in which he included seven genera. His concept of the genus *Grewia* included *Vincentia* Bojer and *Microcos* as synonyms rather than distinct genera. In Hutchinson's (1967) key to the tribe, *Eleutherostylis* was distinguished from

Grewia by a single character, viz. flowers dioecious versus flowers bisexual. Earlier, Burret (1926) had rather pointedly dismissed floral sexuality as a useful systematic character ("Systematischer Wert ist [die Geschlechtsverh] nicht beizumessen"). Hutchinson also noted that he did not follow Burret (1926) who retained *Vincentia* Bojer and *Microcos* as genera separate from *Grewia* because the "stigmatic characters used for distinguishing [these two genera] are scarcely of generic importance". The former is considered now a synonym of *Grewia* (Capuron and Mabberley 1999) while there is strong evidence the latter is distinct (see Brunken and Muellner (2012)).

Few other authors have discussed the relationships of *Eleutherostylis*. Kostermans (1972) considered the genus to be close to both *Grewia* and *Trichospermum* Blume and he placed *G. morotaiensis* Kosterm., described from the Moluccas, in synonymy under *E. renistipulata*. Bayer and Kubitzki (2003) maintained *Eleutherostylis* as a distinct genus, separating it from *Grewia* by the lack of a style in female flowers (versus styles cylindrical or dilated apically) and its heteromorphic (versus usually monomorphic) stipules. The latter is scarcely a generic character and positionally varies within a plant (heteromorphic pairs of reniform plus filiform stipules on lateral plagiotropic branches, but only reniform stipules on orthotropic branches). Brunken and Muellner (2012) included *Eleutherostylis* in their circumscription of the Grewieae and within that tribe in their "Grewia subclade". They based their argument on a morphological phylogenetic analysis, but did not elaborate on either characters or relationships within the subclade they recognised, which also included *Colona* Cav., *Desplatsia* Bocq., *Mollia* Mart., *Tetralix* Griseb. and *Trichospermum*, based on molecular data and *Duboscia* Bocq. and *Vasivaea* Baill., based solely on morphological data. Their phylogenetic analysis did not support the inclusion of *Eleutherostylis* within *Grewia*, although there was not strong support for any of the relationships that they found. Jennings (2021) treated *Eleutherostylis* in a floristic account of the trees of New Guinea, but the key couplet in that work used to separate *Eleutherostylis* from *Grewia* is based only on leaf and stipule characters.

Pollen data presented by Perveen et al. (2004) do not permit one to distinguish *Eleutherostylis* from *Grewia*. The pollen grains of both are described as coarsely reticulate and 3-colporate. The pollen shape ratio (P/E) of the former (1.66) falls within the range (1.27–2.05) of the limited number of species sampled of the latter. Pollen grains of both genera, prolate with long colpi, are described as "Corchorus-type", which can be applied to most Grewioideae, except for *Apeiba* Aubl., which Brunken and Muellner (2012) placed in Apeibeae Benth., a tribe distinct from Grewioideae. Hoorn et al. (2019), relying on the information and images provided by Perveen et al. (2004), noted that, within Malvaceae, the occurrence of prolate–subprolate bireticulate pollen with long colpi and distinct margos is restricted to Grewioideae.

Eleutherostylis was recently sampled with genomic-scale data for the Plant and Fungal Trees of Life Project (PAFTOL) and it was resolved as the strongly-supported sister-group to the single *Grewia* sampled (*G. flavescens* Juss.) (see Tree of Life Explorer, https://treeoflife.kew.org/tree-of-life; Baker et al. (2022)). The PAFTOL generic-exemplar approach to taxon sampling, however, did not test the monophyly of *Grewia*, which requires a more synoptic representation for that genus. The goals of our study, as part of broader phylogenetic work within Grewioideae, were to test the relationships of *Eleutherostylis* more adequately with respect to *Grewia*.

Material and methods

The taxon sampling here of 107 tips was a subset of data from an ongoing broader phylogenetic study and included *Eleutherostylis renistipulata* (*Schodde & Craven 4438*, US [01210662], the neotype designated below), along with a wide geographic sampling of *Grewia* (61 species) and 23/25 genera of Grewioideae (missing *Erinocarpus* Nimmo ex J. Graham and *Goethalsia* Pittier, which have been sampled elsewhere) recognised by Bayer and Kubitzki (2003). Outgroups included three Byttnerioideae (Malvaceae). Appendix 1 provides details of data sources, including vouchers and GenBank accession numbers. The nuclear ribosomal Internal Transcribed Spacer (ITS) region was selected for its ability to resolve the relevant taxa and recoverability from herbarium-specimen sourced DNAs. While single/few locus phylogenetic studies may appear dated in this genomics era, they remain appropriate for the scale of questions addressed here. Molecular methods for the 97 newly-generated sequences and phylogenetic analyses largely followed Dorr and Wurdack (2021) from DNeasy Plant Mini Kit (Qiagen Inc., Valencia, California, USA) extractions through to fluorescent Sanger sequencing of ITS amplification products on an ABI 3730xl DNA Analyzer (Thermo Fisher Scientific, Waltham, Massachusetts). The multiple sequence alignment (MSA) used MAFFT v.7.272 (Katoh and Standley 2013) under the G-INS-i refinement method, followed by minor manual refinements, based on a similarity criterion. Sensitivity analyses with different MAFFT optimality criteria, alignment without the divergent Byttnerioideae outgroups and exclusion sets to reduce missing data (i.e. removal of 119 MSA columns with > 50% missing data that reduced overall missing data from 16.2 to 3.85%) had little impact on the phylogenetic resolution, except in a few poorly-supported nodes. While there is sequence length variation within *Grewia*, there are few ambiguously aligned regions within our sampling for the genus. The MSA with the tested exclusion set is archived in the Dryad data repository (https://doi.org/10.5061/dryad.cnp5hqcbx). Final Maximum Likelihood (ML) analyses using all data were with IQ-TREE v.1.6.12 (Trifinopoulos et al. 2016) under GTR+F+I+G4 (selected by ModelFinder; Kalyaanamoorthy et al. (2017)) and RAxML-NG (Stamatakis 2014) as implemented on CIPRES XSEDE under GTR+I+Γ and clade support estimated by 1000 rapid bootstrap replicates. Bayesian Inference (BI) under GTR+I+Γ was performed using MrBayes v.3.2.7a (Ronquist et al. 2012) with two concurrent runs, each with four Markov chains (three cold and one heated), a 0.2 temperature coefficient and sampling every 1000 generations over 50 million generations and a conservative 25% burn-in. Topology and support value differences between the ML programmes were slight (IQ-TREE values are presented in Fig. 1); however, more pronounced were ML versus BI differences with shifts in some deeper nodes (albeit mostly poorly supported).

Results

Eleutherostylis is resolved as well-nested with multiple strongly-supported nodes (Posterior probability = 1.0, ML bootstrap > 85%) within a paraphyletic *Grewia* (Fig. 1). Its sequence divergence is relatively high amongst *Grewia* species, although it does not present additional alignment problems. Relationships within *Grewia* suggest a complex biogeography, although the small taxon and gene

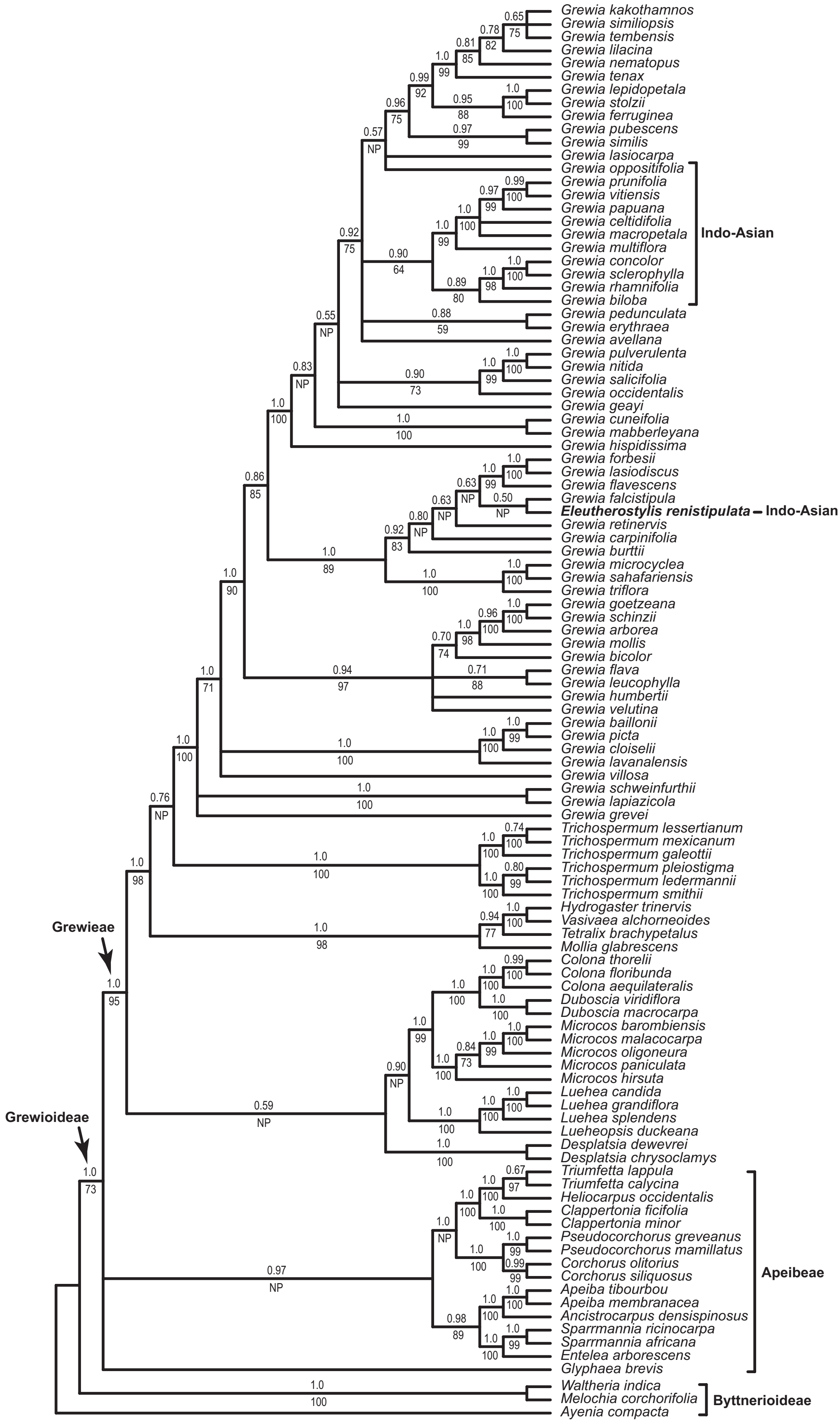

Figure 1. Phylogenetic relationships of *Eleutherostylis* and its Grewioideae relatives. Bayesian 50% majority-rule consensus tree, based on ITS sequences with posterior probability and IQ-TREE ML bootstrap values indicated, above and below branches, respectively. NP = an edge not present with ML.

sampling presented here limit our conclusions. The *Grewia* subclade containing *Eleutherostylis* contains only African species, while all the other Indo-Asian species (11 sampled) are far removed and mostly in a separate well-supported subclade. Relationships amongst the genera of Grewioideae and resolution as two major clades (circumscribed as tribes Apeibeae and Grewieae) largely mirror other studies (Bayer et al. 1999; Brunken and Muellner 2012; PAFTOL), except in the weakly-supported placement here of *Desplatsia* further removed from *Grewia*. *Microcos* is clearly distinct from *Grewia* and groups with *Colona* and *Duboscia*, which are Asian and African genera, respectively. *Desplatsia* and *Duboscia*, both African, are distinct from each other despite prior uncertainty (see Bayer and Kubitzki (2003)). The Neotropical and Palaeotropical taxa of *Trichospermum* group as separate sister subclades.

Discussion

Grewia is a morphologically diverse and biogeographically interesting genus, with species radiations in the Paleotropics, especially in sub-arid and woodland regions of Africa with 60% of the nearly 300 species. This diversification of arid-adapted shrubby species, often with animal dispersed fleshy drupaceous fruit, is especially notable in Madagascar (ca. 65 species, mostly endemic) and Sub-Saharan Africa (124 species) (Gautier et al. 2012). The Indo-Asian (including China) diversity of *Grewia* contains ca. 73 species, with a subset of only 28 species in the Flora Malesiana Region (Peninsula Malaysia, Indonesia, New Guinea, Philippines and Borneo). The relatively isolated nature of *Eleutherostylis* is suggested by sequence divergence and its placement amongst African taxa away from the Indo-Asian clade. However, our limited taxon sampling (ca. 20% of *Grewia* species) and limited phylogenetic resolution prevent us from reliably identifying finer patterns in biogeography, except to note that the Malagasy endemics do not form a monophyletic group. While *Eleutherostylis* fits well within the broad morphological diversity of *Grewia*, it is ecologically unusual in the genus inasmuch as it is a large dioecious tree with dry fruit in lowland tropical forests. Most Malvaceae are hermaphroditic and dioecy is rare. Within Grewioideae, dioecy characterises *Hydrogaster* Kuhlm., *Tetralix*, *Vasivaea* and some *Grewia* (including *Eleutherostylis*). In addition, *Erinocarpus*, *Grewia*, *Heliocarpus* L. and *Triumfetta* L. have some species with alternative breeding systems (e.g. polygamous, gynodioecious) and sometimes unisexual (staminate, pistillate) flowers. While the stipules of *Eleutherostylis* are conspicuous because of their relatively largely size and positional dimorphism, similar large stipules occur in other species of *Grewia* (e.g. *G. falcistipula* K. Schum., an African species).

Taxonomic summary

Grewia renistipulata **(Burret) Dorr, comb. nov.**
urn:lsid:ipni.org:names:77334716-1
Fig. 2

Eleutherostylis renistipulata Burret, Notizbl. Bot. Gart. Berlin-Dahlem 9(88): 630. 1926. Type: New Guinea. Gulf District: West bank of Vailala River, ca. 3 mi south of junction with Lohiki River, ca. 18 m elev., 3 Feb 1966 (fl, fr), *R. Schodde & L.A. Craven 4438* (neotype, here designated: US [01210662]!; isoneotypes: A-2 sheets!, BH!, BO, BRI, CANB [162189.1], CANB [162190.3], CANB [162191.2], G, K [K000062278 as image!], L [L.2349560 as image!], LAE, PNH).

Grewia morotaiensis Kosterm., Reinwardtia 7(5): 444, fig. 5. 1969 (p. 444 as "*raorotaiensis*"; fig. 5 as "*morotaiensis*"). Type: Indonesia. Moluccas, Morotai Isl., Distr. Tobelo near Totodoku [sic], 30 m elev., 2 May 1949 (fr), *A.J.G.H. Kostermans & W. Tangkilisan 44* (= *bb 33752*) (lectotype, here designated: [BO-1331873 as image!]; isolectotypes: A, BM, BO [BO-1331874 as image!], K, L [L 0062741 as image!], LAE, P, PNH, SING [0054550]).

Additional specimens examined. Indonesia. Moluccas, Morotai, Subdistr. Tobelo, north near Totodokoe, 30 m elev., 9 May 1949 (fl), *A.J.G.H. Kostermans & W. Tangkilisan 101* (= *bb 33795*) (A, BO [BO-1331875 as image!], K, L [L.2349554 as image!], L [L.2349555 as image!], SING). New Guinea. [Papua New Guinea]. Gulf District, Delta Divn., Baroi Riv., near Port Romilly, 26 Feb 1951, *M.F.C. Jackson 4119* (BISH, BRI, L [L.2349551 as image!], LAE). Madang District: ca. 5 km SE of Faita Village, along the Ramu River, ca. 150 m elev., 29 Jul 1955 (fl), *R.D. Hoogland 5044* (BRI, CANB [76047.1], CANB [76047.2], L [L.2349552 as image!], L [L.2349561 as image!], LAE, MEL [MEL 2370751A]!). Madang District, Gogol Base, 18 Aug 1969 (♂), *M. Kumul W. 2672* (A!, L [L.2349562 as image!]). Indonesia [Netherlands New Guinea]. Hollandia, 29 Oct 1954 (fr), *A. Brower Bw. 1611* (L [L.2349558 as image!], LAE). Sekoli Plain, Div. Hollandia, ca. 100 m elev., 25 Feb 1960, *G. Th. Iwanggin BW 9206* (BISH (×2), CANB [518317.1], L [L.2349557 as image!], WAG [WAG.1834811 as image!], WAG [WAG.1834812 as image!]). Sekoli- Plain, Div. Hollandia, ca. 100 m elev., 26 Feb 1960, *G. Th. Iwanggin BW 9222* (BISH, CANB [51833.1], L [L.2349564 as image!], LAE). Hollandia, Berap (Nimboeran), 9 Aug 1939, *Neth. Ind. For. Service bb.28959* (L [L.2349556 as image!]). W. Irian, Dozai, E. of Sukarnapura (= Hollandia), 50 m elev., 24 Aug 1966 (♂), *A.J.G.H. Kostermans & W. Soegeng 554* (CANB [339882.1], L [L.2349559 as image!]). Sekoli, O. Afd. Hollandia, 75 m elev., 26 Feb 1960, *A. Noesi BW 8147* (L [L.2349563 as image!], LAE). Tami, Hollandia, 19 Jan 1955, *F. Schram BW 1639* (CANB [51612.1], L [L.2349553 as image!], LAE).

Nomenclatural notes. Burret (1926) based *Eleutherostylis renistipulata* on two collections (syntypes) made by C.L. Ledermann in Sepik, Papua New Guinea: *Ledermann 10535* with male flowers and *Ledermann 10754* with female flowers and fruit. Neither of these syntypes, which were in Berlin (B), survived World War II (Juraj Paule, pers. comm.; see also Hiepko (1987)). Steenis-Kruseman (1950, 1958) noted that, in addition to Ledermann collections deposited in B, duplicate material sometimes can be found in E, K, L and SING, but no duplicates of the syntypes have been located in these Herbaria. Hence, the designation here of a neotype for the name (Fig. 2).

Kostermans (1969) used two different epithets in the original description of *Grewia morotaiensis*: "raorotaiensis" in the text and "morotaiensis" in the figure caption. These epithets have equal priority. Subsequently, Kostermans (1972) effectively made a choice between these competing epithets when he placed *G. morotaiensis* in synonymy under *Eleutherostylis renistipulata* (see Turland et al. (2018; Art. 11.5)).

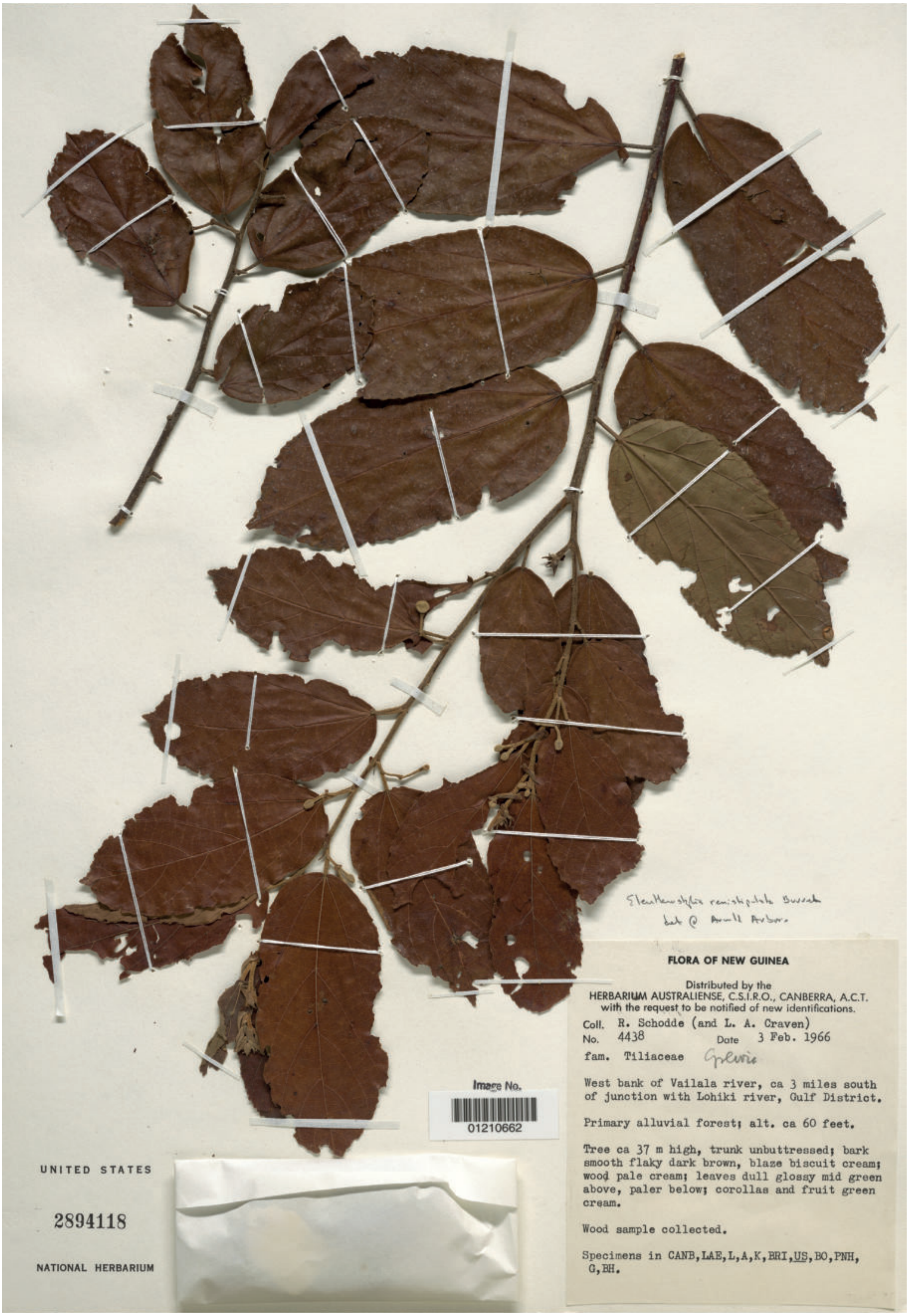

Figure 2. Neotype of *Eleutherostylis renistipulata* Burret (US [01210662]).

Acknowledgements

We thank Gabriel Johnson (US) for generating much of the ITS data and MO and US for relevant specimens.

Additional information

Conflict of interest

The authors have declared that no competing interests exist.

Ethical statement

No ethical statement was reported.

Funding

The molecular phylogenetic work was conducted with support from the Laboratories of Analytical Biology (LAB) of the National Museum of Natural History, Smithsonian Institution.

Author contributions

Conceptualization: LJD, KJW. Formal analysis: KJW. Investigation: KJW, LJD. Methodology: KJW. Writing – original draft: LJD. Writing – review and editing: KJW, LJD.

Author ORCIDs

Laurence J. Dorr https://orcid.org/0000-0001-7157-363X
Kenneth J. Wurdack https://orcid.org/0000-0003-0010-6932

Data availability

All of the data that support the findings of this study are available in the main text or were deposited in archives (Dryad or GenBank).

References

Baker WJ, Bailey P, Barber V, Barker A, Bellot S, Bishop D, Botigué LR, Brewer G, Carruthers T, Clarkson JJ, Cook J, Cowan RS, Dodsworth S, Epitawalage N, Françoso E, Gallego B, Johnson MG, Kim JT, Leempoel K, Maurin O, McGinnie C, Pokorny L, Roy S, Stone M, Toledo E, Wickett NJ, Zuntini AR, Eiserhardt WL, Kersey PJ, Leitch IJ, Forest F (2022) A comprehensive phylogenomic platform for exploring the Angiosperm Tree of Life. Systematic Biology 71(2): 301–319. https://doi.org/10.1093/sysbio/syab035

Bayer C, Fay MF, De Bruijn AY, Savolainen V, Morton CM, Kubitzki K, Alverson WS, Chase MW (1999) Support for an expanded family concept of Malvaceae within a recircumscribed order Malvales: A combined analysis of plastid *atp*B [sic] and *rbc*L [sic] DNA sequences. Botanical Journal of the Linnean Society 129(4): 267–303. https://doi.org/10.1111/j.1095-8339.1999.tb00505.x

Bayer C, Kubitzki K (2003) Malvaceae. In: Kubitzki K, Bayer C (Eds) The Families and Genera of Vascular Plants. V. Flowering Plants. Dicotyledons. Malvales, Capparales and non-betalain Caryophyllales. Springer-Verlag, Berlin, 225–311. https://doi.org/10.1007/978-3-662-07255-4_28

Brunken U, Muellner NA (2012) A new tribal classification of Grewioideae (Malvaceae) based on molecular phylogenetic evidence. Systematic Botany 37(3): 699–711. https://doi.org/10.1600/036364412X648670

Burret M (1926) Beiträge zur Kenntnis der Tiliaceen. Notizblatt des Botanischen Gartens und Museums zu Berlin-Dahlem 9(88): 592–880. https://doi.org/10.2307/3994327

Capuron R, Mabberley DJ (1999) Révision des Malvaceae-Grewioideae ("Tiliacées", p.p.) de Madagascar et des Comores. III. Les *Grewia* du sous-genre *Vincentia* (Benth.) Capuron. Adansonia, sér. 3, 21(1): 7–23. https://biostor.org/reference/245092

Dorr LJ, Wurdack KJ (2021) Indo-Asian *Eriolaena* expanded to include two Malagasy genera, and other generic realignments based on molecular phylogenetics of Dombeyoideae (Malvaceae). Taxon 70(1): 99–126. https://doi.org/10.1002/tax.12370

Gautier L, Chatelain C, Callmander MW, Phillipson PB (2012) Richness, similarity and specificity of Madagascar flora compared with Sub-Saharan Africa. Plant Ecology and Evolution 145(1): 55–64. https://doi.org/10.5091/plecevo.2012.591

Hiepko P (1987) The collections of the Botanical Museum Berlin-Dahlem (B) and their history. Englera 7: 219–252.

Hoorn C, van der Ham R, de la Parra F, Salamanca S, ter Steege H, Banks H, Star W, van Heuven BJ, Langelaan R, Carvalho FA, Rodríguez-Forero G, Lagomarsino LP (2019) Going north and south: The biogeographic history of two Malvaceae in the wake of Neogene Andean uplift and connectivity between the Americas. Review of Palaeobotany and Palynology 264: 90–109. https://doi.org/10.1016/j.revpalbo.2019.01.010

Hutchinson J (1967) The Genera of Flowering Plants (Angiospermae), Dicotyledones (Vol. 2). Clarendon Press, Oxford.

Jennings LVS (2021) Malvaceae subfam. Grewioideae Dippel (Malvaceae). In: Utteridge TMA, Jennings LVS (Eds) Trees of New Guinea. Kew Publishing, Royal Botanic Gardens, Kew, 427–431.

Kalyaanamoorthy S, Minh BQ, Wong TKF, von Haeseler A, Jermiin LS (2017) ModelFinder: Fast model selection for accurate phylogenetic estimates. Nature Methods 14(6): 587–589. https://doi.org/10.1038/nmeth.4285

Katoh K, Standley DM (2013) MAFFT multiple sequence alignment software version 7: Improvements in performance and usability. Molecular Biology and Evolution 30(4): 772–780. https://doi.org/10.1093/molbev/mst010

Kostermans AJGH (1969) New and critical Malesian plants VIII. Reinwardtia 7(5): 433–449.

Kostermans AJGH (1972) A synopsis of the Old World species of *Trichospermum* Blume (Tiliaceae). Transactions of the Botanical Society of Edinburgh 41(3): 401–430. https://doi.org/10.1080/03746607208685242

Perveen A, Grafström E, El-Ghazaly G (2004) World pollen and spore flora 23. Malvaceae Adams. [sic] P.p. Subfamilies: Grewioideae, Tilioideae, Brownlowioideae. Grana 43(3): 129–155. https://doi.org/10.1080/00173130410000730

Ronquist F, Teslenko M, Van der Mark P, Ayres DL, Darling A, Höhna S, Larget B, Liu L, Suchard MA, Huelsenbeck JP (2012) MrBayes 3.2: Efficient Bayesian phylogenetic inference and model choice across a large model space. Systematic Biology 61(3): 539–542. https://doi.org/10.1093/sysbio/sys029

Stamatakis A (2014) RAxML version 8: A tool for phylogenetic analysis and post-analysis of large phylogenies. Bioinformatics 30(9): 1312–1313. https://doi.org/10.1093/bioinformatics/btu033

Trifinopoulos J, Nguyen L-T, von Haeseler A, Minh BQ (2016) W-IQ-TREE: A fast online phylogenetic tool for maximum likelihood analysis. Nucleic Acids Research 44(W1): W232–W235. https://doi.org/10.1093/nar/gkw256

Turland NJ, Wiersema JH, Barrie FR, Greuter W, Hawksworth DL, Herendeen PS, Knapp S, Kusber W-H, Li D-Z, Marhold K, May TW, McNeill J, Monro AM, Prado J, Price MJ, Smith GF [Eds] (2018) International Code of Nomenclature for algae, fungi, and plants

(Shenzhen Code) adopted by the Nineteenth International Botanical Congress Shenzhen, China, July 2017. Regnum Vegetabile 159. Koeltz Botanical Books, Glashütten. https://doi.org/10.12705/Code.2018

van Steenis-Kruseman MJ (1950) Malaysian plant collectors and collections being a cyclopaedia of botanical exploration in Malaysia and a guide to the concerned literature up to the year 1950. Flora Malesiana, ser. 1, 1: 1–639.

van Steenis-Kruseman MJ (1958) Malaysian plant collectors and collections. Suppl. I. Flora Malesiana, ser. 1 5: 1–108. [CCXXV-CCXLII]

Appendix 1

Vouchers

Sources for data used in the phylogenetic analysis of Grewioideae. Ordered as: Taxon, Voucher (new data only; bc = barcode) and GenBank number (new data begin with OR).

Ancistrocarpus densispinosus Oliv., Cameroon, *X. van der Burgt et al. 936* (MO-6147053) OR934538. *Apeiba membranacea* Spruce ex Benth., Bolivia, *E. Stijfhoorn 705* (US-3266700; bc 0053551), OR934539. *Apeiba tibourbou* Aubl., Bolivia, *S. Paredes 427* (US-3684178; bc 01183679), OR934540. *Ayenia compacta* Rose, MF963978. *Clappertonia ficifolia* (Willd.) Decne., Ghana, *D. Harder et al. 3447* (MO-5030390), OR934541. *Clappertonia minor* (Baill.) Bech., Ghana, *H. Schmidt et al. 2081* (MO-5019391), OR934542. *Colona aequilateralis* (C.T.White & W.D.Francis) Merr. & L.M.Perry, New Guinea, *L. Craven & R. Schodde 1014* (US-3320995; bc 01317130), OR934543. *Colona floribunda* (Kurz) Craib, KR531939 (ITS2 only). *Colona thorelii* (Gagnep.) Burret, KR531940 (ITS2 only). *Corchorus olitorius* L., KY968914. *Corchorus siliquosus* L., FJ527604. *Desplatsia chrysochlamys* (Mildbr. & Burret) Mildbr. & Burret, Central African Republic, *D. Harris & J. Fay 680* (US-3404805; bc 01210682), OR934544. *Desplatsia dewevrei* (De Wild. & T.Durand) Burret, Uganda, *ATBP 572* (MO-4935375), OR934545. *Duboscia macrocarpa* Bocq., Gabon, *J. Reitsma & B. Reitsma 2260* (NY), OR934546. *Duboscia viridiflora* (K.Schum.) Mildbr., Ghana, *C. Jongkind et al. 1807* (MO-4667359), OR934547. *Eleutherostylis renistipulata* Burret, New Guinea, *R. Schodde & L. Craven 4438* (US-2894118; bc 01210662), OR934548. *Entelea arborescens* R.Br., FR875089. *Glyphaea brevis* (Spreng.) Monach., Ghana, *H. Schmidt et al. 1618* (MO-504354), OR934549. *Grewia arborea* (Forssk.) Lam., Tanzania, *P. Kuchar 24804* (MO-5688296), OR934550. *Grewia avellana* Hiern, Namibia, *S. Rugheimer et al. 2980* (US-3702461; bc 01183956), OR934551. *Grewia baillonii* R. Vig., Madagascar, *R. Noyes et al. 1011* (MO-5054318), OR934552. *Grewia bicolor* Juss., Namibia, *L. Nanyeni 311* (US-3702456; bc 01183964), OR934553. *Grewia biloba* G. Don, China, *D. Boufford et al. 37887* (MO-6139773), OR934554. *Grewia burttii* Exell, Tanzania, *P. Kuchar 23193* (MO-5583151), OR934555. *Grewia carpinifolia* Juss., Ghana, *C. Jongkind 1707* (MO-4666899), OR934556. *Grewia celtidifolia* Juss., China, *L. Heng 8587* (MO-5320749), OR934557. *Grewia cloiselii* R.Vig., Madagascar, *T. Croat 31963* (MO-2599538), OR934558. *Grewia concolor* Merr., China, *N. Chun & C. Tso 44606* (US-1675394; bc 01173074), OR934559. *Grewia cuneifolia* Juss., Madagascar, *R. Gereau et al. 5733* (US-3335856; bc 00833950), OR934560. *Grewia erythraea* Schweinf., Ethiopia, *D.*

Sebsebe & A. Berhanu 1996 (MO-3887915), OR934561. *Grewia falcistipula* K. Schum., Namibia, *S. Bartsch et al. 1800* (US-3599415; bc 00814074), OR934562. *Grewia ferruginea* Hochst. ex A.Rich., Tanzania, *S. Bidgood et al. 3492* (MO-4925265), OR934563. *Grewia flava* DC., Namibia, *S. Rugheimer et al. 2504* (US-3702462; bc 01183961), OR934564. *Grewia flavescens* Juss., Namibia, *S. Rugheimer et al. 2669* (US-3702455; bc 01183967), OR934565. *Grewia forbesii* Harv. ex Mast., Tanzania, *R. Gereau et al. 6624* (MO-5334011), OR934566. *Grewia geayi* R.Vig., Madagascar, *F. Chauvet 397* (MO-6332845), OR934567. *Grewia goetzeana* K.Schum., Tanzania, *A. Ntemi Sallu 665* (MO-5753794), OR934568. *Grewia grevei* Baill., Madagascar, *P. Phillipson 1680* (MO-3514731), OR934569. *Grewia hispidissima* Wahlert et al., Madagascar, *J. Razafitsalama & Torze 1091* (US-3547850; bc 01205465), OR934570. *Grewia humbertii* Capuron, Madagascar, *P. Phillipson 2536* (MO-3662965), OR934571. *Grewia kakothamnos* K.Schum., Ethiopia, *C. Puff 870423-315* (MO-4010325), OR934572. *Grewia lapiazicola* Capuron, Madagascar, *M. Bardot-Vaucoulon & G. Véné 1782* (MO-6152266), OR934573. *Grewia lasiocarpa* E.Mey. ex Harv., South Africa, *P. Phillipson 4381* (MO-5650943), OR934574. *Grewia lasiodiscus* K.Schum., Mali, *C. Duvall 91* (MO-5333223), OR934575. *Grewia lavanalensis* Baill., Madagascar, *P. Phillipson 3092* (US-3398970; bc 01205481), OR934576. *Grewia lepidopetala* Garcke, Tanzania, *Y. Abeid et al. 1860* (MO-4797160), OR934577. *Grewia leucophylla* Capuron, Madagascar, *P. Phillipson & S. Rabesihanaka 3143* (US-3398976; bc 01205489), OR934578. *Grewia lilacina* K.Schum., Tanzania, *V. Simon & Y.S. Abeid 69* (MO-4902872), OR934579. *Grewia mabberleyana* Phillipson et al., Madagascar, *G. Schatz 3356* (MO-6719378), OR934580. *Grewia macropetala* Burret, China, *Qin Hai-ning et al. 2362* (MO-5746218), OR934581. *Grewia microcyclea* (Burret) Capuron & Mabb., Madagascar, *P. Phillipson 2908* (US-3404759; bc 01207518), OR934582. *Grewia mollis* Juss., Tanzania, *F. Mawi et al. 182* (MO-5731705), OR934583. *Grewia multiflora* Juss., Burma, *R. Belcher* [*US Typhus Comm.*] *671* (US-2213169; bc 00685866), OR934584. *Grewia nematopus* K. Schum., Kenya, *Y. Harvey et al. 60* (MO-5779207), OR934585. *Grewia nitida* Juss., Madagascar, *G. McPherson et al. 14761* (MO-3771574), OR934586. *Grewia occidentalis* L., South Africa, *G. Germishuizen 952* (US-3022273; bc 01207559), OR934587. *Grewia oppositifolia* Buch.-Ham. ex DC., India, *W. Koeltz 4446* (US-1608157; bc 01173134), OR934588. *Grewia papuana* Burret, Australia, *G. Batianoff 900146* (MO-4341230, OR934589. *Grewia pedunculata* K.Schum., Mozambique, *W. Luke et al. 9907* (MO-5761031), OR934590. *Grewia picta* Baill., Comoros, *J.-N. Labat 3198* (MO-6113815), OR934591. *Grewia prunifolia* A.Gray, Fiji, *A. Smith 7910* (US-2190725; bc 00813934), OR934592. *Grewia pubescens* P.Beauv., Guinea, *C. Jongkind 8345* (MO-6185625), OR934593. *Grewia pulverulenta* R.Vig., Madagascar, *G. McPherson & N. Dumetz 14317* (MO-3771579), OR934594. *Grewia retinervis* Burret, Namibia, *L. Hoffman 568* (US-3702466; bc 01183958), OR934595. *Grewia rhamnifolia* B.Heyne ex Roth, Sri Lanka, *A. Robyns 7209* (US-2660528; bc 00813779), OR934596. *Grewia sahafariensis* Capuron & Mabb., Madagascar, *R. Capuron 23036-SF* (MO-6354013), OR934597. *Grewia salicifolia* Schinz, Seychelles (Aldabra), *S. Renvoize 1346* (US-2779483; bc 01207633), OR934598. *Grewia schinzii* K.Schum., Botswana, *P. Smith 4360* (MO-5988288), OR934599. *Grewia schweinfurthii* Burret, Ethiopia, *D. Sebsebe & B. Tamirat 2349* (MO-3855548), OR934600. *Grewia sclerophylla* Roxb. ex G.Don, Nepal, *R. Troth 704* (US-2826357; bc 01173161), OR934601. *Grewia similiopsis*

C.Whitehouse, Tanzania, *P. Kuchar 24245* (MO-5700280), OR934602. *Grewia similis* K.Schum., Tanzania, *L. Ellemann 645* (MO-4859391), OR934603. *Grewia stolzii* Ulbr., Tanzania, *J. Lovett & C. Kayombo 4389* (US-3362978; bc 01207665), OR934604. *Grewia tembensis* Fresen., Saudi Arabia, *T. Miyazaki 990915R5* (MO-6334153), OR934605. *Grewia tenax* (Forssk.) Fiori, Namibia, *H. Kolberg et al. 1215* (US-3702464; bc 01183955), OR934606. *Grewia triflora* (Bojer) Walp., Madagascar, *F. Ratovoson et al. 916* (MO-6034468; bc MO-1059913), OR934607. *Grewia velutina* (Forssk.) Lam., Saudi Arabia, *T. Miyazaki 990905R1* (MO-6334157), OR934608. *Grewia villosa* Willd., Saudi Arabia, *J. Lavranos & I. Collenette 20449* (MO-2952050), OR934609. *Grewia vitiensis* Turrill, Fiji, *O. Degener 15242* (US-1944019; bc 00980012), OR934610. *Heliocarpus occidentalis* Rose, Mexico, *R. McVaugh 20863* (US-2151641; bc 00520160), OR934611. *Hydrogaster trinervis* Kuhlm., Brazil, *J. Paixao et al. 554* (NY-884904), OR934612. *Luehea candida* (DC.) Mart., Mexico, *J. Amith 1843* (US-3635420; bc 00976739), OR934613. *Luehea grandiflora* Mart., Brazil, *B. Amorim et al. 523* (US-3645266; bc 01183510), OR934614. *Luehea splendens* Rusby, Bolivia, *R. López & M. Capra 825* (US-3670168; bc 01183716), OR934615. *Lueheopsis duckeana* Burret, Brazil, *G. Árboez et al. 4305* (US-3419295; bc 00727607), OR934616. *Melochia corchorifolia* L., MH768329. *Microcos barombiensis* (K.Schum.) Cheek, Cameroon, *X. van der Burgt & J. Amambo 379* (MO-5779211), OR934617. *Microcos hirsuta* (Korth.) Burret, Indonesia, *C. Peters 1025* (US-3290456; bc 01208471), OR934618. *Microcos malacocarpa* (Mast.) Burret, Ghana, *H. Schmidt et al. 2022* (MO-5006532), OR934619. *Microcos oligoneura* (Sprague) Burret, Gabon, *J. Boussengui-Nongo 281* (MO-6311890), OR934620. *Microcos paniculata* L., KP092996. *Mollia glabrescens* Benth., Guyana, *K. Redden et al. 6241* (US-3572625; bc 01074205), OR934621. *Pseudocorchorus greveanus* (Baill.) Capuron, Madagascar, *J. & M. Peltier 5196* (MO-6356087), OR934622. *Pseudocorchorus mamillatus* Capuron, Madagascar, *R. Bolliger 337* (MO-6612809), OR934623. *Sparrmannia africana* L.f., South Africa, *R. Brand 228* (MO-5652084), OR934624. *Sparrmannia ricinocarpa* (Eckl. & Zeyh.) Kuntze, FR875088. *Tetralix brachypetalus* Griseb., Cuba, *R. Berazaín et al. [JBNC] 71840* (NY), OR934625. *Trichospermum galeottii* (Turcz.) Kosterm., Mexico, *P. Acevedo-Rdgz. et al. 16062* (US-3697233, bc: 01343493), OR934626. *Trichospermum ledermannii* Burret, Palau (Caroline Islands), *F. Fosberg 50600* (US-3408397; bc 01165395), OR934627. *Trichospermum lessertianum* (Hochr.) Dorr, Mexico, *G. Martínez Calderón 1651* (US-3571535; bc 00976860), OR934628. *Trichospermum mexicanum* (DC.) Baill., Mexico, *J. Amith 1817 (*US-3635429; bc: 00976741), OR934629. *Trichospermum pleiostigma* (F. Muell.) Kosterm., Papua New Guinea, *W. Takeuchi 4559* (US-3306729 [sic] US-3716430 bc: 04214468), OR934630. *Trichospermum smithii* Kosterm., Fiji, *J. Gressitt 2499* (US-2210382; bc: 00977330), OR934631. *Triumfetta calycina* Turcz., Peru, *W. Galiano et al. 4835* (US-3534756; bc 00755457), OR934632. *Triumfetta lappula* L., Panama, *P. Peterson & C. Annable 7242* (US-3114850; bc 00501649), OR934633. *Vasivaea alchorneoides* Baill., Guyana, *M. Jansen-Jacobs et al. 34* (US-3070508; bc 00513683), OR934634. *Waltheria indica* L., MH768330.

PhytoKeys

PhytoKeys 237: 103–116 (2024)
DOI: 10.3897/phytokeys.237.116236

Research Article

Hedysarum qilianshanense sp. nov. (Fabaceae, Hedysareae), a new species from the Qilianshan Mountains in Gansu, China

Pei-Liang Liu[1], Qian-Xi Guo[1], Jian-Qi Zhang[2], Lu-Lu Xun[3], Yuan Lu[1,3], Ming Yue[1,3]

1 *Key Laboratory of Resource Biology and Biotechnology in Western China, Ministry of Education, Northwest University, Xi'an, Shaanxi 710069, China*
2 *Linhai City Natural Resources and Planning Bureau of Zhejiang Province, Linhai, Zhejiang 317099, China*
3 *Shaanxi Engineering Research Centre for Conservation and Utilization of Botanical Resources, Xi'an Botanical Garden of Shaanxi Province (Institute of Botany of Shaanxi Province), Xi'an, Shaanxi 710061, China*
Corresponding author: Ming Yue (yueming@nwu.edu.cn)

Abstract

Hedysarum qilianshanense **sp. nov.** (Fabaceae, Hedysareae) is described and illustrated from the Qilianshan Mountains in Gansu, China. This new species is similar to *H. przewalskii*, but can be distinguished by its corolla being light purple to purple, standard 15–19 mm long, wings 14–16 mm long, keels 16–19 mm long, and the ovary and legume being glabrous. The new species can be easily distinguished from *H. neglectum* Ledeb. by its bract being shorter than the pedicel, and the ovary and legume being glabrous. Phylogenetic tree based on the nuclear ITS and ETS sequences shows that *H. qilianshanense* is sister to *H. przewalskii*, while the tree based on the plastid *psbA-trnH*, *trnC-petN*, *trnL-F*, *trnS-G* and *petN-psbM* sequences shows *H. qilianshanense* as sister to a clade consisting of *H. hedysaroides*, *H. inundatum*, *H. americanum* and *H. neglectum*. The new species is a diploid with the chromosome number $2n = 14$. Based on morphological, phylogenetic and karyotypic evidence, the new species may originate from an ancient homoploid hybrid speciation event.

Key words: Karyotype, phylogeny, Qinghai-Tibetan Plateau, taxonomy

Academic editor: Clifford Morden
Received: 24 November 2023
Accepted: 22 December 2023
Published: 22 January 2024

Citation: Liu P-L, Guo Q-X, Zhang J-Q, Xun L-L, Lu Y, Yue M (2024) *Hedysarum qilianshanense* sp. nov. (Fabaceae, Hedysareae), a new species from the Qilianshan Mountains in Gansu, China. PhytoKeys 237: 103–116. https://doi.org/10.3897/phytokeys.237.116236

Introduction

The genus *Hedysarum* L. (Fabaceae, Hedysareae) consists of more than 160 species, widely distributed in temperate Asia, Europe, northern Africa and North America (Xu and Choi 2010). Previous phylogenetic analyses delimited *Hedysarum* into three sections, *i.e.*, *H.* sect. *Hedysarum*, *H.* sect. *Stracheya* (Benth.) B. H. Choi & H. Ohashi, and *H.* sect. *Multicaulia* (Boiss.) B. Fedtsch. (Duan et al. 2015; Liu et al. 2017b, 2019; Nafisi et al. 2019). Species of *H.* sect. *Hedysarum* mostly inhabit temperate forests, alpine meadows and arctic tundra in Eurasia and North America (Xu and Choi 2010; Duan et al. 2015).

The Qinghai-Tibetan Plateau (QTP) is the largest and highest plateau on the earth. More than 12,000 species of vascular plants inhabit in QTP and such species richness also exhibit a high level of endemism (Wen et al. 2014). The QTP harbors about 24 species of *H.* sect. *Hedysarum*, with 22 species endemic to the QTP. Most of these species are distributed in the Himalayas on the southern border of the QTP, and the Hengduan Mountains on the eastern border of the QTP (Ohashi and Tateishi 1975; Xu and Choi 2010; Choi et al. 2011; Liu et al. 2017a). The Qilianshan Mountains are a huge mountain range that lie on the northeastern border of the QTP, separating the QTP from the deserts in the north. Only one species, *H. algidum* L. Z. Shue, is known from the Qilianshan Mountains. Species diversity in the Qilianshan Mountains remains to be further explored.

When the first author was examining specimens of *Hedysarum* deposited in the herbarium of Northwest Normal University (NWTC), a specimen of *H.* sect. *Hedysarum* collected from the Qilianshan Mountains was found to be different from any of the described species. Field expeditions to the Qilianshan Mountains discovered additional populations of this form and subsequent morphological and phylogenetic analyses indicated that they represent a new species that is described in the present paper.

Materials and methods

Taxon sampling

Samples were collected from three populations of the putative new species, including six individuals from the Xiaogushan population, six individuals from the Wulin'gou population, and five individuals from the Sidalong population. Each of these samples were sequenced for phylogenetic analyses. Other 23 species in *H*. sect. *Hedysarum* were selected to test the phylogenetic position of the putative new species. Species in *H*. sect. *Stracheya* were selected for outgroup comparison because previous studies showed that *H*. sect. *Stracheya* is sister to *H*. sect. *Hedysarum* (Liu et al. 2017a, 2017b, 2019). Voucher information is given in the Appendix 1.

DNA extraction, PCR and sequencing

Silica-gel dried leaves were used to extract genomic DNA by using the Qiagen DNeasy® Plant Mini Kit (Hilden, Germany). The nuclear ribosomal external transcribed spacer (ETS) and internal transcribed spacer (ITS), and the plastid *psbA-trnH*, *trnC-petN*, *trnL-F*, *trnS-G* and *petN-psbM* sequences were amplified using Polymerase chain reaction (PCR). Primers and PCR conditions followed the previous paper (Liu et al. 2017b). Amplicons were sequenced in both directions using the amplification primers. All sequences were deposited in GenBank and the accession numbers are provided in Appendix 1.

Phylogenetic analysis

Phylogenetic trees were reconstructed based on the newly generated sequences together with the previously published data (Duan et al. 2015; Liu et al. 2017a, 2017b, 2019). MUSCLE (Edgar 2004) implemented in Geneious v.9 (Kearse et al. 2012) was used to conduct multiple sequence alignments. The best-fit nucleotide substitution model was determined by jModelTest v.2.1.7 (Darriba et al. 2012). A GTR + G model was applied to the combined nuclear data, and a GTR + G + I model was applied to the combined plastid data. Phylogenetic trees were constructed based on the nuclear and the plastid data separately because of the phylogenetic incongruence between the nuclear and the plastid trees (see results). Bayesian inferences (BI) were conducted in MrBayes v.3.2.5 (Ronquist and Huelsenbeck 2003; Ronquist et al. 2012). We ran BI for 10,000,000 generations, and trees were sampled every 1,000 generations. The first 2,500 trees were discarded, and the remaining trees were used to build a 50% majority-rule consensus tree with posterior probabilities (PP). The maximum likelihood (ML) and maximum parsimony (MP) analyses were conducted using RAxML v.8.2 (Stamatakis 2014) and PAUP* 4.0a169 (Swofford 2002), respectively. The ML and MP bootstrap analyses were each performed with 1,000 replicates. Bootstrap support values (BML, BMP) from the ML and MP analyses were labeled on the corresponding branches of the BI trees.

Chromosome number count

One available seed of the putative new species (voucher: *P. L. Liu 458*, see Appendix 1 for details) was germinated in a culture dish with wet filter paper at room temperature. When root grew to ca. 5 mm long, it was treated in 2 mmol·L^{-1} 8-hydroxyquinoline solution at room temperature for 4 h. It was then fixed with a mixture of acetic acid and ethyl alcohol (1:3 volume) at 4 °C and stored overnight. The root tissue was digested with 1 mol·L^{-1} hydrochloric acid at 60 °C for 3 min, and cleaned thoroughly with tap water. The root tip was stained with carbol fuchsin and squashed on a glass slide. Well-spread mitotic metaphase chromosomes were examined and photographed with 100× oil lens on a Nikon Eclipse 55i microscope.

Results

Nuclear data

The 17 individuals from three populations (Xiaogushan, Wulin'gou and Sidalong) of the putative new species had identical ETS and ITS sequences. The nuclear phylogenetic tree based on the combined ETS and ITS sequences (Fig. 1A) shows the putative new species as sister to *H. przewalskii* Yakovlev (PP = 0.99, BML = 85%, BMP = 79%). These two species formed a clade with *H. taipeicum* (Hand.-Mazz.) K. T. Fu, *H. ussuriense* I. Schischkin & Kom. and *H. citrinum* E. G. Baker (PP = 1, BML = 89%, BMP = 84%).

Plastid data

Three plastid haplotypes, namely AG, Agap and Ggap (Table 1), were found from the combined plastid *psbA-trnH*, *trnC-petN*, *trnL-F*, *trnS-G* and *petN-psbM* sequences of the 17 individuals from three populations of the new species. The sequence variations of the haplotypes and the distribution of the haplotypes in populations and individuals were showed in Table 1. Therefore, each of these three haplotypes were included in the phylogenetic analyses. In the plastid tree based on the combined *psbA-trnH*, *trnC-petN*, *trnL-F*, *trnS-G* and *petN-psbM* sequences (Fig. 1B), the new species was weakly supported (PP = 0.65, BML = 59%, BMP = 41%) to be sister to the circumboreal clade (comprising *H. neglectum* Ledeb., *H. americanum* (Michx.) Britton, *H. inundatum* Turcz. and *H. hedysaroides* Schinz & Thell.). The new species plus the circumboreal clade was sister to the eastern QTP clade (comprising *H. algidum* L. Z. Shue, *H.*

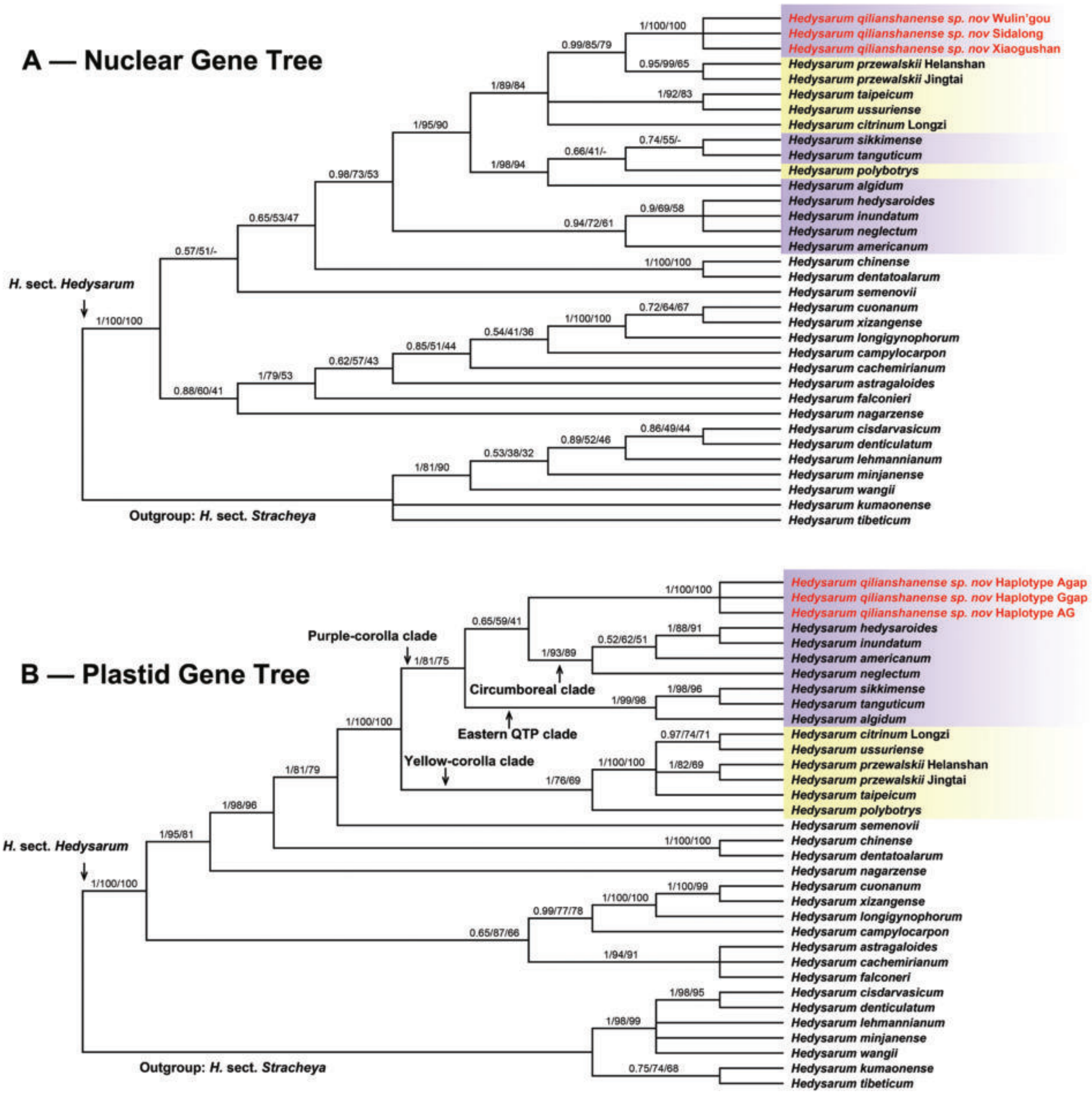

Figure 1. Bayesian trees based on the combined nuclear ETS and ITS sequences (**A**) and the combined plastid *psbA-trnH*, *trnC-petN*, *trnL-F*, *trnS-G* and *petN-psbM* sequences (**B**). The Bayesian posterior probabilities (PP), the maximum likelihood and the maximum parsimony bootstrap supports (BML, BMP) are above the branches. A dash indicates a branch that is not found in the maximum parsimony tree. The purple and yellow shades on taxa names indicates corolla colors.

Table 1. Haplotypes from the combined plastid *psbA-trnH*, *trnC-petN*, *trnL-F*, *trnS-G* and *petN-psbM* sequences of *Hedysarum qilianshanense*.

Haplotype name	Sequence variation					Distribution in populations (number of individuals)
	psbA-trnH	***trnC-petN***	***trnL-F***	***trnS-G***	***petN-psbM***	
AG	A	G	identical	identical	identical	Xiaogushan (6), Wulin'gou (4)
Agap	A	gap	identical	identical	identical	Wulin'gou (2), Sidalong (4)
Ggap	G	gap	identical	identical	identical	Sidalong (1)

tanguticum B. Fedtsch. and *H. sikkimense* Benth. ex Baker), and these clades formed the purple-corolla clade (PP = 1, BML = 81%, BMP = 75%). The purple-corolla clade was sister to (PP = 1, BML = 100%, BMP = 100%) the yellow-corolla clade (comprising *H. polybotrys* Hand.-Mazz., *H. taipeicum*, *H. przewalskii*, *H. ussuriense* and *H. citrinum*).

Chromosome number count

A total of 21 cells with well-spread mitotic metaphase chromosomes were observed. All cells showed that the chromosome number of the new species was $2n = 14$ (Fig. 2).

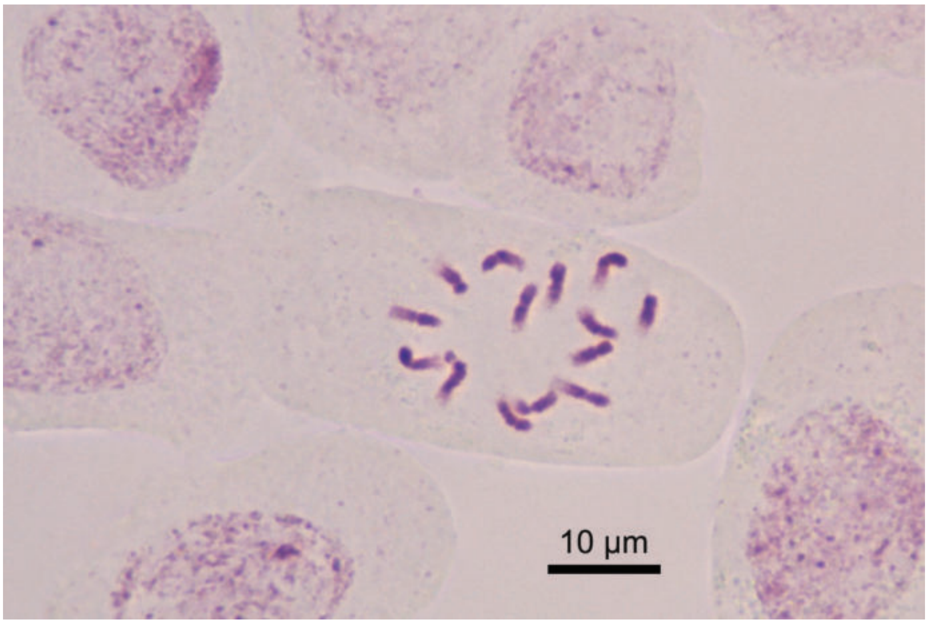

Figure 2. Mitotic metaphase chromosomes from root tip of *Hedysarum qilianshanense.*

Taxonomy

***Hedysarum qilianshanense* P.L.Liu, sp. nov. (*H.* sect. *Hedysarum*)**
urn:lsid:ipni.org:names:77334725-1
Figs 3, 4

Type. China, Gansu Province, Su'nan County, the Heihe River valley, Xiaogushan, in crevice on stony slope, 2053 m above sea level (a. s. l.), 38°41'6.38"N, 110°3'9.98"E, 21 June 2019, *P. L. Liu 458* (Holotype, WUK!, barcode WUK0536471; Isotypes, WUK!, barcodes WUK0536466-WUK0536470, WNU!).

Diagnosis. This new species is morphologically similar to *H. przewalskii*, but can be distinguished by its light purple to purple corolla (vs. light yellow to yellow corolla), 15–19 mm long standard (vs. 10–14 mm long standard), 14–16 mm long wings (vs. 10–14 mm long wings), 16–19 mm long keels (vs. 12–17 mm long keels), and glabrous ovaries and legumes (vs. often pubescent, sometimes glabrate or glabrous ovaries and legumes). The new species can be easily distinguished from *H. neglectum* by its bract shorter than pedicel

Figure 3. Illustration of *Hedysarum qilianshanense* **a** root and basal part of stems **b** upper part of plant **c** calyx tube (split between an adaxial tooth and a lateral tooth) **d** bracteoles **e** standard **f** wing **g** keel **h** androecium **i** pistil **j** infructescence **k** legume. Drawn by Xiu-Zhen Wu.

(vs. bract longer than pedicel), and glabrous ovaries and legumes (vs. pubescent ovaries and legumes) (Table 2).

Description. Perennial herbs, 30–100 cm tall. Main root stout, woody, up to 1.3 cm in diameter. Stems cespitose, ascending, branched; internodes glabrous

Figure 4. Photos of *Hedysarum qilianshanense* from the field **A** habitat **B** plant **C** raceme **D** infructescence. Photographed by Pei-Liang Liu.

Table 2. Morphological comparison of *Hedysarum qilianshanense*, *H. przewalskii* and *H. neglectum*.

	H. qilianshanense	***H. przewalskii***	***H. neglectum***
Bract	shorter than pedicel	shorter than pedicel	longer than pedicel
Corolla color	light purple to purple	light yellow to yellow	purple
Standard length	15–19 mm	10–14 mm	13–14 mm
Wing length	14–16 mm	10–14 mm	13–14 mm
Keel length	16–19 mm	12–17 mm	15–16 mm
Ovary and legume	glabrous	often pubescent, sometimes glabrate or glabrous	pubescent

or loosely pubescent, nodes pubescent. Leaves imparipinnate, alternate, 12–30 cm long; stipules connate, opposite to leaves, wide triangular, membranous, brown, glabrous, apex shallowly bilobed, lower ones 8–17 mm long, becoming smaller in upper part of stem; rachises sulcate, glabrous or sparsely pubescent; leaflets 9–19, opposite or alternate; petiolules ca. 1 mm long, pubescent; leaflet blades elliptic, ovate-elliptic, oblong, 12–40 × 7–25 mm, adaxial surface glabrous, abaxial surface sparsely pubescent along midvein, base wide cuneate or rounded, apex obtuse, rounded or retuse. Racemes axillary, exceeding leaves, 15–42 cm long, with 15–50 flowers, peduncles pubescent; pedicel 3–6 mm long, pubescent; bracts linear, with brown midvein, pubescent, 2–5 mm long;

bracteoles 2, linear, with brown midvein, pubescent, 2–3.5 mm long; calyx tube campanulate, 3–4 mm long, pubescent; calyx teeth 5, pubescent, the two adaxial teeth triangular, ca. 1 mm long, the two lateral teeth narrowly triangular, 1.5–2.5 mm long, the abaxial tooth linear-triangular, 2–3 mm long; corolla light purple to purple; standard obovate, 15–19 × 5.5–7 mm, apex retuse, base attenuate; wings 14–16 × 2–2.5 mm, auricle linear, as long as claw, 2–3 mm long; keels 16–19 × 4–5 mm, auricle triangular, ca. 1 mm long; androecium diadelphous, 12–17 mm long; ovary linear, glabrous, style ca. 13 mm long. Legume a loment, divided into 2–4 articles, with a small beak at apex; articles elliptic, compressed, 8–10 mm × 6–7 mm, glabrous, with reticulate veins, with a narrow wing ca. 0.5 mm wide along the dorsal suture only. Seed reniform, yellow, ca. 3 × 2 mm.

Phenology. Flowering and fruiting in June.

Distribution and habitat. *Hedysarum qilianshanense* is only known from Su'nan, Gansu, China. It grows in stony slope and forest edge in valley, 2053–3000 m a. s. l.

Etymology. The epithet *qilianshanense* is transliterated from the type location, Qilianshan Mountains in China. The Chinese vernacular name for this new species is 祁连山岩黄耆 (qí lián shān yán huáng qí).

Other specimens examined (Paratypes). China, Gansu Province, Su'nan County, Sidalong, Wulin'gou, on stony slope, 3000 m a. s. l., 21 June 1986, *Sheng Huan Bao Dui 86055* (NWTC!); Su'nan County, Sidalong, Wulin'gou, in crevice on stony slope, 2542 m a. s. l., 38°28'1.67"N, 99°56'54.63"E, 21 June 2019, *P. L. Liu 461* (WUK!, barcodes WUK0536462, WUK0536463, WNU!); Su'nan County, Sidalong, on slope on forest edge, 2632 m a. s. l., 38°27'26.6"N, 99°54'52.69"E, 21 June 2019, *P. L. Liu 470* (WUK!, barcodes WUK0536464, WUK0536465, WNU!).

Discussion

The phylogenetic positions of *H. qilianshanense* are different in the nuclear and plastid trees. *Hedysarum qilianshanense* and *H. przewalskii* are similar to each other in well-developed stem and large, elliptic, ovate-elliptic or oblong leaflets. On the other hand, *H. qilianshanense* is clearly different from *H. przewalskii* in flower and fruit features (Table 2). *Hedysarum qilianshanense* is distributed in the central part of the Qilianshan Mountains, whereas *H. przewalskii* is distributed east of the Qilianshan Mountains (Fig. 5). Thus, these two species are isolated from each other. The Badain Jaran Desert and the Tengger Desert may serve as geographic barriers between the two species because they are both mesophytes inhabiting mountainous regions.

In the plastid tree, however, *H. qilianshanense* is a member of the purple-corolla clade (Fig. 1B). All species in this clade have a purple corolla, but are diversified in their morphology of the stem, leaf, flower and fruit. Species of the circumboreal clade are distributed in northern China and Siberia (*H. inundatum* and *H. neglectum*), Europe (*H. hedysaroides*) and North America (*H. americanum*). Species of the eastern QTP clade (*H. sikkimense*, *H. tanguticum* and *H. algidum*) are distributed in the eastern Himalayas and the Hengduan Mountains. Thus, *H. qilianshanense* is isolated from other species of the purple-corolla clade (Fig. 5).

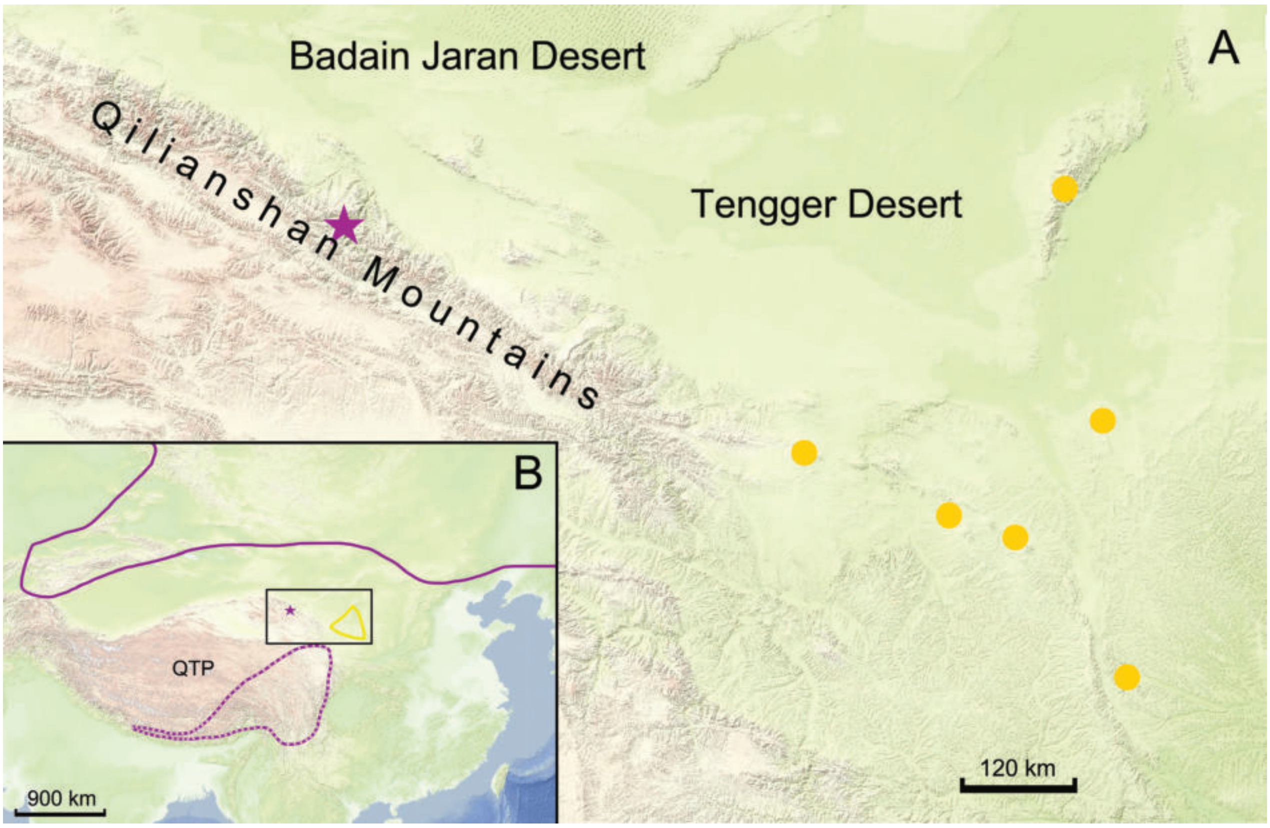

Figure 5. Distributions of *Hedysarum qilianshanense* and related species and clades. The purple star represents *H. qilianshanense*; yellow dots and the area surrounded by yellow line represent *H. przewalskii*; the area surrounded by the purple line represent the circumboreal clade; the area surrounded by the purple dotted line represent the eastern QTP clade. Purple or yellow indicates the corolla color. The black frame in Fig. 5B is enlarged in Fig. 5A. Maps from shaanxi.tianditu.gov.cn.

The incongruent position of *H. qilianshanense* in the nuclear and plastid gene trees indicates that *H. qilianshanense* may have originated from a hybridization event. The nuclear gene tree tracks one potential parent, probably an ancestor of *H. przewalskii*, and the plastid gene tree tracks the other potential parent, probably an ancestor in the purple-corolla clade. Morphologically, *H. qilianshanense* has similar stem, leaf and leaflet features as *H. przewalskii*, and the same corolla color with species of the purple-corolla clade.

A previous study (Choi and Ohashi 2003) concluded that the basic chromosome number of *H.* sect. *Hedysarum* is $x = 7$. Therefore, *H. qilianshanense* is most likely a diploid although chromosome pairing was not observed. *Hedysarum przewalskii* was also reported as diploid, $2n = 14$ [Yan et al. 1995, reported for *H. polybotrys* var. *alaschanicum* (B. Fedtsch.) H. C. Fu & Z. Y. Chu, a synonym of *H. przewalskii*]. In the purple-corolla clade, *H. hedysaroides*, *H. americanum*, *H. neglectum*, *H. sikkimense* and *H. tanguticum* were also reported as diploid, $2n = 14$, (Löve 1979, 1985; Yurkevich et al. 2021), and only *H. inundatum* was reported as tetraploid, $2n = 28$ (Löve 1981). The chromosome number of *H. algidum* is unknown.

In conclusion, based on the morphological, phylogenetic and karyotypic evidences, *H. qilianshanense* may have originated from homoploid hybrid speciation. Because of the allopatric distribution of *H. qilianshanense*, *H. przewalskii*, the circumboreal clade and the eastern QTP clade, the hybrid speciation is most likely to be an ancient, rather than a recent, event.

Acknowledgements

We are grateful to Hua Di in Gansu Qilianshan National Nature Reserve Administration for her great help during field expeditions. We thank curators of NWTC, US, WNU, WUK and XBGH for allowing us to examine the specimens. We thank Xiu-Zhen Wu for preparing the illustration.

Additional information

Conflict of interest

The authors have declared that no competing interests exist.

Ethical statement

No ethical statement was reported.

Funding

This research was funded by the National Natural Science Foundation of China (grant number 31900179) and the Basic Research Program of the Shaanxi Academy of Sciences (grant number 2023K-14).

Author contributions

Conceptualization: PLL, MY. Data curation: PLL, QXG. Funding acquisition: PLL, MY. Investigation: PLL, JQZ, YL, LLX. Methodology: PLL, QXG. Project administration: MY. Resources: PLL, JQZ. Supervision: MY. Visualization: PLL, QXG. Writing - original draft: PLL, QXG. Writing - review and editing: JQZ, YL, LLX, MY.

Author ORCIDs

Pei-Liang Liu https://orcid.org/0000-0001-6566-7824
Qian-Xi Guo https://orcid.org/0009-0002-9144-5752
Lu-Lu Xun https://orcid.org/0000-0002-6861-5883
Yuan Lu https://orcid.org/0000-0002-0329-0803
Ming Yue https://orcid.org/0000-0002-8618-1126

Data availability

The newly generated DNA sequences have been deposited in GenBank and the accession numbers can be found in Appendix 1.

References

Choi BH, Ohashi H (2003) Generic criteria and an infrageneric system for *Hedysarum* and related genera (Papilionoideae-Leguminosae). Taxon 52(3): 567–576. https://doi.org/10.2307/3647455

Choi BH, Endo Y, Zhu XY (2011) A new species of *Hedysarum* (Fabaceae, Hedysareae) from Xizang (Tibet), China. Korean Journal of Plant Taxonomy 41(3): 267–270. https://doi.org/10.11110/kjpt.2011.41.3.267

Darriba D, Taboada GL, Doallo R, Posada D (2012) jModelTest 2: More models, new heuristics and parallel computing. Nature Methods 9(8): 772. https://doi.org/10.1038/nmeth.2109

Duan L, Wen J, Yang X, Liu PL, Arslan E, Ertuğrul K, Chang ZY (2015) Phylogeny of *Hedysarum* and tribe Hedysareae (Leguminosae: Papilionoideae) inferred from sequence data of ITS, *matK*, *trnL-F* and *psbA-trnH*. Taxon 64(1): 49–64. https://doi.org/10.12705/641.26

Edgar RC (2004) MUSCLE: Multiple sequence alignment with high accuracy and high throughput. Nucleic Acids Research 32(5): 1792–1797. https://doi.org/10.1093/nar/gkh340

Kearse M, Moir R, Wilson A, Stones-Havas S, Cheung M, Sturrock S, Buxton S, Cooper A, Markowitz S, Duran C, Thierer T, Ashton B, Meintjes P, Drummond A (2012) Geneious Basic: An integrated and extendable desktop software platform for the organization and analysis of sequence data. Bioinformatics 28(12): 1647–1649. https://doi.org/10.1093/bioinformatics/bts199

Liu PL, Wei Y, Wen J, Chang ZY (2017a) Recognition of a new species of *Hedysarum* (Fabaceae, Hedysareae) from China based on morphological and molecular evidence. Phytotaxa 295(3): 237–245. https://doi.org/10.11646/phytotaxa.295.3.4

Liu PL, Wen J, Duan L, Arslan E, Ertuğrul K, Chang ZY (2017b) *Hedysarum* L. (Fabaceae: Hedysareae) is not monophyletic – Evidence from phylogenetic analyses based on five nuclear and five plastid sequences. PLOS ONE 12(1): e0170596. https://doi.org/10.1371/journal.pone.0170596

Liu PL, Chen XL, Lu Y, Chang ZY, Yue M (2019) New species discovered from old collections, the case of *Hedysarum wangii* sp. nov. (Fabaceae, Hedysareae). Phytotaxa 413(1): 27–38. https://doi.org/10.11646/phytotaxa.413.1.3

Löve Á (1979) IOPB Chromosome Number Reports LXIII. Taxon 28(1, 2/3): 265–279. https://doi.org/10.1002/j.1996-8175.1979.tb00499.x

Löve Á (1981) Chromosome Number Reports LXXIII. Taxon 30(4): 829–861. https://doi.org/10.1002/j.1996-8175.1981.tb04309.x

Löve Á (1985) Chromosome Number Reports LXXXIX. Taxon 34(4): 727–730. https://doi.org/10.1002/j.1996-8175.1985.tb04449.x

Nafisi H, Kazempour-Osaloo S, Mozaffarian V, Schneeweiss GM (2019) Molecular phylogeny and divergence times of the genus *Hedysarum* (Fabaceae) with special reference to section *Multicaulia* in Southwest Asia. Plant Systematics and Evolution 305(10): 1001–1017. https://doi.org/10.1007/s00606-019-01620-3

Ohashi H, Tateishi Y (1975) The Genus *Hedysarum* (Leguminosae) in the Himalayas. In: Ohashi H (Ed.) Flora of Eastern Himalaya Third Report. University Museum, University of Tokyo, Tokyo, 363–392.

Ronquist F, Huelsenbeck JP (2003) MrBayes 3: Bayesian phylogenetic inference under mixed models. Bioinformatics 19(12): 1572–1574. https://doi.org/10.1093/bioinformatics/btg180

Ronquist F, Teslenko M, van der Mark P, Ayres DL, Darling A, Höhna S, Larget B, Liu L, Suchard MA, Huelsenbeck JP (2012) MrBayes 3.2: Efficient Bayesian Phylogenetic Inference and Model Choice Across a Large Model Space. Systematic Biology 61(3): 539–542. https://doi.org/10.1093/sysbio/sys029

Stamatakis A (2014) RAxML version 8: A tool for phylogenetic analysis and post-analysis of large phylogenies. Bioinformatics 30(9): 1312–1313. https://doi.org/10.1093/bioinformatics/btu033

Swofford D (2002) PAUP* Phylogenetic Analysis Using Parsimony (*and Other Methods). Version 4. Sinauer Associates, Sunderland.

Wen J, Zhang J, Nie ZL, Zhong Y, Sun H (2014) Evolutionary diversifications of plants on the Qinghai-Tibetan Plateau. Frontiers in Genetics 5: 4. https://doi.org/10.3389/fgene.2014.00004

Xu LR, Choi BH (2010) *Hedysarum* L. In: Wu ZY, Raven PH, Hong DY (Eds) Flora of China, Vol. 10. Science Press, Beijing, Missouri Botanical Garden Press, St. Louis, 514–525.

Yan GX, Zhang SZ, Xue FH, Yun JF, Wang LY, Fu XQ (1995) The chromosome numbers of 35 forage species and their geographical distribution. Grassland of China 01: 16–20.

Yurkevich OY, Samatadze TE, Selyutina IY, Romashkina SI, Zoshchuk SA, Amosova AV, Muravenko OV (2021) Molecular Cytogenetics of Eurasian Species of the Genus *Hedysarum* L. (Fabaceae). Plants 10(1): 89. https://doi.org/10.3390/plants10010089

Appendix 1

Taxon name, geographical locality, voucher, herbarium code, and GenBank accession number for the sequences used in this study. For each sample, accession numbers are given for the ETS, ITS, *psbA-trnH*, *trnC-petN*, *trnL-F*, *trnS-G* and *petN-psbM* sequences. A dash (–) indicates a missing sequence. New sequences generated in this study are indicated by an asterisk (*).

Hedysarum algidum L. Z. Shue: China, Gansu, W. Q. Yang 2008010 (WUK), KY365837, KP338149, KP338400, KY366037, KP338272, KY365888, KY365987;

Hedysarum americanum (Michx.) Britton: Canada, Tuktut Nogait National Park, L. J. Gillespie et al. 8934 (US), KY365838, KP338150, KP338402, KY366038, KY366134, KY365889, KY365988;

Hedysarum astragaloides Benth. ex Baker: Pakistan, Punjab, W. Koelz 5024 (US), KY367282, KP338153, KP338405, KY367325, KP338275, OR971769*, KY367309;

Hedysarum cachemirianum Benth. ex Baker: Kashmir, Kishenganga Valley and the road to Nanga Parbat, R.R. & I.D. Stewart 18354 (US), KY367283, KY367300, KY367343, KY367326, OR971763*, –, KY367310;

Hedysarum campylocarpon H. Ohashi: China, Xizang, Jilong, Z.Y. Chang et al. 2013073 (WUK), KY367284, KY367301, KY367344, KY367327, –, –, KY367311;

Hedysarum campylocarpon H. Ohashi: China, Xizang, Nielamu, Z.Y. Chang et al. 2011203 (WUK), –, –, –, –, KP338279, OR971765*, –;

Hedysarum chinense (B. Fedtsch.) Hand.-Mazz.: China, Shaanxi, Ningshan, Z. M. Jiang 1565 (WUK), KY365842, KP338159, KP338412, KY366042, KP338280, KY365891, KY365992;

Hedysarum cisdarvasicum Kamelin & Karimova: Tajikistan, Darvaz, Yakhsu river. basin, R. Kamelin s. n. (TAD), MK639303, MK639233, MK639289, –, MK639275, MK639261, MK639247;

Hedysarum citrinum E. G. Baker: China, Xizang, Longzi, Y. S. Chen et al. 13-468. (WUK), OR971731*, OR982385*, OR971741*, OR971748*, OR971757*, OR971778*, –;

Hedysarum cuonanum P. L. Liu, J. Wen & Zhao Y. Chang: China, Xizang, Cuona, Y. S. Chen et al. 13-0948 (WUK), KY367286, KY367302, KY367345, KY367329, OR971764*, OR971767*, KY367312;

Hedysarum dentatoalatum K. T. Fu: China, Henna, Luanchuan, Z. Y. Chang et al. 2013267 (WUK), KY365844, KP338162, KP338415, KY366044, KP338283, KY365893, KY365994;

Hedysarum denticulatum Regel: Kyrgyzstan, Osh, Alay Valley, I. Sodombekov & N. Rogova KPL_00816 (MO), KY365845, KY366156, KY365760, –, KY366137, KY365894, KY365995;

Hedysarum falconeri Baker, Pakistan, Karakoram, O. Polunin 6096 (F), KY367287, KP338163, KP338416, KY367330, KP338284, OR971768*, KY367313;

Hedysarum hedysaroides Schinz & Thell.: Russia, Kamchatka, Tolbachik Volcano, S. McDonald & N. A. Brummitt 23 (US), KY365847, KP338168, KP338421, KY366046, KP338288, KY365896, KY365997;

Hedysarum inundatum Turcz.: China, Shanxi, Huangtudui 01313 (WUK), KY365848, KP338170, KP338423, KY366047, KP338290, KY365897, KY365998;

Hedysarum kumaonense Benth. ex Baker: China, Xizang, Jilong, Z. Y. Chang et al. 2013084 (WUK), KY367288, KP338174, KP338427, KY367331, KP338294, KY365899, KY367314;

Hedysarum lehmannianum Bunge: Tajikistan, Zeravshan range, Pastrud-darya river. basin, Turzun, Abdusalyamova, Zhogoleva & Ovchinnikov 4932 (TAD), MK639308, MK639238, MK639294, –, MK639280, MK639266, MK639252;

Hedysarum longigynophorum C. C. Ni: China, Xizang, Gongbujiangda, Z. Y. Chang. et al. QZ620 (WUK), KY367290, KP338175, KP338428, KY367333, KP338295, KY365900, KY367316;

Hedysarum minjanense Rech. f.: China, Xinjiang, Tashikuergan, Xizhixinjiangdui. 1091 (WUK), KY365852, KY366159, KY365763, –, KY366140, KY365902, KY366001;

Hedysarum nagarzense C. C. Ni: China, Xizang, Langkazi, L.R. Xu 1463 (WUK), KY367292, KY367305, KY367348, KY367335, OR971762*, OR971770*, KY367318;

Hedysarum neglectum Ledeb.: China, Xinjiang, Xinyuan, L. R. Xu 1533 (WUK), KY365853, KY366160, KY365764, KY366050, KY366141, KY365903, KY366002;

Hedysarum polybotrys Hand.-Mazz.: China, Gansu, Xiahe, Z. Y. Chang et al. QZ042. (WUK), KY365854, KP338182, KP338434, KY366051, KP338300, KY365905, KY366003;

Hedysarum przewalskii Yakovlev (Helanshan): China, Ningxia, Helanshan, R. B. Zhu. s. n. (WUK), OR971730*, OR982389*, OR971740*, OR971750*, OR971760*, OR971776*, –;

Hedysarum przewalskii Yakovlev (Jingtai): China, Gansu, Jingtai, Z. Y. Yu & Y. P. Xu 3255 (WUK), OR971729*, OR982390*, –, OR971751*, OR971761*, OR971775*, –;

Hedysarum qilianshanense P. L. Liu (Sidalong or Haplotype Ggap): China, Gansu, Su’nan, Sidalong, P. L. Liu 470 (WUK and WNU), OR971724*, OR982386*, OR971737*, OR971746*, OR971755*, OR971772*, OR971732*;

Hedysarum qilianshanense P. L. Liu (Wulin’gou or Haplotype Agap): China, Gansu, Su’nan, Wulin’gou, P. L. Liu 461 (WUK and WNU), OR971725*, OR982387*, OR971738*, OR971747*, OR971754*, OR971774*, OR971733*;

Hedysarum qilianshanense P. L. Liu (Xiaogushan or Haplotype AG): China, Gansu, Su’nan, Xiaogushan, P. L. Liu 458 (WUK and WNU), OR971726*, OR982388*, OR971739*, OR971745*, OR971756*, OR971773*, OR971734*;

Hedysarum semenowii Regel & Herder: Kazakhstan, Ulken, I. Roldugin 4823 (US), KY365856, KP338183, KP338435, KY366053, KP338301, KY365907, KY366005;

Hedysarum sikkimense Benth. ex Baker: China, Xizang, Yadong Y. S. Chen et al. 13-1772 (WUK), KY367294, KY367306, KY367349, KY367337, OR971753*, OR971771*, KY367320;

Hedysarum taipeicum (Hand.-Mazz.) K. T. Fu: China, Shaanxi, Mt. Taibai, P. L. Liu. 681-1 (WNU), OR971727*, OR982391*, OR971742*, OR971752*, OR971759*, OR971777*, OR971736*;

Hedysarum tanguticum B. Fedtsch.: China, Qinghai, Chengduo, Z. Y. Chang et al. 2010230 (WUK), KY365857, KP338188, KP338440, KY366056, KP338306, KY365910, KY366008;

Hedysarum tibeticum (Benth.) B. H. Choi & H. Ohashi: China, Xizang, Langkazi, Z. Y. Chang et al. 2011111 (WUK), KY367296, KP338189, KP338441, KY367339, KP338307, KY365911, KY367321;

Hedysarum ussuriense I. Schischkin & Kom.: China, Jilin, Mt. Changbai, M. Z. Sun. s. n. (WNU), OR971728*, OR982384*, OR971743*, OR971749*, OR971758*, –, OR971735*;

Hedysarum wangii P. L. Liu & Zhao Y. Chang: China, Gansu, Xiahe, Qu'ao, P. L. Liu. 432 (WUK and WNU), MK639312, MK639242, MK639298, OR971744*, MK639284, MK639270, MK639256;

Hedysarum xizangense C. C. Ni: China, Xizang, Longzi, Sananqulin, Y. S. Chen et al. 13-0886 (WUK), KY367297, KY367307, KY367350, KY367340, KP338310, OR971766*, KY367322.

PhytoKeys 237: 117–139 (2024)
DOI: 10.3897/phytokeys.237.107403

Research Article

Taxonomic dissection based on molecular evidence of the *Eriosyce curvispina* complex (Cactaceae): identifying nine endemic species from Central Chile

Helmut E. Walter[1], Arón Cádiz-Véliz[2,3,4], Beatriz M. Meriño[2,3], Heidy M. Villalobos-Barrantes[2,5,6], Pablo C. Guerrero[2,3,4],

1 *The EXSIS Project: Cactaceae Ex-Situ & In-Situ Conservation, 31860 Emmerthal, Germany*
2 *Departamento de Botánica, Facultad de Ciencias Naturales y Oceanográficas, Universidad de Concepción, Casilla 160C, 4030000, Concepción, Chile*
3 *Institute of Ecology and Biodiversity (IEB), Concepción, Chile*
4 *Millennium Institute Biodiversity of Antarctic and Sub-Antarctic Ecosystems (BASE), Concepción, Chile*
5 *Escuela de Química, Universidad de Costa Rica, CP 11501-2060, San José, Costa Rica*
6 *Centro de Investigación en Biología Celular y Molecular, Universidad de Costa Rica, CP 11501-2060, San José, Costa Rica*
Corresponding author: Pablo C. Guerrero (pabloguerrero@udec.cl)

Academic editor: Alice Calvente
Received: 2 June 2023
Accepted: 8 December 2023
Published: 22 January 2024

Citation: Walter HE, Cádiz-Véliz A, Meriño BM, Villalobos-Barrantes HM, Guerrero PC (2024) Taxonomic dissection based on molecular evidence of the *Eriosyce curvispina* complex (Cactaceae): identifying nine endemic species from Central Chile. PhytoKeys 237: 117–139. https://doi.org/10.3897/phytokeys.237.107403

Abstract

Chile's distinctive flora, geographical isolation, and complex topography collectively contribute to a notable endemic species diversity, particularly within central regions identified as critical areas for biodiversity conservation. The cactus genus *Eriosyce*, as currently circumscribed, encompasses seven sections, with *Eriosyce* sect. *Horridocatus* presenting a notably complex species group. This study investigates the *E. curvispina* complex, a member of the Notocacteae tribe common in central Chile, by incorporating new populations and examining phylogenetic relationships using four plastid and one nuclear molecular marker. The phylogenetic analysis of sampled individuals identified nine independent lineages, each warranting recognition at the species rank. Despite minimal morphological differences among taxa, morphological characters were utilized to support and stabilize the DNA-based phylogenetic hypothesis. The results highlight the high taxonomic diversity in these cactus lineages and have implications for the classification of the *E. curvispina* complex, including new combinations and proposals of conservation status.

Key words: Cactaceae, Caryophyllales, central Chile, *Eriosyce curvispina*, Horridocactus, new combinations, succulent plants, taxonomy

Resumen

La flora distintiva de Chile, su aislamiento geográfico y topografía compleja contribuyen colectivamente a una notable diversidad de especies endémicas, particularmente dentro de las regiones centrales identificadas como áreas críticas para la conservación de la biodiversidad. El género de cactus *Eriosyce*, tal como está circunscrito actualmente, abarca siete secciones, presentando *Eriosyce* sect. *Horridocatus* un grupo de especies notablemente complejo. Este estudio investiga el complejo *E. curvispina*, un miembro de la tribu Notocacteae común en Chile central, incorporando nuevas poblaciones y examinando las relaciones filogenéticas utilizando cuatro marcadores moleculares del cloroplasto y uno nuclear. El análisis filogenético de las poblaciones muestreadas identificó nueve linajes independientes, cada uno mereciendo reconocimiento a nivel de especie. A pesar de las mínimas diferencias morfológicas entre los taxones, se utilizaron caracteres morfológicos para apoyar y estabilizar la filogenia basada en ADN. Los resultados resaltan la alta diversidad taxonómica en estos linajes de cactus y tienen implicaciones para la clasificación del complejo *E. curvispina*, incluyendo nuevas combinaciones y propuestas de estado de conservación.

Palabras clave: Cactaceae, Caryophyllales, Chile central, *Eriosyce curvispina*, Horridocactus, plantas suculentas, taxonomía

Introduction

Chile has a unique flora with a great diversity of endemic species — a condition given by its geographical isolation from the rest of the South American continent (Arroyo et al. 2008; Scherson et al. 2017). Additionally, the complex topography, with two mountain ranges crossing the country from north to south and west to east, joined by transversal mountain ranges in the center of the country, favors the origin of narrow endemisms (Mardones and Scherson 2023). Central Chile has been identified as one of the priority areas of biodiversity worldwide (Myers et al. 2000) and characterized as one of the world's centers of cactus diversity (Hernández-Hernández et al. 2011). Many species belong to the tribe Notocacteae, one of the oldest and most diverse lineages in South America and are estimated to have diverged between 16–14.8 Ma (Arakaki et al. 2011; Hernández-Hernández et al. 2014). They are a heterogeneous tribe of mostly globose, small to medium-sized, mostly unbranched stems, and colorful diurnal flowers, with a great variety of forms (Guerrero et al. 2019a, b).

This study focuses on *Eriosyce* Phil., a genus of the Notocacteae with a long taxonomic with a high level of uncertainty, due to the long history of taxonomic changes since Rodulfo A. Philippi (Philippi 1872). In 1994, F. Kattermann merged five former genera (*Islaya* Backeb., *Pyrrhocactus* A. Berger, *Horridocactus* Backeb., *Neoporteria* Britton & Rose, and *Thelocephala* Y. Ito) into *Eriosyce*. The broad circumscription of *Eriosyce sensu* Kattermann (1994) was supported as monophyletic, only excluding *Rimacactus laui* (Lüthi) Mottram) (Guerrero et al. 2019b), and then all five former genera were regarded in synonym of a broad circumscribed *Eriosyce*. The genus *Eriosyce* harbors more than 50 species, has a relatively wide geographic distribution (between the latitudes of 13°–36°S and longitudes between 70°W and 66°W, altitudes ranging from sea level up to 2800 m.a.s.l.), and a large morphological heterogeneity (Guerrero et al. 2019b). Its current circumscription (Guerrero et al. 2019b) includes the following sections: I. *Eriosyce* sect. *Eriosyce* (Phil.) Katt. (distributed in Chile, Argentina & Peru; 5 accepted taxa), II. *Eriosyce* sect. *Campanulatae* P.C.Guerrero & Helmut Walter (endemic to Chile; 2 accepted taxa), III. *Eriosyce* sect. *Pyrrhocactus* (A. Berger) Katt. (endemic to Argentina; 4 accepted taxa), IV. *Eriosyce* sect. *Horridocatus* (Backeb.) Katt. (endemic to Chile; 12 accepted taxa), V. *Eriosyce* sect. *Diaguita* P.C.Guerrero & Helmut Walter (endemic to Chile; 3 accepted taxa), VI. *Eriosyce* sect. *Neoporteria* (Britton & Rose) Katt. (endemic to Chile; 15 accepted taxa), and VII. Unnamed section (endemic to Chile; 22 accepted taxa) (Guerrero et al. 2011a, b, 2019b).

In 1938, Backeberg erected the genus *Horridocactus* for a group of plants with 22 species from southern central to northern Chile based on a single character state – the lack of hairs on the pericarpel and hypanthium (in contrast to his genus *Neochilenia*) (Backeberg 1938). Yet, the monophyly of *Horridocactus sensu* Backeberg was not supported by molecular data (Guerrero et al. 2019b). Kattermann (1994) merged Backeberg's genera *Horridocactus* and *Neochilenia* into his *Eriosyce* section *Neoporteria*, subsection *Horridocactus*, which includes 14 species from south-central to northern Chile. Conversely, the findings of Villalobos-Barrantes et al. (2022) supported the monophyly of the *Eriosyce* section *Horridocactus*, which is circumscribed to include the following nine species: *E. armata* (F.Ritter) P.C.Guerrero & Helmut Walter, *E. aspillagae* (Söhrens) Katt., *E. cuvispina* (Bertero ex Colla) Katt., *E. duripulpa* (F.Ritter) P.C.Guerrero & Helmut Walter, *E. engleri* (F.Ritter) Katt., *E. garaventae* (F.Ritter) Katt., *E. jussieui* (Monv. ex Salm-Dyck) P.C.Guerrero & Helmut Walter, *E. limariensis* (F.Ritter) Katt. and *E. napina* (F.Ritter) Katt.

The oldest species in *Eriosyce* section *Horridocactus* – *Cactus curvispinus* Bertero ex Colla – was named by Bertero in 1829. However, the type specimen was lost, thus a neotype was designed by Kattermann (1994). During the last 200 years the species was placed in various genera by former authors: Gay (1847): *Echinocactus*; Britton and Rose (1922): *Malacocarpus*; Berger (1929): *Pyrrhocactus*; Kreuzinger (1941): *Hildmannia*; Backeberg (1940): *Horridocactus*; Donald and Rowley (1966): *Neoporteria* and, Kattermann (1994): *Eriosyce*. Various authors merged species and infraspecific taxa mostly erected by F. Ritter into an "*E. curvispina* complex" along several waves of lumping: Donald and Rowley (1966) merged 19 taxa into *Neoporteria curvispina* (Bertero ex Colla) Donald & Rowley. The "*E. curvispina* complex" *sensu* Hoffmann (1989) comprised 6 taxa (i.e. *Neoporteria curvispina* var. *marksiana* (F.Ritter) A. Hoffmann, *N. curvispina* var. *lissocarpa* (F.Ritter) Donald & Rowley, *N. curvispina* var. *engleri* (F.Ritter) A. Hoffmann, *N. curvispina* var. *andicola* (F.Ritter) Donald & Rowley, *N. curvispina* var. *grandiflora* (F.Ritter) Donald & Rowley and, *N. curvispina* var. *garaventae* (F.Ritter) Donald & Rowley.

In 1994, Kattermann merged six Ritter's species into the *E. curvispina* complex: *E. curvispina* var. *aconcaguensis* (F.Ritter) Katt., *E. curvispina* var. *armata* (F.Ritter) Katt., *E. curvispina* var. *choapensis* (F.Ritter) Katt., *E. curvispina* var. *mutabilis* (F.Ritter) Katt., *E. curvispina* var. *robusta* (F.Ritter) Katt. and *E. curvispina* var. *tuberisulcata* (Jacobi) Katt. (=*P. horridus* var. *horridus* F.Ritter). Furthermore, in 2006, Hunt et al. recognized only two of F. Ritter's species—*Pyrrhocactus armatus* F.Ritter and *P. marksiana* F.Ritter—as subspecies of *E. curvispina* and synonymized 11 Ritter´s taxa in *E. curvispina*. However, DNA-based phylogenetic analyses supported the exclusion of *E. armata*, *E. marksiana*, and *E. marksiana* var. *lissocarpa* from the complex (Guerrero et al. 2019b).

A recent study by Villalobos-Barrantes et al. (2022) included the nine species of *Horridocactus* provided new evidence by incorporating new locations and a new population scale molecular dataset (12 new pairs of nuclear microsatellites, SSR). This significantly enhanced our understanding of the evolutionary relationships among the species of the *Eriosyce* section *Horridocactus*. Despite this, no nomenclatural changes were proposed to update the species taxonomy following the genetic analyses. Our objectives were to incorporate more populations ascribed to the *E. curvispina* complex into a DNA-based phylogenetic hypothesis of *Eriosyce*, to evaluate its taxonomic identity, update its taxonomic treatment, and formalize nomenclature changes according to densely sampled phylogenetic inferences based on four plastids and a nuclear molecular marker, and finally, evaluate the conservation status of the delimited species based on IUCN criteria (2017).

Materials and methods

Plant material and DNA extractions

We examined specimens from the *E. curvispina* complex, including *E. curvispina* var. *aconcaguensis*, *E. curvispina* var. *choapensis*, *E. curvispina* var. *mutabilis*, *E. curvispina* var. *robusta*, and *E. curvispina* var. *tuberisulcata*, as proposed by Kattermann (1994), Hunt et al. (2006), and Guerrero et al. (2019b). Our study also revisited taxa previously included within the *E. curvispina* complex, such as *E. armata*, *E. marksiana*, and *E. marksiana* var. *lissocarpa*. The sampling sites (Fig. 1), were chosen to align with the historical localities of populations associated with the *E. curvispina* complex, as described by Ritter (1980) and Kattermann (1994). We included specimens from the type locality of *E. curvispina* near the Cachapoal River at Cerro La Leona (Bertero 1829; Kattermann 1994). Furthermore, we incorporated the nine species of the *Horridocactus* section into a comprehensive dataset of *Eriosyce* species from all sections. Samples were obtained from individuals spaced at least 30 m apart. A total of 105 samples, represented by 535 sequences (105 samples × 5 markers), were utilized. We incorporated 22 new samples, each sequenced for five markers, thereby contributing with 110 new sequences. This complements sequences previously published by our team in Guerrero et al. (2019b) and Villalobos-Barrantes et al. (2022). We collected plant fresh tissue from roots or flowers mainly and kept them in CTAB-NaCl buffer (2%:22%) to transport to the laboratory and store at -80 °C until the extraction.

For DNA extraction we used 40–50 mg of root or flower tissue that first was pulverized to a fine power using an automatic homogenizer and then total DNA was extracted using DNeasy Plant Kit (Qiagen, Valencia, California, USA). For the phylogenetic analysis, we amplified three noncoding chloroplast markers (*rpl32-trnL*, *trnH-psbA*, *trnL-trnF*), one plastid gene (*ycf1*), and one nuclear gene (PHYC) following the protocol described on Guerrero et al. (2019b). PCR products were checked on 1% agarose gels and then sent to Macrogen (Seoul, Korea) for sequencing in both directions. The DNA datasets can be found at the following link: https://github.com/pabloguerrero-cmd/E_curvispina, and the GenBank numbers of unpublished sequence data can be found in Suppl. material 1.

Phylogenetic inferences

A matrix of 105 samples, concatenated from five markers, was assembled, and edited using the program Geneious Prime 2023.1.2 (Biomatters Ltd.). Sequences for each marker were automatically aligned using Muscle and then checked manually. The outgroup consists of 6 species, most from the core Notocacteae. Each marker was aligned separately and then concatenated. A microsat-

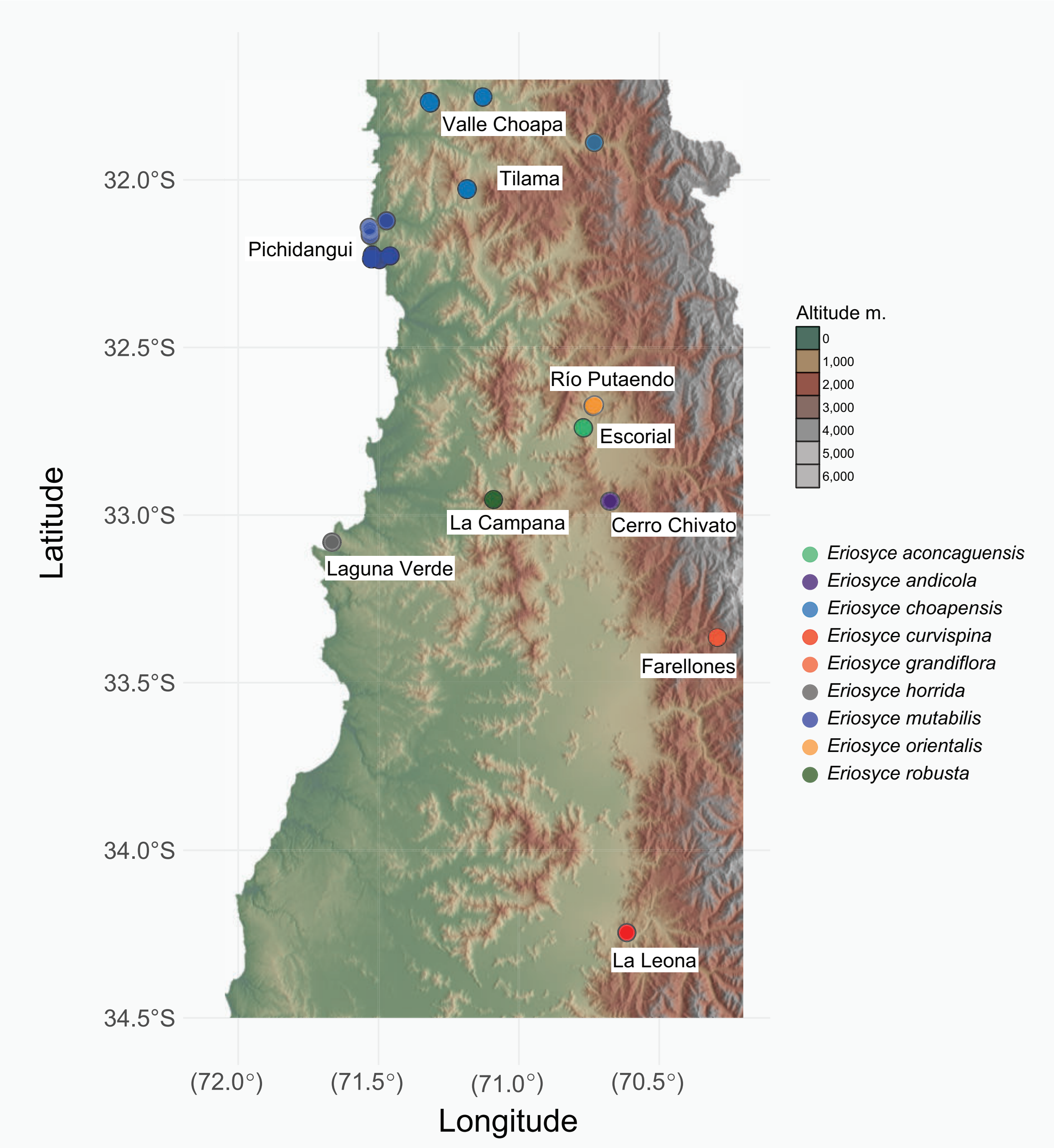

Figure 1. Locations of samples used in the study ascribed to the *Eriosyce curvispina* complex included in phylogenetic inferences.

ellite region in the *ycf1* dataset was excluded (450 bp) because of ambiguous alignment in this region. Best partitions and molecular models were evaluated using PartitionFinder v.2.1.1 as described in Guerrero et al. (2019b).

Bayesian inferences of the concatenated matrix were performed using Mr. Bayes v3.2.7 (Ronquist et al. 2012) using unlinked rate heterogeneity, based frequencies, and substitution rates across partitions. Bayesian ran for 30 million generations across four independent runs with four chains each, sampling every 1000 generations. The best models were GTR+G for *rpl32-trnL* and *trnH-ps-*

bA and GTR+G+I for the rest of the markers. Convergence was monitored using the standard deviation of split frequencies, and when this value stabilized below 0.01, it was considered a strong indication of convergence. The associated likelihood values, effective sample size (ESS) values, and burn-in values of the different runs were verified with the program Tracer v1.7.1 (Rambaut et al. 2018). Trees were visualized using software FigTree v1.4.4 (Rambaut 2016). Maximum likelihood (ML) analyses of the concatenated matrix were also performed using the program raxmlGUI 2.0 v.2.0.6 (Edler et al. 2021). The search for an optimal ML tree run combined with a rapid bootstrap analysis based on 100 trees and 1000 replicates.

Morphological characters

To establish morphological differences between species and build morphological descriptions and an identification key, we used the following diagnostic characters and their (discrete and quantitative) states: stems (habit, size, color); roots (fascicular/ tuberous, size); ribs (shape, size, number); areoles (shape, indumentum, distance, size, color); spines (shape, size, number, color); flowers (pericarpel and hypantium: size, color, indumentum; perianth segments: shape, color; ovary: shape, size; style: size, color); fruit (shape, color, size); seeds (shape, size; testa: color, surface).

Extinction risk assessment

We evaluated the extinction risk of each species by applying the IUCN Red List Categories and Criteria (version 3.1, IUCN 2017). This involved calculating the species' extent of occurrence (EOO) using the spatial tools provided by Google Earth. Additionally, we systematically documented threats based on empirical evidence gathered during fieldwork. The assessments followed a structured approach where the known distribution ranges were analyzed in accordance with Criterion B of the IUCN guidelines. This criterion focuses on geographic range size, the degree of fragmentation, and the level of decline or fluctuation in population size, range, or habitat quality, enabling a comprehensive evaluation of the species' risk of extinction.

Results

The alignment encompasses a total of 4841 nucleotides across 105 individuals, with informative sites varying for each marker, amounting to 2440 for the complete matrix and 1958 for the ingroup (Table 1). The concatenated matrix, which amalgamates all loci, has a total length of 4841 base pairs, with 1565 variable characters within the ingroup, 1754 total variable characters, and 747 parsimony-informative characters. Specifically, the plastid non-coding marker *rpl32-trnL* contributed with 1354 bp (36% of variable sites), *trnL-trnF* contributed with 1084 bp (11%), and *trnH-psbA* contributed with 439 bp (3%). Meanwhile, the plastid gene *ycf1* contributed with 930 bp (24%), and the nuclear gene PHYC contributed with 1034 bp, being the locus with 25% of variable sites.

Table 1. Statistics for the 105-sample DNA sequence alignments.

Locus	Total length	Ingroup, variable characters	Total variable characters	Parsimony-informative characters	Ingroup coverage (%)	Outgroup coverage (%)	% variability
rpl32-trnL	1354	594	640	286	93	11	36
trnL-trnF	1084	161	195	91	83	23	11
trnH-psbA	439	36	55	27	65	18	3
ycf1	930	341	417	223	82	40	24
PHYC	1034	433	447	120	97	7	25
Concatenated matrix	4841	1565	1754	747			

The molecular variation in coding regions is low compared with non-coding regions in general, but all this information was considered in the phylogenetic reconstruction by the Bayesian analysis. A well-supported phylogenetic tree was obtained, indicating nine different lineages of the *E. curvispina* complex (Fig. 2). Two strongly supported clades (A and B) were recovered for the *Eriosyce* section *Horridocactus*: Clade A harbors four independent lineages previously assigned to the *E. curvispina* complex between the latitudes of 32°S and 33°S: The six accessions from the Río Putaendo (HV 34, HV 38, BV 420, BV 422, BC 423, BV 424) were placed as sister to the rest of Clade A. The six accessions from El Escorial (HV 52, HV 56, BV 430, BV 431, BV 432, BV 433) were placed as sister to the four accessions from Pichidangui (PG 513, PG 522, PG 554, and PG 1250) and one from Laguna Verde (BV 230).

Clade B is home to several putative members of the *E. curvispina* complex, which comprises four distinct lineages. Firstly, there is a group of four accessions (PG 1621, PG 1623, PG 1624, PG 1625) collected at the type locality of *E. curvispina* in Cerro La Leona, east of Rancagua at 34°S. This group forms a well-supported subclade. Secondly, there is a robust group comprising three specimens, also identified as members of the *E. curvispina* complex, that were collected from various localities in the hills north of the latitude of 32°S. These specimens include Valle Choapa (PG 1200) and Tilama (PG 1221 and PG 1222). This group is placed sister to *E. limariensis* (F.Ritter) Katt. Finally, there is a subclade that harbors accessions from Farellones, east of Santiago (PG 1317, PG 1318), Cerro Chivato (ACVEA 1, ACVEA 2), and Ocoa (HV 68, HV 70), all located at 33°S. These accessions form a strongly supported group.

The *Eriosyce* section *Horridocactus* contains several taxa that are scattered across various branches. The northernmost species in this section form a subclade that includes *E. napina* (Phil.) Katt, *E. napina* var. *lembckei* Katt., *E. duripulpa* (F.Ritter) P.C.Guerrero & Helmut Walter. This subclade is followed by a subclade consisting of *E. armata* (F.Ritter) P.C.Guerrero & Helmut Walter from the hills southwest of Santiago, as well as the two southern taxa *E. aspillagae* (F. Ritter) Katt. and *E. aspillagae* subsp. *maechlerorum* Helmut Walter (located at 34'30°–36°S). Additionally, *E. garaventae* (F.Ritter) Katt. and *E. engleri* (F.Ritter) Katt., both found in the high coastal mountains at 33°S, form a small subclade. Finally, the sister pair *E. heinrichiana* var. *setosiflora* (F.Ritter) Katt. and *E. jussieui* (Monville ex Salm-Dyck) P.C.Guerrero & Helmut Walter, which occur around the latitude of 30°S, also form a small subclade.

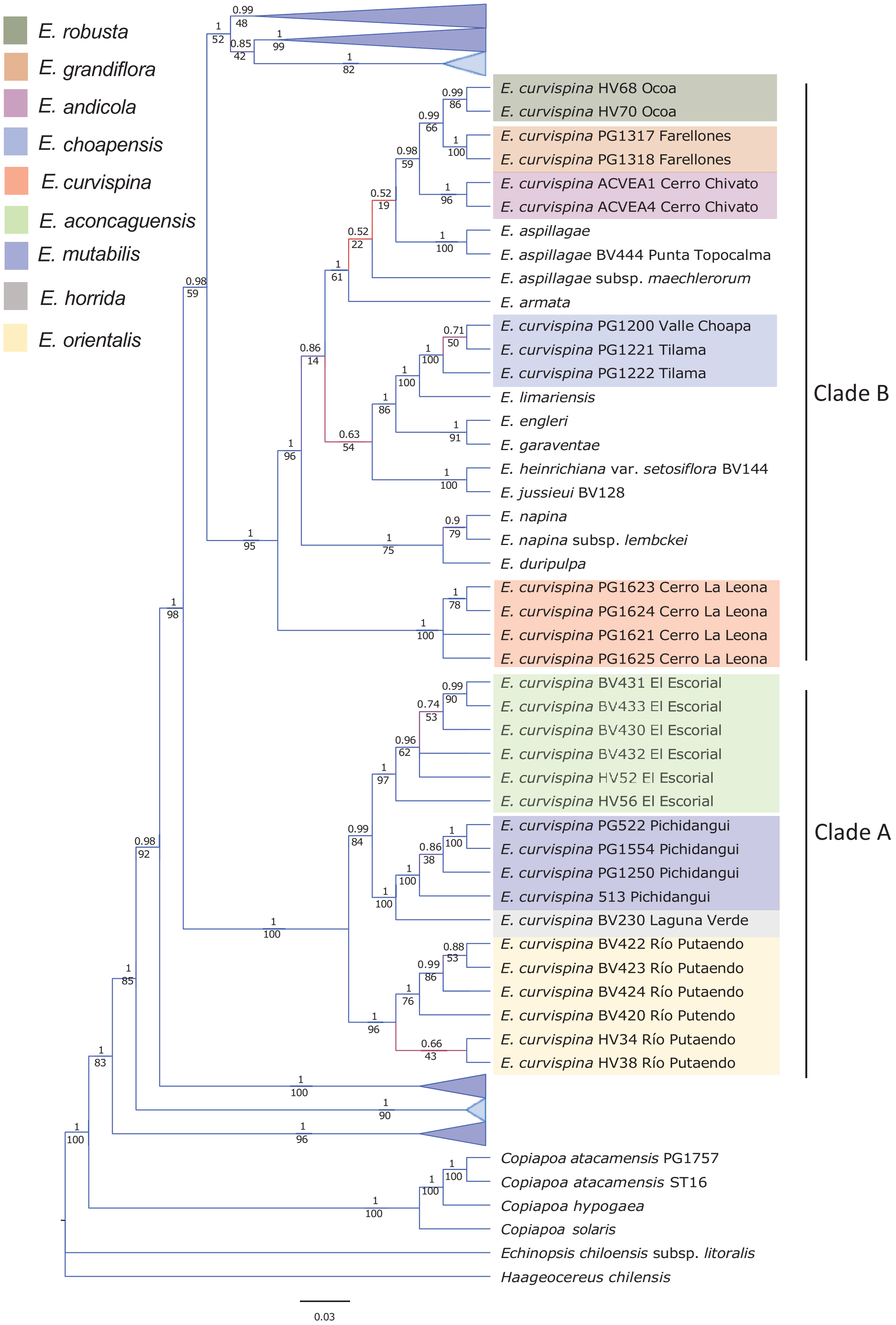

Figure 2. Phylogenetic position of putative members of the *Eriosyce curvispina* species complex. All sections of *Eriosyce* are collapsed, except for the *Eriosyce* section *Horridocactus*.

Discussion

This incorporation of accessions from previously unexplored populations in this study has substantially deepened our comprehension of the *E. curvispina* complex within the *Eriosyce* section *Horridocactus*, leading to a re-evaluation of its taxonomic classification (Guerrero et al. 2019b; Villalobos-Barrantes et al. 2022; Walter and Guerrero 2022). Phylogenetic assessments based on comprehensive sampling reveal that the presumed monophyletic nature of the *E. curvispina* complex is not supported, as certain populations are aligned with different genetic lineages. Additionally, the inclusion of samples from regions such as Cerro Leona in the Province of Cachapoal and in Putaendo in the Province of San Felipe de Aconcagua has prompted significant alterations to the previously established main clades of this complex (Villalobos-Barrantes et al. 2022). While most internal nodes in the phylogenetic tree received strong support, some exhibit only moderate support. To enhance the resolution of these nodes, the application of genomic data is recommended.

In our study, we conducted a focused examination of four accessions from Bertero's (1829) original location "Cachapoal, Chile". This locality is situated approximately 100 km south of Santiago and contrasts with F. Ritter's (1980) type locality "Department Santiago, between 1000 and 2000 m" for his *Pyrrhocactus curvispinus*. Our phylogenetic analyses reveal that the samples from Bertero's locality form a distinct clade, separated from the two accessions collected from east Santiago (Ritter's reported locality for *P. curvispinus*) and other subspecies proposed by Kattermann (1994). These findings support a nomenclatural reevaluation, as the Farellones specimens and Kattermann's subspecies cannot be accurately classified under the epithet *'curvispinus*.' Given that the Farellones specimens' morphology and geographic location align more closely with *Pyrrhocactus grandiflora*, as described by Ritter from 'Cerro Ramón, east of Santiago, above 2000 m,' we propose adopting this name (updating in a new combination) for the Farellones populations to maintain nomenclatural continuity without the need for new taxon names. Our results prompt a significant reorganization of the taxa previously included in the *E. curvispina* complex, ensuring that the nomenclature accurately reflects the phylogenetic relationships and geographical distributions.

Our phylogenetic inference aligns with the study by Villalobos-Barrantes et al. (2022) and provides further insight into the evolutionary relationships within section *Horridocactus*, revealing great complexity in species diversity and their geographic patterns. In that study, at the population level, SSR data revealed substantial genetic divergence even among closely related species, as seen in the case of the Ocoa population (*E. robusta*) and its closest relatives located in Farellones (*E. grandiflora*) and Cerro Chivato (*E. andicola*). High genetic divergence supports their recognition at species rank together with some morphological differences (see section taxonomic treatment and key). Also, the accessions from Tilama and Valle Choapa are supported to be species in their own right (*E. choapensis*) as they are not grouped with other putative members of the *E. curvispina* complex. Furthermore, the populations present low genetic differences inferred from SSR analyses (Villalobos-Barrantes et al. 2022). Some populations distributed in similar habitats can present substantial population genetic divergence, such as the population from

Pichidangui (*E. mutabilis*), compared to the southern population located in Laguna Verde (*E. horrida*) (Villalobos-Barrantes et al. 2022), supporting their recognition as a species in its own. An interesting pair of populations are those from Escorial (*E. aconcaguensis*) and the Putaendo river (*E. orientalis*), they were grouped in different branches in the phylogenetic tree. However, despite the limited morphological differences, we developed a morphological key that circumscribes monophyletic species, according to the results of the phylogenetic analyses, accompanied by detailed descriptions of these taxa. This highlights the importance of confirming previously described morpho-species using molecular data.

The new molecular-based classification of *Eriosyce* section *Horridocactus* demands the search for diagnostic morphological characters to complement the results obtained with the DNA-based phylogenetic tree. This task is challenging because these species possess few distinguishing features, which has led to past taxonomic synonymization. The historically controversial phylogenetic placement of the large *E. curvispina* complex suggests a combination of processes that have led to the current diversity, with species exhibiting similar morphologies but distinct evolutionary trajectories. The previous concept of *E. curvispina* included a wide distribution of its taxonomic entities, from near sea level to above 2000 m.a.s.l. elevation in the Andes, and between the latitudes 30°S and 36°S. The segregation of the *E. curvispina* complex implies a smaller distribution area for the species delimited here; this has consequences for the extinction risk assessment of taxa.

Conclusion

The phylogenetic analysis of the *E. curvispina* complex, together with the phylogeographic analyses by Villalobos-Barrantes et al. (2022) revealed the presence of nine distinct lineages within the complex (Fig. 3). Two major clades, Clade A and Clade B, were strongly supported. Clade A harbored four independent lineages found between the latitudes of 32°S and 33°S (Río Putaendo, El Escorial, Pichidangui, and Laguna Verde). Clade B comprised four lineages previously considered within the *Eriosyce curvispina* complex, such as the accessions from Cerro La Leona, Valle Choapa, Tilama, Farellones, Cerro Chivato and Ocoa. These results challenge the monophyly of previously defined species complexes within *Eriosyce*, including *E. curvispina*, and support the need to revise these complexes taxonomically. Additionally, our results have implications for the conservation status of the species, which we reassess according to the IUCN guidelines.

Taxonomic key to the Eriosyce section *Horridocactus*

1 Perianth segments narrowly lanceolate **2**
– Perianth segments broad, often spathulate with a short tip **14**
2 Stems 2–10 cm diameter, grey-green to grey-brown, often pruinose, fruits elongated, perianth remnant attachment area small; taproots always present.. **3**
– Stems 10–20 cm., usually green, never pruinose; fruits short, ovoid to barrel-shape, perianth remnant attachment area large; roots various **5**

3 Ribs dissolved into tubercles arranged in parastichies; spines very short.... **4**

– Ribs arranged in orthostichies; spines significantly longer .... ***E. jussieui***

4 Stems never elongating, tubercles large; spines black; pericapel and hypanthium covered with brownish wool and black bristles......... ***E. napina***

– Stems extending with age; tubercles small, spines ranging from horn-colored to white; flowers covered with white wool and white bristles............. .... ***E. duripulpa***

5 Stems usually not branching **6**

– Stems with a tendency towards basal branching **13**

6 Stems often elongating, spines numerous, often obscuring the stem...... **7**

– Stems subglobose to globose, with fewer spines..................................... **8**

7 Spines long, from white to yellowish, dark-tipped, turning gray with age; floral bristles few, only near hypanthium rim................................ ***E. engleri***

– Spines shorter, yellow, not turning with age; bristles abundant, covering the hypanthium.. ***E. garaventae***

8 Roots fascicular from short taproots.. **9**

– Roots fascicular (with the exception of *E. aspillagae*) **13**

9 Stems up to 15 cm in diameter; ovary substantially elongated; spines up to 4 cm; taproot thick .... ***E. limariensis***

– Stems to 10 cm; ovary shorter; spines 1–2 cm; taproot thin... ***E. choapensis***

10 Stems 10–20 cm in diameter; ribs 16–24; areoles 1–2 cm long, 1–2 cm apart **11**

– Stems 8–12 cm in diameter; ribs 14–16; areoles smaller of 6 × 4 mm and 6 mm apart; spines 1–2.5 cm; flowers 5–5.5 cm .... ***E. curvispina***

11 Ribs 1.5–2 cm high; areoles 6–10- × 5 mm; pericarpel green.................. **12**

– Ribs to 2.5(-3) cm high; areoles larger, 7–20 × 5–8 mm; pericarpel reddish-grown .... ***E. robusta***

12 Spines numerous, finely acicular with lower portion whitish and upper one brownish-reddish, banded; flowers 5 cm; style white; seed large, 1.5 × 1 mm .... ***E. andicola***

– Spines less numerous, stout, blackish-brown, not bicolored nor banded; flowers up to seven cm; style red; seed small, 1 × 0.7 mm .... ***E. grandiflora***

13 Fruit dry, dehiscing by partial circumscissile splitting; spines finely acicular; ribs broad and low.. ***E. aspillagae***

– Fruit-wall fleshy when ripe, dehiscence not as above; spines thicker; ribs steep and narrower .... ***E. armata***

14 Stems consistently green; spines acicular, curved upwards.................... **15**

– Stems either green or brownish; spines thicker and usually straight **16**

15 Ribs 1.5 cm high; areoles 1.5 cm apart; yellow funnel-form flowers with inner perianth segments lemon yellow without a mid-stripe .... ***E. aconcaguensis***

– Ribs 1 cm high; areoles 0.5–0.7 cm apart; pericarpel and hypanthium tube dark violet; exterior perianth segments purple, inner ones pale yellow with a red mid-stripe.. ***E. orientalis***

16 Stems green,10–20 cm diameter, non-branching; spines 1–2.5 cm, very thick; perianth segments reddish with a dark purple mid-stripe....... ***E. horrida***

– Stems often brownish, often branching, 10–15 cm diameter, spines stout 1–5 cm, perianth segments pale yellowish often with a red midstripe....... .... ***E. mutabilis***

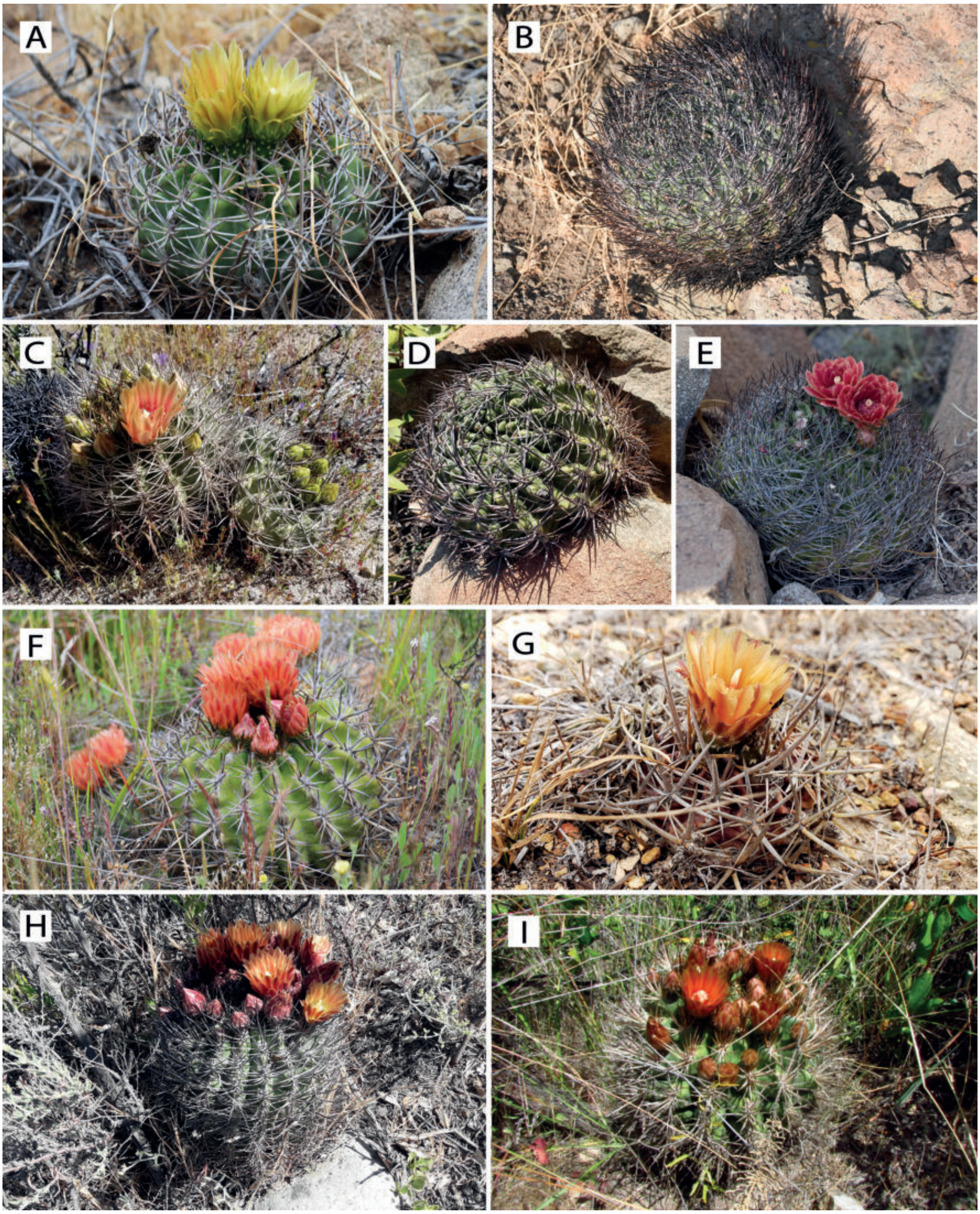

Figure 3. Species of *Eriosyce curvispina* complex **A** *E. aconcaguensis* **B** *E. andicola* **C** *E. choapensis* **D** *E. curvispina* **E** *E. grandiflora* **F** *E. horrida* **G** *E. mutabilis* **H** *E. orientalis* **I** *E. robusta*. Photographs: Arón Cádiz-Véliz (**A, B, F**), Pablo Guerrero (**C, D, G**), Joaquín Keymer (**E**), Heidy Villalobos-Barrantes (**H**), Griselle Guerrero (**I**).

Taxonomic treatment

1. ***Eriosyce aconcaguensis*** (F.Ritter) P.C.Guerrero & Helmut Walter, comb. nov.

urn:lsid:ipni.org:names:77334726-1

Pyrrhocactus aconcaguensis F. Ritter, Succulenta (NL) 9: 108. 1960. Basionym.

≡ *Pyrrhocactus aconcaguensis* F.Ritter in Succulenta (Netherlands) 1960: 108. 1960 syn. sec. Tropicos ≡ *Horridocactus aconcaguensis* (F.Ritter) Backeb., Cactaceae 6: 3791. 1962 syn. sec. Tropicos ≡ *Eriosyce curvispina* var. *aconcaguensis* (F.Ritter) Katt., *Eriosyce* (Cactac.) Gen. Revis. Ampl. 1: 117. 1994 syn. sec. Kew WCVP (2019) ≡ *Neoporteria curvispina* var. *aconcaguensis* (F.Ritter) Donald & G.D.Rowley in Cact. Succ. J. Gr. Brit. 28: 55. 1966 syn. sec. Kew WCVP (2019) ≡ *Pyrrhocactus horridus* var. *aconcaguensis* (F.Ritter) F.Ritter, Kakteen Südamerika 3: 948. 1980 syn. sec. Kew WCVP (2019) ≡ *Pyrrhocactus curvispinus* var. *felipensis* F.Ritter, Kakteen Südamerika 3: 932: 1980 (nom. inval. Art. 34.1, 37.1). In our text, "syn. sec." refers to the source that assigns a synonym to the concept of either the accepted name or one of its homotypic synonyms *sensu* Korotkova et al. (2021).

Type. CHILE, Southern America, Valparaíso Region, Catemu, Chagres, June 1955, *F. Ritter 542* (Holotype: U 0249247, digital image!). (Image available at https://bioportal.naturalis.nl/en/specimen/U__0249247).

Iconography. F. Ritter, Succulenta (NL) 9: 108. 1960 (as *Pyrrhocactus aconcaguensis*); A. Hoffmann & H.E. Walter, Cact. Fl. Sylv. Chile 2nd Ed., Lam. 71a (as *Eriosyce curvispina* var. *aconcaguensis*) 2004.

Morphological notes. Stems globose, 8–12 cm. diameter, sometimes elongating with age. Roots fascicular. Ribs 17–21, 1.5 cm high, obtuse. Areoles 1.5 × 0.6 cm., 1.0–1.5 cm apart. Spines grey, thickly aciculate, mostly straight, or somewhat curved; radial ones 7–12, 1–3 cm long, central ones 4–6, to 4 cm long. Flowers 4–5 cm, funnel-form; pericarpel green, not much elongated, bract-scales small, axils with inconspicuous white hairs; nectary tubular; style white with 14 whitish stigma-lobes; perianth segments yellow, usually with a faint reddish mid-stripe, 0.6–1.2 cm broad. Fruits barrel-form, 1.5–2.5 cm long, reddish, bract-scales as for the pericarpel; perianth remnant attachment area wide, basal pore large. Seeds blackish, 1.2×1 mm; testa finely tuberculate, coarsely ribbed; hilum oval; micropyle in a groove.

Distribution. Endemic species occurring in the middle Río Aconcagua Valley, between Llay-llay and San Felipe (32°S, 70°W) at elevations generally between 500 and 700 m.

Conservation status. The extent of occurrence (EOO) of *E. aconcaguensis* is estimated to be less than 100 km^2, with fewer than 5 known localities. The species range is severely fragmented, and there has been a decrease in population size and the number of localities due to landscape anthropization. Additionally, there has been a loss of habitat quality due to the expansion of the agricultural and mining industry. The population from the type locality at Chagres (Llay-llay) is likely extinct due to the replacement of xerophytic vegetation by extensive cultivation of avocado trees on slopes between Llay-llay and San Felipe. Therefore, we propose to classify the species as Critically Endangered (CR) according to the criteria (2017) B1ab(i,iii,iv).

2. *Eriosyce andicola* (F.Ritter) P.C.Guerrero & Helmut Walter, comb. nov.

urn:lsid:ipni.org:names:77334727-1

Horridocactus andicola F. Ritter, Succulenta (NL) 7: 97. 1959. Basionym.

≡ *Pyrrhocactus andicola* (F.Ritter) F.Ritter in Succulenta (Netherlands) 10: 131. 1959 syn. sec. Hunt (1999) ≡ *Neoporteria curvispina* var. *andicola* (F.Ritter) Donald & G.D.Rowley in Cact. Succ. J. Gr. Brit. 28: 55. 1966 syn. sec. Kew WCVP (2019)

= *Horridocactus andicola* var. *descendens* F.Ritter in Succulenta (Netherlands) 7: 97. 1959 syn. sec. Kew WCVP (2019) ≡ *Neoporteria curvispina* f. *descendens* (F.Ritter) Donald & G.D.Rowley in Cact. Succ. J. Gr. Brit. 28: 55. 1966 syn. sec. Kew WCVP (2019)

= *Horridocactus andicola* var. *robustus* F.Ritter in Succulenta (Netherlands) 7: 97. 1959 syn. sec. Kew WCVP (2019) ≡ *Pyrrhocactus andicola* var. *robustus* (F.Ritter) F.Ritter in Succulenta (Netherlands) 1959: 131. 1959 syn. sec. Kew WCVP (2019) ≡ *Pyrrhocactus andicola* var. *mollensis* F. Ritter, Succulenta (NL) 10: 131. 1959.

Type. Chile, Southern America, Valparaíso Region, Cerro Chivato between Santiago and Los Andes, May 1955, *F. Ritter 468* (Holotype: U 0249335, digital image!). (Image available at https://bioportal.naturalis.nl/en/specimen/U__0249335).

Iconography. F. Ritter, Kakt. Sudam. 3: 1980 (as *Pyrhocactus andicola* var. *robustus*); A.E. Hoffmann, Cact. Fl. Sylv. Chile, Lamina 53 a. 1989 (as *Neoporteria curvispina* var. *andicola*).

Morphological notes. Stems globose, more than 20 cm high with age, apex spiny, 12–16 cm diameter, not branching. Roots fasciculate. Ribs 16–24 cm, 10–15 mm high, notched and somewhat chinned below areoles. Areoles 7–12 mm long and 5–7 mm broad, 1 cm apart. Spines finely aciculate, lower half whitish, upper ones brownish-reddish, dark or light banded; radial spines 10–14, 2–3 cm long, central ones 4–7 cm, somewhat curved upward, 3–4 cm long. Flowers ca. 5 cm, funnel-form; pericarpel and tube green, interior white, bract scales tiny, yellowish, axils with white inconspicuous thin bristles and scarce wool; perianth segments 0.7–1cm broad, spathulate with short tips; lemon- to olive-yellow, often with a narrow pale purple central stripe; style basally widened, whitish; stigma-lobes whitish; filaments whitish; nectary tubular; ovary elongated. Fruit pale red, 1.5 cm, barrel-shape; bract-scales inconspicuous; basal pore large; perianth remnant attachment wide. Seeds ca. 1.5 mm, short ovoid; testa black, opaque, finely tuberculate; ventrally strongly bulged, notched below hilum; hilum shortly ovoid, position ventral.

Distribution. Endemic species occurring between the Rio Molles (30°S, 70°W) and Cerro Chivato (33°S, 70°W) at altitudes between 1000 and 2000 m.

Conservation status. The Extent of Occurrence (EOO) of *E. andicola* is estimated to be < 20.000 km^2, with its populations severely fragmented due to landscape anthropization. There has been an estimated decrease in population size and the number of localities, as well as a loss of habitat quality due to mining activities, stump removal, and livestock. We propose to classify the species as Vulnerable (VU) according to criteria B1ab(i,iii,iv).

3. *Eriosyce choapensis* (F.Ritter) P.C.Guerrero & Helmut Walter, comb. nov.

urn:lsid:ipni.org:names:77334728-1

Pyrrhocactus choapensis F. F.Ritter, Succulenta (NL)12: 133. 1960. Basionym.

≡ *Pyrrhocactus choapensis* F.Ritter in Succulenta (Netherlands) 1960: 133. 1960 syn. sec. Tropicos ≡ *Horridocactus choapensis* (F.Ritter) Backeb., Cactaceae 6: 3793. 1962 syn. sec. Tropicos ≡ *Neoporteria choapensis* (F.Ritter) Donald & G.D.Rowley in Cact. Succ. J. Gr. Brit. 28: 55. 1966 syn. sec. Tropicos ≡ *Eriosyce curvispina* var. *choapensis* (F.Ritter) Katt., *Eriosyce* (Cactac.) Gen. Revis. Ampl. 1: 117. 1994 syn. sec. Kew WCVP (2019).

Type. CHILE, Southern America, Coquimbo Region, Choapa, Illapel, May 1954, *F. Ritter 238* (Holotype: ZSS 005073, Isotypes: SGO, ZSS).

Iconography. F. Ritter, Kakt. Sudam. 3, 1980.

Morphological notes. Stems subglobose, dark green, often burnt brownish, 5–10 cm diameter Roots fascicular with a short thin taproot. Ribs 15–22, obtuse, deeply notched, 1.0–1.5 cm high. Areoles long-oval, 1cm, 1 cm apart. Spines are thin, acicular, grey-brown, short, 1–2 cm; radial ones 8–10, somewhat curved; central ones 4–9, somewhat thicker. Flowers funnel-form, 3.5–4.5 cm; pericarpel and hypanthium bract scales tiny, red, axils with white inconspicuous wool; nectary isodiametric; style pinkish, stigma lobes yellow; perianth segments narrow lanceolate, pale yellow with a faint purple mid-stripe. Fruits 1.5–2 cm, barrel-form, indumentum as for the flower; perianth remnant attachment area wide, basal pore large. Seeds small, 0.8–9 mm, round oval, blackish brown; testa cells arranged in ribs, medium-domed; hilum oval, positioned nearly basal, micropyle in a groove.

Distribution. Endemic species occurring strictly inland, from Illapel (31°S, 71°W) to Tilama (32°S, 71°W) at elevations between 400 and 1200 m.

Conservation status. The Extent of Occurrence (EOO) of *E. choapensis* is estimated at < 5000 km^2, with its populations severely fragmented due to landscape anthropization. There has been an estimated decrease in population size and the number of localities, as well as a loss of habitat quality due to mining activities, stump removal, and livestock. We propose to classify the species as Endangered (EN) according to criteria B1ab(i,iii,iv).

4. *Eriosyce curvispina* (Bertero ex Colla) Katt.

Cactus curvispinus Bertero ex Colla in Mem. Reale Accad. Sci. Torino 37: 76. 1834 syn. sec. Hunt et al. (2006). Basyonym.

≡ *Cactus curvispinus* Bertero ex Colla in Mem. Reale Accad. Sci. Torino 37: 76. 1834 syn. sec. Hunt et al. (2006) ≡ *Echinocactus curvispinus* (Bertero ex Colla) Gay, Fl. Chil. 3: 16. 1848 syn. sec. Kew WCVP (2019) ≡ *Malacocarpus curvispinus* (Bertero ex Colla) Britton & Rose, Cactaceae 3: 203. 1922 syn. sec. Kew WCVP (2019) ≡ *Pyrrhocactus curvispinus* (Bertero ex Colla) A.Berger, Kakteen: 345. 1929 syn. sec. Kew WCVP (2019) ≡ *Horridocactus curvispinus* (Bertero ex Colla) Backeb. in Kakteenkunde 1940: 51. 1940 syn. sec. Kew WCVP (2019) ≡ *Hildmannia curvispina* (Bertero ex Colla) Kreuz. & Buining in Repert. Spec. Nov. Regni Veg. 50: 207. 1941 syn. sec. Kew WCVP (2019) ≡ *Neoporteria curvispina* (Bertero ex Colla) Donald & G.D.Rowley in Cact. Succ. J. Gr. Brit. 28: 55. 1966 syn. sec. Kew WCVP (2019) *Neoporteria curvispina* (Bertero ex Colla) Don. & Rowl., Cact. Succ. J. (GB) 28: 55. 1966; *Pyrrhocactus curvispinus* var. *mostazalensis* F.Ritter, Kakt. Sudam. 3: 932. 1980 (nom.

inval., Art. 34.1, 37.1); *Pyrrhocactus curvispinus* var. *australis* F. Ritter, Kakt. Sudam. 3:932. 1980 (nom. inval., Art. 34.1, 37.1).

Type. Chile, Southern America, O' Higgins Region, Cachapoal (Locotypus). Neotype (designated by F. Kattermann 1994): Colla, l.c.t. 16.2. [132].

Iconography. F. Kattermann, Succ. Pl. Res. 1, Pl. 6.5 and 6.6. 1994.

Morphological notes. Stems dark green, subglobose to globose, not elongating with age; 8–12 cm diameter Roots fascicular. Ribs 14–16, well pronounced, 1–1.5 cm high, notched below areoles, tubercles chinned. Areoles with short wool, oval, 6 × 4 mm, 6 mm apart. Spines horn-coloured, turning grey, acicular, curved; 10–12 radials, curved sideward, 1–2 cm; 1–4 centrals, strongly curved upward, 2–2.5 cm. Flowers diurnal, funnel-form, 5 cm; pericarpel and hypanthium with small bract scales, axils with inconspicuous wool, upper ones with short fine bristles; perianth segments lanceolate, 6 mm wide, yellowish with a reddish mid-stripe of different width; nectary tubular; style reddish, stigma lobes yellow to pale red; ovary isodiametric to elongate. Fruits covered as for the flower, short barrel-shape, 1.5–2 cm, reddish to red brown; perianth remnant attachment area large, basal pore large; fruit wall thick. Seeds oval, 1.3 × 1.2 mm; testa blackish brownish, evenly tuberculate, not ribbed, cells high domed; hilum narrow oval; position oblique; micropyle in a groove.

Distribution. The endemic species occurs from the Rio Maipo Valley (34°S, 70°W) to the Rio Maule Valley (36°S, 70°W) at strictly inland habitats between 1000 and 2000 m.

Conservation status. The Extent of Occurrence (EOO) of *E. curvispina* is estimated at < 20,000 km^2, with its populations severely fragmented due to landscape anthropization. There has been an estimated decrease in population size and the number of localities. Additionally, there has been a loss of habitat quality due to urban expansion, mining activities, forest fires, agriculture, livestock, and stump removal. We propose to classify the species as Vulnerable (VU) according to criteria B1ab(i,iii,iv).

5. *Eriosyce grandiflora* (F.Ritter) P.C.Guerrero & Helmut Walter, comb. nov.

urn:lsid:ipni.org:names:77334729-1

Pyrrhocactus grandiflorus F.Ritter, Succulenta (NL) 4: 41. 1960. Basyonym.

≡ *Pyrrhocactus grandiflorus* F.Ritter in Succulenta (Netherlands) 4: 41. 1960 syn. sec. Kew WCVP (2019) ≡ *Horridocactus grandiflorus* (F.Ritter) Backeb., Cactaceae 6: 3796. 1962 syn. sec. Kew WCVP (2019) ≡ *Neoporteria curvispina* var. *grandiflora* (F.Ritter) Donald & G.D.Rowley in Cact. Succ. J. Gr. Brit. 28: 56. 1966 syn. sec. Kew WCVP (2019) ≡ *Pyrrhocactus curvispinus* var. *santiagensis* F. Ritter, Kakt. Südamerika 3: 932. 1980 (nom. inval., Art. 34.1, 37.1).

Type. Chile, Southern America, Santiago Region, San Ramón, 2000 m, May 1955, *F. Ritter 469* (Holotype: U 0249323, digital image!). (Image available at https://bioportal.naturalis.nl/en/specimen/U__0249323).

Iconography. F. Ritter, Kakt. Südam. 3, 1980.

Morphological notes. Stems simple, grey-green, subglobose, 10–18 cm diameter Roots fascicular. Ribs many, 21–24, 1–1.5 cm high, notched below areoles, tubercles with chin-like protrusions. Areoles 6 × 10 × 5 mm, up to 1.2 cm apart. Spines are acicular, blackish-brown; radial ones 9–12, straight or somewhat curved upward, 1.5–3 cm; central ones 4–7, curved upward, 2–4 cm. Flowers large, 6–7 cm, pericarpel and hypanthium with small bract scales, axils with very short wool, upper ones with short fine bristles; perianth segments lanceolate, 7–10 mm wide and 3.5–4.5 cm long, red with a darker mid-stripe; nectary tubular; style white, superior portion pale reddish, stigma lobes yellow; ovary isodiametric to somewhat elongate. Fruits 1.5 cm, covered as for the flower, short barrel-shape, 1.5 cm, reddish to red brown; perianth remnant attachment area large, basal pore large; fruit wall thick. Seeds 1 × 0.8 mm; testa blackish brownish, evenly tuberculate, not ribbed, cells medium-domed; hilum oval; position oblique.

Distribution. Endemic species occurring from east of Santiago (33°S, 70°W) to the upper Río Aconcagua Valley (32°S, 70°W) at high altitudes, around 2000 m.

Conservation status. The Extent of Occurrence (EOO) of *E. grandiflora* is estimated at < 5000 km^2, with presence in 5 or less locations. It is estimated that there will be a decrease in population size and number of localities, loss of habitat quality due to mining activities, opening of roads, livestock and stump removal. We propose to classify the species as Endangered (EN) according to the criteria B1ab(i,iii,iv).

6. *Eriosyce horrida* (Remy ex Gay) P.C.Guerrero & Helmut Walter, comb. nov.

urn:lsid:ipni.org:names:77334730-1

Echinocactus horridus Remy ex Gay, Fl. Chil. 3: 15. 1848. Basyonym.

≡ *Cactus horridus* Colla in Mem. Reale Accad. Sci. Torino 37: 76. 1834 syn. sec. Hunt et al. (2006) ≡ *Echinocactus horridus* Gay, Fl. Chil. 3: 15. 1848 syn. sec. Tropicos ≡ *Pyrrhocactus horridus* (Colla) Backeb., Kaktus-ABC: 264. 1936 [“1935”] syn. sec. Kew WCVP (2019) ≡ *Horridocactus horridus* (Colla) Backeb. in Kakteenkunde 1940: 51. 1940 syn. sec. Tropicos ≡ *Hildmannia horrida* (Colla) Kreuz. & Buining in Repert. Spec. Nov. Regni Veg. 50: 207. 1941 syn. sec. Kew WCVP (2019) ≡ *Neoporteria horrida* (Gay) D.R.Hunt in Bradleya 5: 93. 1987 syn. sec. Kew WCVP (2019) = *Echinocactus tuberisulcatus* Jacobi in Allg. Gartenzeitung 24: 108. 1856 syn. sec. Korotkova et al. (2006) ≡ *Malacocarpus tuberisulcatus* (Jacobi) Britton & Rose, Cactaceae 3: 202–203. 1922 syn. sec. Korotkova et al. (2006) ≡ *Pyrrhocactus tuberisulcatus* (Jacobi) A.Berger, Kakteen: 215. 1929 syn. sec. Korotkova et al. (2006) ≡ *Horridocactus tuberisulcatus* (Jacobi) Y.Itô, Cacti, ed. 2: 80. 1952 syn. sec. Korotkova et al. (2006) ≡ *Neoporteria tuberisulcata* (Jacobi) Donald & G.D.Rowley in Cact. Succ. J. Gr. Brit. 28: 58. 1966 syn. sec. Korotkova et al. (2006) ≡ *Eriosyce curvispina* var. *tuberisulcata* (Jacobi) Katt., *Eriosyce* (Cactac.) Gen. Revis. Ampl.1: 117. 1994 syn. sec. Korotkova et al. (2006) ≡ *Pyrrhocactus odoriflorus* F.Ritter in Succulenta (Netherlands) 1960: 116. 1960 syn. sec. Kew WCVP (2019) ≡ *Neochilenia odoriflora* (F.Ritter) Backeb., Cactaceae 6: 3778. 1962 syn. sec. Kew WCVP (2019) ≡ *Neoporteria horrida* var. *odoriflora* (F.Ritter) A.E.Hoffm., Cact. Fl. Silvestre Chile: 190. 1989 syn. sec. Kew WCVP (2019).

Type. CHILE, Southern America, Valparaíso Region, Valparaíso (Locotypus). Lectotype (designated by F. Kattermann 1994): Bertero (TO) [171].

Iconography. Kattermann, Succ. Pl. Res. 1, Pl. 7 (5) as “var. *horrida*”(sic!), and as *E. curvispina* var. *tuberisulcata*). 1994; C. Bacheberg, Das Kakteenlexikon, Abb. 170, 171. 1977 (as *Horridocactus tuberisulcatus*).

Morphological notes. Stems green, 10–20 cm diameter Ribs 14–18(-20), ca. 1.5 cm high, deeply notched. Areoles 0.7–1.8 × 0.5–1.0 cm. Spines brown, later grey, usually thick, only slightly curved upward; radials 9–12, 1–2 cm, central ones 4–8, 1.5–3 cm long. Flowers funnel-form, 4–5 cm; pericarpel bract-scales small, axils usually with inconspicuous wool, hypanthium sometimes with tortuous bristles; perianth segments 1–1.2 cm broad with short tips, mostly reddish with a dark purple mid-stripe, sometimes rose with a pale mid-stripe; ovary isodiametric, style reddish, stigma-lobes yellow. Fruits barrel-shape, 1.5 cm, indumentum as for the pericarpel; perianth remnant attachment area wide, basal pore large. Seeds 0.8–1 mm, round oval, opaque, blackish brown; testa finely tuberculate, only slightly ribbed; hilum oval, position ventrally oblique, micropyle in a groove.

Distribution. Endemic species, occurring on low coastal hills between south of Valparaíso (33°S, 71°W) and Papudo (32°S, 71°W).

Conservation status. The Extent of Occurrence (EOO) of *E. horrida* is estimated to be < 5000 km^2, with its populations severely fragmented by urban areas, forest lands, and electric highways. It is estimated that there will be a decrease in the population size and number of localities, loss of habitat quality due to expansion of the real estate industry, forest fires and stump removal. We propose to classify the species as Endangered (EN) according to the criteria B1ab(i,iii,iv).

7. *Eriosyce mutabilis* (F.Ritter) P.C.Guerrero & Helmut Walter, comb. & stat. nov.

urn:lsid:ipni.org:names:77334731-1

Pyrrhocactus horridus var. *mutabilis* F. Ritter, Kakt. Sudam. 3: 946. 1980. Basyionym.
≡ *Eriosyce curvispina* var. *mutabilis* (F.Ritter) Katt., Succ. Pl. Res. 1: 117. 1994.

Type. Chile, Southern America, Coquimbo Region, coastal spur N of Los Vilos, December 1955, *F. Ritter 223b* (Holotype: U 0249320, digital image!). (Image available at https://bioportal.naturalis.nl/en/specimen/U__0249320).

Iconography. F. Ritter, Kakt. Sudam. 3, 1980; F. Kattermann, Succ. Pl. Res. 1, 1994.

Morphological notes. Stems green, often burnt brownish, branching, 8–15 cm diameter Ribs ca. 16, 1.2 cm high, deeply notched. Areoles oval, 0.6–1.0 long. Spines brown, later grey, thickly acicular; radials 9–12, 1–3.5 cm, slightly bent; central ones 3–7, 1.5–4 cm long, shorter ones straight, longer ones bent upward. Flowers funnel-form, 3–4 cm; pericarpal and hypantium bract-scales small, axils with inconspicuous wool; perianth segments 1–1.2 cm broad with short tips, pale yellow or brownish yellowish, often with a pale reddish mid-stripe of various width; ovary isodiametric, style reddish, stigma-lobes yellow. Fruits barrel-shape, 1.5 cm, indumentum as for the flower; perianth remnant attachment area wide, basal pore large. Seeds 0.9–1.1 mm, round oval, opaque, brown; testa tuberculate and ribbed; hilum oval, position ventrally oblique, micropyle in a groove.

Distribution. Endemic species, occurring between Los Vilos (31°S, 71°W) and Los Molles (32°S, 71°W), near the coast.

Conservation status. the extent of occurrence (EOO) of *E. mutabilis* is estimated to be less than 100 km^2, with its populations severely fragmented by population centers and road openings. Additionally, there has been a decrease in population size and the number of localities, as well as a loss of habitat quality due to real estate expansion, forest fires, and destemming. We propose to classify the species as Critically Endangered (CR) according to criteria B1ab(i,iii,iv).

8. *Eriosyce orientalis* (F.Ritter) P.C.Guerrero & Helmut Walter, comb. & stat. nov.

urn:lsid:ipni.org:names:77334732-1

Pyrrhocactus aconcaguensis var. *orientalis* F. Ritter, Succulenta (NL) 9: 109. 1960. Basionym.

≡ *Horridocactus aconcaguensis* var. *orientalis* (F.Ritter) Backeb., Cactaceae 6: 3791. 1962 syn. sec. Kew WCVP (2019) ≡ *Pyrrhocactus horridus* var. *orientalis* (F.Ritter) F.Ritter, Kakteen Südamerika 3: 949. 1980 syn. sec. Kew WCVP (2019) ≡ *Neoporteria curvispina* f. *orientalis* (F.Ritter) Donald & G.D.Rowley in Cact. Succ. J. Gr. Brit. 28: 55. 1966 syn. sec. Kew WCVP (2019).

Type. Chile, Southern America, Valparaíso Region, San Felipe, Las Coimas, June 1955, *F. Ritter 542a* (Holotype: U 0249247, digital image!). (Image available at https://bioportal.naturalis.nl/en/specimen/U__0249247); (Isotype: SGO 121636!).

Iconography. H.M. Villalobos-Barrantes et al., Genes, 2022.

Morphological notes. Stems pale green, globose 7–14 cm diameter, globose. Ribs ca. 20, obtuse, 1 cm high; tubercles small, somewhat chinned. Areoles small, 0.5–0.7 × 0.4–0.5 cm, 1 cm apart. Spines 2–4 cm acicular; radial ones 7–9, 0.5–1.5 cm long, radiating, straight to somewhat curved; centrals 3–6, mostly curved upward, 3–4 cm. Flowers 4–5 cm, funnel-form; pericarpel and hypanthium dark purple, with small scales, axils with inconspicuous white wool; perianth segments 6–8 mm wide with a long tip; interior ones pale yellowish, with a broad faint reddish mid-stripe, exterior ones purple; ovary isodiametric; style white. Fruits ca. 1.5 cm, barrel-form; indumentum as for the flower; perianth remnant attachment area wide, basal pore large.

Distribution. Endemic species, occurring around Putaendo (32°S, 70°W) at elevations between 600–1900 m.

Conservation status. It is estimated that the Extent of Occurrence (EOO) of *E. orientalis* is less than 100 km^2, with its main population restricted to the dry bed of the Putaendo river, severely fragmented by the construction of roads and aggregate extraction centers. A registered population in the Rocín River (Las Tejas Sector) is threatened by mining. There is an estimated decrease in population size and the number of localities, as well as a loss of habitat quality due to the increase in micro-dumps, mining, and vine removal. We propose to classify the species as Critically Endangered (CR) according to criteria B1ab(i,iii,iv).

9. *Eriosyce robusta* (F.Ritter) P.C.Guerrero & Helmut Walter, comb. nov.

urn:lsid:ipni.org:names:77334733-1

Pyrrhocactus robustus F. Ritter, Succulenta (NL) 6: 65. 1960. Basyonym.

≡ *Pyrrhocactus robustus* F.Ritter in Succulenta (Netherlands) 1960: 65. 1960 syn. sec. Tropicos ≡ *Pyrrhocactus horridus* var. *robustus* (F.Ritter) in Kakteen in Südamerika 3: 947 ≡ *Neochilenia robusta* (F.Ritter) Backeb., Cactaceae 6: 3781. 1962 syn. sec. Tropicos ≡ *Eriosyce curvispina* var. *robusta* (F.Ritter) Katt., *Eriosyce* (Cactac.) Gen. Revis. Ampl. 1: 117. 1994 syn. sec. Kew WCVP (2019) ≡ *Neoporteria tuberisulcata* var. *robusta* (F.Ritter) Donald & G.D.Rowley in Cact. Succ. J. Gr. Brit. 28: 58. 1966 syn. sec. Kew WCVP (2019) ≡ *Neoporteria curvispina* f. *robusta* (F.Ritter) Donald & G.D.Rowley in Cact. Succ. J. Gr. Brit. 28: 55. 1966 syn. sec. Kew WCVP (2019) ≡ *Pyrrhocactus horridus* var. *robustus* (F.Ritter) F.Ritter, Kakteen Südamerika 3: 947. 1980 syn. sec. Kew WCVP (2019) = *Pyrrhocactus robustus* var. *vegasanus* F.Ritter in Succulenta (Netherlands) 1960: 65. 1960 syn. sec. Kew WCVP (2019) ≡ *Neochilenia robusta* var. *vegasana* (F.Ritter) Backeb., Cactaceae 6: 3783. 1962 syn. sec. Kew WCVP (2019) ≡ *Neoporteria tuberisulcata* var. *vegasana* (F.Ritter) Donald & G.D.Rowley in Cact. Succ. J. Gr. Brit. 28: 58. 1966 syn. sec. Kew WCVP (2019).

Type. Chile, Southern America, Valparaíso Region, Quillota, Ocoa, *F. Ritter 239a* (Holotype: U 0249318, digital image!). (Image available at https://bioportal.naturalis.nl/en/specimen/U__0249318).

Iconography. F. Ritter, Kakt. Sudam. 3: 1980; A. Hoffmann & H. E. Walter, Cact. Fl. Sylv. Chile 2nd Ed., Lam. 72b (as *Eriosyce curvispina* var. *robusta*) 2004; F. Kattermann, Succ. Pl. Res 1, 1994.

Morphological notes. Stems globose, somewhat elongating with age, 10–20 cm diameter Roots fascicular. Ribs 13–20, broad, obtuse and 1.5–3.0 high, deeply notched, tubercles with a long chin. Areoles 0.7–2 × 0.5–0.8 cm, 1–4 cm apart. Spines mostly stout, gray-brown, the shorter ones mostly straight, the longer ones somewhat curved upward; radial ones 7–12, 1–3 cm long; central ones 1–8, 1–4 cm. Flowers 4–5 cm, funnel-form; pericarpel and hypanthium with small scales, axils with inconspicuous white wool, pericarpel much elongated, brownish-red; perianth segments lanceolate, 0.5–1.0 cm, lower part purple or carmin, superior part pale yellowish; ovary elongated; style whitish, superior part pink. Fruits1–2 × 0.5–1 cm, long barrel-form; indumentum as for the flower; perianth remnant attachment area wide, basal pore large. Seeds 1.2 mm, round ovate, opaque, brownish blackish; testa coarsely tuberculate and ribbed; hilum nearly round, position ventrally oblique, micropyle in a groove.

Distribution. Endemic species occurring in the region around the National Park La Campana (32°S, 71°W).

Conservation status. It is estimated that the Extent of Occurrence (EOO) of *E. robusta* is < 5000 km^2, with its population severely fragmented by urban centers, electric highways and agro-industrial crops. It is estimated there will be a decrease in the population size and number of localities, loss of habitat quality due to urban expansion and agro-industry, forest fires and stump removal. We propose to classify the species as Endangered (EN) according to criteria B1ab(i,iii,iv).

Acknowledgements

We would like to thank Corporación Nacional Forestal (CONAF) for allowing us to work in their protected units through the permit 2/2021. We thank Joaquín Keymer and Griselle Guerrero for allowing us to use their photographs.

Additional information

Conflict of interest

The authors have declared that no competing interests exist.

Ethical statement

No ethical statement was reported.

Funding

This study was funded by the FONDECYT 1211441 grant and the ANID PIA/BASAL FB210006 grant. H.M.V.B. is grateful to the Graduate Scholarship Program of Universidad de Concepción and IAPT research grant Awarded 2019 (www.iaptglobal.org/awarded-grants, accessed on 20 January 2022). A.C.V. is grateful to the ANID Scholarship 21231651. B.M.M is grateful to the ANID Scholarship 20210673.

Author contributions

HEW and PCG conceptualized the project, while BMM, HMVB, and PCG carried out the fieldwork and sampling. The analysis of fieldwork data was conducted collaboratively by BMM, HMVB, and PCG. HEW, ACV, and PCG wrote the manuscript with feedback from all coauthors.

Author ORCIDs

Arón Cádiz-Véliz https://orcid.org/0000-0002-7548-1764
Beatriz M. Meriño https://orcid.org/0000-0002-9518-2331
Heidy M. Villalobos-Barrantes https://orcid.org/0000-0003-3657-4439
Pablo C. Guerrero https://orcid.org/0000-0003-1034-1899

Data availability

All of the data that support the findings of this study are available in the main text or Supplementary Information.

References

Arakaki M, Christin PA, Nyffeler R, Lendel A, Eggli U, Ogburn RM, Spriggs E, Moore MJ, Edwards EJ (2011) Contemporaneous and recent radiations of the world's major succulent plant lineages. Proceedings of the National Academy of Sciences of the United States of America 108(20): 8379–8384. https://doi.org/10.1073/pnas.1100628108

Arroyo MTK, Marquet P, Marticorena C, Simonetti J, Cavieres L, Squeo F, Rozzi R, Massardo F (2008) El hostpot chileno, prioridad mundial para la conservación. In: Ugalde RJ, Stutzin M (Eds) Biodiversidad de Chile, Patrimonio y Desafíos. CONAMA, Ocho Libros Editores, Santiago, 90–93.

Backeberg C (1938) Zur systematischen Uebersicht. Blätt. Kaksteenf 6: 1–13.

Backeberg C (1940) *Pyrrhocactus* und *Horridocactus*. Kakteenkunde: 49–53.

Berger A (1929) Kakteen. Anleitung zur Kultur und Kenntnis der wichtigsten eingeführten Arten. Eugen Ulmer, Stuttgart, 346 pp.

Bertero C (1829) Mercurio Chileno, Santiago 13: e598.

Britton NL, Rose JN (1922) The Cactaceae: descriptions and illustrations of plants of the cactus family (Vol. 3). The Carnegie Institution, Washington DC, 255 pp.

Donald DS, Rowley GD (1966) Reunion of the genus *Neoporteria*. The Cactus and Succulent Journal of Great Britain 28: 54–83.

Edler D, Klein J, Antonelli A, Silvestro D (2021) raxmlGUI 2.0: A graphical interface and toolkit for phylogenetic analyses using RAxML. Methods in Ecology and Evolution 12(2): 373–377. https://doi.org/10.1111/2041-210X.13512

Gay C (1847) Historia física y política de Chile. Botánica 2: 426–466.

Guerrero PC, Arroyo MTK, Bustamante RO, Duarte M, Hagemann TK, Walter HE (2011a) Phylogenetics and predictive distribution modelling provide insights into the geographic divergence of *Eriosyce* subgenus *Neoporteria* (Cactaceae). Plant Systematics and Evolution 297(1–2): 113–128. https://doi.org/10.1007/s00606-011-0512-5

Guerrero PC, Durán AP, Walter HE (2011b) Latitudinal and altitudinal patterns of the endemic cacti from the Atacama desert to mediterranean Chile. Journal of Arid Environments 75(11): 991–997.https://doi.org/10.1016/j.jaridenv.2011.04.036

Guerrero PC, Majure LC, Cornejo-Romero A, Hernández-Hernández T (2019a) Phylogenetic relationships and evolutionary trends in the cactus family. The Journal of Heredity 10(1): 4–21. https://doi.org/10.1093/jhered/esy064

Guerrero PC, Walter HE, Arroyo MTK, Peña CM, Tamburrino I, De Benidictis M, Larridon I (2019b) Molecular phylogeny of the large South American genus *Eriosyce* (Notocacteae, Cactaceae): Generic delimitation and proposed changes in infrageneric and species ranks. Taxon 68(3): 557–5573. https://doi.org/10.1002/tax.12066

Hernández-Hernández T, Hernández HM, De-Nova JA, Puente R, Eguiarte LE, Magallón S (2011) Phylogenetic relationships and evolution of growth form in Cactaceae (Caryophyllales, Eudicotyledoneae). American Journal of Botany 98(1): 44–61. https://doi.org/10.3732/ajb.1000129

Hernández-Hernández T, Brown JW, Schlumpberger BO, Eguiarte LE, Magallón S (2014) Beyond aridification: Multiple explanations for the elevated diversification of cacti in the New World succulent biome. The New Phytologist 202(4): 1382–1397. https://doi.org/10.1111/nph.12752

Hoffmann AE (1989) Cactáceas en la Flora Silvestre de Chile. Ediciones Fundación Claudio Gay, Santiago de Chile, 272 pp.

Hunt D (1999) CITES Cactaceae Checklist. Royal Botanic Gardens Kew, Richmond, 315 pp.

Hunt D, Taylor N, Charles G (2006) The new Cactus Lexicon (1st ed., 2 vols). DH Books, Milborne Port.

IUCN (2017) Guidelines for using the IUCN red list categories and criteria, version 13. Prepared by the Standards and Petitions Subcommittee of the IUCN Species Survival Commission. http://www.iucnredlist.org/documents/RedListGuidelines.pdf

Kattermann F (1994) *Eriosyce* (Cactaceae): The Genus Revised and Amplified. Succulent Plant Research 1. Privately published by David Hunt, Richmond, 176 pp.

Korotkova N, Aquino D, Arias S, Eggli U, Franck A, Gómez-Hinostrosa C, Guerrero PC, Hernández HM, Kohlbecker A, Köhler M, Luther K, Majure LC, Müller A, Metzing D, Nyffeler R, Sánchez D, Schlumpberger B, Berendsohn WG (2021) Cactaceae at Caryophyllales. org–a dynamic online species-level taxonomic backbone for the family. Willdenowia 51(2): 251–270. https://doi.org/10.3372/wi.51.51208

Kreuzinger KG (1941) Bemerkungen zu einigen Gattung der Cactaceae. Repertorium Specierum Novarum Regni Vegetabilis 50: 193–210. https://doi.org/10.1002/fedr.19410501302

Mardones D, Scherson RA (2023) Hotspots within a hotspot: Evolutionary measures unveil interesting biogeographic patterns in threatened coastal forests in Chile. Botanical Journal of the Linnean Society 20(4): 1–16. https://doi.org/10.1093/botlinnean/boad002

Myers N, Mittermeier R, Mittermeier C, Da Fonseca G, Kent J (2000) Biodiversity hotspots for conservation priorities. Nature 403(6772): 853–858. https://doi.org/10.1038/35002501

Philippi RA (1872) Descripción de las plantas nuevas incorporadas últimamente en el herbario chileno. Anales de la Universidad de Chile 41: 663–746.

Rambaut A (2016) FigTree v1.4.4. Institute of Evolutionary Biology, University of Edinburgh, Edinburgh. http://tree.bio.ed.ac.uk/software/figtree/ [Accessed 10.01.2023]

Rambaut A, Drummond AJ, Xie D, Baele G, Suchard MA (2018) Posterior summarization in bayesian phylogenetics using tracer 1.7. Systematic Biology 67(5): 901–904. https://doi.org/10.1093/sysbio/syy032

Ritter F (1980) Kakteen in Südamerika (Vol. 3). Spangenberg: Friedrich Ritter Selbstverlag, 1238 pp.

Ronquist F, Teslenko M, van der Mark P, Ayres DL, Darling A, Höhna S, Larget B, Liu L, Suchard MA, Huelsenbeck JP (2012) MrBayes 3.2: Efficient bayesian phylogenetic inference and model choice across a large model space. Systematic Biology 61(3): 539–542. https://doi.org/10.1093/sysbio/sys029

Scherson RA, Thornhill AH, Urbina-Casanova R, Freyman WA, Pliscoff PA, Mishler BD (2017) Spatial phylogenetics of the vascular flora of Chile. Molecular Phylogenetics and Evolution 112: 88–95. https://doi.org/10.1016/j.ympev.2017.04.021

Villalobos-Barrantes HM, Meriño BM, Walter HE, Guerrero PC (2022) Independent evolutionary lineages in a globular cactus species complex reveals hidden diversity in a Central Chile biodiversity hotspot. Genes 13(2): e240. https://doi.org/10.3390/genes13020240

Walter HE, Guerrero PC (2022) Towards a unified taxonomic catalogue for the Chilean cacti: Assembling molecular systematics and classical taxonomy. Phytotaxa 550(2): 79–98. https://doi.org/10.11646/phytotaxa.550.2.1

WCVP (2019) World Checklist of Vascular Plants. Version 2019. Royal Botanic Gardens, Kew. https://powo.science.kew.org/about-wcvp

Supplementary material 1

New accessions of taxa used in the phylogenetic analyses, including their laboratory code, population locality, and GenBank numbers

Authors: Helmut E. Walter, Arón Cádiz-Véliz, Beatriz M. Meriño, Heidy M. Villalobos-Barrantes, Pablo C. Guerrero

Data type: docx

Link: https://doi.org/10.3897/phytokeys.237.107403.suppl1

PhytoKeys 237: 141–151 (2024)
DOI: 10.3897/phytokeys.237.114704

Research Article

Cyrtandra obliquifolia (Gesneriaceae), a new species from Kaua'i, Hawaiian Islands

Kenneth R. Wood[1], Warren L. Wagner[2]

1 National Tropical Botanical Garden, 3530 Papalina Road, Kalāheo, HI 96741, USA
2 Department of Botany, Smithsonian Institution, PO Box 37012, Washington, DC 20013-7012, USA
Corresponding author: Kenneth R. Wood (kwood@ntbg.org)

Abstract

Cyrtandra obliquifolia K.R. Wood & W.L. Wagner (Gesneriaceae), a new shrub species known only from Kaua'i, Hawaiian Islands, is described and illustrated with notes on its distribution, ecology, and conservation status. The new species is morphologically most similar to *Cyrtandra wawrae* C.B. Clarke but differs by its unique combination of oblique, non-peltate, auriculate leaf bases, more deeply divided calyx lobes, inflorescence with fewer flowers and lacking profusely umbellate cymes. *Cyrtandra obliquifolia* is known from only two localities which have undergone severe habitat degradation from landslides and invasive plants and animals and is determined to be Critically Endangered (CR) when evaluated under IUCN criteria.

Key words: Conservation, critically endangered, *Cyrtandra*, Gesneriaceae, Hawaiian Islands, Kaua'i

OPEN ACCESS

Academic editor: Michael Moeller
Received: 25 October 2023
Accepted: 4 January 2024
Published: 22 January 2024

Citation: Wood KR, Wagner WL (2024) *Cyrtandra obliquifolia* (Gesneriaceae), a new species from Kaua'i, Hawaiian Islands. PhytoKeys 237: 141–151. https://doi.org/10.3897/phytokeys.237.114704

Introduction

Cyrtandra J.R. & G. Forster (Gesneriaceae) is composed of ca. 800 species that range across Southeast Asia and the Pacific (Atkins et al. 2013; Kleinkopf et al. 2019) including ca. 60 species occurring in the Hawaiian Islands, with ca. 50 being single-island endemics (SIE) (Wagner et al. 1999; Wagner and Roalson in prep.). On Kaua'i, oldest of the high islands at ca. 4.7 million years (Price and Clague 2002), there are 14 species of *Cyrtandra*, including 13 SIE, three federally listed endangered, and one considered possibly extinct (i.e., *C. olona* C. Forbes), being last observed in 1909. Of the ca. 134 endemic vascular plants that are thought to be extinct throughout the Hawaiian Islands, five are in the genus *Cyrtandra* (Wood et al. 2019). The current status of all Hawaiian *Cyrtandra* is being investigated as part of ongoing studies by W. L. Wagner, E. Roalson, D. Brokaw, and several Hawaiian field botanists.

The continuing endangerment and loss of global biodiversity, especially in many insular ecosystems, has spurred botanists to rapidly assess and disseminate floristic data and conduct conservation collections to address potential extinctions. Over the last 30 years, ca. 28 new flowering plant and pteridophyte species have been discovered and described on Kaua'i, in addition to about 29 taxa rediscovered after previously being considered possibly extinct. Familiarizing biologists with the distribution and abundance of these unique species is fundamental to our ability to conserve them. One pertinent example is the discovery and description of *Cyrtandra paliku* W.L. Wagner, K.R. Wood & Lorence, an extremely narrow SIE species, restricted to a single cliff face on Kekoiki summit, northeastern Kauaʻi (Wagner et al. 2001), and now being monitored and conserved under the auspices of Hawaii's Plant Extinction Prevention Program (PEPP).

In 2008 an unusual flowering specimen of *Cyrtandra* was collected by National Tropical Botanical Garden (**NTBG**) Science staff with laminae similar to *C. wawrae* C.B. Clarke in overall look and size but differed most notably in having non-peltate leaves. In this specimen the leaf blade base was asymmetrical on most of the leaves, and occasionally with symmetrical base, but not peltate. At the time it was referred to as an atypical *C. wawrae* and put aside for the time being. Further comparison showed additional morphological differences indicated in the diagnosis, most notably having only 3–5-flowered cymes instead of dense umbelliform cymes up to 17-flowered in *C. wawrae*. We included *C. obliquifolia* in ongoing molecular analyses and found it was distinctive yet closely allied to *C. wawrae* (Kleinkopf et al. 2019). During our investigation of this new species, we reexamined other collections in the PTBG and US herbaria and found that there was one additional collection made in 1993 from another locality in Waiʻoli Valley, on the northern slopes of Namolokama, over 10 km from the holotype location (Fig. 1).

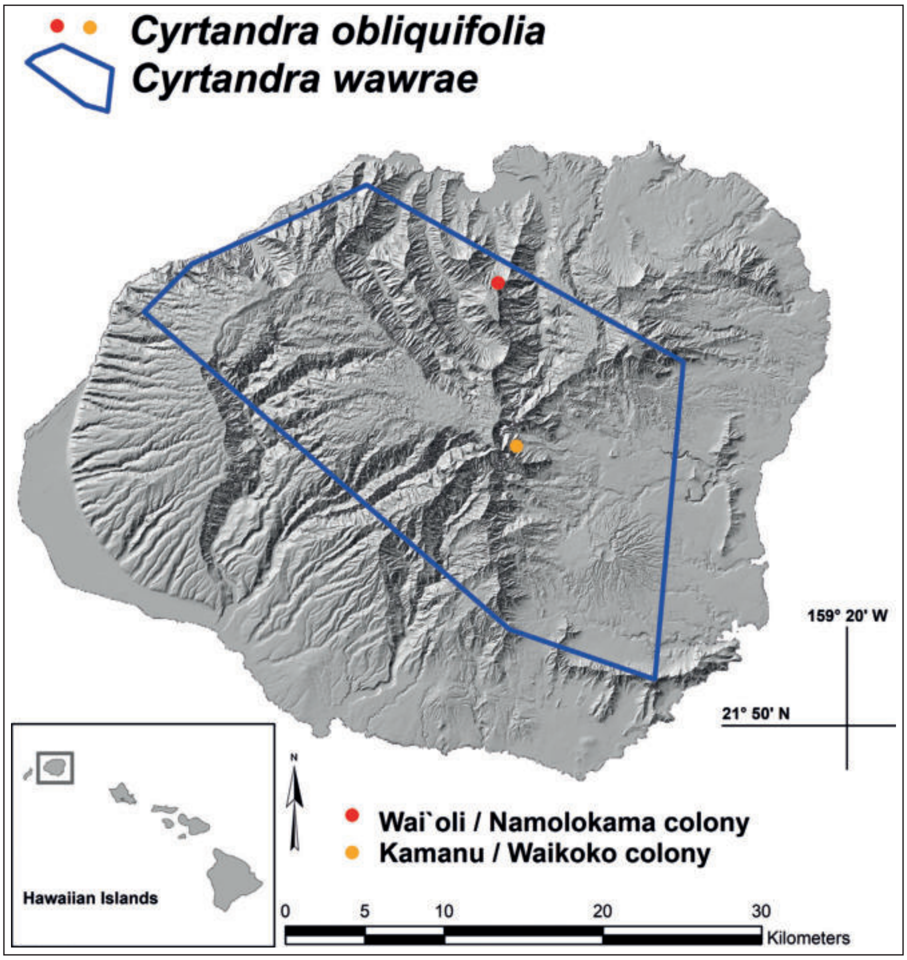

Figure 1. Distribution map (Kauaʻi, Hawaiian Islands) with dots representing the two known locations of *Cyrtandra obliquifolia* K.R. Wood & W.L. Wagner and polygon representing the broad distribution of *C. wawrae* C.B. Clarke.

Methods

All measurements were taken from dried herbarium specimens, while overall plant size and population abundance were taken from field notes. For herbarium research we worked extensively with *Cyrtandra* specimens at BISH, PTBG, and US. The authors have examined all specimens cited in this paper. Measurements are presented in the description as follows: length × width, followed by units of measurements (mm or cm). We assessed the extinction risk for *Cyrtandra obliquifolia* following the IUCN Red List Categories and Criteria (IUCN 2012) and guidelines of the IUCN (2022). The extent of occurrence (EOO) and area of occupancy (AOO) were calculated by using ArcMap 10.6.1 (ESRI 2011) in relation to coordinates recorded while collecting both herbarium specimens.

Taxonomic treatment

***Cyrtandra obliquifolia* K.R.Wood & W.L.Wagner, sp. nov.**
urn:lsid:ipni.org:names:77334870-1
Figs 2, 3

Diagnosis. Morphologically, *Cyrtandra obliquifolia* is similar to *C. wawrae*, differing in having non-peltate leaves (*vs*. peltate), only 3–5-flowered cymes (*vs*. dense umbelliform cymes up to 17-flowered), corolla tube 10–11 mm long (*vs*. 13–17 mm long), and calyx ca. 10 mm long, the lobes lanceolate, 8–9.5 mm long, pilose within (*vs*. calyx 12–32 mm long, enclosing the fruit at maturity, the lobes deltate, 2–6(–10) mm long, glabrate to sparsely pilose).

Type. USA, Hawaiian Islands, Kauaʻi: Līhuʻe District, below Kamanu Ridge, headwaters of Waikoko, 22.058641, -159.484138, 732 m, 12 Jan 2008, *Wood 12775* (holotype: PTBG1000002533!; isotype: BISH1152010!).

Description. Small shrubs ca. 0.5–0.75 m tall; stems few-branched. ***Leaves*** opposite, those of a pair unequal, usually strongly asymmetrical, sometimes nearly symmetrical, coriaceous, very broadly ovate to broadly elliptic or sometimes suborbicular, 20–29 cm long, (7.8–)10–12.8 cm wide, upper surface sparsely to moderately pilose, the hairs with a broad base, lower surface densely velvety pilose, the hairs with a slightly broader base, sometimes gland-tipped, whitish to pale brown, margins dentate or serrate, moderately densely glandular pilose, apex acuminate, base asymmetrically cordate, auriculate, with one side extending 0.3–1.4 cm further than the other, sometimes cordate, petioles 7–13 cm long. ***Flowers*** 3–5 in cymes arising in the axils, glandular pilose throughout, peduncles stout, ca. 45 mm long, pedicels 15–25 mm long, bracts foliaceous, broadly ovate, ca. 20–25 mm long. ***Calyx*** nearly actinomorphic, ca. 10 mm long, the lobes lanceolate, 8–9.5 mm long, pilose, pilose within, apex acuminate, often slightly overlapping near base. ***Corolla*** white, tube cylindrical, 8.5–15 mm long, pilose, upper lobes reniform, ca. 3 mm long, ca. 4 mm wide, lower lobes rhombic-ovate, 3–4 mm long, 6–8 mm wide; ovary glabrous; style 5–10 mm long, glabrous. ***Berries*** not seen. ***Seeds*** not seen.

Additional specimen examined. USA, Hawaiian Islands, Kauaʻi: Hanalei District, Waiʻoli Valley, slopes of Namolokama, hanging valley east of main waterfall, 22.151496, -159.495704, 835 m, 21 Jan 1993, *Perlman, Lorence, Flynn & Wood 13259* (PTBG, US).

Phenology. *Cyrtandra obliquifolia* has been observed with flower during the month of January.

Etymology. The species epithet is from the Latin *obliquus* meaning slanting or unequal sides, and *folius* for leaf.

Affinities. *Cyrtandra obliquifolia* is closely related to *C. wawrae* as shown by the similar morphology when first collected. A sample of it was included as one of the 31 samples in a hyb-seq phylogenomic analysis of the Hawaiian lineage and was strongly supported as sister to *C. wawrae* and the pair an early-diverging one in the Hawaiian lineage (Kleinkopf et al. 2019). Our morphological comparisons indicated there are a number of other differences between these two species (Figs 2–5; Table 1).

Distribution and ecology. *Cyrtandra obliquifolia* is endemic to the volcanic island of Kauaʻi where there is uncertainty whether any surviving plants remain. The oldest of the main Hawaiian Islands and summiting at 1598 m, Kauaʻi contains the highest level of floristic diversity throughout the archipelago with ca. 250 SIE and a total of ca. 673 native vascular plant taxa (Wagner et al. 1999; Vernon and Ranker 2013; Wood et al. 2016; Rønsted et al. 2022). Local botanists estimate around 21 of those Kauaʻi SIE taxa are possibly extinct with no known wild individuals (Wood et al. 2019). Kauaʻi features a highly variable physical geography compared to the younger high Hawaiian Islands, exemplified by deeply eroded and isolated drainages, well-defined canyons, tall coastal seacliffs, along with lowland and montane bogs and interior wet cliff habitats. Although much of the lowland dry habitats had been altered or lost by the time the first European explorer, Captain Cook, made contact on Kauaʻi in 1778, there still remains a fair abundance of mesic and wet forest ecosystems, much of which are extremely rugged and unexplored. It was around Kauaʻi's saturated cliffs and towering waterfalls that *Cyrtandra obliquifolia* was documented.

A vegetative plant of *Cyrtandra obliquifolia* was first documented in 1993 and noted to be occasional around an inaccessible hanging valley above Wai`oli Stream, Kauaʻi, on the isolated northern face of Namolokama Mountain at 835 m elev. (Fig. 1). This survey was facilitated by helicopter. Few botanists have since returned to this exact location, and although no individuals have since been reported around this site, further surveys are recommended along the wet cliffs and surrounding forests of Namolokama's isolated hanging valleys. It should be noted that several rare plant taxa in this area have declined as a result of an influx of weedy invasive plants establishing themselves post-hurricane Iniki (ca. 1992). In Aug 2023, the first author flew into the Wai`oli region and visited the area just below the hanging valley where *Perlman 13259* was

Table 1. Comparison of morphological and ecological characters of two similar Kauaʻi species of Hawaiian *Cyrtandra*.

Character	*C. wawrae*	*C. obliquifolia*
Leaves	Peltate, light green, petioles inserted 1–5.5 cm from base, the base rounded to truncate, occasionally broadly cuneate	Not peltate, dark green, the base asymmetrically cordate, with one side extending 0.3–1.4 cm further than the other, sometimes cordate
Inflorescence	with 6–17 flowers, in dense umbelliform cymes arising in the axils just below the current leaves, peduncles 1–35 mm long	with 3–5 flowers in cymes arising in the axils, peduncles 45 mm long
Calyx	12–32 mm long, enclosing the fruit at maturity, the lobes deltate, 2–6(–10) mm long, glabrate to sparsely pilose within	ca. 10 mm long, the lobes lanceolate, 8–9.5 mm long, pilose within
Corolla tube	13–17 mm long	8.5–15 mm long
Habitat	Mesic to wet forest	Wet forest

Figure 2. *Cyrtandra obliquifolia* K.R. Wood & W.L. Wagner **A** habit **B** pubescence on upper leaf surface and margin **C** pubescence on lower surface and margin **D** flower in early anthesis (male phase) **E** flower in full anthesis (female stage) **F** calyx after flowering showing stigma. Drawn from holotype and augmented with photograph of plant that holotype was taken from (**A–D, F**) and from close-up photo of plant that holotype was taken from (**E**).

Figure 3. *Cyrtandra obliquifolia* K.R. Wood & W.L. Wagner from headwaters of Waikoko Valley where holotype was collected **A, B** habit **C** close-up of early anthesis flower **D** general habitat of type locality. All photos by K.R. Wood.

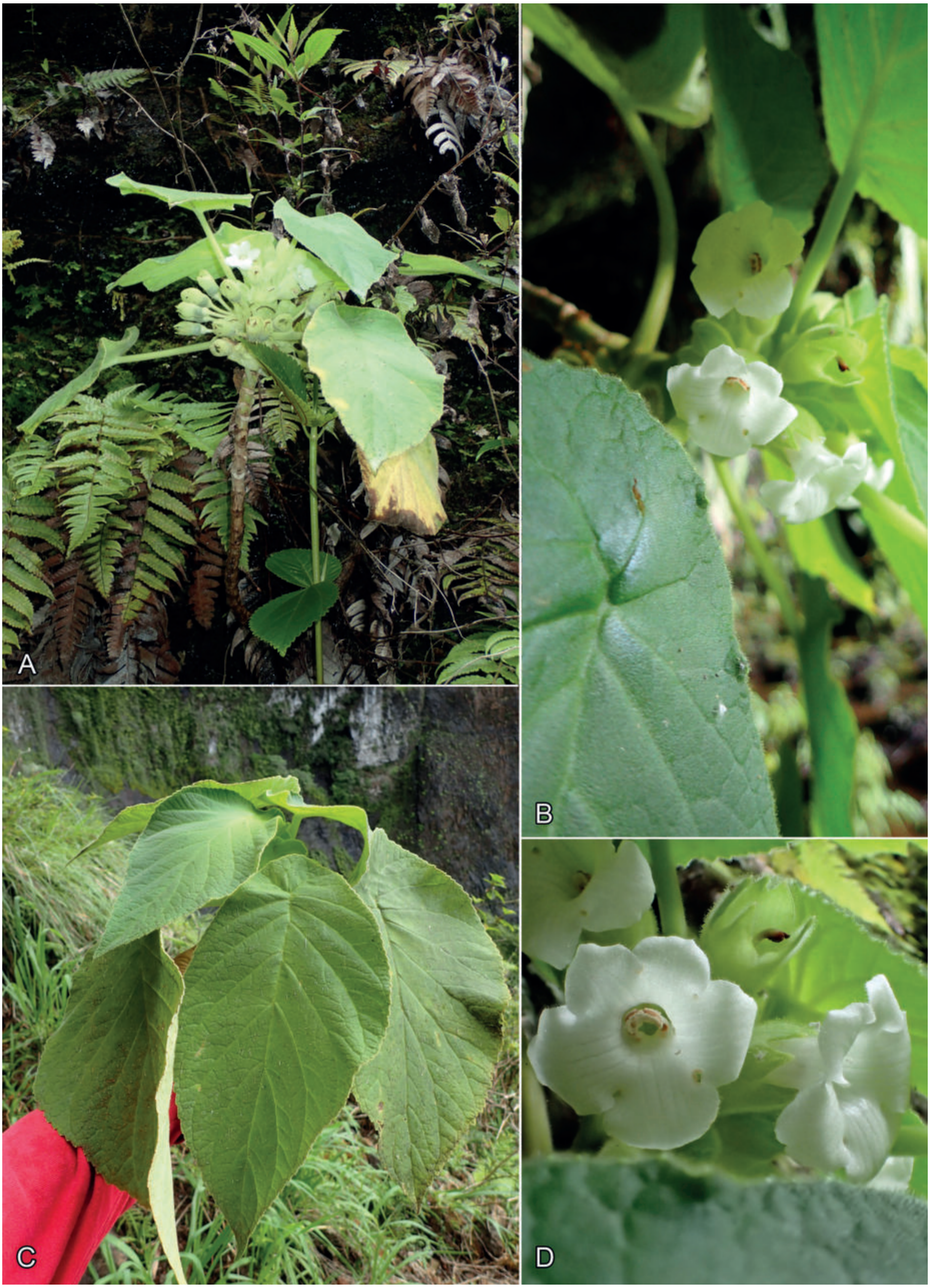

Figure 4. *Cyrtandra wawrae* C.B. Clarke **A** habit with inflorescence **B** close-up of inflorescence and peltate leaf **C** peltate leaves **D** close-up of corolla and side view of calyx. All photos by K.R. Wood **A** 17 June 2017, Wailua **B** Wailua, *Wood 17317* (PTBG) **C, D** Lumahai, *Wood 17398* (PTBG).

collected, and, unfortunately, confirms the serious degradation of the region since the 1990s. A second colony of *C. obliquifolia* was documented in flower 15 years later (i.e., Jan 2008) along the windward headwater drainage of Waikoko Stream at 732 m elev. (east central Kaua'i; Fig. 1). After discovery, this region suffered a devastating landslide which possibly destroyed the known colony of ca. 20 individuals of *C. obliquifolia*, along with the last known Kaua'i colony of *Lysimachia filifolia* C.N. Forbes & Lydgate (Primulaceae). Still, there is extensive habitat surrounding the Waikoko headwaters where additional colonies of *C. obliquifolia* could still occur (Figs 1, 3D).

The plant community where both colonies of *Cyrtandra obliquifolia* were found is a *Metrosideros* Banks ex Gaertn. (Myrtaceae) / *Cheirodendron* Nutt. ex Seem. (Araliaceae) lowland wet forest. These forests are low statured and partially open where they flourish around the bases of seeping vertical basalt wet cliff communities. Associate plant species in the area include a rich mix of endemic native sedges, grasses, ferns, herbs, shrubs, and stunted trees, many of the species being unique single-island endemics. Wood and Knope (2023) defined the general ecology of these wet forests and cliffs in their publication of *Bidens wailele* K.R. Wood & Knope, a recently described endemic perennial herb also documented around the holotype area of *C. obliquifolia*. From our observations, *C. obliquifolia* inhabits the open banks of streams within these lowland wet forests, in addition to the lower walls of the surrounding wet cliff community. Associated genera of trees in the type locality include *Polyscias* J.R. Forst. & G. Forst. (Araliaceae); *Pritchardia* Seem. & H. Wendl. (Arecaceae); *Dubautia* Gaudich. (Asteraceae); *Cyanea* Gaudich., *Lobelia* Plum. ex L. (Campanulaceae); *Perrottetia* Kunth (Dipentodontaceae); *Antidesma* L., *Euphorbia* L. (Euphorbiaceae); *Hydrangea* Gronov. (Hydrangeaceae); *Syzygium* Gaertn. (Myrtaceae); *Bobea* Gaudich., *Coprosma* J.R. Forst. & G. Forst., *Kadua* Cham. & Schltdl. (some being smaller shrubs), *Psychotria* L. (Rubiaceae); *Melicope* J.R. Forst. & G. Forst. (Rutaceae), and *Pipturus* Wedd., *Touchardia* Gaudich., *Urera* Gaudich. (Urticaceae). Genera of sedges and grasses include *Carex* L., *Cyperus* L., *Machaerina* Vahl (Cyperaceae); *Eragrostis* Wolf, *Isachne* R. Br. (Poaceae); ferns of *Asplenium* L., *Hymenasplenium* Hayata (Aspleniaceae); *Deparia* Hook. & Grev., *Diplazium* Sw. (Ath**y**riaceae); *Sadleria* Kaulf. (Blechnaceae); *Cibotium* Kaulf. (Cibotiaceae); *Microlepia* C. Presl (Dennstaedtiaceae); *Hoiokula* S.E. Fawc. & A.R. Sm., *Menisciopsis* (Holttum) S.E. Fawc. & A.R. Sm. (Thelypteridaceae); herbs and shrubs include *Bidens* L. (Asteraceae); *Cyrtandra* J.R. Forst. & G. Forst. (Gesneriaceae); *Gunnera* L. (Gunneraceae); *Plantago* L. (Plantaginaceae); *Lysimachia* Tourn. ex L. (Primulaceae); and the woody climber *Freycinetia* Gaudich. (Pandanaceae).

Preliminary conservation assessment. *IUCN Red List Category*. When evaluated using the World Conservation Union (IUCN 2012, 2022) guidelines and criteria for endangerment, *Cyrtandra obliquifolia* falls into the Critically Endangered (CR) category. Our evaluation following the IUCN hierarchical alphanumeric numbering system of criteria and conditions is CR B1ab(i,ii,iii,iv,v); B2ab(i,ii,iii,iv,v); C2a(i); D; which reflects a severely limited EOO of less than 100 km^2 (i.e., 4 km^2) an AOO of less than 10 km^2 (i.e., 1 km^2), a severely fragmented distribution with two subpopulations separated by 10 km, a continued decline in quality of habitat inferred, and a population of ca. 40 mature plants observed, ranging between 732 and 835 m elev. The continued decline in quality

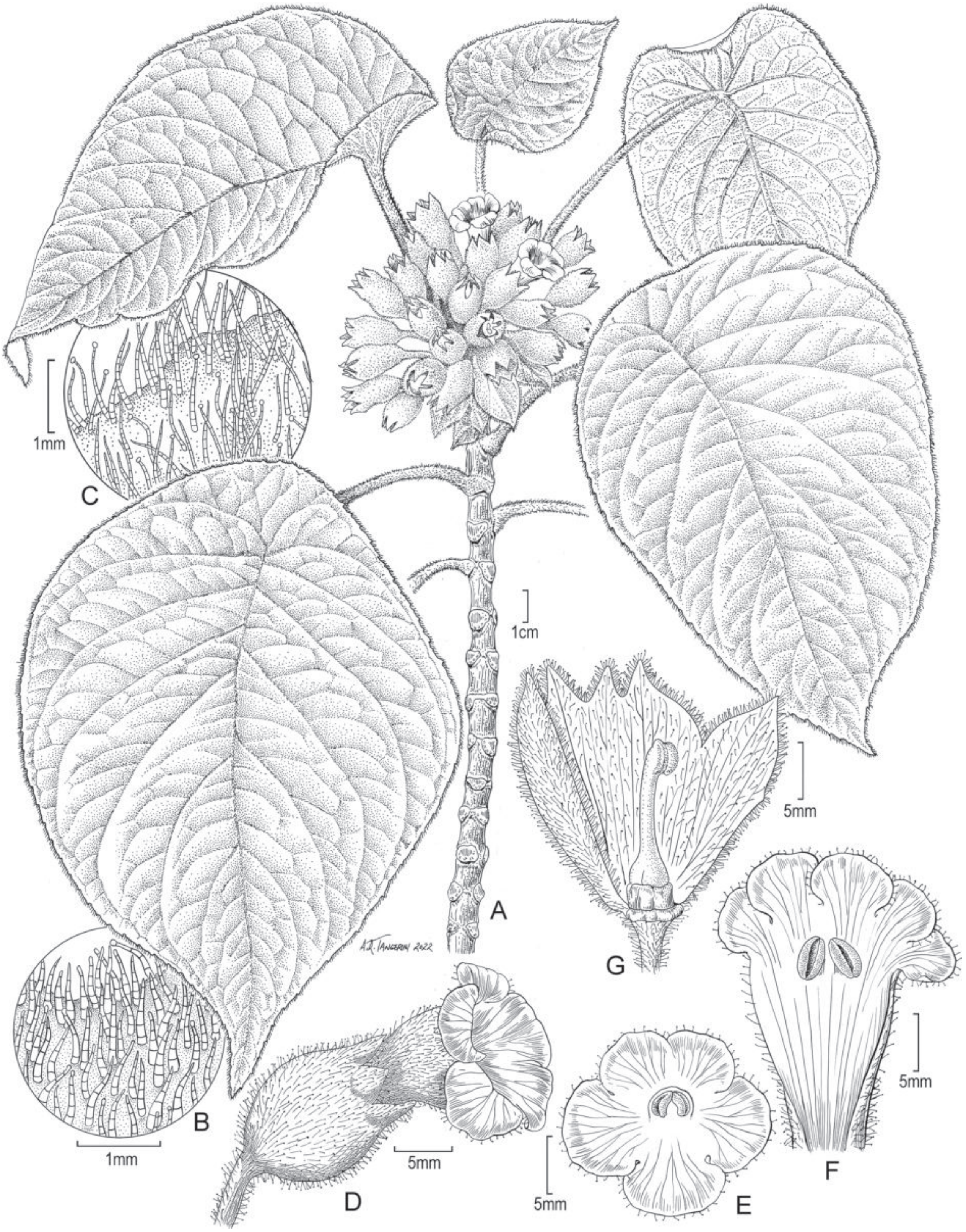

Figure 5. *Cyrtandra wawrae* C.B. Clarke **A** habit showing dense umbelliform cymes **B** pubescence on upper surface and margin **C** pubescence on lower surface and margin **D** flower, lateral view, in full anthesis (female stage) **E** face view of corolla **F** corolla longitudinal section showing inserted stamens **G** calyx longitudinal section after flowering showing stigma. Drawn from *Wood 907* (US), Kalalau Rim (**A–D, F, G**), and photo of *Wood 17398*, upper Lumahai (**E**). Illustration augmented with photos of habit (*Wood 17317*) and leaves from (*Perlman & Wood 13599*) (A), and photos of flowers (*Wood 17398*) (**D**).

of habitat for *Cyrtandra obliquifolia* is evidenced by severe habitat degradation from invasive plants and animals, in addition to hurricane force winds, flash floods and landslides (especially after torrential rains). Destructive non-native animals in the area include (*Sus scrofa* L.), and rats (*Rattus* spp.), along with introduced slugs and insects. Specific invasive non-native plants include *Ageratum conyzoides* L., *Erigeron bonariensis* L., *E. karvinskianus* DC., (Asteraceae); *Buddleja asiatica* Lour. (Buddlejaceae); *Sphaeropteris cooperi* (Hook. ex F. Muell.) R.M. Tryon (Cyatheaceae); *Juncus planifolius* R. Br. (Juncaceae); *Miconia crenata* (Vahl.) Michelang. (Melastomataceae); *Psidium cattleyanum* Sabine (Myrtaceae); *Andropogon glomeratus* (Walter) Britton, Sterns & Poggenb., *Axonopus fissifolius* (Raddi) Kuhlm., *Sacciolepis indica* (L.) Chase (Poaceae); *Adiantum raddianum* C. Presl (Pteridaceae); *Rubus rosifolius* Sm. (Rosaceae); and *Hedychium gardnerianum* Sheph. ex Ker Gawl. (Zingiberaceae).

As exhaustive surveys have not yet been conducted in the surrounding habitats where *Cyrtandra obliquifolia* has been documented, we do not believe this species is extinct in the wild.

We are hoping that this publication with description and illustrations will give botanists incentive and guidance to look for additional colonies of this beautiful gesneriad around the hanging valleys that surround Namolokama, along with searches along the back walls of Waikoko drainage and wet cliffs of Kamanu ridge which rise up to the very summit of Kawaikini, Kauaʻi. We also recommend concerted inventories be initiated deep into the great central, headwater drainage of Olokele, which is quite near the holotype region yet privately owned and in need of special permitting for exploration.

Acknowledgements

We are grateful to Alice Tangerini for her excellent illustrations of this new species to reconstruct its characteristics from limited collection and photographs, and for her illustration of *C. wawrae*. We also thank the staff at the Hawaiʻi State Department of Land and Natural Resources, Division of Forestry and Wildlife for permits, the Kauaʻi Plant Extinction Prevention Program for assistance in conservation efforts, Steve Perlman, David Lorence and Tim Flynn for field assistance, and to Tim Flynn (PTBG) and Nancy Khan (US) for collections' support.

Additional information

Conflict of interest

The authors have declared that no competing interests exist.

Ethical statement

No ethical statement was reported.

Funding

No funding was reported.

Author contributions

Kenneth R. Wood / lead author and field research; Warren L. Wagner / co-author and field research.

Author ORCIDs

Kenneth R. Wood https://orcid.org/0000-0001-6446-1154
Warren L. Wagner https://orcid.org/0000-0001-5012-8422

Data availability

All of the data that support the findings of this study are available in the main text.

References

Atkins HJ, Bramley GLC, Clark JR (2013) The taxonomy of *Cyrtandra* (Gesneriaceae): Current knowledge, future directions. Selbyana 31: 65–253. https://journals.flvc.org/selbyana/article/view/123020

ESRI (2011) ArcGIS Desktop: Release 10.6.1. Environmental Systems Research Institute, Redlands, CA.

IUCN (2012) IUCN Red List Categories and Criteria Version 3.1 (2nd edn.). Prepared by the IUCN Criteria Review Working Group. IUCN, Cambridge.

IUCN (2022) Guidelines for using the IUCN Red List Categories and Criteria. Version 15.1. Prepared by the Standards and Petitions Committee. https://www.iucnredlist.org/documents/RedListGuidelines.pdf [Accessed 17.12.2023]

Kleinkopf J, Roberts W, Wagner WL, Roalson EH (2019) Diversification of Hawaiian *Cyrtandra* (Gesneriaceae) under the influence of incomplete lineage sorting and hybridization. Journal of Systematics and Evolution 57(6): 561–578. https://doi.org/10.1111/jse.12519

Price JP, Clague DA (2002) How old is the Hawaiian biota? Geology and phylogeny suggest recent divergence. Proceedings of the Royal Society B, Biological Sciences 269(1508): 2429–2435. https://doi.org/10.1098/rspb.2002.2175

Rønsted N, Walsh SK, Clark M, Edmonds M, Flynn T, Heintzman S, Loomis A, Lorence D, Nagendra U, Nyberg B, Opgenorth M, Weisenberger L, Williams A, Wolkis D, Wood KR, Keir M (2022) Extinction risk of endemic vascular flora of Kaua'i Island, Hawai'i, based on IUCN assessments. Conservation Biology 36(4): e13896. https://doi.org/10.1111/cobi.13896

Vernon AL, Ranker TA (2013) Current status of the ferns and lycophytes of the Hawaiian Islands. American Fern Journal 103(2): 59–111. https://doi.org/10.1640/0002-8444-103.2.59

Wagner WL, Herbst DR, Sohmer SH (1999) Manual of the Flowering Plants of Hawai'i, revised edition with supplement by Wagner WL and Herbst DR. University of Hawai'i Press (2 Vols). Bishop Museum Special Publication 97, 1919 pp.

Wagner WL, Wood KR, Lorence DH (2001) A new species of *Cyrtandra* (Gesneriaceae) from Kaua'i, Hawaiian Islands. Novon 11(1): 146–152. https://doi.org/10.2307/3393224

Wood KR, Knope ML (2023) *Bidens wailele* (Asteraceae, Coreopsideae): A new critically endangered species from Kaua'i, Hawaiian Islands. International Journal of Plant Sciences 184(5): 378–386. https://doi.org/10.1086/724311

Wood KR, Lorence DH, Kiehn M (2016) *Coprosma kawaikiniensis* (Rubiaceae) a new species from the *Dubautia-Sadleria* shrubland-fernland community on Kaua'i, Hawaiian Islands. PhytoKeys 60: 21–32. https://doi.org/10.3897/phytokeys.60.6406

Wood KR, Oppenheimer H, Keir M (2019) A checklist of endemic Hawaiian vascular plant taxa from the Hawaiian Islands that are considered possibly extinct in the wild. Technical Report 314. The National Tropical Botanical Garden.

PhytoKeys 237: 153–160 (2024)
DOI: 10.3897/phytokeys.237.112270

Research Article

Phalaenopsis zhanhuoensis (Orchidaceae, Vandeae), a new species from Yunnan, China

Shiyu Qin[1,2,3], Hanchen Wang[2,3,4], Yajun Wang[2,3,4], Chongbo Ma[2,3], Zan Li[2,3], Boyun Yang[1], Xiaohua Jin[2,3]

1 School of Life Sciences, Nanchang University, Xuefudadao 999, Shajing, Nanchang, Jiangxi, 330031, China
2 State Key Laboratory of Plant Diversity and Prominent Crops, Institute of Botany, Chinese Academy of Sciences, Nanxincun 20, Xiangshan, Beijing, 100093, China
3 China National Botanical Garden, Beijing, 100093, China
4 University of Chinese Academy of Sciences, Beijing, 100093, China
Corresponding authors: Boyun Yang (yangboyun@163.com); Xiaohua Jin (xiaohuajin@ibcas.ac.cn)

Abstract

A new species of Orchidaceae, *Phalaenopsis zhanhuoensis*, from Xichou County, Yunnan, China, is described and illustrated. The novelty is close to *P. taenialis*, *P. wilsonii*, and *P. stobartiana*, but differs from them by having a distinct, fleshy anterior callus with a deeply lobed apex at the base of the labellum and lateral lobes of labellum reflexed and facing outward.

Key words: China, new species, *Phalaenopsis zhanhuoensis*, Xichou County, Yunnan

Introduction

The moth orchid genus, *Phalaenopsis* Blume, comprises approximately 80 recognized species （https://powo.science.kew.org/） and is extraordinarily prominent in the field of horticulture. *Phalaenopsis* is distributed in India, Southeast to East Asia, and Australia, with most of the diversity in Indonesia and the Philippines (Pridgeon et al. 2014). Recent molecular results based on ITS nrDNA and plastid regions (*trnL* intron, *trnL-F* spacer, and *atpB-rbcL* spacer) indicated that the number of pollinia was not a good morphological character to distinguish *Phalaenopsis* from its alliance, such as *Doritis* Lindl., *Kingidium* P.F.Hunt., and *Nothodoritis* Z.H. Tsi, and proposed broadening *Phalaenopsis* to include its alliance (Christenson 2001; Padolina et al. 2005; Tsai et al. 2005; Yukawa et al. 2005; Tsai et al. 2010; Pridgeon et al. 2014). *Phalaenopsis s.l.* is characterized by roots more or less depressed and verrucose, stem short, leaves usually elliptic and fleshy, lip three lobed, column usually with column foot, pollinia two or four.

Based on molecular data and morphological characters, such as the presence or absence of column foot and the number of pollinia, *Phalaenopsis* was subdivided into four subgenera, subgen. *Parishianae* (Sweet) Christenson (26 spp.), subgen. *Phalaenopsis* Blume (45 spp.), subgen. *Hygrochilus* (Pfitzer) Kocyan & Schuiteman (5 spp.) and subgen. *Ornithochilus* (Lindl.) Kocyan & Schuiteman (4 spp.) (Kocyan and Schuiteman 2014; Pridgeon et al. 2014; Higgins and Alrich 2015).

Academic editor: M. Simo-Droissart
Received: 6 September 2023
Accepted: 31 December 2023
Published: 22 January 2024

Citation: Qin S, Wang H, Wang Y, Ma C, Li Z, Yang B, Jin X (2024) *Phalaenopsis zhanhuoensis* (Orchidaceae, Vandeae), a new species from Yunnan, China. PhytoKeys 237: 153–160. https://doi.org/10.3897/phytokeys.237.112270

The subgenus *Parishianae* is mainly distributed in India, Southeast to East Asia (Pridgeon et al. 2014), with species morphologically characterized by small plant size, few-flowered inflorescence, small scarious floral bracts, and biseriate callus (Pridgeon et al. 2014). There are 25 *Phalaenopsis* species in four subgenera in China (Zhou et al. 2021; Ma et al. 2022), of which 14 species belong to the subgenus *Parishianae* (Chen and Wood 2009; Zhou et al. 2021). During our fieldwork in Yunnan Province, China, in April 2023, a new species of *Phalaenopsis* belonging to subgenus *Parishianae* (Sweet) Christenson was found in evergreen broad-leaved forests and is described here.

Materials and methods

Morphological characters of the new species were observed, measured with a ruler (precision: 1 mm), and photographed based on living plants. Molecular phylogenetic analyses were conducted using one nuclear (nrITS) and four plastid markers (*matK*, *trnL*, *trnL-F*, and *atpB-rbcL*). Genomic DNA was extracted from the newly collected specimen of *Phalaenopsis* (silica dried) using the modified cetyltrimethylammonium bromide (CTAB) method (Li et al. 2013). Sequencing library was generated using Rapid Plus DNA Lib Prep Kit for Illumina and then delivered to Novogene Company (Beijing, China) for 150 bp paired-end sequencing on the Illumina HiSeq 2500 platform. Approximately 5 Gb of raw sequencing data were generated for the collected specimen. Plastid genome and ITS were assembled using GetOrganelle v.1.7.1 with Illumina sequencing reads as input and under default parameters (Jin et al. 2020), respectively. The assembled plastid genome was annotated using Geneious Prime v.2023.0.4 (https://www.geneious.com) and manually checked with *P. lobbii* (NC_059699) and *P. stobartiana* (NC_059917) as references. Four plastid markers (*matK*, *trnL*, *trnL-F*, and *atpB-rbcL*) were extracted from plastid genome using Geneious Prime v.2023.0.4.

Sixty-two species of *Phalaenopsis* were used for phylogenetic analyses. Two species, *Cleisostoma williamsonii* (Rchb. f.) Garay and *Pelatantheria rivesii* (Guillaumin)Tang & F. T.Wang, were used as outgroup based on previous results (Chase et al. 2015; Li et al. 2019; Ma et al. 2022). In total, 225 sequences from 64 Orchidaceae species were downloaded from NCBI (Suppl. material 1: table S1). The combined matrix thus includes 229 sequences for the five markers, belonging to 65 species. Sequence alignment, supermatrix generation, and substitution model selection were performed using PhyloSuite (Zhang et al. 2020). GTR+F+I+G4 was selected as the best model for *matK*, *atpB-rbcL*, *trnL-F*, and *trnL*, and GTR+F+G4 for ITS, respectively. Bayesian Inference of phylogeny was performed using MrBayes v.3.2.7a on XSEDE in the CIPRES Science Gateway online web server (Miller et al. 2010). Two separate Markov Chain Monte Carlo (MCMC) analyses were performed 1,000,000 generations and sampling every 1000 generations. Maximum likelihood (ML) analyses were performed locally using IQTree2 (Minh et al. 2020). Support values for the clade were estimated using 1,000,000 bootstrap replicates.

Results

Phylogram of Maximum Likelihood based on nrITS and plastid DNA markers were used to illustrate the phylogenetic position of the new species. *Phalaenopsis* sp. nov. is nested within subgen. *Parishianae* and sister to *P. taenialis* with

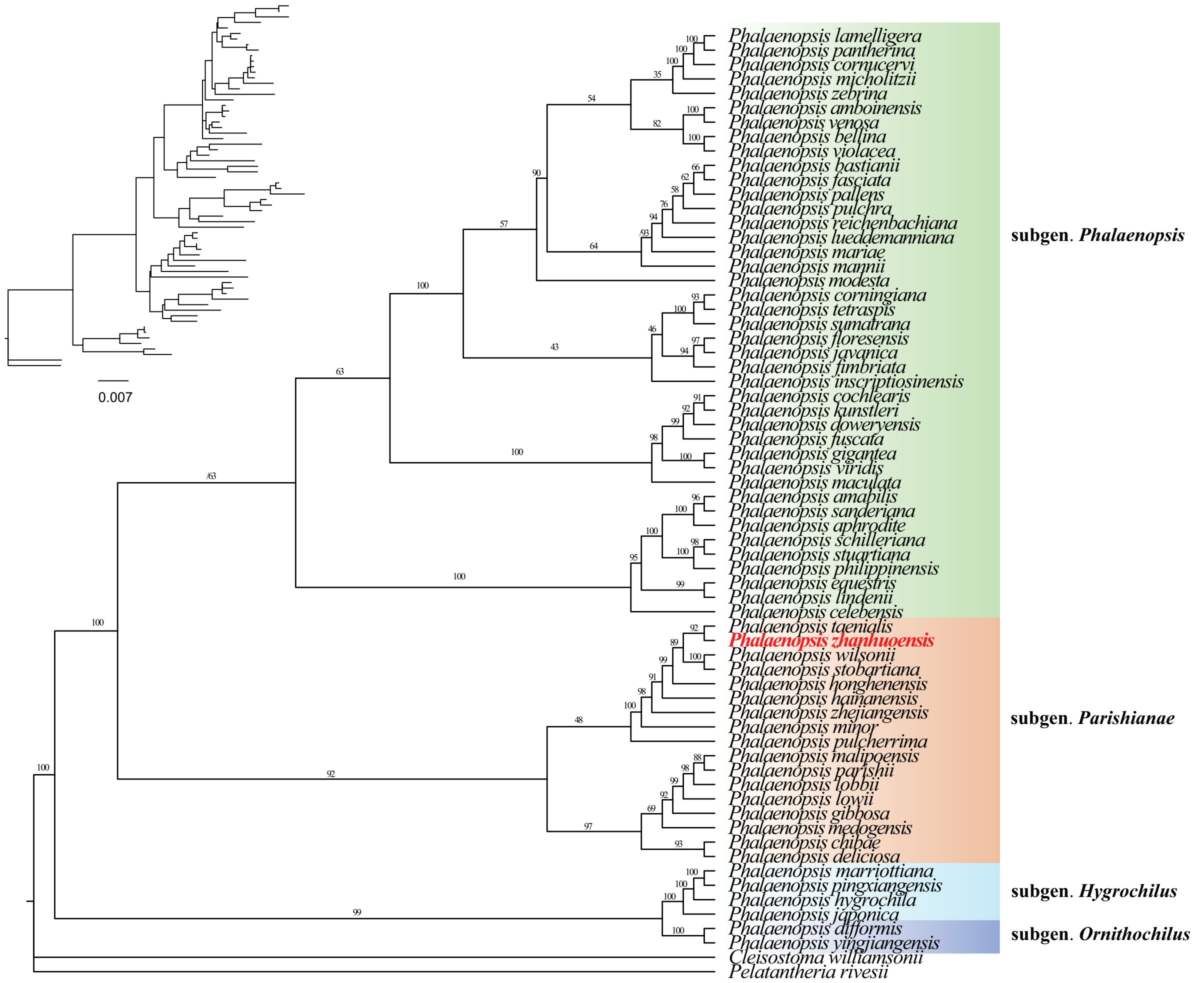

Figure 1. Phylogram of Maximum Likelihood based on nrITS and plastid DNA markers (*matK*, *trnL*, *trnL-F* and *atpB-rbcL*). Numbers above branches indicate bootstrap percentages (BS) for ML.

high support (PP = 1, BSML = 92; Fig. 1, Suppl. material 2: fig. S1). *Phalaenopsis* sp. nov. and *P. taenialis* together formed a clade sister to the clade consisting of *P. stobartiana* and *P. wilsonii* with high support (PP = 0.994, BSML = 89; Fig. 1, Suppl. material 2: fig. S1).

The new species is morphologically close to *P. taenialis*, *P. wilsonii*, *and P. stobartiana* by sharing lip with two seriate of calli at base, lip more or less with spur, lateral lobes more or less erect. *Phalaenopsis* sp.nov., however, differs from its relatives by having a bifurcated, fleshy, yellow anterior callus, and lateral lobes flipping outward and center with large calli.

Key to *Phalaenopsis zhanhuoensis* sp. nov. and its relatives

1a Spur not prominent, apparently absent or forming a small nipple-shaped structure; middle lobe more or less convex..**2a**

2a Lateral lobes flipping backward and centre with large yellow calli; anterior callus yellow, bifurcate.......................................**1. *P. zhanhuoensis* sp.nov.**

2b Lateral lobes without large calli; anterior callus purple, bifid; lobelets linear..**3a**

3a Lip mid-lobe obcordate with a central apical fleshy knob .... **2. *P. wilsonii***
3b Lip mid-lobe not obcordate, without a terminal notch **4a**
4a Petals and sepals deep green, lip purple; mid-lobe without any conspicuous constriction .... **3. *P. stobartiana***
4b Flowers rose-pink; mid-lobe with a conspicuous constriction **5a**
5a Lip mid-lobe flared below apex producing a 3-lobulate mid-lobe .... **4. *P. hainanensis***
5b Lip mid-lobe widest below apex, apical margin reflexed along mid-vein, forming a subtubular apex that may appear emarginate in natural position .... **5. *P. honghenensis***
1b Spur prominent, a continuation of angle formed by junction of lip mid-lobe and lateral lobes; lip midlobe flat .... **6. *P. taenialis***

Taxonomy

Phalaenopsis zhanhuoensis **X.H.Jin & S.Y.Qin, sp. nov.**
urn:lsid:ipni.org:names:77334958-1
Figs 2, 3
吉氏蝴蝶兰

Type. China. Yunnan, Wenshan Ctiy, Xichou County, alt. 1496 m, 11 Apr 2023, *Xiaohua Jin & Shiyu Qin 40050* (holotype, PE!).

Diagnosis. *Phalaenopsis zhanhuoensis* is similar to *P. wilsonii*, but differs from it by having a bifurcated yellow, fleshy anterior callus, lateral lobes with large calli and flipping outward (Table 1).

Description. Epiphytic plants. Roots fleshy, developing from the base or lower parts of the stem, elongated, flattened, densely verrucose and prostrate along

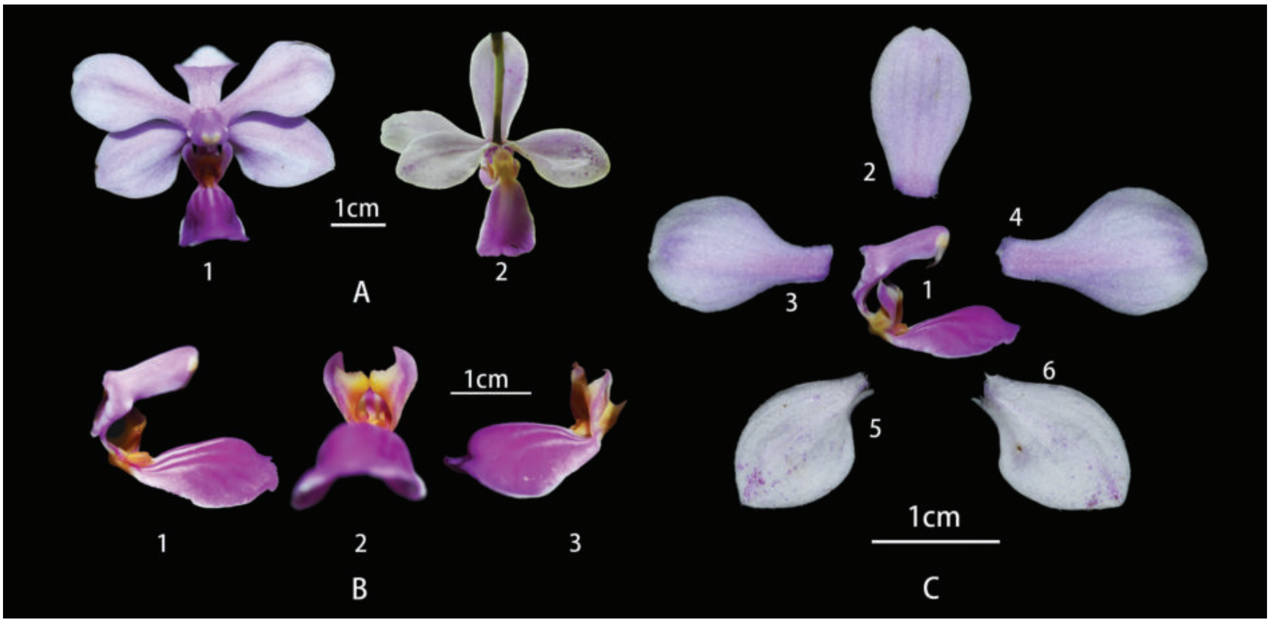

Figure 2. Flowers of *Phalaenopsis zhanhuoensis* X.H.Jin & S.Y.Qin, sp. nov. **A** front view of flower (1) rear view of flower (2) **B** column and lip; lateral view of column and lip, appendage and lateral lobes (1), front view of lateral lobes (2), lateral view of lateral lobes and mid-lobe (3) **C** petal, sepal and lip, lip (1), dorsal sepal (2), petal (3.4), lateral sepals (5.6). Photographed by Xiaohua Jin.

trunks. Stem very short, covered by tubular sheath at base. Leaves unseen. Inflorescence developing from the base of stem, suberect or arching, ca. 4.5 cm long, unbranched, with 3 laxly arranged flowers. Floral bracts ovate-triangular, 4–5 mm long. Flowers white with pale pink rib or white, 3–4 cm in diameter. Dorsal sepal broadly elliptic or spoon-shaped, ca. 2 × 1 cm, with semi-transparent veins abaxially; lateral sepals elliptic, acute at apex, slightly curved toward labellum, lilac spots at the apex in the dorsal, ca.1.8–2.0 × 0.9–1.1 cm, obtuse and notched at base. Petals spathulate, ca. 1.8–2.0 × 0.9–1.1cm, apex obtuse. Labellum three-lobed, clawed at the base, ca. 1–2 mm long; lateral lobes of labellum erect, purple, 0.5 cm long, flipping outward, adaxially center with a big callus; mid-lobe of labellum obcordate, ca. 1.3–1.5 × 0.9–1.1 cm, deep purple, with white stripes at the center, base with a yellow fleshy protuberant anterior callus; anterior callus deeply lobed at apex. Column subparallel to midlobe of labellum, lavender, ca. 0.6 cm long, with triangular wings; pollinarium yellow.

Figure 3. Habitat and plants of *Phalaenopsis zhanhuoensis* X.H.Jin & S.Y.Qin, sp. nov. **A** front view **B** roots **C** lateral view. Photographed by Xiaohua Jin.

Table 1. Morphological comparison of *Phalaenopsis zhanhuoensis* and close taxa.

	P. zhanhuoensis	***P. wilsonii***	***P. stobartiana***	***P. taenialis***
Flower color	white with pale pink ribs	white with pale pink ribs or complete pale pink.	**sepals and petals apple-green to dark olive-green.**	petals pale pink, lip and anther cap rose-purple.
Leaves	**no leaves at anthesis.**	leaves often deciduous in dry season.	leaves often deciduous during dry season, but present at anthesis.	leaves often deciduous at anthesis or during dry season
Lateral sepals	lateral sepals elliptic, acute at apex, obtuse	lateral sepals obovate-elliptic, similar and equal to middle sepal.	lateral sepals slightly oblique, ovate-elliptic, subacute.	lateral sepals subelliptic, **base adnate to column foot**, apex obtuse.
Lateral lobes of lip	lateral lobes **flipping outward**, adaxial center with a big callus	lateral lobes erect, adaxially **with an incised-tipped keel**.	lateral lobes erect, narrow, slightly constricted at middle	lateral lobes **adaxially with a slightly thickened longitudinal ridge close to proximal margin**
callus	**yellow, fleshy, bifurcated.**	purple; anterior callus deeply lobed at apex; lobelets linear and long	purple; concave adaxially and distinctly convex abaxially on disk.	purple; ligulate, deeply bifid; lobelets linear and long, attached to front wall at base of mid-lobe.

Etymology. The epithet *zhanhuoensis* was designated in honor of the Chinese botanist Zhanhuo Tsi.

Distribution and habitat. *Phalaenopsis zhanhuoensis* is currently known only from the type locality in Xichou, Yunnan, China. It is epiphytic on trunks and twigs at elevations 1400–1500 m in evergreen broad-leaved forests.

Phenology. Flowering in March and April.

Conservation status. *Phalaenopsis zhanhuoensis* grows in evergreen broadleaf forests in Xichou County Yunnan Province, China. One subpopulation of about 10 individuals was discovered during our fieldwork. The habitat has been severely fragmented due to the development of agriculture. During our survey in nearby forests, we did not find any additional subpopulation of the new species. According to IUCN criteria v15.1 (IUCN 2022), we putatively assessed this new species as Critically Endangered CR C2a(i).

Additional information

Conflict of interest

The authors have declared that no competing interests exist.

Ethical statement

No ethical statement was reported.

Funding

This research was supported by the Project of Orchid Biodiversity Survey of China, National Forestry and Grassland Administration (2019070714, 2020100707, 2022070702 to XJ) and the National Natural Science Foundation of China (32270214, 31870195 to XJ).

Author contributions

Conceptualization: BY, XJ. Funding acquisition: XJ. Investigation: SQ, XJ. Methodology: CM. Validation: ZL, YW. Writing – original draft: SQ. Writing – review and editing: HW.

Author ORCIDs

Shiyu Qin https://orcid.org/0009-0008-2680-6789
Hanchen Wang https://orcid.org/0000-0002-4690-8052
Yajun Wang https://orcid.org/0009-0001-1035-3964
Chongbo Ma https://orcid.org/0000-0001-5869-8649
Zan Li https://orcid.org/0009-0000-3098-1418
Boyun Yang https://orcid.org/0000-0003-2123-0027
Xiaohua Jin https://orcid.org/0000-0002-9987-5602

Data availability

All of the data that support the findings of this study are available in the main text or Supplementary Information.

References

Chase MW, Cameron KM, Freudenstein JV, Pridgeon AM, Salazar G, Van den Berg C, Schuiteman A (2015) An updated classification of Orchidaceae. Botanical Journal of the Linnean Society 177(2): 151–174. https://doi.org/10.1111/boj.12234

Chen XQ, Wood JJ (2009) *Phalaenopsis* Blume, Bijdr. 294. 1825. In: Wu CY, et al. (Eds) Flora of China, vol. 25. Beijing: Science Press and Missouri Botanical Garden Press, St. Louis, 478–483.

Christenson EA (2001) *Phalaenopsis*: a monograph. Timber Press, Portland, 330 pp.

Higgins W, Alrich P (2015) *Phalaenopsis*: the Genus in Pictures. International *Phalaenopsis* Alliance, Taiwan, 80–83.

IUCN (2022) Guidelines for Using the IUCN Red List Categories and Criteria. Version 15.1. https://www.iucnredlist.org/resources/redlistguidelines [Accessed 4 Dec.2023]

Jin JJ, Yu WB, Yang JB, Song Y, dePamphilis CW, Yi TS, Li DZ (2020) GetOrganelle: A fast and versatile toolkit for accurate de novo assembly of organelle genomes. Genome Biology 21(1): 241. https://doi.org/10.1186/s13059-020-02154-5

Kocyan A, Schuiteman A (2014) New combinations in Aeridinae (Orchidaceae). Phytotaxa 161: 061–085. https://doi.org/10.11646/phytotaxa.161.1.3

Li J, Wang S, Yu J, Ling W, Zhou S (2013) A Modified CTAB Protocol for Plant DNA Extraction. Zhiwu Xuebao 48(1): 72–78. https://doi.org/10.3724/SP.J.1259.2013.00072

Li YX, Li ZH, Schuiteman A, Chase MW, Li JW, Huang WC, Hidayat A, Wu SS, Jin XH (2019) Phylogenomics of Orchidaceae based on plastid and mitochondrial genomes. Molecular Phylogenetics and Evolution 139: 106540. https://doi.org/10.1016/j.ympev.2019.106540

Ma CB, Wang XL, Chen WS, Liu Z, Jin XH (2022) *Phalaenopsis medogensis* (Orchidaceae, Epidendroideae, Vandeae), a new species from Xizang, China. PhytoKeys 214: 39–46. https://doi.org/10.3897/phytokeys.214.93607

Miller MA, Pfeiffer W, Schwartz T (2010) Creating the CIPRES Science Gateway for inference of large phylogenetic trees. In: Gateway Computing Environments Workshop. New Orleans, 1–8. https://doi.org/10.1109/GCE.2010.5676129

Minh BQ, Schmidt HA, Chernomor O, Schrempf D, Woodhams MD, von Haeseler A, Lanfear R (2020) IQ-TREE 2: New Models and Efficient Methods for Phylogenetic Inference in the Genomic Era. Molecular Biology and Evolution 37(5): 1530–1534. https://doi.org/10.1093/molbev/msaa015

Padolina J, Linder C, Simpson B (2005) A Phylogeny of *Phalaenopsis* Using Multiple Chloroplast Markers. Selbyana 26: 23–27.

Pridgeon AM, Cribb PJ, Chase MW, Rasmussen FN (2014) Genera orchidacearum: Epidendroideae, volume 6, Part 3. Oxford University Press, Oxford, 232–241.

Tsai CC, Huang SC, Chou CH (2005) Molecular phylogeny of *Phalaenopsis* Blume (Orchidaceae) based on the internal transcribed spacer of the nuclear ribosomal DNA. Plant Systematics and Evolution 256(1–4): 1–16. https://doi.org/10.1007/s00606-005-0356-y

Tsai C, Chiang Y-C, Huang S, Chen C, Chou C (2010) Molecular phylogeny of *Phalaenopsis* Blume (Orchidaceae) on the basis of plastid and nuclear DNA. Plant Systematics and Evolution 288(1–2): 77–98. https://doi.org/10.1007/s00606-010-0314-1

Yukawa T, Kita K, Handa T, Hidayat T, Ito M (2005) Molecular Phylogenetics of *Phalaenopsis* (Orchidaceae) and allied Genera: Re-evaluation of Generic Concepts. Acta Phytotaxonomica et Geobotanica 56: 141–161. https://doi.org/10.18942/apg.KJ00004623240

Zhang D, Gao F, Jakovlic I, Zou H, Zhang J, Li WX, Wang GT (2020) PhyloSuite: An integrated and scalable desktop platform for streamlined molecular sequence data management and evolutionary phylogenetics studies. Molecular Ecology Resources 20(1): 348–355. https://doi.org/10.1111/1755-0998.13096

Zhou Z, Shi R, Zhang Y, Xing X, Jin X (2021) Orchid conservation in China from 2000 to 2020: Achievements and perspectives. Plant Diversity 43(5): 343–349. https://doi.org/10.1016/j.pld.2021.06.003

Supplementary material 1

GenBank accession numbers for sequences used for phylogenetic analyses

Authors: Shiyu Qin, Hanchen Wang, Yajun Wang, Chongbo Ma, Zan Li, Boyun Yang, Xiaohua Jin

Data type: docx

Link: https://doi.org/10.3897/phytokeys.237.112270.suppl1

Supplementary material 2

Phylogram of Bayesian Inference (BI) based on nrDNA ITS and plastid sequences (***matK***, ***trnL***, ***trnL-F***, and ***atpB-rbcL***)

Authors: Shiyu Qin, Hanchen Wang, Yajun Wang, Chongbo Ma, Zan Li, Boyun Yang, Xiaohua Jin

Data type: pdf

Explanation note: Numbers above branches indicate posterior probabilities (PP) for BI.

Link: https://doi.org/10.3897/phytokeys.237.112270.suppl2

PhytoKeys 237: 161–177 (2024)
DOI: 10.3897/phytokeys.237.103012

Research Article

Phylogenomics reveal *Populus gonggaensis* as a hybrid between *P. lasiocarpa* and *P. cathayana* (Salicaceae)

Wenyan Du[1], Yachao Wang[2], Dajun Xie[3], Enze Li[1], Yuran Bai[1], Ce Shang[1], Zhixiang Zhang[1]

1 *Laboratory of Systematic Evolution and Biogeography of Woody Plants, School of Ecology and Nature Conservation, Beijing Forestry University, Beijing 100083, China*
2 *School of Life Science, Fudan University, Shanghai 200433, China*
3 *Sichuan Academy of Forestry, Chengdu 610000, China*
Corresponding authors: Ce Shang (ce_shang@bjfu.edu.cn); Zhixiang Zhang (zxzhang@bjfu.edu.cn)

Abstract

High levels of intra-specific polymorphism and frequent hybridisation make it difficult to define species and correctly apply their scientific names. *Populus* L. is a challenging genus with plentiful natural and artificial hybrids. This study is a part of the project 'Flora of Pan-Himalaya' and aims to determine the taxonomic identity of *P. gonggaensis* N. Chao & J.R. He and to find out whether it is of hybrid origin. Whole-genome sequencing data were obtained from 57 samples. The SNP matrix was developed for phylogenetic reconstruction, ABBA-BABA statistics, PCA and ADMIXTURE analysis. The results indicate that *P. gonggaensis* is a spontaneous hybrid between *P. lasiocarpa* and *P. cathayana*. This study points out the importance of SNP data and comprehensive analyses for discovering the potential interspecific hybridisation and clarifies the usage of the name. In addition, the lectotype of *P. gonggaensis* was designated.

Key words: hybrid origin, *Populus gonggaensis*, whole genome resequencing

Academic editor: Irina Belyaeva
Received: 5 March 2023
Accepted: 1 January 2024
Published: 23 January 2024

Citation: Du W, Wang Y, Xie D, Li E, Bai Y, Shang C, Zhang Z (2024) Phylogenomics reveal *Populus gonggaensis* as a hybrid between *P. lasiocarpa* and *P. cathayana* (Salicaceae). PhytoKeys 234: 161–177. https://doi.org/10.3897/phytokeys.237.103012

Introduction

The genus *Populus* L. (Salicaceae), embraces ca. 60 tree species that are widely distributed and cultivated throughout the Northern Hemisphere (Dickmann 2001; POWO 2023). Most of the species of this genus play an important role in temperate forest ecosystems and numerous cultivars have arisen through hybridisation and artificial selection (Eckenwalder 1996).

According to morphological features, *Populus* was divided into six sections, i.e. sect. *Abaso* Eckenw., sect. *Turanga* Bunge, sect. *Populus* (= sect. *Leuce* Duby.), sect. *Leucoides* Spach, sect. *Aigeiros* Duby and sect. *Tacamahaca* Spach (Eckenwalder 1996). However, phylogenetic studies, based on nucleotide sequences, showed different results. Both nuclear and plastid sequences inferred that sect. *Tacamahaca* and sect. *Aigeiros* are polyphyletic (Yun et al. 2015; Liu et al. 2017). Using genome-wide nuclear single nucleotide polymorphism and chloroplast genome data, Wang et al. (2022) reconstructed the phylogeny of genus *Populus* and suggested a classification that recognises four subgenera, subg. *Abaso* (Eckenw.) C. Shang, Y.C. Wang and Z.X. Zhang, subg. *Turanga* (Bunge) Dode, subg. *Populus* and subg. *Tacamahaca* (Spach) Kamelin (= subg. *Eupopu-*

lus Dode, *nom. inval.*; containing species of sect. *Leucoides*, sect. *Aigeiros* and sect. *Tacamahaca*). The topology of the main clades of *Populus* is relatively clear; however, the phylogenetic and taxonomic positions of certain species remain problematic. High levels of morphological variation and reticulate evolution have led to a highly controversial species delimitation (Eckenwalder 1996). For instance, Fang et al. (1999) recorded 71 *Populus* species distributed within China, but Eckenwalder (1996) recognised only 29 species all over the world.

Hybridisation occurs amongst species of *Populus* and many species have been proved to be of hybrid origin. When published, *P. wulianensis* S.B. Liang & X.W. Li and *P. ningshanica* Z. Wang & S.L. Tung were regarded as species, but an integrative study, based on molecular evidence and morphological analysis, revealed both of them as hybrid species (Zhang et al. 2018; Liu et al. 2022). *Populus × irtyschensis* Chang Y. Yang was also shown to be a filial generation whose parents should be *P. nigra* L. and *P. laurifolia* Ledeb. (Feng et al. 2013; Shang et al. 2016). Recently, on the basis of whole-genome sequencing, Liu et al. (2022) examined 227 individuals from 12 taxa of the sect. *Populus*, recognised seven species and identified five hybrid taxa. For the genus *Populus*, interspecific hybridisation poses an obstacle to species delimitation and their possible hybrid origin (Belyaeva 2020). Therefore, it is important to conduct studies on some problematic taxa with potential hybridisation phenomena.

High-resolution molecular markers and comprehensive analysis are required in identification of potential hybridisation. Microsatellite (SSR) or a few nuclear/plastid sequences are mostly not enough to provide sufficient informative sites to detect complicated relationships resulting from reticulate evolution (Shang et al. 2022). The first sequenced woody plant genome was *P. trichocarpa* Torr. & A. Gray ex Hook. (Tuskan et al. 2006), a synonym of the earlier name, *P. tristis* Fisch., which is the correct name and currently accepted (Skvortsov 2010; Belyaeva et al. 2020; POWO 2023) and should be used in scientific papers instead of the redundant *P. trichocarpa*. With the continuous development of sequencing technology, whole genome sequence data have been increasingly published and whole-genome resequencing technology could provide sufficient single nucleotide polymorphism (SNP) to deal with taxonomic problems (Hirota et al. 2022). With unique superiority, whole-genome resequencing has also been widely used in phylogenetic and evolutionary studies of *Populus* (Wang et al. 2020; Liu et al. 2022; Wang et al. 2022), especially in detecting hybrids and exploring reticulate evolution.

Populus gonggaensis N. Chao & J.R. He has been described, based on specimens collected from the eastern margin of the Tibetan Plateau (Chao 1991). Several natural *Populus* species are sympatric in the vicinity of where *P. gonggaensis* was found, including two species from sect. *Leucoides*, i.e. *P. lasiocarpa* Oliv. and *P. glauca* Haines [= *P. wilsonii* C.K. Schneid. (Skvortsov 2008; Shang 2017)] and a number of species from sect. *Tacamahaca*, i.e. *P. cathayana* Rehder, *P. trinervis* Z. Wang & S.L. Tung, *P. szechuanica* C.K. Schneid., *P. rockii* (Rehder) H.L. Yang and *P. xiangchengensis* Z. Wang & S.L. Tun (Fang 1985; Fang et al. 1999).

With lobed flower disc, *P. gonggaensis* was thought to be a close relative of *P. lasiocarpa* or *P. glauca* and placed in sect. *Leucoides*. However, hairs on the surface of the abaxial leaf veins and branchlets are relatively short and procumbent, which differ from the long and twisted hairs of *P. lasiocarpa* and *P. glauca*. However, *P. gonggaensis* shows similarity in these characters with species of the sect. *Tacamahaca*.

Shang (2017) argued that *P. gonggaensis* should be treated as an ambiguous species, which needs further research, due to the fact that no wild individuals have been seen since the collection of the type specimen. The follow-up phylogenetic studies on *Populus* species have not taken *P. gonggaensis* into consideration (Wang et al. 2020, 2022). Unfortunately, no more specimens, which conform to the description in the original paper of *P. gonggaensis* or are similar to the type specimen, have been found either in the herbaria collections or digital collections available. Due to the large-scale development of industry in modern China, the locality where the type specimen was collected, has been turned into a newly-built area of Kangding. We also have not found plants that could be identified as *P. gonggaensis* in our recent fieldwork. Thus, it is important to conduct systematic research on *P. gonggaensis*, which can also provide phylogenetic evidence for species definition and taxonomic revision of *Populus* in the future.

Materials and methods

Sample collection and sequencing

A total of 57 samples represent 22 species including three species from sect. *Leucoides* and almost all species of subg. *Tacamahaca* distributed in China (Table 1). Only taxa of the subg. *Tacamahaca* occurring in the *P. gonggaensis* area were included in the study, excluded taxa being summarised in Suppl. material 1. The samples of *P. gonggaensis* were obtained from one of the syntypes stored at the Herbarium of Sichuan Academy of Forestry (**SCFI**, and all herbarium codes follow Thiers (2024)). For other taxa, fresh leaves were collected from adult trees and dried in silica gel. Voucher specimens were deposited at the Herbarium of Beijing Forestry University (**BJFC**). Previous whole-genome resequencing was also downloaded from the National Center for Biotechnology Information (**NCBI**) database and the BIG Data Center, Beijing Institute of Genomics (**BIG**), Chinese Academy of Sciences.

We used the CTAB method with minor modifications to extract the whole-genomic DNA from leaf samples (Doyle and Doyle 1987). All DNA samples were shipped to BerryGenomics (China) for subsequent sequencing. Whole-genome paired-ends reads with a target coverage of 10× were generated using Illumina NovaSeq 6000 platform (Illumina, San Diego, CA, United States).

Read mapping and SNP calling

Nuclear variants were discovered with BWA, SAM tools and GATK tools. First, the resequencing data for each sample was mapped to the reference genome of *P. trichocarpa* (Tuskan et al. 2006) using the default parameters of BWA-MEM v.0.7.17-r1188 (Li and Durbin 2009). Then, the mapped reads were converted to BAM files and sorted and filtered using the SAMtools package v.1.6 (Li et al. 2009). PCR duplications were marked using the Picard tool v.2.1.1. We used GATK v.4.1.4 (McKenna et al. 2010) with HaplotypeCaller to call a single sample of short variants and GATK with CombineGVCFs to combine all samples of short variants. SNPs were called using the SelectVariants tool implemented in GATK. Filters implemented in GATK were applied to the SNPs with the parameters as “QD < 10.0 || FS > 60.0 || MQ < 40.0 || SOR > 3.0 || MQRankSum < -12.5 || ReadPosRankSum < -8.0” (Danecek et al. 2011). Next, the depth of each SNP was counted

Table 1. Summary of the statistics of genome resequencing data for 57 individuals of 22 species and one outgroup.

Species	Individual	Location	BioSample ID	Vouchers	Barcodes or sources
Populus gonggaensis	*Populus gonggaensis*	Kangding, Sichuan, China	SAMN33060399	No.4207, Jiaren He et Neng Z	-
Populus heterophylla	*Populus heterophylla_1*#	Illinois, USA	SAMN17141192	-	Wang et al. (2022) / NCBI
	Populus heterophylla_2	South Carolina, USA	SAMN33178951	-	-
	Populus heterophylla_3#	New York, USA	SAMN17141193	-	Wang et al. 2022 / NCBI
	Populus heterophylla_4	Tennessee, Montgomery, USA	SAMN33178952	-	-
Populus glauca	*Populus glauca_1*#	Yadong, Xizang, China	SAMN17141151	-	Wang et al. 2022 / NCBI
	Populus glauca_2#	Ankang, Shaanxi, China	SAMN17141152	-	Wang et al. 2022 / NCBI
	Populus glauca_3	Weixi, Yunnan, China	SAMN33178953	-	-
Populus rockii	*Populus rockii_1*#	Foping, Shaanxi, China	SAMN17141156	-	Wang et al. 2022 / NCBI
	Populus rockii_2#	Wenxian, Gansu, China	SAMN17141184	-	Wang et al. 2022 / NCBI
	Populus rockii_3#	Zhen'an, Shaanxi, China	SAMN17141174	-	Wang et al. 2022 / NCBI
	Populus rockii_5#	Zhong-Tiao Mountains, Shanxi, China	SAMN17141129	-	Wang et al. 2022 / NCBI
Populus szechuanica	*Populus szechuanica* 1#	Yunnan, China	SAMN17141140		Wang et al. 2020 / NCBI
	Populus szechuanica_2#	Dali, Yunnan, China	SAMN17141153	-	Wang et al. 2022 / NCBI
	Populus szechuanica_3#	Ebian, Sichuan, China	SAMN17141130	-	Wang et al. 2022 / NCBI
Populus haoana	*Populus haoana_1*#	Yunnan, China	SAMN17141167	-	Wang et al. 2022 / NCBI
	Populus haoana_2#	Yunnan, China	SAMN17141185	-	Wang et al. 2022 / NCBI
	Populus haoana_3	Gongshan, Yunnan, China	SAMN33178949	-	-
Populus laurifolia	*Populus laurifolia_1*#	Xinjiang, China	SAMN17141138	-	Wang et al. 2022 / NCBI
	Populus laurifolia_2#	Xinjiang, China	SAMN17141118	-	Wang et al. 2022 / NCBI
	Populus laurifolia_3#	Khunjerab National Park, Pakistan	SAMN17141139	-	Wang et al. 2022 / NCBI
	Populus laurifolia_4#	Aketao, Xingjiang, China	SAMN17141159	-	Wang et al. 2022 / NCBI
Populus cathayana	*Populus cathayana_1*#	Shannxi, China	SAMN17141127	-	Wang et al. 2022 / NCBI
	Populus cathayana_2#	Hebei, China	SAMN17141163	-	Wang et al. 2022 / NCBI
	Populus cathayana_3#	Sichuan, China	SAMN17141172	-	Wang et al. 2022 / NCBI
	Populus cathayana_4	Kangding, Sichuan, China	SAMN33060396	I-3103, Ce Shang	BJFC00112807
Populus koreana	*Populus koreana_1*#	Jilin, China	SAMN17141148	-	Wang et al. 2022 / NCBI
	Populus koreana_2#	Heilongjiang, China	SAMN17141149	-	Wang et al. 2022 / NCBI
	Populus koreana_3#	Chifeng, Nei Mongol, China	SAMN17141162	-	Wang et al. 2022 / NCBI
Populus pseudoglauca	*Populus pseudoglauca_1*#	Mainling, Xizang, China	SAMN17141168	-	Wang et al. 2022 / NCBI
	Populus pseudoglauca_2#	Mainling, Xizang, China	SAMN17141136	-	Wang et al. 2022 / NCBI
Populus ciliata	*Populus ciliata*#	Mainling, Xizang, China	SAMN17141175	-	Wang et al. 2022 / NCBI
Populus xiangchengensis	*Populus xiangchengensis_1*#	Kangding, Sichuan, China	SAMN17141168	-	Wang et al. 2022 / NCBI
	Populus xiangchengensis_2#	Markam, Xizang, China	SAMN17141136	-	Wang et al. 2022 / NCBI
	Populus xiangchengensis_3#	Xiangcheng, Sichuan, China	SAMN17141128	-	Wang et al. 2022 / NCBI
	Populus xiangchengensis_4#	Gongshan, Yunnan, China	SAMN17141166	-	Wang et al. 2022 / NCBI
	Populus xiangchengensis_5	Kangding, Sichuan, China	SAMN33178950	-	-
Populus afghanica	*Populus afghanica*#	Xinjiang, China	SAMN17141165	-	Wang et al. 2022 / NCBI
Populus iliensis	*Populus iliensis*#	Xinjiang, China	SAMN17141158	-	Wang et al. 2022 / NCBI
Populus kangdingensis	*Populus kangdingensis*#	Sichuan, China	SAMN17141132	-	Wang et al. 2022 / NCBI
Populus lasiocarpa	*Populus lasiocarpa_1*#	Sichuan, China	SAMN17141164	-	Wang et al. 2022 / NCBI
	Populus lasiocarpa_2#	Hubei, China	SAMN17141170	-	Wang et al. 2022 / NCBI
	*Populus lasiocarpa_3**	-	SAMC065352	-	Wang et al. 2020 / GSA
	*Populus lasiocarpa_4**	-	SAMC065353	-	Wang et al. 2020 / GSA
	*Populus lasiocarpa_5**	-	SAMC065354	-	Wang et al. 2020 / GSA
Populus nigra	*Populus nigra_1*#	Shannxi, China	SAMN17141114	-	Wang et al. 2022 / NCBI
	Populus nigra_2#	Xinjiang, China	SAMN17141142	-	Wang et al. 2022 / NCBI
Populus qamdoensis	*Populus qamdoensis*#	Qamdo, Xizang, China	SAMN17141117	-	Wang et al. 2022 / NCBI

Species	Individual	Location	BioSample ID	Vouchers	Barcodes or sources
Populus simonii	*Populus simonii_1*#	Taibai, Shaanxi, China	SAMN17141123	-	Wang et al. 2022 / NCBI
	Populus simonii_2#	Aba, Sichuan, China	SAMN17141124	-	Wang et al. 2022 / NCBI
Populus trinervis	*Populus trinervis_3*#	Wenxian, Gansu, China	SAMN17141125	-	Wang et al. 2022 / NCBI
	Populus trinervis_4#	Wuwei, Gansu, China	SAMN17141126	-	Wang et al. 2022 / NCBI
	Populus trinervis_1	Kangding, Sichuan, China	SAMN33060397	I-3107, Ce Shang	BJFC00112810
	Populus trinervis_2	Kangding, Sichuan, China	SAMN33060398	I-3114, Ce Shang	BJFC00112809
Populus yunnanensis	*Populus yunnanensis_1*#	Lijiang, Yunnan, China	SAMN17141154	-	Wang et al. 2022 / NCBI
	Populus yunnanensis_2#	Kunming, Yunnan, China	SAMN17141169	-	Wang et al. 2022 / NCBI
Populus euphratica	*Populus euphratica*#	Qinghai, China	SAMN17141146		Wang et al. 2020 / NCBI

Note: The individuals for which genome sequences were downloaded from the Genome Sequence Archive (GSA) are marked by asterisks, while those downloaded from the NCBI are marked by the hash (#) sign and the rest are data from these two papers (Wang et al. 2020, 2022). Samples without symbol markings are from new data in this study.

and the average depth was calculated. Finally, using GATK, the SNP dataset was generated by filtering by depth the minor allele frequencies. Finally, the "-st" command was used to specify the model when the data used were for DNA.

Phylogenetic analyses

Python v.2.7.5 was used to convert SNPs into phylip format and IQ-tree v.2.0.3 to analyse the dataset (Felsenstein 1993; Nguyen et al. 2015). We used "-alrt" to specify that the number of repetitions of SH-aLRT branch test was 1000 (Guindon et al. 2010). A Maximum Likelihood (ML) phylogenetic tree was constructed by IQ-tree under the most appropriate model selected by ModelFinder (Kalyaanamoorthy et al. 2017). *Populus euphratica* was selected as the outgroup.

PCA and ADMIXTURE analysis

PLINK v.1.9.0 (Purcell et al. 2007) was used for LD-based SNP filtering. A principal component analysis (PCA) of screened species of *Populus* was performed with PLINK, based on whole genome SNPs and graphs were built using the 'ggplot2' package (Wickham 2016) in R. ADMIXTURE software (Alexander et al. 2009) was used for Maximum Likelihood estimation of individual ancestors from multi-locus SNP genotype datasets. Moreover, admixture uses a fast numerical optimisation algorithm that allows for faster calculation of estimates. Then, we used ADMIXTURE v.1.3.0 to study the population structure of some individuals and the number of clusters (K) was set from 1 to 10. Finally, the optimal K value was selected by cross-validation. The cross-validation used by ADMIXTURE is to divide the genotype data into several parts, use one part as the test set and the rest as the training set and then calculate the log-likelihood value. The times of cross-validation can be specified by the -cv=n parameter, where n is the number of splits. ADMIXTURE will output the cross-validation error (CV error). The K value is the most appropriate (most ideal species and population number) when the cross-validation error value is at its lowest.

ABBA-BABA statistics

To detect gene flow from other species into *P. gonggaensis*, we performed ABBA-BABA statistics to calculate gene flow from potential parents. ABBA-BABA

Statistics (also known as D-statistics) provided a model to calculate deviations from a strictly bifurcated evolutionary history using genome-scale SNP data, in order to test for gene penetrance (Martin et al. 2015; Malinsky et al. 2021). Briefly, the relationship amongst three populations and an outgroup was assumed to be (((P_1, P_2), P_3), O) and this model could test whether there was an excess of shared variation between P_2 and P_3 compared to that between P_1 and P_3 (Durand et al. 2011). The D-value was the ratio of the difference in the number of ABBA sites and BABA sites to the sum of the two types of sites. The larger the value of D, the stronger the degree of gene flow from P_2 to P_3. If the absolute value of the Z-score was higher than 3, it would be considered statistically significant (Busing et al. 1999). D software was used for gene flow analysis. The vcf file containing the SNP dataset was imported, a directory was created and the outgroup was specified.

Results

Sequence data processing

We collected and performed whole genome resequencing for nine individuals sampled from *P. heterophylla*, *P. glauca* and *P. haoana*, with an average depth of 10× for each individual. In total, 735.14 GB of clean data of 57 individuals were obtained for single nucleotide polymorphism (SNP) calling. Clean data were mapped against the *P. trichocarpa* reference genome and strict analyses, 4,790,248 high-quality SNPs were obtained. The total SNP dataset was used for all analyses.

Phylogeny based on SNP

The ML tree was built using the total SNP dataset obtained, with *P. euphratica* set as the outgroup and the other 21 species clustered into three clades (Fig. 1A). Two sect. *Leucoides* species, *P. heterophylla* Du Roi and *P. glauca* Haines were firstly divergent. The second clade included some species of the sect. *Tacamahaca* and sect. *Aigeiros*, i.e. *P. trinervis*, *P. kangdingensis* Z. Wang & S.L. Tung, *P. qamdoensis* Z. Wang & S.L. Tung, *P. yunnanensis* Dode, *P. simonii* Carrière, *P. iliensis* Drobow (= *P. usbekistanica* Kom.), *P. nigra* L. and *P. afghanica* (Aitch. & Hemsl.) C.K. Schneid. (= *P. nigra*). *Populus gonggaensis* and *P. lasiocarpa* (sect. *Leucoides*) formed a monophyletic clade, which was sister of other species of sect. *Tacamahaca* represented by *P. cathayana* and *P. szechuanica*. The bootstrap values of all the interspecies nodes in this tree were extremely high.

PCA analysis

To facilitate the observation of the results, the data of the outgroup (*P. euphratica*) were removed from the SNP dataset for PCA analysis. Individuals of sect. *Tacamahaca* were clustered together (upper left corner of the Fig. 2A), while individuals of sect. *Leucoides* were clustered in the lower right corner of the Figure (*P. heterophylla* is the North American-distributed species, which is the right-most off-centre point in Fig. 2A). *P. gonggaensis* was located between the two sections. Combining the ML tree and the result of PCA analysis that involved species that occur in the area within or around the type locality of *P. gonggaensis*, we selected the 12 species closest to *P. gonggaensis* in each of

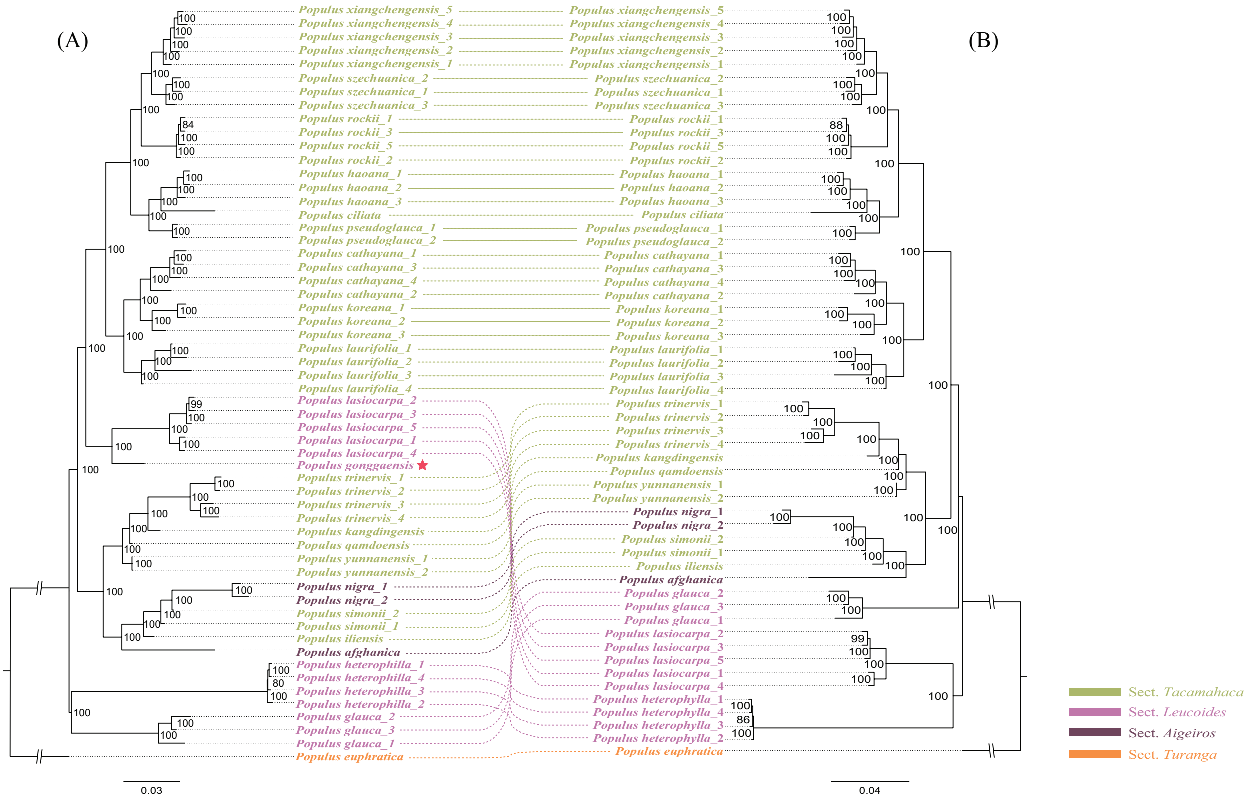

Figure 1. A ML tree of 57 samples of the genus *Populus* reconstructed by IQ-TREE, based on 4,790,248 high-quality SNPs with an outgroup of *P. euphratica* **B** ML tree of 56 samples (*P. gonggaensis* is deleted) of the genus *Populus* reconstructed by IQ-TREE, based on 4,790,248 high-quality SNPs with an outgroup of *P. euphratica*.

the two sections in the PCA, which include *P. glauca*, *P. cathayana*, *P. koreana*, *P. lasiocarpa*, *P. rockii*, *P. laurifolia*, *P. ciliata*, *P. pseudoglauca*, *P. szechuanica*, *P. haoana* and *P. xiangchengensis*. Species of sect. *Tacamahaca* still gathered, but *P. lasiocarpa* became separated from *P. glauca* (Fig. 2B). Fig. 2C was plotted by adding PC3 (Z-axis) to Fig. 2B. Individuals in the blue circles include all samples from *P. cathayana*, and *P. koreana*, while samples in the red circles were *P. lasiocarpa*. *P. gonggaensis* is located between *P. lasiocarpa* and several species of sect. *Tacamahaca* (*P. cathayana* and *P. koreana*)

ADMIXTURE analysis

The SNP dataset for admixture analysis covered 38 individuals of 12 species, amongst which 37 samples were the same as the 37 samples in PCA (Fig. 2B). Besides, *P. euphratica* was added as the outgroup to facilitate the calculation and accuracy for the visualisation of the dataset. The population structure was analysed using K values from 1 to 15 and the optimal K value was calculated as 9 (Fig. 3B). Each of the two assumed parents, *P. lasiocarpa* and *P. cathayana*, was recognised as an independent species separated from other samples (Fig. 3B). Additionally, *P. gonggaensis* was an admixture of these two species.

ABBA-BABA statistics

SNP datasets of 12 species were used for Dsuite calculations. Using *P. euphratica* as the outgroup, the gene flow was calculated for all trios and two result

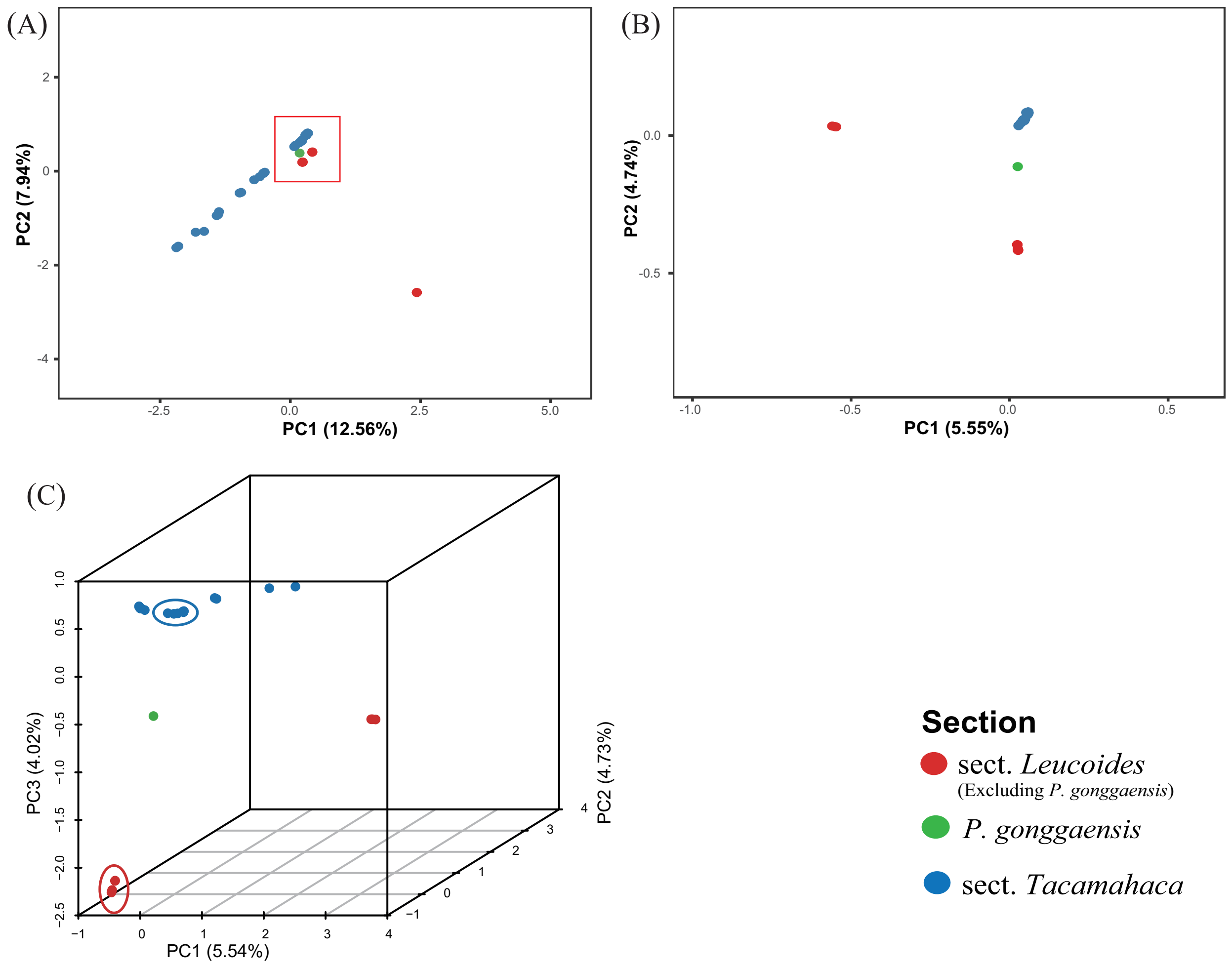

Figure 2. Principal Component Analysis (PCA), based on genetic distance using SNPs data **A** all 57 samples representing 22 species **B** 37 samples representing 12 species, including *Populus gonggaensis* and its most closely-related species **C** plotted by adding PC3 (Z-axis) to **B**. Points inside red circle represents *P. lasiocarpa*, while those inside blue circle represent *P. cathayana* and *P. koreana*.

files (BBAA.txt and Dmin.txt) were generated, reacting to the introgression between P2 and P3 for each trio and containing all combinations with positive D-values after random operations, with the same P2–P3 species corresponding to different D-values depending on the P1 species. The results are shown in Fig. 3A. When *P. gonggaensis* is selected as P3 and the D value is positive, there are a total of 36 combination forms. Amongst the combinations that satisfy the condition, the species that could be located at P2 are *P. cathayana*, *P. koreana*, *P. lasiocarpa*, *P. ciliata*, *P. rockii*, *P. pseudoglauca*, *P. szechuanica* and *P. xiangchengensis*. The formula is used to calculate the results of all negative D-values associated with these eight species and the final data of total D-values are presented in the heat map in Fig. 3A. *Populus cathayana* has the highest D-value amongst all species and when it is P2, all the eight values are positive (Fig. 3A). This means that *P. cathayana* provides more genetic swaps with *P. gonggaensis* than any other species. Hence, the largest proportion of gene flow in *P. gonggaensis* is from *P. cathayana*. When *P. lasiocarpa* is P2, the ratio of gene flow to *P. gonggaensis* is only lower than that caused by *P. cathayana* and all other D-values are positive (Fig. 3A). Thus, *P. cathayana* and *P. lasiocarpa* are the species that swap the most genes with *P. gonggaensis*.

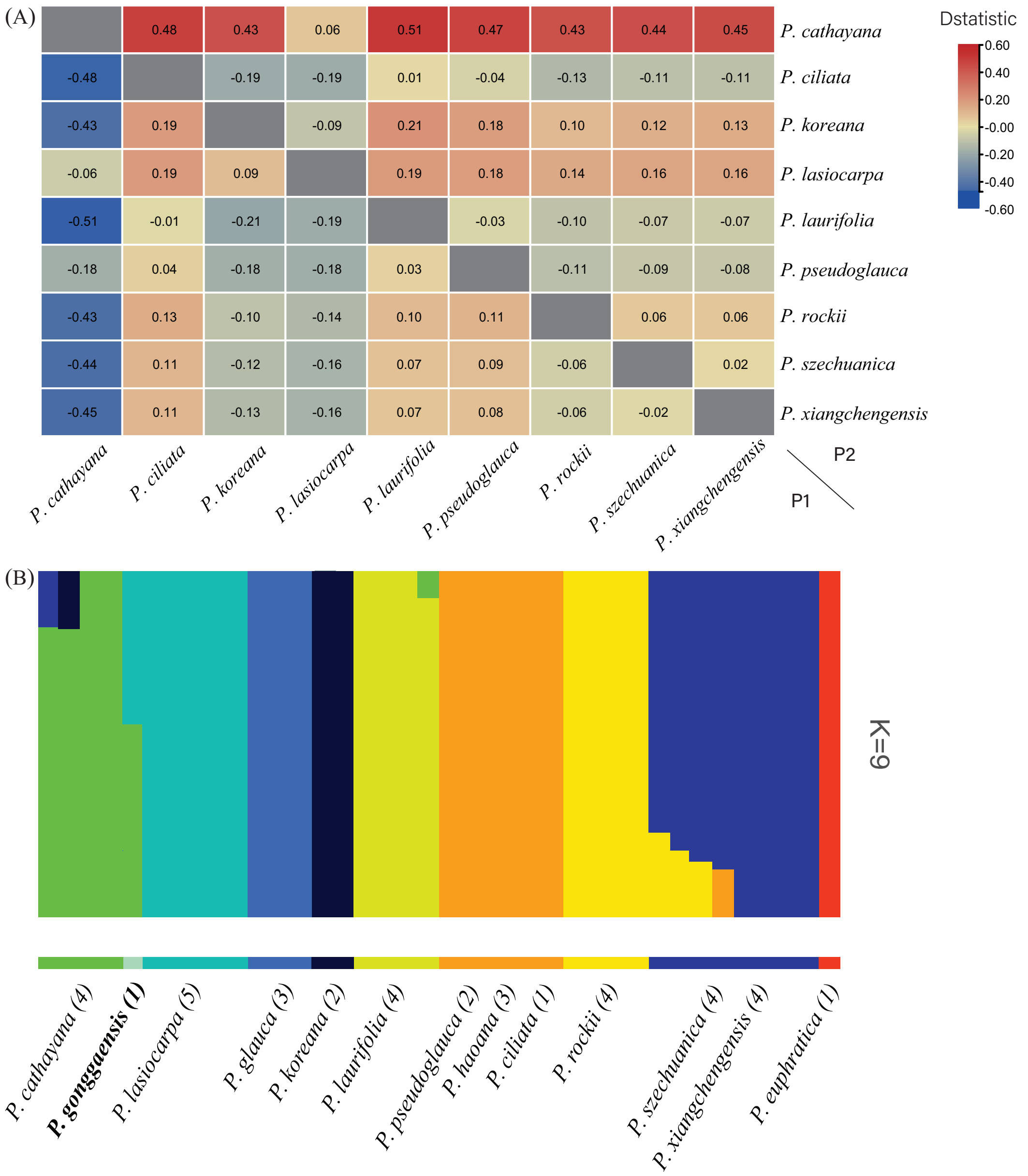

	P. cathayana	*P. ciliata*	*P. koreana*	*P. lasiocarpa*	*P. laurifolia*	*P. pseudoglauca*	*P. rockii*	*P. szechuanica*	*P. xiangchengensis*
P. cathayana		0.48	0.43	0.06	0.51	0.47	0.43	0.44	0.45
P. ciliata	-0.48		-0.19	-0.19	0.01	-0.04	-0.13	-0.11	-0.11
P. koreana	-0.43	0.19		-0.09	0.21	0.18	0.10	0.12	0.13
P. lasiocarpa	-0.06	0.19	0.09		0.19	0.18	0.14	0.16	0.16
P. laurifolia	-0.51	-0.01	-0.21	-0.19		-0.03	-0.10	-0.07	-0.07
P. pseudoglauca	-0.18	0.04	-0.18	-0.18	0.03		-0.11	-0.09	-0.08
P. rockii	-0.43	0.13	-0.10	-0.14	0.10	0.11		0.06	0.06
P. szechuanica	-0.44	0.11	-0.12	-0.16	0.07	0.09	-0.06		0.02
P. xiangchengensis	-0.45	0.11	-0.13	-0.16	0.07	0.08	-0.06	-0.02	

Figure 3. Hybrid introgression analysis using SNP matrix of *Populus* species **A** the results of ABBA-BABA statistics which measured gene flow amongst 12 species when P3 = *P. gonggaensis*. When D > 0 and the D value is further away from 0, it indicates that a gene swap or hybridisation event is more likely to have occurred, which means the genes of P3 is more likely to swap with those of P1 or P2 **B** population structure analysis for 12 species of *Populus* (K = 9). Each coloured bar represents one individual and coloured segments represent proportions of ancestral components. The number of individuals and species names for each lineage are shown at the bottom.

Taxonomic treatment

***Populus* × *gonggaensis* N. Chao & J.R. He in Sichuan Forest. Sci. Techn. 12(3): 1, f. 1. 1991.**

= *Populus cathayana* Rehder × *Populus lasiocarpa* Oliv.

Type. China, Sichuan, Kangding County, Simaqiao, 2700 m elev., 27 May 1991, Neng Chao & Jiaren He 4207 (Lectotype in SCFI!, designated here; isolectotypes in SCFI!).

There were four specimens of ‘Neng Chao & Jiaren He 4207’ found in SCFI and all of them were labelled as ‘TYPUS’. According to Art. 9.6 of ICN (Turland et al. 2018), the four specimens should be syntypes (Suppl. material 3). Hence, we designated the best-preserved one as the lectotype of *P.* × *gonggaensis* (Fig. 5).

Discussion

When published, *P. gonggaensis* was considered as a species that belongs to sect. *Leucoides*, according to morphological characteristics, such as deeply-lobed discs, tomentose leaves and pubescent capsules (Chao 1991). We observed the type specimens and found *P. gonggaensis* shows similarities in both *P. cathayana* and *P. lasiocarpa*. For example, the persistent floral discs on the fruit of *P. gonggaensis* are parted, which is similar to those of *P. lasiocarpa*. On the other hand, the leaves of *P. gonggaensis* are abaxially glabrous, which is similar to those of *P. cathayana*. Additionally, the morphology of *P. gonggaensis* is partly intermediate between that of its parents (Table 2, Fig. 4). Apart from the type specimens, not a single specimen could be indubitably identified as *P. gonggaensis*, based on morphological features. During the field survey, we did not find an individual which is consistent with the original description and protologue. The type of *P. gonggaensis* was collected from Simaqiao, which has now become an urban built-up area of Kangding City. *P. cathayana* has a wide distribution in the area and constitutes a sympatric species with *P. gonggaensis*.

According to the phylogenetic tree, *P. gonggaensis* is clustered with *P. lasiocarpa* with high support, which suggested a close relationship between them. However, the topology differed significantly from another phylogenetic research on the genus *Populus* (Wang et al. 2022). Whether species of sect. *Leucoides* formed a monophyletic clade, *P. lasiocarpa*, *P. glauca* and *P. heterophylla* are always basal taxa of subg. *Tacamahaca* (= subg. *Eupopulus*, *nom. inval.*; Wang et al. (2020); Wang et al. (2022)). In this study, *P. gonggaensis* and *P. lasiocarpa* are clustered in the clade which is composed of sect. *Tacamahaca* and sect. *Aigeiros*, but set apart from *P. heterophylla* and *P. glauca* of sect. *Leucoides*. The introduction of hybrid individuals will alter the topology of the phylogenetic tree (Debray et al. 2022). Almost all the species have been analysed in earlier phylogenetic research (Wang et al. 2020, 2022), except for *P. gonggaensis*. Thus, when we removed *P. gonggaensis* data from the SNP matrix and reconstructed the ML tree, the topology was totally different (Fig. 1B). Simultaneously, we

Table 2. Morphological comparison of *Populus gonggaensis* with *P. cathayana* and *P. lasiocarpa*.

Traits	*P. gonggaensis*	*P. cathayana*	*P. lasiocarpa*
Petiole	Pubescent.	Pilose.	Glabrous.
Leaf blade	Ovate; adaxially glabrous; abaxially glabrous when young; base subcordate; apex acuminate.	Ovate, elliptic-ovate, elliptic or narrowly ovate; adaxially glabrous; abaxially glabrous; base rounded or subcordate; apex acuminate or mucronate.	Ovate; adaxially glabrous; abaxially tomentose when young, and then tomentose along veins; base deeply cordate; apex acuminate.
Male flower	–	Floral disc entire.	Floral disc parted.
Female flower	Floral disc parted, ovary partly pannose.	Floral disc entire; ovary glabrous.	Floral disc parted; ovary pannose.
Capsule	Ovoid, pilose, 3-valved; pedicels 1 mm long, glabrous.	Floral disc persistent, pericarp glabrous.	Floral disc deciduous, pericarp tomentose.

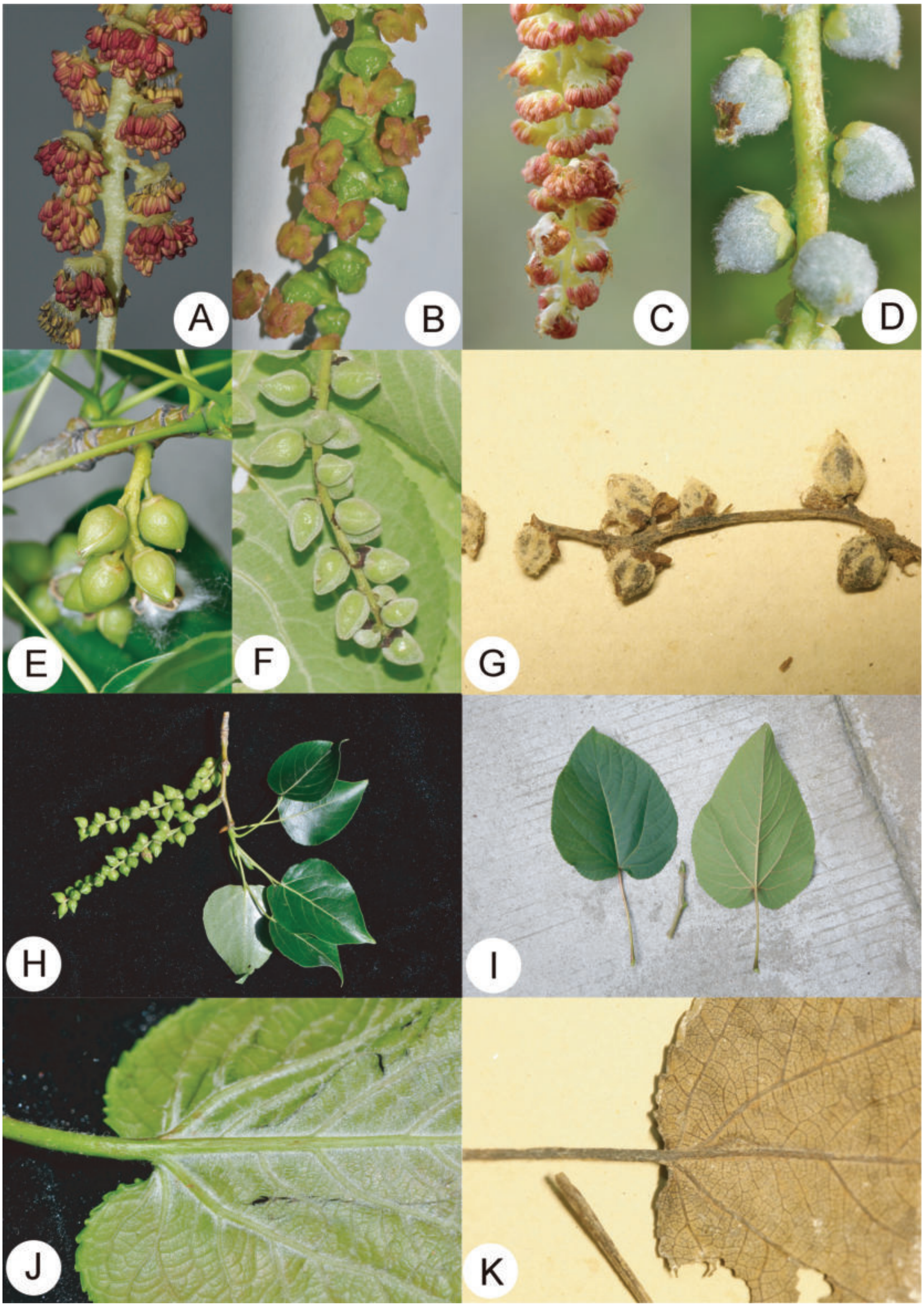

Figure 4. Morphological comparison of *Populus gonggaensis* with *P. cathayana* and *P. lasiocarpa* **A** male flower of *P. cathayana* (floral disc entire) **B** female flower of *P. cathayana* (floral disc entire, ovary glabrous) **C** male flower of *P. lasiocarpa* (floral disc parted) **D** female flower of *P. lasiocarpa* (floral disc parted, ovary pannose) **E** capsule of *P. cathayana* (floral disc persistent, pericarp glabrous) **F** capsule of *P. lasiocarpa* (floral disc deciduous, pericarp tomentose) **G** female flower of *P. gonggaensis* (floral disc parted, ovary partly pannose) **H** fruiting branch of *P. cathayana* (leaf abaxially glabrous, base rounded or subcordate) **I** leaf of *P. lasiocarpa* (base deeply cordate) **J** young leaf of *P. lasiocarpa* (abaxially tomentose) **K** young leaf of *P. gonggaensis* (abaxially glabrous, base subcordate).

四川省林业科学研究所
森林植物分类研究室 植物标本采集记录

标本号：

产地：康定，驷马桥，桥头

海拔高度：2700 米

环境：

乔木、灌木、草本、或藤本

高度：20 米；胸高直径：36 厘米

树皮：

枝：

叶：

花：♀，花盘深裂

果：

用途：

附记：

地方名：

采集人：赵 能 贺家仁

采集号：4207 采集日期：1991 ~~1989~~年 5月 27日

科名：

种名：Populus

赵能

4207

模式标本
TYPUS

Populus gonggaensis, sp. nov.

鉴定人：N. Chao 1991年6月20日

四川省林科所森林植物分类研究室

Figure 5. Lectotype of *Populus gonggaensis* N. Chao & J.R. He.

have reconstructed a species tree, which also solved this problem (Suppl. material 2). *Populus lasiocarpa* no longer clustered with the branches of sect. *Tacamahaca* and sect. *Aigeiros*, but clustered with *P. heterophylla* as a monophyly and all species of sect. *Leucoides*, located at the base of the tree. The PCA analysis showed that *P. gonggaensis* may be an intersectional hybrid and one of the parents could be *P. lasiocarpa*.

Results of ABBA-BABA analysis show that, when *P. lasiocarpa* is P2, the D value is < 0 only compared with *P. cathayana*, so it is more possible that *P. lasiocarpa* is the other parent rather than the remaining *Populus* species. In Fig. 3, when *P. koreana* is P2, the D values of *P. koreana* and *P. lasiocarpa* seem to be close; but when compared with *P. lasiocarpa*, the D value of *P. koreana* is smaller than that of *P. lasiocarpa*. Thus, the probability that *P. koreana* is the other parent is lower than that for *P. lasiocarpa*. There were two other reasons that can also rule out the possibility of *P. koreana* being a parent: firstly, *P. koreana* is distributed in north-eastern China and there is a very large geographical distance from where *P. gonggaensis* is distributed, which means there is no distribution overlap between *P. koreana* and *P. gonggaensis* (we speculate that the high contribution of *P. koreana* is due to the fact that it has a large portion of the gene flow of *P. cathayana* and that they may constitute a complex as found in previous phylogenetic studies); second, what we can find in Fig. 3A is that when *P. cathayana* is P2, the smallest D value occurs when *P. lasiocarpa* is P1, while the D value of *P. cathayana* is still considerable when *P. koreana* is P1 and *P. cathayana* is P2. Therefore, we believe that the D value is close to 0 when P1 and P2 were the two parents of P3, because gene flows occur between *P. gonggaensis* as P3 and both parents. These results suggest that *P. cathayana* and *P. lasiocarpa* are two potential parents for *P. gonggaensis*.

Our PCA study showed that *P. gonggaensis* may be an intersectional hybrid and one of the parents is *P. lasiocarpa* of sect. *Leucoides*, while the contribution of gene flow from *P. koreana* to *P. gonggaensis* is much lower, so the possibility of its being another parent is excluded. Finally, the ADMIXTURE result indicated that *P. gonggaensis* contains nearly equal components of both species, namely *P. cathayana* and *P. lasiocarpa* (Fig. 3B).

In conclusion, multiple methods provided evidence for a supposition that *P. gonggaensis* is a spontaneous hybrid between *P. lasiocarpa* and *P. cathayana*. During our field investigation, not a single individual matching the type specimens was discovered. In addition, *P. gonggaensis* is not a taxon, but a solitary hybrid individual, probably F1, which no longer occurs in the area from which it was described.

Acknowledgements

We thank the curators of SCFI for providing the necessary material. We are also grateful to the reviewers and the editor for constructive comments and suggestions that helped us to improve the manuscript.

Additional information

Conflict of interest

The authors have declared that no competing interests exist.

Ethical statement

No ethical statement was reported.

Funding

This work was financially supported by National Natural Science Foundation of China (grant no. 32001247) and the Second Tibetan Plateau Scientific Expedition and Research Program (grant no. 2019QZKK05020205).

Author contributions

Data curation: WD. Formal analysis: WD. Funding acquisition: ZZ, CS. Methodology: YW. Resources: DX. Software: WD, YW, EL, YB. Visualization: WD. Writing – original draft: WD. Writing – review and editing: CS.

Data availability

All of the data that support the findings of this study are available in the main text or Supplementary Information.

References

Alexander DH, Novembre J, Lange K (2009) Fast model-based estimation of ancestry in unrelated individuals. Genome Research 19(9): 1655–1664. https://doi.org/10.1101/gr.094052.109

Belyaeva IV (2020) Challenges in identification and naming: Salicaceae *sensu stricto*. Skvortsovia: International Journal of Salicology and Plant Biology 5(3): 83–104.

Belyaeva IV, Dutton C, Govaerts RHA, Liesebach H, McGinn K, Taylor G, Pickett J (2020) Verification of names for certain *Populus* L. clones (Salicaceae) commonly grown in the United Kingdom. Skvortsovia: International Journal of Salicology and Plant Biology 6(3): 87–116. https://doi.org/10.51776/2309-6500_2020_6_3_87

Busing FM, Meijer E, Leeden RVD (1999) Delete-m jackknife for unequal m. Statistics and Computing 9(1): 3–8. https://doi.org/10.1023/A:1008800423698

Chao N (1991) New taxa of sect. *Leucoides* Spach of gen. *Populus* L. Sichuan Linye Keji 12(3): 1–3.

Danecek P, Auton A, Abecasis G, Albers CA, Banks E, DePristo MA, Handsaker RE, Lunter G, Marth GT, Sherry ST, McVean G, Durbin R (2011) The variant call format and VCFtools. Bioinformatics 27(15): 2156–2158. https://doi.org/10.1093/bioinformatics/btr330

Debray K, Le Paslier M-C, Bérard A, Thouroude T, Michel G, Marie-Magdelaine J, Bruneau A, Foucher F, Malécot V (2022) Unveiling the Patterns of Reticulated Evolutionary Processes with Phylogenomics: Hybridization and Polyploidy in the Genus *Rosa*. Systematic Biology 71: 547–569. https://doi.org/10.1093/sysbio/syab064

Dickmann D (2001) Poplar culture in north America. NRC Research Press.

Doyle JJ, Doyle JL (1987) A rapid DNA isolation procedure for small quantities of fresh leaf tissue.

Durand EY, Patterson N, Reich D, Slatkin M (2011) Testing for ancient admixture between closely related populations. Molecular Biology and Evolution 28(8): 2239–2252. https://doi.org/10.1093/molbev/msr048

Eckenwalder JE (1996) Systematics and evolution of *Populus*. Biology of *Populus* and its implications for management and conservation 7: 1–32.

Fang W (1985) Salicaceae. In: Editorial Board of 'Flora of Sichuan (Eds) Flora of Sichuan (Vol. 3). Sichuan Publishing House of Science & Technology, Chengdu, 38–143.

Fang ZF, Zhao SD, Skvortsov AK (1999) Salicaceae. In: Wu ZY, Raven PH (Eds) Flora of China (Vol. 4). Science Press, Beijing & Missouri Botanical Garden, St. Louis, 139–274.

Felsenstein J (1993) PHYLIP (phylogeny inference package), version 3.5 c. Joseph Felsenstein.

Feng J, Jiang D, Shang H, Dong M, Wang G, He X, Zhao C, Mao K (2013) Barcoding poplars (*Populus* L.) from western China. PLOS ONE 8(8): e71710. https://doi.org/10.1371/journal.pone.0071710

Guindon S, Dufayard J-F, Lefort V, Anisimova M, Hordijk W, Gascuel O (2010) New algorithms and methods to estimate maximum-likelihood phylogenies: Assessing the performance of PhyML 3.0. Systematic Biology 59(3): 307–321. https://doi.org/10.1093/sysbio/syq010

Hirota SK, Yahara T, Fuse K, Sato H, Tagane S, Fujii S, Minamitani T, Suyama Y (2022) Molecular phylogeny and taxonomy of the *Hydrangea serrata* complex (Hydrangeaceae) in western Japan, including a new subspecies of *H. acuminata* from Yakushima. PhytoKeys 188: 49–71. https://doi.org/10.3897/phytokeys.188.64259

Kalyaanamoorthy S, Minh BQ, Wong TK, Von Haeseler A, Jermiin LS (2017) ModelFinder: Fast model selection for accurate phylogenetic estimates. Nature Methods 14(6): 587–589. https://doi.org/10.1038/nmeth.4285

Li H, Durbin R (2009) Fast and accurate short read alignment with Burrows–Wheeler transforms. Bioinformatics 25: 1754–1760. https://doi.org/10.1093/bioinformatics/btp324

Li H, Handsaker B, Wysoker A, Fennell T, Ruan J, Homer N, Marth G, Abecasis G, Durbin R (2009) The sequence alignment/map format and SAMtools. Bioinformatics 25(16): 2078–2079. https://doi.org/10.1093/bioinformatics/btp352

Liu X, Wang Z, Shao W, Ye Z, Zhang J (2017) Phylogenetic and taxonomic status analyses of the *Abaso* section from multiple nuclear genes and plastid fragments reveal new insights into the North America origin of *Populus* (Salicaceae). Frontiers in Plant Science 7: e2022. https://doi.org/10.3389/fpls.2016.02022

Liu S, Zhang L, Sang Y, Lai Q, Zhang X, Jia C, Long Z, Wu J, Ma T, Mao K, Street NR, Ingvarsson PK, Liu J, Wang J (2022) Demographic history and natural selection shape patterns of deleterious mutation load and barriers to introgression across *Populus* genome. Molecular Biology and Evolution 39(2): msac008. https://doi.org/10.1093/molbev/msac008

Malinsky M, Matschiner M, Svardal H (2021) Dsuite-Fast D-statistics and related admixture evidence from VCF files. Molecular Ecology Resources 21(2): 584–595. https://doi.org/10.1111/1755-0998.13265

Martin SH, Davey JW, Jiggins CD (2015) Evaluating the use of ABBA–BABA statistics to locate introgressed loci. Molecular Biology and Evolution 32(1): 244–257. https://doi.org/10.1093/molbev/msu269

McKenna A, Hanna M, Banks E, Sivachenko A, Cibulskis K, Kernytsky A, Garimella K, Altshuler D, Gabriel S, Daly M, DePristo MA (2010) The genome analysis toolkit: A MapReduce framework for analyzing next-generation DNA sequencing data. Genome Research 20(9): 1297–1303. https://doi.org/10.1101/gr.107524.110

Nguyen L-T, Schmidt HA, Von Haeseler A, Minh BQ (2015) IQ-TREE: A fast and effective stochastic algorithm for estimating maximum-likelihood phylogenies. Molecular Biology and Evolution 32(1): 268–274. https://doi.org/10.1093/molbev/msu300

POWO (2023) Plants of the World Online. Facilitated by the Royal Botanic Gardens, Kew. http://www.plantsoftheworldonline.org/ [Accessed 11.08.2023]

Purcell S, Neale B, Todd-Brown K, Thomas L, Ferreira MA, Bender D, Maller J, Sklar P, De Bakker PI, Daly MJ, Sham PC (2007) PLINK: A tool set for whole-genome association and population-based linkage analyses. American Journal of Human Genetics 81(3): 559–575. https://doi.org/10.1086/519795

Shang C (2017) Taxonomic Review of *Populus* Linnaeus from Pan-Himalaya. PhD Thesis, Beijing Forestry University, China.

Shang C, Zhang L, Zhang Z (2016) New combinations for nothotaxa of *Populus* (Salicaceae) from China. Phytotaxa 253(2): 176–178. https://doi.org/10.11646/phytotaxa.253.2.9

Shang C, Li E, Yu Z, Lian M, Chen Z, Liu K, Xu L, Tong Z, Wang M, Dong W (2022) Chloroplast genomic resources and genetic divergence of endangered species *Bretschneidera sinensis* (Bretschneideraceae). Frontiers in Ecology and Evolution 10: e873100. https://doi.org/10.3389/fevo.2022.873100

Skvortsov AK (2008) The genus *Populus* L. (Salicaceae) of Indian Himalaya. Novosti Sistematiki Vysshikh Rastenii 40: 52–67. https://doi.org/10.31111/novitates/2009.40.52

Skvortsov AK (2010) Taxonomical synopsis of the genus *Populus* L. in East Europe, North and Central Asia. Byulleten'. Glavnogo Botaniceskogo Sada 196: 62–73.

Thiers B (2024) [continuously updated] Index Herbariorum: A global directory of public herbaria and associated staff. New York Botanical Garden's Virtual Herbarium. http://sweetgum.nybg.org/science/ih/ [accessed 23 January 2024]

Turland NJ, Wiersema JH, Barrie FR, Greuter W, Hawksworth DL, Herendeen PS, Knapp S, Kusber W-H, Li D-Z, Marhold K, May TW, McNeill J, Monro AM, Prado J, Price MJ, Smith GF (2018) International Code of Nomenclature for algae, fungi, and plants (Shenzhen Code) adopted by the Nineteenth International Botanical Congress Shenzhen, China, July 2017. Regnum Vegetabile 159. Koeltz Botanical Books, Glashütten. https://doi.org/10.12705/Code.2018

Tuskan GA, Difazio S, Jansson S, Bohlmann J, Grigoriev I, Hellsten U, Rokhsar D (2006) The genome of black cottonwood, *Populus trichocarpa* (Torr. & Gray). Science 313(5793): 1596–1604. https://doi.org/10.1126/science.1128691

Wang M, Zhang L, Zhang Z, Li M, Wang D, Zhang X, Xi Z, Keefover-Ring K, Smart LB, DiFazio SP, Olson MS, Yin T, Liu J, Ma T (2020) Phylogenomics of the genus *Populus* reveals extensive interspecific gene flow and balancing selection. The New Phytologist 225(3): 1370–1382. https://doi.org/10.1111/nph.16215

Wang Y, Huang J, Li E, Xu S, Zhan Z, Zhang X, Yang Z, Guo F, Liu K, Liu D, Shen X, Shang C, Zhang Z (2022) Phylogenomics and biogeography of *Populus* based on comprehensive sampling reveal deep-level relationships and multiple intercontinental dispersals. Frontiers in Plant Science 13:e 813177. https://doi.org/10.3389/fpls.2022.813177

Wickham H (2016) ggplot2: Elegant Graphics for Data Analysis. Springer-Verlag New York. https://doi.org/10.1007/978-3-319-24277-4

Yun T, Li JM, Zhou AP, Yan LX, Zong D, Li D, He CZ (2015) Analysis of phylogenetic relationship of *Populus* based on sequence data of chloroplast regions. Plant Physiology Joumal 51(8): 1339–1346. https://doi.org/10.13592/j.cnkippj.2015.0118

Zhang L, Wang M, Ma T, Liu J (2018) Taxonomic status of *Populus wulianensis* and *P. ningshanica* (Salicaceae). PhytoKeys 108: 117–129. https://doi.org/10.3897/phytokeys.108.25600

Supplementary material 1

Information of taxa that were not used for phylogenetic analysis in *Populus* subg. *Tacamahaca*

Authors: Wenyan Du, Yachao Wang, Dajun Xie, Enze Li, Yuran Bai, Ce Shang, Zhixiang Zhang
Data type: doc

Link: https://doi.org/10.3897/phytokeys.237.103012.suppl1

Supplementary material 2

Species tree of 57 samples of the genus *Populus* constructed by IQ-TREE, based on high-quality SNPs data with an outgroup of *P. euphratica*, using the sliding window method

Authors: Wenyan Du, Yachao Wang, Dajun Xie, Enze Li, Yuran Bai, Ce Shang, Zhixiang Zhang
Data type: pdf

Link: https://doi.org/10.3897/phytokeys.237.103012.suppl2

Supplementary material 3

Syntypes of *Populus gonggaensis* N. Chao & J.R. He

Authors: Wenyan Du, Yachao Wang, Dajun Xie, Enze Li, Yuran Bai, Ce Shang, Zhixiang Zhang
Data type: pdf

Link: https://doi.org/10.3897/phytokeys.237.103012.suppl3

PhytoKeys 237: 179–189 (2024)
DOI: 10.3897/phytokeys.237.116946

Research Article

A new freshwater species of *Pinnularia* (Bacillariophyta) from Hunan Province, China

San-Mei Xu[1,2], Bing Liu[1], Patrick Rioual[3,4], Man-Qi Yi[1], Yi-Dan Ma[1]

1 *College of Biology and Environmental Sciences, Jishou University, Jishou, China*
2 *School of Arts and Science, Huaihua Normal College, Huaihua, China*
3 *Key Laboratory of Cenozoic Geology and Environment, Institute of Geology and Geophysics, Chinese Academy of Sciences, P.O. box 9825, Beijing 100029, China*
4 *CAS Center for Excellence in Life and Paleoenvironment, Beijing 100044, China*
Corresponding author: Bing Liu (jsulb@outlook.com)

Abstract

This study describes a new species of *Pinnularia*, *P. hupingensis* **sp. nov.**, on the basis of light and scanning electron microscope images. *Pinnularia hupingensis* **sp. nov.** is characterised by its linear valve outline, extremely divergent striae, and very large hexagonal central area occupying ca. 1/5–1/8 of the valve length. The primary and secondary sides of the valve and the internal proximal raphe fissures are discussed. The new species is compared to similar taxa of the genus *Pinnularia*.

Key words: Central area, divergent striae, Huping Mountain, *Pinnularia hupingensis*, valvocopula

Academic editor: Kalina Manoylov
Received: 6 December 2023
Accepted: 9 January 2024
Published: 23 January 2024

Citation: Xu S-M, Liu B, Rioual P, Yi M-Q, Ma Y-D (2024) A new freshwater species of *Pinnularia* (Bacillariophyta) from Hunan Province, China. PhytoKeys 237: 179–189. https://doi.org/10.3897/phytokeys.237.116946

Introduction

The genus *Pinnularia* belongs to the artificial category of symmetric biraphid diatoms and is characterised by two girdle-appressed plate-like chloroplasts and alveolate striae (Round et al. 1990). According to the AlgaeBase website, there are 880 accepted species names, 501 accepted varieties and 127 accepted formae in the genus at present (Guiry and Guiry 2023). Hence *Pinnularia* is a very large and speciose genus, with numerous species described from Chinese material (e.g. Zhang et al. (2016); Liu et al. (2018a); Kociolek et al. (2020); Deng et al. (2021); Zhang et al. (2022)). The monograph of Krammer (2000), which provides the descriptions and illustrations of many *Pinnularia* taxa, still represents a very valuable source for taxon identification, although numerous other references are also needed since many new *Pinnularia* species have been described in the 21st century. The different valve sizes, outlines, the arrangements and densities of the striae on the valve surface, the central areas, the shapes of the distal raphe fissures and the ornaments on the valve surface are the most useful characters to discriminate the taxa within the genus *Pinnularia* (e.g. Round et al. (1990); Krammer (2000)).

There are two main types of stria arrangements on the valve surfaces of *Pinnularia* taxa. In one type, the striae are radiate throughout the valve surface, such as in *P. hustedii* F. Meister (Williams et al. 2022). In the other type, the striae are divergent, i.e. the striae are radiate only in the middle of the valve and abruptly become strongly convergent near the two apices, such as in *P. superdivergentissima* H. Germain & Chaumont (Chaumont and Germain 1976; Krammer 2000). If the central area in *Pinnularia* exists, it can be hyaline without any ornaments, such as in *P. lacustrigibba* Poulíčková, D.G. Mann & Kollár (Poulíčková et al. 2018) and *P. qinghainensis* Bing Liu & S. Blanco (Deng et al. 2021) or it may have lunate markings on each side of the central nodule, such as in *P. brandelii* Cleve (Krammer 2000, plate 97, figs 7–12) and *P. stomatophora* (Grunow) Cleve (Krammer 2000, plate 100, figs 1–8). Interestingly, in the closely-related genus *Caloneis*, the lunate markings are more common. Both *Caloneis lewissi* Patrick and *C. schumanniana* (Grunow) Cleve have lunate markings on each side of the central nodule (Stancheva et al. 2009). Levkov and Williams (2014) observed *Caloneis* species from the ancient lakes Ohrid and Prespa and described eighty new species, all of them with lunate markings. The lunate markings seen under the light microscope (LM) are actually lunate depressions as seen under the scanning electron microscope (SEM) (e.g. Krammer (2000), plate 98, figs 7, 8; Stancheva et al. (2009), fig. 39). The stria arrangement and the central area are two important characteristics for the new species described in this paper as they can be used for its distinction from similar species.

Hunan Province is situated in south-central China. Most of the streams/rivers in Hunan are tributaries of four major river systems: the Xiang, Zi, Yuan and Li Rivers. These four major rivers run from the south of Hunan to its north and terminate in Dongting Lake, the largest lake in Hunan that discharges into the Yangtze River (the longest river in China). The diatom flora of Hunan remains underexplored, although Liu and his collaborators have described many new diatom species from Hunan in recent years (e.g. Liu et al. (2018b, 2019, 2020, 2021, 2022); Liu (2023)). This paper further contributes to the investigation of the diatom flora of Hunan by providing the description of a new *Pinnularia* species collected from a river from this Province.

Materials and methods

The diatom samples of this study were collected from the Xie River which originates in the Huping Mountain National Nature Reserve (29°50'–30°09'N, 110°29'–110°59'E, 230 m a.s.l.). The Huping Mountain National Nature Reserve is located in the northwest of Shimen County, Hunan Province and is bordered by the Wufeng and Hefeng Counties of Hubei Province. This reserve was approved by the Chinese government as a national nature reserve in 1994 and it has a total area of 66.6 km^2 and a core area of about 54.5 km^2 (Tian et al. 2019). The Xie River is a headwater tributary of the Li River which is one of the four large rivers in Hunan Province. Epilithic diatom samples were collected on 14 March 2021. The method of collecting the diatom samples is the same as in Yuan et al. (2023) and consists of sampling numerous submerged stones showing yellow-brown surfaces that indicate the presence of diatoms. Each stone was placed on a plastic plate and its surface was brushed using a toothbrush, with the brushed-off diatom samples being washed onto the plate. The diatom samples were transferred into two 100 ml sampling bottles. One bottle was fixed with 70% ethanol and the other was left unfixed. At the time of sample collection, temperature, pH and conductivity were measured in situ with a portable multimeter (HQ40D, HACH Company).

The laboratory methods are also the same as in Liu (2023) and consist as follows: "The collected diatom samples to which 70% alcohol was not added were used to observe the living cells. A total of 100 μl diatom samples were transferred into a round chamber (diameter 14 mm, depth 0.35 mm) located in the middle of a custom-made slide by using a pipette, then examined using a Leica DM3000 light microscope (LM), equipped with a Leica MC190 HD digital camera. The collected diatom samples to which 70% alcohol was added were processed (cleaned) for microscopic examination with 10% hydrochloric acid (HCl) and 30% hydrogen peroxide (H_2O_2). Permanent slides were prepared using Naphrax mountant and examined using the same light microscope as above. Slides are deposited in the Herbarium of Jishou University, Hunan, People's Republic of China (JIU) (Herbarium acronyms follow Index Herbarium http://sweetgum.nybg.org/science/ih/). Samples were also examined using scanning electron microscopy (SEM). Several drops of the cleaned diatom material were air-dried on to glass coverslips. The coverslips were attached to aluminium stubs using double-sided conductive carbon strips and sputter-coated with platinum (Cressington Sputter Coater 108auto, Ted Pella, Inc.). Samples were examined and visualised using a field emission scanning electron microscopy (FESEM) Sigma HD (Carl Zeiss Microscopy) available at Huaihua University, China". The terminology in the diatom descriptions and in the discussion mainly follows Round et al. (1990) and Krammer (2000).

Results

Pinnularia hupingensis **Bing Liu & Rioual, sp. nov.**
Figs 1–5

Holotype. Slide DIA202316, specimen circled on the slide, illustrated here as Fig. 2B, deposited in the Herbarium of Jishou University (JIU), China. Registration: http://phycobank.org/104258.

Type locality. China. Hunan Province, Shimen County, Huping Town, a sampling site (29°57'6"N, 110°45'37"E, 230 m a.s.l.) in a riffle of the Xie River, collected by Bing Liu, 14 March 2021.

Description. ***LM*** (Figs 1, 2). Living cells rectangular in girdle view (Fig. 1A–C), linear with rounded apices in valve view (Fig. 1D–G). Two girdle-appressed, plate-like chloroplasts per cell (Fig. 1D–G). Valves linear with weakly undulate valve margins and broadly rounded apices. Valve dimensions (n = 28): length 28–65 μm, width 6.3–8.4 μm. Axial area narrow, raphe slightly undulate, filiform. Central pores small and bent towards the primary side and distal raphe fissures hooked. Central area very large (ca. 4.5–11.2 μm long), hexagonal, reaching both margins, occupying ca. 1/5–1/8 of the valve length. Striae extremely divergent, strongly radiate in the valve centre, becoming strongly convergent halfway to the apices. Striae 13–14 in 10 μm measured in the middle part of the valve near the central area. Voigt faults sometimes present on the secondary side (Fig. 2A, E, G, H, arrows). Apical hyaline areas well-developed.

SEM (Figs 3–5). Valves linear with broadly rounded apices and flat surface, curving smoothly into relatively deep mantles (Fig. 3A, B). The valve primary and secondary sides can be recognised by the presence of Voigt faults on the secondary side (Fig. 3A, B). Central area very large, with two central pores

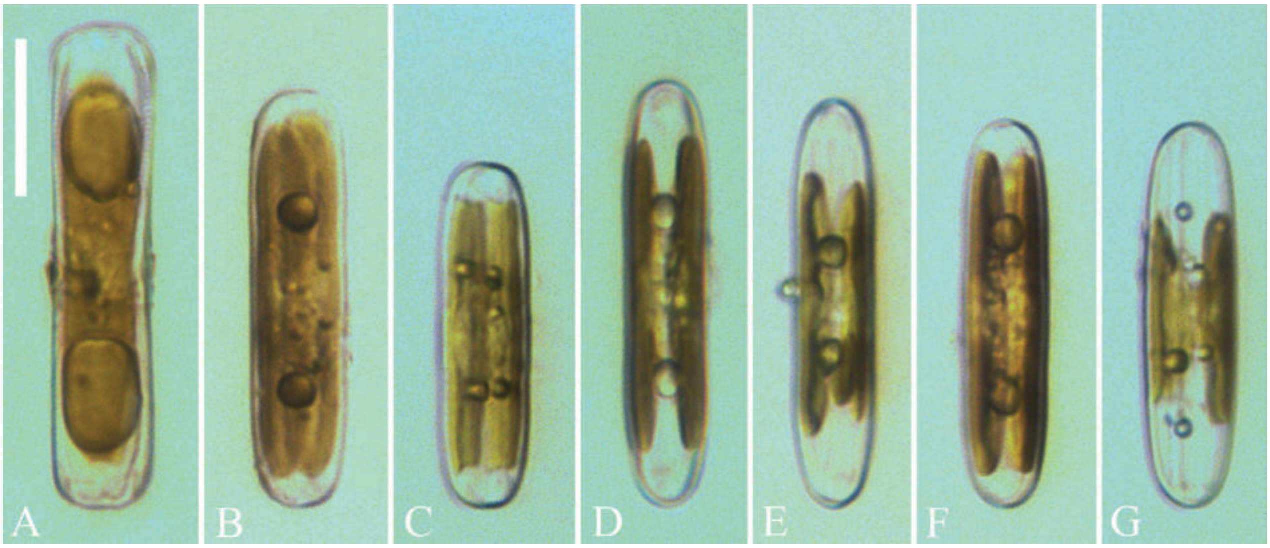

Figure 1. *Pinnularia hupingensis* sp. nov., LM **A–C** three living cells in girdle view, note that the girdle-appressed chloroplast spreads along the apical plane **D–G** four living cells in valve view, note the two plate-like, girdle-appressed chloroplasts. Scale bar: 20 µm.

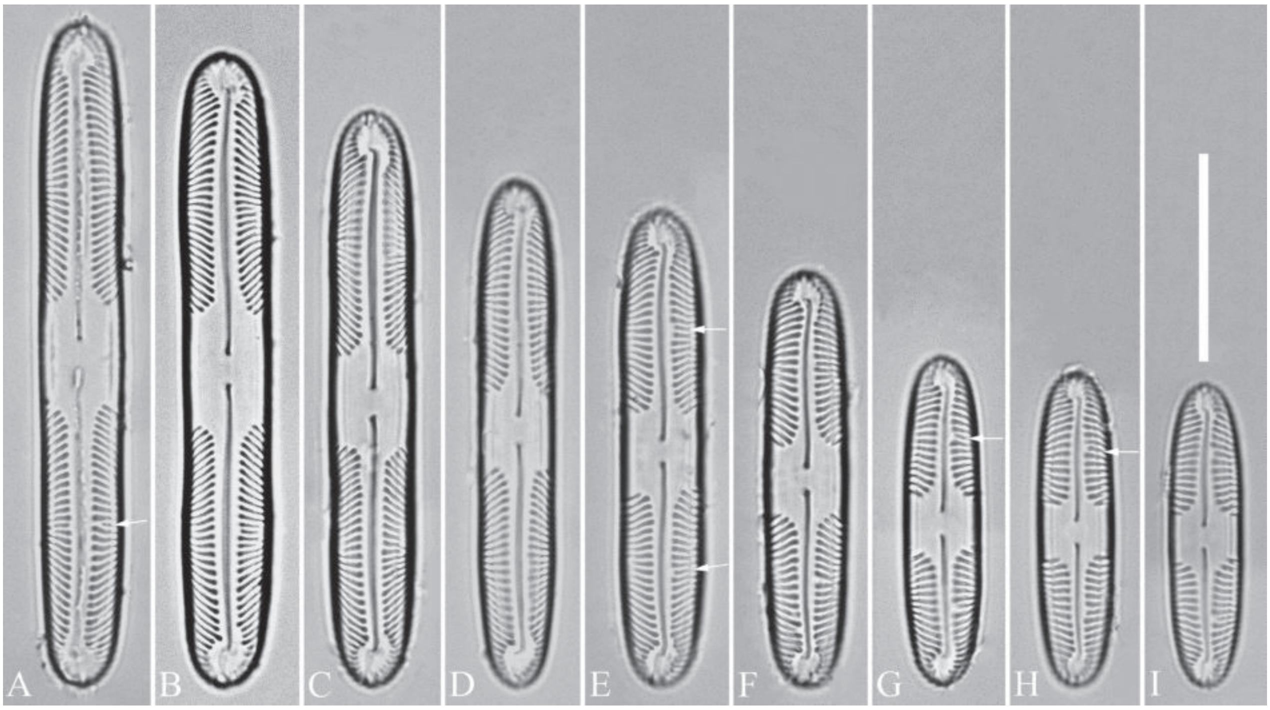

Figure 2. *Pinnularia hupingensis* sp. nov., LM **A–I** nine valves exhibiting a size diminution series, note the Voigt faults present in some of the valves (arrows on **A, E, G, H**) **B** micrograph of the holotype specimen. Scale bar: 20 µm.

both bent towards the primary side (Fig. 3A–C). Internally, proximal raphe endings interrupted by the central nodule, both turning towards the primary side (Fig. 4A–C). The external distal raphe fissures curved (Fig. 3A, B, D, E) while the internal distal raphe fissures run into a small, knob-like helictoglossa (Fig. 4D, E). Apical hyaline areas present (Figs 3D, E, 4D, E). Each alveolate stria comprises 3–5 rows of small rounded poroids externally (Fig. 3C–F) and internally, openings consist of elongate apertures (Fig. 4F, two double-headed arrows).

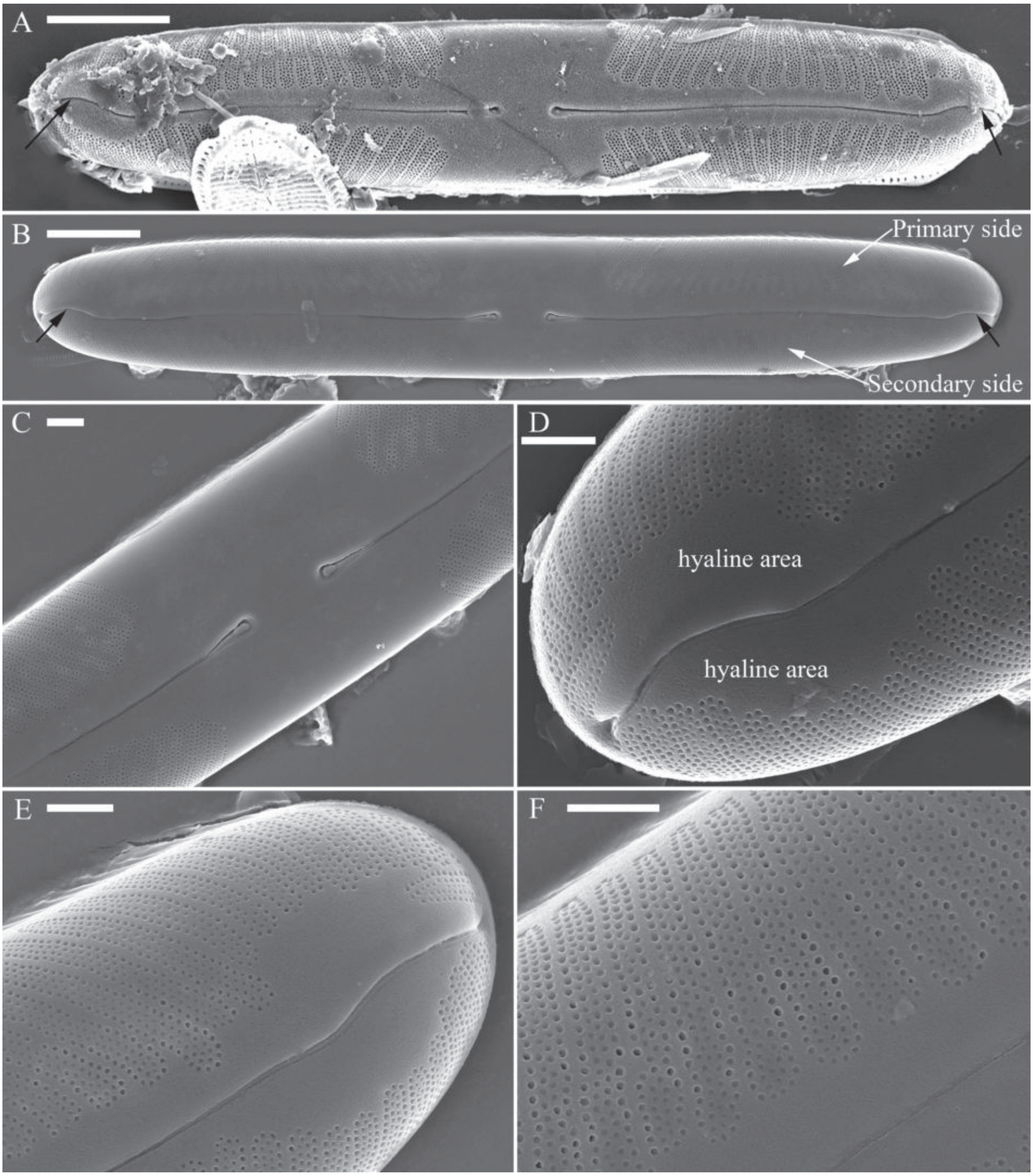

Figure 3. *Pinnularia hupingensis* sp. nov., SEM, valve external view **A, B** two complete valves, note the primary and secondary sides and the curved distal raphe fissures (black arrows) **C** middle part, details from **B** showing the large, hexagonal central area, slightly expanded proximal raphe endings bent in the same direction towards the primary side **D, E** apices, details from **B** showing the curved distal raphe fissures and apical hyaline areas **F** detail of the striae, note each stria comprises 3–5 rows of small round poroids. Scale bars: 5 µm (**A, B**); 1 µm (**C–F**).

Valvocopula has the same outline as that of the valve and is composed of pars interior, suture and pars exterior (Fig. 5A, B). Pars exterior ornamented by a row of elongate poroids (Fig. 5A, white arrows, Fig. 5B, white wavy arrows). Valvocopula closed at one apex and open at the other (Fig. 5C, D).

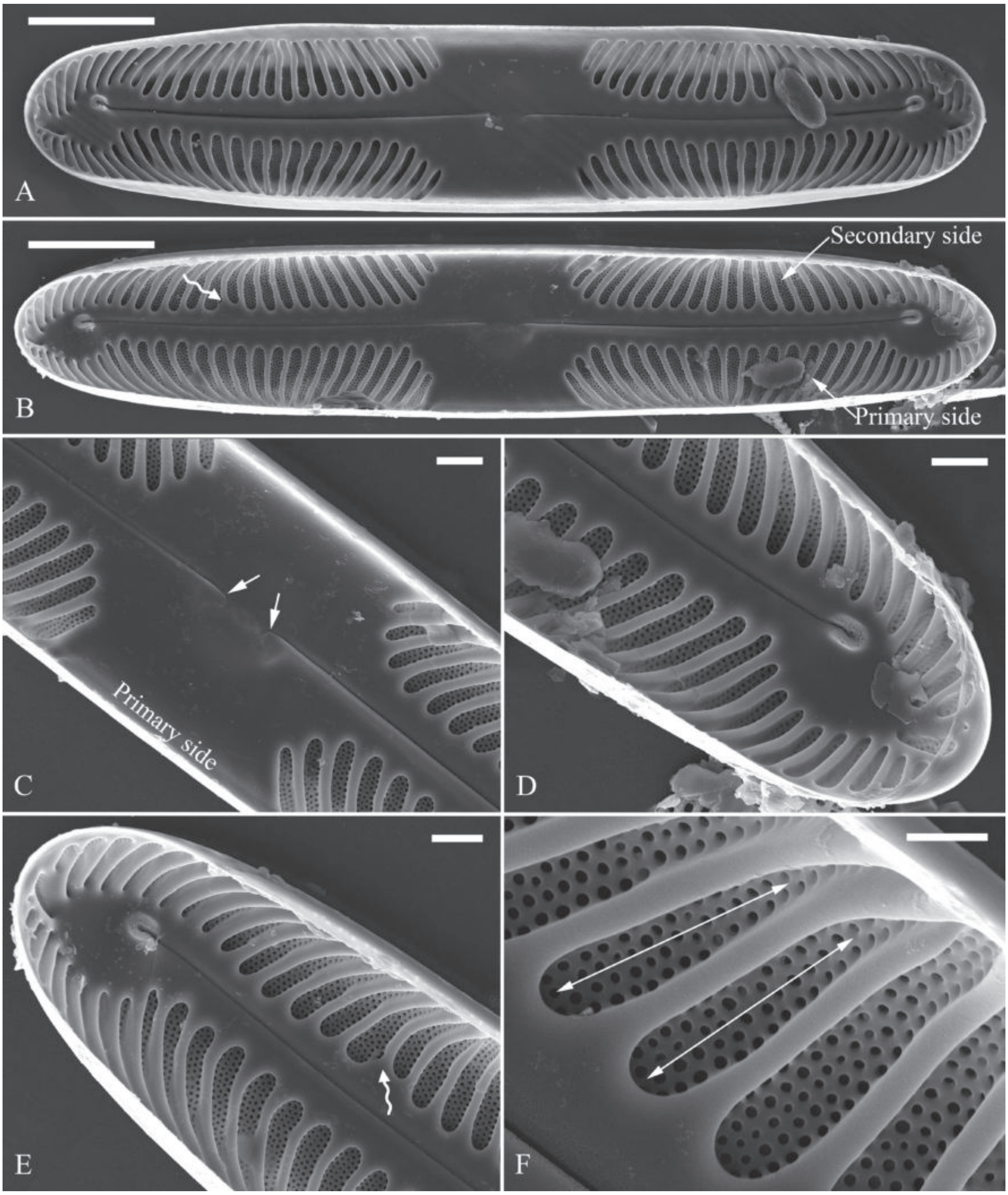

Figure 4. *Pinnularia hupingensis* sp. nov., SEM, valve internal view **A, B** two complete valves, note the primary and secondary sides **C** middle part, details from **B**, note the large, hexagonal central area and the internal proximal raphe fissures both deflecting towards the primary side (two arrows) **D, E** apices, details from **B**, note each internal distal raphe fissure running into a small, knob-like helictoglossa, the hyaline areas and the Voigt fault (**B, E**, wavy arrow respectively) **F** internal detail of the chambers, note the large transapical elongate apertures (two double-headed arrows). Scale bars: 5 μm (**A, B**); 1 μm (**C–F**).

Etymology. The specific epithet *hupingensis* refers to Huping Town where the species was found.

Distribution and ecology. Known only from the type locality in which it is a common species with ca. 4% relative abundance. The samples that included this species were scraped off surface of stones collected in the Xie River.

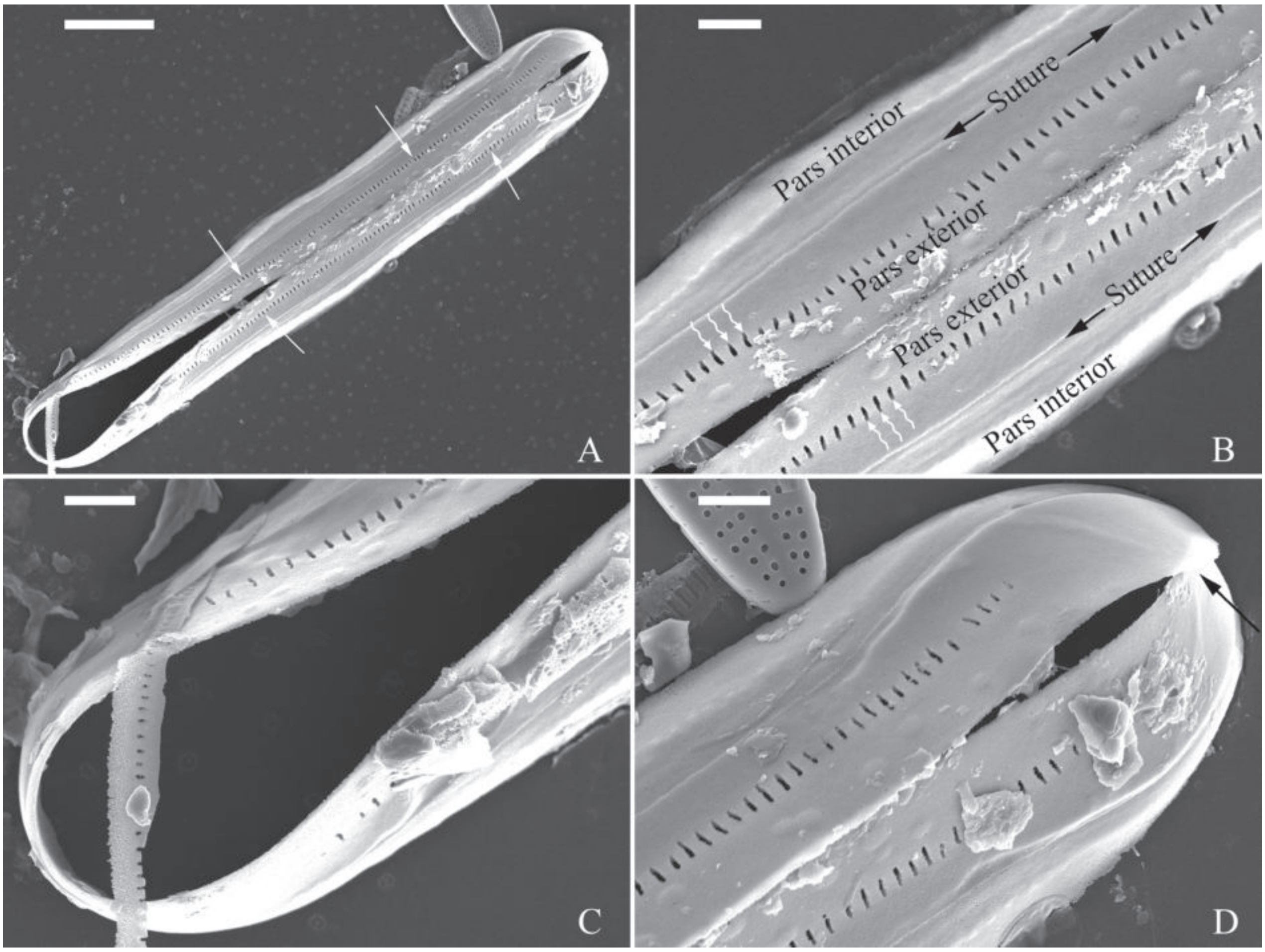

Figure 5. *Pinnularia hupingensis* sp. nov., SEM **A** one complete valvocopula, note a row of elongate poroids are produced in the pars exterior (four arrows) **B** middle part details from **A**, note the pars interior, suture, pars exterior and the elongate poroids (wavy arrows) **C** one apical detail from **A**, note the valvocopula is closed at this apex **D** the other apical detail from **A**, note the valvocopula is open at this apex (black arrow). Scale bars: 5 μm (**A**); 1 μm (**B–D**).

Hence, this is a benthic, epilithic species. The associated taxa include *Navicula reinhardtii* Grunow, *N. radiosa* Kützing, *Ulnaria hupingensis* Bing Liu, *U. xieriverensis* Bing Liu and many unidentified *Cymbella* spp., *Fragilaria* spp., *Gomphonema* spp., amongst others. The following environmental parameters were measured in the field with three replications: Conductivity = 236.3 ± 1.2 μS cm^{-1}; pH = 8.49 ± 0.02; Water temperature = 13.6 ± 0.1 °C.

Discussion

Pinnularia hupingensis sp. nov. is characterised by its linear valve outline, extremely divergent striae and very large, hexagonal central area occupying ca. 1/5–1/8 of the valve length. The characteristics of *P. hupingensis* are summarised in Table 1 and compared to those of similar taxa. At first glance, *P. hupingensis* is similar to *P. brandelii*, but the latter has a lunate marking on either side of the central nodule (see Krammer (2000), plate 97, figs 7–12), whereas *P. hupingensis* does not have such lunate markings. Interestingly, Kezlya et al. (2022) noted that morphological distinctions, such as the surface markings in the central area, are consistent with phylogenic clades defined by genetic markers. The absence of such markings in *P. hupingensis*, therefore, excludes the possibility of this taxon being conspecific with *P. brandelii*. *Pinnularia brebissonii* and *P. krammeri* are more or less similar to *P. hupingensis*, but the former two species have different valve outlines and central areas (Table 1). The relative size of the central area, in particular, has been reported to be a stable character for the recognition of *Pinnularia* species for both small and large specimens (Kollár et al. 2019). *Pinnularia hupingensis* differs from *P. superdivergentissima* by having narrower valves (6.3–8.4 vs. 8–10 μm in width) and much higher stria density (13–14 vs. 7–9 in 10 μm). Furthermore, the ratio between the length of the central area and the length of the valve is ca. 1/5–1/8 in *P. hupingensis*, but ca. 1/9–1/10 in *P. superdivergentissima*.

The most similar taxon to *P. hupingensis* is *Pinnularia* sp1, a taxon morphologically similar to *P. krammeri* illustrated in Zidarova et al. (2012, p.17, figs 44–47). *Pinnularia hupingensis* and *P.* sp1 both have linear valve outline, weakly undulate valve margins, divergent striae, large central area and overlapping valve dimensions and stria density (Table 1). Zidarova et al. (2012) did not provide a formal description and stated: “A few valves could not be identified but have been given a provisional identification as *Pinnularia* sp1 until further observations can be made”. Morphologically, *P. hupingensis* is very similar to *P.* sp1 of Zidarova et al. (2012) and it cannot be excluded that the two taxa may be conspecific.

During the ontogeny of raphid diatoms, the valve side formed from the initial branching of the raphe sternum is termed the primary side and its opposite side is termed the secondary side. The secondary side may include the Voigt faults (or discontinuities) that mark the point of fusion of the sternum during the ontogeny of the valve (Round et al. 1990). Most authors do not discuss the primary and secondary sides of the *Pinnularia* taxa they described (e.g. Krammer

Table 1. Comparisons between *Pinnularia hupingensis* sp. nov. and similar taxa. Information on distribution collated from Algaebase (Guiry and Guiry 2023).

Taxon	*P. hupingensis* sp. nov.	*P. brandelii*	*P. brebissonii*	*P. krammeri*	*P. superdivergentissima*	*P.* sp1
Valve outline	Linear with weakly-undulate valve margins and rounded apices	Linear with broadly-rounded or broadly-capitate apices	Linear-lanceolate to linear-elliptical with broadly-rounded to wedge-shaped apices	Linear to linear-elliptical with wedge-shaped apices	Linear with commonly parallel sides and broadly-rounded apices	Linear with parallel or weakly-undulated margins, non-protracted, broadly-rounded apices
Valve length (L) and width (W) (μm)	L: 28–64, W: 6.3–8.4	L: 51–92, W: 7–10	L: 28–60, W: 9–12	L: 26–45, W: 6.7–7.8	L: 45–80, W: 8–10	L: 25–35, W: 5.0–6.5
Striae in 10 μm	13–14	11–14	10–12	11–13	7–9	11–13
Central area	Hexagonal, large, occupying ca. 1/5–1/7 of the valve length	Moderately broad to broad fascia, 1/7–1/9 of the valve length	More or less broad fascia, rarely with short striae at the fascia edge	Central area variable in shape and size, fascia widening to the valve margin to rhombic	Broad fascia, occupying ca. 1/9–1/10 of the valve length	Large rhombic fascia, occupying ca. 1/3 to 1/4 of the valve length
Lunate markings on each side of central nodule	Absent	Present, elongate	Absent	Absent	Absent	Absent
Type locality	Hubei, China	Finland, fossil	France	Finland, modern	France, Atlantic coast	Livingston Island, Antarctic Region
Distribution	Type locality	Arctic, Europe, N. America, Middle East	Cosmopolitan	Eurasia, N. America, Arctic, Antarctic	France, Britain, Ireland	Type locality
Reference	This study	Krammer (2000)	Krammer (2000)	Krammer (2000)	Krammer (2000)	Zidarova et al. (2012)

(2000)) including in recent publications (Liu et al. 2018b; Moreno et al. 2020; Deng et al. 2021; Kulikovskiy et al. 2023), although there are a few exceptions, such as Zidarova et al. (2012) and Poulíčková et al. (2018). In *P. hupingensis*, the Voigt faults could be seen on the majority of the valves we observed.

In *Pinnularia*, the internal proximal raphe fissures can be continuous or interrupted by the central nodule. The internal proximal raphe fissures are continuous in *Pinnularia lacustrigibba* (Poulíčková et al. 2018) and *P. hustedtii* F. Meister (Williams et al. 2022), but interrupted by the central nodule in *P. hupingensis* as in *P. qinghainensis*. Clearly recognising these morphological structures is crucial to support the establishment of subgroups within the genus *Pinnularia* as discussed by Kulikovskiy et al. (2023).

Acknowledgements

The authors are grateful to Li Yuan, Ji-Yan Long and Wen-Hui Mo for assistance in the field and the laboratory.

Additional information

Conflict of interest

The authors have declared that no competing interests exist.

Ethical statement

No ethical statement was reported.

Funding

This research was supported by the Natural Science Foundation of Hunan Province (grant number 2022JJ30473) and the Scientific Research Project of the Education Department of Hunan Province [grant number 22A0376].

Author contributions

San-Mei Xu: Writing – original draft; Bing Liu: Writing – review and editing; Patrick Rioual: Formal analysis; Man-Qi Yi, Yi-Dan Ma: Investigation.

Author ORCIDs

San-Mei Xu https://orcid.org/0000-0003-1447-4752
Bing Liu https://orcid.org/0000-0002-8516-325X
Patrick Rioual https://orcid.org/0000-0001-9491-9197
Man-Qi Yi https://orcid.org/0000-0002-0503-0626
Yi-Dan Ma https://orcid.org/0009-0005-0636-4168

Data availability

All of the data that support the findings of this study are available in the main text.

References

Chaumont J-P, Germain H (1976) *Pinnularia superdivergentissima* nov. sp., *Achnanthes subsalsoides* Hustedt var. *sterwennensis* nov. var. Bulletin de la Société Botanique de France 123(9): 587–590. https://doi.org/10.1080/00378941.1976.10835714

Deng LY, Blanco S, Liu B, Quan SJ, Long J-Y (2021) *Pinnularia qinghainensis*: A new diatom species (Bacillariophyta) found in the brackish Lake Qinghai, China. Phytotaxa 483(1): 080–084. https://doi.org/10.11646/phytotaxa.483.1.5

Guiry MD, Guiry GM (2023) AlgaeBase. World-wide electronic publication, National University of Ireland, Galway. https://www.algaebase.org [Accessed on 18 November 2023]

Kezlya E, Maltsev Y, Genkal S, Krivova Z, Kulikovskiy M (2022) Phylogeny and fatty acid profiles of new *Pinnularia* (Bacillariophyta) species from soils of Vietnam. Cells 11(15): e2446. https://doi.org/10.3390/cells11152446

Kociolek JP, You QM, Liu Q, Liu Y, Wang QX (2020) Continental diatom biodiversity discovery and description in China: 1848 through 2019. PhytoKeys 160: 45–97. https://doi.org/10.3897/phytokeys.160.54193

Kollár J, Pinseel E, Vanormelingen P, Poulíčková A, Souffreau C, Dvořák P, Vyverman W (2019) A polyphasic approach to the delimitation of diatom species: A case study for the genus *Pinnularia* (Bacillariophyta). Journal of Phycology 55(2): 365–379. https://doi.org/10.1111/jpy.12825

Krammer K (2000) The genus *Pinnularia*. In: Lange-Bertalot H (Ed.) Diatoms of Europe. Diatoms of the European Inland waters and comparable habitats (Vol. 10. A.R.G. Gantner Verlag, K.G., Ruggell, 703 pp.

Kulikovskiy M, Glushchenko A, Kezlya E, Kuznetsova I, Kociolek JP, Maltsev Y (2023) The genus *Pinnularia* Ehrenberg (Bacillariophyta) from the Transbaikal area (Russia, Siberia): Description of seven new species on the basis of morphology and molecular data with discussion of the phylogenetic position of *Caloneis*. Plants 12(20): e3552. https://doi.org/10.3390/plants12203552

Levkov Z, Williams DM (2014) Observations on *Caloneis* Cleve (Bacillariophyceae) species from the ancient lakes Ohrid and Prespa. Nova Hedwigia. Beiheft 143: 141–158.

Liu B (2023) The diatom genus *Ulnaria* (Bacillariophyta) in China. PhytoKeys 228: 1–118. https://doi.org/10.3897/phytokeys.228.101080

Liu Y, Kociolek JP, Wang QX, Fan YW (2018a) The diatom genus *Pinnularia* from Great Xing'an Mountains, China. In: Lange-Bertalot H, Kociolek JP (Eds) Bibliotheca Diatomologica (Vol. 65). J. Cramer, Stuttgart, 298 pp.

Liu B, Williams DM, Ector L (2018b) *Entomoneis triundulata* sp. nov. (Bacillariophyta), a new freshwater diatom species from Dongting Lake, China. Cryptogamie. Algologie 39(2): 239–253. https://doi.org/10.7872/crya/v39.iss2.2018.239

Liu B, Blanco S, Ector L, Liu ZX, Ai J (2019) *Surirella wulingensis* sp. nov. and fine structure of *S. tientsinensis* Skvortzov (Bacillariophyceae) from China. Fottea 19(2): 151–162. https://doi.org/10.5507/fot.2019.006

Liu B, Williams DM, Li Y, Tang ZS (2020) Two new species of *Cymbella* (Bacillariophyceae) from China, with comments on their valve dimensions. Diatom Research 35(1): 99–111. https://doi.org/10.1080/0269249X.2020.1733100

Liu B, Kociolek JP, Ector L (2021) *Surirella dongtingensis* sp. nov. and ultrastructure of *S. undulata* (Bacillariophyta) from China. Botany Letters 168(1): 32–41. https://doi.org/10.1080/23818107.2020.1756908

Liu B, Zhou YY, Blanco S, Williams DM (2022) Three new species of *Delicatophycus* M.J. Wynne (Bacillariophyta) from China, all possessing apical pore fields. Fottea 22(1): 137–151. https://doi.org/10.5507/fot.2021.020

Moreno DF, Luís AT, Vidakovic D, Levkov D, Castillo PMS (2020) *Pinnularia baetica* sp. nov. (Bacillariophyceae): Comparison with other panduriform species in the Mediterranean area. Phytotaxa 435(2): 085–100. https://doi.org/10.11646/phytotaxa.435.2.1

Poulíčková A, Kollár J, Hašler P, Dvořák P, Mann DG (2018) A new species *Pinnularia lacustrigibba* sp. nov. within the *Pinnularia* subgibba group (Bacillariophyceae). Diatom Research 33(3): 273–282. https://doi.org/10.1080/0269249X.2018.1513869

Round FE, Crawford RM, Mann DG (1990) The Diatoms: Biology and Morphology of the Genera. Cambridge University Press, Cambridge, 747 pp.

Stancheva R, Manoylov K, Gillett N (2009) Morphological variation of the *Caloneis schumanniana* species complex (Bacillariophyceae) from different environmental conditions in North American streams. Hydrobiologia 635(1): 157–170. https://doi.org/10.1007/s10750-009-9908-4

Tian SR, Li ZJ, Kang ZJ, Liao QY, Li DQ (2019) Study on readjustment of the area and function zones of Hunan Hupingshan National Nature Reserve and its impacts. Forest Resources Management 2: 21–29, 87. https://doi.org/10.17520/biods.2019334 [In Chinese with English abstract]

Williams DM, Liu B, Taxböck L (2022) *Pinnularia hustedtii* (Bacillariophyta): Notes on specimens from Wuling Mountains, China and from type material. Phytotaxa 536(3): 294–300. https://doi.org/10.11646/phytotaxa.536.3.10

Yuan L, Liu B, Rioual P, Yi M-Q, Zheng Y (2023) Two new species of *Oricymba* (Bacillariophyta) from China, described with reference to the structure of the apical pore field. Phytotaxa 591(3): 181–195. https://doi.org/10.11646/phytotaxa.591.3.1

Zhang W, Pereira AC, Kociolek JP, Liu C, Xu X, Wang L (2016) *Pinnularia wuyiensis* sp. nov., a new diatom (Bacillariophyceae, Naviculales) from the north region of Wuyi Mountains, Jiangxi Province, China. Phytotaxa 267(2): 121–128. https://doi.org/10.11646/phytotaxa.267.2.4

Zhang W, Yang H, Wang N, Cai M, Kociolek JP, Yin S (2022) *Pinnularia dongzhenensis* sp. nov., a new freshwater diatom species (Bacillariophyceae) from Dongzhen Reservoir, Fujian Province, China. Phytotaxa 548(1): 82–90. https://doi.org/10.11646/phytotaxa.548.1.7

Zidarova R, Kopalová K, Van de Vijver B (2012) The genus *Pinnularia* (Bacillariophyta) excluding the section *Distantes* on Livingston Island (South Shetland Islands) with the description of twelve new taxa. Phytotaxa 44(1): 11–37. https://doi.org/10.11646/phytotaxa.44.1.2

PhytoKeys 237: 191–200 (2024)
DOI: 10.3897/phytokeys.237.117071

Research Article

Isodon xiaoluzhiensis (Lamiaceae, Nepetoideae), a new species from Yunnan, southwest China

Shi-Gang Li[1,2], Qiang-Chun Huang[1], Shao-Yun Liu[1], Chun-Lei Xiang[3], Huan-Chong Wang[1,4]

1 *School of Ecology and Environmental Science, Yunnan University, Kunming 650091, Yunnan, China*
2 *Southwest United Graduate School, Kunming 650092, Yunnan, China*
3 *CAS Key Laboratory for Plant Diversity and Biogeography of East Asia, Kunming Institute of Botany, Chinese Academy of Sciences, Kunming 650201, China*
4 *Herbarium of Yunnan University, Kunming 650091, Yunnan, China*
Corresponding author: Huan-Chong Wang (hchwang@ynu.edu.cn)

Abstract

Isodon xiaoluzhiensis, a new species of the tribe Ocimeae in family Lamiaceae, is described and illustrated. The new species is known only from the type locality, Xiaoluzhi village in Luzhijang dry-hot valley of Yimen County, central Yunnan, southwest China. It is characterized by having a procumbent habit, gracile stems and branches, relatively small leaves and flowers, and the phenology of flowering in winter. The morphological comparisons with its putative closest relatives (*I. adenanthus* and *I. hsiwenii*) are also presented.

Key words: Asia, Dry-hot valley, endemism, limestone grassland, phenology, procumbent shrub

Academic editor: Bo Li
Received: 8 December 2023
Accepted: 4 January 2024
Published: 24 January 2024

Citation: Li S-G, Huang Q-C, Liu S-Y, Xiang C-L, Wang H-C (2024) *Isodon xiaoluzhiensis* (Lamiaceae, Nepetoideae), a new species from Yunnan, southwest China. PhytoKeys 237: 191–200. https://doi.org/10.3897/phytokeys.237.117071

Introduction

The genus *Isodon* (Benth.) Schrad. ex Spach is a genus of approximately 100 species widely distributed across tropical and subtropical Asia, and with two endemic species in Africa (Wu and Li 1977; Li 1988; Li and Hedge 1994; Mabberley 2008; Zhong et al. 2010; Chen et al. 2019). It was originally placed under the *Plectranthus* L'Hér. as a section (Bentham 1832). Soon after, it was raised to generic rank by Spach (1840). Nevertheless, Spach's treatment was ignored or overlooked by many later authors (Hasskarl 1842; Bentham 1876; Nakai 1934; Morton 1962), and the name *Rabdosia* (Bl.) Hassk. was widely applied to this genus (e.g. Hara 1972; Li 1975; Wu and Li 1977; Tang and Eisenbrand 1992), until Farr et al. (1979) and Hara (1985) regarded *Isodon* having priority over *Rabdosia*. *Isodon* is now recognized as the only genus in the subtribe Isodoninae (Zhong et al. 2010) and it can be delimited from other genera of the tribe Ocimeae by its bracteolate cymes with a peduncle, actinomorphic or two-lipped (3/2) calyces, strongly two-lipped (4/1) corollas, and stamens with free filaments inserted at the base of the corolla tube (Li 1988; Paton and Ryding 1998; Harley et al. 2004; Chen et al. 2019).

China possesses a rich set of species of *Isodon*, and the center of species diversity of the genus was found in southwest China, especially in the Hengduan

Mountains region (Li 1988; Li and Hedge 1994; Yu et al. 2014). The first comprehensive revision of this genus in China was conducted by Wu and Li (1977) for the "Flora Reipublicae Popularis Sinicae", in which the generic name *Rabdosia.* was applied instead of *Isodon*. Wu and Li (1977) recognized 90 species and 21 varieties in China, and divided these Chinese species into four sections, namely *Isodon* sect. *pyramidium* (Benth.) H. W. Li, *I.* sect. *amethystoides* (Benth.) H. W. Li, *I.* sect. *Isodon*, and *I.* sect. *Melissoides* (Benth.) H. W. Li, and the section *Isodon* was further divided into 10 series. Li and Hedge (1994) reviewed the Chinese species in the *Flora of China*, recognized 77 species in China, 64 being endemics. Recently taxonomic novelties of this genus have been consistently reported from China (Xiang and Liu 2012; Chen et al. 2014, 2016, 2017, 2019, 2021).

In January 2018, during our botanical fieldwork to the Luzhijiang River valley at Yimen County, Yunnan, southwest China, an unknown plant of *Isodon* was encountered and gathered. In 25 September 2021, the same plant was discovered again at the same site. Based on critical comparison with related species, it was confirmed that this plant represents a distinct new species which is described here.

Materials and methods

The study followed the normal practice of plant taxonomic survey and herbarium taxonomy. Morphological studies of the new species were based on observation of living plants and specimens housed at YUKU. Digital images of type specimens of genus *Isodon* available at the JSTOR Global Plants (http://plants.jstor.org/), as well as collections housed at CDBI, KUN, PE, PYU and YUKU, were extensively examined and compared with the new species. Pertinent taxonomic literature (Wu and Li 1977; Li 1988; Xiang and Liu 2012; Chen et al. 2014, 2016, 2017, 2019, 2021) was extensively consulted. Measurements were carried out under a stereomicroscope (Olympus SZX2, Tokyo, Japan) using a ruler and a metric vernier caliper.

Taxonomy

Isodon xiaoluzhiensis **Huan C. Wang & Shi Gang Li, sp. nov.**

urn:lsid:ipni.org:names:77335145-1
Figs 1–4

Type. China. Yunnan Province: Yimen County, Luzhi Town, Xiaoluzhi village, Maomao Mountain, on limestone grasslands, 24°40'N, 101°57'E, alt. 1300–1400 m, 18 January 2018, *H. C. Wang et al. YM8034* (Holotype: YUKU!; isotype: YUKU!, PE!, KUN!).

Diagnosis. *Isodon xiaoluzhiensis* is most similar to *I. adenanthus* (Diels) Kudô in having similar flower shape, but it clearly differs from the latter in its procumbent (vs. erect or ascending in *I. adenanthus*) habit, stems and branches woody (vs. non-woody) with densely white glandular puberulent (vs. densely retrorse gray pubescent), leaves usually narrowly ovate to rhomboid, rarely lanceolate (vs. rhombic-ovate to ovate-lanceolate), small, 0.8–1.4 cm long (vs. 1.5–6.5 cm long), 0.2–0.5 cm wide (vs. 1.0–2.5 cm wide), teeth of calyx subobtose to subacute (vs. apiculate) at apex, posterior lip of corolla non-spotted (vs. purple spotted). Additionally, *I. xiaoluzhiensis* flowers from November to January, nevertheless *I. adenanthus* usually flowers from March to August.

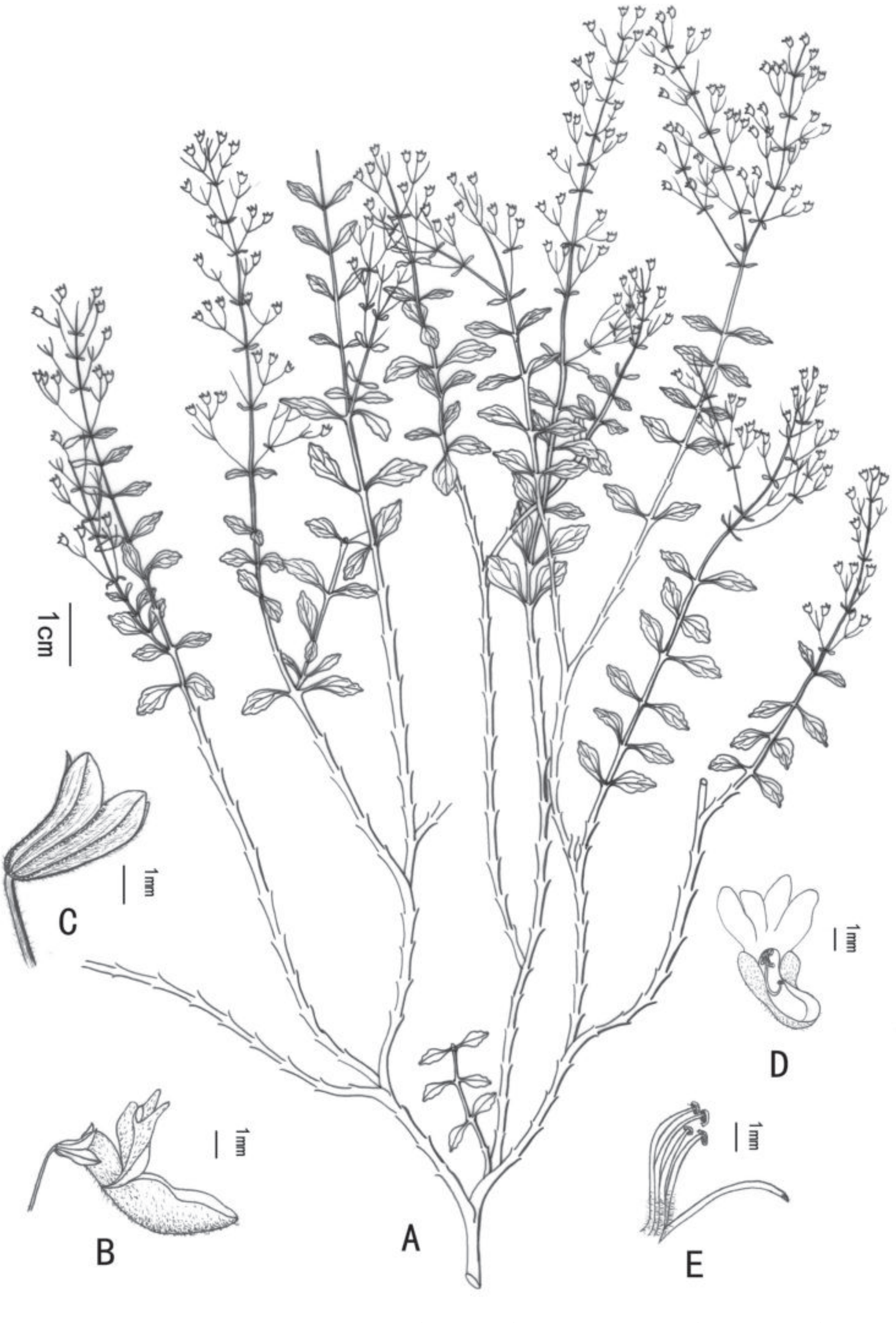

Figure 1. *Isodon xiaoluzhiensis* sp. nov. **A** habit **B** flower (side view) **C** calyx **D** corolla (vertical view) **E** style and stamens.

Description. Small shrubs or subshrubs. Stems woody, procumbent, branched; branches subterete to terete, usually grey, irregularly decorticate, glabrescent; branchlets obtusely quadrangular, purplish, densely white glandular-puberulent. Leaves opposite; petiole 1–3 mm long, rarely subsessile; leaf blades papery or thinly coriaceous, usually narrowly ovate to rhomboid, sometimes lanceolate, 0.8–1.4 cm long, 0.2–0.5 cm wide, apex acute, base cuneate to narrowly cuneate, adaxial surfaces green in young leaves, purplish black when ageing, with pellucid glands, abaxial surfaces gray-green, densely white glandular-puberulent; margin coarsely serrated, with 1–4 teeth on each margin, sometimes entire; veins adaxially depressed, abaxially prominent, with coarse short white hirsute puberulent, lateral veins 2–3 paired. Inflorescences terminal racemose or paniculate, composed of dichasial cymes. Peduncles of cymes gracile, 4–5 mm long, white glandular-puberulent; lax usually with 3–5 flowers; bracts ovate small, subsessile. Flowers small, pedunculate; pedicels gracile, with white glandular-puberulent, 4–5 mm long. Calyx campanulate, conspicuously 10-veined, densely white hirsute outside, 2–3 mm long, 2.0–2.5 mm wide, inconspicuously 2-lipped; posterior lip 3-toothed, subequal, ovate, ca. 1 mm long, usually subobtuse to subacute at apex; anterior lip 2-toothed, equal, ovate, 1.0–1.2 mm long, subobtuse at apex; tube declinate, usually 2 mm long. Corolla purple or light purple, bilabiate, 4–5 mm long; tube tubular, geniculate at base, ca. 2 mm long, densely pubescent outside; posterior lip strongly reflexed, 4-lobed, apex round; anterior lip concave, navicular, obviously longer than the tube, 2.5–3.0 mm long. Stamens 4, didynamous, exserted, inserted at bottom of corolla tube; filaments slender, white villous at base, 5–6 mm long; anthers bluish-purple, elliptic, versatile. Pistil 1, style exserted,7–8 mm long, slightly longer than filaments; ovary superior. Nutlets nearly ovoid, glabrous, sparsely glandular.

Phenology. Flowering from November to January, fruiting from December to February.

Etymology. The specific epithet “*xiaoluzhiensis*” is derived from the type locality of the new species, the Xiaoluzhi village, and the Latin suffix -*ensis*, indicating the place of origin or growth.

Vernacular name. Chinese mandarin: xiao lu zhi xiang cha cai (小绿汁香茶菜).

Distribution and ecology. According to the present investigations, *I. xiaoluzhiensis* is only found in its type locality, i.e. Xiaoluzhi village of Luzhijiang valley, Yimen County, Yunnan Province, southwest China, where the climate is seasonally hot and arid. *Isodon xiaoluzhiensis* occurs in the limestone grasslands between 1,300 m and 1,400 m elevation. In the type locality, its association mainly includes *Dodonaea viscosa* (L.) Jacq. (Sapindaceae), *Indigofera vallicola* Huan C.Wang et Jin L. Liu (Leguminosae) (a new species discovered by Liu et al. (2022)), *Duhaldea lachnocephala* Huan C. Wang et Feng Yang (Compositae) (an endemic species of Luzhijiang valley discovered by Yang et al. (2022)), *Selaginella pulvinata* (Hook. et Grev.) Maxim (Selaginellaceae), *Pterygiella luzhijiangensis* Huan C. Wang (Orobanchaceae) and *Onosma decastichum* Y. L. Liu (Boraginaceae). Among them, the type localities of *I. vallicola*, *D. lachnocephala*, *P. luzhijiangensis*, *O. decastichum* are also in Xiaoluzhi of the Luzhijiang valley (Qiao et al. 2018; Liu et al. 2022; Yang et al. 2022).

Preliminary conservation status. *Isodon xiaoluzhiensis* is a rare species with a restricted distribution and small population size. It is only known from in the upstream region of the Luzhijiang River in the Yimen county, which is no protected area covering. The total population size is estimated at less than 50. According to the IUCN Standards and Petitions Subcommittee (2019), this new species should be considered as "Critically Endangered" (CR).

Additional specimens examined (paratypes): China. Yunnan: Yimen County, Luzhi town, Xiaoluzhi village, Maomao Mountain, elev. ca. 1390 m, 25 Sep. 2021, *H. C. Wang et al. YM14638* (YUKU).

Discussion. *Isodon xiaoluzhiensis* exhibits all the characteristics of *Isodon*, but having a procumbent habit, relatively small leaves, and the phenology of flowering in winter can easily differentiate it from other species in the genus. Especially, the procumbent habit is rare in the entire genus *Isodon*, just *I. xiaoluzhiensis* and *I. hsiwenii*, nevertheless the latter is sometimes arcuate. *Isodon xiaoluzhiensis* is

05008415

云南大学植物标本馆
Herbarium of Yunnan University

采集号：YM8034
Collection number: YM8034
采集人：王焕冲、李世刚、尹明云
Collector: Huan-Chong Wang, Shi-Gang Li
& Ming-Yun Yin
采集时间：2018 年 1 月 18 日
Collection time: 18 January 2018
地点：云南省易门县绿汁镇小绿汁村猫猫山
Location: Maomao Mountain,
Yimen County, Yunnan Province
生境：疏生于石灰山草地中
Habitat: sparsely grown in limestone grasslands
海拔：1300-1400 米
Altitude: 1300-1400 m
GPS: 101°57′E, 24°40′N
附记：5 份
Note: 5 copies
分类：香茶菜属
Classification: *Isodon*

主模式
HOLOTYPUS

YUKU

YM8034

采集号：YM8034 科名：唇形科 Labiatae
小绿汁香茶菜
Isodon xiaoluzhiensis **Huan C. Wang & Shi Gang Li, sp. nov.**
鉴定人：王焕冲、李世刚 日期：2018.4.15

Figure 2. Holotype of *Isodon xiaoluzhiensis* (YUKU-05008415).

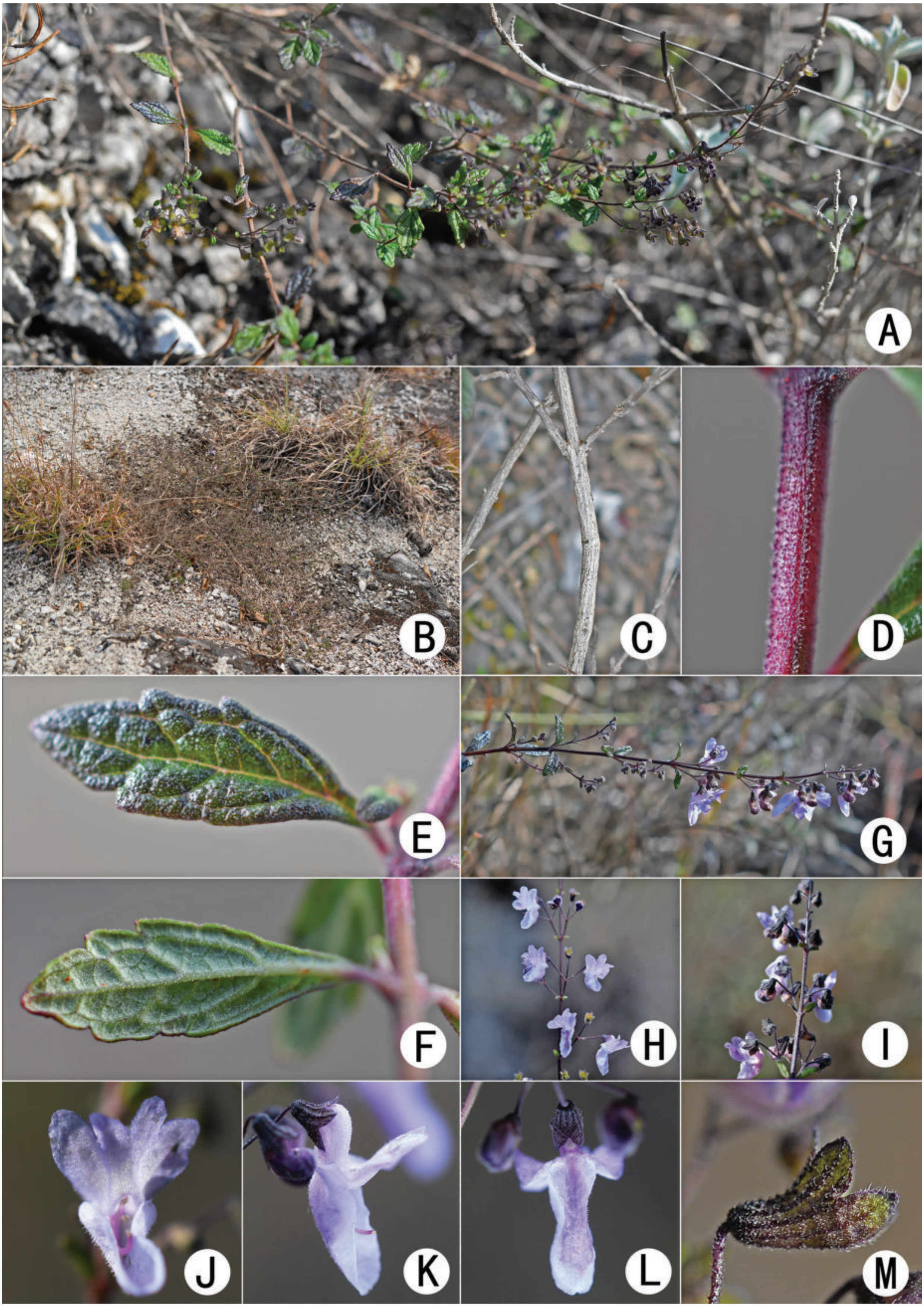

Figure 3. *Isodon xiaoluzhiensis* sp. nov. **A, B** habit **C** perennial stem **D** branchlet **E** adaxial surface of leaf **F** abaxial surface of leaf **G–I** inflorescence **J** corolla (front view) **K** flower (lateral view) **L** corolla (rear view) **M** calyx.

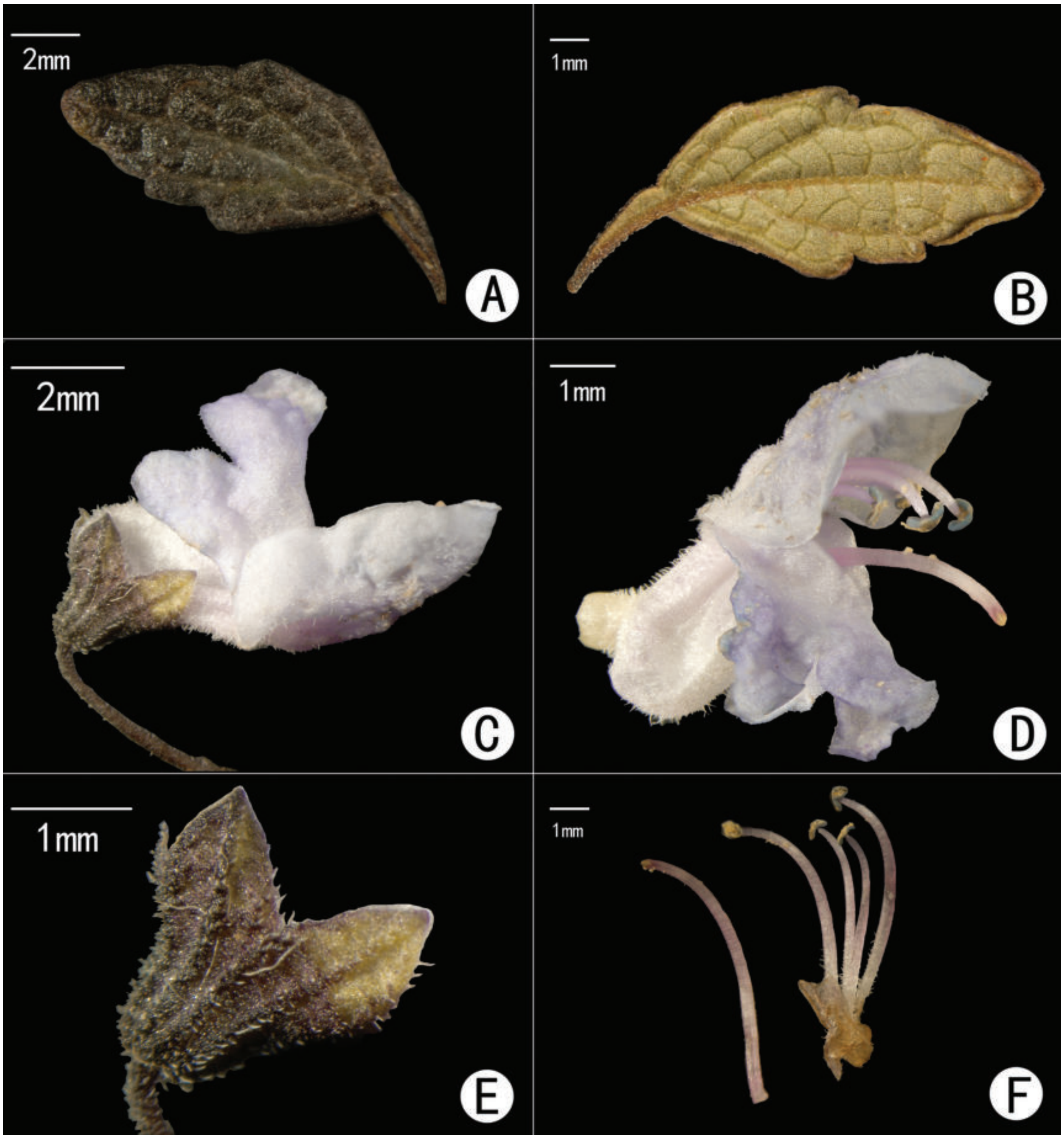

Figure 4. *Isodon xiaoluzhiensis* sp. nov. **A** adaxial surface of leaf **B** abaxial surface of leaf **C** flower (lateral view) **D** flower without calyx **E** calyx **F** pistil and stamens.

very similar to *I. adenanthus* (Diels) Kudô in terms of flower shape and size, but it clearly differs from the latter by its stem woody (vs. non-woody), procumbent (vs. erect or ascending), highly (vs. sparsely) branched, densely white glandular puberulent (vs. densely retrorse gray pubescent), leaves usually narrowly ovate to rhomboid (vs. rhombic-ovate to ovate-lanceolate), papery or thinly coriaceous (vs. herbaceous), small, 0.8–1.4 cm long (vs. 1.5–6.5 cm long), 0.2–0.5 cm wide (vs. 1–2.5 cm wide), teeth of calyx subobtuse to subacute (vs. apiculate) at apex, posterior lip of corolla non-spotted (vs. purple spotted).

Isodon xiaoluzhiensis is somewhat close to *I. hsiwenii* Y. P. Chen et C. L. Xiang in sharing relatively small leaves and procumbent stems. However, *I. xiaoluzhiensis* differs from *I. hsiwenii* by its main stems up to 60 cm long (vs. up to 100 cm for *I. hsiwenii*), leaves adaxially green or purplish black with pellucid glands (vs. dark green, densely puberulent and colorless glandular), leaves abaxially gray-green and densely white glandular-puberulent (vs. light green, densely puberulent colorless glandular on both sides), calyx purple with few green (vs. green outside), veins densely white hirsute outside (vs. densely purplish puberulent on veins), calyces teeth at apex subobtuse to subacute (vs. acute). Additionally, the habitats of these two species are distinctly different and non-overlapping. *Isodon hsiwenii* is only known from northeast Yunnan, situated in Jinshajiang River basin, and grows on stony slopes at an altitude of approximately 1 750 meters. Conversely, *I. xiaoluzhiensis* is discovered in Central Yunnan, located within the Honghe River basin, and inhabits the limestone grasslands between 1300 m and 1400 m at elevation. A morphological comparison of *I. xiaoluzhiensis* with *I. adenanthus* and *I. hsiwenii* is provided in Table 1.

Table 1. A morphological comparison of *Isodon xiaoluzhiensis* with its morphological relatives.

Characters	**Species**		
	I. xiaoluzhiensis	***I. adenanthus***	***I. hsiwenii***
Habit	Shrub or subshrub	herb	shrub
Stems	procumbent	erect or ascending	Procumbent, somewhat arcuate
Stems indumentum	densely white glandular puberulent	densely retrorse gray pubescent	densely purplish puberulent
Stems length (cm)	up to 60	15–40	up to 100
Leaves shape	narrowly ovate to rhomboid	rhombic-ovate to ovate-lanceolate	rhombic-ovate
Leaves size (cm)	0.8–1.4 × 0.2–0.5	1.5–6.5 × 1.0–2.5	1.0–2.0 × 0.5–1.0
Leaves adaxially	green or purplish black with pellucid glands	scattered yellowish glandular	dark green, densely puberulent and colorless glandular
Leaves abaxially	gray-green and densely white glandular-puberulent	white pilose, densely white pubescent on veins	light green, densely puberulent colorless glandular on both sides
Lateral veins	2–3 paired	3–4 paired	2–3 paired
Calyces size (mm)	2–3 × 2–2.5	2–3 × 2–4	2–4 × 2–4
Calyces teeth at apex	subobtuse to subacute	apiculate	acute
Corollas color	light purple	blue, purple, pink, or white	white to light purple
posterior lips of corolla	non-spotted	purple spotted	non-spotted
Phenology	fl. Nov.–Jan., fr. Dec.–Feb.	fl. Jun.–Aug., fr. Jul.–Sep.	fl. Sep.–Nov., fr.Nov.–Dec.

Acknowledgements

We are grateful to the editors of PhytoKeys, and to Dr. Kenneth R. Wood (National tropical botanical Garden, United States) and another anonymous reviewer for critical comments on the manuscript.

Additional information

Conflict of interest

The authors have declared that no competing interests exist.

Ethical statement

No ethical statement was reported.

Funding

This study was supported by grants-in-aid from the National Natural Science Foundation of China (NSFC) (Grant No.31960040) and the Second Tibetan Plateau Scientific Expedition and Research (STEP) program (2019QZKK0502).

Author contributions

Investigation: HCW, SGL, CLX, QCH, SYL. Writing - original draft: SGL. Writing - review and editing: HCW.

Author ORCIDs

Shi-Gang Li https://orcid.org/0009-0000-4041-6236
Qiang-Chun Huang https://orcid.org/0009-0001-9918-9899
Shao-Yun Liu https://orcid.org/0009-0001-6524-7632
Chun-Lei Xiang https://orcid.org/0000-0001-8775-6967
Huan-Chong Wang https://orcid.org/0000-0001-8562-8849

Data availability

All of the data that support the findings of this study are available in the main text.

References

Bentham G (1876) Labiatae. In: Bentham G, Hooker JD (Eds) Genera Plantarum, vol. 2. Lovell Reeve and Co, London, 1160–1223.

Bentham G (1832) Tribe Ocimoideae in Labiatarum genera et species: or, a description of the genera and species of plants of the order Labiatae with their general history, characters, affinities, and geographical distribution. J Ridgway and Sons, London, 151 pp.

Chen YP, Hu GX, Xiang CL (2014) *Isodon delavayi* (Ocimeae, Nepetoideae, Lamiaceae): A new species from Yunnan Province, Southwest China. Phytotaxa 156(5): 291–297. https://doi.org/10.11646/phytotaxa.156.5.5

Chen YP, Xiang CL, Sunojkumar P, Peng H (2016) *Isodon villosus* (Nepetoideae, Lamiaceae), a new species from Guangxi, China. Phytotaxa 268(4): 271–278. https://doi.org/10.11646/phytotaxa.268.4.5

Chen YP, Hu GX, Zhao F, Peng H, Xiang CL (2017) Taxonomic notes on *Isodon* (Lamiaceae) in China, II: *I. aurantiacus*, a new species from Tibet, China. Annales Botanici Fennici 54(4–6): 239–243. https://doi.org/10.5735/085.054.0606

Chen YP, Wilson TC, Zhou YD, Wang ZH, Liu ED, Peng H, Xiang CL (2019) *Isodon hsiwenii* (Lamiaceae: Nepetoideae), a new species from Yunnan, China. Systematic Botany 44(4): 913–922. https://doi.org/10.1600/036364419X15710776741486

Chen YP, Huang CZ, Zhao Y, Xiang CL (2021) Molecular and morphological evidence for a new species of *Isodon* (Lamiaceae) from southern China. Plant Diversity 43(1): 54–62. https://doi.org/10.1016/j.pld.2020.06.004

Farr ER, Leussink JA, Stafleu FA (1979) Index Nominum Genericorum (Plantarum), vol. 2. Bohn, Scheltema and Holkema, Utrecht.

Hara H (1972) On the Asiatic species of the genus *Rabdosia* (Lamiacese). Shokubutsu Kenkyu Zasshi 47: 193–203.

Hara H (1985) Comments on the East Asiatic plants (17). Shokubutsu Kenkyu Zasshi 60: 230–238.

Harley RM, Atkins S, Budantsev AL, Cantino PD, Conn BJ, Grayer BJ, Harley MM, Kok RD, Krestovskaya TV, Morales R, Paton AJ, Ryding O, Upson T (2004.) Labiatae. In: Kubitzki K, Kadereit JW (Eds) The Families and Genera of Vascular Plants, vol. 7. Springer Verlag, Berlin, 167–275. https://doi.org/10.1007/978-3-642-18617-2_11

Hasskarl JK (1842) *Plantarum* genera et species novae aut reforma tae javenses. Flora oder Botanische Zeitung 25(2, Beibl.): 25.

IUCN Standards and Petitions Subcommittee (2019) Guidelines for using the IUCN Red List Categories and Criteria. Version 14. Prepared by the Standards and Petitions Subcommittee. http://www.iucnredlist.org/documents/RedListGuidelines.pdf [Accessed: 11 November 2023]

Li HW (1975) Some changes of botanical name in Chinese Labiatae (continued). Journal of Systematics and Evolution 13(1): 79–94.

Li HW (1988) Taxonomic review of *Isodon* (Labiatae). Journal of the Arnold Arboretum 69(4): 289–400. https://doi.org/10.5962/p.324759

Li HW, Hedge IC (1994) *Isodon* (Schrader ex Bentham) Spach. In: Wu ZY, Raven PH, Hong DY (Eds) Flora of China, vol. 17. Science Press, Beijing. and Missouri Botanical Garden Press, St. Louis, Missouri, 269–291.

Liu JL, Li SG, Yang F, Wang HC (2022) *Indigofera vallicola* (Fabaceae), a new species from Yunnan, southwest China. PhytoKeys 199: 9–16. https://doi.org/10.3897/phytokeys.199.85437

Mabberley DJ (2008) Mabberley's plant-book: A portable dictionary of the plants, 3rd edn. Cambridge University Press, Cambridge.

Morton JK (1962) Cytotaxonomic studies on the West African Labiatae. Journal of the Linnean Society of London, Botany 58(372): 242–249. https://doi.org/10.1111/j.1095-8339.1962.tb00896.x

Nakai T (1934) Notulae ad Plantas Japoniae and Koreae XIIV. Botanical Magazine Tokyo 48(575): 773–792. https://doi.org/10.15281/jplantres1887.48.773

Paton AJ, Ryding O (1998) *Hanceola*, *Siphocranion* and *Isodon* and their position in the Ocimeae (Labiatae). Kew Bulletin 53: 723–731. https://doi.org/10.2307/4110492

Qiao D, He ZR, Ma XD, Wang HC (2018) *Pterygiella luzhijiangensis* (Orobanchaceae), a new species from Yunnan, southwest China. Nordic Journal of Botany 36(4): njb-01680. https://doi.org/10.1111/njb.01680

Spach É (1840) Histoire naturelle des végétaux, vol. 9. Librarie Encyclopédique de Roret, Paris, 1–586.

Tang W, Eisenbrand G (1992). *Rabdosia* spp. In: Tang W, Eisenbrand G (Eds) Chinese Drugs of Plant Origin. Springer, Berlin, Heidelberg, 817–847. https://doi.org/10.1007/978-3-642-73739-8_105

Wu CY, Li HW (1977) *Rabdosia* (Bl.) Hassk. In: Wu CY (Ed.) Flora Reipublicae Popularis Sinicae. vol. 66. Science Press, Beijing, 416–534.

Xiang CL, Liu ED (2012) A new species of *Isodon* (Lamiaceae, Nepetoideae) from Yunnan province, southwest China. Systematic Botany 37(3): 811–817. https://doi.org/10.1600/036364412X648751

Yang F, Ye JY, Huang QC, Wang QP, Wang HC (2022) *Duhaldea lachnocephala* (Asteraceae: Inulinae), a new species from Yunnan, southwest China. Taiwania 67(2): 217–222.

Yu QY, Maki M, Drew BT, Paton AJ, Li HW, Zhao JL, Conran JG, Li J (2014) Phylogeny and historical biogeography of *Isodon* (Lamiaceae): Rapid radiation in south-west China and Miocene overland dispersal into Africa. Molecular Phylogenetics and Evolution 77: 183–194. https://doi.org/10.1016/j.ympev.2014.04.017

Zhong JS, Li J, Li L, Conran JG, Li HW (2010) Phylogeny of *Isodon* (Schrad. ex Benth.) Spach (Lamiaceae) and related genera inferred from nuclear ribosomal ITS, *trn*L-*trn*F region, and *rps*16 intron sequences and morphology. Systematic Botany 35(1): 207–219. https://doi.org/10.1600/036364410790862614

PhytoKeys

PhytoKeys 237: 201–218 (2024)
DOI: 10.3897/phytokeys.237.114461

Research Article

Taxonomic novelties in *Haplopappus* (Asteraceae, Astereae) from Chile

Nicolás García[1], Arón Cádiz-Véliz[2,3], Macarena Villalobos[1], Vanezza Morales[1,4]

1 *Herbario EIF & Laboratorio de Evolución y Sistemática, Facultad de Ciencias Forestales y de la Conservación de la Naturaleza, Universidad de Chile, Avenida Santa Rosa 11315, La Pintana, Santiago, Chile*
2 *Departamento de Botánica, Facultad de Ciencias Naturales y Oceanográficas, Universidad de Concepción, Casilla 160C, 4030000, Concepción, Chile*
3 *Instituto de Ecología y Biodiversidad (IEB), Concepción, Chile*
4 *Museo Nacional de Historia Natural, Interior Quinta Normal s/n, casilla 787, Santiago, Chile*
Corresponding author: Nicolás García (ngarcia@uchile.cl)

Abstract

Two new species of *Haplopappus* (Asteraceae) from central Chile are described in this article. *Haplopappus colliguayensis* **sp. nov.** is restricted to La Chapa hill, Colliguay, Valparaíso Region, and is most similar to *H. undulatus* but differs from the latter in its stem indumentum, leaf shape and margin, and synflorescence arrangement. *Haplopappus teillieri* **sp. nov**. has been recorded from four high-Andean localities in the Choapa, Petorca, Rocín and Aconcagua river basins, and is most similar to *H. punctatus* but differs from the latter in its leaf length and margin, number of peduncles per twig, width of outer phyllaries, number of ray florets per capitulum, and achene dimensions. Additionally, we propose the reinstatement of *H. kingii* in agreement with an exhaustive revision of type material and protologues, as well as the study of herbarium specimens. *Haplopappus kingii* is restricted to mountainous areas in the southern portion of the Atacama Region, and resembles *H. parvifolius* and *H. retinervius* but differs from both by its leaf margin and apex, besides additional differences from each. We provide morphological descriptions, field images, distributional maps, conservation assessments, and taxonomic notes for the three species treated, as well as illustrations for the novel taxa.

Key words: Central Chile, Compositae, IUCN, new species, taxonomy

Academic editor: Alexander Sennikov
Received: 20 October 2023
Accepted: 20 December 2023
Published: 29 January 2024

Citation: García N, Cádiz-Véliz A, Villalobos M, Morales V (2024) Taxonomic novelties in *Haplopappus* (Asteraceae, Astereae) from Chile. PhytoKeys 237: 201–218. https://doi.org/10.3897/phytokeys.237.114461

Introduction

Haplopappus Cassini is a strictly endemic South American genus in the tribe Astereae Cassini (Nesom and Robinson 2007; Funk et al. 2009), composed of 67 specific and intraspecific taxa (Klingenberg 2007; García et al. 2018), distributed in southern South America. Most of the genus diversity is restricted to Chile with 65 taxa, of which 48 (74%) are endemic to this country (Rodríguez et al. 2018).

Haplopappus comprises shrubs, subshrubs and only a few herbaceous taxa (Hall 1928; Cabrera 1934, 1971, 1978; Klingenberg 2007; Nesom and Robinson 2007; Tortosa and Bartoli 2002a, b; Bartoli and Tortosa 2013, 2014). Stems, leaves and phyllaries usually bear glandular trichomes giving them a glutinous to villous-glandular aspect. Phyllaries are organized in numerous series (3–6) and are coriaceous, appressed to recurved, tips acute to spiniform, with an herbaceous portion in a distinct apical green patch. True ray florets are usually yellow, in one series when present and disc florets are usually yellow, numerous, hermaphroditic, narrowly funnelform. Pappus bristles are unequal and numerous, arranged in 2–3 series, slightly connate in a basal ring (Gay 1849; Reiche 1902; Hall 1928; Cabrera 1934; Nesom and Robinson 2007; Klingenberg 2007; Tortosa and Bartoli 2002a, 2003; Bartoli and Tortosa 2013, 2014). An exhaustive phylogeny is lacking for this genus, therefore, its current intrageneric classification is based on morphological similarity, dividing *Haplopappus* in three subgenera and five sections (Klingenberg 2007; García et al. 2018).

Recent floristic studies in the Valparaiso Region of Central Chile led to the discovery of two new *Haplopappus* species. In addition, we also propose the reinstatement of *H. kingii* (Phil.) Reiche, a name that was placed under the synonymy of *H. remyanus* Wedd. by Klingenberg (2007).

Herein, we describe *H. colliguayensis* and *H. teillieri*, two new species from Central Chile, and provide information to support the taxonomic status of *H. kingii*. In addition, we provide illustrations and/or photographs, distribution maps, conservation status assessments, and taxonomic notes for all the species treated here.

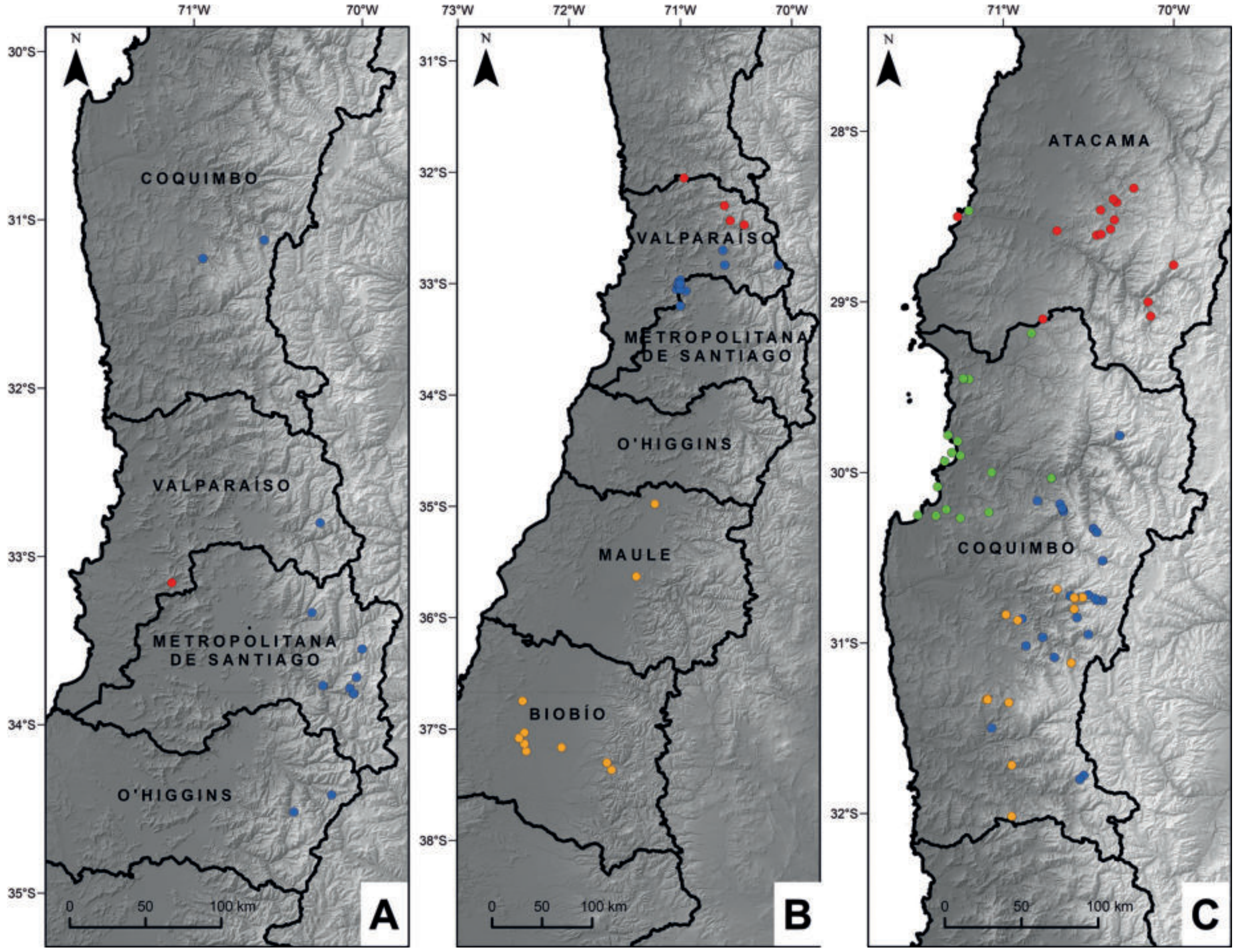

Figure 1. Distribution of *Haplopappus* in central Chile **A** *H. colliguayensis* (red dot), *H. undulatus* (blue dots) **B** *H. teillieri* (red dots), *H. integerrimus* (blue dots), *H. punctatus* (orange dots) **C** *H. kingii* (red dots), *H. parvifolius* (green dots), *H. remyanus* (blue dots), *H. retinervius* (orange dots).

Methods

At first, recently collected material was checked against taxonomic keys and descriptions of *Haplopappus*, which were provided by Gay (1849), Philippi (1858), Reiche (1902), Hall (1928), Brown and Clark (1982) and Klingenberg (2007). Then, the specimens were compared to general and type material held at Chilean herbaria (CONC, EIF, SGO, ULS). Digital images of specimens available on the websites of the following herbaria were also examined: BAA, BM, CAS, E, F, GH, K, LIL, M, MSB, NY, P, PH, S, SI, US, WU. Botanical terminology of the descriptions follows Beentje (2012). Leaf widths were measured over the widest portion of the lamina not considering the teeth, which were described separately. Two capitula per sample were rehydrated in 70% ethanol for 24 hours and were subsequently dissected. The different parts of the capitula (e.g., phyllaries, florets, gynoecium) were mounted on a white cardboard and scanned; measurements of capitulum parts were obtained with the free software ImageJ (Schneider et al. 2012). Distribution maps and the estimation of the area of occupancy and the extent of occurrence (*sensu* IUCN 2022) were generated using the GIS software ArcGis version 10.4 (ESRI 2015).

Taxonomic treatment

Haplopappus colliguayensis **M.A.Villalobos, V.Morales & Nic.García, sp. nov.**
urn:lsid:ipni.org:names:77335209-1
Figs 2, 3

Diagnosis. *Haplopappus colliguayensis* is similar to *H. undulatus* Klingenb., but differs from the latter by its stems with capitate glands and multicellular flagelliform trichomes (vs. sessile glands), leaves oblong to lanceolate (vs. obovate to oblanceolate), leaf margins flat, entire to shortly dentate with up to 5 teeth per side (vs. margins undulate, conspicuously dentate to serrate with 5–9 teeth per side), and paniculiform synflorescences with two or more capitula (vs. solitary capitulum).

Type. Chile. Región de Valparaíso: Provincia de Marga Marga, Comuna de Quilpué, Colliguay, cerro La Chapa, 957 m a.s.l., 33°9'13"S, 71°7'54"W, 27 February 2023, *N. García, M.A. Villalobos, V. Morales, A. Cádiz-Véliz, S. Olfos & O. Ovalle 6783* (holotype: EIF 17304!; isotypes: CONC!, JBN!, SGO!, SI!, VALPL!).

Description. Shrubs 0.4–0.8 m high, 0.1–0.3 m in diameter, ascending to erect, aromatic. Branching at base, some branches dry or with dry leaves and leaf scars on proximal half, leaves green towards the middle and distal portion of branches. Stems slightly corrugated, coppery, densely covered by minute capitate glandular trichomes and scattered multicellular flagelliform (2.0 mm) trichomes (same indumentum up to the peduncles). Leaves (0.5–)1.5–2.5(–4.0) × (0.1–)0.3–0.6(–1.0) cm; laminae oblong to lanceolate, gradually reduced in size towards the tip of branches, usually around five times as long as wide; bases cordate to obtuse; apices acute to acuminate, mucronate; margins entire to irregularly dentate, teeth 0.2–2 × 0.5–1.0 mm at the base, mucronate, (0–)1–3(–5) teeth on each side; leaves densely covered by short capitate glandular trichomes, multicellular, 0.25 mm long, and scattered subulate eglandular trichomes and flagelliform trichomes, membranous-papery to coriaceous,

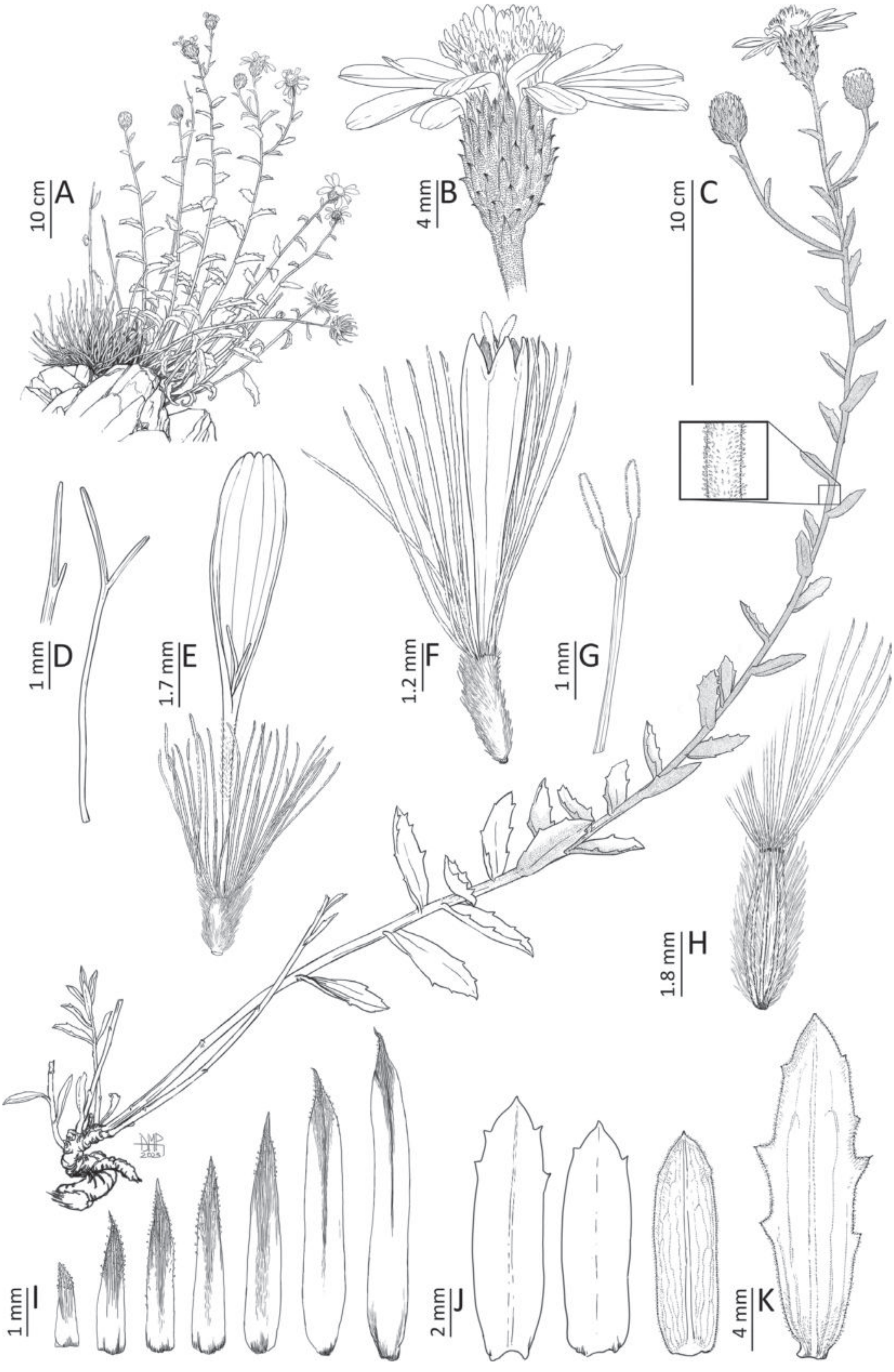

Figure 2. *Haplopappus colliguayensis* M.A.Villalobos, V.Morales & Nic.García **A** habit **B** capitulum **C** flowering branch, inset shows glandular pubescence on stem **D** style and asymmetrical stigmatic branches of true ray florets **E** true ray floret **F** disk floret **G** style and stigmatic branches of disk floret **H** achene **I** series of phyllaries **J** leaves ("bracts") subtending capitula **K** leaf. Drawn by Daniel Martinez Piña from *N. García et al. 6783*, 6785.

simple, sessile, alternate; venation with a dominant midvein and 2–4 basal secondary veins running more or less parallel to it, forming an arch with upper secondaries, overall reticulate due to tertiary veins. Capitula radiate, heterogamous, usually the apices of the main axis and (1–)2–5(–8) short secondary ramifications carry a single capitulum each, less frequently solitary on the main axis or up to 2 capitula per secondary branch, within a paniculiform synflorescence (paniculodium *sensu* Klingenberg 2007), that tends to take the aspect of a pseudoraceme. Peduncles up to 6 mm long or obsolete due to leaves growing up to the capitulum. Involucres 8–11 × 6–10 mm, campanulate to cylindrical. Phyllaries spirally arranged in 6–7 series, covered by short capitate glandular trichomes, border erose, mucronate; external series 2.0–2.5 × 0.5 mm at its widest, linear, mostly green (parenchymatous), sclerenchymatous basally, distal half to two thirds reflexed 30–45°, acute; intermediate series 4–6 × 0.6 mm at its widest, linear, green and reflexed 30–45° on distal half, acute, sclerenchymatous on proximal half; internal series 6.5–7 × 0.9 mm across the middle area, linear, apices straight or shortly reflexed, acute, parenchymatous on distal third, sclerenchymatous elsewhere, margins and below hyaline. Receptacles flat, epaleate, alveolate. True ray florets with tubular portion 4.0 × 0.3 mm and limbs 7.5 × 2.7 mm at its widest, with 4(–6) marked veins, both lateral bifurcating around the middle portion, ending in 2–3 small apical teeth, glabrous, 13–17 per capitulum, pistillate, corollas saffron (yellow-orange), zygomorphic, tubular portion covered with short, multicellular eglandular trichomes, becoming denser towards the throat; styles 4 mm long, divided asymmetrically into two branches; ovaries 1.5 × 0.5 mm, densely strigose. Disk florets 6.5–8.0 × 1.5–1.8 mm at their widest portion, numerous (60–70), perfect, corollas saffron, actinomorphic, infundibuliform, with 5 short lobes, 0.6–0.9 mm deep, edges thickened, shortly papillate; anthers 2.5 mm long; styles 4 mm long, with two style branches, 2.5 mm long each, papillate border on proximal half, differentiated distal half with multicellular collecting trichomes, apical triangular portion papillate; ovaries 1.5–2.5 × ~0.8 mm, densely strigose. Cypselae: achenes 4.0–4.5 × 0.8–1.2 mm, oblong-lanceolate, slightly flattened, asymmetrical, ribbed, only two lateral ribs prominent, covered by white, multicellular, stiff trichomes, 0.5–1 mm long, appressed or slanted up to 45° relative to the exocarp; pappus 3.0–5.5 mm long in ray florets and 3.0–6.0 mm long in disk florets, with numerous bristles (ca. 44), white, persistent, barbellate.

Distribution and habitat. *Haplopappus colliguayensis* has been recorded only in the La Chapa hill, Colliguay (~33.1°S; Fig. 1A), which is part of the coastal mountain range (*cordillera de la Costa*) between the Aconcagua and Maipo rivers. It inhabits rocky outcrops in south- to southwest-facing positions from the base of the hill (680 m a.s.l.) towards its summit (~1680 m a.s.l.). The surrounding zonal vegetation corresponds to sclerophyllous coastal forest; however, the vegetation associated with the rocky outcrops corresponds to a xerophilous scrub with predominance of *Adesmia pirionii* I.M.Johnst., *Gochnatia foliolosa* (D.Don) D.Don ex Hook. & Arn., *Puya coerulea* Lindl., and *Chusquea cumingii* Nees.

Etymology. The specific epithet refers to Colliguay, a locality situated to the south of the city of Quilpué in the Valparaíso Region of Chile.

Phenology. This species has been recorded flowering in February, but the period probably extends between January and March. Fruits have been recorded between February and April.

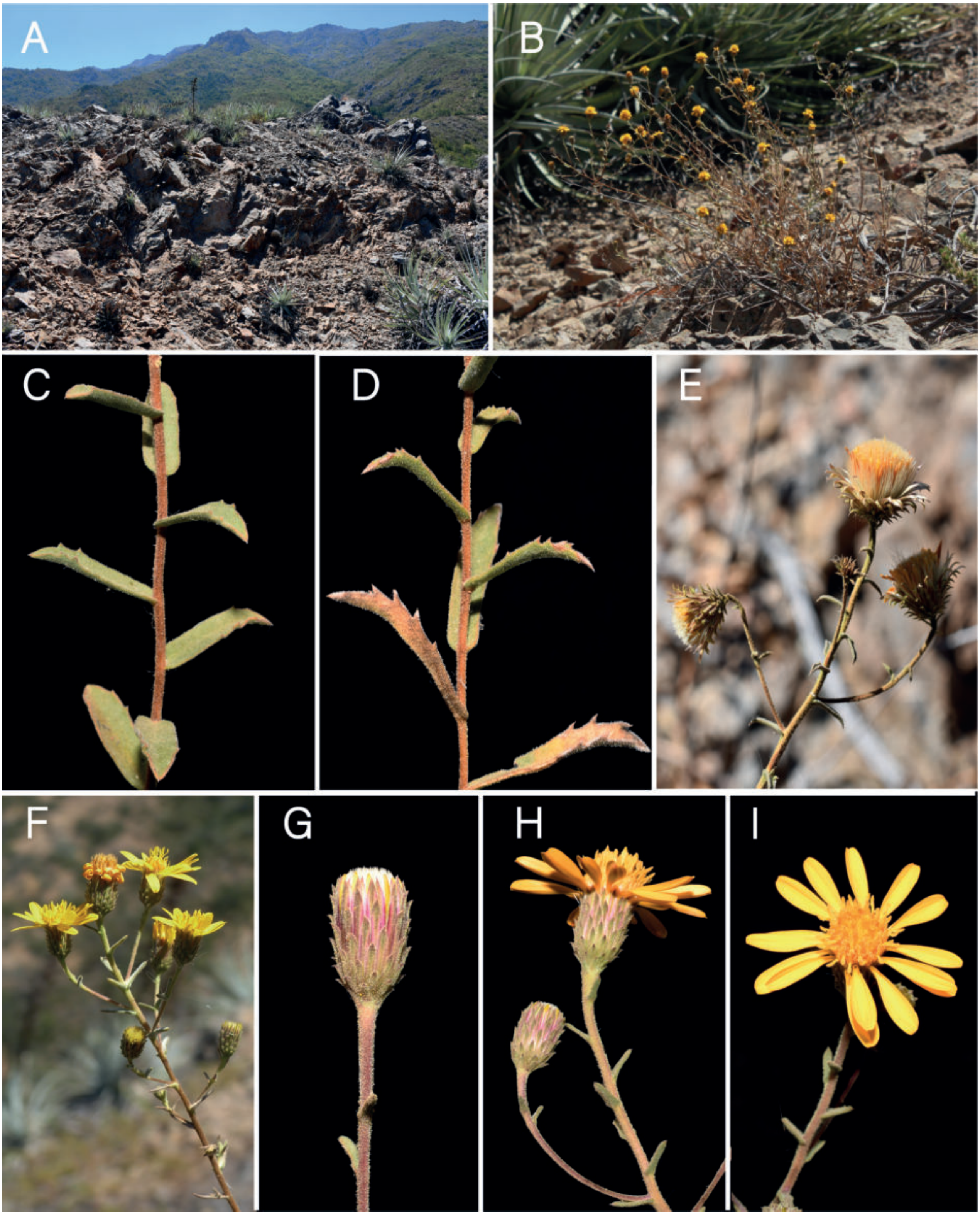

Figure 3. *Haplopappus colliguayensis* M.A.Villalobos, V.Morales & Nic.García **A** habitat **B** habit **C, D** detail of stem and leaves **E** fruiting capitula **F** flowering branch showing paniculiform synflorescence **G** immature capitulum **H** capitulum, side view **I** capitulum, top view. Photographs by Arón Cádiz-Véliz (**A, C–E, G–I**), Macarena Villalobos (**B**), Nicolás García (**F**).

Conservation status. According to IUCN (2022), *Haplopappus colliguayensis* can be considered as Critically Endangered (CR) according to criteria B2ab(iii, v), because its Area of Occupancy (AOO) is <10 km^2 (4 km^2). The criterion “a” was selected because it is known from a single locality. Although it is estimated that the only known population maintains around 1,000 individuals, all of them grow concentrated in a reduced area, which is susceptible to be affected by natural catastrophes or anthropogenic interventions (e.g., fires, droughts). The criterion "b(iii)" was selected because there is an inferred and projected decline in the extent and the quality of the habitat, given projected replacement of the vegetation due to climate change and the high probability of fire occurrence in the area where the species inhabits. According to MMA (2023b), the climate scenarios for 2050 predict an increase in temperature (of 1–2 °C) and a decrease in precipitation (~60–80 mm) in the county of Quilpué, where the species has been recorded. The predicted changes in precipitation allowed to classify this area under high risk of loss of flora (MMA 2023a). Moreover, the region of Valparaíso is one of the Chilean regions that has experienced one of the highest numbers of fires and its burned area was extensive between 1985–2018 (González et al. 2020). As a proof of this risk, a major fire that consumed 10 km^2 in December of 2022, affected a valley contiguous to Colliguay and reached only 2 km away from the location of *H. colliguayensis*. The persistence of this trend with the probability of such future events in La Chapa hill would generate a decrease in the number of mature individuals, affecting the persistence of the species (criterion "b(v)").

Additional specimens examined (paratypes). Chile. Región de Valparaíso: Provincia de Marga-Marga, Comuna de Quilpué, Colliguay, cerro La Chapa, 680 m a.s.l., 17 April 2019, *N. García, M.A. Villalobos & N. Godoy 5561* (EIF); 679 m a.s.l., 15 October 2019, *M.A. Villalobos & J.P. Madriaga 111* (EIF, SGO); 1047 m a.s.l., 10 December 2019, *M.A. Villalobos, V. Farías & P. Villalobos 154* (EIF, SGO, CONC); 1675 m a.s.l., 27 December 2019, *N. García, M.A. Villalobos & V. Villablanca 5720* (EIF); 735 m a.s.l., 27 February 2023, *N. García, M.A. Villalobos, V. Morales, A. Cádiz-Véliz, S. Olfos, O. Ovalle 6785* (EIF, SGO).

Taxonomic notes. Given its phyllaries acute, bracts up to the capitula similar to the cauline leaves, and peduncles not distinctly different from the twigs, *H. colliguayensis* can be assigned to *H.* sect. *Grindelioidae* Klingenb. (Klingenberg 2007). The new species most closely resembles *H. undulatus*, but differs in characters mentioned in the diagnosis and in its distribution restricted to xerophilous/rupiculous scrub in the coastal range, in contrast to the latter which is found in high-montane (i.e., alpine) scrub in the main Andes mountain range between the Valparaíso and O'Higgins regions (Fig. 1A). *Haplopappus colliguayensis* can also be compared to *H. grindelioides* (Less.) DC., which besides having a much southern distribution between the Maule and Los Ríos regions (vs. Valparaíso Region), also has solitary capitula (vs. paniculiform synflorescence with two or more capitula), stems tomentose (vs. glandulose), and outer series of phyllaries 1.7–2 mm wide (vs. 0.5 mm wide) (Klingenberg 2007).

Haplopappus teillieri A.Cádiz-Véliz, V.Morales & Nic.García, sp. nov.

urn:lsid:ipni.org:names:77335471-1

Figs 4, 5

Diagnosis. *Haplopappus teillieri* is similar to *H. punctatus* (Willd.) H.M.Hall, but differs from the latter in its leaves 1–2.5 cm long (vs. 3–6 cm), leaf margin always entire (vs. entire to up to 6 teeth per side), 1–3 peduncles per twig (vs. 2–6 peduncles per twig), outer series of phyllaries 1.2–1.8 mm wide (vs. 0.5–1.0 mm), ~7 ray florets per capitulum (vs. 10–12), and achenes 6.5–7 × 0.8–1.0 mm (vs. 3–4.4 × 1.5–1.8 mm).

Type. Chile. Región de Valparaíso: Provincia de San Felipe de Aconcagua, Comuna de Putaendo, río Rocín, sector Las Tejas, 2530 m a.s.l., 32°28'22"S, 70°25'25"W, 04 January 2023, *A. Cádiz-Véliz, J.L. Álvarez & S. Grau 991* (holotype: EIF 17305!; isotypes: CONC!, JBN!, MO!, SGO!, SI!, VALPL!).

Description. Shrubs 0.25–0.4(–0.5) m high and 0.35–0.7 m in diameter, ascending to erect, with slight citric odor. Stems growing parallel to the ground at first and branching later in an ascending way. Stems furrowed, papery bark at base, greenish near the base, turning yellowish to reddish towards the apex, sparsely covered by sessile glands (same indumentum up to the peduncles), glutinous. Leaves (0.5–)1.0–2.5(–3.0) × (0.1–)0.2–0.3(–0.55) cm; lamina narrowly lanceolate to oblanceolate, rarely linear, gradually reduced in size towards the tip of branches, around five to eight times as long as they are wide; bases attenuate; apices acute to acuminate, ending in a slender seta, 0.2–0,5 mm long; margins entire, scabrid due to short subulate trichomes; leaves glutinous, covered by sessile glands throughout and sparsely by short subulate unicellular trichomes (~0.25 mm long) on margins and upper central vein, coriaceous, simple, sessile, alternate or frequently fasciculate with 3–5 smaller leaves on the axils of major leaves; venation reticulate and inconspicuous. Capitula radiate and heterogamous, rarely discoid and homogamous, with 3–4 small subulate leaf-like bracts at the base, solitary on the apex of a long peduncle. Peduncles up to 28 cm long, 0.6–1.0 mm wide at base, 1–3 per twig, with 3–8 evenly distributed subulate bracts. Involucres 9–14 × 8–12 mm, cylindrical. Phyllaries spirally arranged in 5–6 series, covered by sessile and short capitate glands, glutinous, ending in a slender seta; external series 2.7–4.7 × 1.2–1.8 mm at its widest, ovate to elliptic, mostly green (parenchymatous), sclerenchymatous basally, margin purplish along the middle and towards the tip, straight, acuminate; intermediate series 4.4–7.4 × 1.6–2.0 mm at its widest, lanceolate to oblong, green-purplish on distal half, sclerenchymatous on proximal half, straight or only tip reflexed, acuminate; internal series 7.4–8.3 × 1.5–2.0 mm across the middle area, ligulate, apices straight or shortly reflexed, acuminate, parenchymatous and purplish on distal third, sclerenchymatous elsewhere, margins and below hyaline. Receptacles flat, epaleate, alveolate. True ray florets with tubular portion 4.7–5.5 × ~0.4 mm and limbs 2.3–3.0 × ~1.0 mm at its widest, with 3–4 marked veins ending in 3 small apical teeth, also 2–3 segments fused forming the limb and an extra shorter segment free, glabrous, ~7 per capitulum, pistillate, corollas pale saffron, zygomorphic, tubular portion covered with short, multicellular eglandular trichomes; styles 4 mm long, ending in two asymmetrical style branches 1.2 and 0.7 mm long each or undivided, glabrous; ovaries 1.0–1.5 × ~0.8 mm, densely strigose. Disk florets 5.6–6.6 × 0.7–0.8 mm at their widest portion, numerous (~40), perfect, corollas pale saffron, actinomorphic, infundibuliform, with 5 short lobes, 0.3–0.8 mm deep, edges thickened, shortly papillate; anthers ~2.5 mm long; styles 5.3 mm long, with two style branches, 1.2–1.3 mm long each, apical triangular portion papillate; ovaries 1.0–1.5 × ~0.5 mm, densely strigose. Cypselae: achenes 6.5–7.0 × 0.8–1.0 mm, linear-oblanceolate, slightly flattened, asymmetrical, ribbed, only

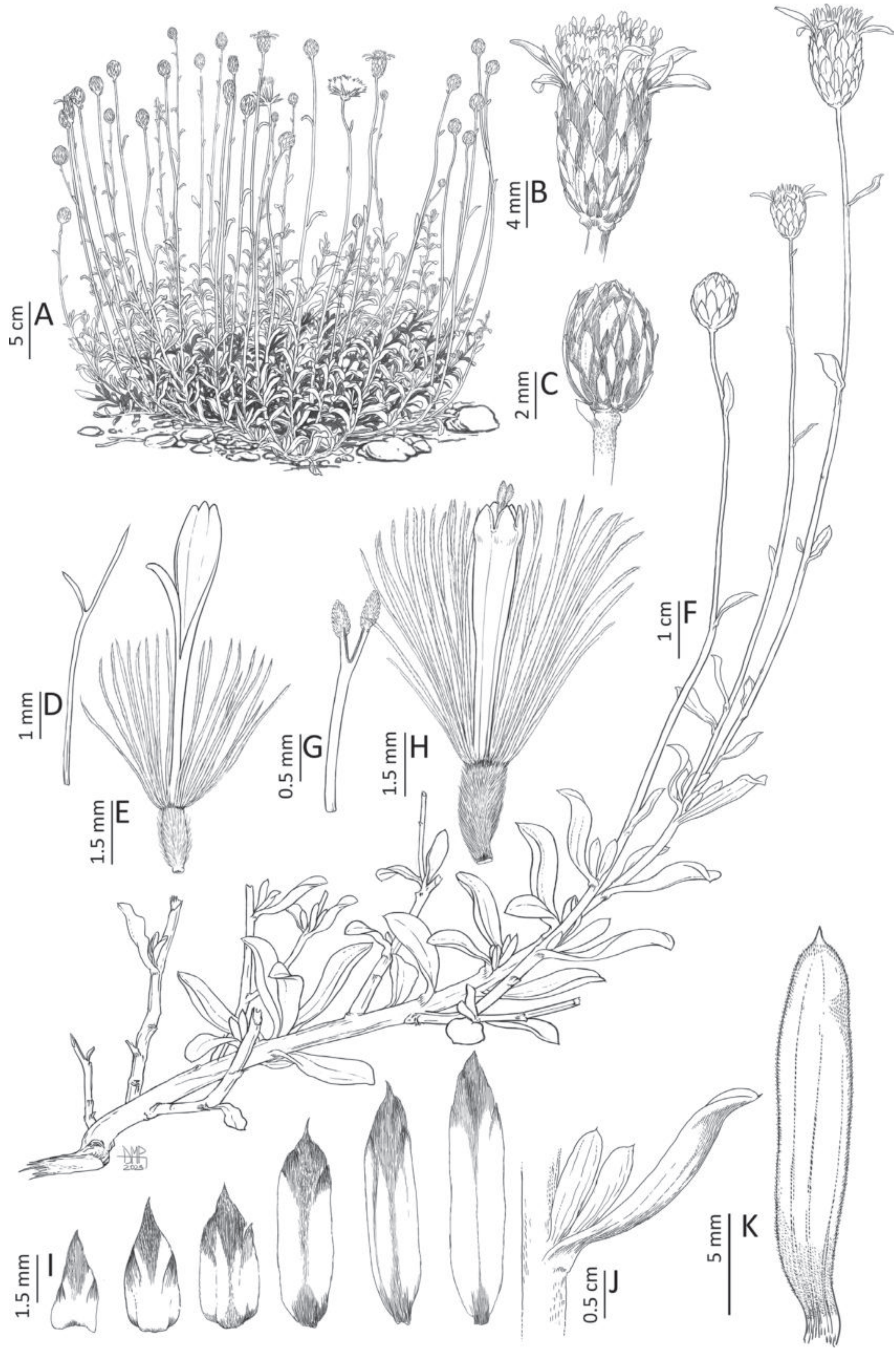

Figure 4. *Haplopappus teillieri* A.Cádiz-Véliz, V.Morales & Nic.García **A** habit **B** capitulum **C** immature capitulum **D** style and asymmetrical stigmatic branches of true ray floret **E** true ray floret **F** flowering branch **G** style and stigmatic branches of disk floret **H** disk floret **I** series of phyllaries **J** fascicle of leaves **K** leaf. Drawn by Daniel Martinez Piña from *A. Cádiz-Véliz et al. 991*.

two lateral ribs prominent, densely covered by white, stiff trichomes, ~0.25 mm long, slanted 20–45° relative to the exocarp; pappus 4.5–5.5 mm long in ray florets and 3.1–7.0 mm long. in disk florets, with numerous bristles (57–58), ochreous, persistent, barbellate.

Distribution and habitat. *Haplopappus teillieri* inhabits the Mediterranean Andean low scrub of *Chuquiraga oppositifolia* D.Don and *Nardophyllum lanatum* (Meyen) Cabrera, between 1500–2600 m a.s.l. (Luebert and Pliscoff 2017). Only four populations have been recorded in the Andes, along the valleys of rivers Choapa, Petorca, Rocín and Aconcagua (Fig. 1B). It seems to be a very rare species but it can become locally dominant.

Etymology. The specific epithet *teillieri* honours the Chilean botanist Sebastián Teillier Arredondo (1956–), who has made significant contributions to the knowledge of the vascular flora of Chile.

Phenology. *Haplopappus teillieri* starts flowering in January, probably extending its bloom until early March. Fruits from February onwards.

Conservation status. *Haplopappus teillieri* was rarely collected since 1924, within a very restricted area in the Andes mountains of the Choapa and San Felipe de Aconcagua provinces (Fig. 1B), which suggests that it is a rare species. Here, we propose the species conservation status as Endangered (EN), considering the criteria B1+B2ab(iii). It has been assessed under the criterion “B1” as its Extent of Occurrence (EOO) is <5,000 km^2 (266 km^2), while the criterion “B2” corresponds to the Area of Occupancy (AOO) <500 km^2 (16 km^2). Criterion “a” is invoked given the species presence in less than five localities (4). Its populations are potentially threatened since all these mountainous areas are located within a zone of high interest for mining development and consequently is fully covered by mining petitions (SONAMI 2023). The criterion “b(iii)” corresponds to the inferred and projected decrease in the quality of the habitat due to the presence of bovine and caprine livestock and mining activities (e.g., opening of roads, prospecting, excavations, removal of soil and vegetation due to installation of facilities). The habitat will also be affected by climate change the consequences of which are a decline in precipitation (35–50 mm) and temperature increase (~2 °C) (MMA 2023a). In this sense, the species inhabits an area that is projected to suffer a moderate to high risk of loss of the flora because of precipitation decrease (MMA 2023a).

Additional specimens examined (paratypes). Chile. Región de Coquimbo: Provincia de Choapa, Comuna de Salamanca, Cuenca Camisas, sector Antena, 2350 m a.s.l., 32°3'S, 70°58'W, 02 July 2000, *G. Arancio & F. Squeo 13236* (ULS 13692, 13693). Región de Valparaíso: Provincia de Petorca, valle del río Alicahue, 1500 m a.s.l., 32°17'56"S, 70°36'10"W, March 2016, *S. Teillier & J. Torres-Mura 8039* (CONC 182727); Provincia de San Felipe de Aconcagua, Laguna del Copín, 3000 m a.s.l., 32°26'S, 70°33'W, April 1924, *C. Joseph 15052* (CONC 59861).

Taxonomic notes. Considering its phyllaries acute ending in a slender seta, bracts subulate, peduncles distinct from the twigs, leaves mostly narrowly lanceolate to oblanceolate, and sterile ray florets, *H. teillieri* clearly belongs in *H.* sect. *Gymnocoma* Nutt. (Brown and Clark 1982; Klingenberg 2007). Due to its capitula with ray florets and tips of the phyllaries straight to slightly spreading, it most closely resembles *H. punctatus*, with which it is directly contrasted in the diagnosis. It also resembles *H. integerrimus* (Hook. & Arn.) H.M.Hall due to its leaves glutinous and scabrid, presence of 1–3 peduncles per twig, and

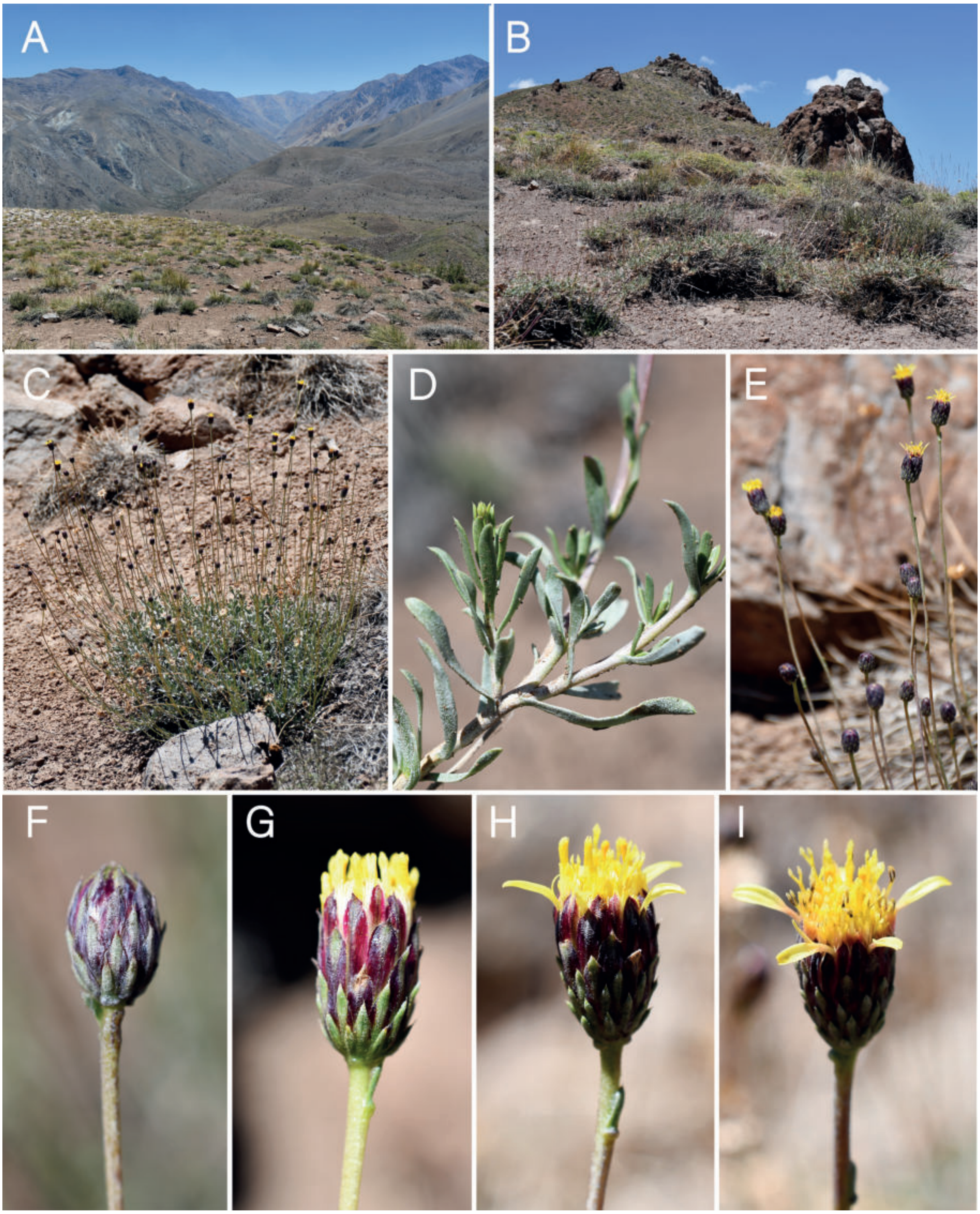

Figure 5. *Haplopappus teillieri* A.Cádiz-Véliz, V.Morales & Nic.García **A** general view of the Rocín valley **B** habitat in Andean scrub-grassland of *Chuquiraga oppositifolia, Festuca acanthophylla* and *H. teillieri* **C** habit **D** detail of branches and leaves **E** flowering branches **F** immature capitulum **G** homogamous mature capitulum **H, I** heterogamous mature capitula. All photographs by Arón Cádiz-Véliz.

ray florets inconspicuous (~7–9 mm long), but *H. teillieri* differs from the latter species by its shorter and narrower leaves ((0.5–)1.0–2.5(–3.0) × (0.1–)0.2–0.3(–0.55) cm vs. 3.0–7.5 × 0.3–0.9 cm), leaf margin always entire (vs. 0–6 teeth per side), peduncles 0.6–1.0 mm wide at base (vs. 1.5–3.0 mm), tips of phyllaries straight to slightly spreading (vs. spreading to recurved), and internal series of phyllaries 1.5–2.0 mm wide (vs. 1.2–1.5 mm) (Klingenberg 2007).

Haplopappus kingii **(Phil.) Reiche, Anales Univ. Chile 109: 41. 1901, as "*kingi*"**
Figs 6, 7

Haplodiscus kingii Phil., Anales Univ. Chile 87: 615. 1894, as "*kingi*".

Type. Chile. Región de Atacama: Provincia de Huasco, Carrizal, 1885, *T. King 62* (holotype: SGO! [SGO000005614]; isotype: E! [E00253112]).

Description. Shrubs, ascending to erect, aromatic. Branching unknown. Stems slightly corrugated, coppery to yellowish, sparsely covered by minute stiff and bulbous trichomes (<0.5 mm) and scattered sessile glands (same indumentum up to the peduncles), glutinous. Leaves (1.0–)1.5–2.6(–3.1) × (0.3–)0.4–1.2(–1.9) cm; laminas oblong to oblanceolate, gradually reduced in size towards the tip of branches, usually around twice as long as they are wide; bases truncate to shortly decurrent; apices acute, rarely obtuse, mucronate; margins strongly dentate, teeth 2.0–3.0 × 1.5–3.0 mm at the base, mucronate, (4–)6–8(–9) teeth on each side; leaves densely covered by minute stiff trichomes, multicellular, 0.2 mm long, and sessile yellowish glands, coriaceous, glutinous, simple, sessile, alternate; venation with a dominant midvein and inconspicuous secondary veins. Capitula discoid, homogamous, usually clustered on short secondary branches, up to 3 capitula per branch, within a paniculiform synflorescence (paniculodium sensu Klingenberg 2007), that tends to take the aspect of a pseudoraceme. Peduncles obsolete due to leaves growing up to the capitulum, rarely up to 3 mm long. Involucres 10–12 × 9–18 mm, cylindrical. Phyllaries spirally arranged in 7–8 series, hyaline margin from the base to the apex, up to 0.5 mm wide on its widest portion, parenchymatous portion covered by minute sessile glands, mucronate; external series 4.2–5.7 × 1.7–2.5 mm at its widest, oblong to obovate, mostly burgundy (parenchymatous), sclerenchymatous basally, acute; intermediate series 5.4–7.6 × 1.8–2.3 mm at its widest, oblong to oblanceolate, acute, sclerenchymatous on proximal half; internal series 7.7–11.0 × 1.3–2.2 mm across the middle area, linear, apices acute, parenchymatous on distal third, sclerenchymatous elsewhere, margins and below hyaline. Receptacles flat, epaleate, alveolate. Disk florets 6.4–7.0 × 0.6–1.0 mm at their widest portion, numerous (38–61), perfect, corollas pale yellow (on herbarium specimens), actinomorphic, infundibuliform, with 5 short lobes, 0.5–0.8 mm deep, edges thickened, glabrous, rarely shortly papillate; anthers 2.9–3.1 mm long; styles 5.4–6.3 mm long, with two style branches, 1.1–1.9 mm long each, papillate on proximal half, differentiated distal half with multicellular trichomes; ovaries 2.5–3.3 × 0.3–0.7 mm, sparsely hispid. Cypselae: achenes 5.0–6.5 × 2.0 mm, linear, wider towards the middle portion, slightly flattened, asymmetrical, ribbed, only two lateral ribs prominent, hispid; pappus 4.1–9.5 mm long, with numerous bristles (55–61), chestnut to cinnamon, persistent, barbellate.

Distribution and habitat. This species is endemic to the Atacama Region in Chile (28°25'–29°05'S), mostly occurring in the middle portions of the Carrizal and

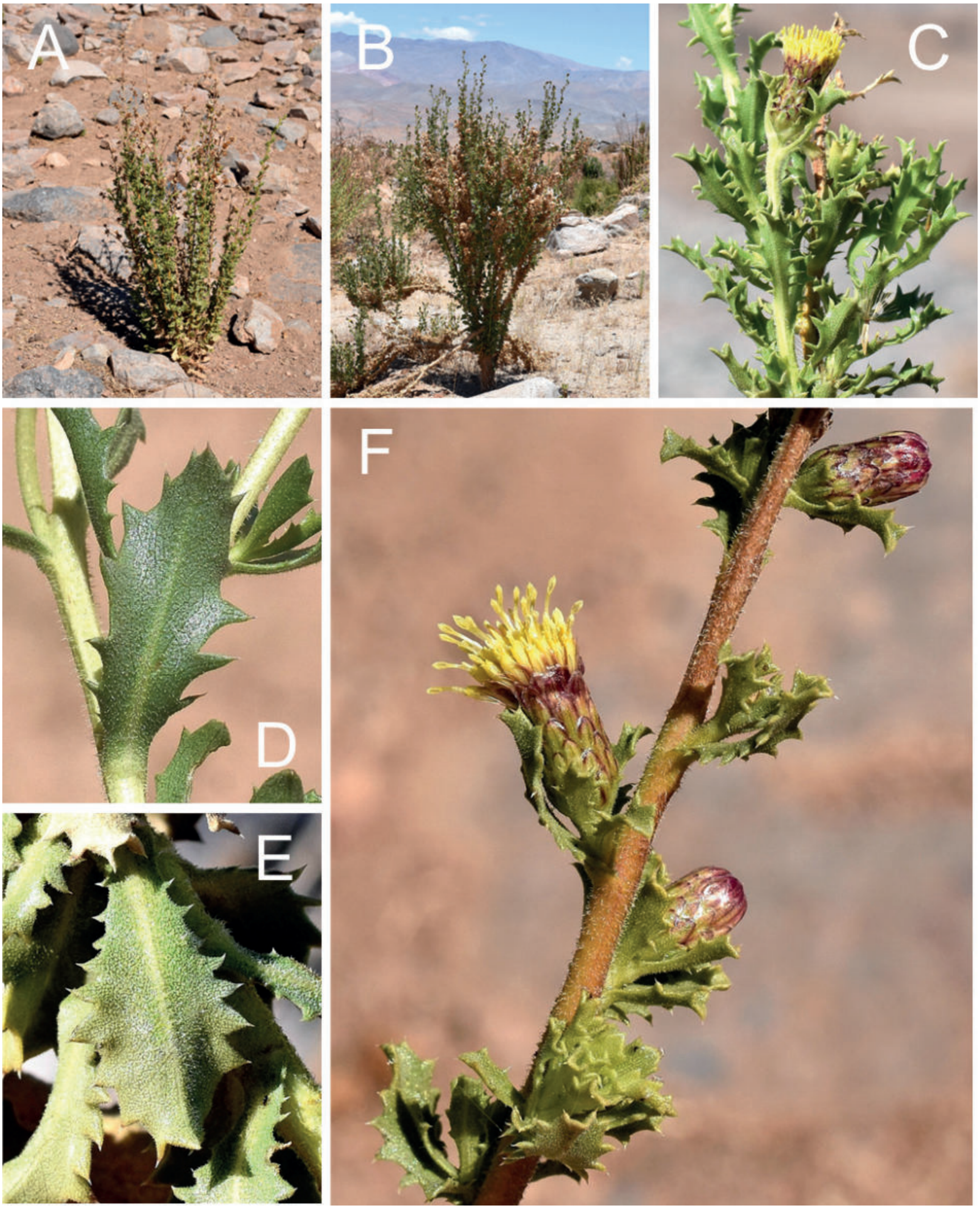

Figure 6. *Haplopappus kingii* (Phil.) Reiche **A, B** habit **C** flowering branch **D, E** detail of the abaxial and adaxial face of leaves, respectively, showing the characteristic hispid pubescence **F** branch showing several sessile capitula, fascicles of leaves and hispid stem. All photographs by Philippe Dandois.

Huasco river basins (Fig. 1C). It has been registered growing mostly on roadsides in mountainous areas, between 1500–3200 m a.s.l. There is a single record in the coast south of Huasco, which we consider may be an accidental occurrence.

Etymology. The specific epithet honours Thomas King, English citizen who collected several specimens in the Atacama Desert during the late 19th century.

Phenology. Flowering from November to January and fruiting from January to March.

Conservation status. *Haplopappus kingii* is only known from few herbarium specimens and field photographs (P. Dandois, personal communication, 7 July 2023). In accordance with the IUCN (2022), the species is known from 12 localities (Fig. 1C), presenting an estimated Extent of Occurrence (EOO) of 7,087 km^2 and Area of Occupancy (AOO) of 56 km^2. Although the estimations of EOO and AOO reach the values of threatened categories (Vulnerable and Endangered, respectively), there is not much information about the current state of the populations. The lack of these data does not allow us to classify the species under any threatened category. However, it is known that the species inhabits an area affected by the development of mining activities (SONAMI 2023) and the severe drought in Central Chile, which has produced a shortfall on normal precipitation of about 20–40% between 2010–2014 in the study area (CR2 2015). Moreover, the projections of climate change to 2050 estimate a decrease in precipitation (2–8 mm) and increase in temperature (1.8–2.5 °C) (MMA 2023b). Consequently, the area where the species is distributed will face a moderate to high risk of the loss of flora given the changes in precipitation (MMA 2023a). Considering all of the above, we inferred a change in the quality of the habitat of *H. kingii* but as the number of known localities exceeds thresholds for threatened categories, we propose the species conservation status as Near Threatened (NT).

Additional specimens examined. CHILE. Región de Atacama: Provincia de Huasco, El Bronce – Mantos Verdes, 1550 m a.s.l., 28°25'S, 70°21'W, November 2007, *S. Teillier & J. Delaunoy 5566* (CONC 166856); Quebrada Jilguero, crece en quebradas y laderas, abundante, 600 m a.s.l., 28°35'S, 70°41'W, 2 December 2008, *J. Reyes 4802* (ULS); Quebrada La Escoria, precordillera, 28°27'40.93"S, 70°25'39.22"W, 14 March 2013, *G. Mieres s.n.* (CONC 179797); Quebrada El Molle, precordillera, 28°31'7.48"S, 70°20'47.86"W, 11 January 2013, *G. Mieres s.n.* (CONC 179877, EIF 17306); Quebrada La Gloria, precordillera, 28°34'24.38"S, 70°22'7.48"W, 23 August 2012, *G. Mieres s.n.* (CONC 179800); Valle del río Laguna Grande, 2100–3000 m a.s.l., 28°49'S, 70°00'W, 14 February 1981, *M.T. Kalin-Arroyo 81565* (CONC 53397); Río Chollay, crece en ladera y lecho de quebrada, escasa, 2050 m a.s.l., 29°05'S, 70°08'W, 17 January 1994, *G. Arancio et al. 94119* (ULS); Huasco, crece entre rocas, 20 m a.s.l., 28°30'S, 71°16'W, 13 December 2008, *J. Reyes 6260* (ULS).

Taxonomic notes. *Haplopappus kingii* had been considered a distinct species in treatments of *Haplopappus* by Reiche (1902) and Hall (1928). However, Klingenberg (2007) reduced *H. kingii* into the synonymy of *H. remyanus* in *H.* sect. *Leiachaenium* DC., a decision that was followed by the latest catalogue of the vascular flora of Chile (Rodríguez et al. 2018). *Haplopappus kingii* can be differentiated from the latter species by its hispid indumentum (vs. glabrous and glutinous), leaves evenly distributed throughout the stem up to the synflorescence (vs. leaves distinctly clustered towards the base of the plant, flowering branches sparsely foliate below the capitula), and outer series of phyllaries 1.7–2.5 mm wide (vs. 2.5–3.0 mm wide).

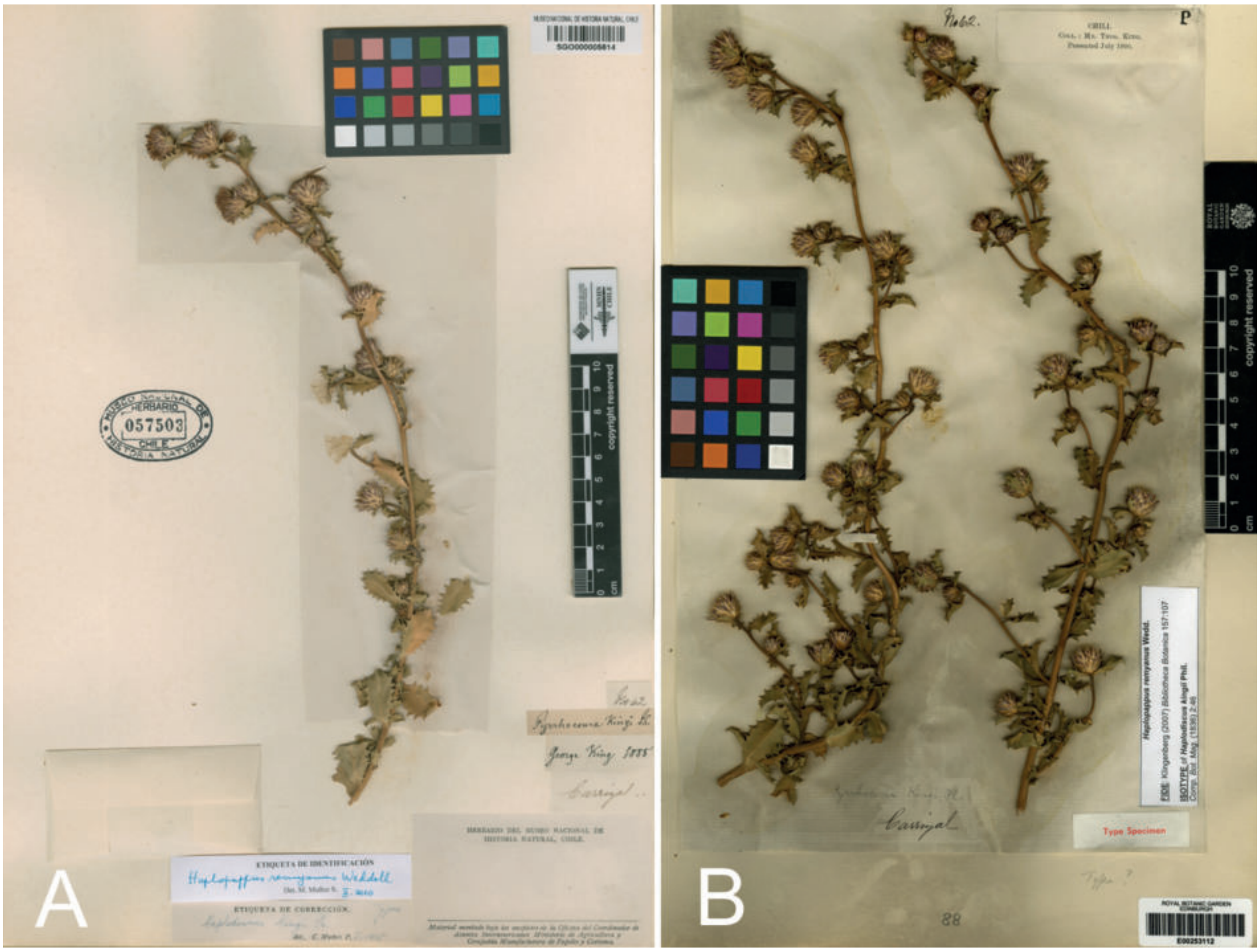

Figure 7. Type specimens of *Haplopappus kingii* (Phil.) Reiche **A** SGO000005614 (holotype) **B** E00253112 (isotype).

However, a close inspection of descriptions and herbarium specimens suggest that *H. kingii* better fits within Klingenberg's (2007) *H.* sect. *Chromochaeta* DC., where it most closely resembles *H. parvifolius* (DC.) A. Gray and *H. retinervius* (Kuntze) Klingenb. *Haplopappus kingii* differs from both species by its leaves with mostly flat margin (vs. margin undulate) and leaf apex acute (vs. obtuse to rounded). More specifically, *H. kingii* differs from *H. parvifolius* by its hispid indumentum (vs. glabrous plants), villous achenes (vs. glabrous achenes) and green leaves (vs. glaucous leaves), and from *H. retinervius* by its leaves oblong to oblanceolate (vs. broadly obovate to nearly orbicular) and more than 35 florets (vs. less than 30 florets) per capitulum (Klingenberg 2007).

In the citation of the type material, we recognize Thomas King as the collector of the sample, which differs from the name mentioned on the protologue, "Georgius King" (Philippi 1894: 615). The holotype at SGO (Fig. 7A) is accompanied by four pieces of paper, each of them with the following information: name of the species ("*Pyrrhocoma kingii* Ph."), the name of the collector and the year of collection ("George King 1885"), the locality ("Carrizal") and what we interpreted as the collection number ("No 62"). On the other hand, the specimen at E (Fig. 7B) is attached to a piece of paper in which it is possible to read "No 62" and "Carrizal". Additionally, there is a printed label saying "Chili. Coll.: Mr. Thos. King. Presented July 1900.", that suggests the sample was sent to Edinburgh by Thomas King himself. The labels with the name of the locality and the collection number seem to have the same handwriting, which suggests they were written by the collector. Thomas (or Tomas) King is a well-known collaborator of R.A. Philippi, who sent him several samples of plants from the Carrizal valley in the Atacama Region and some of these samples were used to describe new species (Philippi 1892; e.g. *Leucocoryne narcissoides* Phil., *Alstroemeria kingii* Phil., *Valeriana senecioides* Phil.). Apart from the description of this species, the name Georgius King has not appeared in other publications. Therefore, we assume that Philippi made a mistake when writing the name of the collector on the label of the holotype specimen of *Haplodiscus kingii* at SGO and in the species protologue.

Acknowledgements

We would like to thank many people for helping us during our research; the curators of the CONC (Alicia Marticorena), SGO (Victor Ardiles) and ULS (Gina Arancio) herbaria, who allowed the access to their collections; José Luis Álvarez and Susana Grau for facilitating the entrance to the Rocín Valley and helping search for *H. teillieri*; José Antonio Rojas for giving us access to Quebrada El Bellotal in La Chapa hill; Mélica Muñoz-Schick for the loan of samples of *Haplopappus* from her personal collection (now at SGO); Claire de Schrevel and Philippe Dandois for sharing photographs and localities of *H. kingii*; Daniel Martinez Piña for illustrating *H. colliguayensis* and *H. teillieri*; Gustavo Heiden for his review of our article. A.C.V. and V.M. are grateful to the ANID Scholarship 21231651 and 21211409, respectively.

Additional information

Conflict of interest

The authors have declared that no competing interests exist.

Ethical statement

No ethical statement was reported.

Funding

The illustrations of both novel species and publication fees for this article were financed by the fund Programa de Estímulo a la Excelencia Institucional (PEEI), Universidad de Chile.

Author contributions

Conceptualization: VM, NG. Investigation: MV, NG, VM, ACV. Methodology: VM. Supervision: NG. Writing – original draft: ACV, NG, VM, MV. Writing – review and editing: VM, NG.

Author ORCIDs

Nicolás García https://orcid.org/0000-0001-9003-1510
Arón Cádiz-Véliz https://orcid.org/0000-0002-7548-1764
Macarena Villalobos https://orcid.org/0000-0001-8897-3429
Vanezza Morales https://orcid.org/0000-0003-3723-8752

Data availability

All of the data that support the findings of this study are available in the main text or upon direct request to the authors.

References

Bartoli A, Tortosa R (2013) *Haplopappus* Cass. In: Kiesling R (Ed.) Flora de San Juan (Vol. IIIb). Asteraceae. Zeta Editores, Mendoza, 200–202.

Bartoli A, Tortosa R (2014) *Haplopappus* Cass. In: Zuloaga F, Belgrano M, Anton A (Eds) Flora Argentina (Vol. 7[1]). Asteraceae: Anthemideae a Gnaphalieae. Estudio Sigma, Buenos Aires, 187–195.

Beentje H (2012) The Kew Plant Glossary. An illustrated dictionary of plant terms. Kew Publishing, 164 pp.

Brown GK, Clark WD (1982) Taxonomy of *Haplopappus* sect. *Gymnocoma* (Compositae). Systematic Botany 7(2): 199–213. https://doi.org/10.2307/2418328

CR2 [Center of Climate and Resilience Research] (2015) Informe a la Nación: La megasequía 2010–2015: una lección para el futuro. Center of Climate and Resilience Research, 26 pp. http://www.cr2.cl/informe-a-la-nacion-la-megasequia-2010-2015-una-leccion-para-el-futuro/

Cabrera AL (1934) Las especies argentinas del género *Haplopappus*. Notas Preliminares del Museo La Plata 2: 233–257.

Cabrera AL (1971) *Haplopappus* Cass. In: Correa MN (Ed.) Flora Patagónica, Parte VII. Compositae. Colección Científica Instituto Nacional Tecnología Agropecuaria (INTA), Buenos Aires, 52–60.

Cabrera AL (1978) *Haplopappus* Cass. In: Cabrera AL (Ed.) Flora Provincia Jujuy, Parte 13(10). Compositae. Colección Científica Instituto Nacional Tecnología Agropecuaria (INTA), Buenos Aires, 197–199.

ESRI [Environmental System Resources Institute] (2015) ArcGis Desktop: Release 10.4. Red- lands, California.

Funk VA, Susanna A, Stuessy TF, Bayer RJ [Eds] (2009) Systematics, evolution and biogeography of Compositae. International Association for Plant Taxonomy, Institute of Botany, University of Vienna, 965 pp.

García N, Medina P, Morales-Fierro V (2018) *Haplopappus mieresii* sp. nov. (Asteraceae) and the reinstatement of *H. reicheanus* from central Chile. Phytotaxa 376(2): e103. https://doi.org/10.11646/phytotaxa.376.2.4

Gay C (1849) Historia física y política de Chile según documentos adquiridos en esta república durante doce años de residencia en ella y publicada bajo los auspicios del supremo gobierno: Botánica (vol. 4[1]). E. Thunot y Ca.; Museo Historia Natural, 516 pp.

González ME, Sapiains R, Gómez-González S, Garreaud R, Miranda A, Galleguillos M, Jacques M, Pauchard A, Hoyos J, Cordero L, Vásquez F, Lara A, Aldunce P, Delgado V, Arriagada R, Ugarte AM, Sepúlveda A, Farías L, García R, Rondanelli RJ, Ponce R, Vargas F, Rojas M, Boisier JP, Carrasco C, Little C, Osses M, Zamorano C, Díaz-Hormazábal I, Ceballos A, Guerra E, Moncada M, Castillo I (2020) Incendios forestales en Chile: Causas, impactos y resiliencia. Center of Climate and Resilience Research (CR)2, Universidad de Chile, Universidad de Concepción, Universidad Austral de Chile, 84 pp. http://www.cr2.cl/wp-content/uploads/2020/01/Informe-CR2-IncendiosforestalesenChile.pdf

Hall HM (1928) The Genus *Haplopappus*: A Phylogenetic Study in the Compositae. Publications of the Carnegie Institution of Washington, 391 pp.

IUCN [International Union for Conservation of Nature] (2022) Guidelines for Using the IUCN Red List Categories and Criteria. Version 15.1. Prepared by the Standards and Petitions Committee. https://www.iucnredlist.org/documents/RedListGuidelines.pdf

Klingenberg L (2007) Monographie der südamerikanischen Gattungen *Haplopappus* Cass. und *Notopappus* L. Klingenberg (Asteraceae – Astereae). Bibliotheca Botanica 157: 1–331.

Luebert F, Pliscoff P (2017) Sinopsis Bioclimática y Vegetacional de Chile (2ª edn.). Editorial Universitaria, 381 pp.

MMA [Ministerio del Medio Ambiente Chile] (2023a) ARClim: Atlas de riesgos climáticos. https://arclim.mma.gob.cl// [Accessed 20.08.2023]

MMA [Ministerio del Medio Ambiente Chile] (2023b) Base Digital del Clima. http://basedigitaldelclima.mma.gob.cl/ [Accessed 29.06.2023]

Nesom G, Robinson H (2007) XV. Tribe Astereae Cass. (1819). In: Kadereit JW, Jeffrey C (Eds) The Families and Genera of Vascular Plants (Vol. VIII): Flowering Plants Eudicots –Asterales. Springer-Verlag, Berlin, 284–341.

Philippi RA (1858) Plantarum novarum Chilensium: centuria secunda, tertia. Linnaea 28(heft 6): 661–704. [705–752.]

Philippi RA (1892) Plantas nuevas chilenas de las familias Crucíferas, Bixáceas, Violáceas, Poligáleas. Anales de la Universidad de Chile 81: 65–86. https://doi.org/10.5962/bhl.title.8592

Philippi RA (1894) Plantas nuevas chilenas de las familias que corresponden al tomo III de la obra de Gay (continuación). Anales de la Universidad de Chile 87: 585–624.

Reiche K (1902) Flora de Chile (Vol. 3[6]). Imprenta Cervantes, 426 pp.

Rodríguez R, Marticorena C, Alarcón D, Baeza C, Cavieres L, Finot VL, Fuentes N, Kiessling A, Mihoc M, Pauchard A, Ruiz E, Sanchez P, Marticorena A (2018) Catálogo de las plantas vasculares de Chile. Gayana. Botánica 75(1): 1–430. https://doi.org/10.4067/S0717-66432018000100001

Schneider CA, Rasband WS, Eliceiri KW (2012) NIH Image to ImageJ: 25 years of image analysis. Nature Methods 9(7): 671–675. https://doi.org/10.1038/nmeth.2089

SONAMI [Sociedad Nacional de Minería de Chile] (2023) Mapa minero de Chile. https://www.sonami.cl/mapaminero/ [Accessed 20.08.2023]

Tortosa R, Bartoli A (2002a) Revisión de las especies argentinas del género *Haplopappus* (Asteraceae, Astereae). Boletín de la Sociedad Argentina de Botánica 37(1–2): 115–133.

Tortosa R, Bartoli A (2002b) Two new species of *Haplopappus* (Astereae, Asteraceae) from Mendoza, Argentina. Brittonia 54(1): 50–53. https://doi.org/10.1663/0007-196X(2002)054[0050:TNSOHA]2.0.CO;2

Tortosa R, Bartoli A (2003) *Haplopappus* Cass. In: Anton AM, Zuloaga FO (Eds) Flora Fanerogámica de la República Argentina. Consejo Nacional de Investigaciones Científicas y Técnicas, Buenos Aires, Argentina 81(16b): 58–64.

PhytoKeys 237: 219–230 (2024)
DOI: 10.3897/phytokeys.237.115003

Research Article

A new species of *Veronica* (Plantaginaceae) from Western Iran

Mahfouz Advay[1], Dirk C. Albach[2], Moslem Doostmohammadi[3]

1 *Central herbarium, Scholar biology, College of Science of Tehran University, Tehran, Iran*
2 *Institut für Biologie und Umweltwissenschaften, Carl von Ossietzky-Universität, 26111 Oldenburg, Germany*
3 *Department of Biology, Shahid Bahonar University of Kerman, Kerman, Iran*
Corresponding author: Dirk C. Albach (dirk.albach@uni-oldenburg.de)

Abstract

A new species, *Veronica kurdistanica* (Plantaginaceae), is described and illustrated. It grows on limestone cliffs in mountainous alpine areas of western Iran (Kurdistan province). The new species belongs to the species group of *V. kurdica* and is considered to be closely related to *V. daranica*, *V. khorassanica* and *V. kurdica*, with which the new species is compared. Molecular phylogenetic analysis of nrDNA (ITS) region confirms this relationship. *Veronica kurdistanica* is distinguished from the mentioned species by its glandular indumentum, length and shape of leaves and bracts, number of flowers per raceme, length and width of calyx and corolla, and size of capsules and seeds.

Key words: Endemic, Hawraman, Kurdistan, Schahu, *Veronica* subg. *Pentasepalae*

Introduction

Veronica L. is the largest genus within the family Plantaginaceae in its current circumscription. The genus has cosmopolitan distribution and includes ca. 450 species (Albach et al. 2004; Fischer 2004). Species of *Veronica* have high ecological diversity and they are found in different habitats that range from arid steppes to aquatic habitats, from the sea level to high alpine regions (Albach et al. 2008). Its centers of diversity are the Eastern Mediterranean and Irano-Turanian regions, as well as in New Zealand (Albach et al. 2004).

Our knowledge of the species diversity of the genus in Iran was summarized in the “Flora Iranica” by Fischer (1981). He recognized 56 species occurring in Iran. However, several new taxa were added afterwards (Saeidi-Mehrvarz et al. 2001; Saeidi-Mehrvarz and Assadi 2003; Saeidi-Mehrvarz 2005, 2011) and the genus includes 61 species with 18 species endemic to the country according to the latest “Flora of Iran” (Saeidi-Mehrvarz 2011). At least two species have since been added to the flora of Iran (Doostmohammadi et al. 2021, 2022). Among these, most species occur in the Zagros and Alborz (also Elburz) Mountains of Iran, which are important centers of diversity of *Veronica*.

Among the recent collections from the northern Zagros Mountains, we identified a small chasmophytic species of *Veronica* which resembles *V. daranica* from central Zagros. Further morphological comparisons and molecular investigations revealed that the new collection belongs to a yet unknown species, which is described below.

Academic editor: Peter de Lange
Received: 31 October 2023
Accepted: 20 December 2023
Published: 29 January 2024

Citation: Advay M, Albach DC, Doostmohammadi M (2024) A new species of *Veronica* (Plantaginaceae) from Western Iran. PhytoKeys 237: 219–230. https://doi.org/10.3897/phytokeys.237.115003

Materials and methods

During a scientific field survey on the western slope of the Zagros Mountains in Western Iran, the first author collected in 2015 specimens of a *Veronica* from Schahu Mountain in the Hawraman region, Kurdistan province. These specimens were compared with diagnostic keys reported in Floras (Fischer 1981; Saeidi-Mehrvarz 2011) and recent new records and species (Saeidi-Mehrvarz et al. 2001; Saeidi-Mehrvarz and Assadi 2003; Saeidi-Mehrvarz 2005). After careful examination with the different floras, we inspected images of type specimens from various online herbaria (BM, K, MPU, P), as well as related taxa in TUH, TARI, HKS and IRAN (herbarium acronyms according to Thiers 2016 and continuously updated). Subsequently, we measured several quantitative and qualitative morphological key traits of our specimens and related species (Table 1).

In order to determine the phylogenetic position of the new species, a phylogenetic analysis was conducted based on the nuclear ITS region. One new sequence of the ITS region of the herbarium specimen of the holotype (NO. 12808 HKS) was generated using ITS1 and ITS4 primers (White et al. 1990). The new sequence was added to a sequence matrix, based on published sequences of Doostmohammadi et al. (2022). All sequences were aligned using MAFFT v. 6.0 (Katoh and Toh 2010) and edited manually using PhyDE v. 0.9971 (Müller et al. 2010). Insertions and deletions (indels) were coded as binary characters using the simple indel coding approach, as implemented in SeqState v. 1.4.1 (Müller 2005). Bayesian inference (BI) was conducted using MrBayes v.3.2.6 (Ronquist et al. 2012) under GTR+Γ+I nucleotide substitution model. Two parallel runs of four MCMC chains including three heated and one cold chain were run simultaneously for four million generations, sampling every 200 generations. After removing 25% of the sampled trees as burn-in, a 50% majority-rule consensus tree was constructed.

Results and discussion

The morphological and phylogenetic analyses indicate a close relationship between *Veronica kurdistanica* sp. nov., and *V. daranica* Saeidi & Ghahr., *V. khorassanica* Czernjak, and *V. kurdica* Benth. in DC. but ample morphological differences to suggest that *V. kurdistanica* is a distinct species.

Taxonomy

***Veronica kurdistanica* M.Advay, sp. nov.**
urn:lsid:ipni.org:names:77335343-1
Fig. 1A–F; Table 1

Type. Iran – Kurdistan province, Kamyaran, Schahu mountain, 34°53'48"N, 46°33'43"E, 2700 m, 7 May 2015, *Advay 12808*. (holotype HKS! (Fig. 2), isotype TUH!).

Diagnosis. *Veronica kurdistanica* is similar to *V. daranica* (Fig. 3A–D) based on simple stems (branched only at the base), terminal racemes (rarely axillary), and purple petals. However, it is distinguished from *V. daranica* by the densely glandular (vs. glabrous) indumentum, obovate, elliptic to spathulate leaves that are 4–10 mm long (vs. narrowly elliptic, elliptic to spathulate and 2.5–5 mm long),

Figure 1. *Veronica kurdistanica* **A–D** habitat and habit **E, F** corolla and inflorescence (photos by M. Advay).

lanceolate bracts that are 2–2.5 mm long (vs. spathulate and 1.5–2 mm long), capsule 1.2–2.2 mm long and 2–2.1 mm wide (vs. 1.8–2.5 mm long and 2–2.5 mm wide), and seeds 0.8–1.2 mm long and 0.3–0.5 mm wide (vs. 0.7–0.9 mm long, 0.5–0.7 mm wide) (Table 1). Also, *V. kurdistanica* is related to *V. khorassanica* but it is distinguished from the latter by the densely glandular indumentum (vs. dense eglandular subcrispate); oblong-obovate, elliptic to spathulate leaves (vs. linear), shorter, terminal racemes with 4–14 flowers (vs. axillary racemes with 15–20 (–60) flowers), longer bracts (2–2.5 mm) and calyces (1.7–2 mm long at anthesis, 2–2.5 mm long in fruit) (vs. bracts 1–1.5 (2.5) mm long, calyces 2–2.5 mm long at anthesis, 2.5–3 mm in fruit), and capsule (1.2–2.2 mm long and 2–2.1 mm wide vs. 2.5–3.5 mm long, 3–3.5 mm wide), and seed size (0.8–1.2 mm long and 0.3–0.5 mm wide vs. 1.5–2.5 mm long, 1–1.5 mm wide) (Table 1). Our new species also differs from *V. kurdica*, specifically by: stems 4–8 cm tall (vs. (5–)10–20(–30) cm), indumentum densely glandular (vs. eglandular or glabrous), raceme terminal and 4–14 flowered (vs. racemes axillary and 5–20 (–25) flowers), pedicels l.5–2 mm long in fruit (vs. 4–8 (–10) mm in fruit), corolla purple, 2.5–3 mm long, 5 mm in diameter (vs. dark to violet blue, 4–6 mm long, 8–10 (–11) mm in diameter) and capsule (1.2–2.2 mm long and 2–2.1 mm wide vs. 2–3.5 mm long, 3–5 mm wide) and seed size (0.8–1.2 mm long and 0.3–0.5 mm wide vs. 1.4–1.8 mm long, 1.1–1.4 (–1.6) mm wide) (Table 1).

Table 1. The morphological differences among *Veronica kurdistanica* and its related taxa.

Characters	*V. kurdistanica*	*V. daranica*	*V. khorassanica*	*V. kurdica* subsp. *kurdica*	*V. kurdica* subsp. *filicaulis*
Stem	4–8 cm	up to 5 cm	6–12 (–25) cm	(5–) 10–20 (–30) cm	5–15 cm
Stem indumentum	densely glandular	glabrous	dense eglandular cinereous- subcrispate	eglandular velvety or rarely glabrous	eglandular pubescent, often glabrous
Leaf	4–10 mm long, 1–2 mm wide, oblong-obovate, elliptic to spathulate	2.5–5 mm long, 1–2 mm wide, narrowly elliptic, elliptic to spathulate	4–11 (–15) mm long, 0.8–1.5 mm wide, linear	5–10 (–16) mm long, 1–5 (–7) mm wide, linear above to elliptic-ovate below	2–6 (–8) mm long, 0.7–3 (–4.5) mm wide, linear to elliptic-ovate
Leaf indumentum	crispulate	glabrous	eglandular cinereous-crispate	eglandular or glabrous	eglandular or glabrous
Inflorescence	terminal, raceme 4–14 flowered	terminal, raceme 4–l2 flowered	axillary, raceme 15–20 (–60) flowered	axillary, raceme 5–**2**0 (–25) flowered	Axillary, raceme 5–15 (–20) flowered
Bract length and shape	2–2.5 mm, lanceolate	1.5–2 mm, spathulate	1–1.5 (–2.5) mm, linear, oblong-subspathulate	(1.5–) 2–3 (– 4) mm, oblong to obovate	1.5–3 mm, oblong
Pedicels length	1–1.5 mm long at anthesis, l.5–2 mm long in fruit	1–1.5 mm long at anthesis, l.5–2 mm long in fruit	2–3 (–4) mm long at anthesis and in fruit	1.5–6 mm at anthesis, 4–8 (–10) mm in fruit	0.5–3 mm at anthesis, 1.5–4 (–6) mm in fruit
Calyx	1.7–2 mm long and 1 mm wide at anthesis, 2–2.5 mm long and 1–1.2 mm wide in fruit	l .3– l .8 mm long and 0.4–0.7 mm wide at anthesis, 1.6–2.5 mm long and 0.5–1.2 mm wide in fruit	2–2.5 mm long at anthesis, 2.5–3 (–4) mm in fruit	1.5–3 mm at anthesis, 2–3 (–4) mm in fruit	1.5–3 mm at anthesis, 2–3 (–4) mm in fruit
Corolla color and size	purple, 2.5–3 mm long, 5 mm in diameter	purple, 2.3–2.5 mm long, 4–6 mm in diameter	purple, 6 mm in diameter	dark blue to violet blue, 4–6 mm long, 8–10 (–11) mm in diameter	Pink or purple or violet purple, 3–4 mm long, (5–)6–8 mm in diameter
Capsule	1.2–2.2 mm long and 2–2.1 mm wide	1.8–2.5 mm long and 2–2.5 mm wide	2.5–3.5 mm long, 3–3.5 mm wide	2.5–4 mm long, 4–5 mm wide	2–3 mm long, 3–4.5 mm wide
Seed	0.8–1.2 mm long, 0.3–0.5 mm wide	0.7–0.9 mm long, 0.5–0.7 mm wide	1.5–2.5 mm long, 1–1.5 mm wide	1.4–1.8 mm long, 1.1–1.4 (–1.6) mm wide	1.4–1.8 mm long, 1.1–1.4 (–1.6) mm wide

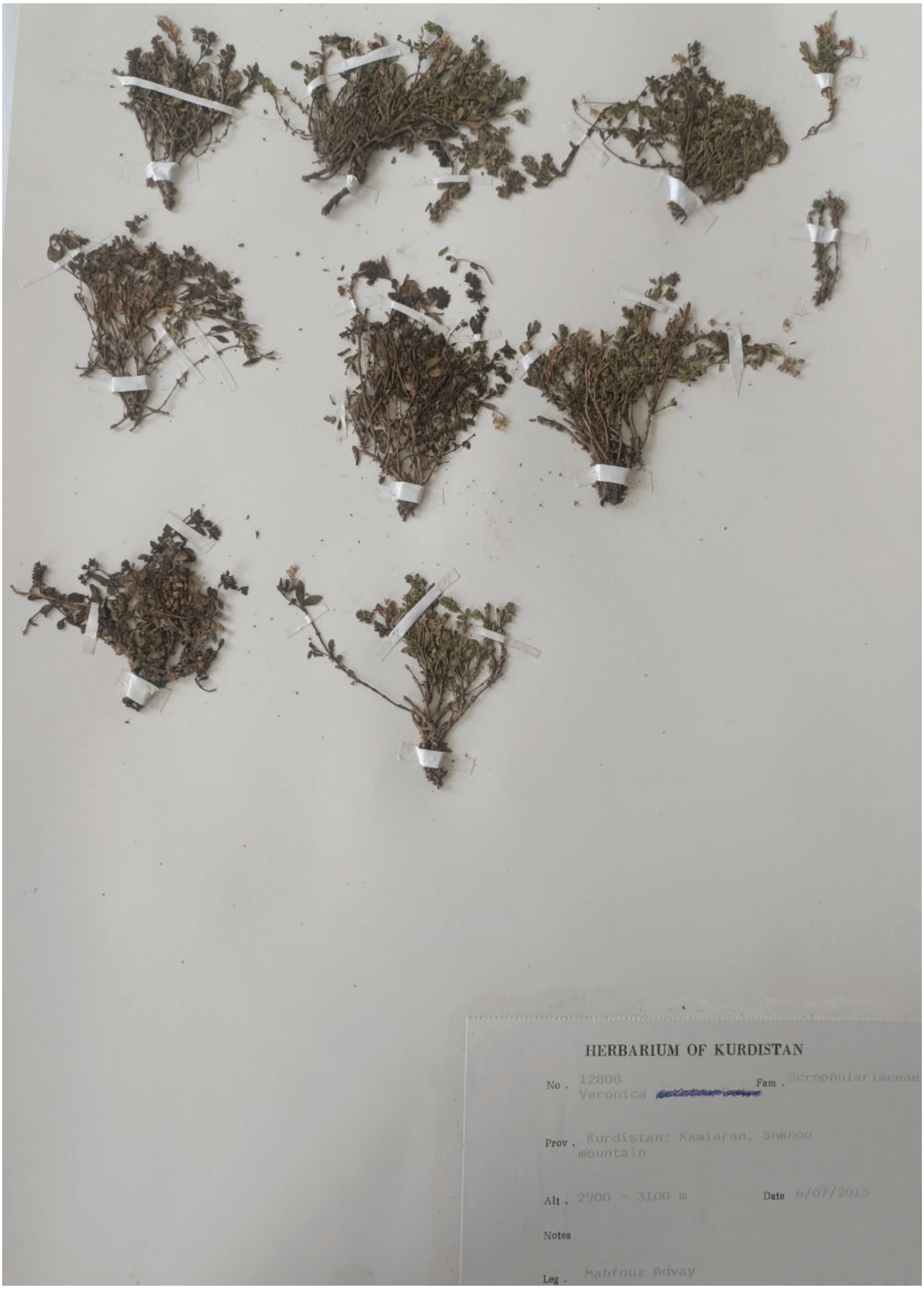

HERBARIUM OF KURDISTAN

No . 12808 Fam . Scrophulariaceae
Veronica [redacted]

Prov . Kurdistan: Kamiaran, Shahoo mountain

Alt . 2900 – 3100 m Date 6/07/2015

Notes

Leg . Mahfouz Advay

Figure 2. Holotype of *V. kurdistanica*.

Figure 3. *Veronica daranica* **A–C** habitat and habit **D** corolla and inflorescence (photos by M. Doostmohammadi).

Description. Perennial plant, rhizome stout, plant 4–8 cm tall; stems woody, ascending at base, erect, ± densely glandular. Leaves 8–10 pairs, fleshy, lower leaves with petiole 8–10 mm long, 4–8 mm wide, gradually attenuate at base, oblong-obovate, elliptic to spathulate, cauline leaves 4–6 mm long, 1–2 mm wide, sessile above, entire, ± glandular, upper side more than lower side. Racemes 1–2, often terminal, 4–14 flowered, 0.5–1 cm long in flowering stage, elongated to 1–1.5 cm long in fruiting stage; hairs 0.3–0.5 mm long, glandular; bracts spathulate, 2–2.5 mm long, shorter than leaves, entire, densely glandular hairy on the upper surface, less so on the lower side; pedicel 1–1.5 mm long at anthesis, 1.5–2 mm long in fruit, pubescent with spreading yellowish glandular hairs. Calyx 1.5–2 mm long and 0.7–1 mm wide at anthesis, 2–2.5 mm long and

Figure 4. A, B habitat of *Veronica kurdistanica* (photos by M. Advay).

1–1.2 mm wide in fruit; lobes oblong, 0.4–0.8 mm long united at base. Corolla purple, 2.5–3 mm long, 4–5 mm in diameter, adaxial and lateral lobes elliptic, obtuse and abaxial lobe oblong, subacuminate, corolla tube white and internally densely pubescent; stamens with filaments 1.5–2 mm long, white; anthers ca. 1 mm, purplish to white; style 1.6–2.7 mm long, purplish, whitish at base. Capsule obcordate, 1.2–2.2 mm long and 2–2.1 mm wide, equaling or slightly overtopping the calyx, glandular hairs sparsely spreading. Seeds flat, oblong-elliptic, 0.8–1.2 mm long, 0.3–0.5 mm wide, brown-yellowish, surface reticulate.

Etymology. Referring to Kurdistan Province (Western Iran), where the new species was discovered.

Distribution, habitat, and phenology. The species is currently known from a few populations in Schahu mountain, Hawraman region, Kurdistan Province, western Iran. It is an Irano-Turanian phytogeographical element that grows on limestone cliffs of mountainous slopes of Schahu mountains, 2500–2950 m a. s. l. (Figs 4, 5). Flowering April to May, fruiting June.

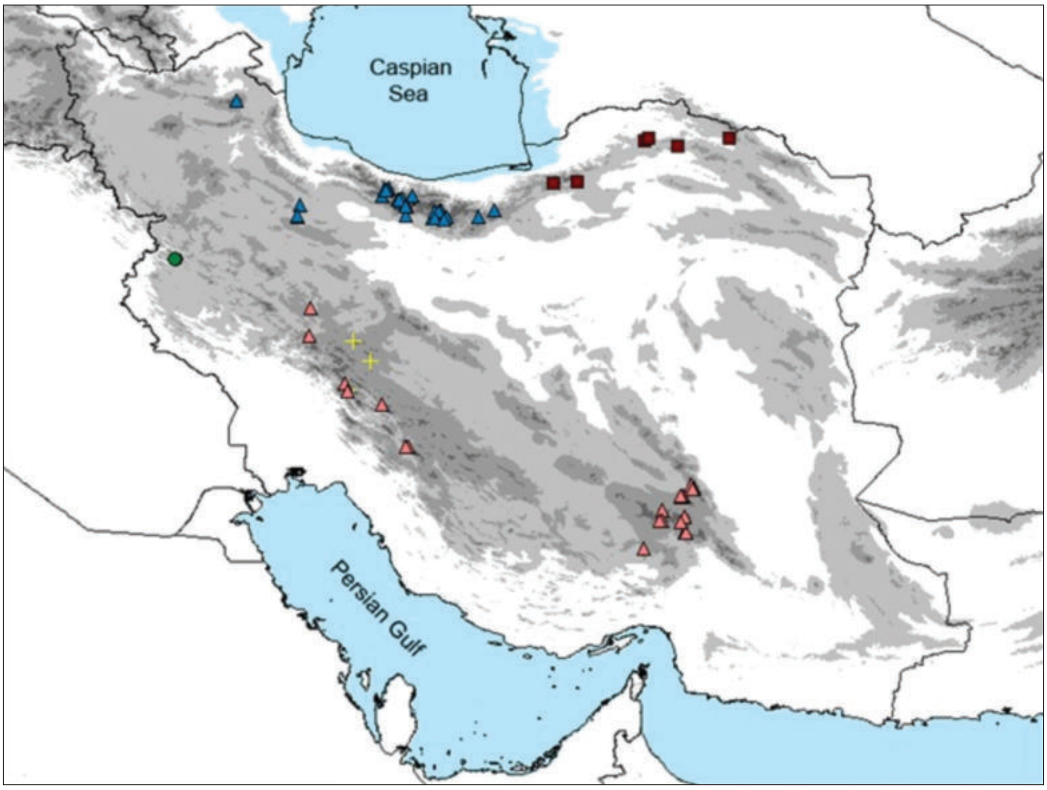

Figure 5. Distribution of *Veronica kurdistanica* (circle) and *V. daranica* (cross), *V. khorassanica* (square), *V. kurdica* subsp. *kurdica* (blue triangle) and *V. kurdica* subsp. *filicaulis* (pink triangle) in Iran.

Conservation status. *Veronica kurdistanica* is observed in a restricted area of the Avroman (Hawraman) region in the province of Kurdistan. The estimated area of occupancy is less than 50 km^2. The species is proposed to be classified as critically endangered (CR) following the IUCN criteria (2022).

Taxonomic notes. *Veronica kurdistanica* belongs to *Veronica* subgenus *Pentasepalae* (Benth.) M. M. Mart. Ort., Albach & M. A. Fisch. (Fig. 6), by far the most species-rich subgenus in Iran, with many perennial, mountainous species. It has been demonstrated that this subgenus has probably originated in the Iranian plateau, with several relict and morphologically isolated species distributed at present along the Zagros and Alborz Mountains (Doostmohammadi et al. 2022).

Veronica kurdistanica belongs to the *V. kurdica* species group and is morphologically closest to *V. daranica* (Fig. 3) but occurs more than 500 km apart (Fig. 5). The group has maximum support in the phylogenetic analysis (Fig. 6), although there is no morphological character setting this group apart from related species. Members of this group are all endemic, perennial species adapted to arid conditions; they are important constituents of the alpine flora of Iran. Species delimitation is sometimes difficult among the members of *V. kurdica* species complex. For instance, *V. daranica* differs from glabrous forms of *V. kurdica* subsp. *filicaulis* (Freyn) M.A. Fisch. only by its dense, compact habit, thinner petals and some other subtle morphometric differences, but the molecular studies confirmed that it is a distinct species (Doostmohammadi et al. 2022). However, *V. kurdistanica* is a unique species within *V. kurdica* complex differing from all others by its glandular indumentum, apart from other subtler differences mentioned above. Other species are either glabrous or have an eglandular indumentum. It is not unusual in

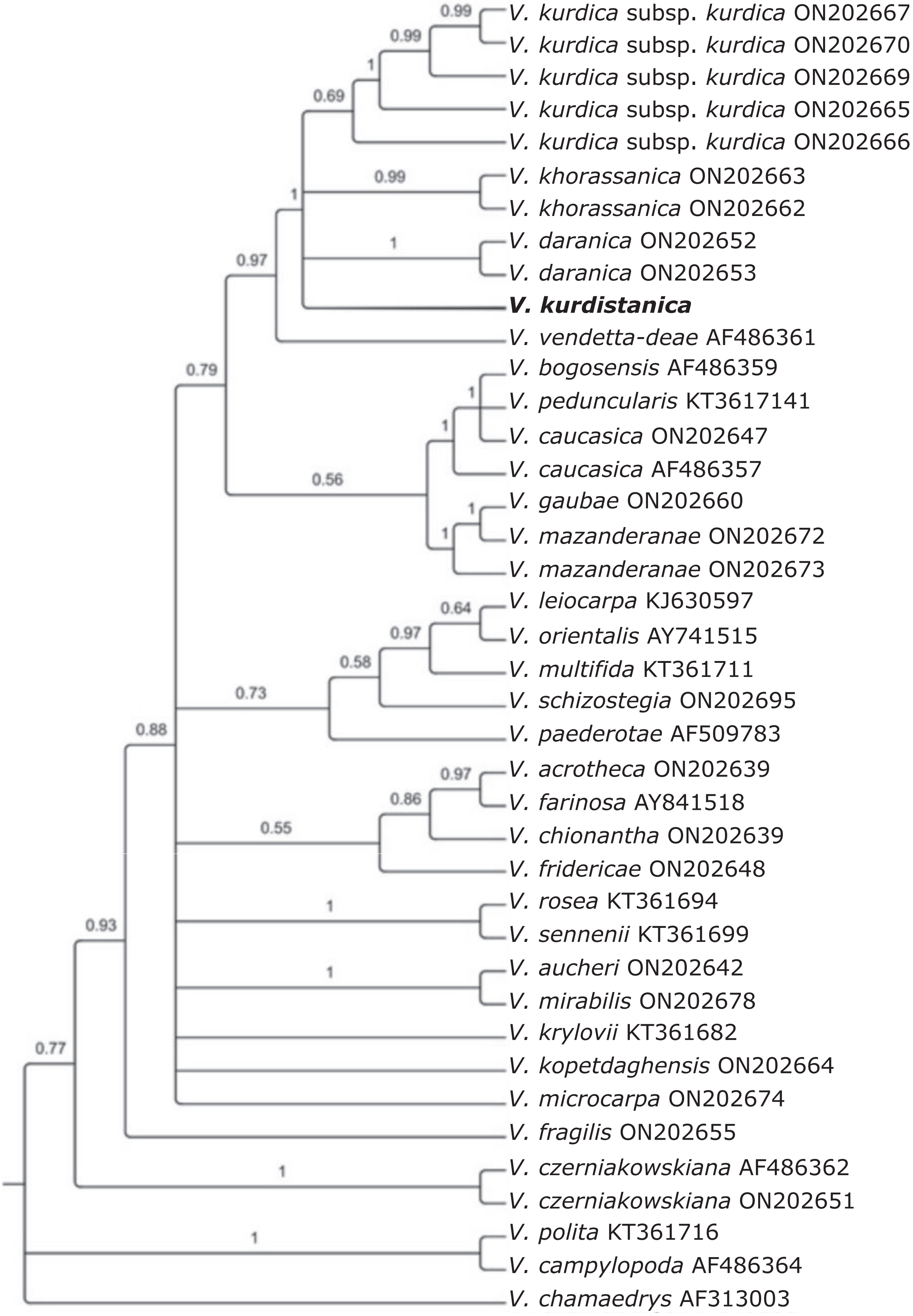

Figure 6. 50% majority-rule consensus tree obtained from the Bayesian analysis of nrDNA ITS sequences. Posterior probabilities are given above the branches.

the genus to differentiate a species mainly on the basis of glandular indumentum and other subtle differences. An example is *V. porphyriana* Pavlov, which has often been included in *V. spicata* L. (*sensu lato*), but has been clearly differentiated based on DNA-based evidence (Khan et al. in press). In the molecular phylogenetic tree, our new species is assembled in a polytomy including *V. daranica*, *V. khorassanica*, and two subspecies of *V. kurdica* (Fig. 6). A comprehensive morpho-molecular study is required to delimitate further the species of this complex, both morphologically and geographically. The finding of this new species is noteworthy since it emphasizes that the Kurdistan region is an important center of diversity, despite being under-investigated. Thus, future field work may further increase the species number of the region.

Additional specimens (paratypes). IRAN – Kurdistan province, Kamyaran, Schahu mountain 34°53'48"N, 46°33'43"E, 2500 m, 10 May 2015, Advay 12829 (HKS), Kamyaran, Schahu mountain 34°54'30"N, 46°32'43"E, 2920 m, 15 May 2023, Advay 48735 (TUH).

Conclusion

We here provide evidence for a new species from Iran, which belongs to the *V. kurdica* group of *Veronica* subg. *Pentasepalae*. This finding emphasizes the need for further detailed floristic investigation of the region and further detailed phylogenetic investigations to find or clarify biogeographic patterns.

Acknowledgements

We thank Dr. Azad Rastegar and Hossein Maroofi (HSK Herbarium) for their help in visiting the Herbarium and providing necessary materials for our research. Also, we thank Dr. Mansour Mirtazdadini for providing photos of the distribution area and habitat of *Veronica daranica*. Critical reviews by Dr. Sergei Mosyakin and an anonymous reviewer are gratefully acknowledged.

Additional information

Conflict of interest

The authors have declared that no competing interests exist.

Ethical statement

No ethical statement was reported.

Funding

No funding was reported.

Author contributions

Conceptualization: MA, DCA, MD. Methodology, Analysis: MA, MD. Data curation: MA, MD. Funding acquisition: MA, DCA, MD. Investigation: MA, DCA, MD. Project administration: MA. Supervision: DCA. Visualization: MA, MD. Writing-original draft: MA. Writing-review and editing: MA, DCA, MD.

Author ORCIDs

Mahfouz Advay https://orcid.org/0000-0002-3542-532X
Dirk C. Albach https://orcid.org/0000-0001-9056-7382
Moslem Doostmohammadi https://orcid.org/0000-0003-1777-6676

Data availability

All of the data that support the findings of this study are available in the main text. The new DNA sequence has been submitted to GenBank.

References

Albach DC, Martinez-Ortega MM, Chase MW (2004) *Veronica*: Parallel morphological evolution and phylogeography in the Mediterranean. Plant Systematics and Evolution 246: 177–194. https://doi.org/10.1007/s00606-004-0148-9

Albach DC, Martínez-Ortega MM, Delgado L, Weiss-Schneeweiss H, Özgökce F, Fischer MA (2008) Chromosome numbers in Veroniceae (Plantaginaceae): Review and several new counts. Annals of the Missouri Botanical Garden 95(4): 543–566. https://doi.org/10.3417/2006094

Doostmohammadi M, Mirtadzadini M, Bordbar F (2021) Chromosome numbers of some annual *Veronica* (Plantaginaceae) with report of *V. tenuissima* from flora of Iran. Feddes Repertorium 132(2): 158–166. https://doi.org/10.1002/fedr.202100002

Doostmohammadi M, Bordbar F, Albach DC, Mirtadzadini M (2022) Phylogeny and historical biogeography of *Veronica* subgenus *Pentasepalae* (Plantaginaceae): Evidence for its origin and subsequent dispersal. Biology 11(5): e639. https://doi.org/10.3390/biology11050639

Fischer MA (1981) *Veronica* L. In: Rechinger KH (Ed.) Flora Iranica (Vol. 147). Graz, Akademische Druck- und Verlagsanstalt, 25–165.

Fischer E (2004) Scrophulariaceae. In: Kadereit JK (Ed.) The Families and Genera of Vascular Plants (Vol. 7). Springer, 333–433. https://doi.org/10.1007/978-3-642-18617-2_21

Katoh K, Toh H (2010) Parallelization of the MAFFT multiple sequence alignment program. Bioinformatics 26(15): 1899–1900. https://doi.org/10.1093/bioinformatics/btq224

Khan G, Mayland-Quellhorst E, Kosachev P, Albach DC (in press) Altai Mountains – cradle of hybrids and introgressants: A case study in *Veronica* subg. *Pseudolysimachium* (Plantaginaceae). TAXON.

Müller K (2005) SeqState: Primer design and sequence statistics for phylogenetic DNA datasets. Applied Bioinformatics 4: 65–69. https://doi.org/10.2165/00822942-200504010-00008

Müller K, Müller J, Quandt D (2010) PhyDE®: Phylogenetic Data Editor, Version 0.9971. http://www.phyde.de/index.html

Ronquist F, Teslenko M, van der Mark P, Ayres DL, Darling A, Höhna S, Larget B, Liu L, Suchard MA, Huelsenbeck JP (2012) MrBayes 3.2: Efficient Bayesian phylogenetic inference and model choice across a large model space. Systematic Biology 61(3): 539–542. https://doi.org/10.1093/sysbio/sys029

Saeidi-Mehrvarz S (2005) *Veronica longipedicellata* (Scrophulariaceae), a new species from Iran. Nordic Journal of Botany 23(5): 559–561. https://doi.org/10.1111/j.1756-1051.2003.tb00435.x

Saeidi-Mehrvarz S (2011) *Veronica*. In: Assadi M, Maassoumi AA, Khatamsaz M, Mozaffarian V (Ed.) Flora of Iran (Vol. 68). Research Institute of Forests and Rangelands Publications, Tehran [in Persian], 75–149. [429–439.]

Saeidi-Mehrvarz S, Assadi M (2003) New *Veronica* (Scrophulariaceae) records for the flora of Iran. Turkish Journal of Botany 27: 339–342.

Saeidi-Mehrvarz S, Ghahreman A, Assadi M (2001) A new species of *Veronica* (Scrophulariaceae) from Iran. Nordic Journal of Botany 21(6): 581–583. https://doi.org/10.1111/j.1756-1051.2001.tb00815.x

Thiers B (2016) [and continuously updated] Index Herbariorum: A global directory of public herbaria and associated staff. New York Botanical Garden's Virtual Herbarium. http://sweetgum.nybg.org/science/ih/

White TJ, Bruns TD, Lee S, Taylor J (1990) Amplification and direct sequencing of fungal ribosomal RNA genes for phylogenetics. In: Innis MA, Gelfand DH, Sninsky JJ, White TJ (Eds) PCR protocols: A guide to methods and applications (Vol. 3). Academic Press, San Diego, 15–22. https://doi.org/10.1016/B978-0-12-372180-8.50042-1

PhytoKeys 237: 231–243 (2024)
DOI: 10.3897/phytokeys.237.111977

Research Article

The identity of *Bupleurum jeholense* (Apiaceae)

Li-Hua Wang[1], Xue-Min Xu[2], Yi He[1], Quan-Ru Liu[1]

1 *Key Laboratory of Biodiversity Science and Ecological Engineering, Ministry of Education, College of Life Sciences, Beijing Normal University, Beijing 100875, China*
2 *School of Life Sciences, Zhengzhou University, Zhengzhou 450001, Henan China*
Corresponding author: Quan-Ru Liu (liuquanru@bnu.edu.cn)

Abstract

Bupleurum jeholense Nakai (Apioideae, Apiaceae), originally found in the Wuling Mountain of China, was initially described as a species but later treated as a variety of *B. sibiricum* Vest ex Spreng. However, researchers have recently found that it is more closely related to *B. chinense* DC. In this study, we conducted morphological and phylogenetic analyses as well as chromosome counting to determine the taxonomic status of *B. sibiricum* var. *jeholense* (Nakai) Chu. Our results showed that *B. sibiricum* var. *jeholense* and *B. chinense* share common features (i.e., bracteoles 5 and stem solid) that distinguish both from *B. sibiricum* var. *sibiricum*. The chromosome number of *B. sibiricum* var. *jeholense* was found to be the same as in *B. chinense* (i.e., 2n = 12), whereas the chromosome number of *B. sibiricum* var. *sibiricum* was 64. A phylogenetic tree based on complete chloroplast genome data revealed a close relationship between *B. sibiricum* var. *jeholense* and *B. chinense*. Finally, *B. sibiricum* var. *jeholense* and *B. chinense* were mainly found to differ in plant height, number of stems, and middle stem leaves. Based on this evidence, we propose a new combination: *Bupleurum chinense* var. *jeholense* (Nakai) Q.R.Liu & L.H.Wang.

Key words: Apiaceae, *Bupleurum chinense* DC. var. *jeholense* (Nakai) Q.R.Liu & L.H.Wang, new combination

Academic editor: Alexander Sennikov
Received: 31 August 2023
Accepted: 9 January 2024
Published: 31 January 2024

Citation: Wang L-H, Xu X-M, He Y, Liu Q-R (2024) The identity of *Bupleurum jeholense* (Apiaceae). PhytoKeys 237: 231–243. https://doi.org/10.3897/phytokeys.237.111977

Introduction

Bupleurum is a monophyletic genus in the tribe Bupleureae (Apioideae, Apiaceae) (Downie et al. 2000). It contains around 180–195 species, is distributed throughout Eurasia and North Africa, with one species each in North America and South Africa, while being adventive in Australasia (Plunkett et al. 2019). China is a major diversity center of *Bupleurum*, containing 42 species and 16 varieties (Sheh and Watson 2005). This genus can be easily recognized based on its entire and single leaves, which usually show parallel venation and distinct bracts and bracteoles. However, the morphological characteristics used for species delimitation of this genus remain limited, thereby rendering species identification difficult. To address this problem, it is necessary to perform detailed examinations and observations in field populations.

Bupleurum jeholense Nakai was initially described on the basis of specimens collected from the Wuling Mountain (China). Nakai stated that the characters of this species are as follows: middle stem leaves oblanceolate, base tapering, apex obtuse or acute, apiculate, bracteoles 5, exceeding flowers (Nakai 1937). Later, Chu (Shan and Li 1974) treated *B. jeholense* as a variety of *B. sibiricum* Vest ex Spreng., i.e., *B. sibiricum* var. *jeholense* (Nakai) Chu. Chu reported that *B. jeholense* was similar to *B. sibiricum*, with the main difference being in bracteole number. For example, *B. jeholense* commonly has five bracteoles, whereas *B. sibiricum* usually has 7–12 bracteoles. This difference was thought to be associated with a geographic distribution, i.e., the transition from the main distribution area in Siberia to the limited populations found in the Wuling Mountain (Liaoning Forestry Soil Research Institute 1977).

During recent fieldwork on Dongling Mountain (Beijing, China), we found that the distribution of *Bupleurum* species was closely linked to altitude. Normally, *B. chinense* is distributed at low altitudes (<1600 m). However, with the increasing altitude, we found a continuous variation in *B. chinense*; for example, plants became shorter; the number of branches decreased; the number of bracteoles gradually changed from 3 to 5 and varied in length from obviously shorter than the umbel to almost equal. Furthermore, as the altitude increased to 1600 m, *B. chinense* was gradually replaced by *B. sibiricum* var. *jeholense*. After checking the specimens, we also found that there were misidentifications between *B. chinense* and *B. sibiricum* var. *jeholense*. Subsequent phylogenetic analyses of Chinese *Bupleurum* spp. based on nrDNA ITS and chloroplast markers (i.e., *trnH-psbA* and *matK*) indicated that *B. sibiricum* var. *jeholense* was more closely related to *B. chinense*, whereas *B. sibiricum* var. *sibiricum* was closely related to *B. smithii* Wolff (Wang et al. 2011b). Hence, we doubt whether *B. sibiricum* var. *jeholense* is a morphological variation of *B. chinense* that is adapted to high-altitude locations in the Yan Mountains.

We therefore collected and checked several specimens from the type locality of *B. jeholense*. We conducted morphological observations, statistical comparisons, cytological studies, and a phylogenetic analysis based on the complete chloroplast genome to clarify the relationship among *B. sibiricum* var. *jeholense*, *B. sibiricum* var. *sibiricum*, and *B. chinense*.

Materials and methods

Morphological observations

Using the existing scientific literature and the relevant type specimens, we collected new specimens from the type locality of *B. sibiricum* var. *jeholense* and compared these with images of the type specimens. Specimens from field collections, CVH (https://www.cvh.ac.cn/), and online herbarium collections (MW, LE) were used to count bracteoles. In total, we obtained bracteole count data for 129 specimens of *B. sibiricum* var. *jeholense*, 183 specimens of *B. sibiricum* var. *sibiricum*, and 183 specimens of *B. chinense*. We analyzed these data using R (beanplot package) to produce boxplots (Kampstra 2008). Morphological terminology was used according to Kljuykov et al. (2004). Voucher specimens were deposited to the BNU herbarium.

Cytology

All materials used for cytological studies were obtained from the Wuling Mountain (*B. sibiricum* var. *jeholense*), Wutai Mountain (*B. chinense*), and Daqing Mountain (*B. sibiricum* var. *sibiricum*). All voucher specimens are listed in Table 1. Chromosome preparations were produced using acid digestion and hypotonic wall removal and photographed. Three technical replicates were obtained for each taxon. This procedure was adapted from Li et al. (2021).

Sampling and molecular analysis

Fresh plant leaves were collected from the field and quickly dried with silica gel for DNA extraction. Specimen voucher information is shown in Table 1. DNA was extracted using an HP Plant DNA hypotonic (D2485-02; Omega Bio-Tek). DNA samples were then sent to Beijing Novogene Corporation for quality testing and resequencing. An Illumina HiSeq X sequencing platform was used to generate approximately 10 GB of data for each sample. The chloroplast genome was then assembled from clean data using GetOrganelle (Jin et al. 2020). PGA (Qu et al. 2019) was used to annotate the resulting chloroplast genome. Sequences for *B. yinchowense* Shan et Y.Li (MT075711) and *B. sikangense* X.J.He & C.B.Wang (NC056803) were downloaded from NCBI (https://www.ncbi.nlm.nih.gov/nucleotide/) to be used as references. All chloroplast genome sequences generated here were deposited in the NCBI GenBank database (accession numbers listed in Table 1). Finally, twenty-one plastid genome sequences were downloaded from NCBI (see Appendix) for phylogenetic comparisons. This included 19 species of *Bupleurum* and two species of *Pleurospermum* Hoffm., which were used as outgroups.

In total, 25 sequences were imported into PhyloSuite (Zhang et al. 2020). The mafft module (Katoh et al. 2019) was used for sequence alignment, and the ModelFinder module (Kalyaanamoorthy et al. 2017) was used to calculate the nucleotide substitution model for all aligned sequences. A maximum likelihood (ML) tree was then constructed using IQ-TREE (Minh et al. 2020), with the nucleotide substitution model set to TVM+F+R2 and a standard bootstrap value of 1000. Results were considered reliable when the bootstrap support value (BS) was ≥70% (Kress et al. 2002). A Bayesian (BI) tree was constructed using MrBayes (Huelsenbeck and Ronquist 2001), with the GTR+F+I+G4 model using the following settings: mcmcp ngen = 2,000,000, printfreq = 10,000, nchains = 4, and burninfrac = 25%. Results were considered reliable when the posterior probability (PP) was ≥0.95. The effective sample size (>200) was determined using Tracer version 1.7 (Rambaut et al. 2018).

Table 1. Voucher information and GenBank accession numbers for newly sequenced plastome sequences.

Taxon	Location	Voucher information	Accession
B. chinense	Dongling Mountain, Beijing, China	BNU2021HB002 (BNU)	OR387523
B. smithii	Xiaowutai Mountain, Hebei, China	BNU2020DT007(BNU)	OR387522
B. sibiricum var. *sibiricum*	Daqing Mountain, Inner Mongolia, China	BNU2021NMG017(BNU)	OR387525
B. sibiricum var. *jeholense*	Wuling Mountain, Hebei, China	BNU2021HB025(BNU)	OR387524

Results

Morphological observations

The bean plot indicated that the number of bracteoles of *B. sibiricum* var. *jeholense* was mostly 5 and occasionally 6, whereas that of *B. sibiricum* var. *sibiricum* was (6)7–8(9). *Bupleurum chinense* had 5, sometimes 4 or even 3 bracteoles at lower elevations or in an understory (Figs 1, 2). The stems of *B. chinense* and *B. sibiricum* var. *jeholense* were solid, lacking a cavity, whereas those of *B. sibiricum* var. *sibiricum* were hollow at all internodes, which led to the formation of a cavity (Fig. 3). *Bupleurum sibiricum* var. *jeholense* and *B. chinense* were found to mainly differ in height, number of stems, and presence of middle stem leaves. The morphological characteristics of *B. sibiricum* var. *jeholense* plants are as follows: height below 40 cm, several stems, with 1–2 branches per stem, middle stem leaves narrower, and middle leaf length to width ratio 10–16. In contrast, *B. chinense* plants had single, occasionally several stem 40–90 cm high, with 2–4 branches per stem, and middle stem leaf length to width ratio 6–10. A comparison of morphological characters is shown in Table 2.

Chromosome numbers

Cytological analysis revealed that the chromosome number of *B. sibiricum* var. *jeholense* was 2n = 12 (x = 6), i.e., the same as *B. chinense* but different from *B. sibiricum* var. *sibiricum* (2n = 64, x = 8) (Fig. 4). We report the chromosome number of *B. sibiricum* var. *jeholense* for the first time, and the chromosome numbers of *B. chinense* and *B. sibiricum* var. *sibiricum* determined here are consistent with previous reports (Pan et al. 1995; Qin et al. 1989).

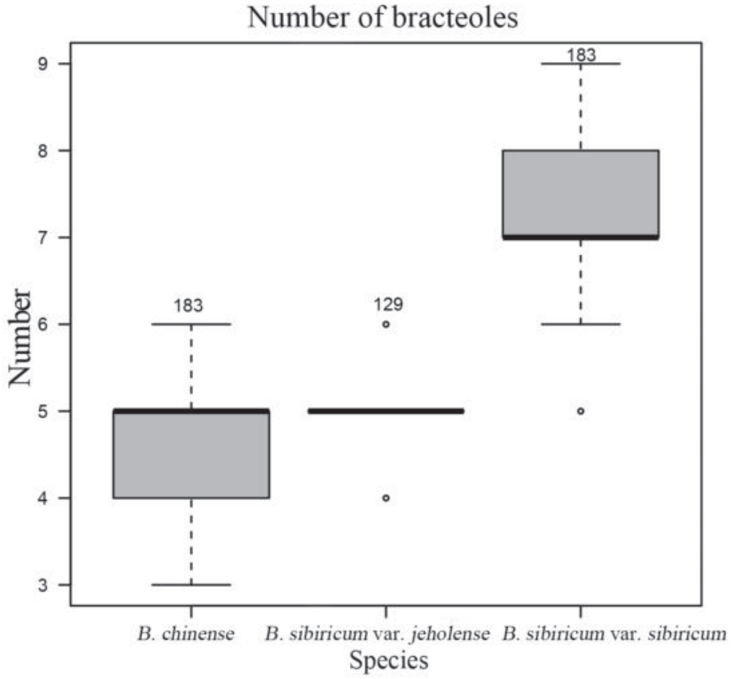

Figure 1. Comparison of the number of bracteoles found in *Bupleurum chinense*, *B. sibiricum* var. *jeholense* and *B. sibiricum* var. *sibiricum*.

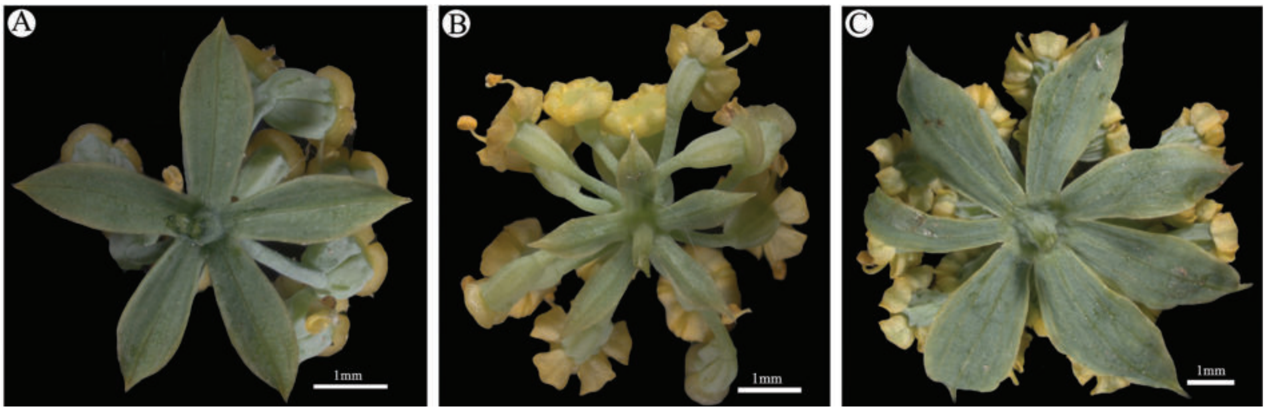

Figure 2. Umbel and bracteoles of the taxa under study **A** *Bupleurum chinense* **B** *B. sibiricum* var. *jeholense* **C** *B. sibiricum* var. *sibiricum*.

Figure 3. Stem transections of the taxa under study **A** *Bupleurum chinense* **B** *B. sibiricum* var. *jeholense* **C** *B. sibiricum* var. *sibiricum*.

Table 2. Comparison of the morphological characteristics and geographic distributions of three taxa under study.

Character	*B. chinense*	*B. sibiricum* var. *jeholense*	*B. sibiricum* var. *sibiricum*
Height	40–90 cm	20–40 cm	30–70 cm
Stem (number)	Single, occasionally several	Many, clustered	Many, clustered
Stem (branching)	2–4-branched	1–2-branched	1–2-branched
Stem (presence of cavity)	Solid	Solid	Hollow in all internodes
Basal leaves	Withering early	Withering early	Persistent, many
Basal leaf size	4–7 × 0.6–0.8 cm	5–10 × 0.3–0.8 cm	12–25 × 0.7–1.6 cm
Middle stem leaves	4–12 × 0.6–1.8 cm	6–12 × 0.5–1.2 cm	6–14 × 0.5–1.6 cm
Middle stem leaf length to width ratio	6–10	10–16	10–14
Upper stem leaves	Not embracing	Not embracing	Rounded-cuneate, embracing
Bracteole relative length	Shorter than flowers	Shorter than or equal to flowers	Exceeding flowers
Bracteoles	(3–4) 5, lanceolate	5 (6–7), lanceolate	(6) 7–12, elliptic-lanceolate
Distribution	Northeast and Central China	Yan mountains (Hebei and Beijing)	Heilongjiang, Liaoning, Inner Mongolia, Mongolia, and Russia

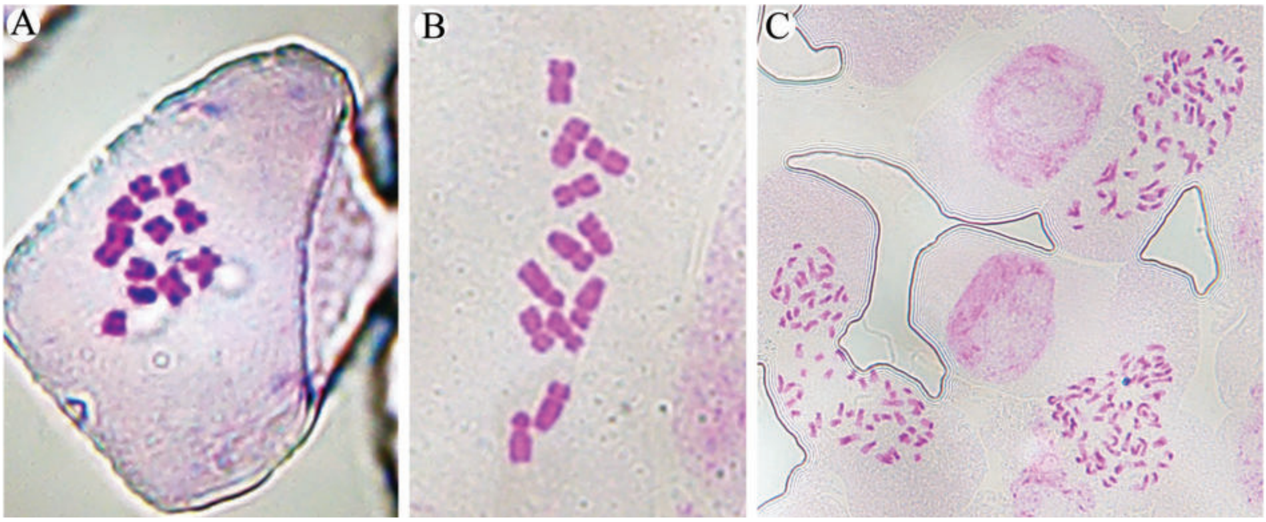

Figure 4. Metaphase chromosomes of the taxa under study **A** *Bupleurum chinense* **B** *B. sibiricum* var. *jeholense* **C** *B. sibiricum* var. *sibiricum*.

Phylogenetic analysis

The size of the four *Bupleurum* chloroplast genomes ranged from 155,706 to 155,858 bp. The complete chloroplast genome had a typical circular quadripartite structure and consisted of a pair of inverted repeat regions separated by the large single copy and small single copy regions. The topologies of the ML and BI trees constructed using the cp genome sequences were consistent. These results showed that the genus *Bupleurum* can be divided into two clades, with all Chinese *Bupleurum* plants belonging to *B.* subg. *Bupleurum*. *Bupleurum sibiricum* var. *sibiricum* was found to cluster with *B. smithii* and *B. bicaule* Helm (BS = 100% PP = 1), whereas *B. chinense* was found to cluster with *B. sibiricum* var. *jeholense* (BS = 100% PP = 1) and was more distantly related to *B. longiradiatum* Turcz., *B. falcatum* L. and *B. boissieuanum* H. Wolff (Fig. 5).

Discussion

Comparative morphology

Botanists have closely monitored the number of bracteoles because this character is essential in the taxonomy of *Bupleurum*. Moreover, bracteole number is an important indicator of the taxonomic position of *B. sibiricum* var. *jeholense* in the genus. Five bracteoles are generally present in both *B. chinense* and *B. sibiricum* var. *jeholense*. However, in environments such as the understory, *B. chinense* may have only three or four bracteoles. Furthermore, 6–7 bracteoles have occasionally been observed in *B. sibiricum* var. *jeholense*. We observed that the number of bracteoles in *B. sibiricum* samples collected from the Daqing Mountain, which were collected at the same latitude and altitude as the samples collected from Wuling Mountain, was not 5, as would be expected for *B. sibiricum* var. *jeholense*. Thus, we speculated that the 5-bracteoled *B. sibiricum* var. *jeholense* may not have evolved from the 12-bracteoled *B. sibiricum* var. *sibiricum*.

In the classification of the genus *Bupleurum*, stem structural characteristics have rarely been examined. After observing numerous specimens, we found

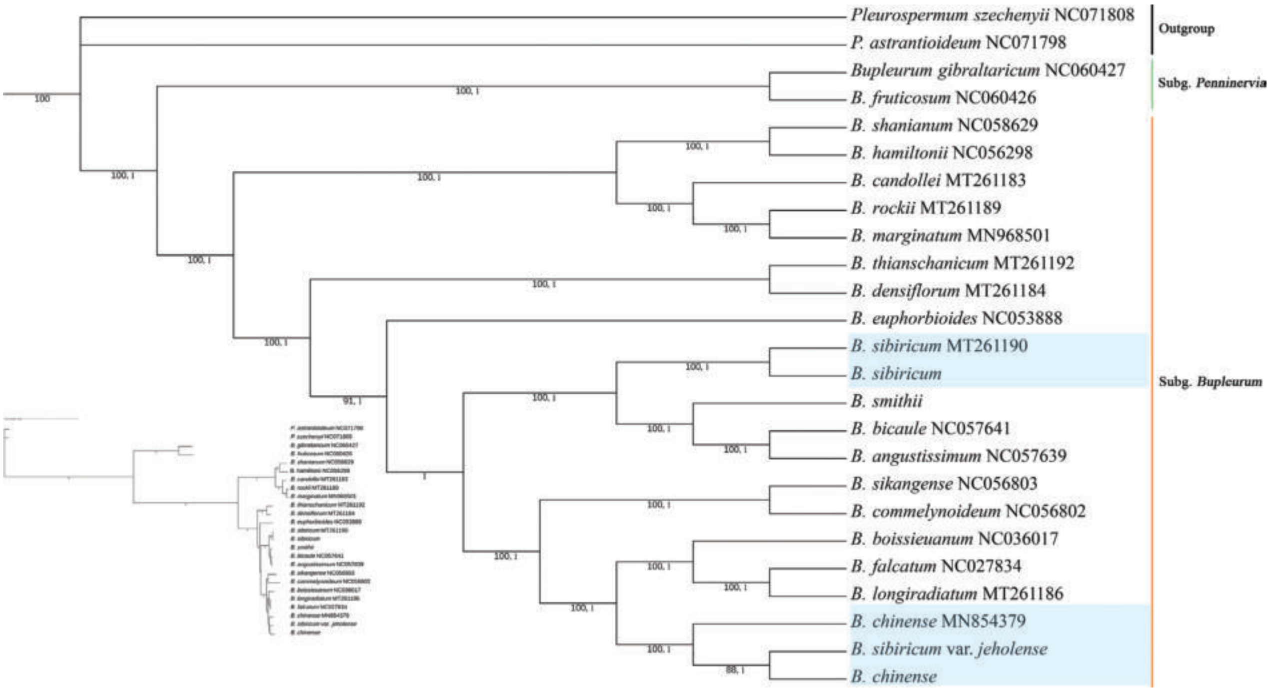

Figure 5. Phylogenetic tree of some Chinese *Bupleurum* species as inferred from chloroplast genomes using ML analyses (numbers below branches represent ML bootstrap values and BI posterior probabilities).

that the stem of *B. sibiricum* var. *sibiricum* was hollow and contained a substantial cavity. In contrast, the stems of *B. chinense* and *B. sibiricum* var. *jeholense* lacked this cavity. The presence or absence of a stem cavity is a stable character and does not change with the period of growth. For example, *B. komarovianum* was once treated as a variety of *B. chinense* (Liaoning Forestry Soil Research Institute 1977) until Wang et al. (2011b) found that the stems of *B. komarovianum* were hollow. The authors combined morphological and chromosomal evidence to argue that *B. komarovianum* should be reinstated as a separate species. Finally, the basal leaves of *B. sibiricum* var. *sibiricum* were found to be persistent, whereas those of *B. sibiricum* var. *jeholense* were found to wither at the flowering and fruiting stages, as in *B. chinense*.

Bupleurum chinense is widely distributed throughout East Asia and is often cultivated as a medicinal plant. The morphology of this species varies with the environment. *Bupleurum sibiricum* var. *jeholense* may be a variant of *B. chinense* that has adapted to the cold environments found in high-altitude mountains. In particular, the bracteole number may have increased to protect flowers at higher altitudes (Kofidis et al. 2007). Compared with *B. chinense* plants, *B. sibiricum* var. *jeholense* plants are shorter, with several stems, fewer stem branches, and narrower middle stem leaves. Overall, the above evidence suggests that *B. sibiricum* var. *jeholense* should be treated as a variety of *B. chinense*.

Cytological analysis

Chromosomal variation plays a vital role in species formation, and the diversity of chromosome size and number is therefore an important character that can be used to track *Bupleurum* species that have adapted to different habitats (Wang 2011a; Weiss-Schneeweiss and Schneeweiss 2013).

Bupleurum sibiricum var. *jeholense* differs from *B. sibiricum* var. *sibiricum* in both chromosome number and basal number, but these values are identical to those of *B. chinense*. In this study, *B. chinense* and *B. sibiricum* var. *jeholense* were both found to have a chromosome number of 12 (diploid), which is the common basic number reported for this genus (Wang 2011a). Regarding the reported chromosome number of 64 in *B. sibiricum* from a population collected in Inner Mongolia, Qin et al. (1989) and Jiang et al. (2002) assumed that *B. sibiricum* was octoploid (i.e., with a basal number of 8), marking the highest level of polyploidy found in this genus. This observation may be due to chromosomal polyploidy, a type common in colder climates (Jiang et al. 2002). Thus, in terms of both chromosome number and basal number, *B. sibiricum* var. *jeholense* appears to be only distantly related to *B. sibiricum* var. *sibiricum*.

Phylogenetic analysis

In this study, a phylogenetic tree was reconstructed using chloroplast genome data. Our findings were consistent with those of Wang et al. (2011b). In particular, we found that *Bupleurum sibiricum* var. *jeholense* was embedded in *B. chinense*, which forms a sister clade with *B. yinchowense*. In addition, *B. sibiricum* var. *sibiricum* is sister to *B. smithii* and *B. bicaule*. In contrast to *B. chinense*, the distributions of *B. sibiricum* and *B. bicaule* are ranging from Siberia to northeastern China.

Distribution

Bupleurum sibiricum is distributed widely throughout temperate Asia. It often co-occurs with *B. scorzonerifolium* in arid meadows in Inner Mongolia and Siberia at elevations of 700–2000 m. In the field, *B. sibiricum* var. *jeholense* is often found to co-occur with *B. chinense* at different altitudes in the same mountain. At present, *B. sibiricum* var. *jeholense* is found only in high-altitude areas of the Yan Mountains. Moreover, it has a narrow distribution area and is confined to altitudes of 1500–2000 m. In contrast, *B. chinense* is widely distributed and is found at altitudes ranging from 200 to 1600 m in Northeast China; however, it has also been found isolated at an altitude of 2100 m in Northwest China. Given these findings, we speculate that *B. sibiricum* var. *jeholense* is a specialized morphological variant of *B. chinense* that has specifically adapted to high altitudes. Overall, in terms of distribution and habitat, *B. sibiricum* var. *jeholense* differs considerably from *B. sibiricum* and is more similar to *B. chinense*.

Taxonomic treatment

***Bupleurum chinense* var. *jeholense* (Nakai) Q.R.Liu & L.H.Wang, comb. nov.**
urn:lsid:ipni.org:names:77335467-1

– *Bupleurum jeholense* Nakai in J. Jap. Bot. 13: 482 (1937) – *Bupleurum sibiricum* var. *jeholense* (Nakai) Chu in Shan & Li, Acta Phytotax. Sin. 12 (3): 272 (1974).
= *Bupleurum jeholense* var. *latifolium* Nakai in J. Jap. Bot. 13: 482 (1937). Type. China. Hebei: Wuling Mountain, 1800 m, 2 Sept 1933, *Nakai*, *Honda et Kitagawa s. n.* (holotype: TI0082957!).

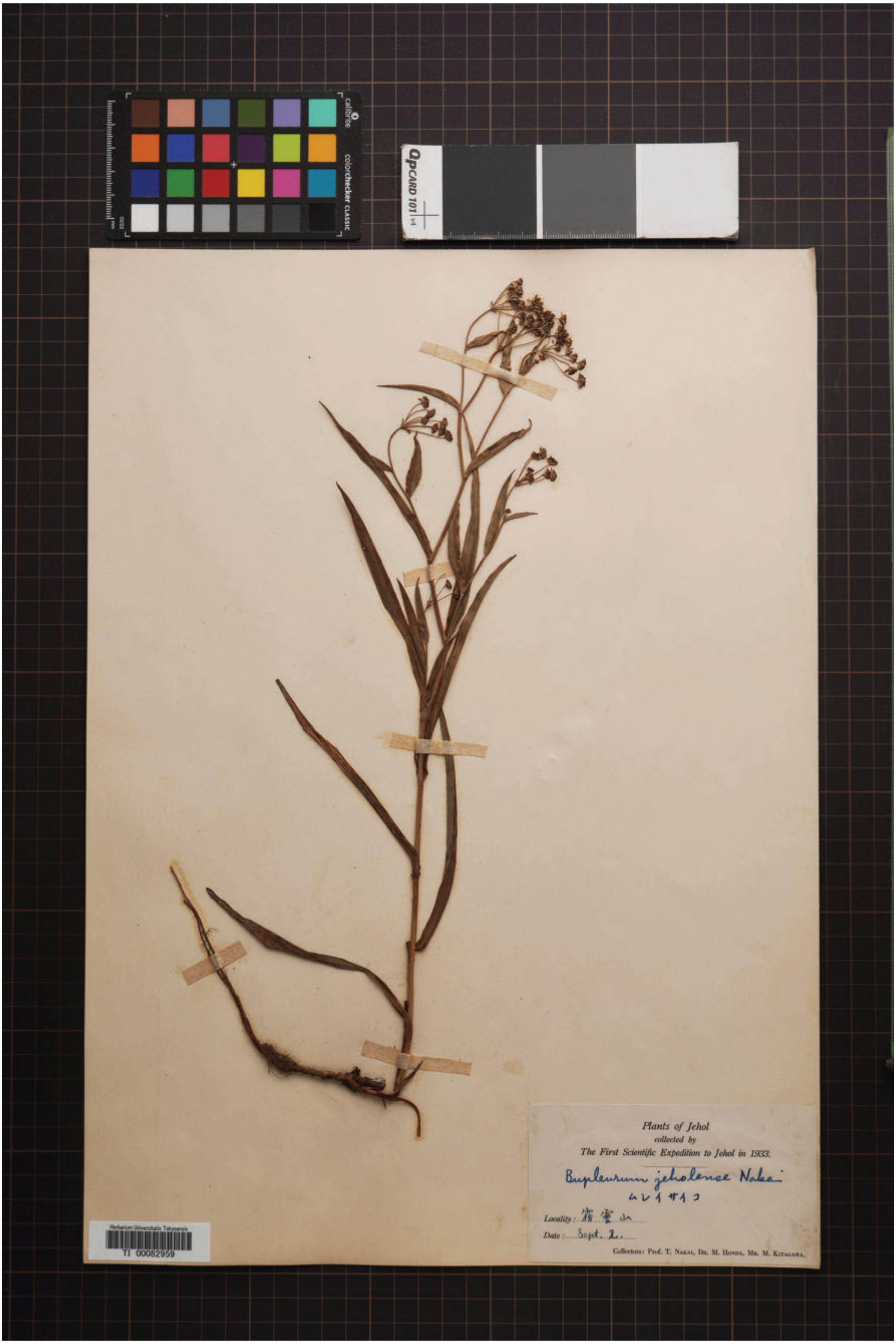

Figure 6. Isotype of *Bupleurum chinense* var. *jeholense* (Photo from TI Herbarium).

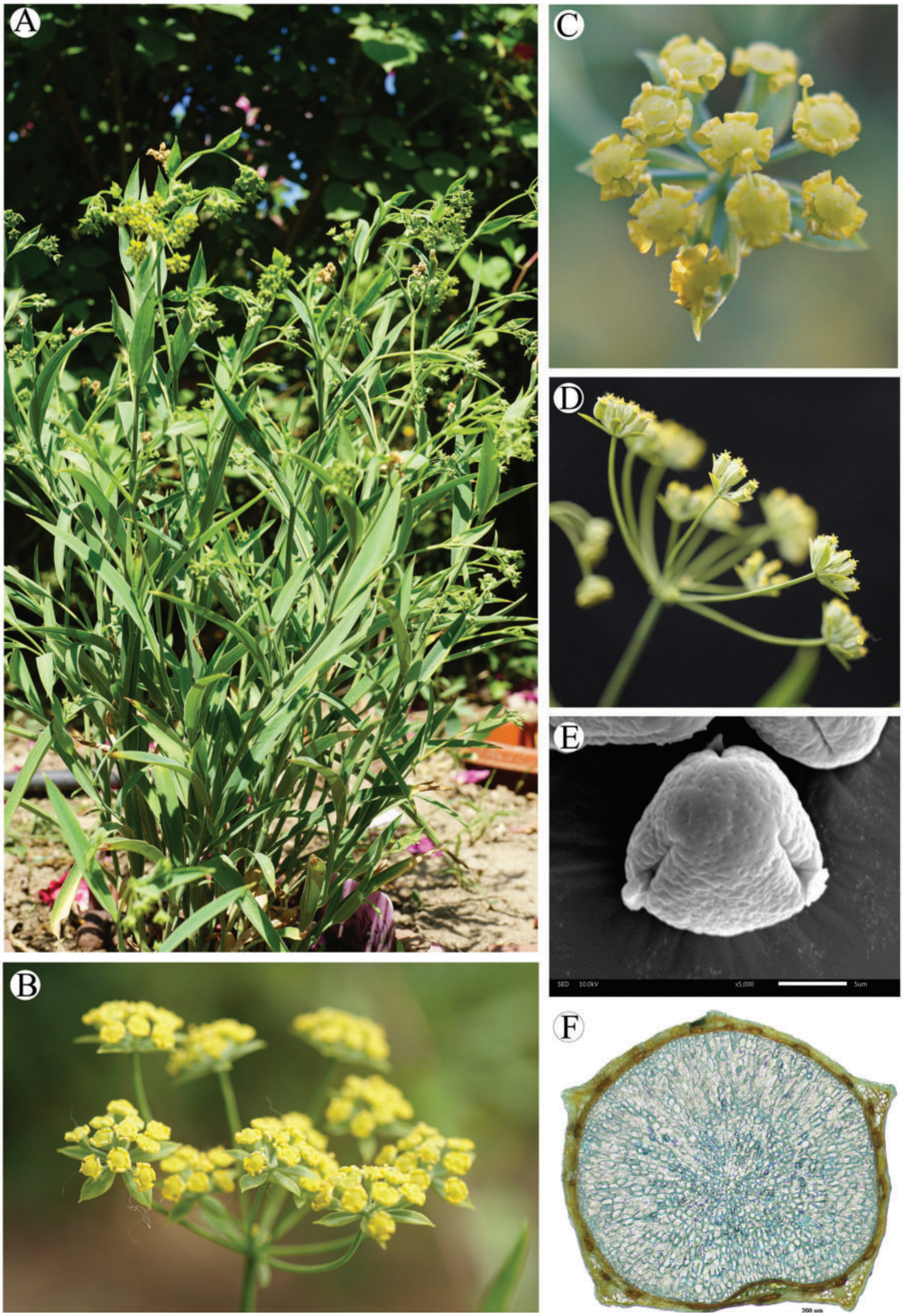

Figure 7. *Bupleurum chinense* var. *jeholense* **A** plant **B** umbel and bract **C** flowers **D** umbel (side view) **E** pollen **F** transverse section of mericarp.

Type. China. Hebei: Wuling Mountain, 1500–2000 m, 2 Sept 1933, *Nakai*, *Honda et Kitagawa*, *s. n.* (holotype: not barcode, fig in protologue pp 481!; isotypes: TI0082958! TI0082959! (Fig. 6) TI0082960! TI0082961!],

Diagnosis. *Bupleurum chinense* var. *jeholense* is morphologically similar to var. *chinense* and can be distinguished from the latter by plant size (>40 cm), the presence of multiple stems, with 1–2 branches per stem, thinner middle stem leaves, leaf length to width ratio 10–16, and the presence of 5 bracteoles.

Description. Plants 20–40 cm, perennial. Root stout, brown, woody. Stem solitary or several, solid, petioles often purplish-red, clasping base without fibrous remnant sheaths. Basal leaves oblanceolate, 5–10 × 0.3–0.8 cm, base petioles, apex acuminate. Middle leaves sessile, oblanceolate, 4.5–12 × 0.4–1.4 cm, 7–9-nerved, base tapering, apex obtuse or acute, apiculate. Apical leaves small. Umbels 5–12, nearly equal or unequal rays 0.4–4 cm long; bracts of 1–5 unequal leaflets, often obsolete or deciduous, 3–15 × 0.6–11 mm, 4–7-nerved; bracteoles 5, lanceolate, 3–7 × 0.6–0.8 mm, exceeding flowers; umbellule 4–12 mm across, 8–14-flowered. Petals bright yellow. Stylopodium low-conic, discoid, dark yellow. Fruit oblong, brown, ca. 2.2–3.5 × 0.9–1.5 mm; ribs prominent, narrowly winged, wings pale brown; vittae 3(–4) in each furrow, 4 on commissure (Fig. 7). Fl. July–August and Fr. August–October. $2n = 12$.

Phenology. Flowering and fruiting from August to October.

Distribution and habit. Hebei, Beijing. It grows in mountains at elevations of 1500–2000 m.

Additional specimens examined. China. **Beijing**: Fangshan county, *Jin-Wu Wang s.n.* (PEY!); Mentougou county, *Xiao-Liu QS-186* (BJFC!); *Quan-Ru Liu 200609009* (BNU!); *Xue Lin 05 05-4-114* (BJFC!); *Gang-Min Zhang 201008036* (BJFC!); *Xian-Yun Mu 1821* (BJFC!); *Duan-Zheng Lu s.n.* (BJFC!); *Quan-Ru Liu DL025-2* (BNU!); *Quan-Ru Liu DL026-2* (BNU!); *Quan-Ru Liu DL027-1*(BNU!); Miyun county, *Xian-Yun Mu 1924* (BJFC!). **Hebei**: Xinglong county, *Li-Hua Wang BNU2021HB029* (BNU!); *Li-Hua Wang BNU2021HB025* (BNU!); *Jia-Yi Liu 0845 2190* (TIE!); *Jin-Wu Wang s.n.* (PEY!); *Zhen-Fu Fang 825* (NAS!); *Ze-Hui Pan 83940* (NAS!); *Ze-Hui Pan 83939* (NAS!); *Shen-E Liu 4833* (IFP!); *Zhen-Fu Fang 826* (IFP!); *Quan-Ru Liu WLS068* (BNU!); *Xin-Yuan Liu 1652* (KUN!); *Jia-Yi Liu 08450* (TIE!); *Jia-Yi Liu 00485* (TIE!); *Biaobenshi 2190* (PE!); *Wu-Xiu Zhang 91* (PE!).

Acknowledgements

We gratefully acknowledge the collaboration of the curators and staff of the herbaria mentioned in the text for their assistance upon visits, as well as for access to digital specimen images. Special thanks are due to Professor Akiko of the University of Tokyo for kindly providing photographs of the type specimens. We thank Dr. Dan-Hui Liu for the analyses of molecular sequence data and Xun Sun for the field assistance.

Additional information

Conflict of interest

The authors have declared that no competing interests exist.

Ethical statement

No ethical statement was reported.

Funding

This research was funded by the Biodiversity survey and assessment project of the Ministry of Ecological Environment (2019HJ2096001006).

Author contributions

Funding acquisition: QRL. Investigation: LHW. Software: XMX, LHW. Supervision: QRL. Writing – review and editing: YH, XMX, LHW.

Author ORCIDs

Yi He https://orcid.org/0000-0002-6925-7299
Quan-Ru Liu https://orcid.org/0000-0003-4270-4746

Data availability

All of the data that support the findings of this study are available in the main text.

References

Downie SR, Katz-Downie DS, Watson MF (2000) A phylogeny of the flowering plant family Apiaceae based on chloroplast DNA rpl16 and rpoC1 intron sequences: Towards a suprageneric classification of subfamily Apioideae. American Journal of Botany 87(2): 273–292. https://doi.org/10.2307/2656915

Huelsenbeck JP, Ronquist F (2001) MRBAYES: Bayesian inference of phylogenetic trees. Bioinformatics (Oxford, England) 17(8): 754–755. https://doi.org/10.1093/bioinformatics/17.8.754

Jiang CM, Lu F, Peng YL (2002) Chromosomal study on *Bupleurum* L. in Northeast China. Journal of Heilongjiang Nongken Normal College (4): 50–60.

Jin JJ, Yu WB, Yang JB, Song Y, de Pamphilis CW, Yi TS, Li DZ (2020) GetOrganelle: A fast and versatile toolkit for accurate de novo assembly of organelle genomes. Genome Biology 21(1): 1–31. https://doi.org/10.1186/s13059-020-02154-5

Kalyaanamoorthy S, Minh BQ, Wong TKF, Haeseler A, Jermiin L (2017) ModelFinder: Fast model selection for accurate phylogenetic estimates. Nature Methods 14(6): 587–589. https://doi.org/10.1038/nmeth.4285

Kampstra P (2008) Beanplot: A Boxplot Alternative for Visual Comparison of Distributions. Journal of Statistical Software 28(1): 1–9. https://doi.org/10.18637/jss.v028.c01

Katoh K, Rozewicki J, Yamada KD (2019) MAFFT online service: Multiple sequence alignment, interactive sequence choice and visualization. Briefings in Bioinformatics 20(4): 1160–1166. https://doi.org/10.1093/bib/bbx108

Kljuykov EV, Liu M, Ostroumova TA, Pimenov MG, Tilney PM, Wyk B-E (2004) Towards a standardised terminology for taxonomically important morphological characters in the Umbelliferae. South African Journal of Botany 70(3): 488–496. https://doi.org/10.1016/S0254-6299(15)30233-7

Kofidis G, Bosabalidis AM, Moustakas M (2007) Combined effects of altitude and season on leaf characteristics of *Clinopodium vulgare* L. (Labiatae). Environmental and Experimental Botany 60(1): 69–76. https://doi.org/10.1016/j.envexpbot.2006.06.007

Kress WJ, Prince LM, Williams KJ (2002) The phylogeny and a new classification of the gingers (Zingiberaceae): evidence from molecular data. American Journal of Botany 89(11): 1682–1696. https://doi.org/10.3732/ajb.89.10.1682

Li HM, Zhou W, Song CF (2021) Karyotype analysis of two species in *Pternopetalum* Franch. of Apiaceae. Journal of Plant Resources and Environment 30(1): 69–71.

Liaoning Forestry Soil Research Institute (1977) Flora Plantarum Herbacearum Chinae Boreali-Orientalis vol. 6. Science Press, Beijing, 188–200.

Minh BQ, Schmidt HA, Chernomor O, Schrempf D, Woodhams M, Haeseler A, Lanfear R (2020) IQ-TREE 2: New models and efficient methods for phylogenetic inference in the genomic era. Molecular Biology and Evolution 37(5): 1530–1534. https://doi.org/10.1093/molbev/msaa015

Nakai T (1937) Notulae ad plantas asiae orientale. Shokubutsu Kenkyu Zasshi 13: 471–491.

Pan ZH, Zhuang TD, Zhou XL, Yao XM (1995) Karyotype analysis of four taxa of *Bupleurum* used in Chinese drugs. Jorrnal of Plant Resources and Environment 4(4): 41–45.

Plunkett GM, Pimenov MG, Reduron JP, Kljuykov EV, Wyk BE, Ostroumova TA, Henwood MJ, Tilney PM, Spalik K, Waston MF, Lee BY, Pu FD, Webb CJ, Hard JM, Mitchell AD, Muckensturm B (2019) Apiaceae. In: Kadereit JW, Bittrich V (Eds) The families and genera of vascular plants, vol. 15, Flowering plants, Eudicots: Apiales, Gentianales (except Rubiaceae). Springer, Cham, 109 pp.

Qin HZ, Pan ZH, Sheh ML, Wu ZJ (1989) A Report on Chromosome Numbers of Chinese Umbelliferae. Zhiwu Fenlei Xuebao 27(4): 268–272.

Qu XJ, Moore MJ, Li DZ, Yi TS (2019) PGA: A software package for rapid, accurate, and flexible batch annotation of plastomes. Plant Methods 15(1): 1–12. https://doi.org/10.1186/s13007-019-0435-7

Rambaut A, Drummond AJ, Xie D, Baele G, Suchard MA (2018) Posterior summarisation in Bayesian phylogenetics using Tracer 1.7. Systematic Biology 67(5): 901–904. https://doi.org/10.1093/sysbio/syy032

Shan RH, Li Y (1974) On the Chinese species of *Bupleurum* L. Zhiwu Fenlei Xuebao 12: 261–294.

Sheh ML, Watson MF (2005) *Bupleurum* L. In: Wu ZY, Raven PH, Hong DY (Eds) Flora of China, vol. 14. Missouri Botanical Garden Press & Science Press, Beijing & St. Louis, 60–74.

Wang CB (2011a) Systematic and taxonomical studies on Chinese *Bupleurum* L. (Apiaceae) Sichuan University.

Wang CB, Ma XG, He XJ (2011b) A taxonomic re-assessment in the Chinese *Bupleurum* (Apiaceae): Insights from morphology, nuclear ribosomal internal transcribed spacer, and chloroplast (*trnH-psbA, matK*) sequences. Journal of Systematics and Evolution 49(6): 558–589. https://doi.org/10.1111/j.1759-6831.2011.00157.x

Weiss-Schneeweiss H, Schneeweiss GM (2013) Karyotype diversity and evolutionary trends in angiosperms. In: Leitch IJ, Greilhuber J, Doležel J, Wendel JF (Eds) Plant Genome Diversity 2: Physical Structure, Behaviour and Evolution of Plant Genomes, Springer, Wien, 209–230. https://doi.org/10.1007/978-3-7091-1160-4_13

Zhang D, Gao FL, Jakovlić I, Zou H, Zhang J, Li WX, Wang GT (2020) PhyloSuite: An integrated and scalable desktop platform for streamlined molecular sequence data management and evolutionary phylogenetics studies. Molecular Ecology Resources 20(1): 348–355. https://doi.org/10.1111/1755-0998.13096

PhytoKeys 237: 245–255 (2024)
DOI: 10.3897/phytokeys.237.114768

Research Article

Camellia zijinica (Theaceae), a new species endemic to Danxia landscape from Guangdong Province, China

Min Lin[1*], Qin-Liang Ye[2*], Zhi-Jian Zhang[2], Wen-Bo Liao[1], Qiang Fan[1]

1 State Key Laboratory of Biocontrol and Guangdong Provincial Key Laboratory of Plant Resources, School of Life Sciences, Sun Yat-sen University, Guangzhou 510275, China
2 Zijin Baixi Provincial Nature Reserve of Guangdong, Heyuan 517400, China
Corresponding author: Qiang Fan (fanqiang@mail.sysu.edu.cn)

Abstract

A new species of the genus *Camellia* (Theaceae), *Camellia zijinica*, discovered in the Danxia landscape from Guangdong Province, China, is characterized and illustrated. Phylogenetic analysis based on chloroplast genomes suggested its affinity with *C. drupifera*, *C. oleifera* and *C. fluviatilis*, however, it morphologically differs from all of the latter by leaf shape and size. Phonologically, it most closely resembles *C. microphylla*, but can be distinguished from the latter by its young branchlets glabrous (vs. densely pubescent), fewer bracteoles and sepals, diverse leaf shape, midvein raised slightly with sparsely pubescent or glabrous (vs. prominently with densely pubescent) and leaf adaxially matt (vs. vernicose) when dried. By morphological and molecular analyses, *Camellia zijinica* represented a distinct new species of *C.* sect. *Paracamellia*.

Key words: *Camellia*, Danxia landscape, morphology, new species, phylogeny

Academic editor: Bing Liu
Received: 26 October 2023
Accepted: 17 January 2024
Published: 31 January 2024

Citation: Lin M, Ye Q-L, Zhang Z-J, Liao W-B, Fan Q (2024) *Camellia zijinica* (Theaceae), a new species endemic to Danxia landscape from Guangdong Province, China. PhytoKeys 237: 245–255. https://doi.org/10.3897/phytokeys.237.114768

Introduction

Camellia L. is the largest genus in Theaceae, widely distributed across eastern and southern Asia (Chang 1981; Ming et al. 2000). More than twenty new *Camellia* species have been predominantly reported and described in China and Vietnam in recent years (Shi et al. 2018; Hu et al. 2019; Le et al. 2020; Nguyen et al. 2020; Xu et al. 2020; Yu et al. 2021; Ly et al. 2022; Quach et al. 2022; Ye et al. 2022). Moreover, China has the highest richness of *Camellia* species with over 80% of *Camellia* species, mainly distributed in Yunnan Province, Guangdong Province, Guangxi Province and Sichuan Province (Chang and Ren 1998; Ming and Bartholomew 2007). Among them, more than 60% of *Camellia* species were endemic to China (Ming and Bartholomew 2007).

The sect. *Paracamellia* was initially constructed by Sealy, and the sect. *Oleifera* was proposed by Chang (1981). Chang and Ren (1998) and Ming (1999) both observed morphological similarities between sect. *Paracamellia* and sect. *Oleifera*, and Ming merged sect. *Oleifera* into sect. *Paracamellia*. However, Chang and Ren (1998) highlighted certain distinguishing features of sect. *Paracamellia*, such as smaller flowers, tinier fruits, shorter styles, shorter stamens,

---

[*] These authors contributed equally to this work.

and thinner trunks compared to sect. *Oleifera*. In recent years, based on molecular analyses represented sect. *Paracamellia* was not monophyletic and nested with taxa of several sections, such as sect. *Camellia*, sect. *Oleifera* and sect. *Archecamellia*, etc., which the phylogenetic relationship of sect. *Paracamellia* and relatives need to be further explored and reconstructed through integrated means (Pang et al. 2022; Wu et al. 2022; Zan et al. 2023; Zhao et al. 2023).

During our field investigation of Guangdong Province in 2018, we noticed an unknown *Camellia* species, which can be easily misidentified as *C. microphylla* (Merr.) Chien. After several years of field observations and a precise comparison of relevant herbarium specimens, we confirmed it as a new member of the *Camellia* sect. *Paracamellia* based on morphological characteristics and molecular traits. In this study, we described and illustrated this new species.

Materials and methods

Morphological study

Field observations and collections of the new species were carried out from 2018 to 2023 in Zijin County, Guangdong Province, China. Morphological comparisons of the putative new species with the related species based on living plants, relevant literature and herbarium specimens, including "Flora Reipublicae Popularis Sinicae" (Chang and Ren 1998), "A Taxonomy of the Genus Camellia" (Chang 1981), "Flora of China" (Ming and Bartholomew 2007), the Chinese Virtual Herbarium (https://www.cvh.ac.cn/) and other recently described species and infraspecies of *C.* sect. *Paracamellia* (Ma et al. 2012; Lee and Yang 2019). Then we used nine morphological characters to distinguish each other. All the characters were measured and described by dissecting microscopes.

Molecular analysis

Fresh leaf materials of individuals were collected and stored in silica gel for subsequent molecular experiments. Whole genomic DNA for each sample was extracted using the modified CTAB method (Doyle and Doyle 1987) and then purified using magnetic beads. A library was constructed for each sample by TruePrep DNA Library Prep Kit, which was then sent for Illumina sequencing on the Novaseq 6000 platform under standard operation procedure. Raw sequencing data were filtered with fastp v0.23.4 (Chen et al. 2018) to obtain clean data. Chloroplast genomes were assembled by GetOrganelle v1.7.7.0 (Jin et al. 2020) and annotated with cpGAVAS (Liu et al. 2012). The complete chloroplast sequences of *C. zijinica* were submitted to NCBI (https://www.ncbi.nlm.nih.gov/) and deposited with the accession number OR567094, OR567095, OR567096. Additionally, we extracted, sequenced, filtered, annotated the total DNA of *C. microphylla* with the accession number OR567093. Voucher specimens were deposited in the herbarium of Sun Yat-sen University (**SYS**).

We downloaded 50 accessions of chloroplast genomes containing 44 *Camellia* species and two related species as outgroups from the NCBI. The chloroplast genome sequences were aligned using MAFFT v7 (Katoh and Standley 2013). TrimAl v1.2 was applied to trim the alignment with the "gap out" model setting (Capella-Gutiérrez et al. 2009). Maximum likelihood (ML) and Bayesian inference (BI) were used to derive and construct their phylogenies respectively. ML tree was constructed using IQ-TREE v2.2.3 under 5,000 replicates of SH approximate likelihood ratio test (SH-aLRT) and 10,000 ultrafast bootstrap (UFBS) replicates (Nguyen et al. 2015). BI analysis was using MrBayes v.3.2.6 (Ronquist et al. 2012), and Markov chain Monte Carlo (MCMC) simulations were run for 1.6 million generations with one cold chain and three heated chains until the average standard deviation of split frequencies of these runs was <0.01 starting from random trees and sampling 1 of 100 generations, discarding the first 25% and the posterior probabilities were then estimated.

Results

Based on morphological observations, *C. microphylla*, *C. brevistyla* (Hayata) Coh. St and *C. fluviatilis* Hand.-Mazz. exhibited morphological similarities with the new species. Among them, *C. microphylla* most resembles the new species, but *C. zijinica* has a more diverse leaf shape compared with *C. microphylla*, including elliptic, oblong-elliptic, obovate-elliptic or oblong-lanceolate, while *C. microphylla* displays oblong-elliptic or obovate-elliptic leaves, moreover, the leaf adaxially matt when dried (vs. vernicose). Differences between *C. zijinica* and *C. fluviatilis* are leaf shape and size, and the latter is lanceolate to narrowly lanceolate leaves, 5–9 × 1–1.5 cm (vs. 2–4.8 × 0.8–1.9 cm). Additionally, the leaf apex of *C. fluviatilis* is caudate-acuminate, which is a distinctive feature that sets it apart. *C. zijinica* and *C. brevistyla* differ not only in the shape and size of their leaves but also in having longer stamens and ovaries in the case of *C. brevistyla*. Furthermore, the young branchlets of *C. zijinica* are glabrous, while those of the other species are usually pubescent or glabrescent (Table 1).

Phylogenetic analysis by Maximum likelihood (ML) and Bayesian inference (BI) inferred from chloroplast genomes showed generally common results with highly supported values. The phylogenetic result using ML proved that this new species was sister to *C. drupifera*, *C. oleifera*, and successively grouped with *C. fluviatilis*, *C. yuhsienensis*, *C. granthamiana*, *C. semiserrata* in clade CAI with

Table 1. Morphological comparisons amongst *C. zijinica*, *C. brevistyla*, *C. microphylla* and *C. fluviatilis*.

Characters	*C. zijinica*	*C. brevistyla*	*C. microphylla*	*C. fluviatilis*
Leaf shape and size	elliptic, oblong-elliptic, obovate-elliptic or oblong-lanceolate , 2–4.8 × 0.8–1.9 cm	elliptic, obovate-elliptic, obovate-oblong or obovate, 3–5.5 × 1.5–3 cm	oblong-elliptic or obovate-elliptic , 2–3.5 × 1–1.3 cm	lanceolate to narrowly lanceolate, 5–9 × 1–1.5 cm
Leaf apices	rounded, acute or acuminate	acute	obtuse, rounded, acute	caudate-acuminate
Young branchlets	glabrous	pubescent to hirtellous	densely pubescent	puberulent, soon glabrescent
Petiole length	1–3 mm	3–5 mm	1–2 mm	2–5 mm
Bracteoles and sepals	4–6	7–8(-10)	6–7	8–9
Petals, shape and size	4–6, oblong-elliptic to obovate-elliptic, apex retuse, 0.7–1.1 × 0.4–0.5 cm	5–7, obovate to obovate-spatulate, apex retuse to deeply emarginate, 1–2.5(-3) × 0.4–1(-1.5) cm	5–7, broadly obovate, apex retuse, 0.8–1.1 × 0.5–0.8 cm	5–6, oblong-elliptic to oblanceolate, apex rounded to slightly retuse, 0.8–3 × 0.4–2 cm
Stamens	4–5 mm	5–10 mm	5–6 mm	5–7 mm
Capsule shape and size (diameter)	ovoid or subglobose, 1.2 cm	subglobose, 1.5–1.8 cm	ovoid, 1.5 cm	ovoid, 1.5–1.7 cm
Styles	3–4, 1–2 mm	3–4, 4–7 mm	3, 2–3mm	3, 4 mm

*Comparative data from: Chang and Ren (1998); Ming and Bartholomew (2007); Merrill (1927).

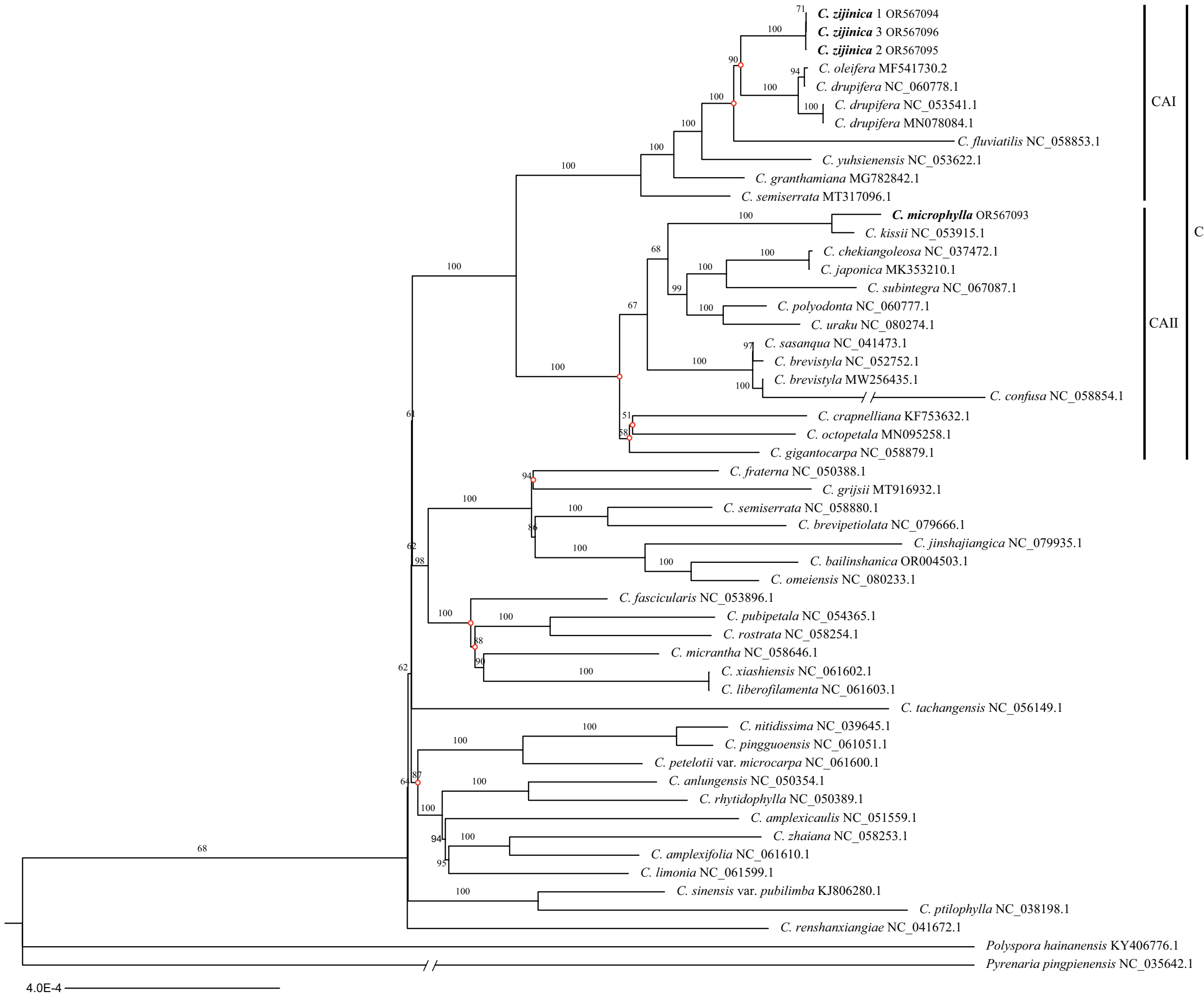

Figure 1. Maximum likelihood phylogenetic tree of *C. zijinica* and other 46 related species based on chloroplast genomes. Above the nodes of the tree, maximum likelihood ultrafast bootstrap support values were shown. The new species and *C. microphylla* were highlighted in bold. The red circles marked on the tree nodes indicated differences between the maximum likelihood and Bayesian inference. "CAI" and "CAII" refer to the two clades within CladeA.

robust support values (BS = 100) (Fig. 1). However, the BI analysis presented a different arrangement in clade CAI, where the new species initially grouped with *C. fluviatilis* (PP = 0.90), and subsequently formed a clade with *C. drupifera*, *C. oleifera* (PP = 1.00) (Appendix 1). The species *C. microphylla* and *C. brevistyla* were nested within clade CAII, which was sister to clade CAI, together forming CladeA with highly supported values (PP = 1.00; BS = 100).

Taxonomic treatment

Camellia zijinica **M.Lin, Q.L.Ye & Q.Fan, sp. nov.**
urn:lsid:ipni.org:names:77335468-1
Figs 2, 3
Chinese name: 紫金短柱茶

Type. China. Guangdong: Zijin County, Guzhu Town, Mount Yuewang, in mixed forests, 23°29'N, 114°44'E, 294 m a.s.l., 22 September 2018, *H.W. Wang* & *Q.*

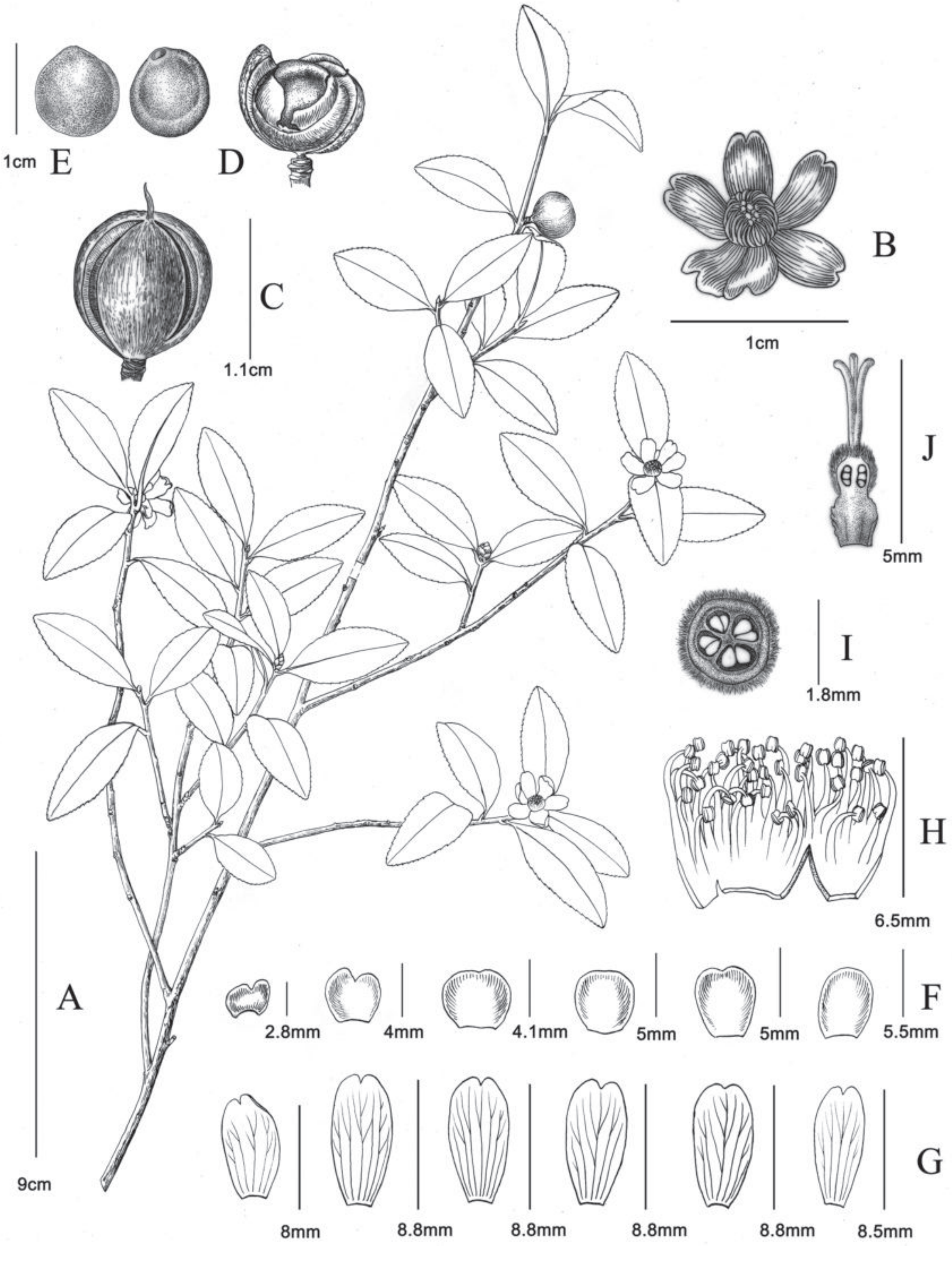

Figure 2. *Camellia zijinica* sp. nov. **A** flowering and fruiting branch **B** flower in front view **C** fully ripe fruit, tending to split **D** young fruit in longitudinal section **E** seeds in obverse and reverse sides **F** bracteoles and sepals **G** petals **H** stamens (incomplete) **I** ovary in transverse section **J** pistil in longitudinal section. Illustrated by Yun-Xiao Liu.

Fan 18084 (holotype: SYS00236945! isotypes: IBSC1010670! SYS00236946! SYS00236947! SYS00236948!)

Diagnosis. *Camellia zijinica* is morphologically similar to *C. microphylla* in the flower shape and size, but differs from the latter by its young branchlets glabrous (vs. densely pubescent), the diverse leaf shape (elliptic, oblong-elliptic,

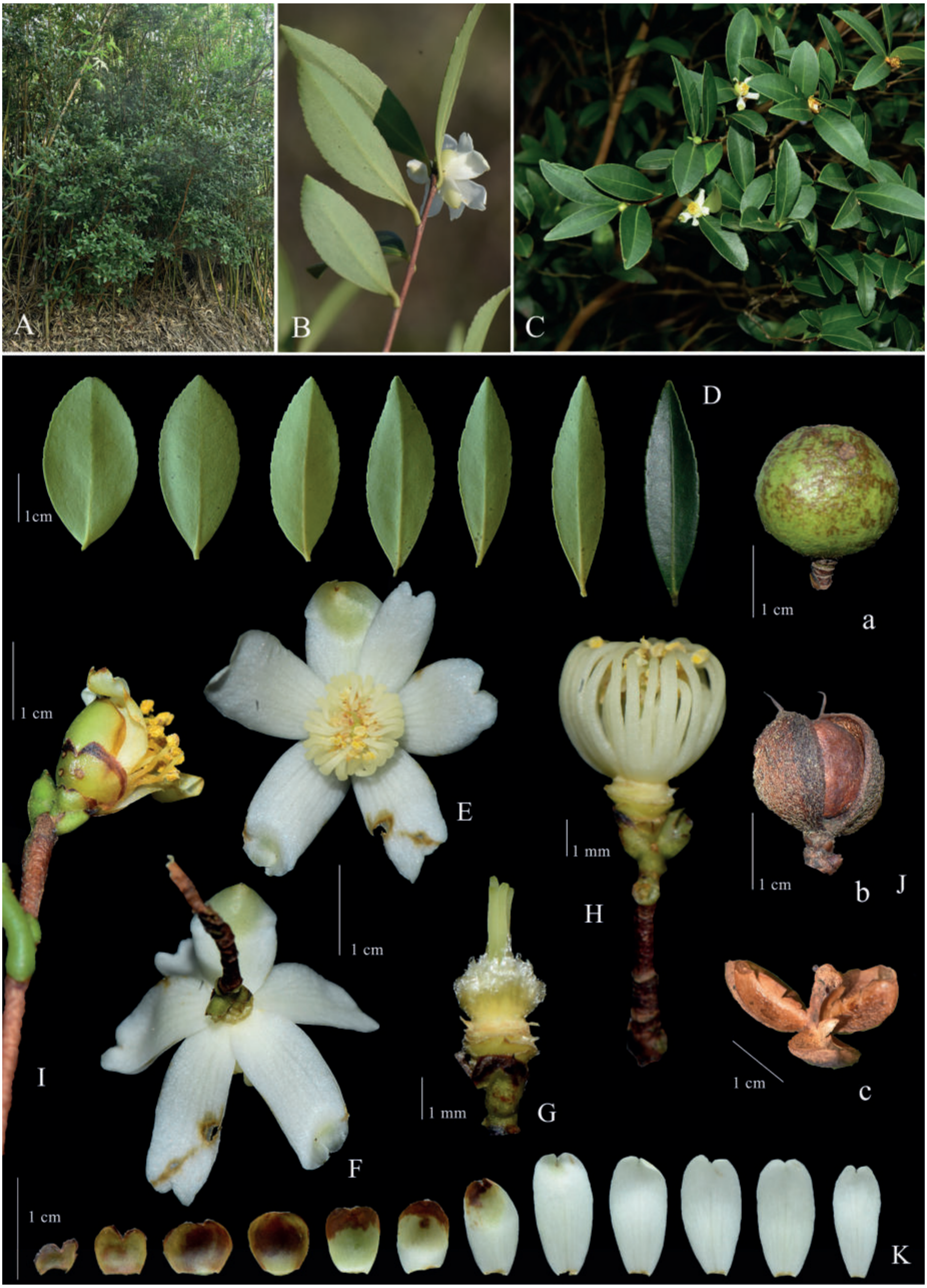

Figure 3. *Camellia zijinica* sp. nov. **A** habit **B, C** flowering branch **D** leaf shape **E** flower in front view **F** flower in back view **G** pistil and ovary **H** flowering branch, showing the stamens **I** flowering branch, showing the bracteoles and sepals **J** fruits, showing young to ripe (a-c) **K** bracteoles, sepals and petals. Photographed by Zhi-Ming Zhong, Qiang Fan and Min Lin.

obovate-elliptic or oblong-lanceolate vs. oblong-elliptic or obovate-elliptic), midvein raised slightly with sparsely pubescent or glabrous (vs. prominently with densely pubescent), fewer bracteoles and sepals (4–6 vs. 6–7), leaf adaxially matt when dried (vs. vernicose).

Description. Small evergreen shrubs, 2–5 m tall; bark yellowish brown; young branchlets reddish brown, glabrous. ***Leaf*** blades elliptic, oblong-elliptic, obovate-elliptic or oblong-lanceolate, 2–4.8 × 0.8–1.9 cm, adaxially dark green, abaxially light green, thick papery to coriaceous; petiole 1–3 mm long, pubescent; midrib prominent on both surfaces, glabrous and sometimes adaxially sparsely pubescent, secondary veins 6–7 on each side, invisible; apex rounded, acute or acuminate; margin serrulate; base cuneate. ***Flowers*** solitary, terminal or axillary, 1.5–2.3 cm in diameter, subsessile. bracteoles and sepals 4–6, caducous, outside pubescent at base, inside glabrous, margin ciliate; outer bracteoles and sepals broadly semiorbicular, partial apex bifid; inner bracteoles and sepals suborbicular to oblong-elliptic. Petals 4–6, white, distinct, glabrous, oblong-elliptic to obovate-elliptic, apically 2-lobed, 7–11×4–5 mm. ***Stamens*** 33–40, 4–5 mm long, glabrous; outer filament whorl basally connate for 1–1.5 mm. ***Ovary*** 3–4-loculed, with 2 ovules per locule, about 2 mm in diameter, tomentose. ***Styles*** 3 or 4, 1–2 mm long, connate half from the base, apically 3–4-lobed. ***Capsule*** ovoid or subglobose, ca. 1.2 cm in diameter; pericarp 1–2 mm thick, splitting into 3–4 valves. ***Seeds*** semiglobose or globose, 9–10 mm in diameter, brown, glabrous.

Phenology. Flowering from September to December, fruiting from January to September.

Etymology. The specific epithet refers to Zijin County of Guangdong Province, the type locality of the new species.

Distribution and habitat. Presently, *Camellia zijinica* is only known from its type locality, Zijin County of northeastern Guangdong. It is distributed in mixed forests of Danxia landscape at altitudes of 200–400 m a.s.l.

Conservation status. Only two populations of a total of about 90 mature individuals were found currently. Thus, the species could be considered as Endangered (EN; D) status according to IUCN Red List criteria (IUCN Standards and Petitions Subcommittee 2022).

Additional specimens examined (paratypes). China. Guangdong: Zijin County, Guzhu Town, near Mount Yuewang, 23°37'N, 115°10'E, 234 m a.s.l., 12 Oct. 2022 (fl. and fr.), *Z.M. Zhong 1012* (SYS); Zijin County, Guzhu Town, near Mount Yuewang, 23°29'N, 114°44'E, 310 m a.s.l., 7 June 2023 (young fr.), *Z.M. Zhong 0607* (SYS), the type locality, 21 July 2023 (young fr.), *Z.M. Zhong 0721* (SYS).

Discussion

Geographically, *C. drupifera* and *C. oleifera* are distributed in southern China, belonging to sect. *Oleifera*. Although they share a similar distribution area with the new species, they exhibit distinct morphological characteristics, such as larger leaves, flowers and fruits compared to *C. zijinica*. Furthermore, *C. fluviatilis*, a sympatric species of the new species, shows similarities in gross morphology but can be easily distinguished by leaf shape and size. Instead, *C. microphylla* is distributed in a different distribution area from the new species, located in the Jiangxi, Guizhou, Zhejiang, Hunan and Anhui Provinces, China, but they most resembled in morphology. Traditionally, the identification of *C. microphylla* is associated with having the smallest leaves within the sect. *Paracamellia* (Chang and Ren 1998). Nevertheless, our careful comparisons revealed that its leaves were similarly small to those of *C. zijinica*.

The phylogenetic tree generated using ML and BI showed *C. zijinica* was grouped with *C. drupifera*, *C. oleifera* (BS = 90) and *C. fluviatilis* (PP = 0.90) with low support values, implying an unclear relationship among them. However, these species collectively exhibited the closest relationship to the new species. The species within CladeA belong to the sect. *Oleifera*, sect. *Paracamellia*, sect. *Camellia*, sect. *Archecamellia*, sect. *Furfuracea*, as classified in Flora Reipublicae Popularis Sinicae (Chang and Ren 1998). Additionally, they are classified in the sections of *Paracamellia*, *Camellia*, and *Heterogenea* based on Flora of China (Ming and Bartholomew 2007), suggesting a close relationship among these sections. Moreover, recent phylogenetic analyses of *Camellia* based on low-copy nuclear genes and chloroplast genomic regions have suggested that further investigation is needed to clarify the relationships among these *Camellia* sections (Zan et al. 2023; Wu et al. 2022). Nevertheless, our comprehensive comparisons and analyses revealed that *C. zijinica* was a distinct new species of sect. *Paracamellia*.

Acknowledgments

We are deeply grateful to Dr. Xianggang Shi for his suggestions on our manuscript, Mrs. Yun-Xiao Liu for her excellent illustration and kindly thank Mr. Zhi-Ming Zhong for his great assistance in sampling.

Additional information

Conflict of interest

The authors have declared that no competing interests exist.

Ethical statement

No ethical statement was reported.

Funding

This study was supported by the Guangdong Provincial Special Research Grant for the Creation of National Parks (2021GJGY034) and Guangdong Provincial Ecological Forestry Development Project (2020141).

Author contributions

Formal analysis: ML. Funding acquisition: WBL. Investigation: QLY, QF, WBL, ZJZ. Methodology: ML. Resources: QLY. Software: ML. Supervision: WBL. Validation: QF. Writing – original draft: ML. Writing – review and editing: QF.

Author ORCIDs

Min Lin https://orcid.org/0000-0001-6342-1978
Wen-Bo Liao https://orcid.org/0000-0001-6839-9511
Qiang Fan https://orcid.org/0000-0003-4254-6936

Data availability

All of the data that support the findings of this study are available in the main text.

References

Capella-Gutiérrez S, Silla-Martínez JM, Gabaldón T (2009) trimAl: A tool for automated alignment trimming in large-scale phylogenetic analyses. Bioinformatics 25(15): 1972–1973. https://doi.org/10.1093/bioinformatics/btp348

Chang HT (1981) A Taxonomy of the Genus *Camellia*. Sunyatsen University Natural Science 1: 1–43.

Chang HT, Ren SX (1998) Theaceae. In: Chang HT (Ed.) Flora Reipublicae Popularis Sinicae (Vol. 49(3)). Science Press, Beijing, 3–34.

Chen SF, Zhou YQ, Chen YR, Gu J (2018) fastp: An ultra-fast all-in-one FASTQ preprocessor. Bioinformatics 34(17): 884–890. https://doi.org/10.1093/bioinformatics/bty560

Doyle JJ, Doyle JL (1987) A rapid DNA isolation procedure for small quantities of fresh leaf tissue. Phytochemical Bulletin 19: 11–15.

Hu RC, Wei SJ, Liufu YQ, Nong YK, Fang W (2019) *Camellia debaoensis* (Theaceae), a new species of yellow camellia from limestone karsts in southwestern China. PhytoKeys: 49–58. https://doi.org/10.3897/phytokeys.135.38756

IUCN Standards and Petitions Subcommittee (2022) Guidelines for Using the IUCN Red List Categories and Criteria. Version 15. Prepared by the Standards and Petitions Subcommittee. https://nc.iucnredlist.org/redlist/content/attachment_files/RedListGuidelines.pdf

Jin JJ, Yu WB, Yang JB, Song Y, dePamphilis CW, Yi TS, Li DZ (2020) GetOrganelle: A fast and versatile toolkit for accurate de novo assembly of organelle genomes. Genome Biology 21(1): e241. https://doi.org/10.1186/s13059-020-02154-5

Katoh K, Standley DM (2013) MAFFT Multiple Sequence Alignment Software Version 7: Improvements in Performance and Usability. Molecular Biology and Evolution 30(4): 772–780. https://doi.org/10.1093/molbev/mst010

Le NHN, Luong VD, Nguyen VC, Pham TTD, Luu TT, Pham VT (2020) An updated checklist of Theaceae and a new species of from Vietnam. Taiwania 65: 216–227. https://doi.org/10.6165/tai.2020.65.216

Lee SL, Yang TYA (2019) *Camellia chinmeii*, a new species of *Camellia* sect. *Paracamellia* in Taiwan. Taiwania 64: 321–325. https://doi.org/10.6165/tai.2019.64.321

Liu C, Shi LC, Zhu YJ, Chen HM, Zhang JH, Lin XH, Guan XJ (2012) CpGAVAS, an integrated web server for the annotation, visualization, analysis, and GenBank submission of completely sequenced chloroplast genome sequences. BMC Genomics 13(1): e715. https://doi.org/10.1186/1471-2164-13-715

Ly NS, Luong VD, Le TH, Do ND, Tran N, Nguyen AD, Nguyen TL, Uematsu C, Katayama H (2022) *Camellia annamensis* (Theaceae), a new species from central Vietnam. Taiwania 67: 243–249. https://doi.org/10.6165/tai.2022.67.243

Ma JL, Ye H, Ye CX (2012) A new species of *Camellia* sect. *Paracamellia*. Guihaia 32(6): 753–755. https://doi.org/10.3969/j.issn.1000-3142.2012.06.007

Merrill ED (1927) New Chinese Ligneous Plants. Journal of the Arnold Arboretum 8(1): 3–19. https://doi.org/10.5962/p.318021

Ming TL (1999) A systematic synopsis of the genus *Camellia*. Acta Botanica Yunnanica 21: 149–159.

Ming TL, Bartholomew B (2007) Theaceae. In: Wu ZY, Raven PH (Eds) Flora of China (Vol. 12). Science Press, Beijing & Missouri Botanical Garden Press, St. Louis, 367–412.

Ming TL, Gu ZJ, Zhang WJ, Xie LS (2000) Ming TL (Ed.) Monograph of the Genus *Camellia*. Yunnan Science and Technology Press, Yunnan, 310 pp.

Nguyen LT, Schmidt HA, von Haeseler A, Minh BQ (2015) IQ-TREE: A fast and effective stochastic algorithm for estimating maximum-likelihood phylogenies. Molecular Biology and Evolution 32(1): 268–274. https://doi.org/10.1093/molbev/msu300

Nguyen DH, Luong VD, Le TH, Tran QT, Do ND, Ly NS (2020) *Camellia puhoatensis* (Sect. *Archecamellia* – Theaceae), a new species from Vietnam. PhytoKeys 153: 1–11. https://doi.org/10.3897/phytokeys.153.49388

Pang Z, Wang YL, Mantri N, Wang Y, Hua XJ, Quan YP, Zhou X, Jiang ZD, Qi ZC, Lu HF (2022) Molecular phylogenetic relationships and taxonomy position of 161 *Camellia* species in China. Taiwania 67: 560–570. https://doi.org/10.6165/tai.2022.67.560

Quach VH, Hoang TT, Truong QC, Le VH, Luong VD, Vo QT, Nong VD, Curry AS (2022) *Camellia phuongchiana* (Theaceae, section *Piquetia*), a new species from Lam Dong Province, southern Vietnam. Brittonia 74(4): 339–345. https://doi.org/10.1007/s12228-022-09716-w

Ronquist F, Teslenko M, van der Mark P, Ayres DL, Darling A, Hohna S, Larget B, Liu L, Suchard MA, Huelsenbeck JP (2012) MrBayes 3.2: Efficient Bayesian Phylogenetic Inference and Model Choice Across a Large Model Space. Systematic Biology 61(3): 539–542. https://doi.org/10.1093/sysbio/sys029

Shi XG, Li WX, Wu HD, Guo WX, Ye CX, Liao WB, Huang YL (2018) *Camellia psilocarpa* (Theaceae), a new species from Guangdong, China, based on morphological and molecular data. Phytotaxa 338(2): 209–215. https://doi.org/10.11646/phytotaxa.338.2.6

Wu Q, Tong W, Zhao H, Ge R, Li R, Huang J, Li F, Wang Y, Mallano AI, Deng W, Wang W, Wan X, Zhang Z, Xia E (2022) Comparative transcriptomic analysis unveils the deep phylogeny and secondary metabolite evolution of 116 *Camellia* plants. The Plant Journal 111(2): 406–421. https://doi.org/10.1111/tpj.15799

Xu Z, Yuan D, Tang Y, Wu L, Zhao Y (2020) *Camellia hainanica* (Theaceae) a new species from Hainan, supported from morphological characters and phylogenetic analysis. Pakistan Journal of Botany 52(3): 1025–1032. https://doi.org/10.30848/PJB2020-3(31)

Ye PM, Huang YS, Huan JF, Liu ED, Ma JL, Yang SX (2022) *Camellia hainingii*, a new species of Theaceae in China. Phytotaxa 558(3): 291–296. https://doi.org/10.11646/phytotaxa.558.3.5

Yu XQ, Liu ED, Liu ZW, Xiao B, Ma JL, Yang SX (2021) *Camellia luteocalpandria* (Theaceae), a new species and the first discovery of sect. *Calpandria* in China. Phytotaxa 489(2): 223–228. https://doi.org/10.11646/phytotaxa.489.2.11

Zan T, He YT, Zhang M, Yonezawa T, Ma H, Zhao QM, Zhang WJ, Huang CH, Kuo WY (2023) Phylogenomic analyses of *Camellia* support reticulate evolution among major clades. Molecular Phylogenetics and Evolution 182: 1–13. https://doi.org/10.1016/j.ympev.2023.107744

Zhao DW, Hodkinson TR, Parnell JAN (2023) Phylogenetics of global *Camellia* (Theaceae) based on three nuclear regions and its implications for systematics and evolutionary history. Journal of Systematics and Evolution 61(2): 356–368. https://doi.org/10.1111/jse.12837

Appendix 1

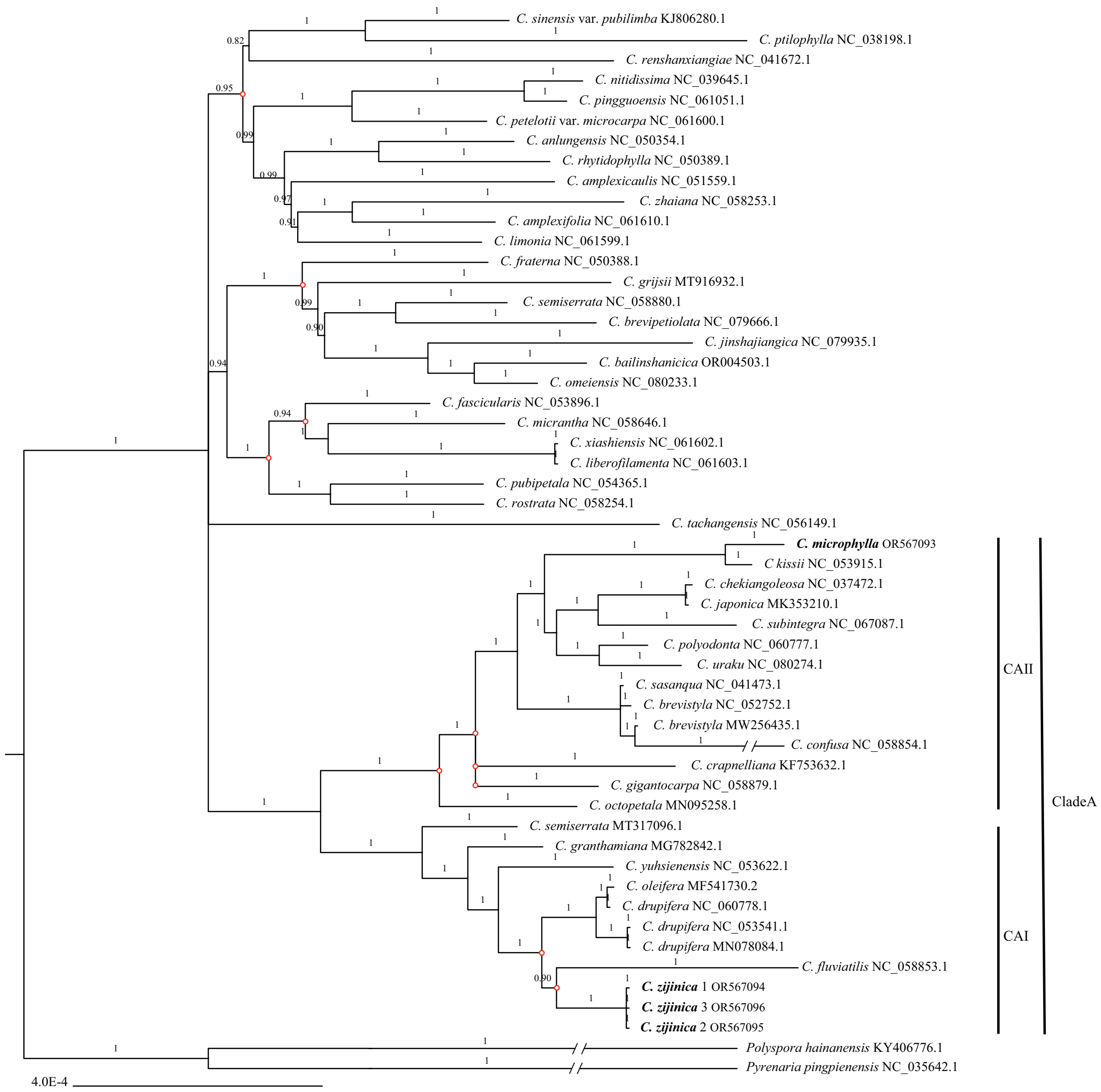

Figure A1. Bayesian inference phylogenetic tree of *C. zijinica* and other 46 related species based on chloroplast genomes. Above the nodes of the tree, Bayesian posterior probabilities support values were shown. The new species and *C. microphylla* were highlighted in bold. The red circles marked on the tree nodes indicate differences between the maximum likelihood and Bayesian inference. "CAI" and "CAII" refer to the two clades within CladeA.

PhytoKeys

PhytoKeys 237: 257–268 (2024)
DOI: 10.3897/phytokeys.237.114484

Research Article

Lysimachia danxiashanensis, a new species of Primulaceae from Guangdong, China

Xing-Yue Zhang[1,2], Jing-Min Dai[1,2], Qiang Fan[1,2], Zai-Xiong Chen[3], Guang-Da Tang[4], Wen-Bo Liao[1,2]

1 *State Key Laboratory of Biocontrol and Guangdong Provincial Key Laboratory of Plant Resources, School of Life Sciences, Sun Yat-sen University, Guangzhou 510275, China*
2 *National Park and Nature Education Research Institute, Sun Yat-sen University, Guangzhou 510275, China*
3 *Administrative Commission of Danxiashan National Park, Shaoguan 512300, China*
4 *College of Forestry and Landscape Architecture, South China Limestone Plants Research Center, South China Agricultural University, Guangzhou 510642, China*
Corresponding authors: Wen-Bo Liao (lsslwb@mail.sysu.edu.cn); Guang-Da Tang (gdtang@scau.edu.cn)

Abstract

Lysimachia danxiashanensis, a new Primulaceae species, endemic to the Danxia landscape in Guangdong Province, China, is described and illustrated. This new species is morphologically similar to *L. pseudohenryi*, *L. phyllocephala*, *L. congestiflora* and *L. kwangtungensis*, but it differs from the similar species by its purplish-red plants, petiole without wings, calyx with orange glandular and the corolla margin serrated on upper half with orange-red glandular punctates. This new species belongs to *Lysimachia* subgen. *Lysimachia* sect. *Nummularia*. Phylogenetic analysis confirmed that *L. danxiashanensis* is a distinct clade, based on the combined data of ITS and *rbc*L sequences. The conservation status of the new species was evaluated as Endangered (EN) according to IUCN Red List Categories and Criteria.

Key words: Danxia landscape, IUCN Red List, *Lysimachia*, taxonomy

Academic editor: Avelinah Julius
Received: 20 October 2023
Accepted: 17 January 2024
Published: 31 January 2024

Citation: Zhang X-Y, Dai J-M, Fan Q, Chen Z-X, Tang G-D, Liao W-B (2024) *Lysimachia danxiashanensis*, a new species of Primulaceae from Guangdong, China. PhytoKeys 237: 257–268. https://doi.org/10.3897/phytokeys.237.114484

Introduction

Lysimachia L. is a member of the tribe Lysmachieae (Primulaceae) and is composed of over 200 species (Chen and Hu 1979; Hu and Kelso 1996; Wang et al 2018). This genus is the most widely distributed genera of Primulaceae and is mainly distributed in the temperate and subtropical regions of the Northern Hemisphere, but there are also a few species in Africa, Australia and South America (Hu 1994; Hao and Hu 2001; Hao et al. 2004; Kodela 2006). China is considered to be the origin and diversity centre of *Lysimachia*, with 138 native species having been recorded in Flora of China and nearly 80% of them are endemic species (Chen and Hu 1979; Hu and Kelso 1996; Hao and Hu 2001). In recent years, many new species of this genus have been described and this highlights more opportunities for discoveries in China (Wang et al 2018; Huang et al 2020; Yan et al 2022).

An unknown species of *Lysimachia* was discovered during a field floristic investigation from May 2022 to August 2023 in Danxiashan National Park, Renhua County, Guangdong Province. It is most similar to *L. congestiflora* Hemsl., but its purplish-red plants, petiole without wings, corolla lobes serrated on upper half and calyx with orange glandular punctates clearly distinguish from the latter. After careful morphological comparison by specimens and consultation with relevant literature and molecular phylogenetic analysis, we confirmed that it represented a new species, described and illustrated here. The threat status of the new species is assessed according to the IUCN Red List Categories and Criteria (IUCN Standards and Petitions Committee 2022).

Materials and methods

Morphological study

The morphological characters of the new species were observed and measured, based on fresh and dry specimens using a micrometer and a stereomicroscope and were compared with its related species, based on herbarium specimens deposited at the Herbarium of SYS and IBSC (the herbarium acronyms follow Thiers (2023)), as well as the digital images on the Chinese Virtual Herbarium (https://www.cvh.ac.cn/) and the China Field Herbarium (https://www.cfh.ac.cn/). Morphological observation and examination were conducted in the SYS.

Taxon sampling and molecular analysis

Leaf tissue of the putative new species and related species was collected from one population and silica dried in zip-lock plastic bags until use for comparisons and taxonomic treatment. Total DNA was extracted with a modified CTAB method (Doyle and Doyle 1987). Regions of the partial internal transcribed spacer 1, the 5.8S ribosomal RNA gene and partial internal transcribed spacer 2 were amplified using the previously-reported primers ITS1 and ITS4 (White et al. 1990) and the ribulose-1,5-bisphosphate carboxylase/oxygenase large subunit (*rbc*L) gene was amplified using the primers *rbc*La-f (Kress and Erickson 2007) and 724R (Fay et al. 1997). PCR amplifications were performed following Fan et al. (2015). Following the studies of *Lysimachia* (Zhang et al. 2011; Yan et al. 2018), we retrieved 67 ITS and *rbc*L accession of 30 species from GenBank, which belong to subgenus *Lysimachia* L., subgenus *Palladia* (Moench) Hand.-Mazz., subgenus *Heterostylandra* (Hand. -Mazz.) Chen et C.M.Hu. and subgenus *Idiophyton* Hand.-Mazz. Two accessions of the putative new species (GenBank Acc. ITS No.: OR665389, OR665390; *rbc*L No: PP025352, PP035354) and one accession of *Lysimachia kwangtungensis* (GenBank Acc. ITS No.: OR941025; *rbc*L No: PP025355) were sequenced for this study. *Ardisia verbascifolia* was selected as outgroup. The sequences were aligned using MAFFT v.7 (Katoh and Standley 2013) and subsequently manually adjusted. Phylogenetic constructions were based on Maximum Likelihood (ML) and Bayesian Inference (BI) and were respectively run by IQ-TREE v. 2.0.3 (Minh et al. 2020) and MrBayes version 3.1.2 (Huelsenbeck and Ronquist 2001), selecting best-fit model as SYM+I+G4 with 2000 bootstraps (BS) for ML analysis. ModelFinder v.2.2.0 (Kalyaanamoorthy et al. 2017) was used to select the best-fit partition model (Edge-linked) using the BIC criterion. The best-fit models according to BIC were SYM+G4 for ITS and K2P+I+G4 for *rbc*L. BI analysis employed random starting trees and four Markov Chain Monte Carlo (MCMC) simulations were run simultaneously and sampled every 1000 generations for 10 million generations. The average standard deviation of split frequencies (< 0.01) was used to assess the convergence of the two runs. Bayesian posterior probabilities (PP) were calculated as the majority consensus of all sampled trees with the first 25% discarded as burn-in.

Results and discussion

Morphological comparison

According to the classification of Chen and Hu (1979), *L. danxiashanensis* is a member of subgenus *Lysimachia* sect. *Nummularia*, which is characterised by stems prostrate to erect on the upper part, leaves opposite, racemes shortened to subcapitate, filaments longer than anthers, lower part connate into a tube, corolla and calyx with coloured glandular punctates (Fig. 2). In China, there are over 50 species of sect. *Nummularia* and it widely distributed from southwest to the east and south China. Morphologically, *Lysimachia danxiashanensis* is similar to *L. phyllocephala* Hand.-Mazz., *L. pseudohenryi* Pamp., *L. congestiflora* Hemsl. and *L. kwangtungensis* (Hand.-Mazz.) C.M.Hu by sharing the following morphological features: stems with multicellular hairs, leaves opposite and racemes terminal. However, the new species can be easily distinguished from similar species by combination characters including its purplish-red plants (vs. green), petiole without wings (vs. narrowly winged in *L. pseudohenryi* and *L. congestiflora*, narrowly margined and auriculate at base in *L. kwangtungensis* and absent in *L.phyllocephala*) and the corolla lobes serrated on upper half (vs. entire margin in all four species). A more detailed morphological comparison of these species is summarised in Table 1.

Molecular analysis

The combined aligned matrix had a length of 1268 bp (ITS: 650, *rbc*L: 615), including 373 variable sites, of which 291 were parsimony-informative. The two accessions of the new species were from the same population and formed a separate monophyletic lineage (Fig. 1: BS = 93%, PP = 0.72), the sister group of *L. rubiginosa*. Although *L. danxiashanensis* and *L. rubiginosa* both belong to

Table 1. Morphological comparison of *Lysimachia danxiashanensis* with its four closely-related species.

Characters	*L. danxiashanensis*	*L. phyllocephala*	*L. pseudohenryi*	*L. congestiflora*	*L. kwangtungensis*
Stems	upper erect, creeping at base	erect to ascending-erect, prostrate at base	erect or arcuate at base	prostrate and branches ascending	erect
Colour of plants	purplish-red	green	green	green	green
Leaf shape	ovate to broadly ovate or oval	ovate to ovate-lanceolate	rhomboid-ovate to ovate, rarely ovate-lanceolate	ovate to broadly ovate or suborbicular	ovate-lanceolate to lanceolate
Petiole wings	absent	absent	narrowly winged	narrowly winged	narrowly margined and auriculate at base
Corolla lobes	margin serrated on upper half with orange-red glandular punctates	margin entire, with sparsely transparent glandular punctates	margin entire, with transparent glandular punctates	margin entire, with dull red or black glandular punctates	margin entire, with red to dark purple glandular punctates
Style	6–8 mm; glabrous	*c.* 8 mm; puberulous	5–6 mm; lower part with pubescent	5–7 mm; glabrous	5–6 mm; glabrous
Glandular dots on Calyx	orange, dense	absent	absent	absent	orange, sparse

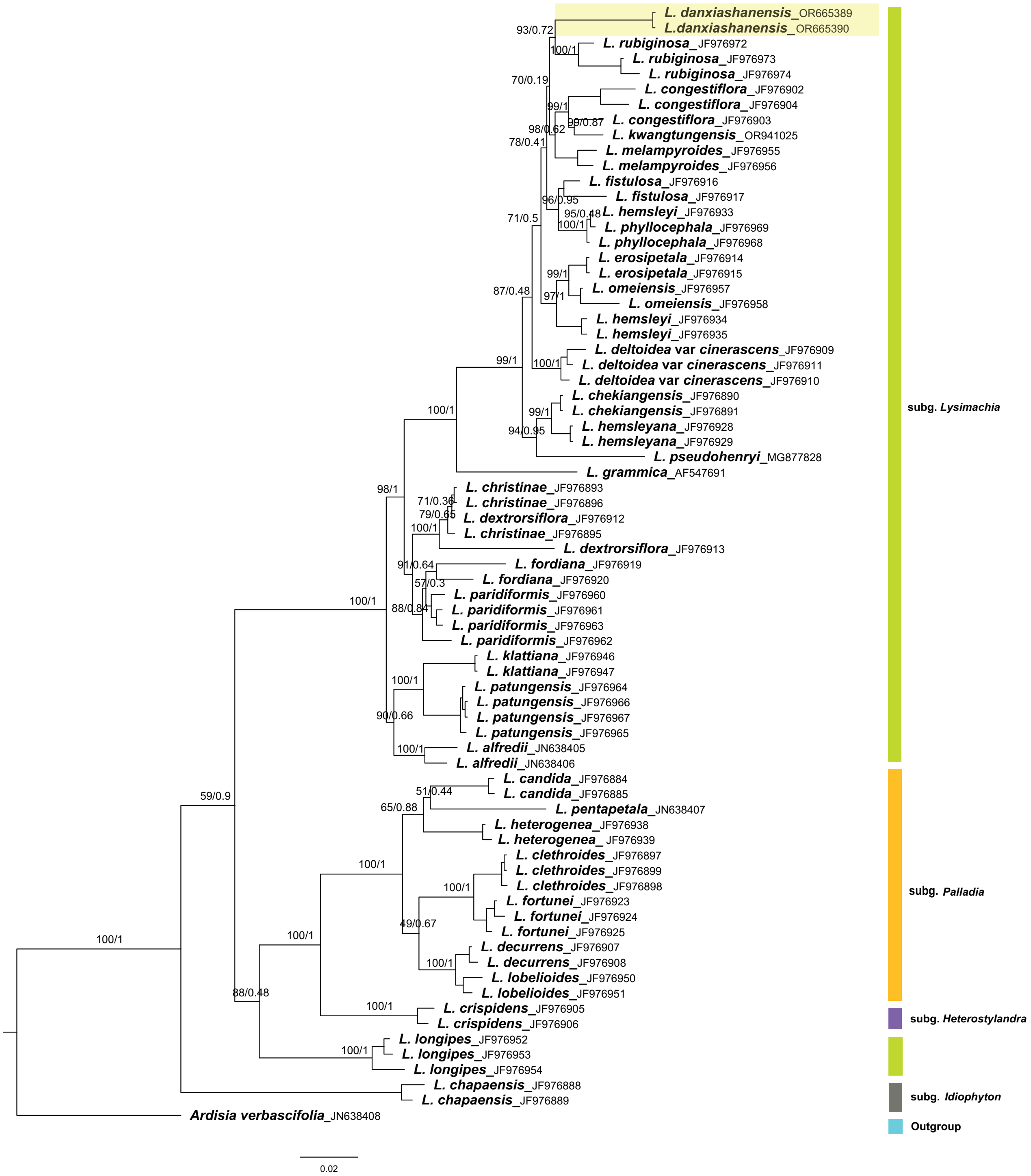

Figure 1. Phylogenetic tree of *Lysimachia danxiashanensis* and related species generated by Bayesian Inference (BI) of the combined dataset (ITS, *rbc*L). Bootstrap values of the ML and BI posterior probabilities are shown along the branches. The new species in yellow shaded area, green indicates subgen. *Lysimachia*, orange is subgen. *Palladia*, purple is subgen. *Heterostylandra* and grey is subgen. *Idiophyton*. Blue indicates outgroup, *Ardisia verbascifolia*.

subgen. *Lysimachia* sect. *Nummularia*, the new species can be easily distinguished from the latter by its shorter plants (10–28 cm vs. 30–60 (100) cm), orange glandular punctates on corolla lobes and calyx (vs. black or brown glandular striate on leaves, corolla lobes and calyx), 5–9 flowered on branches and stems axis (vs. 3–5 flowered on branches, seldom on main axis).

Geographically, *L. rubiginosa* is distributed in Guangxi, Guizhou, Hubei, Hunan, Sichuan, Yunnan and Zhejiang and it mainly grows in limestone. In contrast, the new species is distributed in Danxia landscape, Guangdong. The geographical distribution of these two taxa does not overlap.

Although the infrageneric phylogenetic relationships within Chinese *Lysimachia* remain controversial (Zhen and Chen 2012; Liu et al. 2023), the phylogenetic tree placed *L. danxiashanensis* distant from other species in this genus (Fig. 1). Based on the morphological and molecular evidence, we confirmed that *L. danxiashanensis* is a distinct species. Therefore, we describe and provide illustrations for the new species below.

Taxonomic treatment

***Lysimachia danxiashanensis* W.B.Liao, Q.Fan & G.D.Tang, sp. nov.**
urn:lsid:ipni.org:names:77335469-1
Figs 2, 3

Diagnosis. *Lysimachia danxiashanensis* can be distinguished from *L. congestiflora* by its purple-red plants (vs. green), petiole without wings (vs. narrowly winged), corolla lobes yellow with serrations on upper half (vs. dull red at base with entire margin) and calyx with orange glandular (vs. without glandular) (Fig. 4).

Type. China. Guangdong Province, Danxiashan National Park, 25°0'N, 113°37'E, 311 m a.s.l., 12 May 2023 (fl.), *Xing-Yue Zhang, Zai-Xiong Chen* DNPC 3801 (holotype SYS!; isotypes CANT! SYS!).

Description. Perennial herb, 10–28 cm tall. ***Stems*** prostrate, rooting at nodes, upper part ascending, purplish-red, terete, with dense white multicellular hairs. ***Leaves*** opposite, upper 2 or 3 pairs usually crowded, papery, ovate to broadly ovate or oval, wavy margin, 1.6–3.8 × 1.2–2.4 cm, apex acute, base broadly cuneate; adaxial surface dark green with antrorse strigose, abaxial surface purple-red, with strigose and densely pilose along the mid-rib vein; lateral veins 2–4-paired; petiole without wings, 0.5–2.7 cm, densely villous. ***Racemes*** terminal, abbreviated, capitate, 5–9 flowered; pedicel 3–5 mm long, densely pilose. ***Calyx*** 5, parted nearly to base; lobes lanceolate, 2–2.5 × 7–8.5 mm long, sparsely orange glandular on both surfaces, pilose outside. ***Corolla*** yellow; tube 1.5–2 mm; lobes 5, obovate-elliptical, 3–5 × 9–10 mm, serrate on upper half, apex acute to obtuse, abaxially glabrous, sparsely orange-red glandular, adaxially glabrous with orange-reddish glandular. ***Stamens*** 5, filaments glabrous, connate basally into a 2–3 mm high tube, free parts 2.8–4.5 mm; anthers ovate-lanceolate, dorsifixed, opening by lateral slits, ca. 2.8 mm long. ***Ovary*** white, terete, apex puberulous, glabrous at lower part; style glabrous, 6–8 mm long, stigma obtuse with papillae. ***Capsule*** subglobose, green, apex puberulous, 3–5 mm in diam.

Phenology. The flowering of *Lysimachia danxiashanensis* is from May to June; and the fruiting in June.

Distribution. *Lysimachia danxiashanensis* is currently known only from the type locality, Danxiashan National Nature Reserve, Guangdong, China.

Habit. *Lysimachia danxiashanensis* was observed to grow on wet rocks of Danxia landform at elevations 270 to 320 m.

Etymology. The specific epithet refers to the type locality, Danxiashan National Nature Reserve in Guangdong Province, China.

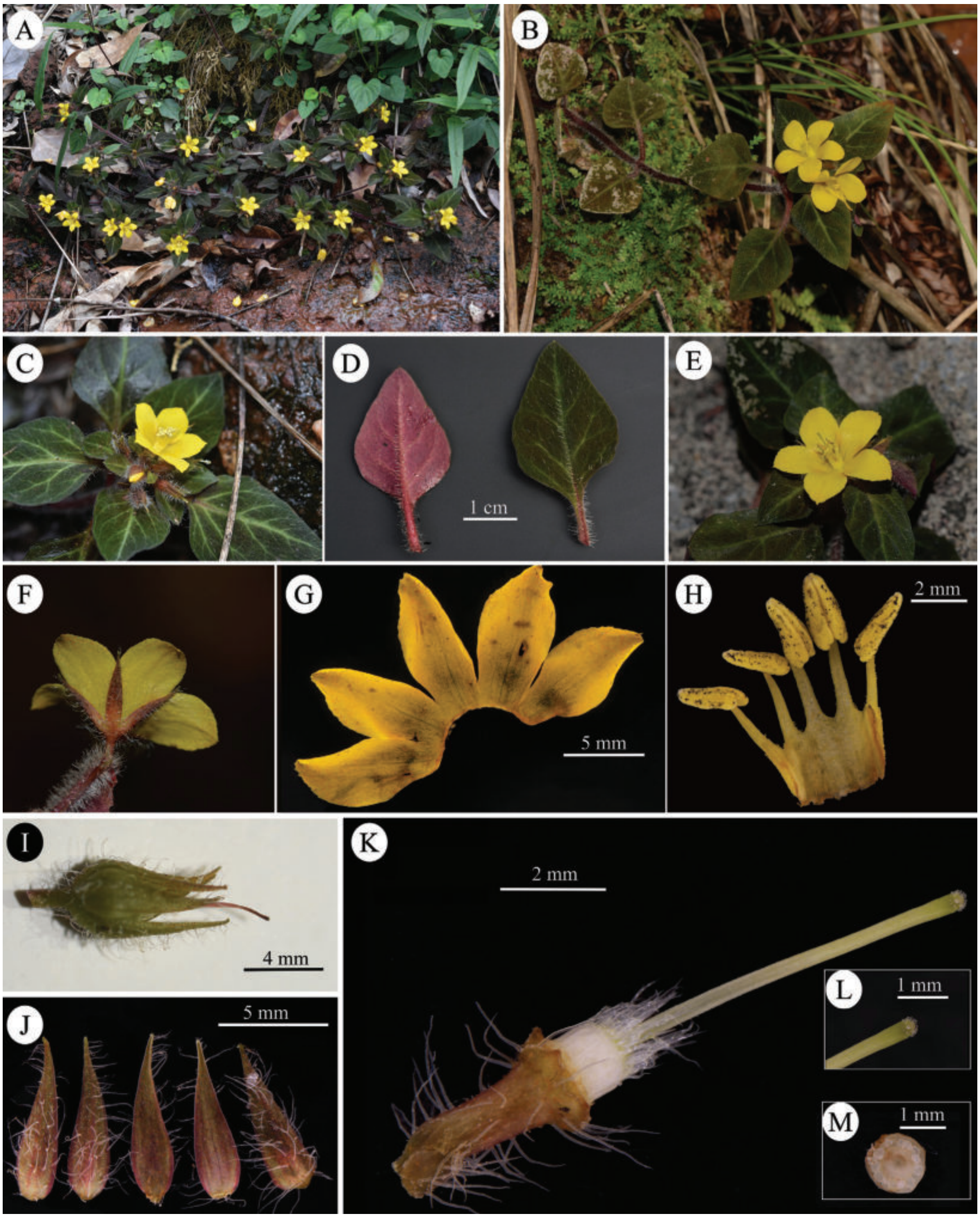

Figure 2. *Lysimachia danxiashanensis* W.B.Liao, Q.Fan & G.D.Tang, sp. nov. **A** habit **B** flowering branch **C** inflorescence **D** abaxial and adaxial views of leave **E** lateral view of flower **F** dorsal view of flower **G** adaxial side of corolla lobes **H** stamens **I** immature capsule **J** abaxial (1st, 2nd, 5th) and adaxial (3rd, 4th) views of calyx lobes **K** pistil and densely pilose pedicel **L** stigma **M** cross-section of ovary (Photographers: **A, C, D, I** by Xing-Yue Zhang; **B, E, F** by Qiang Fan; **G, H, J–M** by Jing-Min Dai).

Local name. The Chinese name of the new species is here given as 丹霞山过路黄 (Dān xiá Shān Guò Lù Huáng).

Provisional conservation status. Endangered (EN). In the past two years, we have conducted several field investigations on the Danxia landscapes in Guangdong Province, with only four populations of *Lysimachia danxiashanensis* being found in Danxiashan National Nature Reserve and the number of mature individuals is stable (total < 200 individuals); However, its habitat is on the side of the road, which is vulnerable to human disturbance. *L. danxiashanensis*

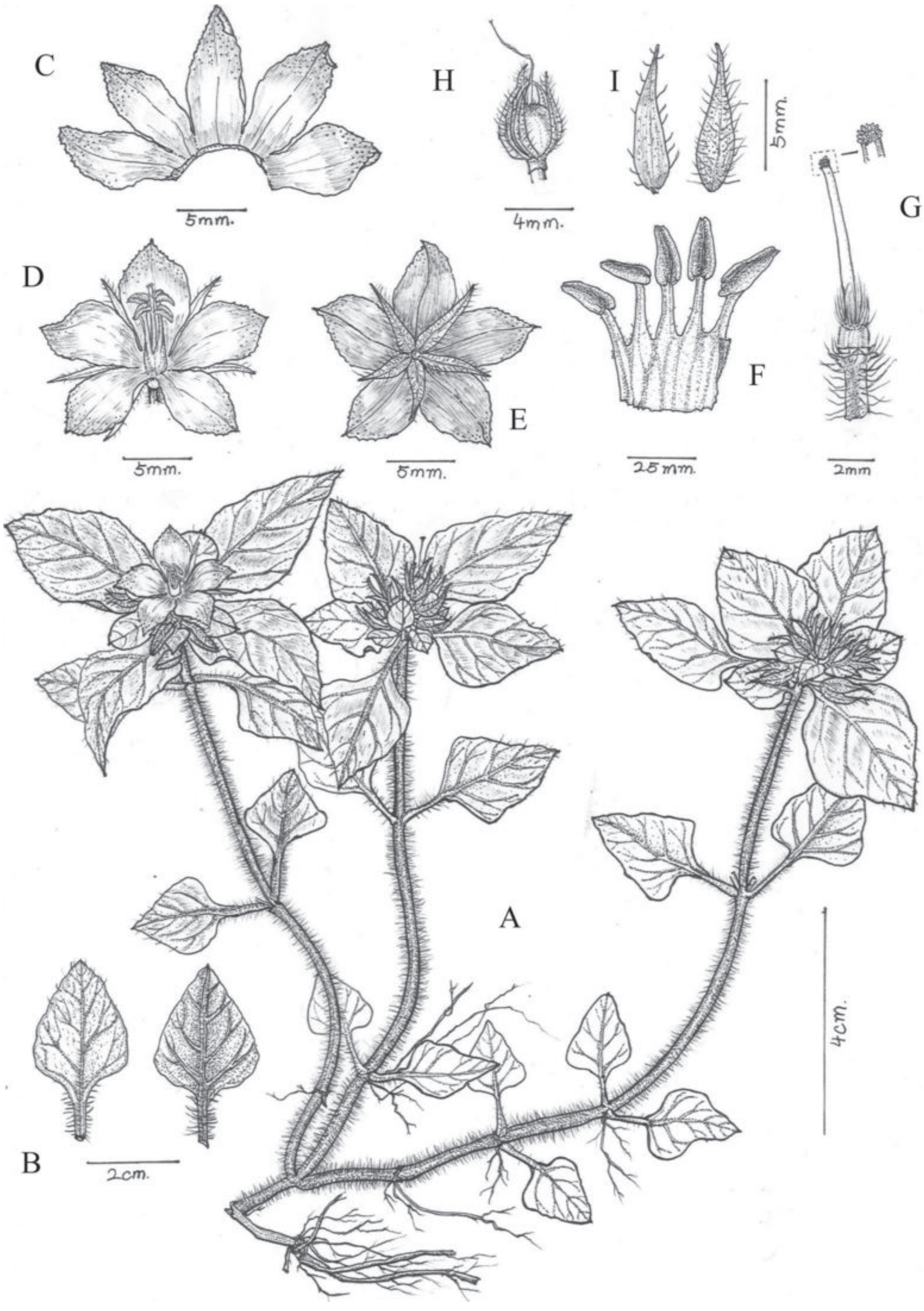

Figure 3. *Lysimachia danxiashanensis* W.B.Liao, Q.Fan & G.D.Tang, sp. nov. **A** habit **B** abaxial (left) and adaxial (right) views of leaf **C** adaxial side of corolla lobes **D** lateral view of flower **E** dorsal view of flower **F** stamens **G** pistil and stigma **H** fruit **I** adaxial (left) and abaxial (right) views of calyx (Drawn by Rong-En Wu).

is regarded as Endangered (EN) according to D (the number of mature individuals in the population < 250) (IUCN Standards and Petitions Committee 2022).

Additional specimens examined (*paratypes*). China, Guangdong: Danxiashan National Park, 25°0'N, 113°38'E, 298 m a.s.l., 12 June 2023 (fr.), *Jie-Hao Jin* DNPC 3803 (SYS!); Danxiashan National Park, 25°0'N, 113°38'E, 14 August 2023, *Qiang Fan, Jie-Hao Jin & Li-Juan Liao* DNPC 3845 (SYS!).

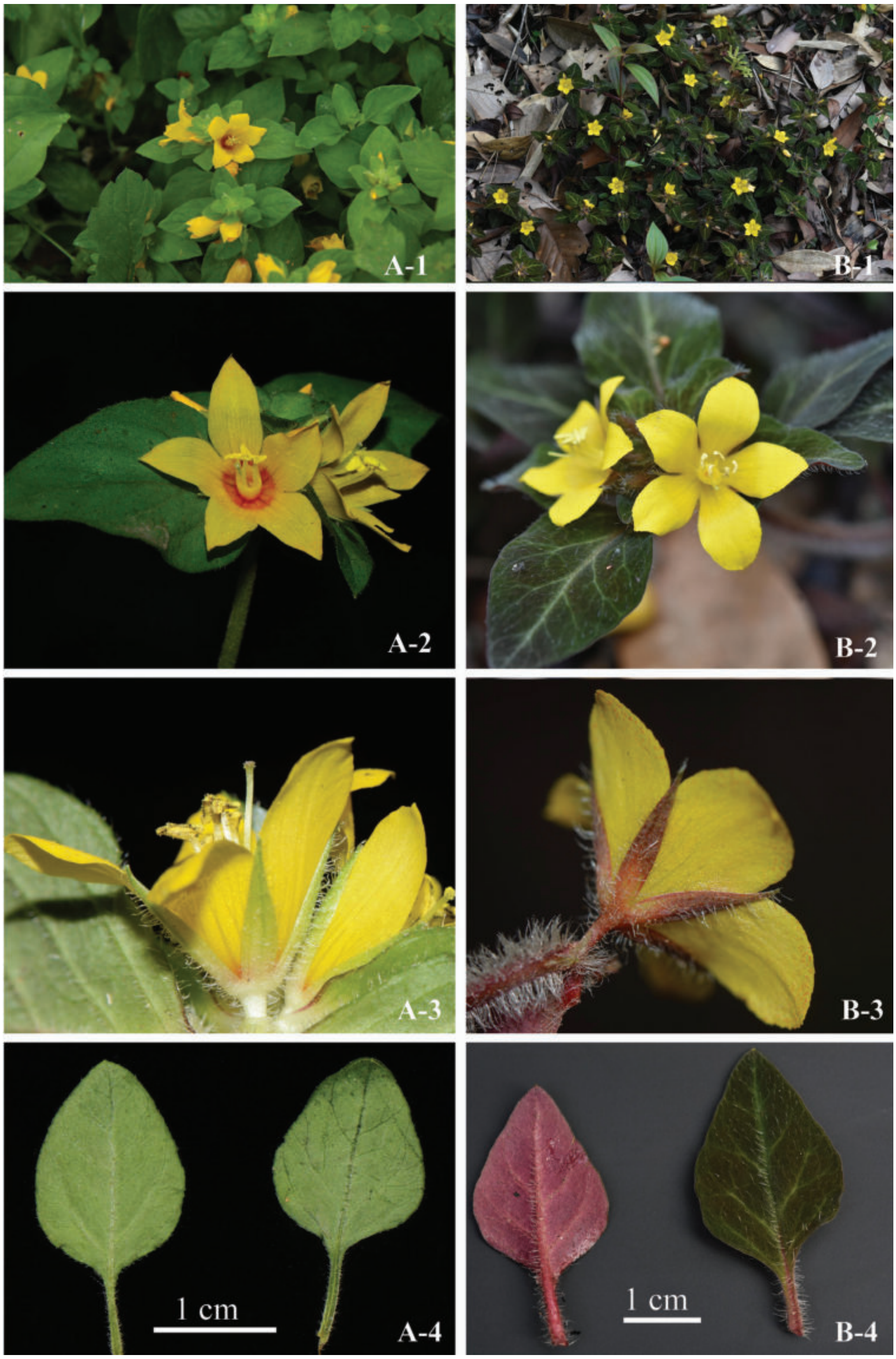

Figure 4. Morphological differences between *L. congestiflora* and *L.danxiashanensis* **A** *L. congestiflora* **B** *L. danxiashanensis* **1** plants **2** corolla lobes **3** calyx lobes **4** petiole (Photographers: **A–1** by Wan-Yi Zhao **A2–4** by Xin-Xin Zhu **B1, 2, 4** by Xing-Yue Zhang **B–3** by Qiang Fan).

Acknowledgments

We are grateful to Jie-Hao Jin and Li-Juan Liao for their assistance during field collections. We are deeply grateful to Mrs Rong-En Wu for her excellent illustrations in the manuscript. We are grateful for the photos provided by Xin-Xin Zhu and Wan-Yi Zhao. We appreciate Dr Wan-Yi Zhao and Dr Cui-Ying Huang for their help and suggestions for this article.

Additional information

Conflict of interest

The authors have declared that no competing interests exist.

Ethical statement

No ethical statement was reported.

Funding

This study was supported by the Guangdong Provincial Special Research Grant for the Creation of National Parks (2021GJGY034) and the Foundation of Administrative Committee of Danxiashan National Park (K22-33000-060, 2016-0293).

Author contributions

Xing-Yue Zhang participated field investigation, taxonomic confirmation and wrote the original draft. Jing-Min Dai performed the molecular analysis. Zai-Xiong Chen and Qiang Fan participated field investigation and collected the plants. Wen-Bo Liao and Guang-Da Tang are project leaders and contributed to paper writing.

Author ORCIDs

Xing-Yue Zhang https://orcid.org/0009-0007-5398-7100
Jing-Min Dai https://orcid.org/0009-0002-1090-4823
Qiang Fan https://orcid.org/0000-0003-4254-6936
Zai-Xiong Chen https://orcid.org/0009-0002-0475-6414
Guang-Da Tang https://orcid.org/0000-0001-5623-3928
Wen-Bo Liao https://orcid.org/0000-0001-6839-9511

Data availability

The newly-obtained sequences of Lysimachia danxiashanensis and L. kwangtungensis have been submitted to the NCBI website. The ITS and rbcL sequence data supporting the findings of this study are available within Appendix 1. The morphological data used in the study are included in this paper.

References

Chen FH, Hu CM (1979) Taxonomic and phytogeographic studies on Chinese species of *Lysimachia*. Acta Phytotaxonomica Sinica 17: 21–53.

Doyle JJ, Doyle JL (1987) A rapid DNA isolation procedure for small quantities of fresh leaf tissue. Phytochemical Bulletin 19: 11–15.

Fan Q, Chen SF, Wang LY, Chen ZX, Liao WB (2015) A new species and new section of *Viola* (Violaceae) from Guangdong, China. Phytotaxa 197(1): 15–26. https://doi.org/10.11646/phytotaxa.197.1.2

Fay MF, Swensen S, Chase MW (1997) Taxonomic affinities of *Medusagyne oppositifolia* (Medusagynaceae). Kew Bulletin 52(1): 111–120. https://doi.org/10.2307/4117844

Hao G, Hu CM (2001) Phylogenetic relationships in *Lysimachia* (Primulaceae): A cladistic analysis. Journal of Tropical and Subtropical Botany 9(2): 93–100. https://doi.org/10.3969/j.issn.1005-3395.2001.2.001

Hao G, Yuan YM, Hu CM, Ge XJ, Zhao NX (2004) Molecular phylogeny of *Lysimachia* (Myrsinaceae) based on chloroplast *trn*L-F and nuclear ribosomal ITS sequences. Molecular Phylogenetics and Evolution 31(1): 323–339. https://doi.org/10.1016/S1055-7903(03)00286-0

Hu CM (1994) On the geographical distribution of the Primulaceae. Journal of Tropical and Subtropical Botany 04: 1–14. https://doi.org/10.3969/j.issn.1005-3395.1994.4.001

Hu CM, Kelso S (1996) Primulaceae. In: Wu ZY, Raven PH (Eds) Flora of China (Vol. 15). Science Press, Beijing, and Missouri Botanical Garden Press, St Louis, Missouri, 39–189.

Huang RZ, Liao M, Han W, Yang YZ, Zhou MY, Feng HH, Tang GD (2020) *Lysimachia daqiaoensis* (Primulaceae), a new cave species from Guangdong, China. Phytotaxa 430(1): 41–45. https://doi.org/10.11646/phytotaxa.430.1.6

Huelsenbeck JP, Ronquist F (2001) MRBAYES: Bayesian inference of phylogenetic trees. Bioinformatics 17(8): 754–755. https://doi.org/10.1093/bioinformatics/17.8.754

IUCN Standards and Petitions Committee (2022) Guidelines for using the IUCN Red List categories and criteria. Version 15.1: Prepared by the Standards and Petitions Subcommittee. https://www.iucnredlist.org/resources/redlistguidlines

Kalyaanamoorthy S, Minh BQ, Wong TKF, von Haeseler A, Jermiin LS (2017) ModelFinder: Fast model selection for accurate phylogenetic estimates. Nature Methods 14(6): 587–589. https://doi.org/10.1038/nmeth.4285

Katoh K, Standley DM (2013) MAFFT multiple sequence alignment software version 7: Improvements in performance and usability. Molecular Biology and Evolution 30(4): 772–780. https://doi.org/10.1093/molbev/mst010

Kodela PG (2006) *Lysimachia* (Myrsinaceae) in New South Wales. Telopea 11(2): 147–154. https://doi.org/10.7751/telopea20065718

Kress WJ, Erickson DL (2007) A two-locus global DNA barcode for landplants: The coding *rbc*L gene complements the non-coding *trn*H-*psb*A spacer region. PLOS ONE 2(6): e508. https://doi.org/10.1371/journal.pone.0000508

Liu TJ, Zhang SY, Wei L, Lin W, Yan HF, Hao G, Ge XJ (2023) Plastome evolution and phylogenomic insights into the evolution of *Lysimachia* (Primulaceae: Myrsinoideae). BMC Plant Biology 23(1): e359. https://doi.org/10.1186/s12870-023-04363-z

Minh BQ, Schmidt HA, Chernomor O, Schrempf D, Woodhams MD, von Haeseler A, Lanfear R (2020) IQ-TREE 2: New models and efficient methods for phylogenetic inference in the genomic era. Molecular Biology and Evolution 37(5): 1530–1534. https://doi.org/10.1093/molbev/msaa015

Thiers B (2023) [continuously updated]: Index Herbariorum: A global directory of public herbaria and associated staff. New York Botanical Garden's Virtual Herbarium. http://sweetgum.nybg.org/science/ih/ [Accessed 23.01.2024]

Wang Y, Ma W, Zhou SB, Liu K (2018) *Lysimachia tianmaensis* (Primulaceae), a new species from Anhui, China. PhytoKeys 98: 117–124. https://doi.org/10.3897/phytokeys.98.23751

White TJ, Bruns T, Lee S, Taylor J (1990) Amplification and Direct Sequencing of Fungal Ribosomal RNA Genes for Phylogenetics. In: Innis MA, Gelfand DH, Sminsky J, White TJ (Eds) PCR protocols: A Guide to Methods and Applications. Academic Press, San Diego, 315–322. https://doi.org/10.1016/B978-0-12-372180-8.50042-1

Yan HF, Zhang CY, Anderberg AA, Hao G, Ge XJ, Wiens JJ (2018) What explains high plant richness in East Asia? Time and diversification in the tribe Lysimachieae (Primulaceae). The New Phytologist 219(1): 436–448. https://doi.org/10.1111/nph.15144

Yan HF, Huang Y, Zhang HJ, Yi SR (2022) *Lysimachia coriacea* (Primulaceae, Myrsinoideae), a new species from Chongqing, China. PhytoKeys 215: 87–94. https://doi.org/10.3897/phytokeys.215.91488

Zhang CY, Wang FY, Yan HF, Hao G, Hu CM, Ge XJ (2011) Testing DNA barcoding in closely related groups of *Lysimachia* L. (Myrsinaceae). Molecular Ecology Resources 12(1): 98–108. https://doi.org/10.1111/j.1755-0998.2011.03076.x

Zhen W, Chen LQ (2012) Phylogenetic relationship of sect. *Nummularia* (*Lysimachia*): Evidence from ITS sequences. Guihaia 32(2): 163–166. https://doi.org/10.3969/j.issn.1000-3142.2012.02.005

Appendix 1

Table A1. List of the GenBank accession numbers of the *rbc*L and ITS sequences of sampled species in this study.

Taxon	Voucher	Locality	*rbc*L	ITS
Lysimachia alfredii Hance	Hao394	Lianping, Guangdong, China	JF942344	JN638405
	Y2009279	Ruyuan, Guangdong, China	JF942343	JN638406
Lysimachia candida Lindl.	Ge2010001	Yangchun, Guangdong, China	JF942346	JF976885
	Y2010016	Tongbai, Henan, China	JF942345	JF976884
Lysimachia chapaensis Merrill	GBOWS704	Maguan, Yunan, China	JF942350	JF976889
	GBOWS878	Hekou, Yunnan, China	JF942349	JF976888
	Hao209	Wuhan, Hubei, China	JF942392	AF547691
Lysimachia chekiangensis C.C.Wu	Y2009263-1	Longquan, Zhejiang, China	JF942352	JF976891
	Y2009263-2	Longquan, Zhejiang, China	JF942351	JF976890
Lysimachia christinae Hance	Y2009209	Jiujiang, Jiangxi, China	JF942357	JF976896
	Y2009235	Shucheng, Anhui, China	JF942356	JF976895
	Y2009272	Jiangle, Fujian, China	JF942354	JF976893
Lysimachia clethroides Duby	Y2009157	Tongbai, Henan, China	JF942362	JF976899
	Y2009248	Lin'an, Zhejiang, China	JF942360	JF976898
	Hao955	Wuxi, Chongqing, China	JF942359	JF976897
Lysimachia congestiflora Hemsl.	Y2009196	Xinjian, Jiangxi, China	JF942367	JF976904
	Y2009266	Longquan, Zhejiang, China	JF942366	JF976903
	GBOWS262	Malipo, Yunnan, China	JF942365	JF976902
Lysimachia crispidens Hemsl.	Hao212	Yichang, Hubei, China	JF942369	JF976906
	Y2010029	Xinhua, Hubei, China	JF942368	JF976905
Lysimachia decurrens Forst.F.	GBOWS1234	Hekou, Yunnan, China	JF942371	JF976908
	Ye et al. 3980	Lianshan, Guangdong, China	JF942370	JF976907
Lysimachia deltoidea var. *cinerascens* Franch.	Hao & Yan1033	Dali, Yunnan, China	JF942374	JF976911
	Hao731	Yongsheng, Yunnan, China	JF942373	JF976910
	GLM081121	Zhongdian, Yunnan, China	JF942372	JF976909
Lysimachia dextrorsiflora X.P.Zhang, X.H.Guo & J.W.Shao	Y2009265-1	Longquan, Zhejiang, China	JF942376	JF976913
	Y2009265-2	Longquan, Zhejiang, China	JF942375	JF976912
Lysimachia erosipetala Chen et C.M.Hu	Y2010037-1	Emeishan, Sichuan, China	JF942378	JF976915
	Y2010037-2	Emeishan, Sichuan, China	JF942377	JF976914
Lysimachia fistulosa var. *wulingensis* Chen et C.M.Hu	Ye et al. 3561	Lianshan, Guangdong, China	JF942381	JF976917
	Ning20101	Jinggangshan, Jiangxi, China	JF942380	JF976916

Taxon	Voucher	Locality	*rbc*L	ITS
Lysimachia fordiana Oliv.	Ye et al. 3940	Lianshan, Guangdong, China	JF942384	JF976920
Lysimachia fortunei Maxim	Y2009285	Ruyuan, Guangdong, China	JF942383	JF976919
Lysimachia hemsleyana Maxim	Guo20001	Ningguo, Anhui, China	JF942398	JF976932
	Y2009245	Lin'an, Zhejiang, China	JF942395	JF976929
	Y2010008	Tongbai, Henan, China	JF942394	JF976928
Lysimachia hemsleyi Franch.	Hao713	Huili, Sichuan, China	JF942402	JF976935
	Hao730	Yongsheng, Yunnan, China	JF942401	JF976934
Lysimachia heterogenea Klatt	Y2009199	Jiujiang, Jiangxi, China	JF942407	JF976939
	Y2010009	Tongbai, Henan, China	JF942405	JF976938
Lysimachia klattiana Hance	Y2010014-1	Tongbai, Henan, China	JF942415	JF976947
	Y2010014-2	Tongbai, Henan, China	JF942414	JF976946
Lysimachia lobelioides Wall.	Hao303	Menglian, Yunnan, China	JF942419	JF976951
	Y2010001	Jingping, Yunan, China	JF942418	JF976950
Lysimachia longipes Hemsl.	Y2009255-1	Kaihua, Zhejiang, China	JF942422	JF976954
	Y2009255-2	Kaihua, Zhejiang, China	JF942421	JF976953
	Guo xinhu200012	Shitai, Anhui, China	JF942420	JF976952
Lysimachia melampyroides R.Knuth	Lichanghan8174	Shangzhi, Hunan, China	JF942424	JF976956
	Dengyunfei15945	Xinning, Hunan, China	JF942423	JF976955
Lysimachia omeiensis Hemsl.	Y2010033	Emeishan, Sichuan, China	JF942426	JF976958
	Hao224	Emeishan, Sichuan, China	JF942425	JF976957
Lysimachia paridiformis var. *paridiformis* Franch.	Chen s.n.	Enshi, Hubei, China	JF942429	JF976961
Lysimachia paridiformis var. *stenophylla* Franch.	Deng15921	Xinning, Hunan, China	JF942431	JF976963
	Y2010044	Emeishan, Sichuan, China	JF942430	JF976962
	GLM07658	Zhenxiong, Yunnan, China	JF942428	JF976960
Lysimachia patungensis Hand.-Mazz.	Y2009187	Jinggangshan, Jiangxi, China	JF942435	JF976967
	Y2009258	Kaihua, Zhejiang, China	JF942434	JF976966
	Y2009280	Ruyuan, Guangdong, China	JF942433	JF976965
	Ye et al. 3851	Lianshan, Guangdong, China	JF942432	JF976964
Lysimachia pentapetala Bunge	Y2010013-1	Tongbai, Henan, China	JF942437	JN638407
Lysimachia phyllocephala Hand.-Mazz.	Y2010030	Emeishan, Sichuan, China	JF942439	JF976969
	Y2010048	Nanchuan, Chongqing, China	JF942438	JF976968
	GLM07662	Yanjin, Yunnan, China	JF942399	JF976933
Lysimachia pseudohenryi Pamp.	Guo XH 20007	East Asia	MG950600	MG877828
Lysimachia rubiginosa Hemsl.	Hao704	Hongya, Sichuan, China	JF942444	JF976974
	Y2010036	Emeishan, Sichuan, China	JF942443	JF976973
	Hao419	Dujiangyan, Sichuan, China	JF942442	JF976972
Lysimachia danxiashanensis	DNPC-3711	Danxiashan, Guangdong, China	PP025352	OR665389
	DNPC-3711	Danxiashan, Guangdong, China	PP025354	OR665390
Lysimachia kwangtungensis (Handel-Mazzetti) C.M.Hu	DNPC-3743	Danxiashan, Guangdong, China	PP025355	OR941025
Ardisia verbascifolia Mez.	GBOWS1216	Hekou, Yunnan, China	JN638410	JN638408

PhytoKeys 237: 269–279 (2024)
DOI: 10.3897/phytokeys.237.115098

Research Article

Molecular and morphological evidence support a new species of Rosaceae *Prunus* subg. *Cerasus* from Wuyishan National Park, southeast China

Xiangui Yi[1*], Jingjing Dong[1*], Jie Chen[1], Huajin Zhou[1], Tong Wu[1], Shucheng Gao[1], Xiangzhen Chen[1], Meng Li[1], Xianrong Wang[1]

1 *Co-Innovation Center for the Sustainable Forestry in Southern China, College of life sciences, Cerasus Research Center, Nanjing Forestry University, Nanjing 210037, Jiangsu, China*

Corresponding author: Xiangui Yi (yixiangui@njfu.edu.cn)

Abstract

Prunus tongmuensis, a new species of cherry blossom, is described and illustrated from Wuyishan National Park, southeast China. This species is characterized by its tubular to nearly bottle-shaped receptacles and dark purple drupes. It can be distinguished from other wild cherry trees by its flowers and leaves, reddish brown young leaves, presence of 1–2 glands at the base of leaves, petioles densely covered with yellowish brown villi, longer pedicels (0.6–2.5 cm), villous pistil, and dark purple drupes. In the present study, we conducted a comprehensive morphological study based on specimens of the new species and its morphologically close species, field observations, and examination of pollen morphology. In addition, our phylogenetic analysis based on the complete plastid genome sequences further confirms the status of the new species and indicates that it is closely related to *Prunus clarofolia*, however, it notably differs in leaf shape, size, petiole villus color, gland location, timing of flower and leaf openings, and reflexed or spread sepals, as well as drupe color.

Key words: molecular phylogeny, morphological comparison Rosaceae, subgenus. *Cerasus*, taxonomy

Academic editor: Hanno Schaefer
Received: 2 November 2023
Accepted: 19 January 2024
Published: 31 January 2024

Citation: Yi X, Dong J, Chen J, Zhou H, Wu T, Gao S, Chen X, Li M, Wang X (2024) Molecular and morphological evidence support a new species of Rosaceae *Prunus* subg. *Cerasus* from Wuyishan National Park, southeast China. PhytoKeys 237: 269–279. https://doi.org/10.3897/phytokeys.237.115098

Introduction

Prunus L. subg. *Cerasus* (Mill.) A. Gray, a member of the family Rosaceae (Li and Bartholomew 2003), is characterized by its densely lenticelled bark, young leaves frequently folded in half, and the presence of glands at the tip of the petiole or along the leaf blade edge (Wang 2014). This subgenus comprises approximately 150 species distributed in the temperate to subtropical zone of the Northern Hemisphere, including Asia, Europe, and North America (Iwatsuki et al. 2001; Li et al. 2022). China has a high species diversity of the subgenus (Zhu et al. 2018), with over 50 species mainly distributed in the western, southwestern, and eastern regions of the country. Most of these species exhibit a broad distribution range and significant morphological variation. Notably, there

---

* Contributed equally as the first authors.

are distinct differences observed both between different species and between different populations of the same species (Bortiri et al. 2006).

The Wuyi Mountains are situated on the boundary of the provinces Fujian and Jiangxi with an average elevation of 1100 m. The highest point in the region is Huanggang Mountain, reaching an altitude of 2158 m, making the area abundant in resources for cherry blossom (Xie et al. 2007). During 2018–2021, we conducted several botanical expeditions in Wuyishan National Park and its adjacent areas. A population of *Prunus* was discovered in Tongmuguan. However, this species was found to have notable differences from any known species in the genus. In-depth morphological comparison and examination of specimens revealed that the morphology of this species closely resembled that of *Prunus dielsiana* (Schneid.) Yü et Li; however, it notably differs in the location of glands, timing of flower and leaf openings, reflexed or spread sepals, and drupe color (Wang 2014). Further morphological comparisons with other relatives based on herbarium specimens clearly distinguish the Tongmuguan population as a new species due to its distinctive reddish brown young leaves, the presence of 1–2 glands at the base of the leaves, petioles densely covered with yellowish brown villi, longer pedicels (0.6–2.5 cm), pubescent pistil, and dark purple drupes. Hence, we describe, illustrate, and name it as *Prunus tongmuensis*, providing a description, accompanied by photographs and a morphological comparison with closely-related species, as well as an exploration of its phylogenetic position within the genus.

Materials and methods

Morphological study

Morphological observations were conducted based on living plants in the field and dried specimens in herbaria. A total of 20 specimens were collected from seven species, of which two were the new species and 18 specimens from six closely related species. The closely related species are *Prunus clarofolia* (Schneid.) Yü et Li, *P. dielsiana* (Schneid.) Yü et Li, *P. discoidea* Yü & Li, *P. pseudocerasus* (Lindl.) G. Don, *P. conradinae* (Koehne) Yü et Li and *P.* × *subhirtella* (Miq.) Sok. The material for morphological study is listed in Table 1. Measurements were conducted manually with rulers or using ImageJ software (Version 1.54b, Bethesda, MD, USA, Rasband 1997–2017). Morphological comparison was carried out among six closely related species based on 18 specimens deposited in herbaria or digital specimens provided by the National Plant Specimen Resource Center, NPSRC (available at https://www.cvh.ac.cn/ accessed 8 March 2019), Global Biodiversity Information Facility (available at https://www.gbif.org/ accessed 9 April 2019), and JSTOR (available at https://plants.jstor.org/ accessed 20 May 2019). Two specimens of the new species were deposited in the Herbarium of Nanjing Forestry University (Voucher specimens *X.G. Yi-201832301*; *X.G. Yi-201832302* (NF)). An identification key of *Prunus* L. subg. *Cerasus* (Mill.) for seven species is also provided.

The observation of pollen morphology analysis was carried out using pollen samples of specimen *X.G. Yi-201832302* collected from Wuyishan National Park. Mature and well-developed pollen grains were selected for observation. The morphology of pollen grains was scanned and photographed using an electron microscope (ZEISS EVO LS10, Germany) after being sputter-coated with gold.

Table 1. Species names and voucher specimen information.

Species name	Voucher specimen	Locality
Prunus clarofolia	Chen Ze-Ying PE01802945(PE)	Si Chuan, China
	Zhao Qing-sheng & Tan Zhong-ming CDBI0045472(CDBI)	Si Chuan, China
	Xiao Shun-chang CDBI0045468(CDBI)	Si Chuan, China
Prunus dielsiana	He Xian-yu NAS00357009(NAS)	An Hui, China
	C.T.Hwa NAS00357021(NAS)	Si Chuan, China
	H.Migo NAS00357093(NAS)	Zhe Jiang, China
Prunus discoidea	H.Migo NAS00357008(NAS)	Jiang Xi, China
	Li Pan CSH0073332(CS)	Zhe Jiang, China
	Zhang Fang-gang ZMNH0061126(ZMNH)	Zhe Jiang, China
Prunus pseudocerasus	J. I. Jeon et al. PE01928048(PE)	Si Chuan, China
	Lin Qin-Zhong CSFI011626(CSFI)	Hu Nan, China
	Tan Ce-ming SZG00026422	Jiang Xi, China
Prunus conradinae	Zhou Shi-liang PE2062176(PE)	Yun Nan, China
	T.T.Yu et H.T.Hsai PE01296356(PE)	Gui Zhou, China
	Zhang Dai-gui JIU23231 (JIU)	Hu Bei, China
Prunus × subhirtella	Chen Zhi-Yuan CCAU0009236(CCAU)	Hu Bei, China
	C.T.Hwa NAS00358355(NAS)	Si Chuan, China
	Zhang Dai-gui JIU25570(JIU)	Hu Nan, China
Prunus tongmuensis	Xiangui Yi(NF)	Fu Jian, China
	Xiangui Yi(NF)	Fu Jian, China

Phylogenetic study

Genomic DNA was extracted from fresh leaves of the new species from the specimens *X.G. Yi-201832301* and *X.G. Yi-201832302* (NF) using the DNA extraction kit DP305 (Tiangen Biotechnology (Beijing) Co., LTD.) following the manufacturer's instructions. DNA quality was measured using a NanoDrop 2000 spectrophotometer (NanoDrop Technologies; Thermo Fisher Scientific, Inc., Wilmington, DE, USA). The qualified DNAs (≥50 ng) were sent to Novogene Bioinformatics Technology Co., Ltd. (Beijing, China) for paired-end (PE) library construction and genome-skimming sequencing. The generated reads were assembled using the GetOrganelle pipeline (Jin et al. 2020). The genome annotation was performed with CpGAVAS (Liu et al. 2012), then the inverted repeat (IR) boundaries were manually adjusted and confirmed using Geneious prime version 2021.0.4 (https://www.geneious.com/). In total, two plastid genomes of the new species were assembled and annotated. In order to determine the phylogenetic position of this species in *Prunus* L. subg. *Cerasus* (Mill.), complete plastid genomes of 34 plastid genomes were downloaded from NCBI and aligned with the two plastid genomes of the new species to reconstruct the phylogenetic trees with *P. serotina* and *P. padus* as outgroups (Fig. 1). The 36 plastid genomes were initially aligned using MAFFT version 7 (Katoh and Standley 2013), and then manually checked and edited using PhyloSuite version 1.2.2. Maximum likelihood (ML) analyses were conducted using IQ-tree version 1.6.12 (Trifinopoulos et al. 2016) with 10,000 ultrafast bootstrap (UFBS) replicates. The Bayesian Information Criterion (BIC) was employed to calculate the best fitting substitution models using PhyloSuite version 1.2.2. (Lu et al. 2018; Fu et al. 2020; Medeiros et al. 2020).

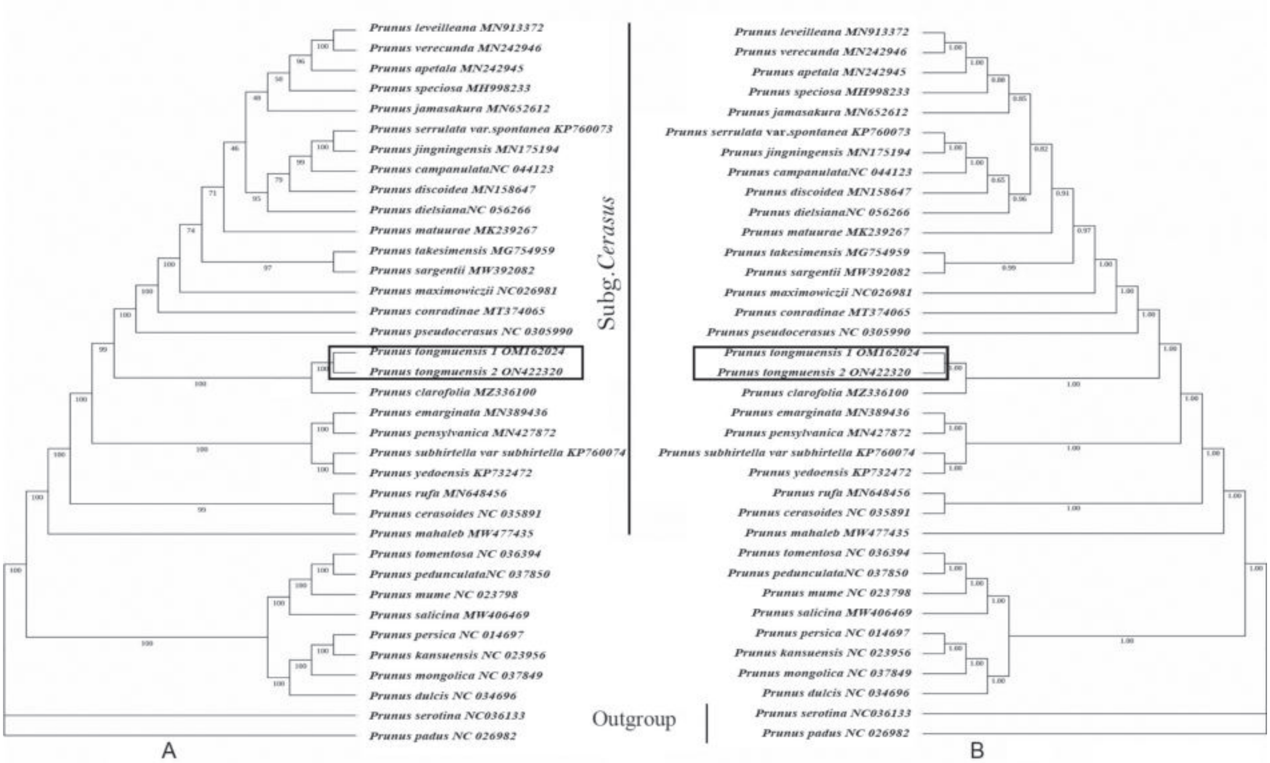

Figure 1. Maximum Likelihood (ML) tree (**A**) and Bayesian inference (BI) tree (**B**) of cherry blossom inferred from the plastid genome. The numbers associated with branches are maximum likelihood bootstrap (MLBS) values of **A** and Bayesian posterior probabilities (PP) of **B**.

Bayesian inference (BI) analysis was carried out using MrBayes version 3.2.2 (Ronquist et al. 2012). The Markov chain Monte Carlo analysis was executed for 2,000,000,000 generations, with one cold and three heated chains, each starting with a random tree, and sampled at every 1000 generations. Convergence of runs was accepted when the average standard deviation (*d*) of split frequencies was < 0.01. The first 25% of the trees were discarded as burn-in, and the remaining trees were used to construct majority-rule consensus trees. The final trees obtained from ML and BI analyses were visualized using FigTree v.1.4.2 (Rambaut 2009).

Results and discussion

Morphological study

The morphological study revealed distinctive characteristics of the new species *P. tongmuensis*, including elongated oval leaves with doubly serrated edges lacking glands. Additionally, the leaves are densely covered with fine villi on both surfaces. The young leaves display a reddish-brown color and are adorned with small yellow villi on the petioles. There are one to two glands situated at the base of each leaf blade. The bracts of the new species appear oblong or fan-shaped, distinguished by their short pedicels. Its hypanthium displays a tubular-campanulate form, as its sepals vary between triangular or long lanceolate shapes with entire margins. Notably, the style slightly surpasses the stamens in length. Based on these traits, it is inferred that the new species pertains to *Prunus* Subg. *Cerasus*. Morphologically, the new species bears the closest resemblance to *P. dielsiana* in terms of leaf shape. However, the new species can be easily distinguished from *P. dielsiana* by having 1–2 glands at the base of the leaves and the sepals are not reflexed (Table 2). In addition, we compared the new species to other morphologically similar species and revealed significant differences among them (see the key).

Key to the new species and its morphologically similar species in the genus

1 Sepals reflexed **2**
– Sepals erect or spread **4**
2 Petals rounded and obtuse, hypanthium glabrous, style base sparsely pubescent, bracts with conical or capitate glands at tooth ends, stipules linear.. **1. *P. clarofolia***
– Petals sharply lobed or conspicuously concave, hypanthium outside pilose, style glabrous; stipules narrowly banded.. **3**
3 Flowers opening before leaves.. **2. *P. discoidea***
– Flowers opening at same time as leaves .... **3. *P. dielsiana***
4 Leaf margins bluntly notched and double serrated, hypanthium tubular, drupe ripening red **5**
– Leaf edges sharply double serrated, hypanthium suburceolate, drupe ripening black or dark purple **6**
5 Hypanthium outside sparsely pilose, flowers white.....**4. *P. pseudocerasus***
– Hypanthium smooth and glabrous, flowers white, pink or red .... **5. *P. conradinae***
6 Flowers opening before leaves, petiole with 1–3 glands, densely white pubescent .... **6. *P. subhirtella***
– Flowers opening at same time as leaves, leaf blade base with 1–2 glands, petiole densely yellow pilose .... **7. *P. tongmuensis***

Plastid genome structure of *Prunus tongmuensis*

The plastid genome of *P. tongmuensis* (voucher specimen *X.G. Yi-201832301*) exhibits a ring tetrad structure typical for higher plants. The total length of the

Table 2. Diagnostic macro-morphological characteristic of *P. tongmuensis*, *P. clarofolia* and *P. dielsiana*.

	P. tongmuensis	***P. clarofolia***	***P. dielsiana***
Leaf shape	no glands at the end of teeth	tooth end with small glands or glands not obvious	obvious glands at the end of tooth
Leaf size(cm)	4–10 /2–4	3–6 /2–4	6–14 /2.5–4.5
Petiole villi color	Yellow	white	white
Glands	1–2 glands at leaf base	1–2 glands on the petiole	1–3 glands on the petiole
Inflorescence	Flowers 1-(2, 3)-4, flowers opening at same time as leaves	Flowers 2–4(-5), flowers opening at same time as leaves	Flowers 3–6, flowers opening before leaves
Hypanthium	tubular-campanulate	campanulate	campanulate
Sepal	erect or spread	reflexed	reflexed
drupe color	ripening dark purple	ripening red	ripening red

genome is 157,926 bp, consisting of a large single-copy region (LSC) with the length of 86,025 bp, a small single-copy region (SSC) with the length of 19,117 bp, and two inverted repeat regions with combined length of 26,392 bp. The total GC content is 36.7%, while the AT content is 63.3% (Fig. 2). The plastid genome of *P. tongmuensis* totally contains 130 genes, which can be categorized into three groups: 85 protein-coding genes (PCGs), 37 transfer RNA (tRNA) genes, and 8 ribosomal RNA (rRNA) genes. 21 genes are duplicated in the two inverted repeat regions.

Among the 130 genes, 81 genes can be attributed to two categories: genes involved in photosynthesis, such as Photosystem Ⅰ, Photosystem Ⅱ, Cytochrome b/f 6 complex, ATP synthase; and NADH dehydrogenase and genetically related genes, including RubisCO large subunit, RNA polymerase, Ribosomal

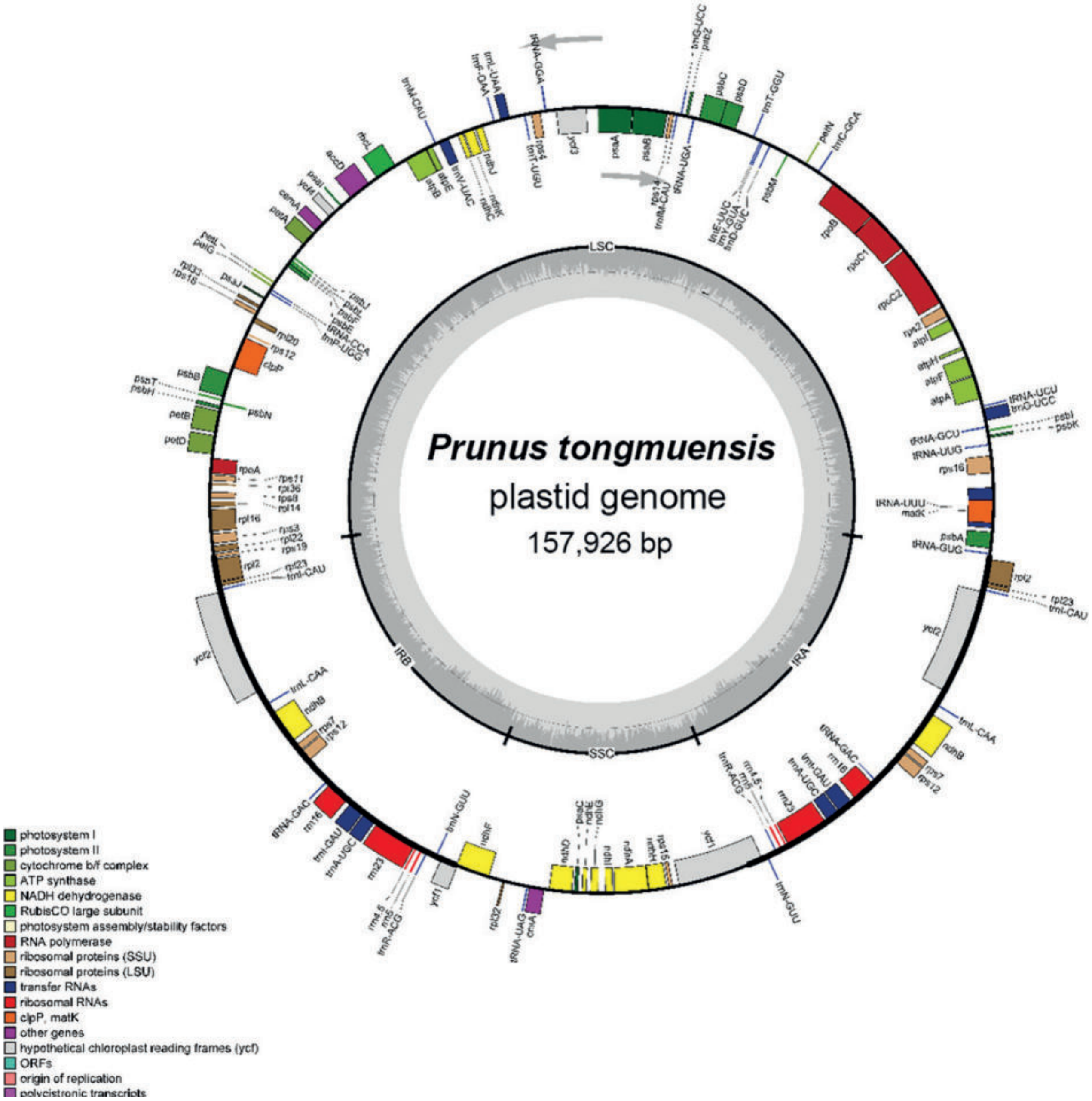

Figure 2. Plastid genome map of *Prunus tongmuensis*.

proteins-SSU, Ribosomal proteins-LSU, transfer RNAs, and Ribosomal RNAs. Additionally, there are 11 genes, which consist of *clpP*, *matk*, and genes related to the hypothetical chloroplast reading frames.

Molecular phylogenetic study

The alignment of the plastid genomes was 164,917 bp long. The model TVM+F+R2 for ML analysis and GTR+F+I+G4 for BI analysis was used according to the Bayesian information criteria (BIC). Our results show that *Prunus* subg. *Cerasus* is resolved as a clade with strong support values (BS = 99%, PP = 1), which is consistent with previous studies (Shi et al. 2013; Shen et al. 2023). Two accessions of the new species *P. tongmuensis* were well resolved as a distinct clade, which is sister to the species *P. clarofolia* (BS = 100%, PP = 1) (Fig. 1).

Taxonomic treatment

***Prunus tongmuensis* X.G.Yi & X.R.Wang, sp. nov.**
urn:lsid:ipni.org:names:77335470-1
Figs 3, 4

Diagnosis. This species closely resembles *P. dielsiana* in leaf shape, however, it can be distinguished by no glands at the end of teeth (obvious glands at the end of tooth in *P. dielsiana*), petiole yellow villous (petiole white villous in *P. dielsiana*), 1–2 glands at leaf base (1–3 glands on the petiole in *P. dielsiana*), Flowers 1–4 (2, 3), flowers opening at same time as leaves (flowers 3–6, flowers opening before leaves in *P. dielsiana*), sepal erect or spread (sepal reflexed in *P. dielsiana*), ripening dark purple (ripening red in *P. dielsiana*).

Type. China. Fujian Province: Tongmuguan, Wuyishan National Park, 27°74.91'N, 117°67.49'E, elev. ca. 728 m, 10 March, 2018, *X.G. Yi 201832301* NF-201832302 (Holotype).

Description. Trees or shrubs, 3–10 m tall. Bark grayish brown. Young branchlets yellow-green, densely yellow villous. Winter buds ovoid, 2–4 mm. Stipules narrowly lorate, slightly shorter than petiole, caducous, margin glandular-serrate. Petiole 5 × 8 mm, densely covered with yellow villi. Leaf blade obovate, elliptic, or obovate-oblong, 4–10 × 2–4 cm, base rounded to broadly cuneate, margin biserrate or sharply serrulate, teeth with no gland; main and secondary veins densely covered with villous, secondary veins 7–12. Inflorescences umbellate, 1–4-flowered, involucral bracts brown, long elliptic, 6–8 mm long, ca. 3 mm in width, adaxially densely covered with appressed villous; bracts ovate, 1–3 mm in diam., margin strongly fimbriate, fimbria with a long-stalked gland. Flowers opening before leaves or nearly at the same time. Pedicel 0.5–1(–2) cm, spreading white villous. Hypanthium tubular-campanulate, 3–5 × 3–4 mm, outside densely villous, pubescent. Sepals usually reddish, triangular, 0.4–5.5 cm, erect, margin entire, apex acute to obtuse. Petals white or pink, ovate to obovate, apically entire or emarginate. Stamens 35–40, shorter than petals. Style as long as stamens, glabrous, stigma disciform. Drupe dark purple, ovoid, 1–1.2 × 0.5–0.8 cm; endocarp ovoid, 0.6–0.8 × 0.4 cm, deeply furrowed and pitted on the lateral sides, apex obtuse. Flowers Mar.–Apr., fruits in May.

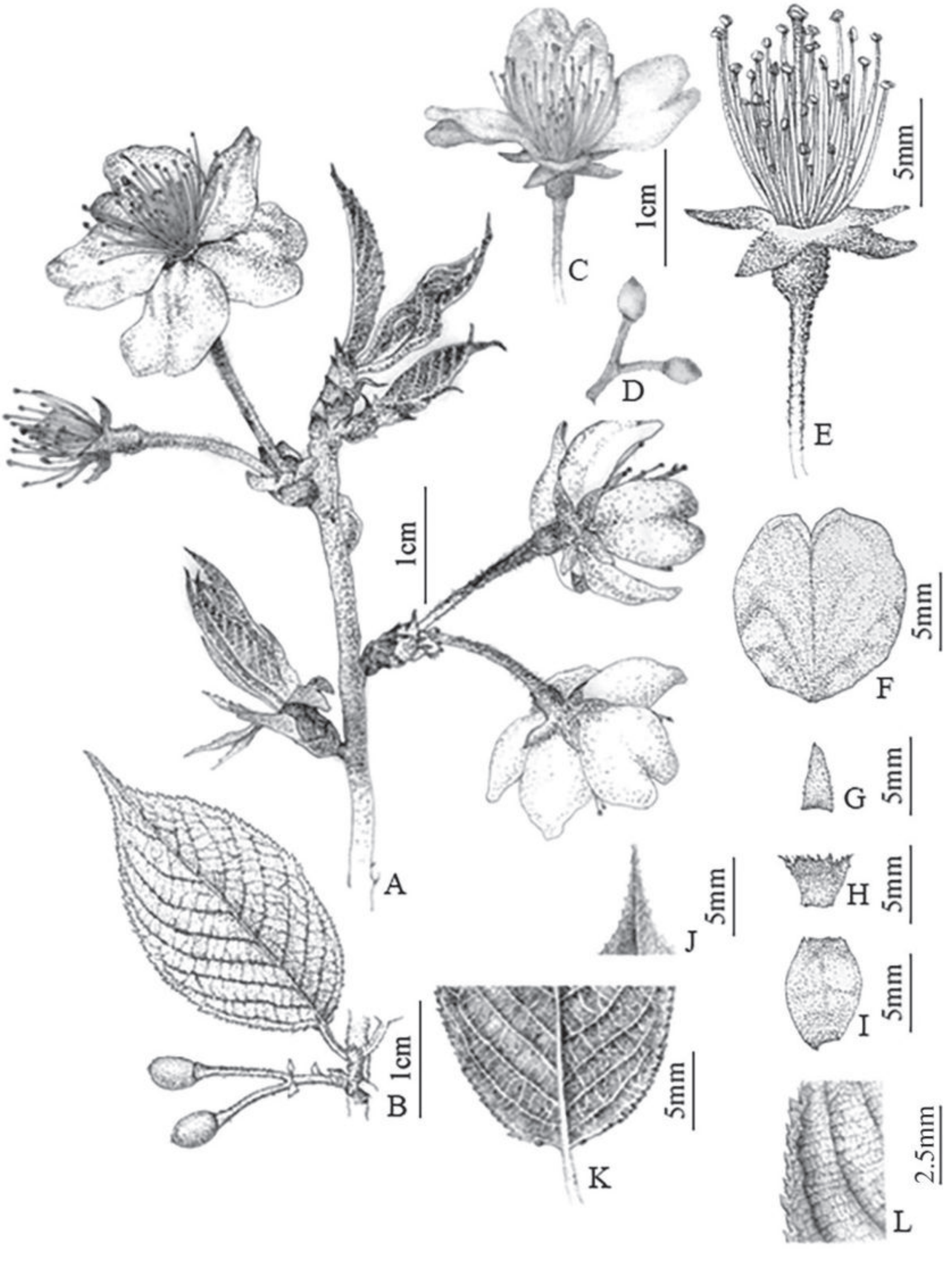

Figure 3. *Prunus tongmuensis* X.G.Yi & X.R.Wang **A** flowering branch **B** fruiting branch **C** flower **D** fruit **E** pistil and stamen **F** petal **G** sepal **H** bract **I** involucral bract **J** leaf apex **K** two glands at the base of leaf **L** teeth.

Etymology. Referring to the locality (Tongmuguan) where this new species was found.

Distribution and habitat. This species is currently known only from Wuyishan National Park, Fujian and Jiangxi Province. This species grows in various habitats such as the margins of evergreen broad-leaved forests, valleys, or roadsides, at an altitude of 600–1000 m.

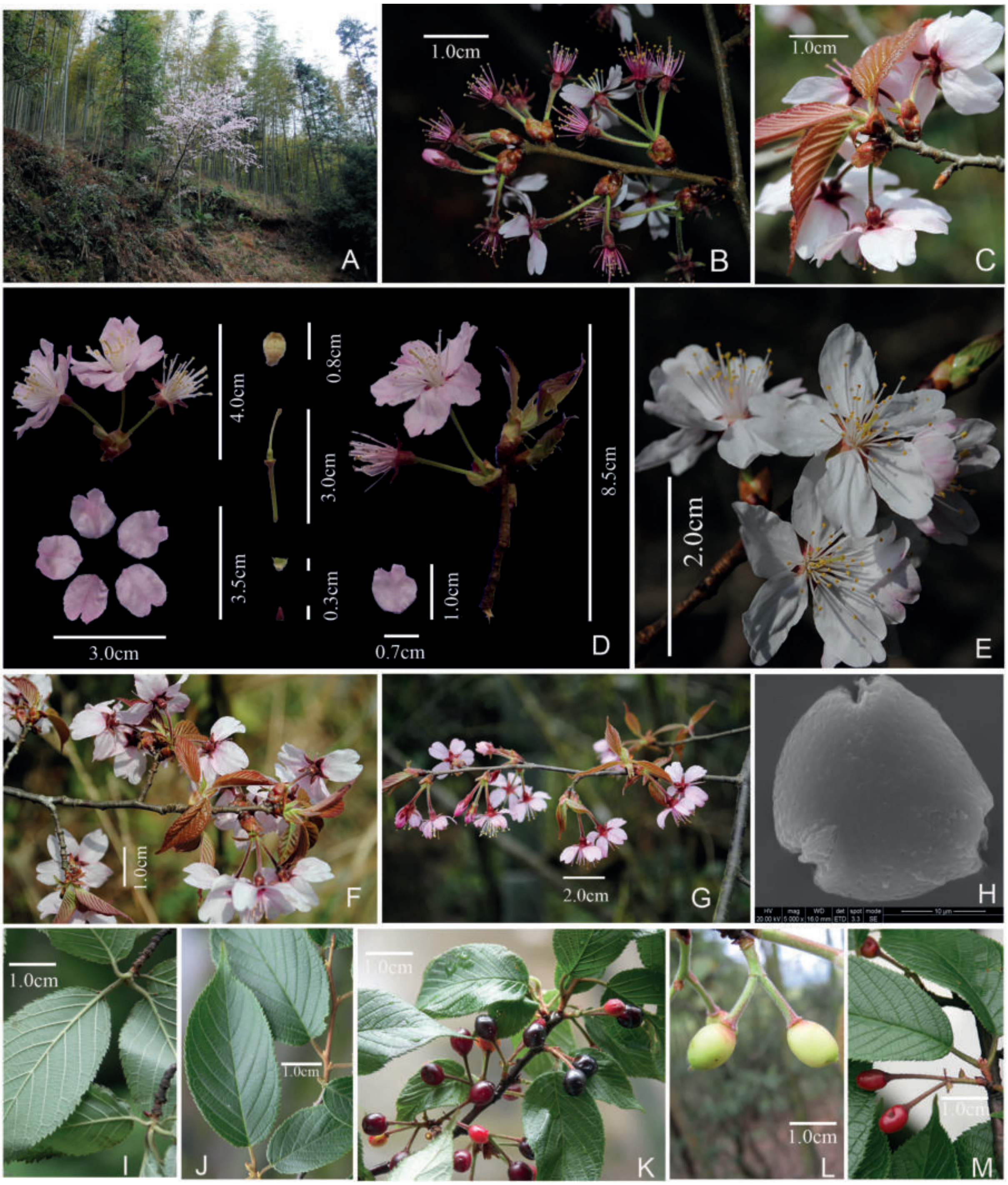

Figure 4. *Prunus tongmuensis* X.G.Yi et X. R.Wang **A** habitat **B–G** flowering branch **H** pollen grain **I, J** leaves **K** fruiting branch **L** young fruit branch **M** dark purple fruits.

Conclusions

We have described and illustrated a new species of *Prunus* L. subg. *Cerasus* (Mill.) within the family Rosaceae in Tongmuguan, Tongmu Village situated on the border of Jiangxi and Fujian provinces in China. Additionally, we have presented evidence for its phylogenetic position through the whole plastid genome data. Following comprehensive field research, we have determined that *Prunus tongmuensis* is confined to a narrow range within Tongmuguan, located in the break pass of the Wuyi Mountains. On the edge of the forest, four large populations of nearly 60 individuals, each with about 15 individuals, were observed scattered. It is quite interesting that morphologically, this species bears the closest resemblance to *P. dielsiana*, with significant differences in the location of glands, timing of flower and leaf openings, reflexed or spread sepals, and drupe color. Phylogenetically, the new species is closely linked to *P. clarofolia*; however, it notably differs in leaf shape, size, petiole villus color, gland location, timing of flower and leaf openings, and reflexed or spread sepals, as well as drupe color. Our study not only contributes to the diversity of *Prunus* subg. *Cerasus* species in China but also underscores the importance of conducting a comprehensive survey of biodiversity in the Jiangxi and Fujian provinces and the Wuyi Mountains.

Acknowledgements

We thank Zikun Xu, Caixia Shi, Chunping Xie, and Jing Qiu for their assistance in the field, Yifan Duan and Yong Yang for their valuable suggestions in data analysis. Thanks to the painter: Nannan Wang. Special thanks are extended to Ming Zhang and Lin Chen for his assistance when assembling the plastid genome.

Additional information

Conflict of interest

The authors have declared that no competing interests exist.

Ethical statement

No ethical statement was reported.

Funding

This study was funded by the Jiangsu Province Modern Agriculture Key Project [BE2020343] and the Xuzhou Science and Technology Project [KC21336].

Author contributions

Conceptualization: XGY, JJD. Sample collection: XGY. Data curation: SCG, HJZ, TW, XZC. Valuable advice: MZ, KWX, LM. Painting: NNW. Writing – review and editing: XGY, JJD.

Author ORCIDs

Xiangui Yi https://orcid.org/0000-0003-3123-9076
Jingjing Dong https://orcid.org/0000-0001-5269-4778
Meng Li https://orcid.org/0000-0003-2085-3388
Xianrong Wang https://orcid.org/0000-0002-7940-909X

Data availability

All of the data that support the findings of this study are available in the main text.

References

Bortiri E, Heuvel BV, Potter D (2006) Phylogenetic analysis of morphology in *Prunus* reveals extensive homoplasy. Plant Systematics and Evolution 259(1): 53–71. https://doi.org/10.1007/s00606-006-0427-8

Fu LF, Liao R, Lan DQ, Lan DQ, Wen F, Liu H (2020) A new species of *Chrysosplenium* (Saxifragaceae) from Shaanxi, north-western China. PhytoKeys 159: 127–135. https://doi.org/10.3897/phytokeys.159.56109

Iwatsuki K, Boufford DE, Ohba H (2001) Flora of Japan. Science Press 2: 435–148.

Jin JJ, Yu WB, Yang JB, Song Y, de Pamphilis CW, Yi TS, Li DZ (2020) GetOrganelle: A fast and versatile toolkit for accurate de novo assembly of organelle genomes. Genome Biology 21(1): e241. https://doi.org/10.1186/s13059-020-02154-5

Katoh K, Standley DM (2013) MAFFT multiple sequence alignment software version 7: Improvements in performance and usability. Molecular Biology and Evolution 30(4): 772–780. https://doi.org/10.1093/molbev/mst010

Li CL, Bartholomew B (2003) *Cerasus* in Flora of China. Science Press 9: 404–420.

Li M, Song YF, Sylvester SP, Sylvester SP, Wang XR (2022) Comparative analysis of the complete plastid genomes in *Prunus* subgenus *Cerasus* (Rosaceae): Molecular structures and phylogenetic relationships. PLOS ONE 17(4): e0266535. https://doi.org/10.1371/journal.pone.0266535

Liu C, Shi LC, Zhu YJ, Chen HM, Zhang JH, Lin XH, Guan XJ (2012) CpGAVAS, an integrated web server for the annotation, visualization, analysis, and GenBank submission of completely sequenced chloroplast genome sequences. BMC Genomics 13(1): e715. https://doi.org/10.1186/1471-2164-13-715

Lu Z, Li Y, Yang X, Liu J (2018) *Carpinus tibetana* (Betulaceae), a new species from southeast Tibet, China. PhytoKeys 98: 1–13. https://doi.org/10.3897/phytokeys.98.23639

Medeiros H, de Carvalho Lopes J, Acevedo-Rodríguez P, Forzza RC (2020) A new species of *Thinouia* (Paullinieae, Sapindaceae) from the Amazon and its phylogenetic placement. PhytoKeys 165: 115–126. https://doi.org/10.3897/phytokeys.165.57341

Rambaut A (2009) FigTree 1.3.1. http://tree.bio.ed.ac.uk/software/figtree

Ronquist F, Teslenko M, van der Mark P, Ayres DL, Darling A, Höhna S, Larget B, Liu L, Suchard MA, Huelsenbeck JP (2012) MrBayes 3.2: Efficient Bayesian phylogenetic inference and model choice across a large model space. Systematic Biology 61(3): 539–542. https://doi.org/10.1093/sysbio/sys029

Shen X, Zong W, Li Y, Liu X, Zhuge F, Zhou Q, Zhou S, Jiang D (2023) Evolution of Cherries (*Prunus* Subgenus *Cerasus*) based on chloroplast genomes. International Journal of Molecular Sciences 24(21): we15612. hhttps://doi.org/10.3390/ijms242115612

Shi S, Li J, Sun J, Yu J, Zhou SL (2013) Phylogeny and classification of *Prunus sensulato* (Rosaceae). Journal of Integrative Plant Biology 55(11): 1069–1079. https://doi.org/10.1111/jipb.12095

Trifinopoulos J, Nguyen L, von Haeseler A, Minh Q (2016) W-IQ-TREE: A fast online phylogenetic tool for maximum likelihood analysis. Nucleic Acids Research 44(W1): W232–W235. https://doi.org/10.1093/nar/gkw256

Wang XR (2014) An illustrated monograph of cherry cultivars in China. Science Press 12: 24–28.

Xie CP, Yi XG, Wang XR (2007) Population structure and dynamics of Cerasus subhirtella var. ascendens in Wuyi Mountain, Fujian. Shihezi Daxue Xuebao. Ziran Kexue Ban 25(6): 732–736.

Zhu H, Yi XG, Zhu SX, Wang HC, Wang XR (2018) Application of the molecular marker technology to *Cerasus* Mill. (Rosaceae). World Forestry Research 31: 16–24.